

FINAL REPORT

Designing, Assessing, and Demonstrating Sustainable
Bioaugmentation for Treatment of DNAPL
Sources in Fractured Bedrock

ESTCP Project ER-201210

MARCH 2017

Charles Schaefer, Ph.D.
CDM Smith

Graig Lavorgna
CB&I Federal Services

Michael Annable, Ph.D. and Erin White
University of Florida

Distribution Statement A
This document has been cleared for public release



Page Intentionally Left Blank

This report was prepared under contract to the Department of Defense Environmental Security Technology Certification Program (ESTCP). The publication of this report does not indicate endorsement by the Department of Defense, nor should the contents be construed as reflecting the official policy or position of the Department of Defense. Reference herein to any specific commercial product, process, or service by trade name, trademark, manufacturer, or otherwise, does not necessarily constitute or imply its endorsement, recommendation, or favoring by the Department of Defense.

Page Intentionally Left Blank

REPORT DOCUMENTATION PAGE

Form Approved
OMB No. 0704-0188

Public reporting burden for this collection of information is estimated to average 1 hour per response, including the time for reviewing instructions, searching existing data sources, gathering and maintaining the data needed, and completing and reviewing this collection of information. Send comments regarding this burden estimate or any other aspect of this collection of information, including suggestions for reducing this burden to Department of Defense, Washington Headquarters Services, Directorate for Information Operations and Reports (0704-0188), 1215 Jefferson Davis Highway, Suite 1204, Arlington, VA 22202-4302. Respondents should be aware that notwithstanding any other provision of law, no person shall be subject to any penalty for failing to comply with a collection of information if it does not display a currently valid OMB control number. **PLEASE DO NOT RETURN YOUR FORM TO THE ABOVE ADDRESS.**

1. REPORT DATE (DD-MM-YYYY) 01-27-2017		2. REPORT TYPE Final		3. DATES COVERED (From - To) April 2012 to January 2017	
4. TITLE AND SUBTITLE Designing, Assessing, and Demonstrating Sustainable Bioaugmentation for Treatment of DNAPL Sources in Fractured Bedrock				5a. CONTRACT NUMBER W912HQ-12-C-0062	
				5b. GRANT NUMBER NA	
				5c. PROGRAM ELEMENT NUMBER NA	
6. AUTHOR(S) Schaefer, Charles E., Ph.D. (CDM Smith) Lavorgna, Graig M. (CB&I Federal Services) Annable, Michael D., Ph.D. (University of Florida) White, Erin B. (University of Florida)				5d. PROJECT NUMBER NA	
				5e. TASK NUMBER NA	
				5f. WORK UNIT NUMBER NA	
7. PERFORMING ORGANIZATION NAME(S) AND ADDRESS(ES) CB&I Federal Services, LLC. 17 Princess Road Lawrenceville, NJ 08648				8. PERFORMING ORGANIZATION REPORT NUMBER NA	
9. SPONSORING / MONITORING AGENCY NAME(S) AND ADDRESS(ES) Environmental Security Technology Certification Program 4800 Mark Center Drive, Suite 17D08 Alexandria, VA 22350-3605				10. SPONSOR/MONITOR'S ACRONYM(S) ESTCP	
				11. SPONSOR/MONITOR'S REPORT NUMBER(S) NA	
12. DISTRIBUTION / AVAILABILITY STATEMENT Distribution Statement A: Approved for Public Release, Distribution is Unlimited					
13. SUPPLEMENTARY NOTES None					
14. ABSTRACT Bioaugmentation was applied to treat the DNAPL sources present in the fracture zones that were targeted for investigation using the partitioning tracer testing. Nine months of active treatment (using groundwater re-circulation with electron donor and nutrient delivery) was followed by a 10-month rebound period. While enhanced dissolution of the DNAPL sources was observed in both the shallow and deep fractures intervals, a greater extent of DNAPL mass removal (approximately 100%) was observed in the shallow fracture zone, while only 45% of the DNAPL was removed in the deep zone. The difference in DNAPL mass removal between the two zones was attributed to the DNAPL architecture, as the flow field in the deep zone was more complex, and a greater extent of the DNAPL was present in mass transfer controlled zones. Furthermore, while no increases in chlorinated ethenes or ethene was observed in the shallow zone during the 10-month rebound period, data suggest the sum of chlorinated ethenes and ethene concentrations were increasing during rebound in the deep zone, likely due to the persistence of residual DNAPL sources. This highlights the relationship between DNAPL architecture and remedial performance.					
15. SUBJECT TERMS PCE, DNAPL, bedrock, bioaugmentation, bioremediation					
16. SECURITY CLASSIFICATION OF:			17. LIMITATION OF ABSTRACT UU	18. NUMBER OF PAGES 363	19a. NAME OF RESPONSIBLE PERSON Dr. Charles Schaefer
a. REPORT U	b. ABSTRACT U	c. THIS PAGE U			19b. TELEPHONE NUMBER (include area code) 732-590-4633

Page Intentionally Left Blank

FINAL REPORT

Project: ER-201210

TABLE OF CONTENTS

	Page
EXECUTIVE SUMMARY	ES-1
1.0 INTRODUCTION	1
1.1 BACKGROUND	1
1.2 OBJECTIVE OF THE DEMONSTRATION.....	2
1.3 REGULATORY DRIVERS	2
2.0 TECHNOLOGY	3
2.1 TECHNOLOGY DESCRIPTION	3
2.1.1 Background – Bioaugmentation	3
2.1.2 Bioaugmentation for Treatment of DNAPL	3
2.2 TECHNOLOGY DEVELOPMENT	4
2.2.1 DNAPL in Fractured Bedrock – Discrete Fracture Scale Studies	4
2.2.2 DNAPL in Fractured Bedrock – Intermediate Scale Fracture Network Studies.....	7
2.2.3 DNAPL Source Strength Function in Fractured Bedrock	9
2.3 ADVANTAGES AND LIMITATIONS OF THE TECHNOLOGY	10
2.3.1 Advantages.....	10
2.3.2 Limitations	10
3.0 PERFORMANCE OBJECTIVES	11
3.1 EFFECTIVENESS OF BIOAUGMENTATION FOR PCE DNAPL REMOVAL... 11	
3.1.1 Data Requirements for DNAPL Removal	12
3.1.2 Success Criteria for DNAPL Removal	12
3.2 BIOAUGMENTATION EFFECTIVENESS FOR FLUX REDUCTION..... 12	
3.2.1 Data Requirements for Flux Reduction	12
3.2.2 Success Criteria for Flux Reduction	12
3.3 COMPLETE PCE DECHLORINATION	13
3.3.1 Data Requirements for Complete PCE Dechlorination	13
3.3.2 Success Criteria for Complete PCE Dechlorination	13
3.4 DHCDISTRIBUTION AND GROWTH..... 13	
3.4.1 Data Requirements for DHC Distribution and Growth	13
3.4.2 Success Criteria for DHC Distribution and Growth	13
3.5 EASE OF IMPLEMENTATION	13
3.5.1 Data Requirements to Assess Ease of Implementation.....	13

TABLE OF CONTENTS (Continued)

	Page
3.5.2 Success Criteria for Ease of Implementation	14
4.0 SITE DESCRIPTION	15
4.1 SITE SELECTION	15
4.2 SITE LOCATION AND HISTORY	18
4.3 SITE GEOLOGY AND HYDROGEOLOGY	19
4.3.1 Site Geology	19
4.3.2 Groundwater Monitoring Wells	21
4.3.3 Hydrogeology and Fracture Network	23
4.3.4 Groundwater Flow	23
4.3.5 Groundwater Geochemistry	25
4.4 CONTAMINANT SOURCE AND DISTRIBUTION	27
4.5 TEST PLOT LOCATION	31
5.0 TEST DESIGN	33
5.1 CONCEPTUAL EXPERIMENTAL DESIGN	33
5.2 BASELINE CHARACTERIZATION ACTIVITIES	33
5.2.1 Preliminary Assessment of DNAPL Distribution and Hydrogeology	34
5.3 LABORATORY TREATABILITY STUDY	54
5.3.1 Objectives	54
5.3.2 Sample Collection	55
5.3.3 Treatability Study Methodology	55
5.3.4 Treatability Study Results	57
5.3.5 Treatability Study Conclusions	60
5.4 DESIGN AND LAYOUT OF TECHNOLOGY COMPONENTS	62
5.4.1 Basis and Rationale for Demonstration Layout	62
5.4.2 Layout and Well Construction	63
5.4.3 Packer Installation and Sampling Assembly	68
5.4.4 Enhanced Bioremediation Treatment System	71
5.4.5 Power	74
5.5 FIELD TESTING	74
5.5.1 Short-term Hydraulic Testing and Baseline Sampling– STAGE 1	76
5.5.2 Groundwater Recirculation and Partitioning Tracer Testing – STAGE 2	76
5.5.3 Bioaugmentation Treatment and Monitoring – STAGE 3	78
5.5.4 Post-Treatment Monitoring and Assessment – STAGE 4	80
5.5.5 Demobilization	81
5.6 DATA ANALYSIS	82
5.6.1 Determination of Flow Field and DNAPL Architecture	82

TABLE OF CONTENTS (Continued)

	Page
5.6.2 Determination of DNAPL Mass Removal	83
5.7 SAMPLING METHODS	84
5.7.1 Groundwater Sampling	84
5.7.2 Decontamination	85
5.7.3 Analytical and Sample Preservation for Groundwater Samples	85
5.7.4 Groundwater Sampling Locations and Frequency	86
5.7.5 Quality Assurance for Groundwater Sampling and Analysis	87
5.8 RESULTS	91
5.8.1 Results of STAGE 1 Testing.....	91
5.8.2 Results of STAGE 2 Testing.....	92
5.8.3 Results of STAGE 3 Testing: Bioaugmentation Treatment and Monitoring.....	95
5.8.4 Results of STAGE 4 Testing: Post Treatment Monitoring and Assessment.....	101
6.0 PERFORMANCE ASSESSMENT	105
6.1 DNAPL ARCHITECTURE	105
6.2 BIOAUGMENTATION TREATMENT	107
6.2.1 DNAPL Mass Removal	107
6.2.2 Rebound	108
6.2.3 Implications for Groundwater Quality	109
7.0 COST ASSESSMENT.....	111
7.1 COST MODEL.....	111
7.1.1 Capital Costs	111
7.1.2 O&M Costs	111
7.1.3 Demonstration-Specific Costs	113
7.2 COST DRIVERS.....	113
7.2.1 General Considerations.....	113
7.2.2 Competing Treatment Technologies.....	113
7.3 COST ANALYSIS	114
7.3.1 Base Cost Template	115
7.3.2 Bioremediation Recirculation System	116
7.3.3 Thermal Conductive Heating.....	118
7.3.4 Active Pump and Treat	119
8.0 IMPLEMENTATION ISSUES	123
9.0 REFERENCES	125
APPENDIX A POINTS OF CONTACT.....	A-1
APPENDIX B BORING LOGS.....	B-1

TABLE OF CONTENTS (Continued)

	Page
APPENDIX C	BOREHOLE GEOPHYSICAL LOGS..... C-1
APPENDIX D	FIELD OPERATIONS SUMMARY TABLE..... D-1
APPENDIX E	PERMIT FOR INDUSTRIAL WASTEWATER DISCHARGEE-1
APPENDIX F	ANALYTICAL DATA TABLES..... F-1

LIST OF FIGURES

		Page
Figure 2.1.	Laboratory Studies - PCE DNAPL.....	5
Figure 2.2.	Dissolution and Dechlorination in Fractures - Laboratory Scale.....	5
Figure 2.3.	Bioaugmentation in Fractured Sandstone.....	6
Figure 2.4.	Simulated Bioaugmentation.....	6
Figure 2.5.	DNAPL Removal - Bioaugmentation versus Persulfate.....	7
Figure 2.6.	Fracture Network – Colorado School of Mines.....	8
Figure 2.7.	DNAPL Dissolution Enhancement Colorado School of Mines.....	8
Figure 4.1.	Bench Scale Microcosm Testing.....	16
Figure 4.2.	Partitioning Tracer Test- Push Pull Results.....	17
Figure 4.3.	Edwards AFB Research Laboratory OU4 and OU9.....	18
Figure 4.4.	Edwards AFB Geology. Modified from Dibblee, 1960 (25).....	20
Figure 4.5.	South AFRL Monitoring Well Network.....	22
Figure 4.6.	South AFRL Potentiometric Surface 2010. (26).....	24
Figure 4.7.	Building 8595 Facilities.....	28
Figure 4.8.	Plume Boundary VOC Current Groundwater and Projected 30-year Vapor.....	29
Figure 4.9.	Geologic Cross Section and PCE Concentration circa 2005.....	30
Figure 4.10.	Site 37 Bioaugmentation Test Area.....	32
Figure 5.1.	Well Installations, Bioaugmentation Test Phase I.....	35
Figure 5.2.	Geologic Core 37-B06: 69 ft bgs to 82.5 ft bgs.....	37
Figure 5.3.	Borehole Televiewer Log 37-B06 (71 to 88 ft bgs interval).....	41
Figure 5.4.	Generalized Geologic Cross Section A-A’.....	44
Figure 5.5.	Results of Short-Term Pumping Test.....	46
Figure 5.6a.	Shallow Push-Pull PTT Results for 37-B06.....	49
Figure 5.6b.	Deep Push-Pull PPT Results for 37-B06.....	49
Figure 5.6c.	Push-Pull PPT Results for 37-B07.....	50
Figure 5.7.	Interwell Tracer Test Results.....	52
Figure 5.8.	Conceptual Model Showing Likely DNAPL Locations.....	53
Figure 5.9.	Chlorinated Ethenes and Ethene Results for Treatments 1-6.....	61
Figure 5.10.	Groundwater Recirculation and Amendment Delivery System.....	64
Figure 5.11.	Typical Well Completion Diagram.....	66

LIST OF FIGURES

	Page
Figure 5.12. Inflatable Packers.....	69
Figure 5.13. Packer and Pump Placement.....	71
Figure 5.14. Enhanced Bioremediation Treatment System P&ID	72
Figure 5.15. Post-Treatment Rock Core Location	81
Figure 5.16. Chain of Custody Form.....	89
Figure 5.17. PCE Concentration within the Rock Matrix at 37-B10	91
Figure 5.18. Bromide and DMP Tracer Elution in 37-B11s	93
Figure 5.19. Bromide and DMP Tracer Elution in 37-B11d.....	94
Figure 5.20. Groundwater Re-circulation Flow Rate.....	95
Figure 5.21. Chlorinated Ethene+Ethene, Sulfate, and Dhc Levels at 37-B07d.....	96
Figure 5.22. Propionic Acid Concentration Measured in the Shallow Interval of 37-B11	97
Figure 5.23. Propionic Acid Concentration Measured in the Deep Interval of 37-B11.....	97
Figure 5.24. Chlorinated Ethene and Ethene Concentrations at 37-B11s.....	98
Figure 5.25. Chlorinated Ethene and Ethene Concentrations at 37-B11d.....	99
Figure 5.26. Generated Chloride (above background chloride levels) at 37-B11.....	99
Figure 5.27. Sulfate and Dissolved Iron Concentrations Measured in 37-B11s and 37-B11d 100	
Figure 5.28. DHC Concentrations Measured in 37-B11s (top) and 37-B11d (bottom).....	101
Figure 5.29. Ferrous mineral content within the rock matrix at 37-B14.....	102
Figure 5.30. Acoustic Televiewer Results Focusing on the Deep Fracture Zone at 37-B06 ..	103
Figure 7.1. Base Plume Characteristics.....	115
Figure 7.2. Bioremediation Recirculation System Alternative	117
Figure 7.3. Thermal Conductive Heating Alternative.....	118
Figure 7.4. Active Pump and Treat Alternative	120

LIST OF TABLES

	Page
Table 1.1. Federal and California State Maximum Contaminant Levels.....	2
Table 3.1. Performance Objectives	11
Table 4.1. Site Selection Criteria	17
Table 4.2. Water Quality Parameter Concentrations from Inorganic Study	26
Table 5.1. VOCs in Geologic Core, PID Examination	39
Table 5.2. Groundwater PCE Concentration Measured at the Boreholes.....	43
Table 5.3. Summary of 37-B07 Pump Test Analysis	46
Table 5.4. Geochemical Results for Treatability Study	58
Table 5.5. Alcohol Results for Treatments 3 and 6	59
Table 5.6. Alcohol Sorption Test Results	59
Table 5.7. Discrete Intervals for Monitoring, Injection and/or Extraction	63
Table 5.8. Timeline of Field Operations	75
Table 5.9. Purge Volumes for Groundwater Sampling.....	85
Table 5.10. Analytical Methods, Preservation, and Containers -Groundwater	86
Table 5.11. Groundwater Sampling Schedule	87
Table 5.12. Modeling Results Based on the PTT	94
Table 7.1. Demonstration Cost Components	112
Table 7.2. Summary of Base Case Site Characteristics and Design Parameters	116
Table 7.3. Cost Components for Bioremediation Recirculation System	117
Table 7.4. Cost Components for Thermal Conductive Heating.....	119
Table 7.5. Cost Components for Active Pump and Treat	120
Table 7.6. Summary of Costs for Treatment Alternatives	121

Page Intentionally Left Blank

ACRONYMS AND ABBREVIATIONS

µg/L	micrograms per liter
µM	micromolar
AFB	Air Force Base
AFP	Air Force Plant
AFRL	Air Force Research Laboratory
AGW	Artificial Groundwater
As	Arsenic
AST	Aboveground Storage Tank
ASTM	American Society for Testing and Materials
bgs	below ground surface
Blvd	Boulevard
°C	degrees Celsius
CB&I	Chicago Bridge and Iron Federal Services
Cl ⁻	Chloride
COC	Chain-of-Custody
CSM	Conceptual Site Model
cVOC	Chlorinated Volatile Organic Compound
DAP	Diammonium Phosphate
DCE	<i>cis</i> -1,2-Dichloroethene
DHC	<i>Dehalococcoides</i> sp.
DMP	2,4-dimethyl-3-pentanol
DNAPL	Dense Non-Aqueous Phase Liquid
DO	Dissolved Oxygen
DoD	U.S. Department of Defense
ESTCP	Environmental Security Technology Certification Program
EVO	Emulsified Vegetable Oil
Fe	Iron
ft	foot or feet
g	gram
GAC	Granular Activated Carbon
GC-FID	Gas Chromatography-Flame Ionization Detector
GETS	Groundwater Extraction and Treatment System
gpm	gallons per minute
IDW	Investigation Derived Waste
IPR	In-Progress Review

Kg	kilogram
L	liter
LNAPL	Light Non-Aqueous Phase Liquid
MCL	Maximum Contaminant Level
mg/kg	milligrams per kilogram
mg/L	milligrams per liter
mL	milliliters
mL/min	milliliters per minute
mM	millimolar
Mn	Manganese
MNA	Monitored Natural Attenuation
MOM	Method of Moments
MRF	Mass Recovery Fraction
NDMA	N-nitrosodimethylamine
NPV	Net Present Value
O&M	Operation and Maintenance
OD	Outer Diameter
ORP	Oxidation-Reduction Potential
OU	Operable Unit
P&ID	Piping and Instrumentation Diagram
P&T	Pump and Treat
PCE	Tetrachloroethene
PID	Photoionization Detector
PLC	Programmable Logic Controller
ppb	parts per billion
ppm	parts per million
PTT	Partitioning Tracer Test
QA	Quality Assurance
QC	Quality Control
QED	QED Environmental Systems
qPCR	Polymerase Chain Reaction
RDG	Reductive Dehalogenase Genes
SCADA	Supervisory Control and Data Acquisition
SERDP	Strategic Environmental Research and Development Program
SO ₄ ⁻	Sulfate
SOP	Standard Operating Procedure
SVE	Soil Vapor Extraction

TCE	Trichloroethene
TCH	Thermal Conductive Heating
TeCA	1,1,2,2-Tetrachloroethane
USEPA/EPA	U.S. Environmental Protection Agency
USGS	United States Geological Survey
UV	Ultraviolet
VC	Vinyl Chloride
VFA	Volatile Fatty Acid
VOA	Volatile Organic Analysis
VOC	Volatile Organic Compound
ZVI	Zero-Valent Iron

Page Intentionally Left Blank

ACKNOWLEDGEMENTS

We wish to thank the environmental staff at Edwards Air Force Base, CA for their support during this demonstration. In particular, special thanks to Nashat Salet and Ai Duong for their dedication to the project and its success. We also wish to thank ESTCP for their financial support, and Dr. Andrea Leeson, the Environmental Restoration Program Manager at ESTCP, for her guidance. We would also like to thank Mark Henkes and his team at AECOM for their on-site logistical support during the demonstration; in particular John Oltion, who provided system operations and monitoring support throughout the duration of the field testing. Finally, we wish to acknowledge the capable staff at CB&I that conducted site assessment, laboratory studies, well installation, system design and installation, substrate injection, data management, and analytical support. In particular, Tim Ault, Randi Rothmel, Christina Andaya, Antonio Soto, Paul Hedman, and Sheryl Streger of CB&I were vital to project success. Their efforts ultimately lead to the quality experimental results and findings demonstrated during this project.

Page Intentionally Left Blank

EXECUTIVE SUMMARY

Management of fractured rock sites impacted with chlorinated solvents remains one of the top environmental challenges for the Department of Defense (DoD). Due to the use of chlorinated solvents such as tetrachloroethene (PCE) and trichloroethene (TCE) as industrial degreasers and cleaners, many unintended discharges and improper disposal practices have occurred, resulting in subsurface impacts that have produced regulatory exceedances in both soil and groundwater. Many studies have examined these dense non-aqueous phase liquid (DNAPL) sources in unconsolidated subsurface media. These studies have shown that DNAPL typically serves as a long-term contaminant source for groundwater, as the DNAPL slowly dissolves into surrounding groundwater. Unfortunately, even within unconsolidated media, treatment of DNAPL sources has proven challenging. These challenges have been due to identification and quantification of the DNAPL itself, mass transfer limitations with respect to DNAPL mass removal, concerns regarding uncontrolled DNAPL mobilization, and/or inhibition of complete microbial dechlorination. Thus, for many DNAPL-impacted sites, the DNAPL source area is the focus of site management and remedial efforts.

The challenges associated with DNAPL in fractured rock are similar to those encountered in unconsolidated media. However, these challenges are exacerbated by the complexities associated with the dual porosity nature of fractured rock, as well as the lack of insight into the highly complex DNAPL architecture at the field scale. The work performed as part of ESTCP Project ER-201210 focused on the detailed characterization of PCE DNAPL sources within the fracture flow field, and the subsequent treatment of those PCE DNAPL sources using bioaugmentation. For this effort, a small, well defined portion of a (presumably) much larger DNAPL source area was targeted at Edwards AFB in California. Using a series of conventional hydraulic and geophysical tools, along with partitioning tracer testing, the DNAPL distribution was quantified relative to the fracture flow field in both a shallow and deep fracture interval. Key results demonstrated that very low levels of DNAPL (<1% of the fracture volume) persisted in several of the fracture zones, and that DNAPL was present in both the lower and higher transmissivity zones. The DNAPL present in the low transmissivity zones is likely to remain long after DNAPL sources in the higher transmissivity zones are removed.

Bioaugmentation was applied to treat the DNAPL sources present in the fracture zones that were targeted for investigation using the partitioning tracer testing. Nine months of active treatment (using groundwater re-circulation with electron donor and nutrient delivery) was followed by a 10-month rebound period. While enhanced dissolution of the DNAPL sources was observed in both the shallow and deep fractures intervals, a greater extent of DNAPL mass removal (approximately 100%) was observed in the shallow fracture zone, while only 45% of the DNAPL was removed in the deep zone. The difference in DNAPL mass removal between the two zones was attributed to the DNAPL architecture, as the flow field in the deep zone was more complex, and a greater extent of the DNAPL was present in mass transfer controlled zones. Furthermore, while no increasing trend in the sum of chlorinated ethenes and ethene was observed in the shallow zone during the 10-month rebound period, data suggest the sum of chlorinated ethenes and ethene concentrations were increasing during rebound in the deep zone, likely due to the persistence of residual DNAPL sources. This highlights the relationship between DNAPL architecture and remedial performance.

Page Intentionally Left Blank

1.0 INTRODUCTION

1.1 BACKGROUND

Management of dense non-aqueous phase liquid (DNAPL) tetrachloroethene (PCE) and trichloroethene (TCE) source areas in fractured bedrock is a challenging environmental concern for the U.S. Department of Defense (DoD). Several DoD facilities, including Air Force Plant 4 (AFP4), AFP6, Edwards Air Force Base (AFB), Loring AFB, and Redstone Arsenal, likely contain DNAPL sources in bedrock. These DNAPL sources in bedrock are particularly problematic to treat and manage because defining the nature and extent of the DNAPL source is difficult, DNAPL can sustain groundwater plumes for several decades, and intrinsic mass transfer limitations hinder source removal. Cost-effective treatment technologies for these DNAPL sources in fractured rock are not available. Conventional technologies such as pump-and-treat or chemical oxidation typically are not effective, and the cost and effectiveness of innovative technologies (e.g., thermal, surfactant flushing) have yet to be fully demonstrated. Thus, many DoD fractured bedrock DNAPL sites persist without any active treatment to remove the source.

Another obstacle in addressing DNAPL sources in fractured rock is uncertainty regarding the relationship between contaminant mass removal and the dissolved contaminant flux emanating from the source area. This uncertainty has made it difficult to treat and manage these DNAPL sites, as the extent of mass removal (or “remediation”) that is required typically is unknown. Without knowing the extent of mass removal that is required to attain remedial goals for groundwater, or even how to assess this based on pilot scale testing, selecting an appropriate path forward is often difficult.

Because of these difficulties, field applications demonstrating the successful implementation of a selected technology that is both technically and economically effective for treating DNAPL sources in fractured rock have been very limited. As a result, impacts to aquifers from these DNAPL sources continue to occur, and the implementation of long-term containment approaches (e.g., pump-and-treat) for mitigating the downgradient plume are often employed. Demonstration and verification of a cost-effective technology for treating DNAPL sources in bedrock would provide a great benefit to the DoD.

As part of our completed Strategic Environmental Research and Development Program (SERDP) Project ER-1554, the use of bioaugmentation for treatment of PCE DNAPL sources in laboratory scale rock fracture experiments was demonstrated. However, there are currently no demonstrated examples of the successful application of biostimulation or bioaugmentation for treatment of DNAPL sources at the field scale in fractured bedrock so that a final monitored natural attenuation (MNA) remedy can be employed. No field studies have shown that bioaugmentation is effective in fractures containing residual DNAPL. While laboratory studies have demonstrated that bioaugmentation can substantially enhance DNAPL removal in rock fractures and reduce the dissolved flux emanating from the source area, a field scale study demonstrating that bioaugmentation can enhance DNAPL dissolution and mitigate dissolved contaminant flux both within and downgradient of the DNAPL source has not been performed. Furthermore, methods to optimize implementation (in terms of sustainability, limiting carbon consumption, and minimizing costs) of bioaugmentation in bedrock have not been demonstrated; the ability to target specific fracture zones where DNAPL sources are present would facilitate this.

Thus, a demonstration and assessment of this cost-effective remedial approach is needed to determine the efficacy of this technology for treatment of DNAPL sources at fractured bedrock sites.

1.2 OBJECTIVE OF THE DEMONSTRATION

The overall objectives of this project were to evaluate the use of bioaugmentation for treatment of PCE DNAPL sources in fractured rock, to assess treatment impacts on the dissolved downgradient plume, to demonstrate effective reductive dechlorination in DNAPL-filled fractures, and develop and verify design parameters to optimize sustainability. Specifically, this evaluation consisted of an assessment of the DNAPL architecture (including identification of specific fracture or fractures zones that contain DNAPL sources), DNAPL dechlorination and dissolution rates in DNAPL-containing fractures, distribution and growth of dechlorinating bacteria both within and downgradient of the DNAPL source area, impact on dissolved contaminant flux emanating from the DNAPL source, and evaluation of electron donor demand during treatment. The relationship between incremental DNAPL mass removal and dissolved PCE concentrations also was assessed, with the ultimate goal of demonstrating that bioaugmentation can facilitate a final MNA remedy in bedrock. This demonstration was performed at the Site 37 PCE source area at Edwards AFB.

1.3 REGULATORY DRIVERS

PCE, along with its reductive dechlorination daughter products TCE, *cis*-1,2-dichloroethene (DCE), and vinyl chloride (VC), are regulated in drinking and ground water by both the U.S. Environmental Protection Agency (USEPA) and the state of California. The applicable groundwater standards are provided in Table 1.1.

Expected PCE concentrations in DNAPL source areas, assuming concentrations of at least 1% solubility, are 300-times above both state and federal regulatory levels. PCE groundwater concentrations in the demonstration source area at Edwards AFB are in excess of 1% solubility. It is significant to note that partial dechlorination of PCE, resulting in near-stoichiometric accumulation of either TCE, DCE, and/or VC, would result in regulatory exceedances of these compounds as well.

Table 1.1. Federal and California State Maximum Contaminant Levels

Constituents	USEPA MCL (µg/L)	California MCL (µg/L)
Tetrachloroethene (PCE)	5	5
Trichloroethene (TCE)	5	5
<i>cis</i> -1,2-dichlorethene (DCE)	70	6
Vinyl Chloride (VC)	2	5

2.0 TECHNOLOGY

2.1 TECHNOLOGY DESCRIPTION

2.1.1 Background – Bioaugmentation

Bioaugmentation involves the subsurface delivery of bacteria, along with electron donor (e.g., lactate, vegetable oil) and nutrients, that are capable of completely dechlorinating PCE and TCE. For chlorinated ethenes, bioaugmentation typically involves the use of mixed anaerobic cultures that contain *Dehalococcoides* sp. (DHC), or closely related strains, that can reductively dechlorinate the chlorinated ethenes. Bioaugmentation has been successfully applied at several DoD and industrial facilities using both passive (single or periodic injection of amendments) and active (continual or intermittent recirculation of groundwater) *in situ* remedial approaches. Thus, bioaugmentation is a proven and well-demonstrated technology with respect to treatment of chlorinated ethenes in groundwater.

Our work as part of Environmental Security Technology Certification Program (ESTCP) Project ER-0515 demonstrated that DHC are rapidly distributed in the aquifer as the bacteria grow. The *in situ* dechlorination kinetics, as well as DHC growth and migration, were well described using an attachment-detachment type model coupled with Monod kinetics (1,2). This work has enabled us to improve our design of *in situ* bioaugmentation systems (with respect to dosage and well spacing), as well as to better assess remedial performance.

2.1.2 Bioaugmentation for Treatment of DNAPL

While several laboratory and field studies have demonstrated the effectiveness of bioaugmenting with DHC for treating dissolved phase PCE and TCE (1-5), the use of this approach for treating DNAPL sources has received far less attention. However, since the treatment of DNAPL source areas has increasingly become a focus at many contaminated sites (6-8), there has been a recent increased focus on application of bioaugmentation for DNAPL sources. Batch and column studies have indicated that the presence of PCE DNAPL can have an inhibitory effect on the reductive dechlorination of PCE during bioaugmentation (9-11). Adamson et al. (10) noted the accumulation of TCE and *cis*-1,2-DCE in the DNAPL source zone, without further dechlorination to VC or ethene until PCE concentrations decreased to approximately 10 μM .

Despite this apparent inhibitory effect of DNAPL on the reductive dechlorination of PCE, bioaugmentation has been shown to enhance the rate of PCE DNAPL dissolution in sand columns and flow cells by factors ranging from approximately 1.1 to 21 (11-13); enhancement rates generally were on the high end of this range when the dissolved concentration of PCE was less than approximately 300 μM (approximately 30% of the PCE solubility in water) (11,13). This enhancement occurs in the DNAPL source zone, despite the fact that (in some cases) only partial dechlorination to DCE occurs, because DCE is approximately 30-times more soluble than PCE. Thus, enhanced solubilization of the DNAPL occurs, with subsequent complete dechlorination of the DCE occurring immediately downgradient of the DNAPL zone.

Field scale applications of bioaugmentation or biostimulation to treat PCE or TCE DNAPL in unconsolidated materials have been performed (6,14). Results generally have been consistent with the laboratory studies described in the previous paragraphs; enhanced dissolution of the DNAPL occurred as evidenced by increases in total ethene molar concentrations and/or reduction in soil phase PCE/TCE concentrations. Accumulation of DCE also was observed. These results (6,14) suggest that biostimulation/bioaugmentation can be effective for treating DNAPL sources in unconsolidated materials.

2.2 TECHNOLOGY DEVELOPMENT

2.2.1 DNAPL in Fractured Bedrock – Discrete Fracture Scale Studies

While application of bioaugmentation for treatment of DNAPL in unconsolidated media has been demonstrated, as well as application of bioaugmentation to treat dissolved phase chlorinated ethenes in fractured bedrock (SERDP Project ER-1555), application of bioaugmentation to treat DNAPL sources in fractured bedrock has not yet been demonstrated. The architecture and dissolution of DNAPL in fractured bedrock can be substantially different than in unconsolidated media. The role of fracture intersections (15), preferential flow in discrete fractures (16), and low (relative to sands) DNAPL-water interfacial area and dissolution rates (17) are among the factors that differentiate DNAPL dissolution in fractured bedrock from that in unconsolidated media.

As part of our recently completed SERDP project (ER-1554), we have evaluated the use of bioaugmentation for treating PCE in bench-scale discretely fractured sandstone blocks containing residual DNAPL. Bioaugmentation resulted in dechlorination of PCE, as evidenced by generation of DCE, ethene, and chloride; chloride was shown to be the best indicator of dechlorination due to back-partitioning of volatile organic compounds (VOCs) into the DNAPL (18). Furthermore, results of our discrete fracture experiments showed that bioaugmentation enhanced DNAPL dissolution by up to 3.5-times (relative to dissolution into groundwater alone) with dissolved PCE concentrations at or near solubility (18) (Figure 2.1). Applying these DNAPL dissolution and dechlorination rates to a comparable field scale system (the short length scales in the bench scale systems amplified the importance of abiotic dissolution and masked the importance of biotic dissolution), the estimated DNAPL dissolution enhancement attained via bioaugmentation would be on the order of 30-times greater than via dissolution (e.g., pump-and-treat) alone (Figure 2.2). In addition, based on the observed DNAPL dechlorination kinetics observed in our bench scale testing, application of bioaugmentation for treatment of DNAPL sources can result in a 98% reduction (without rebound) in dissolved PCE concentration and flux within approximately 2.5 years of bioaugmentation treatment (Figures 2.3 and 2.4). Bioaugmentation was also shown to be more effective than chemical oxidation with respect to long-term mass removal, due to accumulation of precipitates at the DNAPL-water interface during chemical oxidation (Figure 2.5).

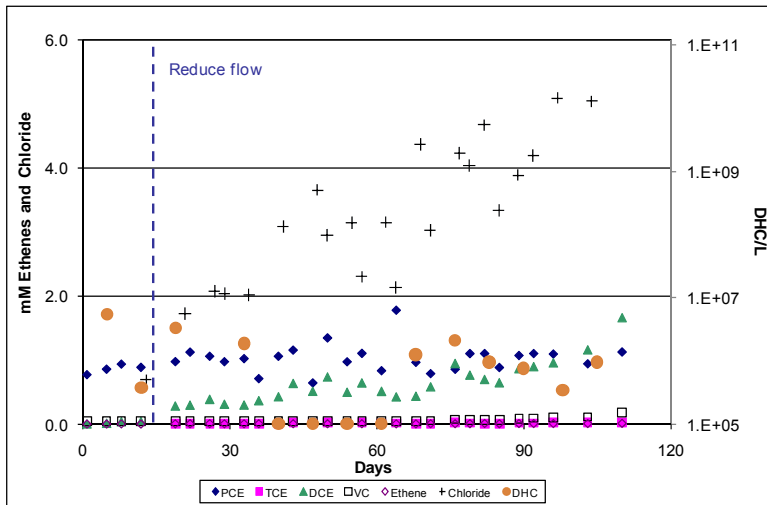


Figure 2.1. Laboratory Studies - PCE DNAPL

Shown are results from laboratory studies where bioaugmentation was used to treat PCE DNAPL in fractured sandstone blocks (18). Dissolved concentrations emanating from the fracture are shown. Reductive dechlorination was observed. Based on the chloride generation, DNAPL dissolution was enhanced during bioaugmentation by 3.5-times across the 29-centimeter fracture length.

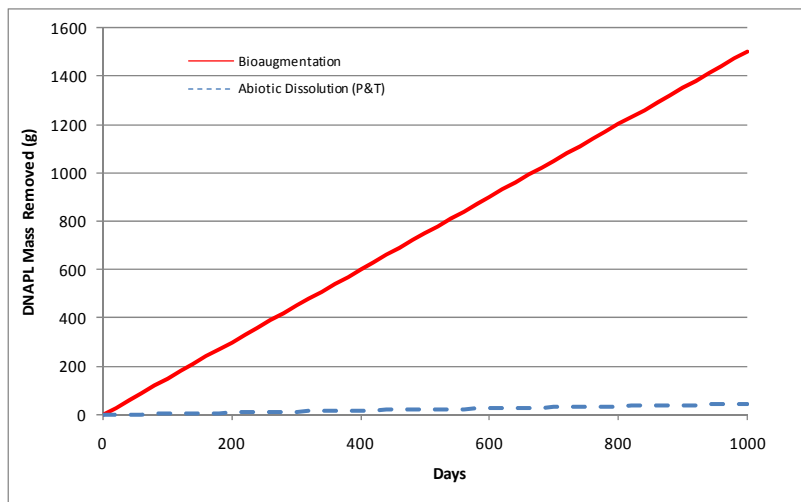


Figure 2.2. Dissolution and Dechlorination in Fractures - Laboratory Scale

Based on the dissolution and reductive dechlorination rates observed during bioaugmentation for PCE DNAPL in laboratory scale fracture systems (Figure 2.1), DNAPL mass removal in a single fracture (10 feet [ft] long, parallel to groundwater flow) would be enhanced 30-times over that obtained via dissolution only during pump-and-treat.

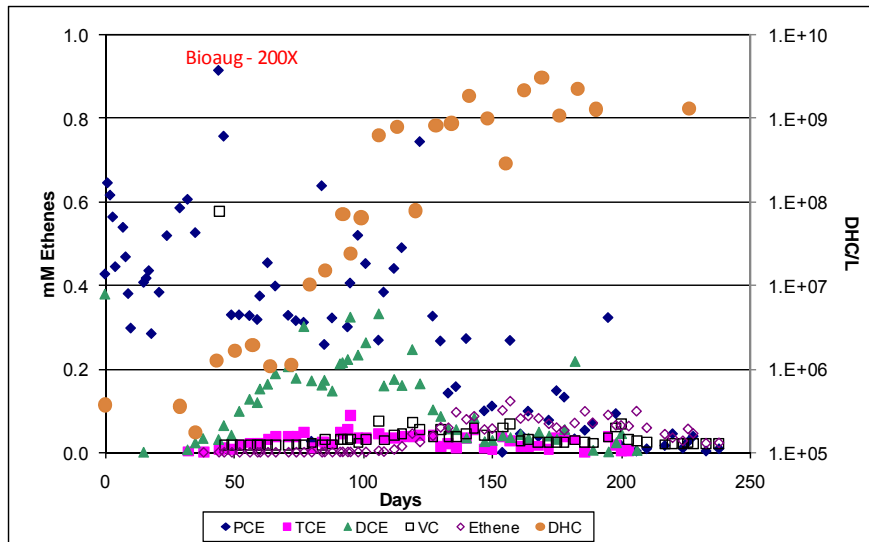


Figure 2.3. Bioaugmentation in Fractured Sandstone

Results from laboratory studies where bioaugmentation was used to treat PCE DNAPL in fractured sandstone blocks (18). Dissolved concentrations emanating from the fracture are shown. This experiment was performed for a longer duration and increased flow rate compared to the experiment shown on Figure 2.1. Results indicate that within 200 days, dissolved effluent PCE concentrations decreased by 98% (no rebound following treatment) with only 16% of the DNAPL mass removed.

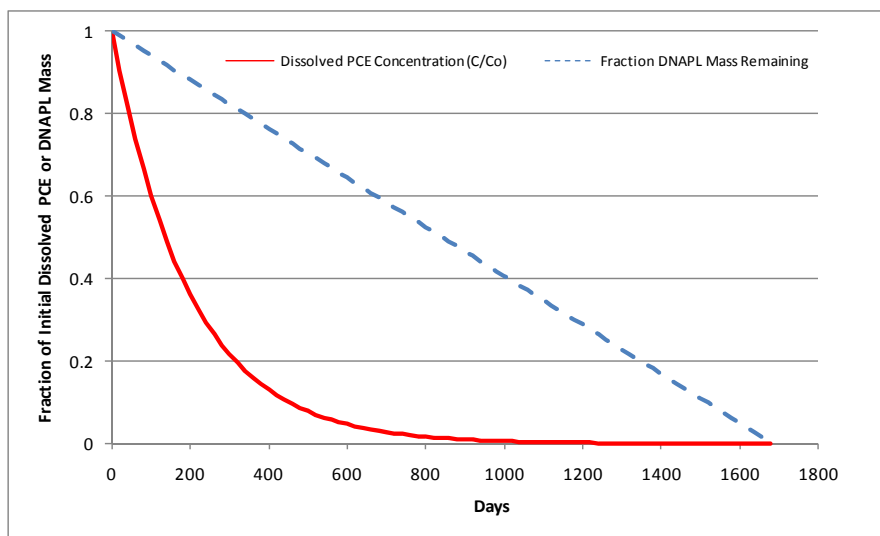


Figure 2.4. Simulated Bioaugmentation

Simulated DNAPL mass removal and dissolved PCE concentrations during bioaugmentation. Simulations are based on DNAPL dissolution kinetics measured in our laboratory experiments.

The observed dechlorination in our bench scale fracture systems, despite the elevated and potentially inhibitory levels of PCE, was attributed to growth of biofilms within the fractures (18). Increasing the flow rate resulted in increased migration of DHC from the fracture effluent, presumably due to increased shear and detachment of bacteria from the biofilms. These DHC migrating downgradient of the DNAPL source area will continue to treat the dissolved contaminant plume. At the field scale, these migrating DHC would provide a means to treat dissolved PCE in the downgradient plume and further reduce the concentration of dissolved chlorinated ethenes (1,2).

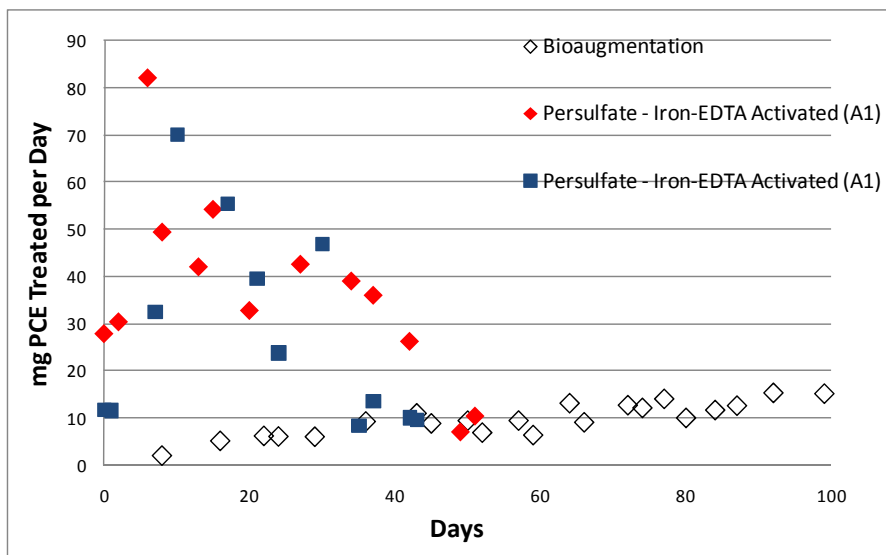


Figure 2.5. DNAPL Removal - Bioaugmentation versus Persulfate

Comparison of DNAPL removal rates between bioaugmentation and persulfate chemical oxidation (recently completed SERDP Project ER-1554). Mass removal using chemical oxidants initially are greater than that observed during implementation of bioaugmentation. However, due to increase in biomass, DNAPL mass removal rates begin to exceed that of chemical oxidation.

2.2.2 DNAPL in Fractured Bedrock – Intermediate Scale Fracture Network Studies

In the second phase of our SERDP Project ER-1554, we evaluated bioaugmentation for treatment of PCE DNAPL in an intermediate scale fracture network (Figure 2.6). This fracture network was used as an intermediate between a discrete fracture and a field scale fracture network. The intermediate scale fracture network consisted of multiple horizontal, vertical, and dead-end fractures, and was intended to capture (in part) the complex flow and DNAPL heterogeneities that likely exist at the field scale.

DNAPL dissolution studies showed that residual DNAPL in the fracture network was better contacted by groundwater compared to the discrete fractures, likely owing to enhanced contact of DNAPL at the fracture intersections. Furthermore, dissolution was enhanced by a factor of approximately 100 during bioaugmentation in the intermediate scale fracture network (Figure 2.7).

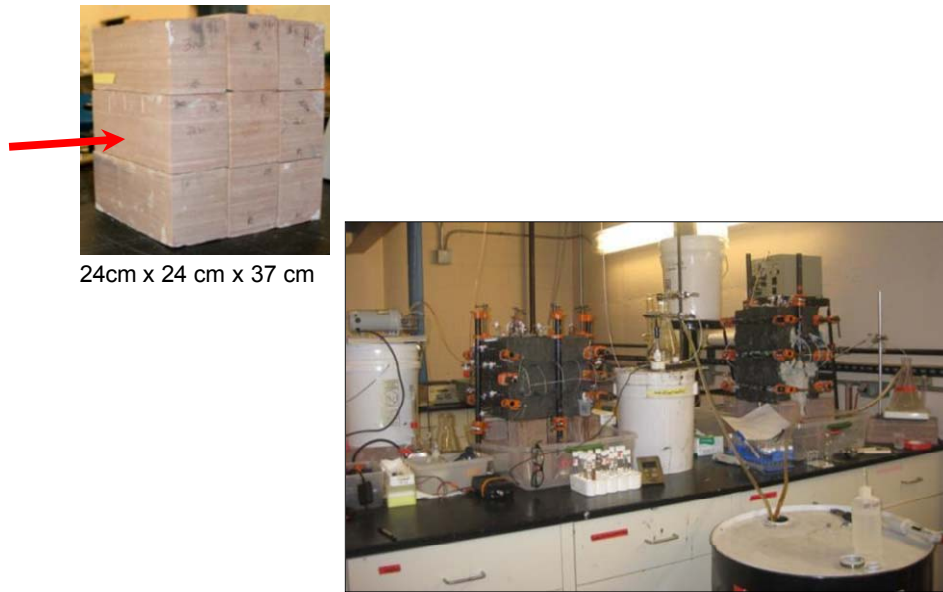


Figure 2.6. Fracture Network – Colorado School of Mines

Fracture network, constructed and photographed at the Colorado School of Mines, as part of recently completed SERDP Project ER-1554. The fracture network consists of vertical and horizontal fractures, dead-end fractures, and fracture intersection. DNAPL dissolution during application, similar to that evaluated in the discrete fracture experiments (18), has been evaluated in this intermediate scale system.

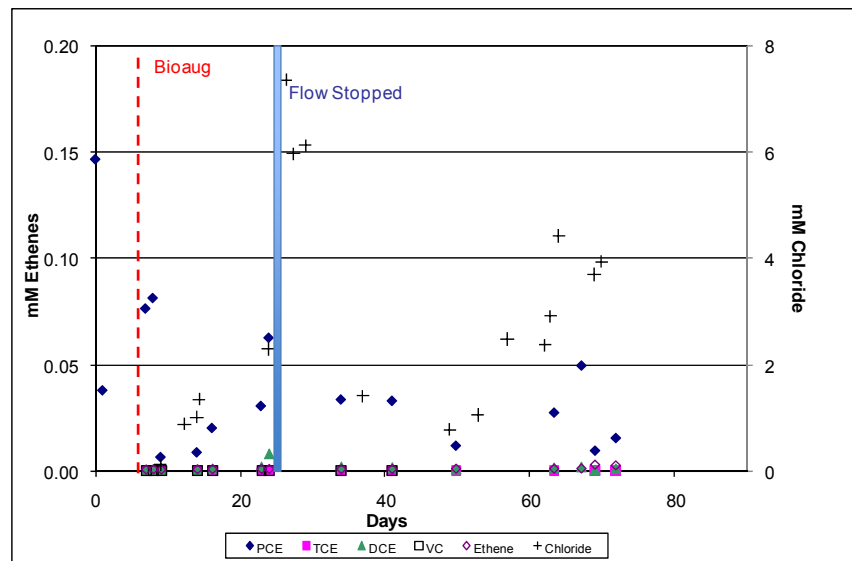


Figure 2.7. DNAPL Dissolution Enhancement Colorado School of Mines

DNAPL dissolution enhancement measured during bioaugmentation in the fracture network (data courtesy of the Colorado School of Mines). Molar chloride concentrations (plotted on the secondary y-axis) indicate that bioaugmentation enhanced DNAPL dissolution by approximately 100-times. The residence time in the fracture network was only 10 hours.

The reason for the relatively large increase in bioaugmentation effectiveness at the fracture network scale, compared to the discrete fracture scale, likely is due to the fact that the dissolved PCE concentrations were lower in the fracture network (due to dilution from flow heterogeneity). Larger fracture apertures in the fracture network also may have enhanced bioaugmentation effectiveness by facilitating biomass growth. Thus, intermediate scale fracture network experiments confirm that bioaugmentation is a potential treatment option for DNAPL sources in fractured bedrock.

2.2.3 DNAPL Source Strength Function in Fractured Bedrock

Several recent studies have evaluated DNAPL source strength (i.e., the relationship between DNAPL mass removed and dissolved flux emanating from the source) in unconsolidated materials (19-22). These studies have shown that the fraction of DNAPL mass removed is not necessarily proportional to the decrease in dissolved contaminant concentration and flux. The relationship between DNAPL mass removal and dissolved concentration/flux is typically determined by the DNAPL architecture.

As indicated on Figures 2.2 and 2.4, DNAPL source strength can be important for assessing potential effectiveness of a remedial technology, or for determining the longevity of the DNAPL source. Thus, proper assessment of bioaugmentation for treatment of bedrock DNAPL sources requires an assessment of DNAPL architecture within the fracture network, as these coupled physical and biological processes will determine the potential limits of success not only of bioaugmentation, but of most other remedial technologies (including MNA) implemented for treatment of DNAPL in fractured bedrock. We demonstrated that DNAPL architecture plays an important role in DNAPL dissolution kinetics and during bioaugmentation (17,18). We have shown that much of the DNAPL present in bedrock fractures has limited impact on groundwater quality. This finding has important implications for field scale management of DNAPL sources, as it implies that only a small fraction of the DNAPL mass may need to be removed in order to improve groundwater quality and facilitate an MNA remedy. However, DNAPL architecture in fractured bedrock is poorly understood at the field scale, as the relationship between DNAPL mass and dissolved flux emanating from DNAPL sources has not been evaluated in field scale bedrock fracture systems.

The findings discussed in the paragraphs above suggest that the effectiveness of bioaugmentation is dependent upon DNAPL architecture, and that only partial treatment of DNAPL sources may be sufficient for reducing contaminant flux so that an MNA remedy can be achieved. While our discrete fracture and intermediate fracture network scale studies evaluating DNAPL architecture and dechlorination rates in fractures have demonstrated that bioaugmentation for treatment of DNAPL sources in bedrock (and in fractures containing DNAPL) is feasible, there currently are no reported field studies that have focused on assessing bioaugmentation for treating PCE/TCE DNAPL sources in bedrock fractures, particularly as it relates to DNAPL dissolution kinetics, DNAPL architecture, and dissolved plume response. Furthermore, the relationship between partial DNAPL mass removal and contaminant flux in fractured bedrock is unclear, and the extent to which bioaugmentation can reduce contaminant mass and flux has not been demonstrated or assessed at the field scale. As a result, the efficacy of bioaugmentation for addressing DNAPL sources in bedrock has not been demonstrated. In addition, screening and management tools for assessing DNAPL sources in bedrock are lacking, and improved understanding is needed to determine DNAPL source longevity and flux response on the dissolved plume.

2.3 ADVANTAGES AND LIMITATIONS OF THE TECHNOLOGY

2.3.1 Advantages

The primary advantages of utilizing an *in situ* approach for treatment of PCE DNAPL sources in fractured bedrock are as follows:

1. Appreciably reduced cost, infrastructure, and timeframe compared to traditional pump-and-treat approaches; and,
2. Transformation to species that do not have maximum contaminant levels (MCLs) (i.e., ethene, ethane) in groundwater, rather than transferred to a secondary medium such as granular activated carbon (GAC).

In addition, the use of an active bioaugmentation approach for treatment of the PCE DNAPL sources provides several advantages over alternate *in situ* approaches, such as:

1. The addition of bacteria capable of enhancing the complete dechlorination of PCE is expected to enhance DNAPL dissolution and mitigate accumulation of daughter products.
2. The biological reactions are slower and longer lasting than other *in situ* approaches (e.g., chemical oxidation), and thus are well suited for treatment under the expected mass transfer controlled conditions in the DNAPL source area.
3. Energy requirements are substantially less than an aggressive *in situ* thermal treatment approaches.
4. Due to residual carbon and biomass, enhanced reductive dechlorination is expected to occur long after active treatment ceases.

2.3.2 Limitations

As with all technologies, there are also limitations with bioaugmentation:

1. Biofouling is a potential concern, especially at the injection well(s). Well re-development and more aggressive methods (e.g., application of a biocide) were required during the demonstration in an attempt to maintain active treatment design flowrates.
2. The groundwater oxidation-reduction potential (ORP) will be significantly reduced, which is necessary to create conditions conducive to reductive dechlorination of PCE. However, such a reduction in ORP also causes secondary geochemical impacts, such as mobilization of metals (e.g., dissolved Fe [II] and Mn [III] from dissolution of Fe and Mn oxides), sulfide production, and other changes in groundwater geochemistry that impact local groundwater quality. Arsenic mobilization is another potential concern.

Transient generation of chlorinated ethenes such as DCE and VC was expected and did occur during the demonstration.

3.0 PERFORMANCE OBJECTIVES

Performance objectives are summarized in Table 3.1, and details are provided in Sections 3.1-3.5.

Table 3.1. Performance Objectives

Performance Objective	Data Requirements	Success Criteria	Results
Quantitative Performance Objectives			
Effectiveness of bioaugmentation for PCE DNAPL removal	Pre- and post-treatment measurement of DNAPL using partitioning tracer tests, and determination of DNAPL mass removal rates by measuring rates of daughter product generation	>9% DNAPL mass removal per month	This objective was attained for the shallow zone, but fell short (~5% / month) in the deep zone due to mass transfer limitations.
Effectiveness of bioaugmentation for reducing dissolved chlorinated ethene flux from the DNAPL source area	Pre- and post-treatment contaminant concentrations in groundwater wells using EPA Method 8260, and measurement of dissolved chlorinated ethene flux pre-and post-treatment using passive flux meters	>90% reduction in chlorinated ethene flux by the end of active treatment	This objective was attained for both the shallow and deep zones, but chlorinated ethene rebound may have been masked by ongoing reductive dechlorination in the deep zone.
Complete PCE dechlorination	Measurement of ethene and ethane	Ethene and/or ethane detected above background levels within or downgradient of the DNAPL source area	This objective was attained for both the shallow and deep zones.
Distribution and growth of <i>Dehalococcoides</i> sp. (DHC) following bioaugmentation	Measurements of DHC via qPCR in groundwater	Minimum 100-fold increase in DHC levels at least 20 ft downgradient of bioaugmentation injection point	This objective was attained.
Qualitative Performance Objectives			
Ease of Implementation	Time needed to maintain system during active treatment Amendment delivery rate Feedback from field technician	Biofouling Ability to operate in semi-passive mode Minimal costs	Biofouling in the injection well was a challenge, but otherwise system was operated with ease and minimal O&M.

3.1 EFFECTIVENESS OF BIOAUGMENTATION FOR PCE DNAPL REMOVAL

The effectiveness of bioaugmentation for removal of DNAPL sources is a critical performance objective that was evaluated during this demonstration. The time and effort needed to remove the DNAPL sources to the point where groundwater impacts are greatly reduced played a large role in determining the overall success of this technical approach.

3.1.1 Data Requirements for DNAPL Removal

Partitioning tracer tests (PTTs) performed prior to treatment were used to provide an estimate of the DNAPL mass initially within the source area. The rate of DNAPL mass removal (via reductive dechlorination) during the demonstration was determined by calculating the rate of DNAPL mass removal based on daughter product (chloride, ethene/ethane, DCE, and VC) generation in the groundwater. Measured groundwater concentrations, multiplied by the volumetric groundwater flow rate through the DNAPL source area, provide a measure of the DNAPL mass removal. A final partitioning tracer test was originally planned to provide a second means to determine DNAPL mass removal, but the loss of transmissivity in the injection well during active treatment prevented this final PTT from being performed.

3.1.2 Success Criteria for DNAPL Removal

The objective was considered to be met if the rate of DNAPL mass removal by the end of the demonstration attained a rate of 9% DNAPL removal per month (i.e., 9% of the initial DNAPL mass removed per month). It is recognized that initial DNAPL mass removal rates may be much less than this, as several weeks may be needed for biomass growth and DHC distribution. A DNAPL mass removal rate of 9% per month was expected to provide a sufficient treatment rate so that the active treatment timeframe is reasonable (i.e., approximately 1 year of treatment). For the shallow zone, approximately 100% of the DNAPL mass was removed in 9 months, which is approximately 11% DNAPL mass removal per month. This was calculated based on chloride generation during active treatment, along with the initial DNAPL mass as determined via PTT. For the deep zone, DNAPL mass removal occurred at a rate of approximately 5% per month. As explained in Section 5, the lower rate of DNAPL mass removal in the deep zone likely was due to mass transfer limitations.

3.2 BIOAUGMENTATION EFFECTIVENESS FOR FLUX REDUCTION

In addition to removing DNAPL mass, bioaugmentation is expected to reduce the chlorinated ethene flux migrating downgradient. This reduction is expected to occur within, or immediately downgradient of, the DNAPL source area. Mitigating the downgradient flux of chlorinated ethenes was an important aspect of this demonstration.

3.2.1 Data Requirements for Flux Reduction

Reduction in chlorinated ethene flux was determined by direct measurement of groundwater concentrations, where concentrations before, during, and after the demonstration were performed. Monitoring points both within the DNAPL source area were evaluated, as complexity in the fracture flow field prevented assessment of the downgradient plume (i.e., the wells placed downgradient were not along the groundwater flow path, as indicated by tracer testing).

3.2.2 Success Criteria for Flux Reduction

The success criterion for flux reduction was a 90% decrease in the chlorinated ethene flux (or, dissolved chlorinated ethene concentration) by the end of the demonstration. This was attained for both the shallow and deep fractured zone. However, because biogeochemical conditions favorable to reductive dechlorination persisted in the deep zone throughout the rebound period, and ethene concentrations continued to increase, it is possible that increases in chlorinated ethene concentrations were “masked”.

3.3 COMPLETE PCE DECHLORINATION

Successful treatment of PCE requires its complete dechlorination. While some accumulation of daughter products is expected, particularly within the DNAPL source area, evidence that complete dechlorination is occurring is needed to ensure that increases in DCE and VC will not impact downgradient water quality.

3.3.1 Data Requirements for Complete PCE Dechlorination

The parameters that were measured to assess complete PCE dechlorination were reduced gases (ethene/ethane) via laboratory gas chromatography-flame ionization detector (GC-FID) analysis of groundwater samples.

3.3.2 Success Criteria for Complete PCE Dechlorination

The success criterion for complete PCE dechlorination was measureable ethene/ethane generation (i.e., measureable increases above background). Measurable ethene generation was observed in both the shallow and deep zones.

3.4 DHCDISTRIBUTION AND GROWTH

Bioaugmentation success is typically dependent upon successful distribution and growth of the injected microbial culture. Evidence of DHC growth and distribution are therefore important parameters to assess during this demonstration.

3.4.1 Data Requirements for DHC Distribution and Growth

DHC distribution and growth was assessed by performing polymerase chain reaction (qPCR) analyses on groundwater samples. These analyses will be performed on samples collected from within the source area, as well as samples collected downgradient.

3.4.2 Success Criteria for DHC Distribution and Growth

DHC distribution and growth will be considered adequate if an increase (from baseline) in DHC levels of at least two orders of magnitude is observed at least 20 ft downgradient of the bioaugmentation injection point. This criterion was met at one of the monitoring wells.

3.5 EASE OF IMPLEMENTATION

The level of effort needed to maintain effective treatment of the DNAPL sources following bioaugmentation will determine, in part, the plausibility of this approach for treating DNAPL sources in bedrock. This effort was assessed throughout the demonstration.

3.5.1 Data Requirements to Assess Ease of Implementation

Information such as required labor time, effort needed to address potential biofouling issues, amendment consumption, and the extent to which the system can be passively operated all were considered when assessing the overall ease of implementation of this approach.

3.5.2 Success Criteria for Ease of Implementation

The success criteria are qualitative, but the level of effort was compared (to the extent possible) to other *in situ* approaches with respect to time, resources, and effectiveness.

4.0 SITE DESCRIPTION

4.1 SITE SELECTION

Site selection was performed by first attaining a list of potential sites with known PCE or TCE contamination in fractured bedrock. This list, which was developed during the proposal phase of the project, was developed based on CB&I Federal Services' (CB&I's) experience at DoD sites, a literature review, and by discussions with site contractors, regulators, and DoD personnel. Additional candidate sites were provided via Mr. Charles Coyle, the DoD liaison for this project. The list of sites that were initially screened with respect to suitability for this project included: Pease AFB (Site 32 source area), Loring AFB (GMZ4 Quarry area), AFP4 (Landfill 3 area), AFP6 (Building B-76 area), Edwards AFB (Site 37 source area, which is part of the South Air Force Research Laboratory), and the former Nike Battery PR-58 site (RI). Of these sites, AFP6 was excluded because of the depth to bedrock (~170 ft) and due to the planned implementation of *in situ* chemical oxidation. Pease AFB was excluded because, based on current groundwater concentrations within bedrock, DNAPL likely is not present (DNAPL sources are likely limited to the overburden materials). Loring AFB was excluded due to site access issues, as often the site is inaccessible due to snow. The site selection criteria for which the remaining three sites (Edwards AFB, AFP4, and PR-58) were evaluated included the following:

- Confirmed (or very likely) presence of DNAPL;
- Shallow depth to saturated bedrock (<100 ft below ground surface [bgs]);
- Immobile DNAPL (i.e., no recoverable DNAPL from existing bedrock wells);
- No co-contaminants present that would significantly inhibit DNAPL dissolution and PCE/TCE bioremediation;
- pH between 6 and 8;
- Well-connected network of conductive fractures;
- Presence of existing monitoring wells and site data; and
- Site accessibility.

Because of the substantial costs associated with implementing a bedrock investigation, particular care and attention was given to the site selection phase of this ESTCP project. At each of the three sites that remained on the candidate list, preliminary screening tests were performed to assess their suitability for the demonstration.

At PR-58, a screening level laboratory microcosm test was performed in site groundwater to assess the effectiveness of bioaugmentation (using CB&I's SDC-9 culture) to treat the elevated dissolved concentrations of TCE and 1,1,2,2-tetrachloroethane (TeCA) present near the presumed bedrock DNAPL source area. Results, shown on Figure 4.1, showed that TCE was rapidly biodegraded. However, TeCA was not treated, as the presence of even relatively low concentrations of TCE inhibited TeCA removal. Since the DNAPL, if present, likely contains a mixture of these two compounds, it was determined that bioaugmentation using SDC-9 would be efficient for enhancing DNAPL dissolution.

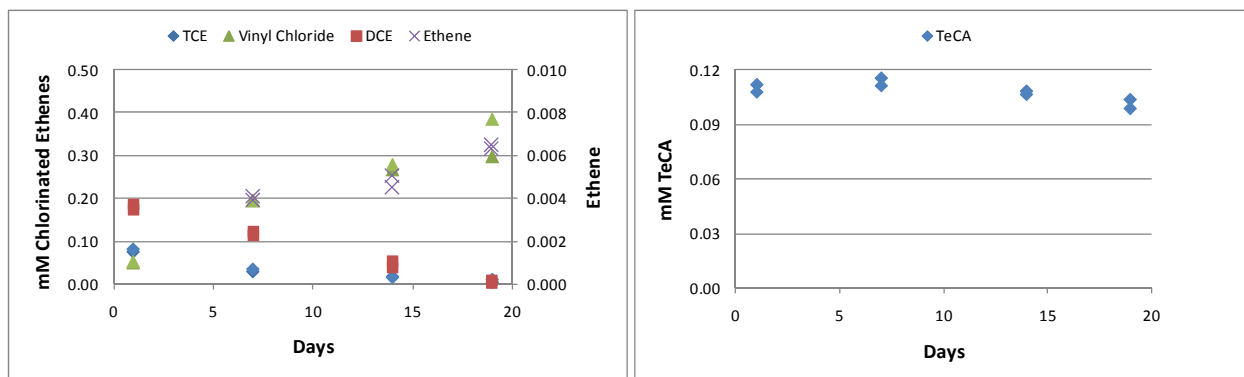


Figure 4.1. Bench Scale Microcosm Testing

Results of bench-scale microcosm testing using groundwater collected from the suspected bedrock source area at PR-58. After amending with lactate, nutrients (diammonium phosphate and yeast extract), and CB&I's DHC-containing SDC-9 culture, complete dechlorination of TCE and DCE were observed (as evidenced by generation of ethene – left figure). However, no significant removal of TeCA was observed (right figure). Microcosms were prepared in duplicate. Controls, prepared with no amendments, showed no measurable biodegradation of either the chlorinated ethenes or TeCA.

At AFP4, bedrock samples were graciously collected by URS for CB&I as part of their sampling program. Both groundwater samples and samples of DNAPL were collected. During collection, mobile DNAPL or light non-aqueous phase liquid (LNAPL) was observed in all wells. The presence of mobile DNAPL would make assessment of DNAPL dissolution challenging, as mobile DNAPL would prohibit the use of techniques such as partitioning tracer tests for quantifying DNAPL mass. The risk of spreading DNAPL (or LNAPL) mass during the demonstration also makes this site problematic and unsuitable for the technology demonstration.

At Edwards AFB, AECOM (the current site contractor) provided field assistance to CB&I in performing a partitioning tracer test in a bedrock monitoring well located within the suspected DNAPL source area, and with dissolved PCE concentrations greater than 1% solubility. This monitoring well, 37-EW07, is located near Building 8595, which is in the vicinity of the reported PCE DNAPL release. For simplicity, the partitioning tracer test was performed as a push-pull test at a bedrock well located within the presumed PCE DNAPL source area. The test involved injecting approximately 20 gallons of an aqueous solution containing sodium bromide, methanol, 1-hexanol, and 2-octanol. After waiting approximately 12 hours, groundwater was extracted from the bedrock well over a 24-hour period. Approximately 25 gallons were extracted. Results of the testing are shown on Figure 4.2. While results are intended to provide only qualitative information with regards to the presence of DNAPL in the fractures, the retardation of the 2-octanol (the most hydrophobic of the tracers employed for this test) relative to the other tracers suggests that residual DNAPL is present in the vicinity of the test well.

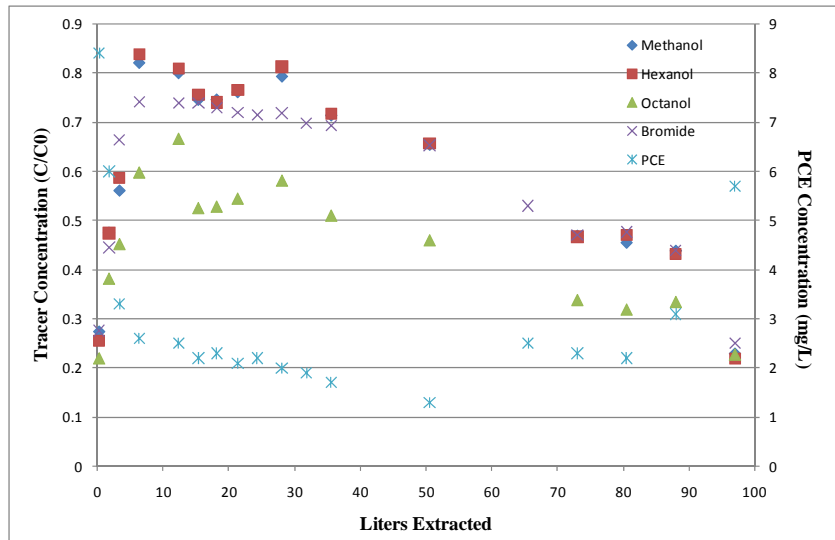


Figure 4.2. Partitioning Tracer Test- Push Pull Results

Results from the partitioning tracer test (performed as a push-pull test) at bedrock monitoring well 37-EW07, located approximately 50 ft bgs in the suspected source area in Site 37 at Edwards AFB.

Site selection criteria were applied to PR-58, AFP4, and Edwards AFB, and each site was ranked with respect to attainment of each of these criteria. Table 4.1 below provides an overall assessment of site suitability. Based on the overall ranking, Edwards AFB was the most suitable location for this demonstration. Thus, Edwards AFB, Site 37, was the selected site. The Air Force had expressed an interest and willingness to host this demonstration at Edwards AFB; and during a site meeting in the fall of 2012, site regulators also expressed interest in this project. Site selection criteria and the corresponding data from potential demonstration sites are provided in Table 4.1.

Table 4.1. Site Selection Criteria

Parameter	Preferred Value(s)	Relative Importance (1-5, with 1 being highest)	PR-58	AFP4	Edwards AFB
Likely presence of DNAPL ³	NA ¹	1	Yes	Yes	Yes
Shallow depth to bedrock	< 100 ft	3	Yes	Yes	80-125 ft ²
Immobile DNAPL	NA ¹	1	Yes	No	Yes
No inhibitory co-contaminants	NA ¹	1	No	Uncertain	Yes
pH	6<pH<8	3	Yes	Yes	Yes
Well-connected fractures	NA ¹	2	Yes	Yes	Yes
Existing site data and wells	NA ¹	3	Yes	Yes	Yes
Site accessibility	NA ¹	2	Yes	Yes	Yes

¹ NA; Not Applicable

² Likely treatment interval where DNAPL and water-bearing fractures are present.

³ PCE/TCE groundwater concentrations >1% solubility or visual DNAPL observations.

4.2 SITE LOCATION AND HISTORY

Edwards AFB is located approximately 30 miles northeast of the city of Lancaster in the Antelope Valley of the Mojave Desert (refer to Figure 4.3). The Air Force Research Laboratory (AFRL), in the eastern portion of Edwards AFB, has been used as a rocket research and testing facility since the 1950s. The Environmental Restoration Program has divided the base into 10 operable units (OUs); OU4 and OU9 encompass the AFRL on the eastern side of Rogers Dry Lake. In general, OU4 includes test areas along Leuhman Ridge, the major AFRL support facilities clustered southeast of the ridge, and Test Area 1-46 along Mars Boulevard (Blvd).

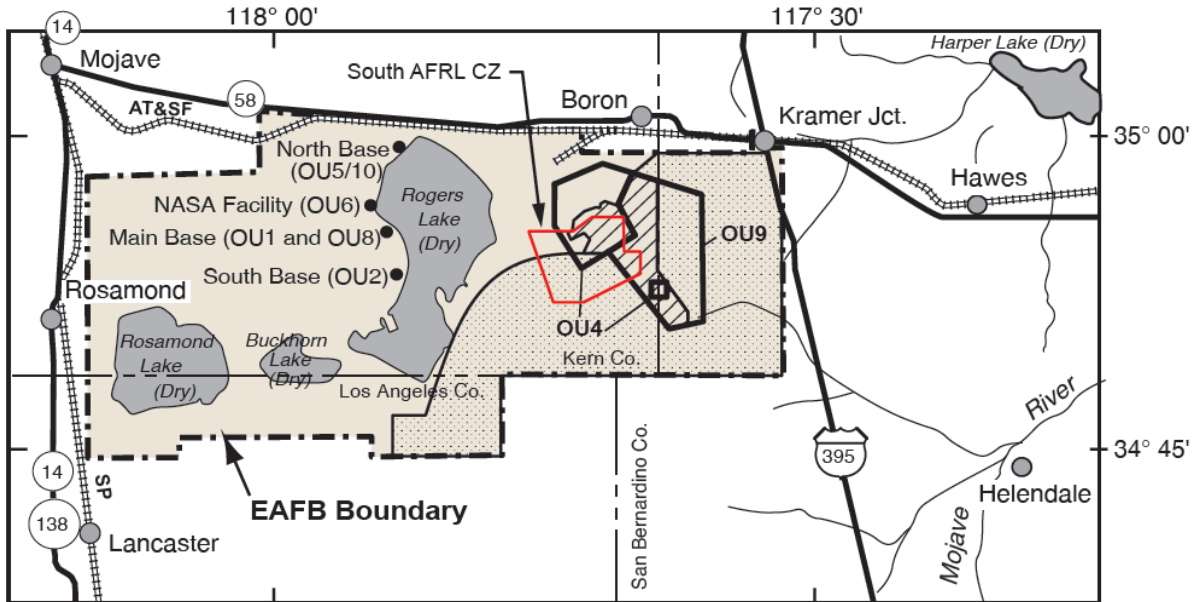


Figure 4.3. Edwards AFB Research Laboratory OU4 and OU9

Contaminant plumes in OU4 and OU9 have been assigned to one of four areas based on geographic location and the direction of groundwater flow: the South AFRL, AFRL Arroyos, Northeast AFRL, and Mars Blvd. The South AFRL includes Environmental Remediation Program Sites 37, 120, and 133 in OU4 and Site 321 in OU9 where facilities are (or were) associated with rocket component maintenance (Site 37), the AFRL wastewater treatment plant (Site 120), civil engineering shops (Site 133), and chemicals storage (Site 321). The groundwater plumes associated with these sites located on the southwestern side of Leuhman Ridge share a regional groundwater flow direction toward the southwest.

The hydrogeology of the AFRL is greatly influenced by Leuhman Ridge, a prominent northeast-southwest trending topographic high on which the earliest AFRL test areas were located. The highest point on the ridge is 3,360 ft above mean sea level. The South AFRL contamination zone encompasses groundwater to a depth of 500 ft in a 16.4-square-mile area that extends southwest from the southern flank of Leuhman Ridge. Surface flow from both sides of the ridge ultimately drains to Rogers Dry Lake, located to the west of the AFRL. Throughout the AFRL, and particularly along Leuhman Ridge and its southeastern flank, weathered and competent fractured granitic bedrock crops out at the ground surface. Site 37 and Building 8595 at the south AFRL is roughly 275 ft above the valley floor.

4.3 SITE GEOLOGY AND HYDROGEOLOGY

The regional subsurface geology at the AFRL is characterized in the South AFRL First Five-Year Review (23) as a crystalline granitic bedrock complex overlain in areas by a thin veneer of unconsolidated material, which increases in thickness down slope from the crest of Leuhman Ridge. Approximately 3.5 miles downgradient of the Sites 37 and 133 source areas, the thickness of the alluvium gradually increases to hundreds of feet as alluvial material transitions to lacustrine deposits. Figure 4.4 presents the surface geology of the site.

The unconsolidated material originates from the erosion and weathering of exposed and shallow bedrock, and the reworking of older alluvium, windblown sand, and gravel deposits. It consists of fine-grained, quartzo-feldspathic, rock-fragment sand with varying percentages of low plasticity clay, silt, and gravel (24). These deposits are loose to very dense and typically dry to slightly moist. The unconsolidated material grades into fractured, weathered bedrock below which fractured, competent bedrock. The bedrock underlying the AFRL consists of two types of crystalline rock: a quartz monzonite host rock that has been intruded by the granite that forms Leuhman Ridge. The intrusive granite that forms Leuhman Ridge is distinguished from quartz monzonite by an increase in the potassium feldspar constituent and a decrease in the plagioclase feldspar to near zero. Scattered mafic dikes and pegmatite-aplite dikes also occur in the AFRL.

4.3.1 Site Geology

The subsurface geology at Site 37 is typical of the AFRL with crystalline granitic bedrock overlain by unconsolidated alluvium. The thickness of the alluvium within the treatment area in the vicinity of Building 8595, as observed project drilling to date, ranges from less than 5 to 24 ft. The alluvium consists of fine-grained quartzo-feldspathic, rock fragmented sand derived from weathering and decomposition of the underlying bedrock. The alluvium also contains varying percentages of low plasticity clay, silt, and gravel. The unconsolidated layer is loose to very dense and generally dry to slightly moist.

The bedrock beneath the alluvium is below the site and is composed of two types of pre-tertiary plutonic crystalline rock. The first (quartz monzonite) is composed of varying percentages of quartz, plagioclase, and potassium feldspar. The monzonite host rock is intruded in places by a granite that is distinguished from the monzonite by increased percentages of potassium feldspar and decreased plagioclase. Drilling in the immediate area of the proposed treatment area encountered both the quartz monzonite and granite material with the monzonite representing the predominant rock encountered rock type. The bedrock competence varies from very competent to incompetent and is impacted by fractures, and chemical alteration to clay along fracture planes. Both mafic and pegmatite-aplite dikes are present in the bedrock beneath the AFRL.

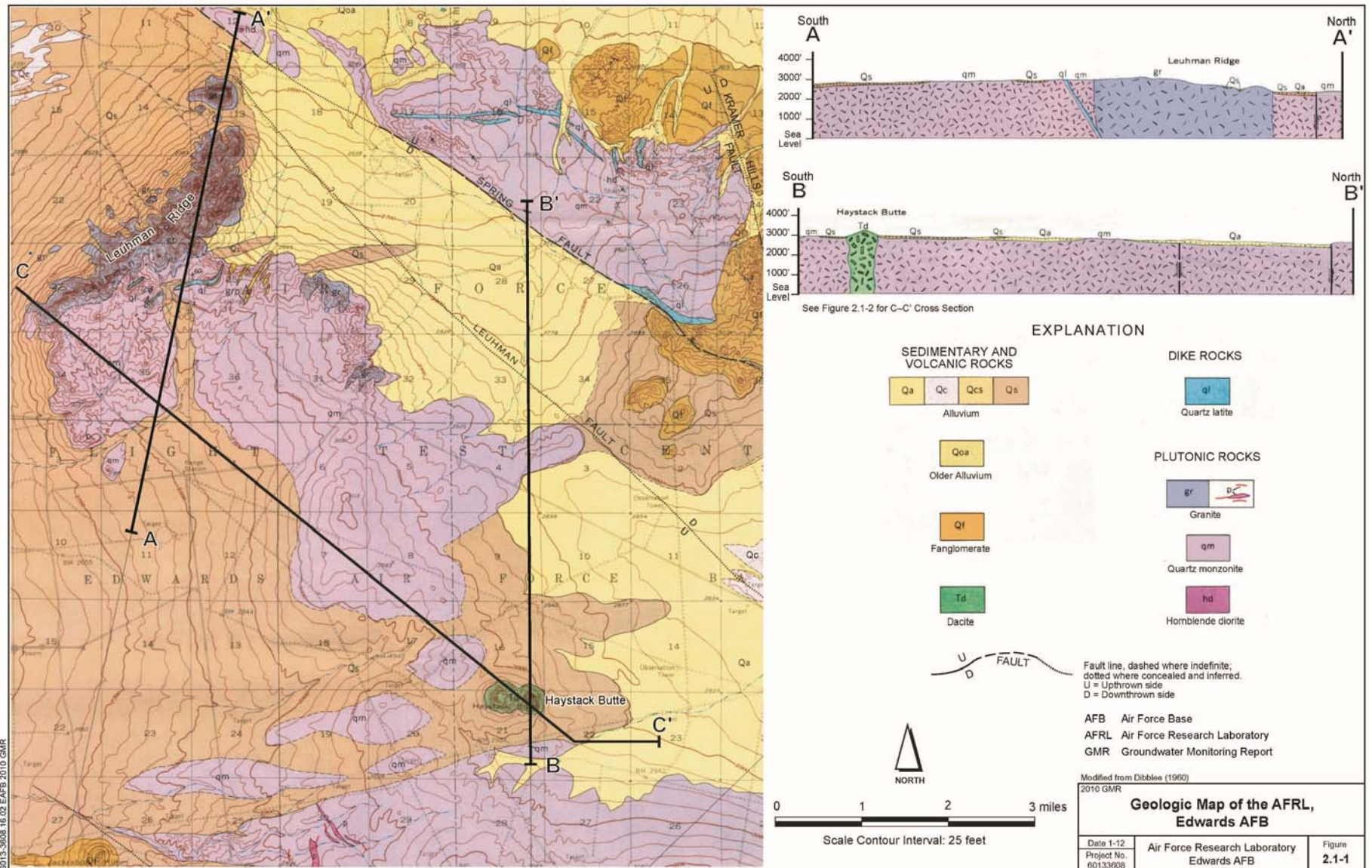


Figure 4.4. Edwards AFB Geology. Modified from Dibblee, 1960 (25)

4.3.2 Groundwater Monitoring Wells

The well inventory for the Southern AFRL as of 2010 included 192 wells of various functions and depths. The inventory includes groundwater monitoring, extraction, and injection wells, as well as vapor monitoring and extraction wells. Sixty-three (63) of the wells are designated as Site 37 wells. For wells within Site 37, the completion depths range from 35 to 290 ft bgs. Figure 4.5 presents the network of wells in the vicinity of Site 37.

In 2010, the Air Force developed the *2010-2015 AFRL Long-Term Monitoring Strategy* (26). The purpose of the document was to update the AFRL sampling strategy. A sufficient number of wells were selected to be sampled annually, biennially, or less frequently in order to achieve the critical objectives: these included;

- Confirmation of the rate of movement of the leading edge of plumes. The chemicals with the most widespread distribution (PCE, TCE, and perchlorate plumes for Sites 37 and 133) were targeted for sampling and transport modeling and sampling.
- Monitor the internal contours of plumes at a sufficient frequency to allow testing (or “validation”) of groundwater transport models.
- Monitor the groundwater contaminant plumes at a sufficient frequency to identify any departures from the conceptual site model (CSM) or the predicted direction of groundwater flow and contaminant plume transport.

The revised sampling program included only a fraction of the wells routinely sampled as of 2010. The sampling program for the Southern AFRL in 2010 included a total of 12 wells which include both five existing and seven newly installed wells. The Site 37 wells currently included in the program are as follows:

- 37-MW40;
- 37-MW44;
- 37-MW46S; and,
- 37-MW47.

The wells are located at the distal end of the defined plume or southwest of the known plume boundary. None of the wells designated for long-term monitoring are in the immediate area of the demonstration.

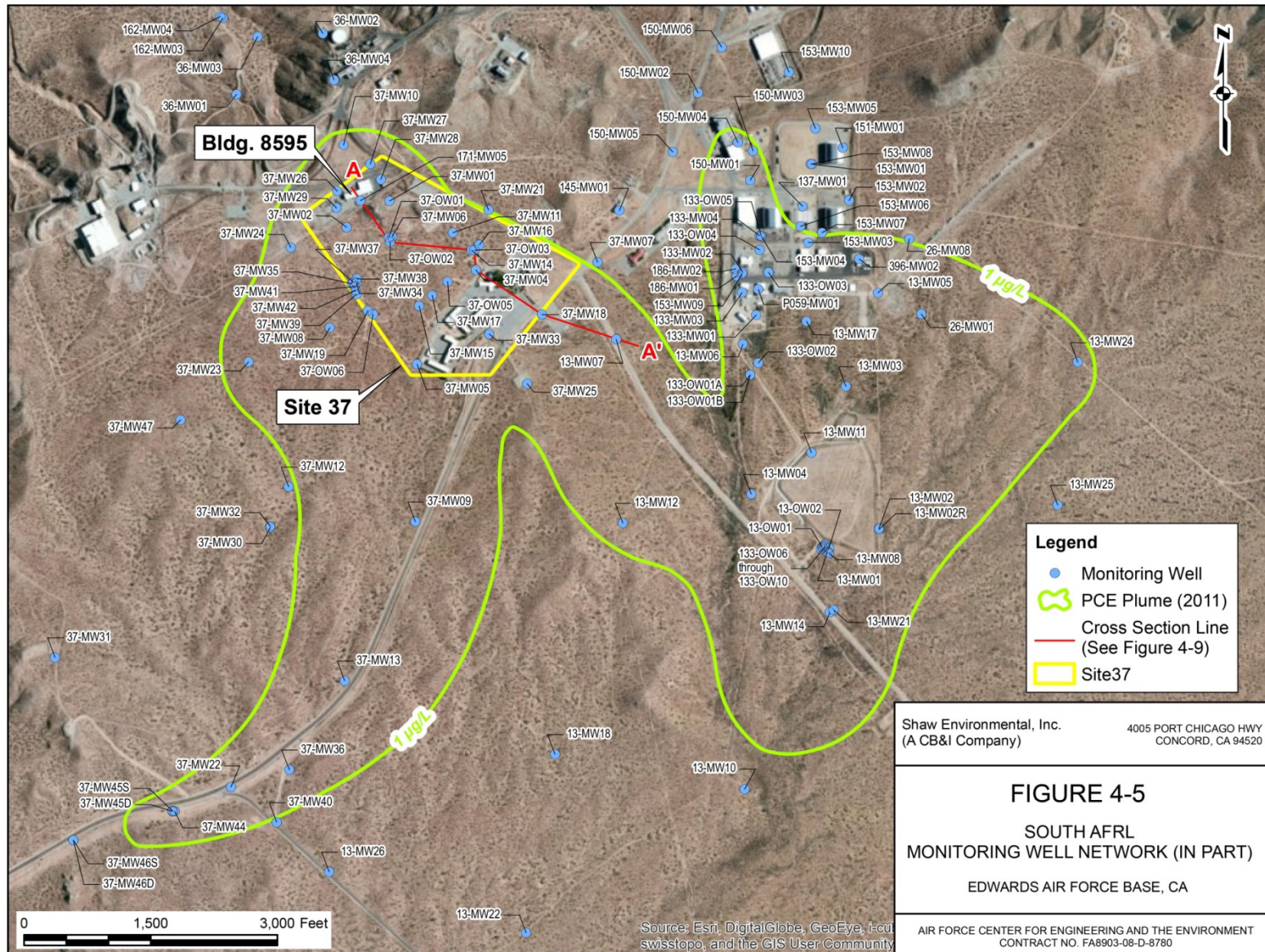


Figure 4.5. South AFRL Monitoring Well Network

4.3.3 Hydrogeology and Fracture Network

The Antelope Valley is underlain by a large groundwater basin that has been divided into several subbasins bounded laterally by consolidated rock, faults, and groundwater divides; or in some cases by arbitrary boundaries (23). The AFRL is located within the Hi Vista sub area of the basin. Hydrogeology at the AFRL is typified by shallow crystalline bedrock with low groundwater yield. Bedrock at the AFRL is not an aquifer (i.e., it does not yield useable quantities of groundwater) and is not within a basin as delineated by the United States Geological Survey (USGS) based on geophysical evidence (27). However, the California Regional Water Quality Control Board, Lahontan Region (Water Board) considers the AFRL to fall within the Antelope Valley hydrologic basin 6-44. The following beneficial uses are designated for this basin: municipal, agricultural, industrial, and freshwater replenishment.

Fracture Characteristics

Hydrogeology at the AFRL is characterized by shallow granitic bedrock with low groundwater yields from fracture flow. Groundwater occurs under hydrostatic pressure within fractures in both weathered and competent granitic bedrock. The fracture network does not yield usable quantities of groundwater with typical flow rates of less than 0.5 gallons per minute. Groundwater gradients mimic the surface topography, with little asymmetry that would suggest strong fracture control (24). The draft *Groundwater Modeling Report for the Northeast AFRL* (28) concluded the following based on an evaluation of results from eight at the AFRL between 1991 and 2009:

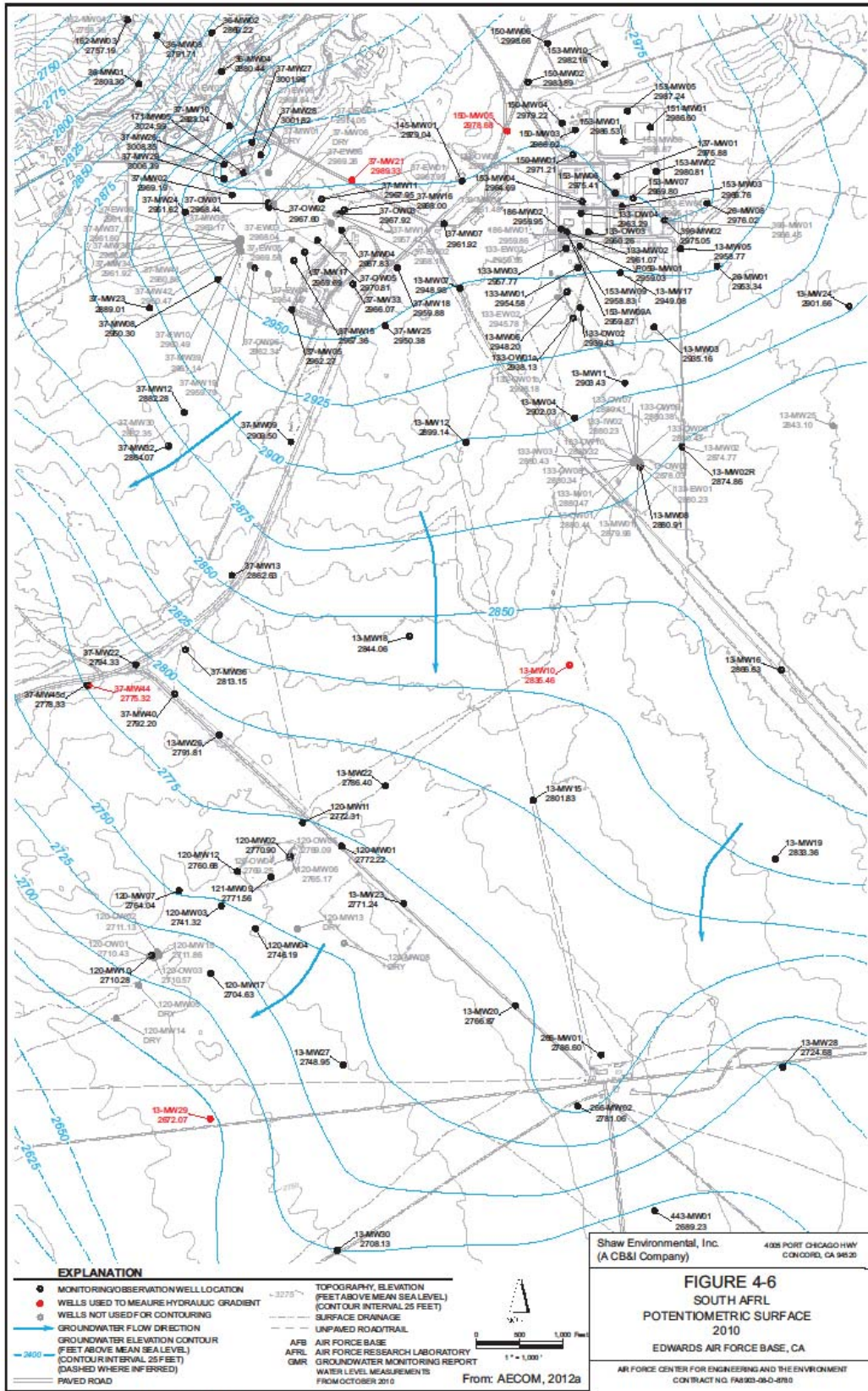
- Fracture orientations at the AFRL are highly variable; and,
- Previous fracture mapping has proven ineffective in predicting preferred groundwater flow pathways at the scale of bulk contaminant transport.

On a local scale the movement of groundwater is expected to be fracture-controlled, as confirmed by results of tracer studies conducted in pilot study areas at Site 162 in the AFRL Arroyos and Sites ITI/325 in the Northeast AFRL (29,30). The extent and continuity of fractures is probably controlled by the structural and intrusive history.

Investigations conducted by CB&I during the first phase of this investigation provide additional insight into the character and variation of fracturing at Site 37. The work included geologic coring and borehole geophysical logging, which provide a detailed qualitative and quantitative evaluation of the fracture system (see Section 5.2). Despite the presence of a number of fracture sets within the bedrock, there appears to be one prevalent northeast dipping fracture set that is present across Site 37.

4.3.4 Groundwater Flow

In the South AFRL, groundwater flows ultimately into the Lancaster Subbasin, recharging the aquifer. The groundwater potentiometric surface for October 2010 is displayed on Figure 4.6. The flow of groundwater, based the potentiometric contours, is radially outward from the Building 8595 and Main Gate area (i.e., flow to southeast, south and northwest).



\\S0102\work\AFRL\GIS_06_Document\Output\Contours Oct2010.PDF ONLY

Figure 4.6. South AFRL Potentiometric Surface 2010. (26)

A groundwater divide appears to be present in the vicinity of Building 8595, which would explain the southeastern migration of contaminants away from the original tank leak location. The potentiometric surface (an assumed flow direction) is only generally controlled by topography, with low elevation variations in the topographic surface not necessarily reflected in the potentiometric surface. Based on the potentiometric surface and from the configuration of plumes originating at Site 37, the flow directions appear to be south, southeast, and southwest away from Building 8595.

During 2010, the depth to the first water-bearing zone encountered during drilling of wells at Sites 37, 120, and 133 ranged from 12 ft bgs in Well 396-MW02 to 420 ft bgs in Well 13-MW32 (24). The average hydraulic gradient is 0.03 vertical feet per horizontal foot (ft/ft) as measured between Wells 37-MW21 and 37-MW44 (0.03 ft/ft), Wells 150-MW05 and 13-MW10 (0.02 ft/ft), and Wells 13-MW10 and 13-MW29 (0.02 ft/ft). Hydraulic conductivities ranging from 1.1 x 10 feet per day (ft/day) to 8.5 ft/day were estimated using aquifer test data collected between 1996 and 2007 as summarized in a focused feasibility study prepared for the South AFRL (31) and the *Site 37 Fractured Bedrock Lime Treatability Study Evaluation Report* (32).

4.3.5 Groundwater Geochemistry

The groundwater geochemistry of the AFRL was evaluated in an Assessment of Inorganic Groundwater Quality and was included as an appendix in the 2008 annual groundwater report (26). The document provides an assessment of inorganic groundwater quality conducted at OUs 4 and 9.

The study was conducted to evaluate the chemical evolution of groundwater as precipitation enters the groundwater at the higher elevations (Leuhman Ridge) and infiltrates into the ground water-bearing bedrock fracture zones. Based on the report, two different water types are present at OUs 4 and 9. Group 1, the South AFRL (including Site 37), AFRL Arroyos, and Northeast AFRL areas; and Group 2, which includes the Mars Blvd area. Group 1 groundwater chemistry ranges from a chloride-type to no-dominant type for anions. Group 2 groundwater ranges from a no-dominant type to bicarbonate-type for anion constituents. Both Groups 1 and 2 trend from no-dominant cation type near the groundwater source area to a sodium-type with increasing distance from groundwater source areas. Average water quality parameters were calculated for the various locations relative to the wells position relative to the crest of Leuhman Ridge and this variation is presented on Table 4.2. Additional parameters measured during the Assessment of Inorganic Groundwater Quality study (26) add further insight into groundwater chemistry. These include the following for 23 wells at Site 37:

- pH range – 6.9 to 10.2;
- Dissolved oxygen range – 0.3 to 5 milligrams per liter (mg/L);
- Arsenic background value (AFRL) – total 0.081 mg/L and dissolved 0.058 mg/L;
- Iron background value (AFRL) – total 109 mg/L and dissolved 0.42 mg/L; and,
- Manganese background value (AFRL) – total 2.8 mg/L and dissolved 0.49 mg/L.

Site-specific measurements were available from the study for three wells in the vicinity of Building 8595 and are included in Table 4.2.

No trend in chloride concentration was readily apparent based on level of VOC contamination that was not explained by distance from a recharge area. Evidence for intrinsic bioremediation at the AFRL is limited and, where observed, extremely localized. The results of field measurements (ORP, dissolved oxygen [DO]) and sulfate concentrations in wells with elevated chloride concentrations generally do not suggest anaerobic, geochemical conditions conducive to reductive dechlorination.

Table 4.2. Water Quality Parameter Concentrations from Inorganic Study

Regional Averages

Location	n	Ca ²⁺	Mg ²⁺	Na ⁺	K ⁺	CO ₂	HCO ₃	Cr ⁶⁺	SO ₄
Sierra Snow (39)	79	0.4	0.17	0.46	0.32	0	2.88	0.5	0.95
OU4 ridge average	6	166	124	417	12	3	430	587	610
OU4 below ridge average	27	90	41	389	11	9	342	395	396
Mars Blvd average 17	17	63	92	358	15	4	701	218	306
Alluvial average	6	52	15	289	4	1	160	278	263

Site-Specific Elements and Chemistry

Well	Location (Relative to Building 8595)	Well Depth (ft bgs)	pH	Dissolved Oxygen-total (mg/L)	Iron-total (mg/L)	Manganese-total (mg/L)
37-MW26	Upgradient 200 ft	98	7.5	2.4	<0.10	0.238
37-W02	Downgradient 500 ft	155.3	6.8	0.6	5.28	0.169
37-W06	Downgradient 1000 ft	125	7.6	2.7	.0321	0.0637

Data Source: AECOM (26)

Notes:

All concentrations are given as mg/L.

Wells used for average concentrations are those in which the concentration of VOCs was less than 80 µg/L.

µg/L - micrograms per liter

mg/L - milligrams per liter

n - number of samples included in average

VOC - volatile organic compound

4.4 CONTAMINANT SOURCE AND DISTRIBUTION

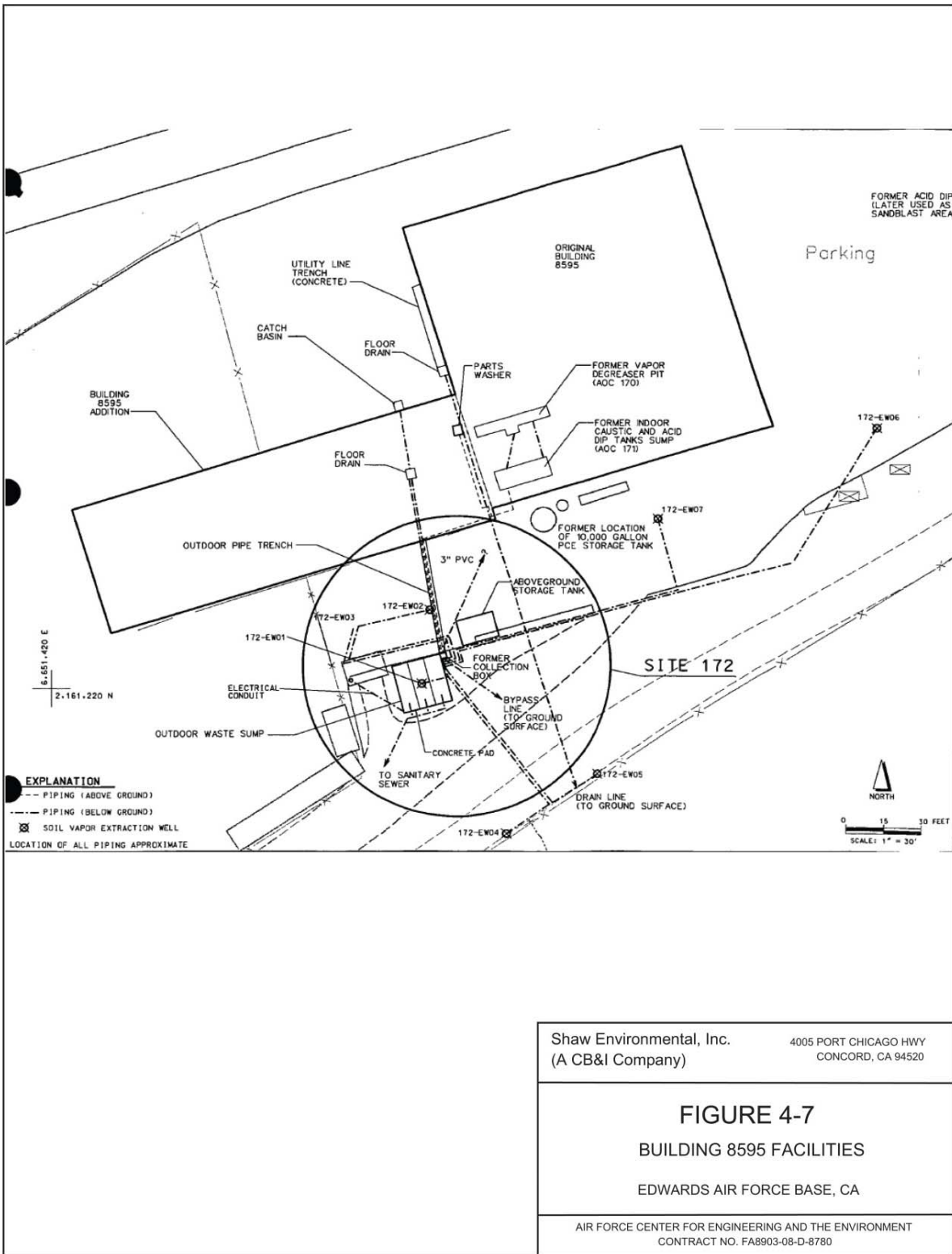
The 16 groundwater sites in OU4 and OU9 have been assigned to one of four areas based on geographic location and the direction of groundwater flow. The South AFRL area encompasses OU4 Sites 37, 120, and 133 (including wells monitored at Site 13, the closed AFRL landfill), and OU9 Site 321. The plumes from these areas form a complex pattern of groundwater plumes, which include PCE, TCE, 1-2-DCE, and perchlorate. Contaminants 1,4-dioxane and N-nitrosodimethylamine (NDMA) are present with the South AFRL, but with limited distribution.

The PCE groundwater plume at Site 37 originates at Building 8595 (Figure 4.5), located on the southwestern flank of Leuhman Ridge, approximately 300 ft southwest of the intersection of Mars Blvd and Ara Street. Building 8595 was used from 1960 to 1997 for maintenance and repair of rocket components. Since 1998, Building 8595 has been used as a laboratory and not for rocket component maintenance.

Past activities that led to the release of chemicals to the groundwater include development and testing of rocket motors using either liquid or solid propellants; and cleaning of rocket components using chlorinated solvents (particularly TCE and PCE). Due to former operational practices (discontinued since the early 1980s) and spills or leaks from storage units, significant quantities of solvents and fuels were released to the ground surface or subsurface. PCE, previously used in a vapor degreaser, is the most widespread contaminant of concern at Site 37. Past releases that contributed to groundwater contamination at Site 37 include a spill from a 10,500-gallon aboveground storage tank (AST) and leakage of wastewater from indoor and outdoor waste sumps (Figure 4.7). The 10,500-gallon AST supplied PCE to a vapor degreaser. The AST was located on the south side of the building. Reportedly, the tank's contents spilled onto the ground surface when a valve was inadvertently left open sometime in the early 1980s. The AST was later refilled and used until its removal in 1994.

The lateral and vertical extent of the VOC constituents at Site 37 have been examined through an extensive network of monitoring wells (Figure 4.5). The lateral extent has been largely defined with the extend reaching roughly 7,000 ft downgradient (south and southwest) of the site. Although the number and complexity of VOC plumes makes the isolation of an individual plume difficult, the plume segment with the most clear relationship to Site 37 (Building 8595) is represented by the smaller (western most) lobe as depicted on Figure 4.8.

The deepest well drilled to date at Site 37 is 37-MW14, which was drilled in 1998 to determine the depth extent of contamination and is depicted on cross section A-A' (Figure 4.9) from the Focused Feasibility Study (31). The deepest detection posted on the figure is from this well (37-MW14: circa 2003) with the sample yielding a 330 µg/L PCE detection.



S:\GIS\GIS_Documents\Output\Building 8595 facility PDF ONLY

Figure 4.7. Building 8595 Facilities

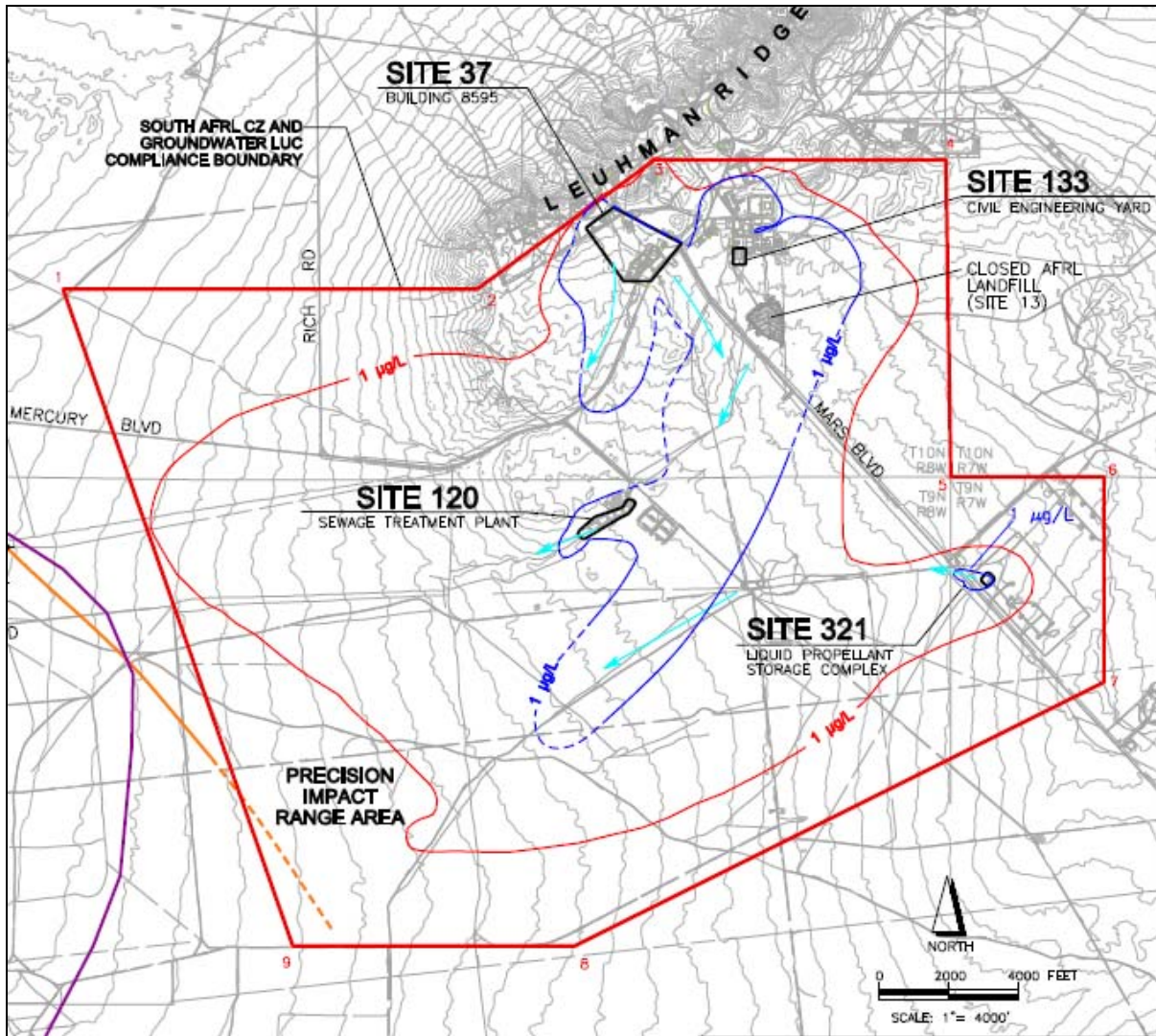


Figure 4.8. Plume Boundary VOC Current Groundwater and Projected 30-year Vapor

Legend

----- Extent of South AFRL VOC Plume (2010) at 1 µg/L concentration -groundwater: Dashed where inferred.

----- Estimated Vapor Intrusion Boundary at Projected 30-year timeframe (risk at 10⁻⁶).

Source: AECOM (24)

The CSM for the South AFRL assumes that low hydraulic conductivity of groundwater in the fractured bedrock will contain contaminants vertically within the control zone. The South AFRL Control Zone extends to a depth of 500 ft and is in the 2010 Annual Report (24) depicts a conceptual distribution of dissolved contaminants to a depth of nearly 400 ft bgs. The maximum extent of the Site 37 plume is defined by wells placed at the distal end of the plume. No VOCs were detected in the three wells (37-MW40, 37-MW46S, and 37-MW47) at the plume front, leading to the conclusion that the existing monitoring well network provides control for the outer extent of PCE; however, the extent of perchlorate is not fully delineated (24).

Active Groundwater and Soil Vapor Remediation

A groundwater extraction and treatment system (GETS) consisting of seven extraction wells and aboveground treatment by liquid phase granular-activated carbon was operated as a treatability study at Site 37 from 1999 through November 2007. A similar GETS with four extraction wells operated at Site 133 east of Site 37 from 2001 through November 2007. Both of these systems were no longer operating as of early 2008.

A soil vapor extraction (SVE) system, originally installed as an interim response action at Site 172, operated south of Building 8595 from 2000 through April 2011 (except during an extended period of downtime for rebound monitoring in 2007). This system when operational, extracts vapors from up to seven shallow vapor extraction wells screened in the unconsolidated soil below and surrounding the former outdoor waste sump.

4.5 TEST PLOT LOCATION

The sustainable bioaugmentation treatment demonstration was conducted south of and adjacent to Building 8595 near Site 37 (Figure 4.10). The treatment test plot includes the area encompassed by both the groundwater extraction and SVE wells. The dimensions of the test plot are roughly 160 ft by 200 ft. The test plot area currently contains Site 37 monitoring and extraction wells that were part of the (now decommissioned) groundwater pump and treat system, soil gas extraction wells that were installed for the SVE system, and monitoring, injection, and extraction wells installed during the current project.



C:\GIS\EdwardsAFB\GIS_Documents\Project_Maps\EAFB_014_Proposedv2.mxd • Date: 08/08/13

Figure 4.10. Site 37 Bioaugmentation Test Area

5.0 TEST DESIGN

The following subsections provide detailed descriptions of the system design and testing conducted to address the performance objectives described in Section 3.0.

5.1 CONCEPTUAL EXPERIMENTAL DESIGN

A demonstration of bioaugmentation to treat DNAPL sources in fractured bedrock was performed to assess overall dissolution and dechlorination rates within targeted DNAPL-filled fractures, to evaluate the overall effectiveness of bioaugmentation for reducing DNAPL mass and reducing dissolved contaminating flux emanating from the source area, to determine the impacts on the downgradient dissolved plume, and to develop and verify design parameters to optimize sustainability (e.g., limit electron donor). Additional bedrock open borehole wells were installed within the DNAPL source area, as determined during the initial DNAPL investigation (Section 5.4). After installation, geophysical testing was performed on the newly installed wells, followed by a series of short-term discrete interval pumping tests to confirm intervals and locations that are hydraulically connected. Discrete interval groundwater sampling was also performed.

Following this initial testing, a tracer test (conservative tracers and partitioning tracers) was performed across the demonstration area. This testing was used to verify the flow field (i.e., conductive fractures), to provide an estimate of the DNAPL mass, and to identify the locations of the DNAPL sources. Dissolved contaminant flux was measured via use of passive flux meters installed to intercept water-bearing fractures within (and downgradient of) the DNAPL source zone.

After baseline characterization was completed, bioaugmentation amendments were distributed through the targeted monitoring zone, which consists of discrete interval sampling points within the array of open borehole bedrock wells, where conductive fractures containing residual DNAPL sources are targeted. Groundwater monitoring was used to measure bioaugmentation effectiveness, as well as dissolved contaminant mass flux and discharge, in the specific fractures (or fracture zones) that contain the DNAPL source. Groundwater monitoring was used to assess the extent and rate of microbially-enhanced reductive dechlorination of PCE, the extent of electron donor distribution, and the extent to which DHC growth and distribution occurs through the fractured bedrock. Daughter product generation (including chloride) was used to determine the extent of DNAPL mass removed during treatment. A rebound assessment was also performed. Combined, this information provides insight into the relationship between DNAPL mass removal and groundwater quality, and ultimately the efficacy of bioaugmentation for treatment of DNAPL sources in fractured bedrock.

5.2 BASELINE CHARACTERIZATION ACTIVITIES

Prior to site selection, CB&I reviewed existing site investigation documents and all available hydrogeologic and contaminant distribution data for the Site 37 source area at Edwards AFB. The screening partitioning tracer test that was performed using an existing monitoring well (as discussed in Section 4.1) suggested that DNAPL was likely present in the vicinity of Building 8595 and monitoring well 37-EW07, and the demonstration test plot was selected in this general area (see Figure 5.1). However, as described in Section 5.2.1 below, initial characterization activities were performed to verify the suitability of this location, and to confirm the effectiveness of bioaugmentation for treatment of PCE under site biogeochemical conditions.

5.2.1 Preliminary Assessment of DNAPL Distribution and Hydrogeology

5.2.1.1 Rationale and Objectives

An initial investigation was performed in the presumed PCE DNAPL source area in the vicinity of 37-EW07 (based on the results of the screening-level partitioning tracer test that suggested DNAPL was present in bedrock at this location, and based on the proximity of this location to reported PCE DNAPL releases, as discussed in Section 5.2). The overall goal of this preliminary assessment was to verify that the site was suitable for the proposed demonstration, and to provide a design basis for the Demonstration Work Plan that followed this initial testing. Specific objectives of this preliminary assessment included the following:

- Verify that DNAPL is present;
- Identify approximate locations and depths where DNAPL is located;
- Identify primary conductive fractures, and connectivity of wells;
- Determine well capacity (to estimate recirculation flow rates during bioaugmentation); and,
- Collect aquifer solids for the bench scale treatability study (Section 5.3).

5.2.1.2 Approach

The approach employed was intended to provide a preliminary assessment of DNAPL distribution and bedrock hydrogeology in the suspected DNAPL source area. The approach consisted of collection of rock core from four locations, installation of open-borehole bedrock wells at these four locations, geophysical testing, discrete interval rock and groundwater sampling, pump testing, and implementation of partitioning tracer tests (PTTs). Rock core sampling and discrete interval groundwater sampling were used to identify potential DNAPL locations (Section 5.2.1.3). The geophysical testing and pump testing were used to identify conductive fracture zones, and to assess connectivity among the monitoring wells. PTTs were used to determine which conductive zones contained DNAPL.

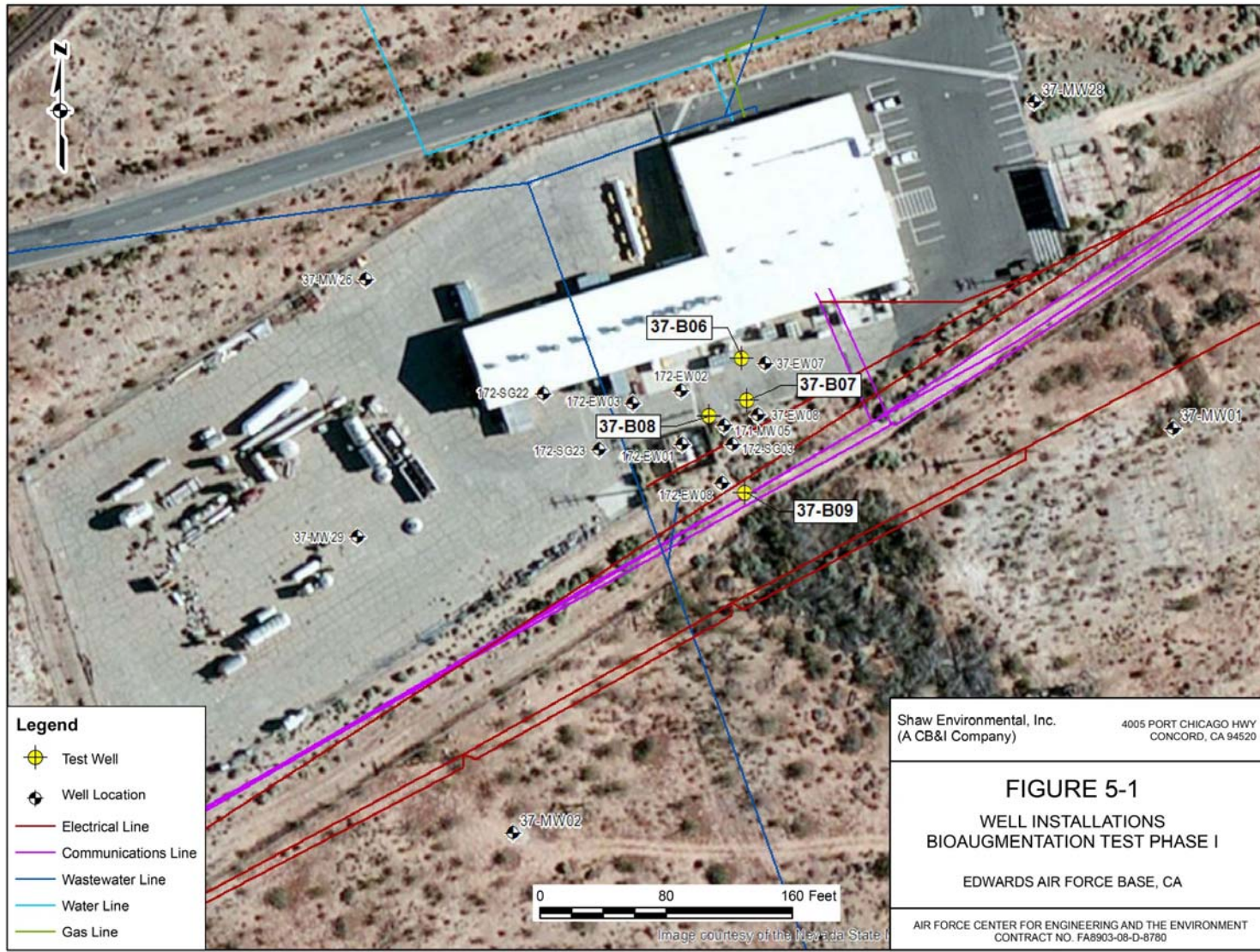


Figure 5.1. Well Installations, Bioaugmentation Test Phase I

5.2.1.3 Rock Core Collection, Rock Core Screening, and Well Installation

The site testing included the drilling of four boreholes into site bedrock to depths of approximately 100 ft bgs. The location of the boreholes relative to Building 8595 is illustrated on Figure 5.1. Geologic characterization, borehole geophysical logging, groundwater sampling, and hydrologic testing were conducted in these boreholes. The boreholes were completed as open annulus monitoring wells within the bedrock. The wells were designed to facilitate further testing and use in the bioaugmentation demonstration.

Drilling and Coring

The four wells were drilled at locations adjacent to the original product tank location (suspected source) and at locations as far as 105 ft downgradient from the former product tank. The wells were permitted through the Kern County Public Health Services Department (permits #37-B06, 37-B07, 37-B08 and 37-B09). The locations of the wells are illustrated on Figure 5.1. Well 37-B06 is located closest to the suspected source and 37-B09 the greatest distance downgradient near the facility fence line.

Well installation was conducted between January 10 and January 23, 2013, using a Brainard-Killman (BK-81) drill rig with HQ wire line diamond core (3.781-inch outside diameter). The surficial sediments were isolated by setting a 6-inch conductor casing into the upper bedrock surface. The conductor casing depths ranged from 7 ft bgs (37-B06 and 37-B07) to 24 ft bgs in well 37-B08. Drilling fluids (potable water) and cuttings were contained analyzed and disposed of according to State of California requirements.

Water levels were monitored in the adjacent well 37-B06 while drilling 37-B07 to evaluate whether there was hydraulic connection. No measurable influence was observed until the drilling reached a depth of approximately 78 ft bgs in 37-B07 at which point an increase of 0.15 ft was observed.

Geologic Logging

The HQ geologic core was logged, boxed, photographed, and retained in on-site storage. Figure 5.2 illustrates a typical sequence of geologic core as returned from boring 37-B06 (69 to 82.5 ft bgs). Geologic logging was conducted according to CB&I Procedure EID-GS-024 “Standards for Conducting Rock coring.” The wells were drilled to varying depths indicated below:

- 37-B06 – 115 ft bgs;
- 37-B07 – 95.5 ft bgs;
- 37-B08 – 101 ft bgs; and,
- 37-B09 – 89 ft bgs.

The geologic log for boring 37-B06 is presented in Appendix B. Geologic logging included determination of mineralogical content, percent recovery, rock quality designation. The core recovery was generally excellent, with 80% to 100% recovery common for most intervals. Three of the borings, 37-B06, 367-B07 and 36-B09, contained similar lithological sequences, with the rock consisting of the commonly present quartz monzonite with intruded zones of granite. Occasional thin layers of dark mafic material were also observed in the wells. Distinct fracture sets were observed in the core with at least four sets present. The dip of the fractures ranged from nearly vertical (within 10 degrees of vertical) to nearly horizontal.

IMAGE	X-REF	OFFICE	DRAWN BY	CHECKED BY	APPROVED BY	DRAWING NUMBER
		CONCORD	SAZ	4/8/13	TA	4/8/13
						148185-B3



NOTES:
 1. FRACTURE ZONE 78 TO 79 FT-BGS.
 2. FRACTURE ZONE 81.5 TO 82.5 FT-BGS

	EDWARDS AFB
FIGURE 5-2 GEOLOGIC CORE 37-B06 69 FT-BGS TO 82.5 FT-BGS	

Figure 5.2. Geologic Core 37-B06: 69 ft bgs to 82.5 ft bgs

- Notes: 1. Fracture zone: 78 to 79 ft bgs
 2. Fracture zone: 81.5 to 82.5 ft bgs

The presence and orientation of fractures is discussed further in relation to the borehole geophysics testing (Section 5.2.1.4). The contrasting lithologies (quartz monzonite versus granite) were encountered repetitively, with zonal thickness ranging from 5 ft to greater than 20 ft. The two lithologies appeared to be the result of multiple intrusions and not the result of structural juxtaposition (e.g., faulting) or secondary fracture filling. Quartz monzonite is the primary lithology with the granite representing a secondary (later stage intrusion). Lithological transitions ranged from gradual to abrupt. In contrast, the somewhat rare, but distinct mafic (dark) lithology appears as thin tabular bodies that may have exploited existing fracture plains. Well 37-B08 contained somewhat distinct characteristics: having considerably more clay and broken material. Two other distinguishing features of well 37-B08 were the considerably greater depth to the bedrock surface (27 ft bgs) and lack of available groundwater.

The geologic core was examined for VOC constituents as it was removed from the core barrel, upon separation of the split spoon using a handheld photoionization detector (PID). The full length of the core was examined with the PID and the locations with detectable concentrations were recorded. The PID readings are presented in Table 5.1 below.

Boring 37-B06, which is adjacent to the original source (tanks) location, produced only one depth interval (82.2 ft bgs) with total VOCs detected by the PID at 2.6 parts per million [ppm]. The reading is coincident with a fracture zone observed in core (Figure 5.2). VOC readings in Boring 37-B07, roughly 30 ft downgradient (from 37-B06) were detected at two depths (63-64 ft bgs and 71.5 ft bgs) spanning an interval of between 8 and 9 ft.

The vertical distribution of detectable VOCs was observed over a wider vertical interval with increasing distance from the original Building 8595 source location. VOCs were detected in PID readings from core from boring 37-B07 (downgradient from 37-B06), at three depths. The PID readings at 63 and 64 ft bgs depths were 19 and 5.2 ppm, respectively. A reading at 71.5 ft bgs was observed but at a concentration of less than 1 ppm.

Boring 37-B08, which is positioned 40 ft southwest of 37-B06, produced PID responses at 86 ft bgs and 96 ft bgs depths with concentrations of less than 1 ppm. The furthest downgradient well, 37-B09, located roughly 80 ft downgradient produced the highest and widest distribution PID readings with concentrations as high as 52 ppm and a vertical depth distribution over roughly 30 ft. The VOC concentrations as observed using the PID are strongly correlated to the presence of rock fractures in all four borings.

Rock samples were collected for analysis, using methanol extraction, at two locations. This collection occurred shortly after the rock cores were collected. The first location, collected at approximately 63 ft bgs at 37-B07, corresponded to the location of the most elevated PID reading at this borehole location. The resulting value was 7 milligrams per kilogram (mg/kg) PCE, which is indicative of residual DNAPL and/or substantial PCE mass sorbed to the rock matrix. The second rock sample analyzed, collected at approximately 57 ft bgs at 37-B09, was collected at the location with the most elevated PID reading (approximately 430 parts per million by volume) at this borehole. The resulting PCE concentration was 195 mg/kg, which is indicative of the presence of residual PCE DNAPL.

Table 5.1. VOCs in Geologic Core, PID Examination

Phase I Well Installation

Well	Depth (ft bgs)	PID Reading (ppm)
37-B06	82.2	2.6
37-B07	63	19
	64	5.2
	71.5	0.2
37-B08	86	0.7
	96	0.4
37-B09	46	7.7
	48.25	15.5
	49	11.4
	50	45
	50.5	33
	51	52
	51.5	1
	52	1
	54	31
	56.5	7
	57	0.4
	57.5	0.1
	65	2
67.5	7	
77.5	3.0	
78	6.8	

Although the two locations noted above suggest that DNAPL is or may be present at the sampled intervals, we note that observing and verifying the presence of residual DNAPL in rock fractures via rock sampling is very difficult, as residual DNAPL mass may be lost during the coring process and inspection of the rock core. An improved approach for assessing the potential presence of residual DNAPL is via in situ partitioning tracer tests, as discussed in Section 5.2.1.7.

Periodic water level measurements were made in the open boreholes as well installation progressed using a handheld water Solinst level meter. The static water table in borehole 37-B06 was 51.5 ft bgs upon completion of drilling. The static water table in borehole 37-B09 was 78.7 ft bgs.

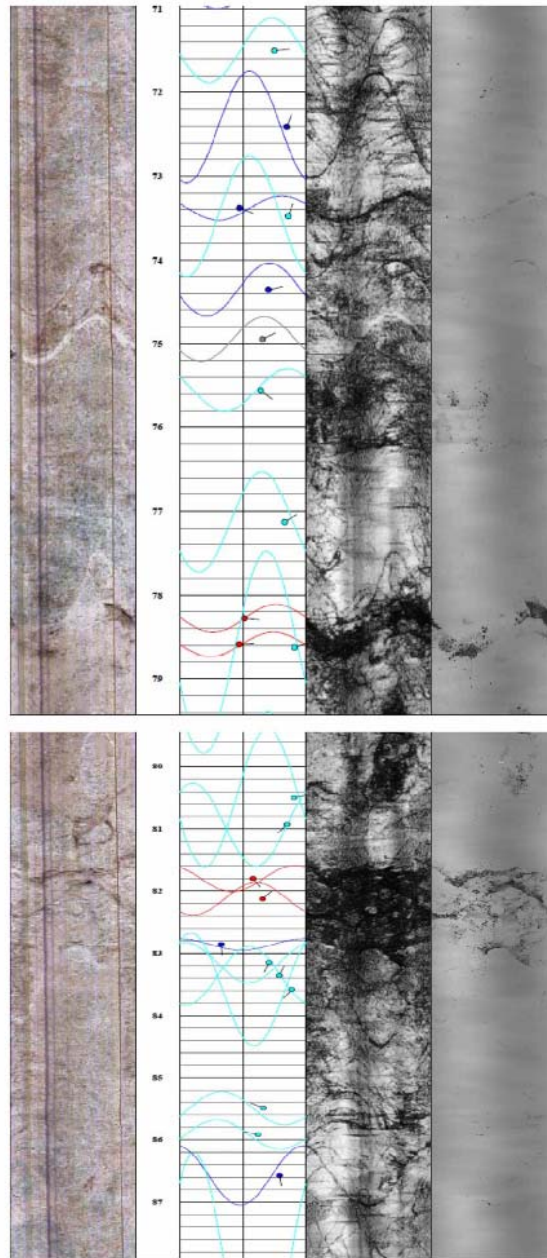
5.2.1.4 Geophysical Logging

Geophysical testing was performed on January 17 and 18, 2013, in borings 37-B06 and 37-B09. The geophysical methods performed in borehole 37-B06 included: the optical televiewer, acoustic televiewer, natural gamma, single point resistance, spontaneous potential, and heat pulse flow meter. A limited suite of logs was performed in 37-B09 due to a limited column of water in the boring with the spontaneous potential and heat pulse flow meter omitted. A representative segment of the optical and acoustic televiewer log is presented on Figure 5.3 and the complete logging suite for 37-B06 is presented in Appendix C. Optical televiewer and acoustic televiewer logging in was performed in 37-B06 from 4.1 to 108.1 ft bgs and from 51.1 to 110.1 ft bgs, respectively. In boring 37-B09 the optical televiewer run was from 11.8 ft to a depth of 88.9 ft but the acoustic televiewer logging was conducted from only 78.6 to 89.3 ft bgs. The reduced interval for the acoustic televiewer, compared to the optical televiewer, was due to the need for a fluid filled borehole. The following observations were made by Colog (the geophysical logging contractor):

- The method identified fractures/features with open aperture at suspected water producing zones. Dip directions analysis indicates that approximately 32.4% of the identified features in 37-B06 dip in the direction of 50 to 100 degrees (East-Northeast and East-Southeast). Dip Angles indicated that approximately 86% of the features in 37-B06 are dipping at more than 40° from horizontal while the remaining features are dipping at less than 40° from horizontal.
- There are 103 high-angle fractures or features (dip angles greater than 45°) identified in 37-B06 out of a total of 135 fractures. These high-angle features are qualitatively ranked 0 to 3, suggesting minimal flow potential from these features. Optical televiewer and acoustic televiewer data depict features at depths which correlate well with the water-bearing intervals identified from the heat pulse flow meter data (see below).
- Dip Directions analysis in borehole 37-B09 indicate approximately 26% of the identified features dip in the direction of 320 to 360 degrees (Northwest) and 25.5% dip in the direction of 140 to 200 degrees (Southeast). Dip Angles image indicate over approximately 66% of the features in 37-B09 are dipping at more than 50° from horizontal, while the remaining features are dipping at less than 50° from horizontal. There are 97 high-angle fractures or features (dip angles greater than 45°) that were identified in 37-B09. These 97 high-angle features represent 79.5% of all identified features from the optical televiewer and acoustic televiewer data set. The 97 high-angle features are qualitatively ranked 0 to 3, suggesting minimal flow potential from these features, with the exception of one high-angle feature ranked 4, suggesting a nominal flow potential.

IMAGE	X-REF	OFFICE	DRAWN BY	CHECKED BY	APPROVED BY	DRAWING NUMBER
---	---	CONCORD	S.G.	6/8/13	TR	6/8/13

		Acoustic and Optical Telemetry		COLOG Main Office 639 West Street, Suite E, Lakewood, CO 80226 Phone: (303) 274-6171, Fax: (303) 274-6151 www.colog.com	
COMPANY: Sham	PROJECT: Hermosa	DATE LOGGED: 17-18 Jan 2013	WELL: 37-B06	Optical Image: MN	Depth: 18.120'
Projection: MN		Acoustic Amplitude: MN		Acoustic Travel Time: MN	
0° 90° 180° 270° 0° 90° 180° 270° 0° 90° 180° 270° 0° 90° 180° 270° 0° 90° 180° 270°					



	EDWARDS AFB
	FIGURE 5-3 BOREHOLE TELEVIEWER LOG 37-B06 71 TO 81 FT-8GS

Figure 5.3. Borehole Televiewer Log 37-B06 (71 to 88 ft bgs interval)
COLOG fracture flow potential: Lowest: Black (1), Blue (2), Purple (3), Highest: Red (4)

Marginal conductive zones as identified by a quantitative “feature rank” of “3” were interpreted by the logging contractor at 78, between 81.8 to 82.1, and at 99.5 ft bgs (rank 3) in 37-B06. These zones are also potentially productive water-producing zones based on core logging as well. One potentially productive fracture in borehole 37-B09 was ranked in the feature rank “4” category but is located above the water table (20.9 ft bgs). No other fractures below water table depths were rated above category “2” or “3” in borehole 37-B09.

Rose diagrams of dip direction indicate the direction of dip for fractures in each logged well (Appendix C). The fracture directions observed in the two borings, as discussed above, reflect different stress regimes. Potentially significant features not discussed by the contractor are fracture sets that are oriented 50 to 60 degrees from the north in both 37-B06 and 37-B09. The fracture set represents 10% of the fractures in each borehole and represent a common fracture set that potentially have significance with respect to groundwater flow.

The heat-pulse flowmeter logging in 37-B06 indicated no flow during ambient conditions between approximately 51 and 58 ft bgs. Minor flow was indicated at 60.7, 66.1, 71.0, 76.6, 96.0, and 102.0 ft bgs with flow ranging from 0.02 to 0.04 gallons per minute (gpm) (see Appendix C). During pumping, water was drawn up the borehole and extracted at 1.07 gpm. The Heat-Pulse tests in the deeper borehole, during pumping, indicated upflow with a maximum of 0.03 gpm at 71.0 ft bgs and a minimum of 0.01 gpm at 83.9 ft bgs. This decreasing flow with depth indicates that the entire interval was contributing to the flow of fluid into the borehole and adding to the flow rate with successively shallower tests.

Key findings, as they relate to the presence of conductive fractures and fracture connectivity in the demonstration area, are summarized below:

Borehole 37- B06

- Many fractures, at various dip direction and angle;
- East-Northeast and East-Southeast direction are predominant;
- Most of the fractures are poorly- or non-conductive;
- Conductive fractures exist between 78 and 83 ft bgs; and

Borehole 37-B09

- Many fractures, at various dip direction and angle;
- Northwest and southeast directions predominate;
- Most of the fractures are poorly or non-conductive; and
- The boring is less conductive (hydraulically) than 37-B06.

Based on the analysis of the acoustic and optical televiewer logs, both boreholes contain a northeast dipping set of fractures that account for about 10 percent of observed fractures. This set of fractures, given their common presences in both boreholes represents a potential conduit for DNAPL migration. Figure 5.4 shows a conceptualized cross-section between 37-B06 and 37-B09, where conductive fractures are shown. The conductive fractures shown are based on the geophysical testing at 37-B06. For 37-B06, only the interval from 59 to 83 ft bgs is shown, as this zone represents the fracture planes that will be investigated during the demonstration. The conductive fracture pair at ~78 ft bgs that intersects both boreholes provides an explanation for the hydraulic response observed in 37-B06 when coring at 37-B07 reached a depth of 78 ft bgs.

Well Installation

The borings were converted into open interval monitoring wells (see Section 5.4 for specifications). The open borings were retained with the addition of a surface completion to prevent the entry of surface water. The surface conductor casings were retained in place and flush mount surface completions were constructed to protect the wells. The well's bedrock intervals are unscreened and open, without sand pack or well casing. The retention of the full open interval will allow continued depth specific testing throughout the whole well interval.

Well development included extensive recirculation of drilling fluids through the drill stem after the borehole reached total depth and extensive pumping during specific capacity and short-term pump tests. Conventional swab and bail techniques were not applied due to the open hole configuration of the borehole and the presence of distinct fracture sets. Aggressive development could potentially dislodge fractured rock fragments and obstruct the borehole.

5.2.1.5 Initial Groundwater Sampling

Initial groundwater sampling was performed at 37-B06, 37-B07, and 37-B09. No groundwater sampling or testing was performed in 37-B08, as this well could not be developed due to the lack of flow and production. Results of the initial groundwater sampling are summarized in Table 5.2. These results all show PCE concentrations greater than 1% of the PCE solubility, which suggests that DNAPL may be present. The PCE concentrations shown in Table 5.2 are consistent with historical groundwater data collected in the source area (24).

Table 5.2. Groundwater PCE Concentration Measured at the Boreholes

Borehole	Interval	PCE Concentration (mg/L)
37-B06	Top of packer at ~87 ft bgs, and pump intake ~1 ft above packer	18
37-B07	Pump intake at 90.5 ft bgs	34
37-B08	<i>Not Sampled</i>	
37-B09	Pump intake at ~86 ft bgs	21

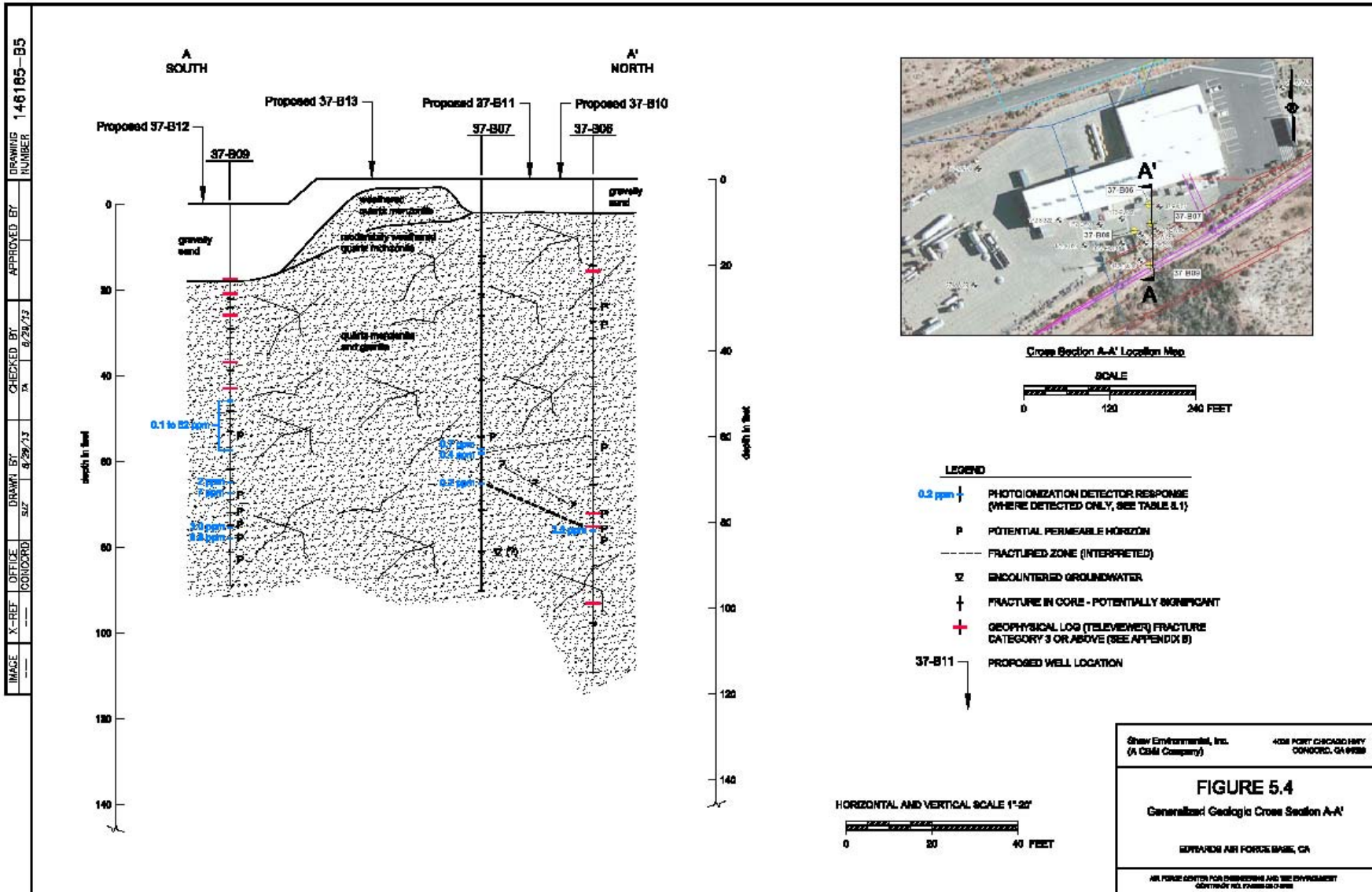


Figure 5.4. Generalized Geologic Cross Section A-A'

5.2.1.6 Well Capacity and Short-Term Pumping Tests

To perform the bioaugmentation demonstration, and to effectively distribute bioremediation amendments throughout the demonstration area, bedrock wells with the capacity to inject and deliver amendments are required. For fractured bedrock with low effective porosities, even very low well capacities (e.g., 100 milliliters per minute [mL/min]) can be sufficient for distributing amendments over reasonable (i.e., tens of feet) distances. Testing was performed on boreholes 37-B06, 37-B07, and 37-B09 to estimate the capacity (i.e., sustainable flow rate) at selected depth intervals. As previously discussed, no measurable flow was measured in 37-B08, as the well would not develop; thus, no well production testing was performed in 37-B08.

With the bottom of the pump lowered to approximately 108 ft bgs in 37-B06, the open borehole sustainable groundwater extraction flow rate was 238 mL/min. To estimate the flow rate in the shallow portion of borehole 37-B06, a packer was inserted in the well so that the top of the packer was at 86 ft bgs. Drawing the water down to the top of the packer and measuring recharge above the packer, the well capacity was 156 mL/min. These results are consistent with the geophysical testing (Section 5.2.1.4) for 37-B06, where the most conductive fractures were located between 78 and 83 ft bgs.

The initial capacity test for 37-B07 was performed by setting the top of the packer at approximately 70 ft bgs, and the pump intake approximately 1 foot above the top of the packer. The groundwater was extracted to the depth of the pump intake, and the maximum recharge rate of 50 mL/min was used to estimate the capacity. This test was repeated with the top of the packer set to approximately 80 ft bgs, with the pump intake at approximately 79 ft bgs. The estimated well capacity for this test was 110 mL/min. Thus, the fracture pair that intersects both 37-B06 and 37-B07 at 77 to 78 ft bgs appears to be responsible for a large fraction of the well capacity at 37-B07.

For borehole 37-B09, the extraction pump was lowered to approximately 86 ft bgs (open borehole). After drawing the water down to the pump intake, the recharge rate of the well was measured. The calculated flow rate into the well was approximately 24 mL/min, which is substantially less than the well capacities measured in 37-B06 and 37-B07. The low well capacity observed in 37-B09 is in qualitative agreement with the geophysical data (Section 5.2.1.4), which showed less prominent fractures (and presumably less conductive) than what was observed for 37-B06.

CB&I field personnel conducted a short-term pumping test on 37-B07 while collecting drawdown observation data from 37-B06. The data collected were used to calculate approximate horizontal hydraulic conductivity (K_h), storativity, and transmissivity. To collect pumping data while also gaining information about which zones in 37-B07 were most connected to 37-B06, a packer was placed in 37-B07 with the pump placed above the packer. Initially, the pump intake in 37-B07 was at 69 ft bgs and the top of the packer was at 70 ft bgs. After 1 hour of extraction at this depth, CB&I personnel lowered the pump and packer to 79 and 80 ft bgs, respectively. Pumping continued at 79 ft bgs for another hour until personnel removed the packer and lowered the pump to the bottom of 37-B07. Extraction continued at this depth for another 2.5 hours, for a total pumping time of 4.5 hours (Figure 5.5). After pump shut down, CB&I personnel observed recharge in 37-B07 for an hour and a half. Noticeable drawdown of 37-B06 began to occur after 1 hour of pumping in 37-B07. CB&I analyzed the data collected from this test using AquiferTest V3.5 software and two analysis methods: The Moench Solution for flow in fractured media aquifers and the Cooper-Jacob solution which is typically used for porous aquifers. The results of the test are summarized below.

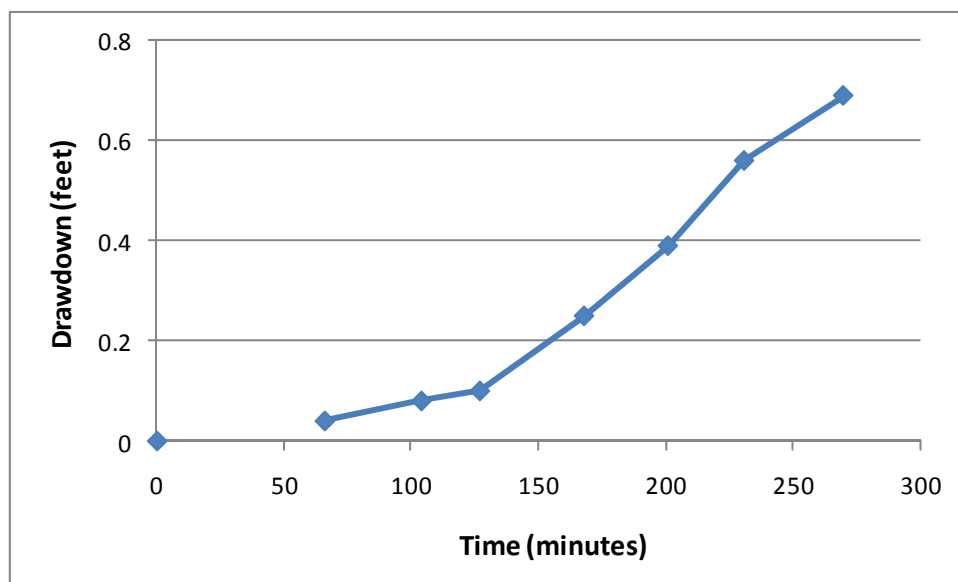


Figure 5.5. Results of Short-Term Pumping Test

The data show drawdown in borehole B06 while extracting at 100 mL/min in borehole B07.

The results of the analysis are presented in Table 5.3. The conductivity values were derived from multiple analytical methods that are applicable to various flow scenarios. The values reflect the very low groundwater flow rates that are expected in a fractured bedrock environment.

Table 5.3. Summary of 37-B07 Pump Test Analysis

Parameter	Theis	Theis Recovery	Moench Fracture	Cooper-Jacob	Average
Conductivity (ft/day)	0.00642	0.00022	0.00755	0.01830	0.00812
Storativity	0.00015	N/A	0.00017	0.00011	0.00014
Transmissivity (ft ² /day)	0.328	0.011	0.385	0.933	0.414

5.2.1.7 Partitioning Tracer Tests

PTTs involve the use of both hydrophilic and hydrophobic groundwater tracers to estimate DNAPL mass (34). The hydrophilic tracers are used to estimate the groundwater velocity and dispersion, while the hydrophobic tracers will partition into DNAPL encountered along the groundwater flow path and will be used to estimate the effective DNAPL mass. We note here that PTTs are a useful tool for estimating DNAPL mass along hydraulically conductive pathways (in this case, within conductive fractures). However, DNAPL residing in low permeability regions may not be fully identified using PTTs, as mass transfer will limit uptake of the tracers into DNAPL sources. Thus, DNAPL mass estimated via PTTs should be considered as “hydraulically accessible” DNAPL mass. While this may not include the totality of DNAPL mass, the DNAPL mass identified via PTTs will likely identify the DNAPL which has the greatest impacts (with respect to contaminant flux) impacting groundwater.

PTTs were performed in two phases. The first phase implemented PTTs as push-pull tests (similar to the methods used by Istok et al. [35]) at selected boreholes and depth intervals to provide a qualitative indicator of DNAPL, thereby serving as a means to verify the presence of DNAPL within the demonstration area. The second phase of the PTTs was implemented as an inter-well tracer test.

For the first phase PTTs performed as push-pull tests, the selected hydrophilic tracers for the tracer testing were bromide and methanol; the selected hydrophobic tracers included 1-hexanol and 2-octanol. Concentrated stock solutions of the tracers were prepared in 5-gallon stainless steel soda kegs in the CB&I laboratory in Lawrenceville, NJ. The stock tracer solutions were diluted in tap water in 55-gallon drums in the field to obtain the following concentrations (approximate – actual concentrations were measured in the 55-gallon drums during injection into the wells):

- 500 mg/L bromide;
- 400 mg/L methanol;
- 200 mg/L 1-hexanol; and,
- 80 mg/L 2-octanol.

A total of three push-pull PTTs were performed. The first test was performed at 37-B06 and targeted the interval between 78 and 88.5 ft bgs using a straddle packer. The tracer solution for this test was gravity fed into the borehole and metered with a valve in the injection line. The injection began at 13:00 on January 23, 2013, at a rate of approximately 110 mL/min and ended around 21:50. This equates to an 8.8-hour injection duration and 15.4 gallons of injected tracer solution. The extraction of water from 37-B06 began roughly 12 hours later at 10:20 on January 24, 2013, and ended at 14:50 on January 25, 2013. However, the active extraction time is significantly less because the pump shut off at the end of the day on January 24 and resumed at 08:20 on January 25. This means that the actual extraction time was 6 hours on January 24 and 6.5 hours on January 25, for a total of 12.5 hours of extraction. A QED Environmental Systems (QED) pneumatic extraction pump was used to extract groundwater and tracer solution from 37-B06. A total of 66.7 gallons (252 Liters) of groundwater was purged from 37-B06 with an average flow rate of 336 mL/min. This average rate is significantly higher than the 100 to 150 mL/min rate used throughout most of the extraction time because higher rates were used to purge the borehole the morning after the pump was shut down on January 24.

The second test, performed concurrently with the first push-pull PTT, was performed at 37-B07. The PTT performed at this well was performed in the open borehole with no packer. The pump intake in 37-B07 was placed at 90.5 ft bgs. Injection in 37-B07 began by gravity at 15:20 on January 23 and lasted 7.3 hours. The volume of tracer injected into B07 was 12.7 gallons. 37-B07 extraction began at 10:35 on January 24 and continued for just under 7 hours until the pump was shut off at the end of the day. Extraction resumed at 08:20 on January 25 and lasted 5 hours. The total combined extraction time in B07 was 12 hours. A pneumatic QED pump was also used in 37-B07. A total of 57.2 gallons (216 Liters) of groundwater was purged from 37-B07 with an average flow rate of 300 mL/min. This average rate is significantly higher than the 100 to 150 mL/min rate used throughout most of the extraction time because higher rates were used to purge the borehole the morning after the pump was shut down on January 24.

During these two tests, CB&I personnel sampled each well at 20-minute intervals for the first 3 hours and then every 30 minutes until the end of the day on January 24. On January 25, samples were collected every 2 hours. Field bromide screening was conducted periodically during the extraction period.

The third push-pull PTT was performed at 37-B06. This test was performed using a single packer, but utilized the same type of tracer solution as in the first two tests. The testing occurred above the packer, where the top of the packer was located at approximately 77 ft bgs and the pump intake was placed at approximately 76 ft bgs. Thus, this PTT focused on the shallow conductive zone in 37-B06, including the conductive fracture at 60 ft bgs (as indicated by the geophysical testing). Injection of tracer began on January 28, 2013, and a total of 7.5 gallons of tracer was injected into 37-B06. The tracer was allowed to mix with formation water overnight and extraction and sampling began on January 29, 2013. Purging of 37-B06 continued for approximately 7 hours at an average extraction rate of 115 mL/min. A total of 20 gallons of groundwater and tracer was purged from 37-B06 during the test, although approximately 6.5 gallons of the 20 was attributed to the borehole volume. Therefore, the volume of groundwater purged from the formation was approximately 13.5 gallons. Sample collection occurred every 30 minutes during the 7-hour extraction period. After completion of the extraction period, the pump was shut off. Samples were screened in the field for bromide and analytical samples were sent off site to laboratories for analysis.

PCE and bromide were analyzed at CB&I's laboratory in Lawrenceville, NJ using EPA Method 8260 and 300.0, respectively. Alcohols were analyzed at the University of Florida using direct liquid injection gas chromatography (Perkin Elmer GC, Autosystem XL) using a flame-ionization detector.

Results from the three push-pull PTTs are summarized on Figures 5.6a through 5.6c. The bromide mass recovery was greater than 99% for the shallow PTT performed at 37-B06. This high recovery is likely due to the fact that only limited migration of the tracers occurred between the injection and extraction stages of the test, as the primary conductive fractures resided below the packer and only the less conductive packers were evaluated during this shallow test (based on the heat pulse flowmeter testing performed at 37-B06). Bromide mass recoveries were approximately 58% for the PTT performed at 37-B07 and the deep PTT test performed at 37-B06. Migration of tracers through conductive fractures at depths greater than 77 ft bgs likely resulted in more substantial migration of tracers between the injection and extraction stages than that which occurred during the shallow PTT at 37-B06, thereby inhibiting the rate of tracer recovery. A substantially longer extraction stage would have been needed to recover >90% of the injected tracers.

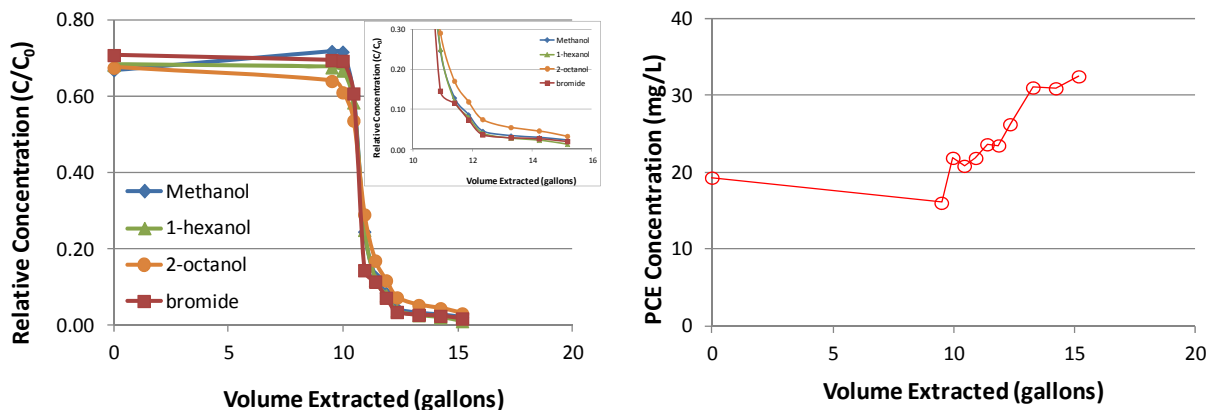


Figure 5.6a. Shallow Push-Pull PTT Results for 37-B06

Results from the shallow push-pull PTT performed at 37-B06. Tracer results are shown on the left, and dissolved PCE concentrations are shown on the right. The inset showing the tracer concentrations at late times highlights the tailing of the hydrophobic 2-octanol tracer, indicating the presence of DNAPL.

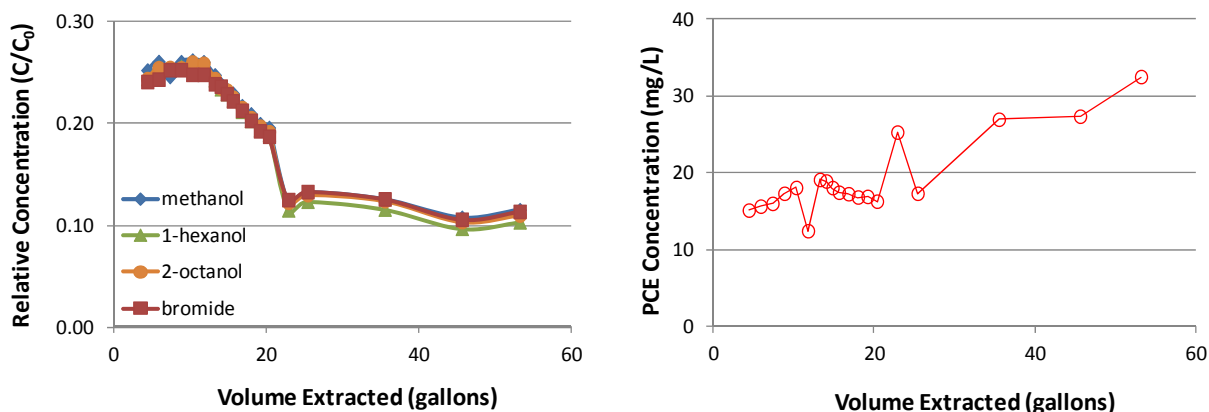


Figure 5.6b. Deep Push-Pull PTT Results for 37-B06

Results from the deep push-pull PTT performed at 37-B06. Tracer results are shown on the left, and dissolved PCE concentrations are shown on the right. At both early and late times, the 2-octanol and 1-hexanol elute with the conservative tracers, indicating that DNAPL was not observed during this test. However, an increased extraction time may have been needed to observe tailing of the 2-octanol.

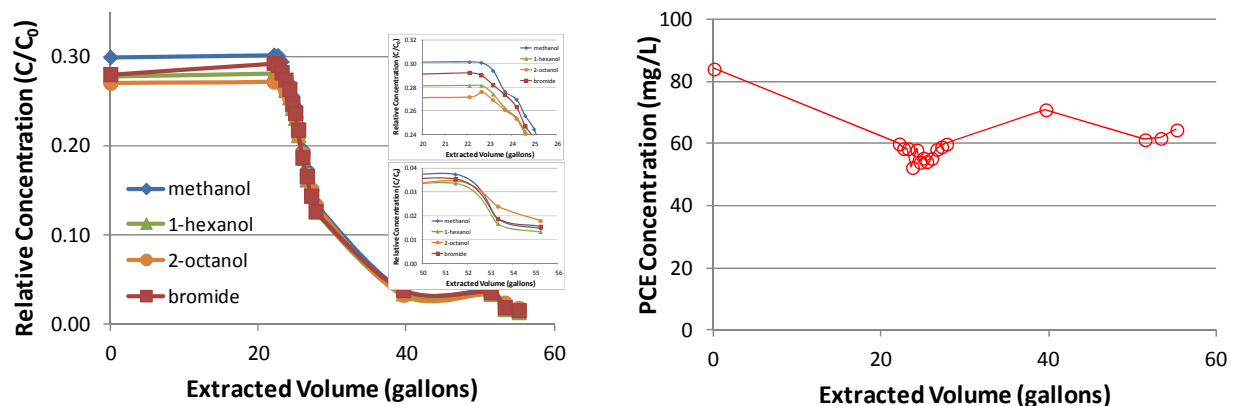


Figure 5.6c. Push-Pull PTT Results for 37-B07

Tracer results are shown on the left, and dissolved PCE concentrations are shown on the right. The insets showing tracer elution at early and late times clearly show that 2-octanol (and 1-hexanol at early times) shows an increase in the apparent dispersion, which is indicative of the presence of DNAPL (35).

Upon initiation of the extraction stage of the PTTs, the initial conservative (i.e., bromide and methanol) tracer concentrations measured in the extracted groundwater during the shallow PTT at 37-B06 were approximately 70% of the injected concentrations. For the other two PTTs, the initial extracted conservative tracer concentrations were 25 to 30%. This difference likely is due to the fact that (as discussed in the previous paragraph) tracer concentrations were flushed from the borehole during the time interval between injection and extraction stages for the deep PTT at 37-B06 and the PTT at 37-B07; based on the results of the heat pulse flow meter testing, substantially less flow occurs in the shallow portion of 37-B06, which is why tracer concentrations remained comparatively high for this PTT, as less tracer was flushed from the borehole during the time interval between injection and extraction stages.

For both the shallow PTT at 37-B06, and the PTT at 37-B07, the behavior of the 2-octanol differs from that of the conservative tracers (i.e., bromide and methanol). The 2-octanol is the most hydrophobic tracer and will be the most responsive and show the highest affinity to DNAPL. At early times, the relative 2-octanol concentrations, and to a lesser extent 1-hexanol, were less than those of the conservative tracers. At later times, “tailing” of the 2-octanol was observed, as relative 2-octanol concentrations were greater than those of the other tracers. This behavior is consistent with the apparent increase in dispersion observed for a partitioning tracer when DNAPL is present (35). Thus, fracture flow paths contacted during the PTT in the shallow interval for 37-B06 and for 37-B07 exhibit behavior consistent with the presence of residual DNAPL.

Differences in the elution of 2-octanol is not observed for the deep interval PTT at 37-B06, suggesting that DNAPL may not be present in this zone. The absence of any observable differences in the elution of 2-octanol at this location provides assurance that the observed differences at the other PTT locations likely was not due to any sorption to aquifer solids (especially at early times). However, the tailing of the 2-octanol in the other two PTTs was not observed until tracer concentrations decreased to below 4 to 8% of their initial injection concentrations.

Tracer concentrations were at approximately 11% of their injection concentration by the end of the deep PTT at 37-B06; tailing of the 2-octanol, suggesting the presence of DNAPL, may have been observed if the test duration was increased. It is important to note that the interval isolated by the straddle packer for the deep PTT at 37-B06 intercepted conductive fractures at both 78.5 and 82 ft bgs. If the permeability in one of these fracture sets was substantially greater than the other, and DNAPL only existed in the less permeable fracture set, than the presence of residual DNAPL would not have been detected using the PTT.

The second phase of PTTs consisted of an interwell tracer test between 37-B06 and 37-B07. 37-B06 served as the injection well, and 37-B07 served as the extraction well. CB&I personnel, along with assistance from the University of Florida, began the interwell tracer test on March 5, 2013. This test involved injecting tracer solution into two intervals in 37-B06 and extracting from two intervals in 37-B07. Inflatable packers were placed within the test borehole to isolate specific test intervals. The upper interval in 37-B06 was from approximately 50 to 76 ft bgs, and the lower interval was from 78 to 83 ft bgs. In 37-B07, the upper interval was from the top of the potentiometric surface (49.2 ft bgs) to 73 ft bgs and the lower interval was from 75 to 82 ft bgs. Two pneumatic QED bladder pumps extracted water from 37-B07; the top interval had a 1.75-inch diameter bladder pump, and the bottom interval a 3-inch diameter extraction pump.

Two batches of tracer solution were prepared for this test. The solution injected into the upper interval in 37-B06 used a bromide tracer (field tracer) and isopropyl alcohol; and the lower interval solution included a fluorescent rhodamine dye for the field tracer mixed with methanol. Extraction of water from 37-B07 began 30 minutes prior to the initiation of injection in 37-B06 in order to facilitate flow between the two wells. Approximately 5.7 gallons of tracer was injected in the upper zone in 37-B06 and 11 gallons of tracer was injected into the lower interval. The tracer injection into the upper interval of 37-B06 was stopped early because field personnel observed little to no flow into the formation from the upper interval. Following the completion of tracer injection, tap water was injected down 37-B06 during extraction and sampling of 37-B07 to maintain a head differential between 37-B06 and 37-B07 and encourage the flow of tracer towards 37-B07.

During working hours, personnel collected field screening and analytical samples for alcohols from both intervals in 37-B07 every 30 minutes for the first day and then every hour for the next two days. Due to access restrictions, continuous (24 hours/day) extraction and sampling of groundwater from 37-B07 was not possible. Pumping 37-B07 overnight without regular sampling was avoided during the initial phase of testing as a precaution against missing the appearance of tracers (i.e., missing the tracer pulse). Pneumatic bladder pumps brought the samples to the surface with extraction rates varying between 30 and 125 mL/min. The use of bladder pumps isolates the drive gas from the water and prevents stripping VOCs from the sample. During the initial phase, field screening was conducted with a digital field bromide probe and a YSI 6920 probe equipped with a fluorometer to detect Rhodamine dye. Upon sample collection, CB&I staff placed the samples in a cooler for holding until shipment to the off-site laboratories at Lawrenceville, NJ, and the University of Florida, Gainesville.

The testing initially ended on March 8, 2013. Because field screening of water extracted from 37-B07 did not show increasing concentrations of the tracers, it was thought that the tracers may have been missed overnight or the effective porosity was much higher than predicted causing a longer travel time between the boreholes. However, analysis of the laboratory samples indicated increasing concentrations of alcohols from the latter part of the testing. Because of these results, personnel resumed testing after a 10-day interruption due to the time required to process samples and the scheduling to re-deploy staff to the AFRL. On March 18, 2013, CB&I personnel resumed groundwater extraction and sampling in 37-B07. Groundwater samples were collected from 37-B07 three to four times daily for the next 5 days with the last samples collected on March 22, 2013. During this period, groundwater extraction occurred continuously to maintain a hydraulic gradient towards 37-B07. No field screening was performed and all samples were sent off site for laboratory analysis. CB&I terminated field activities for the interwell tracer test on March 22, 2013.

Results of the interwell tracer test are summarized on Figure 5.7. Only very low levels of tracers injected into the deep zone were observed at 37-B07; these tracer concentrations were rapidly increasing prior to the 10-day interruption in testing. These results suggest that the effective porosity was much greater than expected (a value of 0.00015 was estimated based on the storativity value determined during the pumping test), where breakthrough of the tracer would have been expected within a few hours. Based on the observed tracer velocity between 37-B06 and 37-B07, the effective porosity likely is between 0.001 and 0.01, which still is within the plausible range for fractured bedrock. This result also suggests that the storativity value determined during the pumping test (Section 5.2.1.6) likely reflects a response for a confined aquifer, rather than an extremely low effective porosity in an unconfined aquifer (40).

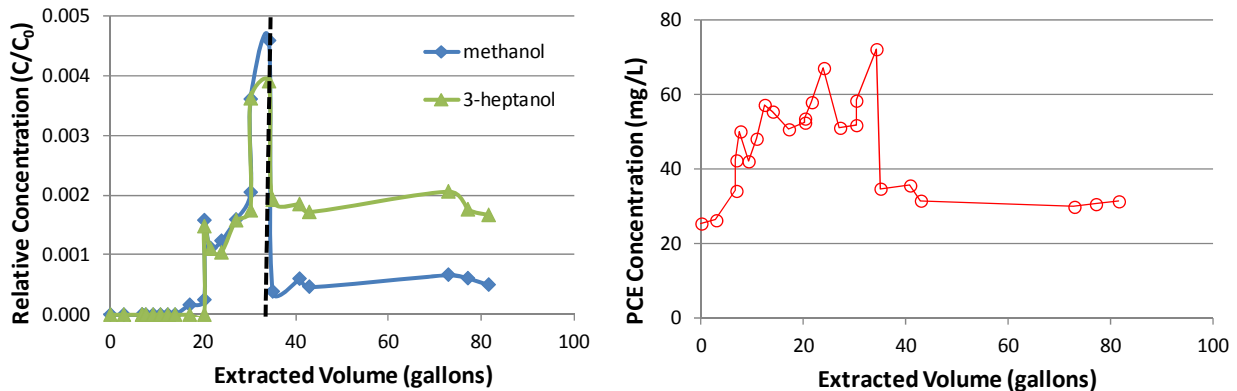


Figure 5.7. Interwell Tracer Test Results

Tracer and PCE results from the interwell tracer test between 37-B06 and 37-B07. The vertical dashed line represents the 10-day interruption in testing, which is likely when the majority of the tracer pulse migrated beyond 37-B07.

After resuming the interwell tracer testing after the 10-day interruption, tracer concentrations decreased substantially compared to concentrations observed prior to the interruption. Results suggest that the pulse of tracers had migrated beyond 37-B07, and that only the slow decreasing “tail” of the tracers were captured. However, the 3-heptanol (which partitions strongly into the PCE DNAPL) clearly exhibited a greater extent of tailing than the conservative methanol tracer, indicating that DNAPL likely was present along the flow path connecting the deep zone in 37-B06 and 37-B07.

The absence of any measurable tracer in 37-B07 from the tracer mix injected in the shallow interval of 37-B06 is likely due to the reduced transmissivity of this zone, causing the shallow-injected tracers to become diluted in the extraction well and decreasing to below their detection limits. Additional investigation and tracer testing within this shallow interval will be performed as part of baseline characterization (Section 5.5).

The dissolved PCE concentrations measured during the push-pull and interwell PTTs are also consistent with the presence of PCE DNAPL, as concentrations remain above 10% of the PCE solubility in water. By the end of the test for each location, PCE concentrations were greater than 20% solubility.

Figure 5.8 provides a conceptual model of the location of residual PCE DNAPL sources in the vicinity of 37-B06 and 37-B07. It is reassuring to note potential correlations between fracture flow paths and measured PID readings/analytical data collected from the rock core at 37-B07. This preliminary conceptual model would serve as the basis for the remaining well installation, and design of future pump and tracer testing described in Section 5.5.1.

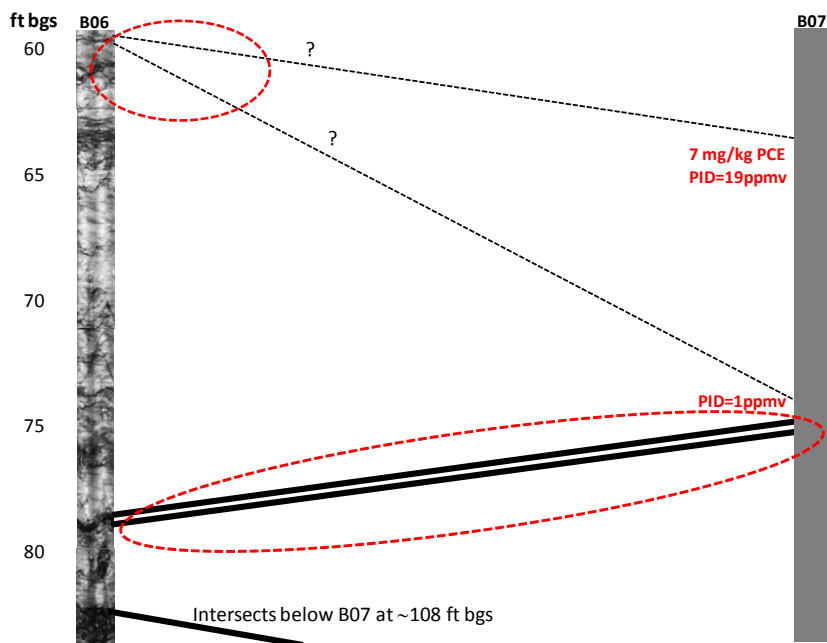


Figure 5.8. Conceptual Model Showing Likely DNAPL Locations

Dashed red circles indicate locations that PTT suggest DNAPL is present. PID screening and rock analyses at 37-B07 appear to correlate with locations of potentially DNAPL-impacted fracture paths.

5.2.1.8 Conclusions from the Preliminary Characterization Activities

The preliminary assessment of DNAPL distribution and hydrogeology performed for this project supported the implementation of the proposed bioaugmentation demonstration within the targeted Site 37 source area at Edwards AFB. A summary of the key preliminary characterization results are as follows:

- Well capacities within the source area are relatively low (<250 mL/min), but likely are sufficient for distribution of bioaugmentation amendments in conductive fractures. This was verified by observing the travel times during the interwell tracer test.
- Groundwater flow and solute migration is controlled by a complex fracture flow path, which consists of many fractures at varying orientation and angle.
- Hydraulic connectivity was observed for at least two wells (37-B06 and 37-B07), located 30 ft apart, within the DNAPL source area. This connectivity was attributable to a conductive fracture-plane that intersects these wells at a similar elevation. Less conductive fractures also likely intersect these two well locations.
- DNAPL was identified within the source area. Results of the PTTs indicate that DNAPL was present within the conductive fractures that intersect 37-B06 and 37-B07. PID and VOC analysis of rock fragments at 37-B07 were consistent with the PTT results. DNAPL also was observed, based on rock VOC fragment analysis, in a low permeable zone at 37-B09.
- PCE groundwater concentrations measured during the preliminary investigation were all consistent with the presence of PCE DNAPL (i.e., greater than 1% solubility).

The conclusions of the preliminary DNAPL and hydrogeologic characterization for this project marked a Go/No-Go decision point to move onto the field demonstration phase of the project at Edwards AFB. Results clearly showed that PCE DNAPL is present, that wells are hydraulically connected, and that conductive fractures containing DNAPL can be contacted by injected amendments (as indicated by the PTTs).

5.3 LABORATORY TREATABILITY STUDY

5.3.1 Objectives

Laboratory treatability studies were conducted with samples obtained during the initial site characterization and DNAPL investigation, which occurred in January 2013. The overall goal of the laboratory treatability study was to evaluate the effectiveness of bioaugmentation for treatment of PCE under site conditions. The specific objectives of the treatability studies were as follows: 1) to verify that bioaugmentation using CB&I's commercially available SDC-9 culture will be effective, 2) to assess the need for additional amendments (e.g., nutrients and/or pH buffer), and 3) to determine the extent to which the alcohols that will be used as partitioning tracer might be inhibitory or toxic to the dechlorinating bacteria in SDC-9 (as this would determine whether or not partitioning tracer tests were performed during the active treatment phase of the field demonstration).

5.3.2 Sample Collection

Groundwater and aquifer solids were collected during the site characterization activities described in Section 5.2.1 during January 2013. Rock fragments were collected from borehole B07 between a depth of 74 and 79 ft bgs; these fragments were collected after the core was logged and screened with the handheld PID. Rock fragments were placed in a glass 1-liter (L) amber jar with a Teflon lined cap. Groundwater samples were collected from borehole B06 with the pump intake at approximately 84 ft bgs. Groundwater samples were collected in three glass 1-L amber jar with a Teflon lined cap.

Collected rock and groundwater samples were shipped in coolers on ice to CB&I's laboratory in Lawrenceville, NJ. Samples were stored at approximately 5°C until treatability setup was initiated.

5.3.3 Treatability Study Methodology

The treatability study for this project consisted of a batch microcosm study to evaluate bioaugmentation effectiveness under site conditions. The details of setup, sampling, and evaluation are provided in the subsequent sections. A Treatability Study Report was submitted to ESTCP in June 2013.

5.3.3.1 Microcosm Set-up

Evaluation of Biodegradation

Site soil containing bedrock and groundwater were collected during the site characterization/ DNAPL investigation in January 2013. Homogenized site crushed bedrock solids (15g) were combined in 160-milliliter (mL) serum bottles with 145 mL of site groundwater. Headspace in the bottles was negligible (<1mL). Bedrock fragments used were <20mm in size. All treatments were prepared in duplicate. A total of 18 bottles were prepared, and were sealed with Teflon[®]-lined butyl rubber stoppers and crimp caps. After setup, all microcosms were incubated with gentle shaking at 15°C in the dark.

The following treatments were included in the microcosm test (all prepared in duplicate):

Treatment 1: KILLED CONTROL: This treatment was amended with a formaldehyde solution (final concentration in groundwater approximately 0.5% by volume) and mercuric chloride (final concentration in groundwater approximately 300 mg/L) to inactivate microbial activity, and was used to evaluate abiotic loss of VOCs. An additional spike of PCE to 1 part per billion (ppb) was amended as well.

Treatment 2: LIVE CONTROL: This treatment received an amendment of 1 ppb PCE and no others except for deionized water (to simulate the volumetric addition of amendments performed for the other treatments). This treatment served as a control to monitor VOC loss in the absence of any amendments.

Treatment 3: LIVE CONTROL WITH ALCOHOLS: This treatment was amended with the following alcohol tracers: methanol (to a concentration of 250 mg/L), 1-hexanol (to a concentration of 250 mg/L), and 2-octanol (to a concentration of 100 mg/L), as well as a 1 ppb PCE spike.

This treatment was used to assess the sorption of the alcohols that will be used for the partitioning tracer test to the aquifer solids. This treatment was also used to assess any biodegradation of the alcohols that might occur under ambient conditions.

Treatment 4: BIOSTIMULATION: This treatment was used to evaluate the effects of biostimulation (i.e., electron donor and nutrient addition, but no addition of *Dehalococcoides* sp.) on biodegradation of the target chlorinated ethenes. Bottles were amended with sodium lactate to a concentration of 1,000 mg/L, diammonium phosphate at a concentration of 100 mg/L, yeast extract at a concentration of 50 mg/L, and a 1 ppb PCE spike.

Treatment 5: BIOAUGMENTATION: This treatment was used to evaluate the effects of anaerobic bioaugmentation on PCE biodegradation. Treatment 5 was prepared identically to Treatment 4, except that CB&I's *Dehalococcoides* sp. –containing culture SDC-9 was added to the bottles so that an optical density of 0.01 was attained.

Treatment 6: BIOAUGMENTATION WITH ALCOHOL TRACERS: This treatment was used to evaluate the effects of the alcohols that were used for the partitioning tracer tests on anaerobic PCE biodegradation during bioaugmentation. Treatment 6 was prepared identically to Treatment 5, except that bottles were amended with the following alcohol tracers: methanol (to a concentration of 250 mg/L), 1-hexanol (to a concentration of 250 mg/L), and 2-octanol (to a concentration of 100 mg/L).

In addition, a parallel set of bottles consisting of one bottle for each treatment was prepared for monitoring volatile fatty acids (VFAs), pH, and anions during the course of the study.

Evaluation of Alcohol Fate

A supplemental experiment was performed to verify that the alcohols used for the partitioning tracer experiments in the field (methanol, 1-hexanol, and 2-octanol) were not susceptible to rapid biodegradation or sorption to aquifer solids. Such conservative behavior is desired in order to effectively determine DNAPL mass residing in the bedrock fractures. This testing was performed over a 2-week period.

Microcosms were prepared by adding 15g of crushed bedrock (<20mm) with artificial groundwater (AGW). AGW was prepared using Deionized water amended with the following reagent grade chemicals from Sigma-Aldrich (St. Louis, MO): 120 mg/L CaCl₂ · 2H₂O, 70 mg/L NaHCO₃, 0.1 mg/L NaNO₃, 60 mg/L MgSO₄ · 7H₂O, 4 mg/L KCO. The AGW solution was further amended with alcohol tracers that were (and will be) used as part of the partitioning tracer field testing: methanol, 1-hexanol, and 2-octanol. Tests were prepared in triplicate in glass serum bottles (approximate volume, 160 mL), and filled so that headspace was negligible (<1 mL). After setup, all microcosms were incubated with gentle shaking at 15°C in the dark.

The following treatments were included in the alcohol sorption test (prepared in triplicate):

Treatment 1: NO ROCK CONTROL: This treatment was amended with the following alcohol tracers: methanol (to a concentration of 100 mg/L), 1-hexanol (to a concentration of 100 mg/L), and 2-octanol (to a concentration of 100 mg/L) and with mercuric chloride (final concentration in AGW approximately 300 mg/L) to inactivate microbial activity. This treatment was used to evaluate alcohol sorption.

Treatment 2: KILLED CONTROL: This treatment was amended with mercuric chloride (final concentration in AGW approximately 300 mg/L) to inactivate microbial activity, alcohol tracers: methanol (to a concentration of 100 mg/L), 1-hexanol (to a concentration of 100 mg/L), and 2-octanol (to a concentration of 100 mg/L). This treatment also contained 15g crushed bedrock. This treatment was used to evaluate alcohol sorption to the rock.

Treatment 3: LIVE CONTROL: This treatment was also used to assess any biodegradation of the alcohols that might occur under ambient conditions. Treatment 3 was prepared identically to treatment 2, except that no mercuric chloride was added.

5.3.3.2 *Microcosm Sampling and Analysis*

At each sampling event, microcosm bottles were removed from the shaker and allowed to settle, so that the aqueous supernatant could be sampled. Sampling was performed in a glove bag with a nitrogen headspace. Aqueous samples were collected at approximately $t = 24$ hours (to serve as an initial condition), 2 weeks, 5 weeks, 10 weeks, and 16 weeks.

At each of these sampling events, groundwater was analyzed for VOCs, reduced gases, pH, and anions (pH and anions were monitored in the parallel set of bottles only). All analytical was conducted in-house in CB&I's laboratory. In addition, for treatments amended with alcohols, samples were collected at $t = 24$ hours and 10 weeks for analysis of the alcohols via GC-FID in the parallel set of bottles only. VFAs also were monitored in the lactate-amended treatments (Treatments 4 through 6) to ensure that electron donor levels remained sufficiently high (VFAs were measured in the parallel set of bottles only). Additional lactate was amended to the bottles at 5 weeks and 8 weeks. Nutrients, in the form of yeast extract were also amended at 8 weeks. Treatments 5 and 6 were re-bioaugmented with SDC-9 at 8 weeks. Glass beads were placed in the bottles after each sampling to maintain zero headspace.

For the alcohol sorption testing, sampling for alcohols was performed similarly to the aqueous sampling described above. Samples were collected a $t = 24$ hours, 4 days, and 14 days. Samples were sent to Dr. Michael D. Annable at the University of Florida for alcohol analysis using a GC-FID.

5.3.4 Treatability Study Results.

5.3.4.1 *Geochemical Results*

Geochemical results for the biodegradation experiments are provided in Table 5.4. Due to elevated background concentrations of chloride, chloride generated via reductive dechlorination could not be determined.

Values for the pH ranged from 7.3 to 8.2, which is within the range where reductive dechlorination of PCE to ethene can occur. It is noted, however, that reported pH values within the demonstration area measured in the field typically were in the range of 6.5 to 7, suggesting that the slightly elevated pH levels measured in the laboratory may be an artifact of sample handling and exposure to the atmosphere. The lack of any decreasing trend in pH in the biostimulation or bioaugmentation treatments suggests that generation of any organic acids are likely being naturally buffered by the rock alkalinity.

Table 5.4. Geochemical Results for Treatability Study

Chloride (mg/L)						
Time (weeks)	Killed Control	Live Control	Live w/ Alcohols	Biostimulation	Bioaugmentation	Bioaug w/ Alcohols
0	381	367	345	333	348	346
2	411	345	373	360	375	398
5	446	401	402	404	417	424
10	409	366	380	392	429	359
16	418	410	354	383	396	404
Sulfate (mg/L)						
Time (weeks)	Killed Control	Live Control	Live w/ Alcohols	Biostimulation	Bioaugmentation	Bioaug w/ Alcohols
0	327	360	332	322	332	328
2	357	346	359	360	310	362
5	424	418	422	407	4.6	425
10	354	355	379	2.7	1.0	322
16	399	417	362	4.4	1.7	23
pH (SU)						
Time (weeks)	Killed Control	Live Control	Live w/ Alcohols	Biostimulation	Bioaugmentation	Bioaug w/ Alcohols
0	7.3	7.8	8.0	7.9	7.9	7.9
2	7.6	8.0	8.0	8.0	8.0	8.0
5	8.0	8.0	8.1	8.1	8.1	8.0
10	8.2	8.2	8.3	8.2	8.2	8.1
16	8.2	8.1	8.4	8.2	8.2	8.2

Sulfate values in the Killed and Live controls were approximately 350 to 400 mg/L. No sulfate reduction was observed in any treatments that were not amended with lactate. Sulfate reduction was most rapid in the Bioaugmentation treatment (Treatment 5), where sulfate reduction was observed within 5 weeks. Sulfate reduction for the Biostimulation treatment was observed within 10 weeks. The addition of the SDC-9 culture, which is known to contain sulfate-reducing bacteria, likely is the reason why sulfate reduction was more rapid in the bioaugmented treatment. Interestingly, sulfate reduction was delayed until greater than 10 weeks when alcohols were present in the bioaugmented treatment. This suggests that the presence of the alcohols may inhibit sulfate reduction.

5.3.4.2 Alcohol Fate

Alcohol concentrations, measured at time 0 and 10 weeks in the biodegradation study, are provided in Table 5.5. Results show negligible (less than approximately 10%) difference in alcohol concentrations between the un-amended and bioaugmented treatments, suggesting that the bioaugmentation culture did not biotransform the alcohols within the 10-week timeframe. However, in both treatments, slight to moderate decreases in the alcohol concentrations were observed. This decrease may be due to slow adsorption of the alcohols into the rock, and/or biodegradation of the alcohols due to indigenous bacteria.

Table 5.5. Alcohol Results for Treatments 3 and 6

Methanol (μM)		
Time (weeks)	Live w/ Alcohols	Bioaug w/ Alcohols
0	8.6	8.3
10	7.8	8.0
1-Hexanol (μM)		
Time (weeks)	Live w/ Alcohols	Bioaug w/ Alcohols
0	2.4	2.4
10	1.3	1.6
2-Octanol (μM)		
Time (weeks)	Live w/ Alcohols	Bioaug w/ Alcohols
0	0.6	0.7
10	0.2	0.4

The alcohol concentrations over a time period of 2 weeks (which was representative of the expected duration of the partitioning tracer tests that would be performed in the field) is provided in Table 5.6. Data from this supplemental experiment show that, for a 14-day duration, no measurable sorption or biodegradation of the tracers occurred. Thus, it was reasonable to assume that these tracers would behave conservatively in the field with respect to sorption to aquifer solids and any biodegradation processes over a 2-week period.

Table 5.6. Alcohol Sorption Test Results

Methanol (μM)			
Time (days)	Control	Killed	Live
0	2.6 ± 0.4	2.6 ± 0.1	2.6 ± 0.1
4	2.7 ± 0.2	2.6 ± 0.1	2.6 ± 0.2
14	2.7 ± 0.1	2.5 ± 0.1	2.7 ± 0.1
1-Hexanol (μM)			
Time (days)	Control	Killed	Live
0	0.7 ± 0.1	0.8 ± 0.1	0.8 ± 0.0
4	0.8 ± 0.0	0.8 ± 0.1	0.8 ± 0.1
14	0.8 ± 0.0	0.8 ± 0.1	0.7 ± 0.0
2-Octanol (μM)			
Time (days)	Control	Killed	Live
0	0.2 ± 0.1	0.4 ± 0.1	0.4 ± 0.1
4	0.4 ± 0.1	0.5 ± 0.0	0.5 ± 0.0
14	0.4 ± 0.1	0.5 ± 0.0	0.5 ± 0.0

5.3.4.3 PCE Biodegradation

Results summarizing the PCE biodegradation testing are provided on Figure 5.9. Results showed no evidence of reductive dechlorination in any of the controls or biostimulation treatments. However, evidence of the complete reductive dechlorination of PCE was observed in both (with and without the alcohols) bioaugmentation treatments.

Both bioaugmentation treatments showed substantial decreases in PCE concentration, along with increases in both DCE and VC. Ethene concentrations, although relatively low on a molar basis, were rapidly increasing over the last two sampling events. Surprisingly, transformation of PCE to DCE and VC occurred more rapidly in the treatment where the alcohols were added. The reason for this observation is unclear, but may be due to the fact that sulfate reduction was initially inhibited in the presence of the alcohols, which may have allowed for a greater availability of electron donor for reductive dechlorination. At the very least, comparison between the bioaugmentation treatments with and without the alcohols indicate that the presence of any residual alcohols following completing of the partitioning tracer experiments is not expected to have any adverse effects on biodegradation of PCE.

5.3.5 Treatability Study Conclusions

Results from the treatability study indicate that bioaugmentation is effective for the reductive dechlorination of PCE. Furthermore, the complete dechlorination of PCE to ethene was observed in site groundwater with rock fragments. It is important to note that our previous research has shown that dechlorination of PCE DNAPL in closed microcosm systems may occur much more slowly than in the field or other “open” systems. The fact that substantial PCE dechlorination, and even ethene generation, was observed in this treatability study was very encouraging. Thus, the results of the treatability study supported our approach to perform the bioaugmentation demonstration at Site 37 at Edwards AFB.

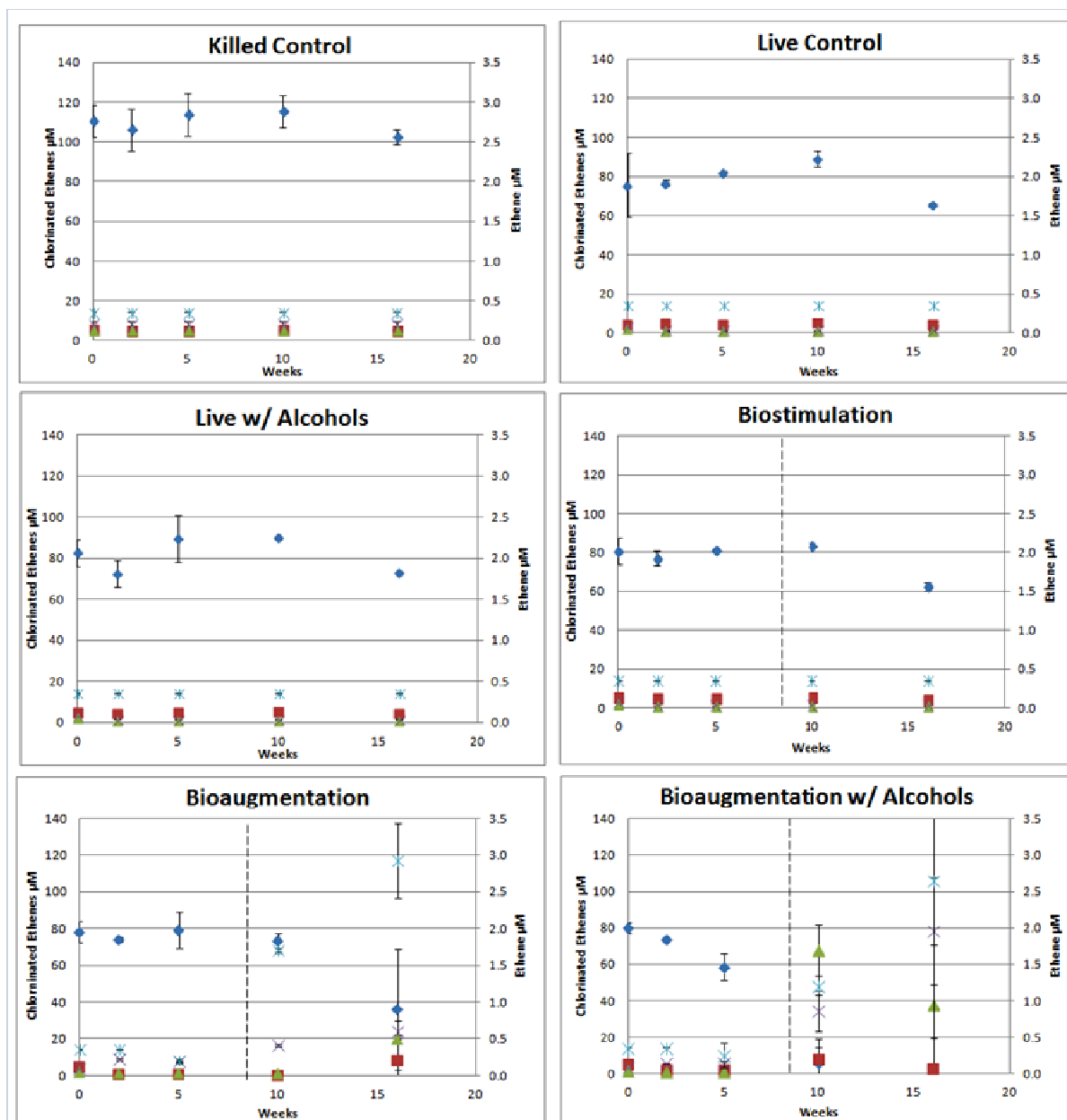


Figure 5.9. Chlorinated Ethenes and Ethene Results for Treatments 1-6 where \blacklozenge = PCE, \blacksquare = TCE, \blacktriangle = *cis*-1,2-DCE, \times = Vinyl Chloride, and $*$ = Ethene. The dotted line represents additional nutrients (yeast extract and lactate), as well as re-bioaugmentation of SDC-9 for treatments 5 and 6, was performed.

5.4 DESIGN AND LAYOUT OF TECHNOLOGY COMPONENTS

During this field demonstration, a series of discreet interval borehole sampling locations were used to assess the effectiveness of bioaugmentation for treatment of PCE DNAPL sources in fractured bedrock. Bioaugmentation treatment was preceded by performance of a partitioning tracer test to assess DNAPL architecture and the fracture flow field. The bioaugmentation amendments were distributed using injection and extraction wells. Bioaugmentation amendments included CB&I's commercially available DHC-containing culture SDC-9, lactate, nutrients, and a bicarbonate buffer. Amendments were distributed across a targeted region within the DNAPL source zone. Amendment distribution, reductive dechlorination rates, microbial growth and transport, and DNAPL dissolution rates were evaluated. By monitoring electron donor and hydrogen levels, efforts were made to limit excess electron donor delivery during the demonstration. Following the almost 12-month demonstration period, rebound testing was performed.

5.4.1 Basis and Rationale for Demonstration Layout

The demonstration layout shown on Figure 5.10 is based on the testing described in Section 5.2. Key aspects that served as design basis and rationale for the selected locations included the following:

- *Demonstration Centered within PCE DNAPL Zone.* The PTTs described in Section 5.2.1.7 verified the presence of DNAPL within the footprint of the demonstration layout, and within the target interval of approximately 60 to 85 ft bgs.
- *Hydraulic Connectivity between Demonstration Bedrock Wells.* Hydraulic connectivity was observed between B06 and B07; this connectivity occurred primarily through the fractures that intersect these wells at approximately 78 ft bgs. Based on the dip and strike of these fractures, boring locations 37-B12 and 37-B13 should be intercepted by the same fracture pair.
- *Well Capacity.* In general, bedrock wells near the Building 8595 source area are low (<500 mL/min) producing wells, limiting potential injection and extraction flow rates. However, due to the relatively low effective porosities associated with fractured bedrock system, flow rates as low as 100 mL/min can be sufficient for remedial amendment delivery and distribution. Boreholes B06 and B07 showed well capacities >100 mL/min, and the results of the pump and tracer testing showed that these flow rates were sufficient for distributing amendments (tracer injected at B06 reached B07 within 15 hours of pumping). Since the fractures at approximately 78 ft bgs appeared to be (based on the testing described in Section 5.2) the primary conductive fractures, the wells shown on Figure 5.10 were expected to also have sufficient well capacity; this was verified during the testing described in Section 5.5.
- *Radius of Influence and Intersection of Multiple Fractures.* The well layout shown on Figure 5.10 was intended to provide an assessment of the radius of influence with respect to bioaugmentation amendments. Distances of up to approximately 70 ft downgradient from the injection well were evaluated. As indicated on Figures 5.4 and 5.8, the older existing and these newer boreholes intersect multiple fractures and fracture zones, which will allow assessment of treatment in multiple zones.

5.4.2 Layout and Well Construction

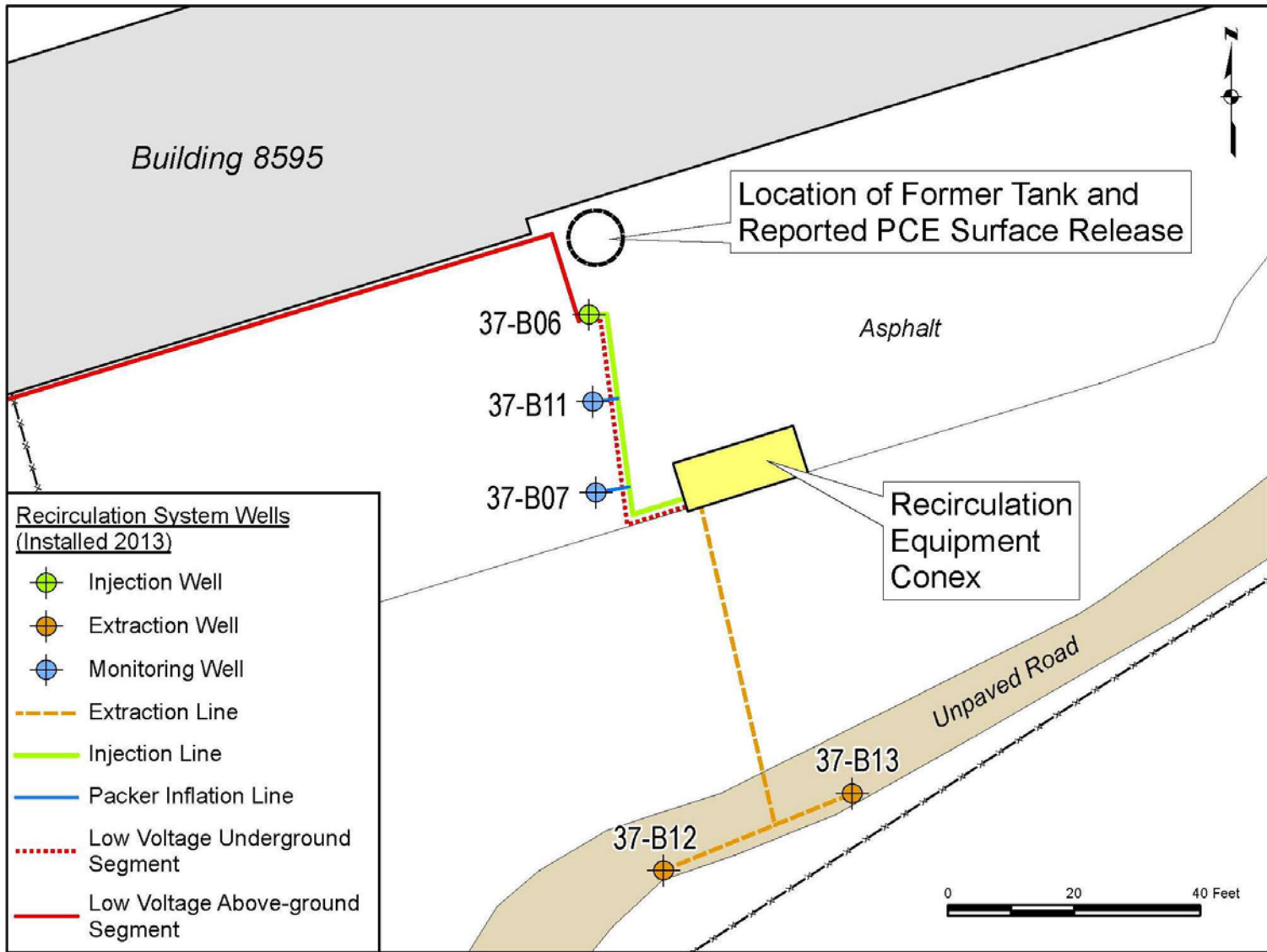
The treatment test plot includes groundwater extraction, injection, and monitoring wells in an area south of Building 8595. The demonstration layout, which includes open borehole wells installed during the preliminary characterization, as well as more recent wells installed for treatment system operation, is shown on Figure 5.10. The test and treatment system consists of one injection, two extraction, and two monitoring wells. Borehole B06 was used as an injection well for tracer and amendment injection, and boreholes B12 and B13 were used as extraction wells. Borehole B07 and B11 were used as monitoring wells, with multiple sample intervals within each borehole. 37-EW07 is a source area monitoring well that was installed prior to this demonstration, and was periodically sampled, though not included in the monitoring program for the demonstration. The depth intervals that were monitored at each well location are presented in Table 5.7. These intervals were based upon our knowledge of the connective fracture pathways and DNAPL distribution as determined during the characterization activities described in Section 5.2, as well as the results from additional geophysical and hydraulic testing performed as part of system installation (see Sections 5.4.2.2 and 5.5.1, respectively).

Table 5.7. Discrete Intervals for Monitoring, Injection and/or Extraction

Borehole or Well Location	Well Status	Number of Depth Intervals for Monitoring	Sampling or Packered Intervals (ft bgs)
37-B06	Existing	2	< 59 59-85
37-B07	Existing	3	<70 70-85 85-97
37-B11	Proposed	2	<83 83-105
37-B12	Proposed	1	120-132
37-B13	Proposed	1	79-99
37-EW07*	Existing	1	37.4-57.4

* Existing source area monitoring well. The depth interval is the screen interval of the well.

NOTE: For the initial Stage 1 hydraulic testing described in Section 5.5.1, the isolated intervals were modified to facilitate initial testing.



S:\GIS\EdwardsAFB\GIS_Documents\Project_Maps\EAFB_023_presentation3.mxd 6/15/2016

Figure 5.10. Groundwater Recirculation and Amendment Delivery System

5.4.2.1 Well Installation

The installation of the final four demonstration wells (37-B10, 37-B11, 37-B12, and 37-B13) were constructed in a manner similar to those installed during the initial phase of the project: as open borings drilled into the solid bedrock with surface conductor casing installed through the upper sediment interval. Note that 37-B10 was installed at an incorrect location for the demonstration, thus an additional monitoring well (37-B11) was installed and used for performance monitoring.

The system wells were drilled at locations shown on Figure 5.10 at locations as far as 105 ft downgradient from the former product tank. The wells were permitted through the Kern County Public Health Services Department (permits #37-B11, 37-B12 and 37-B13). Well 37-B11 is located closest to the suspected source, approximately 15 feet downgradient of injection well 37-B06, while 37-B12 and 37-B13 are the greatest distance downgradient near the facility fence line.

Geophysical utility clearance was conducted by a CB&I subcontractor (Spectrum Geophysics) prior to any intrusive work. Geophysical methods for utility clearance included electromagnetic induction and geomagnetics. The drilling subcontractor (Woodward Drilling) also used air vacuum equipment to visually clear borehole of underground obstructions to a depth of 5 ft bgs.

Geologic Logging

The monitoring wells were drilled and completed under the supervision of a California-licensed Professional Geologist who was responsible for all borehole logging, well installation, and development. The logging was conducted in accordance with the Unified Soil Classification System and American Society for Testing and Materials (ASTM) D1586-84. During drilling, selected rock cores were also logged and screened for DNAPL using a handheld PID and a hydrophobic dye (e.g., Sudan IV). Boring logs are presented in Appendix B.

Rock Matrix Sample Collection

Slices of the rock matrix were collected adjacent to a PCE containing conductive fracture at 37-B10 (along the conductive fractures at approximately 76 and 98 ft. bgs). These slices were collected immediately upon retrieval in the field. Each slice was approximately 1 to 2 cm thick, crushed, then placed into capped glass jars containing methanol. Up to 5 rock slices (i.e, 5 slices going inwards towards the rock matrix from the conductive fractures) were collected. The methanol was analyzed for PCE at approximately 2 and 5.5 weeks; PCE concentrations did not show an increase going from 2 to 5.5 weeks, thereby confirming equilibrium was attained at 2 weeks. This information was used to assess the extent of contaminant mass present in the rock matrix in close proximity to the fracture interface.

Well Construction

Well installation was conducted between December 10 and December 16, 2013 using a Brainard-Killman (BK-81) drill rig with HQ wire line diamond core (3.781-inch outside diameter). A surface conductor casing was installed through the overburden and keyed into bedrock. The surface conductor was constructed using a 6-inch steel casing that was set through the overburden and grouted in place prior to initiating core drilling, to prevent sloughing of overburden in the well-bore. Each well was completed without the installation of sand pack or well casing, and grouting was limited to the completion of the surface conductor casing.

A typical well construction diagram is presented as Figure 5.11. The conductor casing depths ranged from approximately 7 ft bgs (37-B11 and 37-B13) to 24 ft bgs in well 37-B12. Each boring was completed with a traffic-rated flush-mount well box. Drilling fluids (potable water) and cuttings were contained analyzed and disposed of according to State of California and Edwards AFB requirements (as discussed in Section 5.5.3).

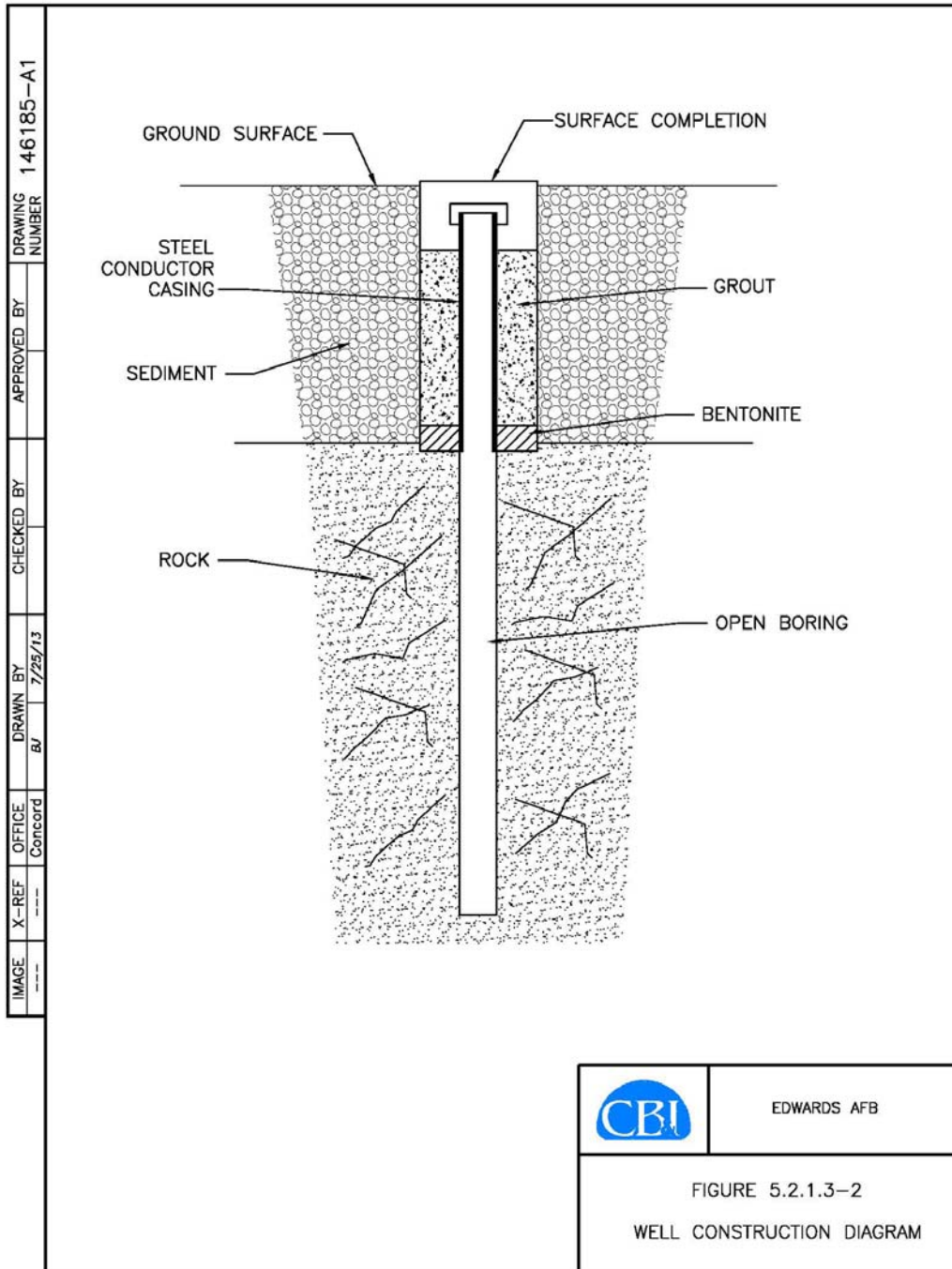


Figure 5.11. Typical Well Completion Diagram

The wells and completion depths, as shown on the boring logs presented in Appendix B are as follows:

- 37-B11 = 105 ft bgs;
- 37-B12 = 132 ft bgs; and,
- 37-B13 = 99 ft bgs.

Well Development

The wells were pumped by the drilling contractor to facilitate the removal of cuttings from fracture zones. The low production rates of fracture zones prevented the removal of typically required volumes of groundwater. The wells were pumped dry quickly and did not allow for the collection of meaningful purge parameters. At least one well volume was removed from each well, with additional withdrawals required if relative clarity was not achieved. Further development would be conducted during subsequent specific capacity and aquifer testing (see Section 5.5.1).

5.4.2.2 Geophysical Testing

Geophysical logging was conducted in five test boreholes to further characterize bedrock fracture zones. The logging was conducted immediately after the well installation activity. The logging was conducted in three of the final demonstration wells (37-B10, 37-B12, and 37-B13) wells and in one well installed in the first phase of the project (37-B07); geophysical logging also was performed in 37-B06 as part of the initial characterization performed. The objective of the geophysical logging was to identify fracture zones that may contain dissolved or DNAPL phase chlorinated solvents.

The logging included the collection of borehole geophysical data throughout saturated and unsaturated zones: giving due consideration to operating conditions (fluid filled versus air filled intervals) required for the respective geophysical tools. The methods applied to the logging were as follows:

- Optical Borehole Imager;
- Acoustic Borehole Imager;
- Single point Resistivity; and,
- High resolution heat pulse flow meter.

The granite bedrock at the site contains water-filled fracture zones, which formed potential migration pathways for chlorinated solvent (DNAPL) from a large spill that occurred at the site. It was not clear at the time whether or not DNAPL was still present in the fractures. The investigation's goal was to locate, characterize, and test the flow characteristics of the fractured zones.

The optical televiewer geophysical logging was conducted from the top of bedrock to the total depth of the borehole. The televiewer provides recorded indicators of the tool output (visual observation of the boring), relative orientation, and depth of the televiewer tool. The televiewer was run over the total open whole interval as long as visual clarity was able to be maintained.

The acoustic televiewer geophysical logging was conducted from the water table to the total depth of the borehole. The acoustic televiewer provides recorded indicators of the fractures, relative orientation, and depth of the televiewer. The high resolution heat pulse flow meter logs selected intervals of the open borehole from the water table to the total depth of boreholes. Both stressed (pumped) and non-pumping conditions were logged as directed by the on-site CB&I Geologist. Pumping equipment was used to induce stressed conditions. The contractor also provided basic field interpretation of the result with respect to the test effectiveness at specific intervals.

Geophysical Testing Results

Geophysical logs are presented in Appendix C. The key results from the geophysical testing showed that potentially conductive fracture zones were present in 37-B07 at approximately 78 and 90 ft bgs. These fracture zones, based on their depth and orientation, appeared to correspond to fracture zones identified in 37-B06 located at 79 and 83 ft bgs, respectively. Thus, this information was used to determine the discrete interval sampling points discussed in the following sections, and in Section 5.4.3.2.

5.4.3 Packer Installation and Sampling Assembly

The pre-installation testing and operation of the treatment system targeted specific intervals within wells containing fracture zones. The drilling and geophysical logging described above provides access to and identifies potentially conductive fracture zones. Based upon our knowledge of the connective fracture pathways and DNAPL distribution as determined during the characterization activities described in Section 5.2, as well as the results from additional geophysical and hydraulic testing performed as part of system installation (Sections 5.4.2.2 and 5.5.1, respectively), the intervals for which the packers were used to isolate targeted intervals are listed in Table 5.7. Note that for the initial Stage 1 hydraulic testing described in Section 5.5.1, the isolated intervals were modified to facilitate initial testing.

The basic inflatable straddle packer assembly is illustrated on Figure 5.12. The assembly is constructed of two single inflatable packers ganged together to form a single unit which can be used to isolate specific borehole intervals. The unit also was applied in a single packer mode (where appropriate, as shown in Table 5.7) with the removal of one packer segment. The straddle packer can isolate the borehole into three segments, although the upper and lower borehole segments are open to the entire intervals above and below the straddle packer assembly.

The basic assembly includes the packers, wireline suspension cable, tubing used for inflation of the packer, and additional ports and tubing connectors that facilitate the primary operational functions. The packers were placed via the suspension wire using a manually operated tripod and winch assembly. The packers were inflated through the application of air pressure to the down-hole inflation tube.

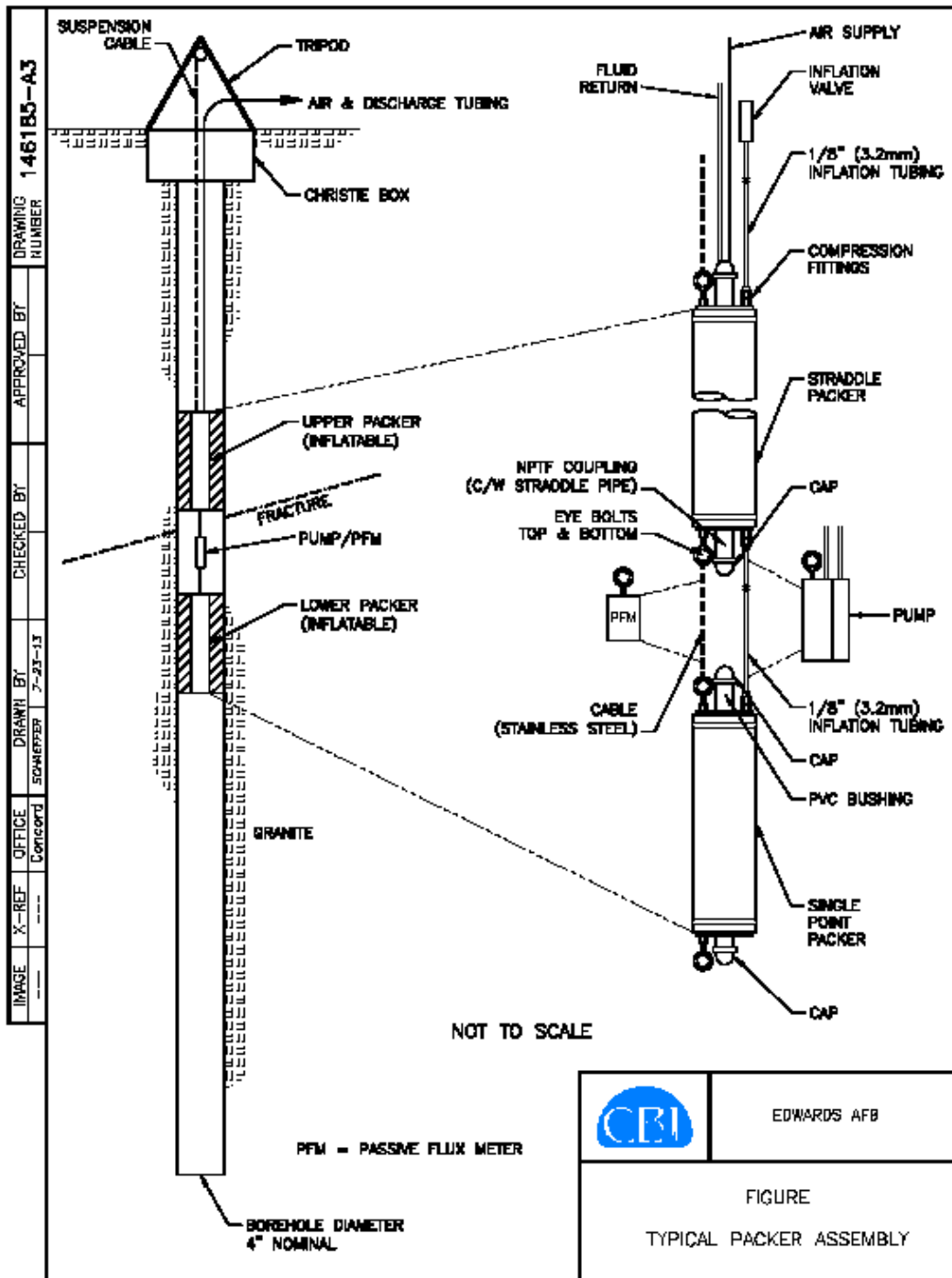


Figure 5.12. Inflatable Packers

5.4.3.1 Injection Well Packers

Groundwater injection in well 37-B06 required the isolation of one zone, though the installation consisted of two packers, the top packers set at 59 ft bgs and the bottom packer at 85 ft bgs (see Figure 5.13). One injection drop-pipe was utilized to inject recirculated water into this interval, through the packer placed at 59 ft bgs.

5.4.3.2 Extraction Well Packers

The groundwater extraction wells (37-B12 and 37-B13) utilized bladder pumps designed for continuous service. The pump mechanism consisted of the following:

- QED Well Wizard Model T1200M stainless steel bladder pump with Teflon bladder;
- ¼-inch OD UV protected Nylon 12 air supply tubing; and
- 3/8-inch OD Teflon-lined polyethylene discharge tubing.

Each of the extraction wells withdrew water from one zone, requiring the installation of the pump below a single packer, between the packer and the bottom of the borehole (see Figure 5.13). 37-B12 had a single packer installed at 120 ft bgs, with the pump below, extracting water from the interval from 120 ft bgs to 132 ft bgs. 37-B13 had a single packer installed at 79 ft bgs, with the pump below, extracting water from the interval from 79 ft bgs to 99 ft bgs.

5.4.3.3 Monitoring Well Packers

Dedicated groundwater sampling bladder pumps were installed in treatment system monitoring wells 37-B07 and 37-B11, while portable bladder pumps (decontaminated between sample intervals/wells) were used to sample existing site wells when needed. The pump setups consisted of the following:

- QED Well Wizard Model T1250 stainless steel bladder pump with Teflon bladder;
- ¼-inch OD UV protected Nylon 12 air supply tubing; and
- 3/8-inch OD Teflon-lined polyethylene discharge tubing.

Sampling pumps installed into wells with multiple sampling intervals were installed using packers and were left in place for the entire duration of the demonstration. See Figure 5.13 for the pump and packer placement depths for monitoring wells 37-B07 and 37-B11.

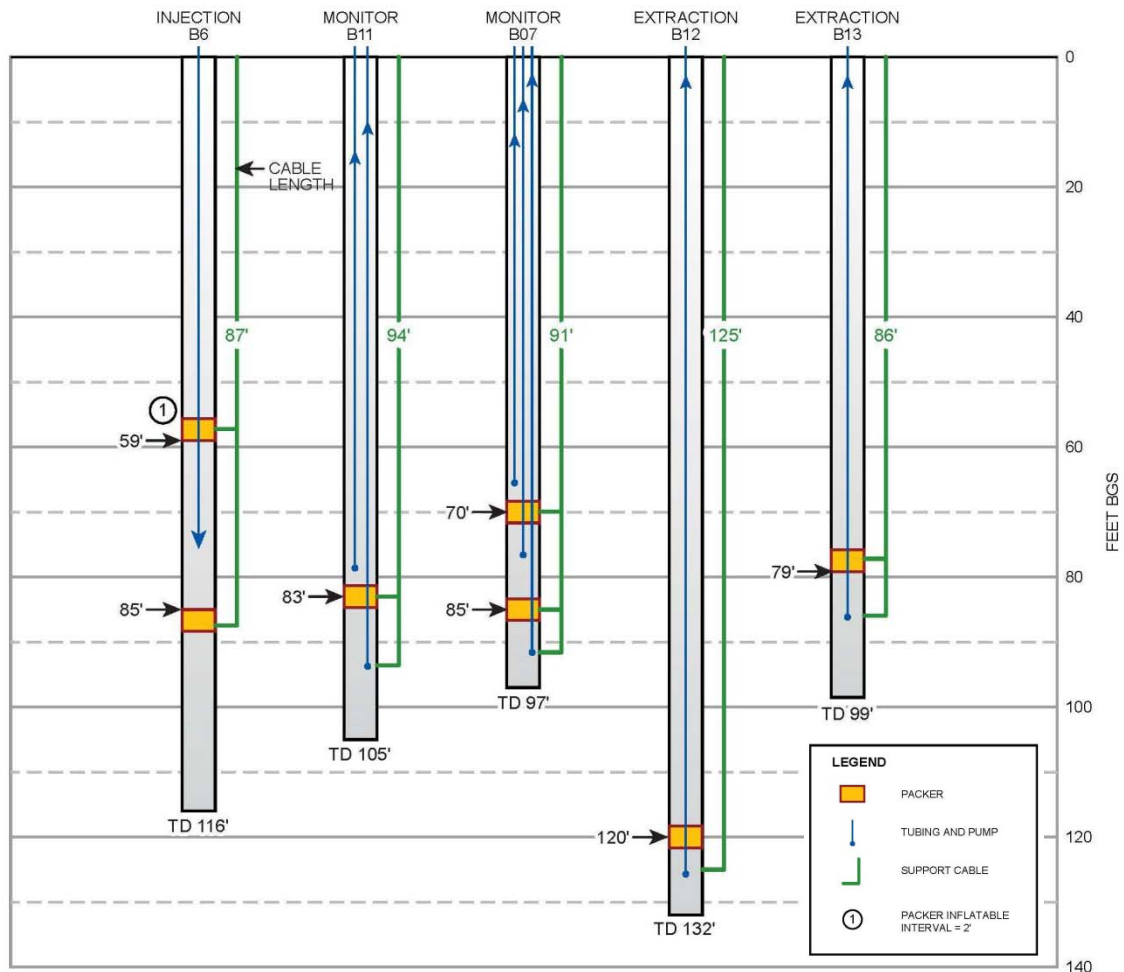


Figure 5.13. Packer and Pump Placement

5.4.4 Enhanced Bioremediation Treatment System

The components of the enhanced bioremediation treatment system include the recirculation system, the tracer and amendment injection system, and ancillary equipment to power the recirculation system. The physical layout of the system is depicted on Figure 5.10, and the components of the system are identified on the piping and instrumentation diagram (P&ID), presented as Figure 5.14. The recirculation system was installed to transport downgradient groundwater and substrate upgradient to the head of the source plume. The design maximum system flow was 300 mL/min; however, flow was dictated by what the injection well could receive (as discussed in Section 5.5.3). The tracer and amendment injection system is a subsystem to the recirculation system. Initially, this sub system was utilized to mix and inject tracer media into the injection wells (see Section 5.5.2). During enhanced bioremediation activities, the sub system was used to inject substrate and amendments to maintain reducing conditions in the treatment area. The specification and installation of these components are described in detail in the following subsections.

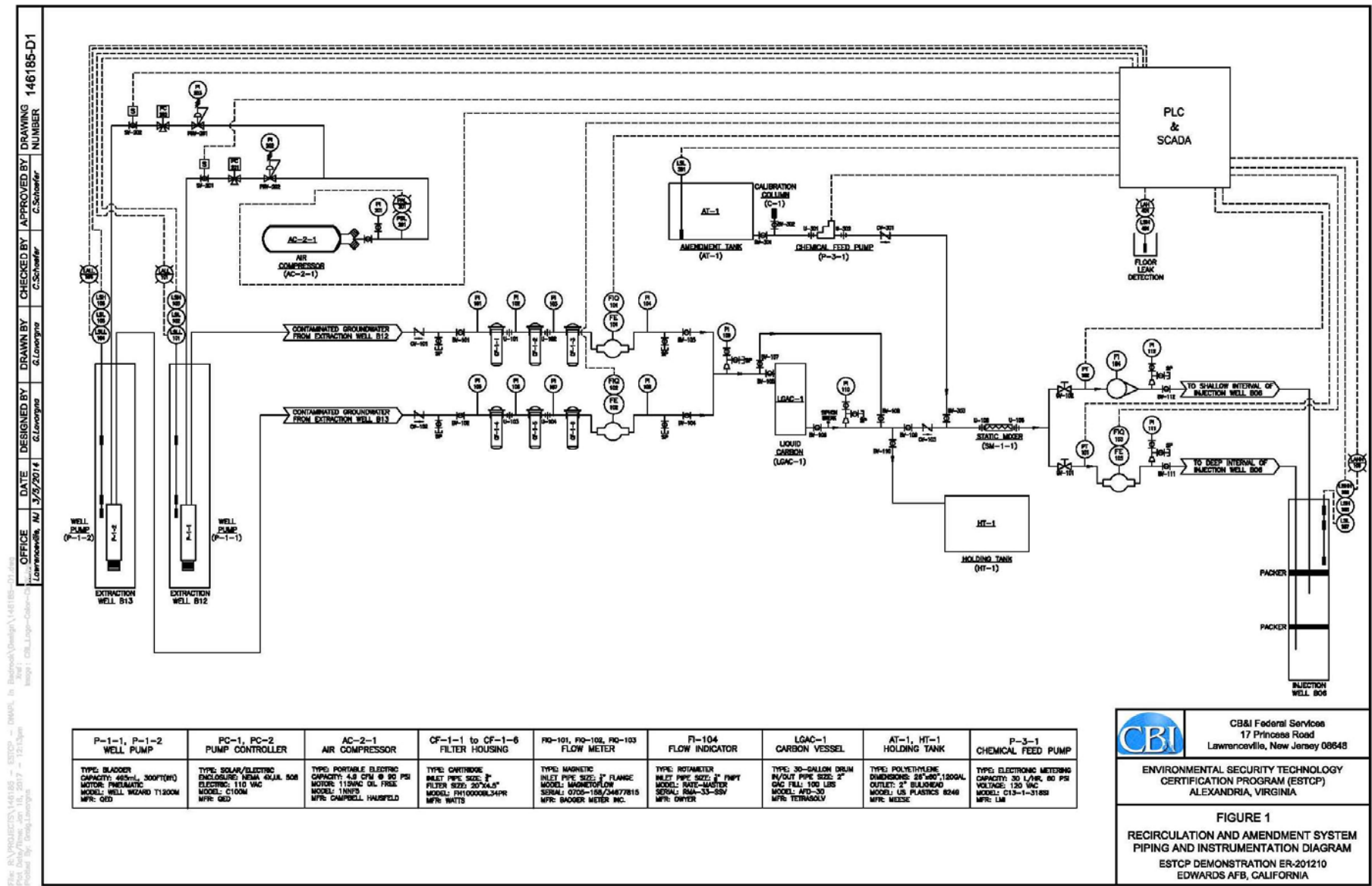


Figure 5.14. Enhanced Bioremediation Treatment System P&ID

5.4.4.1 Recirculation System

The recirculation system was installed as a single unit housed in a 20-foot long conex box, and included the Tracer and Amendment Delivery System. This unit included a programmable process controller, piping, instrumentation, inline mixers, and manual control valves, as presented in Figure 5.14. Figure 5.14 also shows the process flow of the entire system, including the tracer and amendment delivery subsystem.

Groundwater extraction occurred through the pneumatic bladder pumps identified in Section 5.4.3.2). Each pump was fully submersible and be capable of maintaining flows over the 300 mL/min design flow for the system. The pumps were controlled through a programmable process controller, which was powered through ancillary equipment. Once groundwater was extracted from the wells, the groundwater was processed through cartridge filters. These filters were utilized to prevent biofouling particulates from entering the system. A lead and a lag filter were included in the system, the lead filter being a 50 micron size and the lag a 20 micron size. The groundwater from the two extraction wells was then combined after the flow meters/totalizers.

During the tracer test, as discussed in Section 5.5.2, groundwater was passed through a liquid GAC unit prior to collection in the holding tank (HT-1) for characterization and proper disposal. ***The use of GAC and diversion to the holding tank was only employed while the tracer slug was being injected in 37-B06 – otherwise the extracted groundwater was re-injected in the injection well (37-B06) without passing through GAC.***

During enhanced bioremediation, as discussed in Section 5.5.3, groundwater bypassed the carbon and was directed to the injection wells. Prior to the injection wells, groundwater was mixed with amendments from the amendment delivery system and tank AT-1.

5.4.4.2 Ancillary Equipment

Ancillary equipment was utilized to operate the pneumatic bladder pumps. It consisted of an air compressor, desiccant filter, and programmable process controller (QED C100M). The piping and instrumentation is shown on Figure 5.14. This subsystem controls the groundwater extraction flow rate through the process controllers.

5.4.4.3 Tracer and Amendment Delivery System

The tracer and amendment delivery system will be a subsystem to the recirculation system. This subsystem will introduce tracer media or amendments at each individual well injection line. The components of the delivery system will consist of a tank, control valves, pressure gauges, and a positive displacement variable speed metering pump. The tank will be a minimum of 55 gallons, and the pump will be able to maintain maximum flow speeds of 75 to 300 mL/min.

During the tracer test, groundwater will be extracted from the two extraction wells. Groundwater will be processed through filters to remove any particulates in the stream and passed to liquid GAC to remove any VOCs before being stored. While groundwater is being extracted, tracer material will be injected from the delivery system into the injection well. Tracer injection volume and mass are described in Section 5.5.2. The mixing will occur in the delivery system tank.

During enhanced bioremediation treatment, the recirculation system will bypass the liquid GAC. Groundwater will recirculate from the extraction wells to the injection wells while pulsed injections of amendments enter the system. Amendment quantities will be adjusted based on data received in the field to optimize the system performance.

5.4.4.4 Instrumentation and Monitoring

Process instrumentation including pressure, level, and flow switches were installed at critical locations in the system to ensure safe and controlled operation. The supervisory control and data acquisition (SCADA) system and associated programmable logic controller (PLC) contain all the process control logic to monitor and regulate the operation of the various system components, both locally and remotely through a cellular-based telemetry system. The SCADA/PLC enables the application of power to the pneumatic pump solenoid valves and chemical feed pump, and also monitors the system safety interlocks, calling out when the system is in alarm or offline.

5.4.5 Power

Power requirements for the system operation were supplied by on base grid power. Power was available from Building 8595. Edwards AFB electrical personnel installed a disconnect switch on the main panel within Building 8595 and a transformer to supply power to the 220-volt system disconnect mounted on the side of the system conex box. The availability of 220-volt, 100 ampere power was sufficient to effectively power the system.

5.5 FIELD TESTING

The field testing was performed in 4 stages, with data from each stage being carefully evaluated prior to proceeding to the next phase. A general timeline of field operations is provided as Table 5.8, with additional details and operations data presented in Appendix D. The first stage consisted of short term hydraulic testing to verify the extraction well capacity, and to assess hydraulic influence among the injection, monitoring, and extraction wells in the targeted depth intervals. Stage 1 also consisted of baseline sampling (VOC, reduced gases, anions, DHC, metals) at the monitoring and injection wells (Table 5.7) under ambient (no groundwater re-circulation) conditions; this baseline sampling was performed several months after the hydraulic testing. The second stage involved the initiation of groundwater re-circulation, and performance of the partitioning tracer test. This stage continued unto groundwater conditions (VOCs, etc.) equilibrated. The third stage was the active bioremediation phase, which lasted 9 months. The fourth stage was the rebound period, which lasted 10 months.

Table 5.8. Timeline of Field Operations

Timeline of Field Operations ESTCP Project ER-201210					
ID	Task Name	Duration	Start	Finish	Qtr 1, 2 Qtr 2, 2 Qtr 3, 2 Qtr 4, 2 Qtr 1, 2 Qtr 2, 2 Qtr 3, 2 Qtr 4, 2 Qtr 1, 2 Qtr 2, 2 Qtr 3, 2
1	Stage 1 - Short-Term Hydraulic Testing and Baseline Testing	128 days	Mon 1/6/14	Wed 7/2/14	
2	Short-term Pump Testing at 37-B06, 37-B07, 37-B12, 37-B13	4 days	Mon 1/6/14	Thu 1/9/14	
3	Baseline Sampling Event No. 1	1 day	Wed 5/28/14	Wed 5/28/14	I
4	Baseline Sampling Event No. 2	1 day	Wed 7/2/14	Wed 7/2/14	I
5	Stage 2 - Groundwater Recirculation and Partitioning Tracer Testing	41 days	Wed 7/2/14	Wed 8/27/14	
6	Start Groundwater Recirculation	0 days	Wed 7/2/14	Wed 7/2/14	7/2
7	Partitioning Tracer Test	32 days	Tue 7/15/14	Wed 8/27/14	
8	Pre-Bioaugmentation Sampling Event	1 day	Wed 8/27/14	Wed 8/27/14	I
9	Stage 3 - Bioaugmentation Treatment and Monitoring	188 days	Thu 8/28/14	Tue 5/19/15	
10	Initial Lactate/Nutrient Pulse Injection	1 day	Thu 8/28/14	Thu 8/28/14	I
11	Bioaugmentation Injection	1 day	Fri 8/29/14	Fri 8/29/14	I
12	Post-Bioaugmentation Sampling Event No. 1	1 day	Tue 9/9/14	Tue 9/9/14	I
13	Redevelop 37-B06 with surge and pumping	1 day	Thu 10/2/14	Thu 10/2/14	I
14	Post-Bioaugmentation Sampling Event No. 2	1 day	Mon 10/13/14	Mon 10/13/14	I
15	Post-Bioaugmentation Sampling Event No. 3	1 day	Wed 11/19/14	Wed 11/19/14	I
16	Post-Bioaugmentation Sampling Event No. 4	1 day	Wed 12/17/14	Wed 12/17/14	I
17	Redevelop 37-B06 with Nu-Well products	4 days	Mon 2/9/15	Thu 2/12/15	I
18	Post-Bioaugmentation Sampling Event No. 5	1 day	Thu 3/5/15	Thu 3/5/15	I
19	Redevelop 37-B06 with surging and wire brush	1 day	Fri 3/27/15	Fri 3/27/15	I
20	Post-Bioaugmentation Sampling Event No. 6	1 day	Mon 4/13/15	Mon 4/13/15	I
21	Shut-down Groundwater Recirculation	0 days	Tue 5/19/15	Tue 5/19/15	5/19
22	Stage 4 - Post-Treatment Monitoring and Assessment	358 days	Tue 5/19/15	Thu 9/29/16	
23	Rebound Baseline Sampling Event	1 day	Tue 5/19/15	Tue 5/19/15	I
24	Rebound Sampling Event No. 1	1 day	Wed 8/5/15	Wed 8/5/15	I
25	Rebound Sampling Event No. 2	1 day	Mon 10/19/15	Mon 10/19/15	I
26	Rebound Sampling Event No. 3	1 day	Tue 1/12/16	Tue 1/12/16	I
27	Rebound Sampling Event No. 4	1 day	Wed 3/9/16	Wed 3/9/16	I
28	Post-Treatment Rock Core Collection	2 days	Wed 9/28/16	Thu 9/29/16	I

Date: Tue 1/17/17 	Task		External Tasks		Manual Task		Finish-only	
	Split		External Milestone		Duration-only		Deadline	
	Milestone		Inactive Task		Manual Summary Rollup		Progress	
	Summary		Inactive Milestone		Manual Summary			
	Project Summary		Inactive Summary		Start-only			

Page 1

5.5.1 Short-term Hydraulic Testing and Baseline Sampling– STAGE 1

During installation of the monitoring wells used for the Stage 1 testing, a rock core was collected to determine the extent of PCE migration into the rock matrix, as described in Section 5.4.2.1. This was performed during the installation on 37-B10.

Initial short-term hydraulic testing was performed to assess the hydraulic connection among the injection, extraction, and monitoring wells, and also to assess the extraction well capacity. The following tests were performed January 8-13, 2014 (one test per day):

- *Pump test at 37-B13 (open borehole for all wells).* The test was performed for approximately 3 hours. Pressure transducers placed in 37-B06 and 37-B07 were used to assess hydraulic influence. Extraction well capacity also was determined.
- *Pump test at 37-B12 (open borehole for all wells).* The test was performed for approximately 3 hours. Pressure transducers placed in 37-B06, 37-B07, and 37-B11 were used to assess hydraulic influence. Extraction well capacity also was determined.
- *Pump test at 37-B06.* The test was performed for approximately 3 hours. Single packers were placed in 37-B06 and 37-B07 so that the top of the packer was at 80 ft bgs. A pressure transducer was placed in 37-B07 above the packer. The pump was placed above the packer in 37-B06 for the pump test.
- *Pump test at 37-B07.* The test was performed for approximately 3 hours. A single packer was placed in 37-B07 so that the bottom of the packer was at approximately 83 ft bgs. A pressure transducer was placed in 37-B06 (no packer in 37-B06). The pump was placed below the packer in 37-B07 to test the connectivity associated with the deeper fracture zone.

Approximately 4 months following the short-term hydraulic testing, and after placing the packers in the boreholes as shown in Table 5.7, two rounds of baseline groundwater sampling were performed (May 28 and July 2, 2014) for analysis of VOCs, reduced gases, anions, DHC, and dissolved iron.

5.5.2 Groundwater Recirculation and Partitioning Tracer Testing – STAGE 2

This second stage of the field testing was performed using the well network in the demonstration area, and provided baseline (pre-bioaugmentation) conditions with respect to DNAPL mass, flow field, and dissolved contaminant concentrations. Stage 2 testing, except where noted, was performed using the packer intervals described in Table 5.7.

5.5.2.1 Initiation of Groundwater Re-Circulation

As discussed in Section 5.4.4, the vast majority of the components making up the groundwater recirculation system (i.e., air compressor, solenoid and other control, valves, filters, flow meters, tanks, chemical feed pumps, etc.) were housed in a shipping container (conex box), which was delivered to the Site on April 15, 2014. This conex box also contained an electrical control and logic system for operation of the groundwater recirculation system.

Once placed at the site, CB&I personnel, in conjunction with an electrical subcontractor, finalized the connections to the conex box, including the main electrical power from the Site Building 8595 transformed (installed by base personnel), the air and water line connections to and from the injection and extraction wells, and the compressed air lines leading to the packers installed in each of the five bedrock wells being used for the demonstration. The main electrical power line, along with piping runs to the injection and monitoring wells, were installed within a trench below the main driveway of Building 8595, as required by the base (shown on Figure 5.10). Shakedown testing and startup of the groundwater recirculation system was completed by a CB&I engineer and Calcon Systems, Inc. (electrical controls support) on July 2, 2014.

Groundwater recirculation began on July 2, 2014, with an average recirculation rate during the first week of operation of approximately 113 milliliters per minute (mL/min). Groundwater was extracted from 37-B12 and 37-B13 at approximately 76 and 37 mL/min, respectively. All groundwater was re-injected into 37-B06.

5.5.2.2 Partitioning Tracer Testing

Following nearly two-weeks of groundwater re-circulation, the PTT was initiated. The PTT was used to determine the flow field, verify connectivity between boreholes, determine travel times across the demonstration plot, and estimate the mass of DNAPL present. The PTT was performed similarly to the interwell PTT described in Section 5.2.1.7, with 37-B06 used as the injection well and boreholes 37-B12 and 37-B13 will be used as extraction wells.

PTT activities began the week of July 14, 2014 (conducted by personnel from the University of Florida), with injection of the tracer (mixture of bromide and alcohols) occurring on July 15 and 16, 2014. Addition of the tracer amendments was performed using the amendment delivery system described in Section 5.4.4. Tracer amendments were delivered to the injection interval of B06 (as specified in Table 5.7). The 34 gallon tracer solution was prepared using tap water and the following solute concentrations (verified by sampling the tracer solution during the injection process):

- 517 mg/L bromide (from sodium bromide);
- 1,480 mg/L methanol; and
- 663 mg/L 2,4-dimethyl-3-pentanol (DMP).

The tracer solution was injected into the target interval in B06 over 1.1 days, thereby attaining an average injection flow rate of 83 mL/min, which was similar to that during the previous 10 day recirculation period. During tracer injection, the extracted groundwater from the extraction wells (37-B12 and 37-B13) was directed to a tank in the system Conex box to maintain groundwater flow conditions. The Conex box served as a location to monitor system flows and was ultimately used to facilitate the delivery of remedial amendments for planned bioremediation testing. Groundwater recirculation was reinitiated (i.e., the reinjection of the extracted groundwater from 37-B12 and 37-B13 into 37-B06) after the delivery of the tracer pulse and continued throughout the duration of the tracer test at a combined recirculation rate of approximately 111 mL/min.

Groundwater sampling for bromide and the alcohols commenced just prior to tracer addition and continued throughout the 92-day tracer test. Monitoring locations were sampled by using dedicated pneumatic bladder pumps installed in each of the sampled borehole intervals on Table 5.7.

The extraction wells were sampled by diverting the flow to collect 40 mL samples of the recirculating groundwater. The recirculation flow was monitored throughout the tracer test and remained relatively constant at 111 mL/min prior to bioaugmentation (see Section 5.5.3). It is noted that no tracers were detected at any time in the extraction wells; thus, no tracers were reinjected into the injection well following the initial tracer slug.

The PTT results are presented in detail in Section 5.8.2.2.

Upon completion of the PTT, operation of the groundwater recirculation continued with an average flow rate of approximately 115 mL/min through the end of August 2014. Groundwater sampling rounds were conducted on July 31, August 7, August 14 and August 27, 2014, prior to aquifer amendment and bioaugmentation. Sampling was performed at 37-EW07 and all system wells except the injection well 37-B06 (i.e., 37-B07s, 37-B07i, 37-B07d, 37-B11s, 37-B11d, 37-B12, and 37-B13). This monitoring and continued re-circulation was performed to allow for equilibration throughout the demonstration area, as PCE concentrations were increasing for several weeks after initiating re-circulation.

5.5.3 Bioaugmentation Treatment and Monitoring – STAGE 3

Aquifer amendment activities were initiated on August 28, 2014, with personnel from the University of Florida injecting 59 liters of a mixture of sodium lactate and nutrients (diammonium phosphate [DAP] and yeast extract) in water into injection well B06 at approximately 500 mL/min. The mixture was injected with average concentrations of 2,000 mg/L lactate and 100 mg/L DAP and yeast extract.

The following day, August 29, 2014, bioaugmentation was conducted, with 19 liters of CB&I's concentrated SDC-9 bacteria culture injected into injection well 37-B06. Following bioaugmentation, 38 liters of water amended with 2,000 mg/L sodium lactate and 100 mg/L DAP and yeast extract was injected into the injection well as chase water. Groundwater recirculation continued upon completion of chase water injection. Extraction well bladder pump controller refill/discharge settings are provided in Appendix D, along with corresponding groundwater extraction flowrates and totalized flow. Numerous groundwater monitoring events were conducted throughout Stage 3 of the demonstration at wells within the treatment zone, as presented in Table 5.8 and Appendix D.

Upon completion of the amendment and bioaugmentation injections, subsequent observations of system performance showed that the water level in the injection well rose significantly, from approximately 30 feet below ground surface (ft-bgs) prior to the injections to less than 10 ft-bgs. The recirculation system's automated controls go into an alarm condition when the water level in the injection well becomes less than 10 ft-bgs, shutting the extraction well pumps down until the water level decreases down to 20 ft-bgs, at which time the extraction well pumps are reinitiated. This cycle of the extraction wells operating for a certain period (approximately 7 hours), followed by down-time to let the water levels drop in the injection well continued throughout system operation.

In an attempt to remedy this loss in injection well yield, 37-B06 was redeveloped. Environmental field technicians from AECOM (O&M subcontractor to CB&I) performed the well development on October 2, 2014. The packer string was deflated and removed from the borehole. The borehole was surged using a plastic surge block (sized for the 3.78-inch diameter borehole) for approximately 15 minutes for every 10 feet within the injection interval. The borehole was then pumped for approximately one half hour until the water level dropped to the target pump depth of 85 feet below ground surface. Water level recharge was then monitored, calculated to be approximately 0.05-0.06 feet/minute (a little over 100 mL/min). The packer string was then reinserted into the borehole at the proper depth and re-inflated.

On December 17, 2014, potassium bicarbonate was added to the amendment tank in an attempt to buffer the pH and keep it from dropping below 6.0. It was estimated that 0.2 g/L of bicarbonate was required to raise the pH from 6.0 to 7.0; therefore approximately 7 kg of potassium bicarbonate was added to the amendment tank and the dosage rate was adjusted to account for the additional volume.

System operation continued, and on January 13, 2015, the amendment (lactate, nutrients, bicarbonate) dosage was increased from 60 mL every 2 hours to 60 mL every 30 minutes, as the volatile fatty acid results from the December 17, 2014 groundwater sampling event showed decreased concentrations relative to prior sampling events at monitoring well 37-B11s.

It was also observed on January 13, 2015 that the injection well (37-B06) recharge rate had dropped to less than 10 mL/min. Therefore, a second well development scope of work was generated, consisting of the addition of well development chemicals (Nu-Well 120 Liquid Acid in combination with Nu-Well 310 Bioacid Dispersant, manufactured by Johnson Screens) to remove any scaling or biofouling that may have occurred in the borehole or near fractures. Well surging and pumping were used in combination with the chemicals to develop the borehole and ensure that the low pH water created by the chemicals was removed. The development activities were conducted from February 9 through February 12, 2015. 37-B06 well recharge was measured to be approximately 40 mL/min after development, which was considered acceptable for continued system operation. 2 liters of bioaugmentation bacteria culture (SDC-9), diluted to 19 liters with water, was injected into 37-B06 on February 13, 2015.

By March 1, 2015, the recharge rate in 37-B06 was down to approximately 13 mL/min, and remained at that rate for the next few weeks. An additional well development scope of work was generated, consisting of having a drilling subcontractor mobilize to the site to brush the sides of the borehole with a wire brush, surge the borehole within the injection interval with a surge block and pump the borehole. Upon removal of the packer string (2 packers isolating the injection interval) from the borehole to complete the development work on March 27, 2015, the glands of both packers were observed to be bulging, which did not allow their reinsertion back into the borehole. One spare packer was located on-site, which was installed into the packer string as the bottom packer. Because injected water was getting around and above the top packer of the original configuration, as evidenced by the water level rise above the top packer during recirculation/injection, it was decided to not reinstall a top packer into the packer string. The replacement packer was set in the borehole at the same elevation as the original bottom packer, and the injection tubing was lowered to the same depth as the original. The only difference is that the new configuration did not include a top packer.

Upon packer replacement and inflation, the recharge rate was again measured in the borehole. Very little improvement was observed following the recent well development activities. Therefore, the decision to deflate the bottom packer was made on March 28, 2015, to allow the recirculation system to operate at a more reasonable (higher) flow. Recharge rates of greater than 200 mL/min were observed upon packer deflation. Careful consideration was taken when evaluating the results of subsequent groundwater sampling events, to determine the connectivity of the deeper portion of the 37-B06 to the monitoring well depth intervals.

System operation continued through May 19, 2015, at which time the system was shut-down and the rebound assessment phase of the project began. Groundwater monitoring was performed on that day, to serve both as the final Stage 3 groundwater results and as a baseline for post-treatment monitoring. Data justifying shut-down of the system was presented to ESTCP in a technical memorandum dated May 7, 2015.

Coordination of investigation derived waste (IDW) handling was performed with base personnel from Edwards. Soil IDW was approved by the base for on-site disposal. The soil was spread along the ground at the site on October 20 and 21, 2015. The asphalt/concrete generated during the system installation activities was drummed and transported to the on-base landfill on October 27, 2015. The water IDW was pumped through carbon, collected in tanks, and sampled (sample date was November 9, 2015). A permit to discharge the water IDW was approved by the base, allowing discharge of the water to the on-base industrial wastewater system. A copy of the discharge permit is included in Appendix E. The water was discharged to the industrial system by AECOM site personnel on July 12, 2016.

5.5.4 Post-Treatment Monitoring and Assessment – STAGE 4

To assess the feasibility of performing a final partitioning tracer test at the site, an injection well recharge test was performed on January 13, 2016. The water column in injection well 37-B06 was pumped down to just above the inflated packer (approximately 80 ft-bgs), and the well recharge rate was observed by measuring depth to water periodically during borehole recharge. The test duration was approximately 2.5 hours, with well recharge measurements ranging from 8.68 mL/min near the beginning of the test to 3.67 mL/min at the end of the test. These low borehole recharge measurements provide sufficient data to conclude that performing a final partitioning tracer test at the site is not feasible, as initial well capacity for injection (used during the initial tracer testing) was approximately 100 mL/min.

As mentioned above, the post-treatment monitoring baseline groundwater samples were collected on May 19, 2015. Four additional sampling events were conducted during the post-treatment assessment phase, as presented in Table 5.8 and Appendix D.

One final post-treatment rock core was also collected during this Stage. A California-licensed drilling company (Woodward Drilling) mobilized to the site on September 28, 2016, along with a senior geologist from CB&I, to advance the borehole and collect the rock cores. Hollow-stem-auger and rock coring (HQ) techniques were used to advance the boring. The surficial sediments were isolated by setting a 6-inch conductor casing into the upper bedrock surface. The conductor casing depth was approximately 7 feet below ground surface (ft-bgs). The borehole was located between the injection well (37-B06) and the first monitoring well (37-B11), as shown in Figure 5.15.

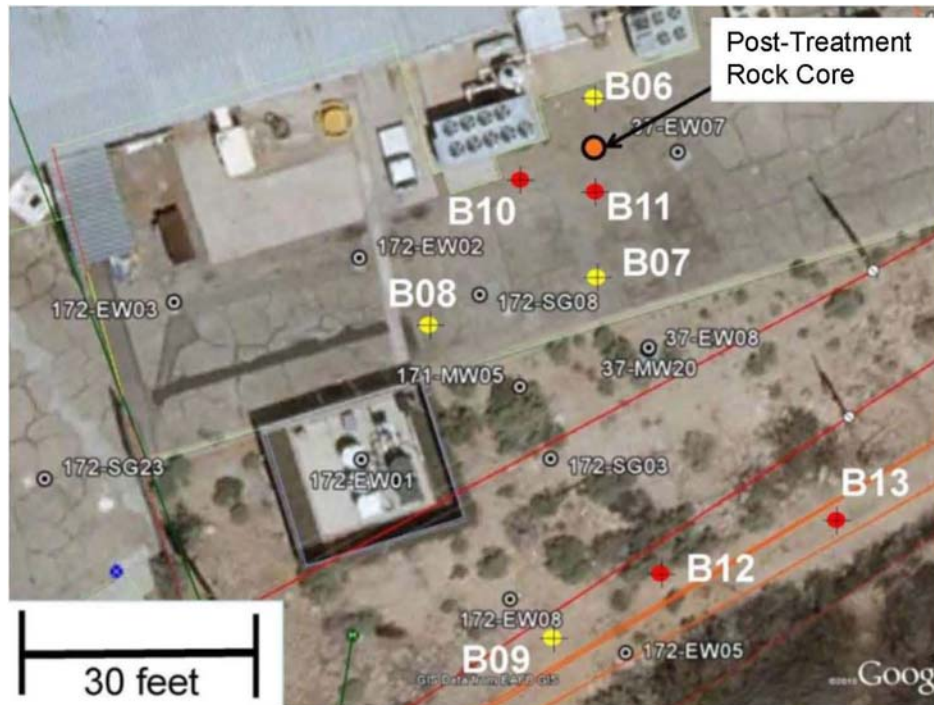


Figure 5.15. Post-Treatment Rock Core Location

The focus of the rock core collection was centered on the conductive fractures observed in nearby injection well 37-B06 at approximately 78 and 83 feet below ground surface. The observed fractures in the new borehole (37-B14), which may be connected to the fractures observed in 37-B06, were located approximately 81.4 ft-bgs and 86.4 ft-bgs. Slices of rock (approx. 1 cm thick) were cut in the field with a diamond blade saw, adjacent to both fractures, from the fracture interface into the rock matrix (up to 8 cm distance). The rock was crushed and immediately placed into soil jars with methanol for extraction. The methanol was to be analyzed as a function of time (up to 3 sampling events over a 3 month period) for VOCs to ensure extraction equilibration, and to assess the concentration profile within the rock. On the other face of each of the two fractures, samples were collected for mineral analysis (ferrous iron using the 1,10-phenanthroline method, which was employed in our recently completed SERDP project ER-1685). Samples were collected as a function of distance from the fracture interface (up to 5 cm distance). This allowed for assessing the extent to which reducing conditions impacted the rock matrix. The borehole was abandoned with neat cement upon completion of coring and rock sample collection.

5.5.5 Demobilization

Decommissioning of the recirculation system and demobilization activities include the removal of recirculation pumps and piping from the boreholes and the disassembly of the control system. The conex shipping container was disconnected from base power and removed from the site. Wells were left in place for future use by the Base.

5.6 DATA ANALYSIS

5.6.1 Determination of Flow Field and DNAPL Architecture

The hydraulically conductive fracture flow field and DNAPL architecture relative to the flow field were assessed by evaluating tracer elution at both the shallow and deep intervals at monitoring well 37-B11 (denoted 37-B11s and 37-B11d). The method of moments (MOM) approach (38,39) was used to evaluate the elution data and estimate the DNAPL fracture saturation S_n (DNAPL volume/fracture volume). The mean residence time for each tracer was determined for each tracer breakthrough curve (corresponding to each fracture zone) as follows (38,39):

$$m_n = \int t^n C(x,t) dt \quad \text{Eq. 1}$$

where m_n is the absolute n^{th} temporal moment of the tracer breakthrough curve at a monitoring well located at distance x from the tracer injection well, $C(x,t)$ is the tracer concentration, and t is time. Breakthrough curves were exponentially extrapolated through 100 days to minimize truncation errors for moment analysis (34,39), and the trapezoidal rule was used to approximate the integral at each time step. The partitioning tracer retardation factor, R , is the ratio of the mean residence time of the partitioning tracer to the nonpartitioning tracer:

$$R = \frac{\bar{t}_p}{\bar{t}_{np}} \quad \text{Eq. 2}$$

where \bar{t}_p and \bar{t}_{np} represent the mean residence times for the partitioning and non-partitioning tracers (respectively) to the monitoring well. Mean residence time is determined by the first normalized moment of each tracer with a correction for the duration of tracer pulse injection:

$$\bar{t} = \frac{m_1}{m_0} - \frac{\bar{t}_0}{2} \quad \text{Eq. 3}$$

where \bar{t}_0 is the duration of the injected tracer pulse (1.1 days). For the partitioning tracer, the average DNAPL saturation (S_n , defined as DNAPL volume per fracture volume) was calculated using (39)

$$S_n = \frac{R-1}{R+K_{NW}-1} \quad \text{Eq. 4}$$

where the DNAPL–water partitioning coefficients (K_{NW}) were used from previous estimates from batch laboratory experiments (40,44); K_{NW} is 35 m^3/m^3 for DMP and approximately 0 for the bromide and methanol.

To estimate the DNAPL volume in the vicinity of 37-B06, we employed a simplifying assumption of radial flow outward from the injection well (following hydraulically conductive fractures). This radius was defined by the mean residence time needed to travel from the injection well to 37-B11; thus, the volume of DNAPL was calculated for the radial length r of 4.3 m from the injection well and over the 7.6 m vertical interval b of the packed injection zone. The volume of DNAPL (V_n) was then estimated for each breakthrough curve using (39)

$$V_n = \frac{S_n V_f}{1-S_n} \quad \text{Eq. 5}$$

where V_e is the effective fracture volume swept by the injected tracer solution. V_e was calculated per fracture flowpath as follows:

$$V_e = Q_i \bar{t}_{np} \quad \text{Eq. 6}$$

where Q_i is the flow rate [m³ d⁻¹] associated with each fracture flow path (or, breakthrough curve). Q_i was calculated as follows:

$$Q_i = Q_{\text{total}} \times \text{MRF} \quad \text{Eq. 7}$$

where Q_{total} is the recirculation flow rate (equal to the re-circulation flow rate) and MRF is the mass recovery fraction, which is the relative fraction of the total injected flow associated with each of the fracture zones (or, breakthrough curves). MOM analysis was used to determine the tracer mass associated with each fracture zone. Based on the tracer elution results, one fracture zone was assumed for the shallow depth interval at 37-B11s. Since the 37-B11d breakthrough data exhibited three distinct tracer elution regimes, three fracture zones were assumed to be associated with 37-B11d. MOM analyses at 37-B11d employed a sectional method of moment analysis. The tracer breakthrough curve at 37-B11d was divided into three sections to examine the relative contribution of each portion of the curve to the total DNAPL saturation at 37-B11d using the method of moments: (1) initial peak, (2) main peak, and (3) slowly eluting tail. The relative fraction of flow to each of the fracture zones was determined using zeroth temporal moments to calculate a mass recovery fraction (MRF) for each zone.

The fracture porosity for each of the four fracture zones (ϵ) was calculated using Equation 8:

$$\epsilon = \frac{V_e}{\pi r^2 b} \quad \text{Eq. 8}$$

where r is the radial distance between the injection and monitoring well, and b is the packered interval of the injection well.

It is recognized that, due to the complexity of the fracture flow path, the assumption of radial flow along conductive fractures from the injection well is likely not a completely accurate assumption. However, failure of this assumption would only impact the total volume of DNAPL, fracture volume, and fracture porosity estimated. The values of S_n , \bar{t}_p , \bar{t}_{np} , and MRF associated with each of the fracture zones are not dependent on this assumption. Thus, the DNAPL distribution relative to the flow field is not impacted by the radial flow assumption.

5.6.2 Determination of DNAPL Mass Removal

DNAPL mass removal along the radial fracture flow path between the injection well, 37-B06, and the circumference defined by the distance to 37-B11 was determined using a mass balance approach based on the estimated DNAPL mass from the partitioning tracer test (described in section 5.6.1) and the chloride generated during active treatment. Using this approach, the DNAPL mass along the shallow and deep radial flowpaths was estimated at 1.1 and 1.3 kg, respectively (Schaefer et al., 2016). The mass of PCE DNAPL removed was determined based on chloride generation (2, 41) using the following equation:

$$M_D^* = \frac{C_{Cl}}{2} V_f MW_{PCE}$$

Eq. 9

where M_D^* is the mass of PCE DNAPL removed during bioaugmentation, C_{Cl} is the average molar increase in chloride observed at the monitoring well due to the reductive dechlorination of PCE to DCE from DNAPL sources, V_f is the swept volume of water based on the partitioning tracer test that flowed through either the shallow or deep fracture zones during active (i.e., groundwater re-circulation) treatment, and MW_{PCE} is the molecular weight of PCE. The PCE extracted from the extraction wells and re-injected into 37-B06 is assumed to be completely converted to DCE upon re-injection, and the chloride derived from this dissolved PCE mass is subtracted from the average molar increase in chloride so that C_{Cl} is attributable to DNAPL dissolution only. The value for V_f (for both the shallow and deep fracture zones) is 205 m^3 , which is determined based on the total recirculated flow during treatment multiplied by the fraction of flow going to both the shallow and deep fracture zones. It is noted that the radial flow assumption used to determine the initial DNAPL mass by Schaefer et al. would also be employed in the calculated value of M_D^* . Thus, the fraction of DNAPL mass removed during bioaugmentation treatment becomes independent of the radial flow assumption. Eq. 9 was applied to both the shallow (37-B11s) and deep (37-B11d) zones.

5.7 SAMPLING METHODS

Groundwater sampling was conducted in order to characterize the distribution of chemical constituents in groundwater, to evaluate the hydrochemistry of the aquifer, and to determine formation travel times (tracer testing). The varied objectives of the sampling required multiple sampling schemes: each analytical suite and sequencing reflecting the individual goals. The completion of wells at multiple levels with single wells also necessitated variations in sampling protocol.

5.7.1 Groundwater Sampling

Groundwater samples which analyzed for VOCs and/or other site-related analytes were collected using modified low-flow sampling methods to limit purge volumes and to accommodate monitoring points located in low permeability zones. Sampling procedures also varied depending on whether the sampling was being conducted for analysis of constituent of concern or for the analysis of tracers. The physical installation of sampling equipment (e.g., packer interval versus open borehole) affected sampling procedures as well. Groundwater samples were collected from dedicated sampling equipment, portable sampling pumps, and from direct discharge ports within the recirculation system.

Groundwater bladder sampling pumps were installed in selected treatment system wells, and portable pumps will be used to sample peripheral treatment system and existing site wells. The sample pump setups consisted of the following pieces of equipment:

- Bladder Pump-QED Well Wizard T1250;
- Polyethylene air supply tubing (1/4-inch) – P5000;
- Teflon-lined polyethylene (3/8-inch) – PT5000; and
- Pump Controller QED MicroPurge Low-Flow Pump Control.

Sampling pumps installed into wells with packers were left in place the entire duration of the treatment. Peripheral site wells and single sample interval wells that were infrequently sampled did not have dedicated pumps, and portable pumps were decontaminated before and after sampling each of these well locations.

Purge volumes within isolated (packer) intervals during groundwater sampling for site-related constituents were calculated based on the internal volume of the sample tubing and pump bladder. The isolation provided by the packers assured that fresh formation water was sampled. A sufficient volume was purged to remove stagnant water from the sampling tubing. The purge volume will be the interior volume of the sampling hose that is within the well's saturated interval, plus the volume of the bladder. Purge volumes are presented on Table 5.9.

Table 5.9. Purge Volumes for Groundwater Sampling

	Bladder	Tubing	Tubing	Purge
Well	Volume	Length	Volume	Volume
ID	(mL)	(ft)	(mL)	(mL)
37- B07s	100	68	1,476	1,576
37-B07i	100	73	1,585	1,685
37-B07d	100	88	1,910	2,010
37-B11s	100	81	1,758	1,858
37-B11d	100	85	1,845	1,945
37-B12	495	123	2,670	3,165
37-B13	495	82	1,780	2,275

5.7.2 Decontamination

Decontamination of all non-dedicated groundwater sampling and measurement equipment included washing with an Alconox soap and a subsequent rinse with deionized water. Dedicated sampling equipment did not require pre-sampling decontamination once installed into wells. Decontamination was required for all measurement or sampling equipment prior to reuse in any site wells.

5.7.3 Analytical and Sample Preservation for Groundwater Samples

The analytical methods and sample preservation used for the analyses that were part of this demonstration are summarized in Table 5.10 below.

Table 5.10. Analytical Methods, Preservation, and Containers -Groundwater

Analyte	Method/ Laboratory	Preservative	Bottle
VOCs	EPA 8260 CB&I	4°C with HCl	40 mL VOA vial (x2)
Reduced Gases	EPA 3810 CB&I	4°C with HCl	40 mL VOA vial (x2)
Anions	EPA 300.0 CB&I	4°C	100 mL polyethylene screw-cap (x1)
Alcohols	GC-FID Univ. Florida	4°C with HCl	40 mL VOA vial (x2) cap (x2)
<i>Dehalococcoides</i> sp. (DHC)	qPCR (Schaefer et al. [1]) CB&I Microbial Insights	4°C	1 L glass bottle
Reductive dehalogenase genes (RDG) (<i>tceA</i> , <i>vcrA</i> and <i>bvcA</i>)	qPCR Microbial Insights	4°C	1 L glass bottle
Volatile Fatty Acids	EPA 300m CB&I	4°C	40 mL VOA vial (x2)
Hydrogen	RSK175 CB&I	4°C with HCl	125 mL glass serum bottle with Teflon-lined cap and crimp seal
Metals (Fe, As)	EPA 200.7 Chemtech	Capsule filter, 4°C with HNO ₃	100 mL polyethylene screw- cap (x1)
Bromide	Field Meter	--	--
pH	Field pH Test Strips	--	--

5.7.4 Groundwater Sampling Locations and Frequency

The analytical sampling described in Sections 5.5.1 through 5.5.4 was performed, in general, at the locations and frequency described in Table 5.11. Sampling locations were, in large part, based upon the results of the tracer test.

Table 5.11. Groundwater Sampling Schedule

Stage	Analyte	Locations	Frequency
Stage 1 (Section 5.5.1)	VOCs	B10, B11, B12, B13	1 event
Stage 2 (Section 5.5.2)	VOCs	B06, B07, B10, B11, B12, B13	1 event
	Alcohols	B06, B07, B10, B11, B12, B13, 37-EW07	Multiple events (up to 27)
Stage 3 (Section 5.5.3)	VOCs Reduced Gases Anions VFAs DHC	B07, B11, B12, B13, 37-EW07*	2 baseline, 2, bi-weekly, 5 monthly events
	Hydrogen	B07, B11, B12, B13	1 baseline, 1 bi-weekly, 2 monthly
	RDG	B07, B12, B13 B11	1 baseline event Stage 3 - Month 8
	Total/dissolve Fe As	B07, B11, B12, B13	1 baseline, 1 bi-weekly, 3 monthly
Stage 4 (Section 5.5.4)	VOCs Reduced Gases Anions VFAs DHC Total/Dissolved Metals (Fe, Ar, Na, K)	B07, B11	4 events (3, 5, 8, and 10 months post-Stage 3 treatment)

* Select sampling frequency at this location (pre-bioaugmentation baseline, post-bioaugmentation round no 1)

5.7.5 Quality Assurance for Groundwater Sampling and Analysis

5.7.5.1 Calibration Procedures and Frequency

Calibration refers to the checking of physical measurements of both field and laboratory instruments against accepted standards. It also refers to determining the response function for an analytical instrument, which is the measured net signal as a function of the given analyte concentration. These determinations have a significant impact on data quality and are performed regularly. In addition, preventative maintenance is important to the efficient collection of data. For preventative maintenance purposes, critical spare parts were obtained from the instrument manufacturer.

All field and laboratory instruments were calibrated according to manufacturers' specifications. All CB&I laboratory instruments were calibrated in accordance with established Standard Operating Procedures (SOPs). Calibration was performed prior to initial use, during periods of extended use, and after periods of non-use. Certified standards were used for all calibrations and calibration check measurements. A calibration logbook was maintained by CB&I field and laboratory QA personnel.

5.7.5.2 Quality Control Samples

Internal quality control (QC) data provides information for identifying and defining qualitative and quantitative limitations associated with measurement data. Analysis of trip blanks provided the primary basis for quantitative evaluation of field data quality. Trip blanks are often used to evaluate the presence of contamination from handling errors or cross-contamination during transport, particularly for VOCs. Trip blanks are often not necessary when the contaminants of concern are non-volatile or have low volatility (e.g., anions, alcohols). Trip blanks were analyzed for VOCs, reduced gases, and hydrogen.

5.7.5.3 Sample Documentation

CB&I Lawrenceville, NJ project staff coordinated shipment and receipt of sample bottles, coolers, ice packs, chain of custody (COC) forms, and custody seals. Upon completion of sampling, the COC was filled out and returned with the samples to the CB&I and University of Florida laboratories. An electronic copy of each COC form was placed in the project database. An important consideration for the collection of environmental data is the ability to demonstrate that the analytical samples have been obtained from predetermined locations and that they have reached the laboratory without alteration. Evidence of collection, shipment, laboratory receipt, and laboratory custody until disposal must be documented to accomplish this. Documentation was accomplished through a COC Record that recorded each sample and the names of the individuals responsible for sample collection, transport, and receipt. A sample is considered in custody if it is:

- In a person's actual possession;
- In view after being in physical possession;
- Sealed so that no one can tamper with it after having been in physical custody; or
- In a secured area, restricted to authorized personnel.

Sample custody was initiated by field personnel upon collection of samples. Samples were packaged appropriately to prevent breakage or leakage during transport, and shipped to the laboratory via either hand delivery or commercial carrier.

5.7.5.4 Sample Identification

A discrete well number was assigned to each sample. This discrete identifier was placed on each bottle and was recorded, along with other pertinent data in a field notebook dedicated to the project. The sample identification number designated the sample location (e.g., "37-B11s" for this specific monitoring well). The bottle label also contained the site name, the sampling date and time, any preservatives added to the bottle, and the initials of the sampler.

5.7.5.5 Chain-of Custody Forms

The COC Record used by CB&I's laboratory is shown in Figure 5.16. All samples collected for off-site analysis were physically inspected by the Field Engineer prior to shipment.

Each individual who had sample in their possession signed the COC Record. Preparation of the COC Record was as follows:

- The COC Record was initiated in the field by the person collecting the sample, for every sample. Every sample was assigned a unique identification number entered on the COC Record.

5.7.5.6 Laboratory Sample Receipt

Following sample receipt, the Laboratory Manager or qualified personnel:

- Examined all samples and determined if proper temperature has been maintained during transport. If samples had been damaged during transport, the remaining samples were carefully examined to determine whether they were affected. Any samples affected were considered damaged. It was noted on the COC record that specific samples were damaged and that those samples were removed from the sampling program.
- Compared samples received against those listed on the COC record.
- Verified that sample holding times were not exceeded.
- Signed and dated the COC record.
- Recorded samples in the laboratory sample log-in book containing, at a minimum, the following information:
 - Project identification number
 - Sample numbers
 - Type of samples
 - Date and time received.

The COC Record was placed in the project file.

5.7.5.7 Other Documentation

Following sample receipt at the laboratory, the Laboratory Manager or sample custodian clearly documented the processing steps applied to the sample. The analytical data from laboratory QC samples were identified with each batch of related samples. The laboratory log book includes the time, date, and name of the person who logged each sample into the laboratory system. This documentation is thorough enough to allow tracking of the sample analytical history without aid from the analyst. At a minimum, laboratory documentation procedures provide the following:

- Recording in a clear, comprehensive manner using indelible ink.
- Corrections to data and logbooks made by drawing a single line through the error and initialing and dating the correction.
- Consistency before release of analytical results by assembling and cross-checking the information on the sample tags, custody records, bench sheets, personal and instrument logs, and other relevant data to verify that data pertaining to each sample are consistent throughout the record.
- Observations and results identified with the project number, date, and analyst and reviewer signatures on each line, page, or book as appropriate.
- Data recorded in bound books or sheaf of numbered pages, instrument tracings or hard copy, or computer hard copy.
- Data tracking through document consolidation and project inventory of accountable documents: sample logbook, analysis data book, daily journal, instrument logbook, narrative and numerical final reports, etc.

5.8 RESULTS

5.8.1 Results of STAGE 1 Testing

5.8.1.1 Rock Matrix Assessment

Results of the rock matrix assessment are provided in Figure 5.17. The results clearly show PCE diffusive uptake into the rock matrix. Although there is scatter in the data, no clear gradient of PCE migration (high concentration to low concentration) emanating from the fracture face is observed. These results suggest that there is a high storage potential of PCE within the rock matrix. It is noted that the rock matrix porosity was 4.9%, as measured using the water uptake method (49).

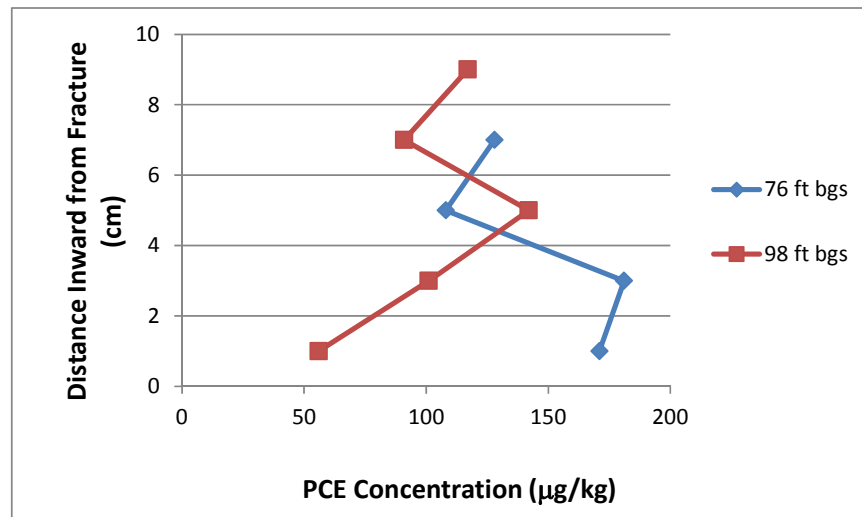


Figure 5.17. PCE Concentration within the Rock Matrix at 37-B10

Adjacent to fracture zones at approximately 76 and 98 ft bgs.

5.8.1.2 Short-Term Hydraulic Testing

Results of the short term hydraulic testing yielded the following qualitative and quantitative results:

- *Pump test at 37-B13.* Test results showed that the open borehole extraction capacity was approximately 70 to 90 mL/min, based on steady draw-down testing and the rate of recharge observed within the borehole after the pump test was completed. No measurable drawdown was observed in 37-B06 or 37-B07 during the test, suggesting that a strong hydraulic connection between the test well and the injection/monitoring wells was not present.
- *Pump test at 37-B12.* Test results showed that the open borehole extraction capacity was approximately 110 to 130 mL/min, based on steady draw-down testing and the rate of recharge observed within the borehole after the pump test was completed. No measurable drawdown was observed in 37-B06 or 37-B07 during the test, suggesting that a strong hydraulic connection between the test well and the injection/monitoring wells was not present.

- *Pump test at 37-B06.* Test results showed that the open borehole extraction capacity was approximately 25 to 50 mL/min, based on steady draw-down testing and the rate of recharge observed within the borehole after the pump test was completed. Due to decreases in water table elevation in 37-B07 prior to the test, the extent of hydraulic influence in the shallow (above 80 ft bgs) fracture zone could not be assessed.
- *Pump test at 37-B07.* Test results showed that the open borehole extraction capacity was approximately 400 mL/min, based on steady draw-down testing. Rapid drawdown was observed at 37-B06 during testing, indicating a strong hydraulic influence in the deep (below 80 ft bgs) fracture zone.

5.8.1.3 Baseline Sampling

Results of the baseline groundwater sampling under ambient (no re-circulation) conditions indicated significant (>1% solubility) PCE concentrations at all the monitoring locations shown in Table 5.7. Ambient (prior to recirculation) dissolved groundwater PCE concentrations ranged from 4 to 25 mg/L in the monitoring wells and as high as 85 mg/L in the extraction wells. Further results of the baseline sampling are presented and discussed in the context of the initiation of groundwater re-circulation and bioaugmentation treatment in Section 5.8.3.

5.8.2 Results of STAGE 2 Testing

5.8.2.1 Partitioning Tracer Test

Results showed that only 37-B11s and 37-B11d had appreciable quantities of tracer, indicating complete breakthrough of the tracer pulse. No tracer was observed at either of the extraction wells (37-B12 and 37-B13), or in the shallow and intermediate intervals of 37-B07. Very low levels (less than 1% of the injected tracer concentrations) were measured in B07d, making any meaningful interpretation of results with respect to DNAPL architecture difficult at this location. Thus, assessment of DNAPL architecture and flow field is focused on the strong tracer signatures observed at 37-B11s and 37-B11d. The lack of hydraulic influence observed at B06 and B11 (shallow and deep intervals) while pumping at the extraction wells likely limited the tracer zone of influence to the immediate vicinity of the injection well (which included 37-B11s and 37-B11d), where the tracer flow was largely controlled by the hydraulic gradient emanating from the injection well. It is suspected that the fracture plane that was shown to hydraulically connect the deep zone between 37-B06 and 37-B07 is likely intersected by another fracture plane that diverted most of the tracer flow.

Tracer breakthrough curves for 37-B11s and 37-B11d are shown in Figures 5.18 and Figure 5.19, respectively. For both 37-B11s and 37-B11d, and also for 37-B07d, methanol concentrations are lower than bromide (bromide concentrations were normalized to the background bromide concentration of 1.3 mg L⁻¹). If both methanol and bromide were conservative tracers, they would co-elute, even in the presence of DNAPL. These observations suggest that slow biodegradation of methanol was likely, which is consistent with previous observations of methanol biodegradation in groundwater (43). Thus, bromide was likely the only conservative tracer in this study.

Observation of the tracer elution data shows a distinct pulse of tracer breakthrough at 37-B11s, an initial small pulse of tracer at 37-B11d (located at 1.1 days), followed by a second much larger pulse of tracer (located at 2.5 days), and a final slowly eluting tracer mass (or, “tail”) late in 37-B11d. Qualitative observations also show that the conservative bromide tracers have lower peak concentrations and/or show less tailing than the hydrophobic alcohol tracer at 37-B11s, the initial small peak at 37-B11d, and slightly in the “tail” at 37-B11d, suggesting that partitioning into DNAPL is occurring along the flow path in these flow regimes. In contrast, the bromide appears to co-elute with the hydrophobic tracer at the primary pulse in 37-B11d, suggesting that DNAPL is not present along this flow path. The absence of any measureable difference in the elution of bromide and hydrophobic tracers at the large pulse in 37-B11d also confirms that hydrophobic tracer sorption to the aquifer solids is negligible, thus DMP uptake (where observed) is assumed attributable to DNAPL in the fractures.

5.8.2.2 Assessment of Flow Field

Applying the MOM model, the fracture volume and the fraction of the injected flow associated with each of the regimes depicted in Figures 5.18 and 5.19 are presented in Table 5.12; other model regressed parameters also are provided in Table 5.12. The mass of bromide eluting through 37-B11s and d is consistent (within approximately a factor of 2) with the radial fracture flow assumption, thus indicating that this assumption is reasonable given the conditions of the tracer experiment.

The distribution of flow among the four fracture zones is proportional to the transmissivity of each of these zones. Results show that most of the tracer mass, and flow, that reached the target 37-B11 intervals eluted through 37-B11s and the tracer tail at 37-B11d. The relatively large fracture porosity, and associated low tracer velocities, is responsible for the tailing peak at 37-B11d. In contrast, the initial peak at 37-B11d has a relatively low transmissivity (compared to the other 3 fractures), but has a low fracture porosity; these factors are what cause the low flow and short elution time relative to the other fracture zones. The implications of this immobile porosity and DNAPL architecture and dissolution are discussed in the following sections.

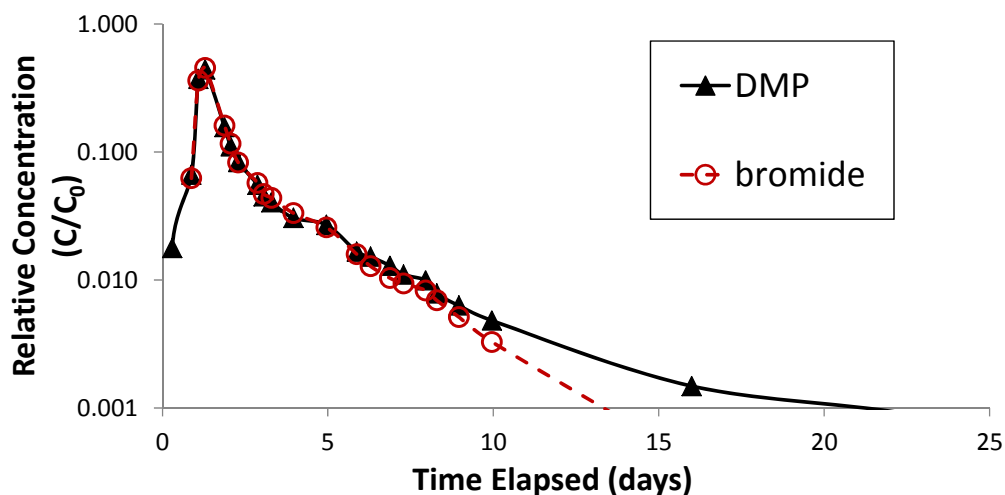


Figure 5.18. Bromide and DMP Tracer Elution in 37-B11s Bromide and DMP tracer elution through the 37-B11s monitoring interval. Concentrations are plotted relative to the injection concentration. A semi-log plot is used to show the difference in tracer behavior.

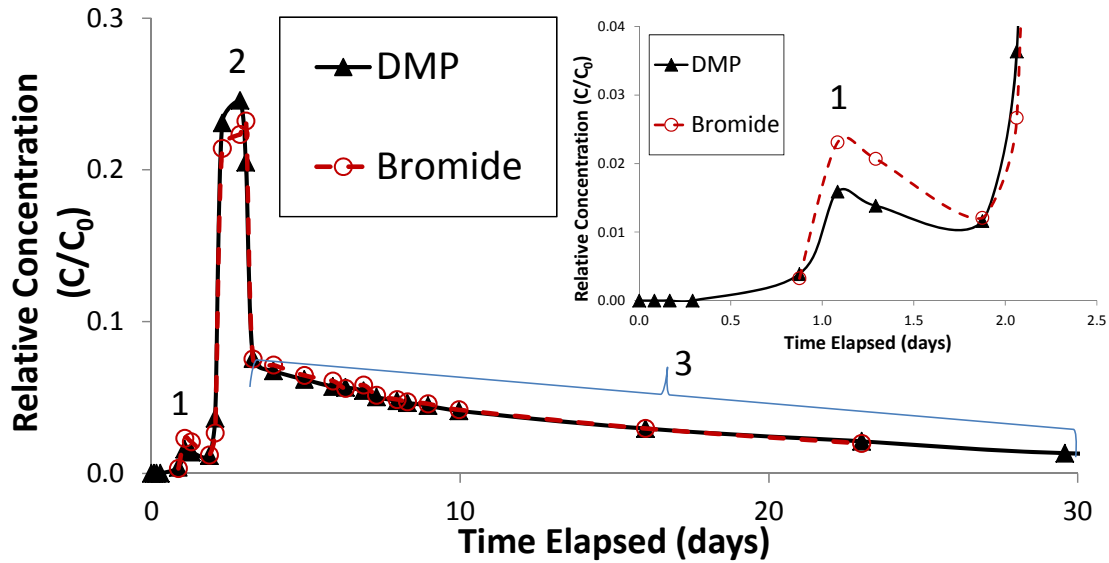


Figure 5.19. Bromide and DMP Tracer Elution in 37-B11d Bromide and DMP tracer elution through the 37-B11d monitoring interval. Concentrations are plotted relative to the injection concentration. Early and middle peaks are observed (denoted by the 1 and 2, respectively), followed by the late tail (denoted by the 3). The inset figure highlights the initial peak.

Table 5.12. Modeling Results Based on the PTT

The relative flow for each fracture zone is calculated as the fraction of eluted bromide mass through each zone divided by the eluted bromide mass for the sum of the 4 zones.

Parameter	37-B11s	37-B11d (initial)	37-B11d (middle)	37-B11d (last)
Relative Flow (MRF)	0.50	0.011	0.087	0.40
Velocity (m/day)	1.5	7.5	1.6	0.2
Mean residence time (days)	2.7	0.6	2.5	21
Fracture Porosity	0.00069	3.0×10^{-6}	0.00080	0.0042
R	1.08	1.24	0.99	1.02
S _n	0.002	0.007	0.0	0.0004
DNAPL volume (m ³ x 1000)	0.66	0.0091	0.0	0.82
DNAPL Dissolution Time (ambient) (years)	44	200	0.0	13

5.8.2.3 DNAPL Architecture

The DNAPL fracture saturation associated with each zone is presented in Table 5.12. The DNAPL saturation in each of the fracture zones is quite low, ranging from 0 (no measurable DNAPL) to a maximum of 0.007. These saturations are likely 1 to 2 orders of magnitude below levels needed for DNAPL mobility (13, 21). DNAPL is observed in both high and low transmissivity (or, flow) zones within the fracture network. The majority (55%) of the DNAPL resides in the relatively transmissive zone in 37-B11d (final peak), which also is associated with the largest fracture porosity. The greatest DNAPL saturation is located in the low transmissivity fracture zone (initial peak in 37-B11d), but only 0.6% of the DNAPL mass is present in this zone due to its low fracture porosity.

5.8.3 Results of STAGE 3 Testing: Bioaugmentation Treatment and Monitoring

5.8.3.1 Re-circulation Flow and Amendment Distribution

The groundwater re-circulation flow rate prior to and after bioaugmentation is shown in Figure 5.20. Immediately after adding the bioaugmentation culture, the re-circulation flow rate diminished by approximately 40% without any recovery in the flow rate as groundwater re-circulation continued. The reason for this immediate and sustained decrease is unclear, but it is unlikely that any biofouling impacts would have occurred so quickly based on prior experience using similar bioaugmentation approaches (2). It is possible a physical blockage of the fractures occurred during injection, perhaps due to instability or crumbling along the borehole wall, or any solids potentially present in the injection. Following the culture injection, slow decreases in re-circulation flow rate were observed over time following bioaugmentation and during delivery of biological amendments. These slow decreases in flow, in contrast to the step-decrease observed during the initial bio-amendment delivery, were due to slowly diminishing capacity of the injection well, and were likely due to biomass growth and/or microbially-enhanced mineral precipitation. The re-circulation flow rate decreased to as low as approximately 10 to 20% of the original flow rate for several months of the demonstration. Attempts to re-develop the injection well only resulted in marginal improvement to the well capacity; *the relatively large improvement at 303 days was primarily due to deflating the packer in the injection well.*

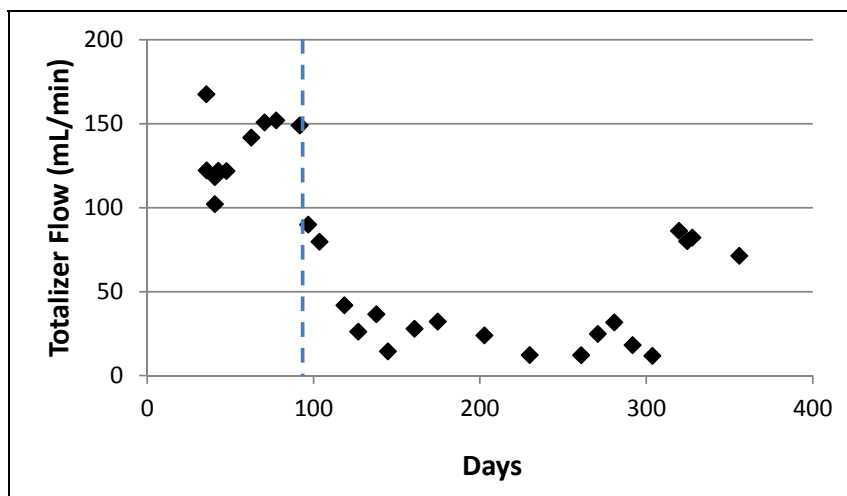


Figure 5.20. Groundwater Re-circulation Flow Rate.

The vertical dashed line indicates the start of biological amendment addition. Attempts to re-develop the well were performed on days 127, 256 and 303.

PCE concentrations within the two extraction wells 37-B12 and 37-B13 remained elevated during the duration of the demonstration, with PCE concentrations averaging 0.7 and 0.4 mM (120 and 70 mg/L), respectively. Analytical results are presented in tabular form in Appendix F. These dissolved PCE concentrations were several times greater than the dissolved PCE concentrations observed (under ambient conditions prior to initiation of groundwater re-circulation) at the injection well or monitoring wells 37-B11 and 37-B07. The elevated PCE concentrations in the two extraction wells suggest that PCE DNAPL potentially may also be present further downgradient in the vicinity of the extraction wells.

No remedial amendments or biodegradation impacts (e.g., decreases in PCE, chlorinated ethene daughter products, lactate fermentation products, increases in DHC) were observed at either of the extraction wells during the demonstration. These results are consistent with the previously performed tracer tests, where no tracers were observed at the extraction wells (42). In addition, no remedial amendments or biological impacts were observed at the shallow and intermediate intervals of 37-B07 (although one sample at the shallow interval of 37-B07s did show a 1 to 2-log increase in DHC). Trace impacts of biological treatment were observed at the deep interval in 37-B07d, located approximately 5 m downgradient from 37-B11. Lactate fermentation products typically were between 50 and 200 mg/L, which were approximately 10-times less than what was observed in the 37-B11 intervals. As shown in Figure 5.21, DCE generation, decreases in PCE concentration, and DHC increases were minimal at 37-B07d; all of these data indicate that no bioremediation of PCE occurred at this location due to insufficient delivery of remedial amendments. By the end of the demonstration, sulfate levels also had decreased by approximately a factor of 2, suggesting that sulfate reduction was only starting to occur. The sum of detected volatile fatty acids at 37-B07d never exceeded 200 mg/L. The minimal impacts observed at 37-B07d (as well as the other shallower 37-B07 intervals) were consistent with the previous tracer testing, which indicated that this monitoring location was not along the primary fracture flow paths emanating from the injection well. The lack of a strong amendment response at 37-B07, located only 8.8 m downgradient of the injection well, highlights the complexity of fracture flow at this site.

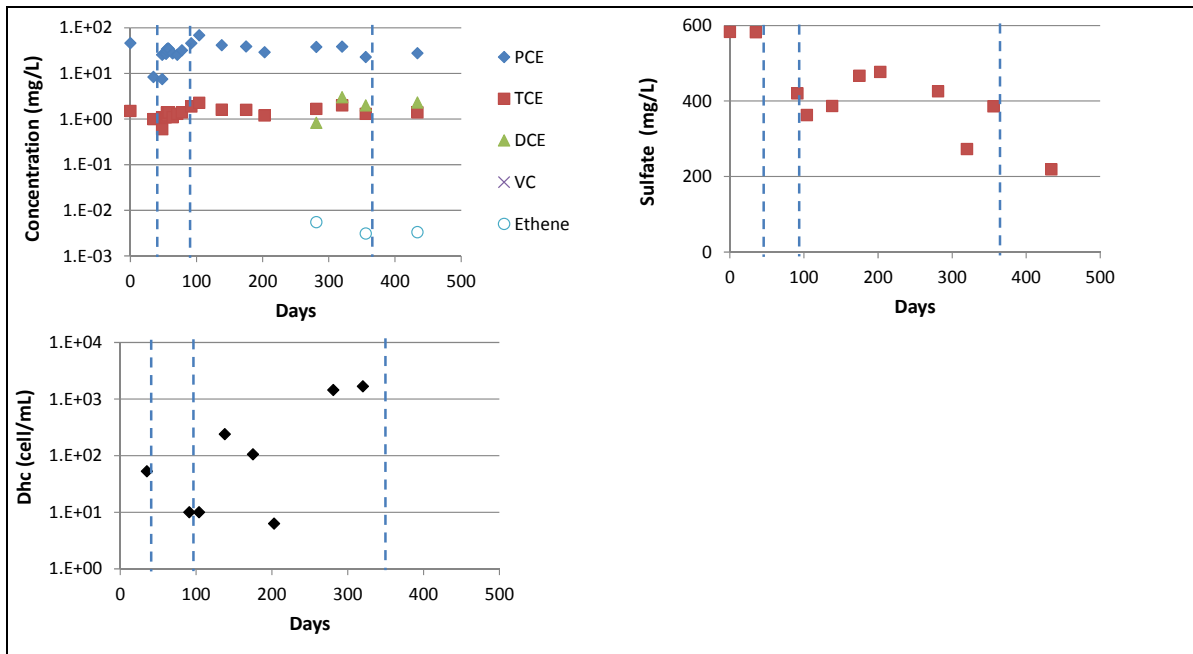


Figure 5.21. Chlorinated Ethene+Ethene, Sulfate, and Dhc Levels at 37-B07d

Vertical dashed lines represent the start of groundwater re-circulation, the initiation of bioremediation amendment addition, and the cessation of groundwater recirculation. For the chlorinated ethenes, only detections are shown. For the Dhc, data at 10 cell/mL represent the analytical detection limit.

Consistent with the pre-remedial tracer test, migration of remedial amendments and biological impacts were most clearly observed at both the shallow and deep monitoring intervals of 37-B11. Figures 5.22 and 5.23 show the relatively high levels of propionic acid (a lactate fermentation daughter, and also a fermentable volatile fatty acid) observed in the shallow and deep intervals of 37-B11 throughout the demonstration; propionic acid typically was the most abundant volatile fatty acid detected. Other biological impacts at 37-B11, including an assessment of PCE dechlorination and DNAPL removal, are discussed in the following subsections.

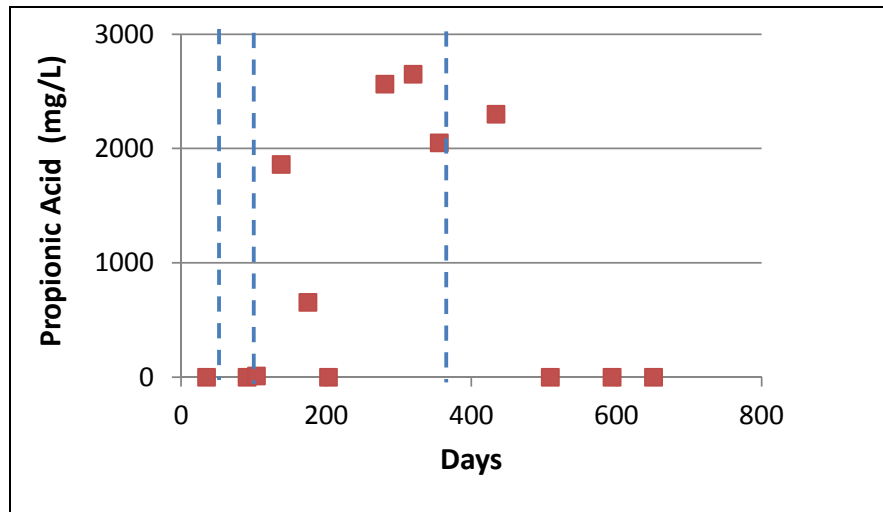


Figure 5.22. Propionic Acid Concentration Measured in the Shallow Interval of 37-B11

Vertical dashed lines represent the start of groundwater re-circulation, the initiation of bioremediation amendment addition, and the cessation of groundwater re-circulation.

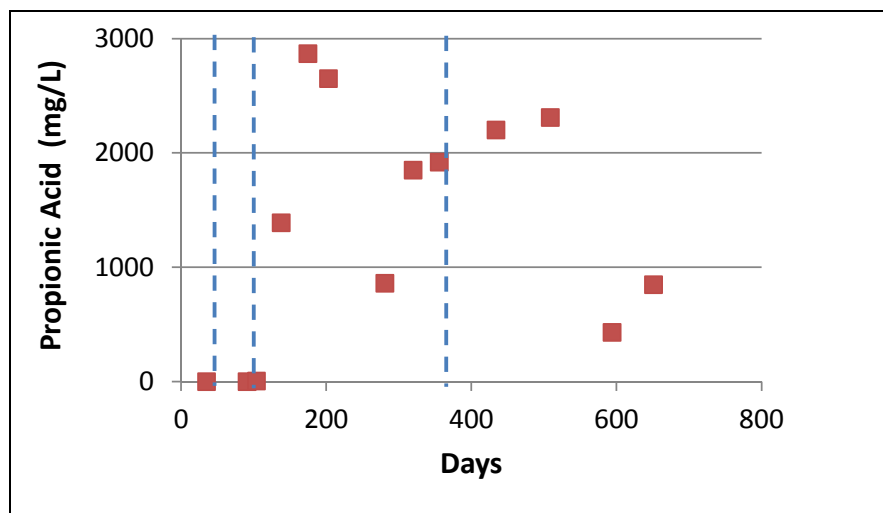


Figure 5.23. Propionic Acid Concentration Measured in the Deep Interval of 37-B11.

Vertical dashed lines represent the start of groundwater re-circulation, the initiation of bioremediation amendment addition, and the cessation of groundwater re-circulation.

5.8.3.2 Reductive Dechlorination

Figures 5.24 and 5.25 summarize the chlorinated ethenes and ethene observed at 37-B11s and 37-B11d, respectively. The increases in PCE concentrations after initiating groundwater re-circulation were due to the elevated PCE concentrations in the downgradient extraction wells. Results indicate that, within 7 weeks following bioaugmentation and biological amendment delivery, PCE concentrations showed a substantial (~90%) decrease, with an approximate stoichiometric increase in DCE (although the DCE concentrations in 37-B11s at 46 days following bioaugmentation appear anomalously low). These results are consistent with previous studies that show DCE as the primary dechlorination daughter product when PCE DNAPL is present (18,45,46). The increases in chloride concentrations, particularly between 130 and 205 days, also confirm reductive dechlorination is occurring (Figure 5.26).

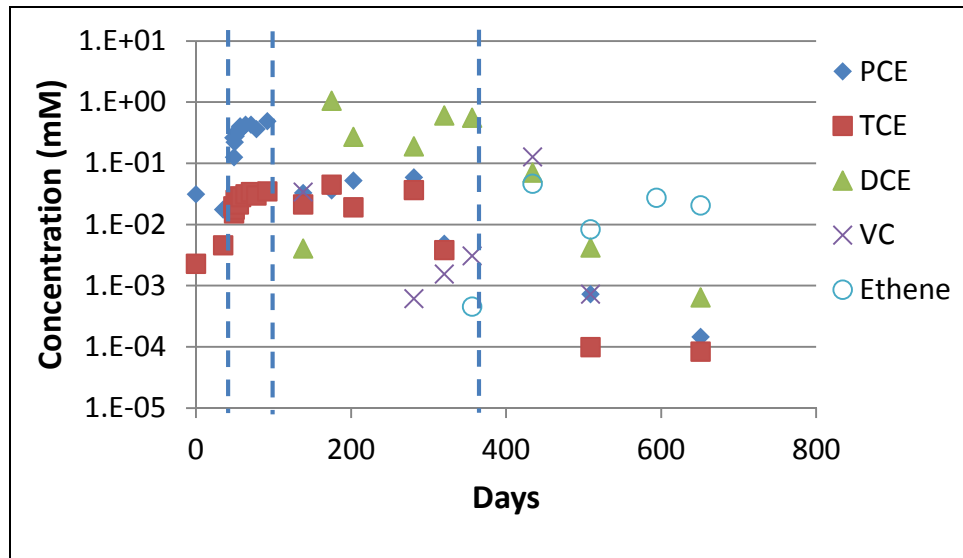


Figure 5.24. Chlorinated Ethene and Ethene Concentrations at 37-B11s

Only detections of chlorinated ethenes and ethene are shown. Vertical dashed lines represent the start of groundwater re-circulation, the initiation of bioremediation amendment addition, and the cessation of groundwater re-circulation.

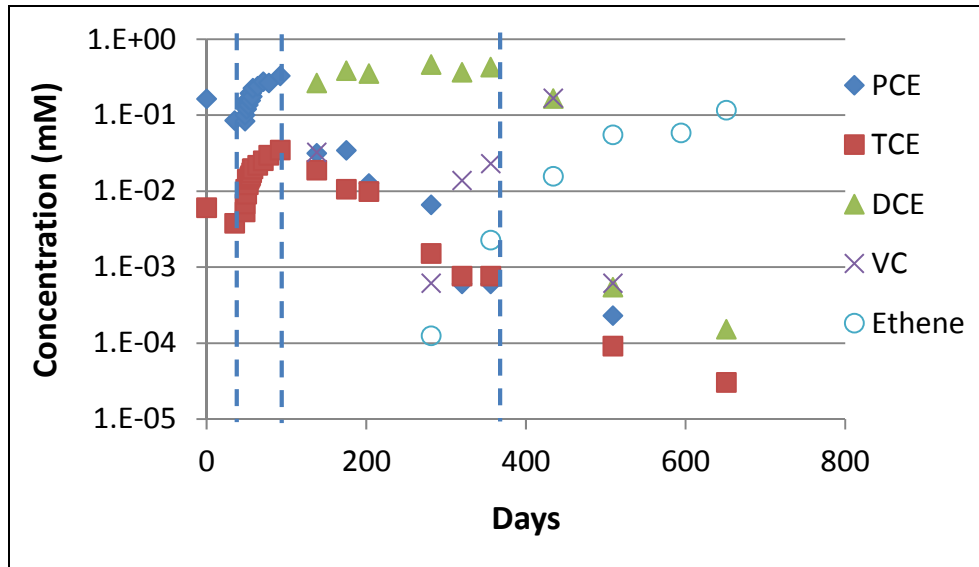


Figure 5.25. Chlorinated Ethene and Ethene Concentrations at 37-B11d

Only detections of chlorinated ethenes and ethene are shown. Vertical dashed lines represent the start of groundwater re-circulation, the initiation of bioremediation amendment addition, and the cessation of groundwater re-circulation.

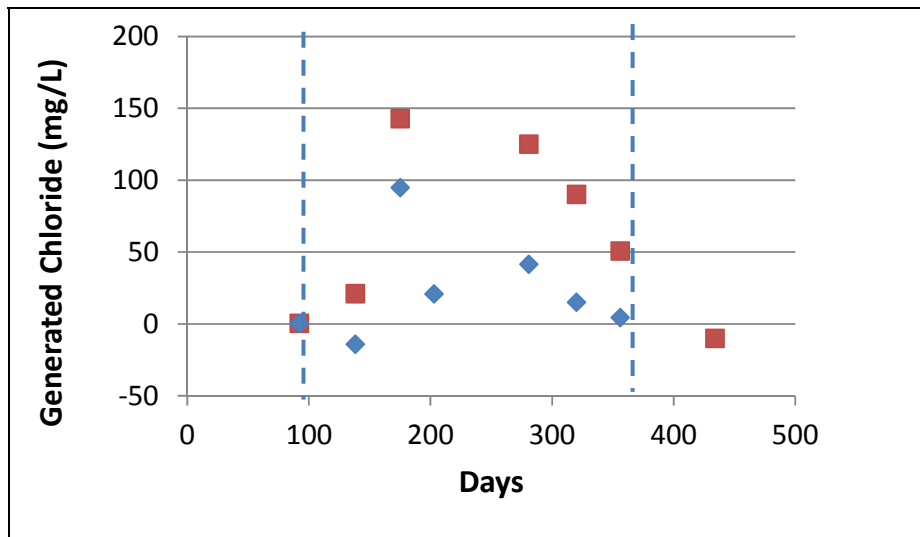


Figure 5.26. Generated Chloride (above background chloride levels) at 37-B11.

37-B11s (■) and 37-B11d (◆). Vertical dashed lines represent the initiation of bioremediation amendment addition and the cessation of groundwater re-circulation. Dilution and mixing from extraction wells are accounted for in determining the generated chloride.

5.8.3.3 Microbial Growth and Geochemical Impacts

Figure 5.27 shows the sulfate and dissolved iron levels for 37-B11s and 37-B11d. Results indicate that sulfate reduction occurred in both zones. Increases in dissolved iron also occurred. Methane levels typically were non-detect or less than 5 µg/L, suggesting that bulk methanogenic conditions likely were not attained during active treatment.

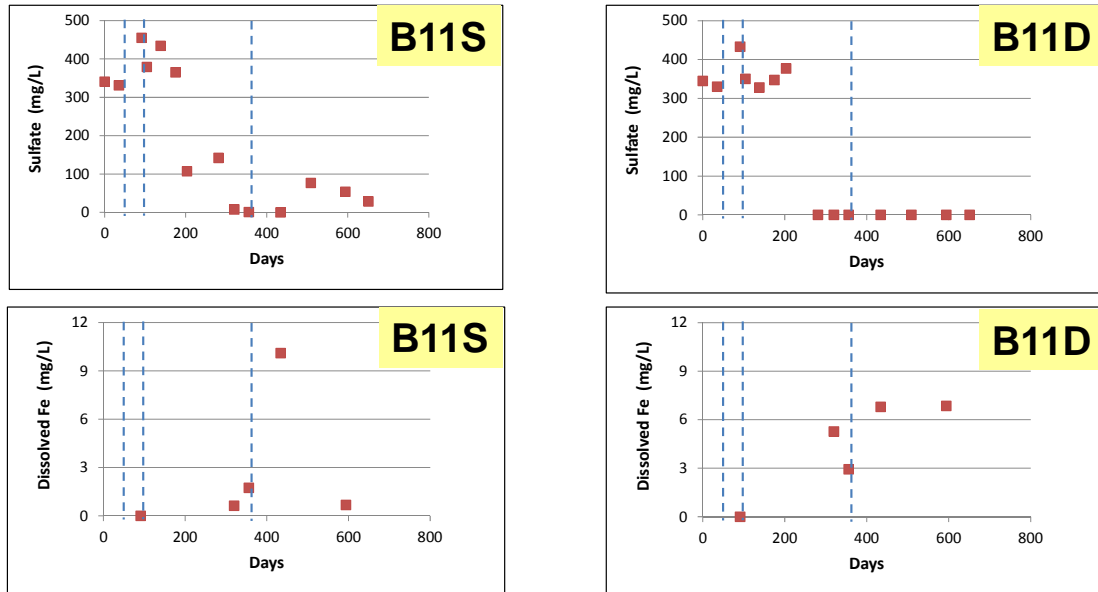


Figure 5.27. Sulfate and Dissolved Iron Concentrations Measured in 37-B11s and 37-B11d

Vertical dashed lines represent the start of groundwater re-circulation, the initiation of bioremediation amendment addition, and the cessation of groundwater re-circulation.

Figures 5.28 shows the Dhc concentrations for 37-B11s and 37-B11d as a function of time. Results indicate that the Dhc were able to migrate to this well. The increasing Dhc levels overtime also indicate that Dhc growth occurred. Dhc concentrations on the order of 10^3 Dhc/mL were observed at 37-B07d. However, because the primary fracture flow path beyond 37-B11 was not well defined, the downgradient extent of Dhc migration could not be determined.

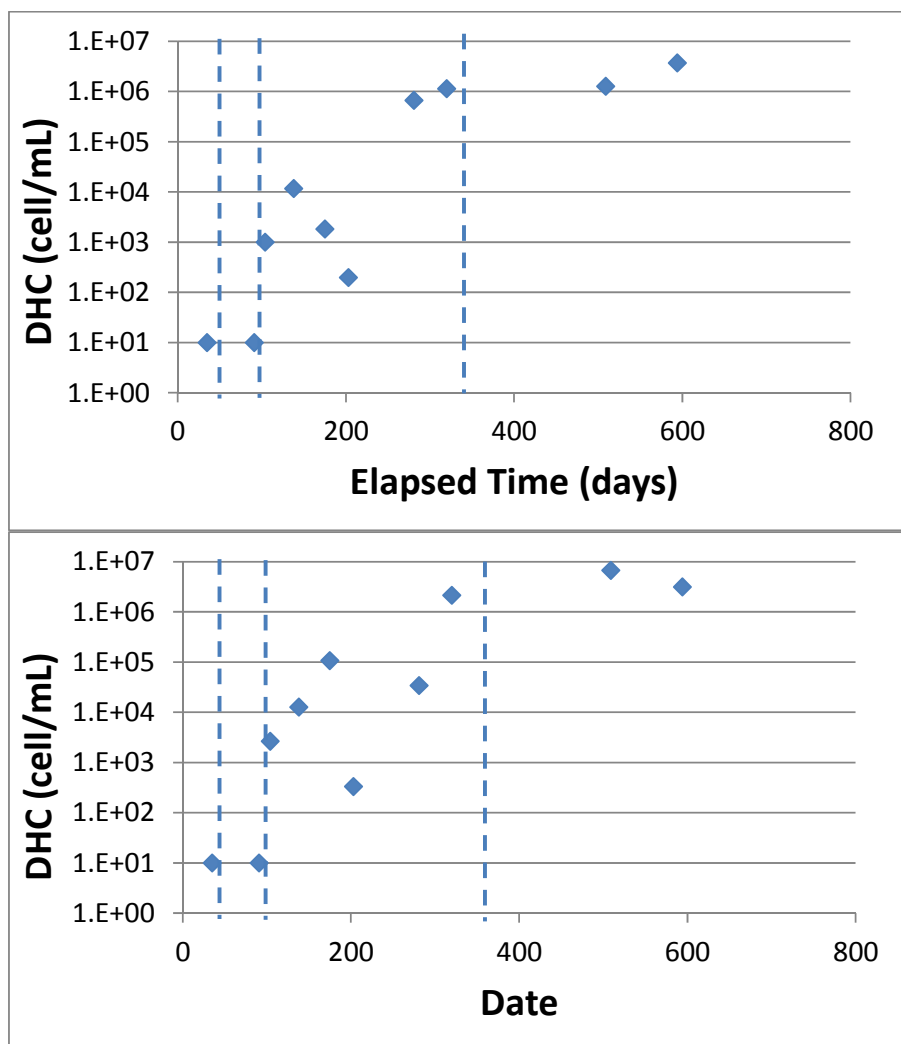


Figure 5.28. DHC Concentrations Measured in 37-B11s (top) and 37-B11d (bottom)

Vertical dashed lines represent the start of groundwater re-circulation, the initiation of bioremediation amendment addition, and the cessation of groundwater re-circulation.

5.8.4 Results of STAGE 4 Testing: Post Treatment Monitoring and Assessment

5.8.4.1 Groundwater Monitoring

After cessation of the groundwater re-circulation and amendment delivery at 356 days, DCE concentrations in 37-B11(s and d) began to rapidly decrease, with a transient increase in VC and increased ethene generation (Figures 5.24 and 5.25). An increasing trend in total molar chlorinated ethene + ethene was observed over the rebound period for 37-B11d, while no increasing trend was observed for 37-B11s. Sulfate levels remained low (Figure 5.27) and ferrous iron levels remained elevated at 37-B11d; volatile fatty acid levels also remained elevated (Figure 5.23). These data indicate that strongly reducing conditions favorable to the complete dechlorination of PCE were maintained at 37-B11d throughout the rebound period.

In contrast, by 5 months into the rebound period at 37-B11s, volatile fatty acids became depleted, sulfate levels had increased from non-detect levels (Figure 5.27), and dissolved iron levels decreased, which together suggest that strongly reducing conditions were not maintained throughout the rebound period at this location.

5.8.4.2 Post Treatment Rock Core Collection

Results of the rock core collection for ferrous iron content are shown in Figure 5.29. These ferrous mineral contents are orders of magnitude below those previously observed in rock matrices that showed abiotic dechlorination of chlorinated ethenes (59). Consistent with this observation, abiotic reactivity on the rock matrix using collected rock core showed no abiotic dechlorination. The ferrous iron content showed a decreasing trend going into the rock matrix, particularly for the shallow zone. It is unclear if this trend existed prior to bioremediation, or if bioremediation facilitated the formation of ferrous mineral phases at or near the fracture interface.

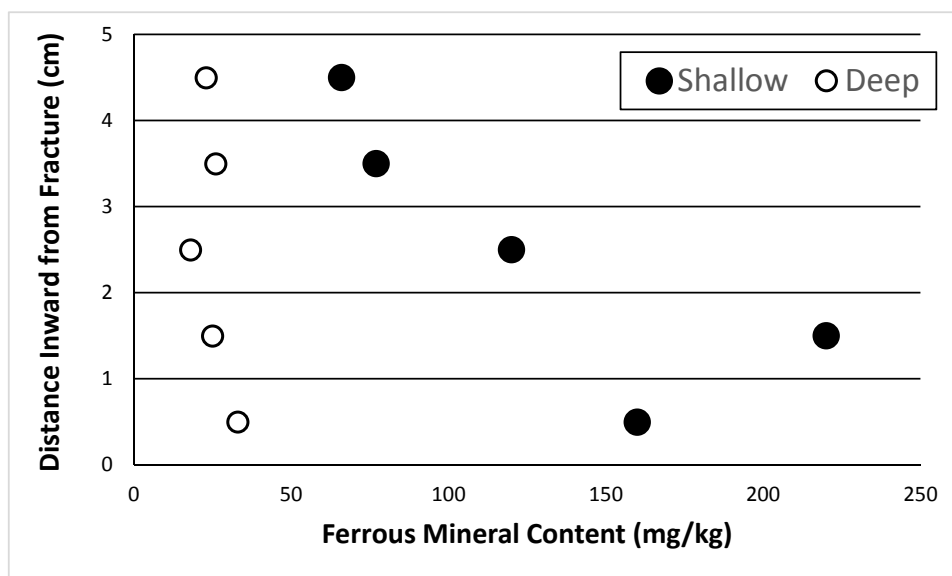


Figure 5.29. Ferrous mineral content within the rock matrix at 37-B14.

Shown as a function of distance from the fracture interface. Both the shallow (~76 ft bgs) and deep (~85 ft bgs) fracture zones were evaluated.

PCE concentrations within the rock matrix (up to 8 cm into the rock matrix) were below the analytical detection limit (<80 $\mu\text{g}/\text{kg}$). Thus, in comparison to the PCE concentrations within the rock matrix prior to bioremediation, the concentrations decreased by at least a factor of 2. Based on the conceptual model of rapid treatment and removal of PCE in the fractures by biological treatment, and corresponding removal of PCE from the rock matrix via aqueous diffusion, impacts of treatment would not have been expected beyond 1 to 2 cm. Thus, the absence of measureable PCE in the rock matrix is not readily explained. One possibility is that the presence of microfractures in vicinity of the fracture zone may have allowed remedial amendments to migrate into what appeared to be a competent rock matrix (see Figure 5.30); this would have greatly reduced the diffusion length, and would explain how PCE removal occurred at such relatively large distances from the primary fracture interfaces.

Acoustic Televiewer – identifies fractures to ~0.1 mm

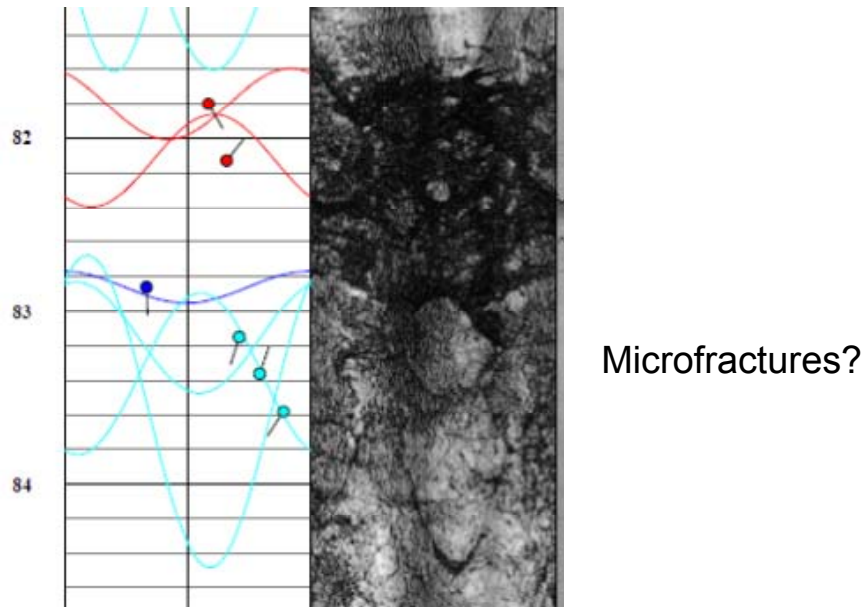


Figure 5.30. Acoustic Televiewer Results Focusing on the Deep Fracture Zone at 37-B06

Microfractures may exist adjacent to the primary fracture. These microfractures may have allowed remedial amendments to distribute further into the rock matrix than what would have been predicted based on diffusion alone.

Page Intentionally Left Blank

6.0 PERFORMANCE ASSESSMENT

6.1 DNAPL ARCHITECTURE

Due to high groundwater flow velocities and low matrix porosity, tracer elution likely was controlled by convection through the fractures, with limited impacts from matrix diffusion. To verify this, assuming diffusion controlled uptake into the rock matrix as described by Parker et al. (48), the ratio of convective tracer migration through the fractures to diffusive uptake into the rock matrix ($F_{\text{frac}}/F_{\text{matrix}}$) is defined as follows:

$$F_{\text{frac}}/F_{\text{matrix}} = \frac{A_{\text{cs}}V}{A_{\text{fs}}\sqrt{\frac{D_{\text{eff}}}{\pi t}}} \quad \text{Eq. 10}$$

where A_{cs} is the fracture cross sectional area, V is the average tracer velocity, A_{fs} is the interfacial area between the fracture and the rock matrix, D_{eff} is the effective diffusion coefficient of tracer in the rock matrix, and t is time. Applying Eq. 10 to the DMP tracer pulse at 37-B11s, A_{cs} is estimated by multiplying the fracture porosity by the vertical injection interval, then multiplying this value by the circumference around 37-B06 with a radius extending to 37-B11s (this assumes radial flow out from the injection well). A_{fs} is estimated by twice the surface area (top and bottom fracture faces) of this injection radius. With a rock matrix porosity of 4.9%, determined using rock core samples via the water uptake method (49), D_{eff} is estimated at $4.3 \times 10^{-8} \text{ m}^2 \text{ d}^{-1}$ (50,51). Using the value of the tracer velocity V listed in Table 5.12, along with a characteristic time of 2.7 days (Table 5.12), the value of $F_{\text{frac}}/F_{\text{matrix}}$ for 37-B11s is 65, indicating that matrix diffusion effects are minimal. A similar result (150) is attained for the tail of 37-B11d.

The impacts of matrix diffusion on mean retention time (or, retardation) is related to the tracer diffusion coefficient, where tracers with large diffusion coefficients show more retardation due to uptake into the rock matrix than tracers with small diffusion coefficients (52). For our system, where the aqueous diffusion coefficient for bromide is approximately 2-times greater than that of DMP (51,53), matrix diffusion would lead to a potential underestimation of DNAPL mass, as the difference in mean retention time between bromide and DMP would be greater if bromide exhibited enhanced retardation due to matrix diffusion. However, because the impacts of matrix diffusion in our system is small (Eq. 10), a factor of two difference for the aqueous diffusion coefficient has minimal impact on the mean residence time, resulting in less than a 10% error in the DNAPL estimates calculated via the MOM.

While the role of matrix back diffusion in sustaining groundwater plumes in fractured bedrock has been examined (54,55), the role of DNAPL in low permeability fracture zones on plume longevity has received little attention. The ambient (prior to initiating groundwater recirculation) PCE concentrations in 37-B11s and 37-B11d were 4 mg L^{-1} and 21 mg L^{-1} , respectively. The 21 mg L^{-1} dissolved PCE concentration is associated primarily with the dissolved PCE concentration in the “tail” portion of the fracture zone, as the majority of the fracture flow and porosity is associated with this fracture zone. The difference in dissolved PCE concentration between 37-B11s and 37-B11d is approximately proportional to the difference in residence time (i.e., travel time between 37-B06 and 37-B11), as increased residence time allows for more DNAPL dissolution.

This observation is consistent with laboratory-scale studies examining the DNAPL dissolution in single fracture planes, where the residence time (and not DNAPL fracture saturation) was the controlling factor in determining the dissolution rate (56). Assuming the dissolved PCE concentration is approximately proportional to the residence time, the dissolved concentration in the low transmissivity zone associated with the initial tracer peak in Figure 5.19 is estimated as 0.6 mg L⁻¹, which is calculated by multiplying the 21 mg L⁻¹ concentration by the ratio of the velocity in the initial fracture zone divided by the velocity in the “tail” portion of the fracture zone.

The estimated average ambient groundwater linear velocity (V_{amb}) of 0.031 m d⁻¹ through the fractured bedrock (based on hydraulic conductivity and gradient data (17)) is 6.5-times less than the mean (based on distribution of tracer mass) groundwater velocity observed during the tracer study. Assuming a constant DNAPL dissolution rate, the time needed for DNAPL removal is:

$$t_d = \frac{V_n \rho_n}{C Q_i} \quad 6.5 \quad \text{Eq. 11}$$

where t_d is the DNAPL dissolution time, ρ_n is the PCE DNAPL density, and C is the average aqueous concentration of PCE in either 37-B11s or 37-B11d (initial or tail). It is noted that Eq. 11 is not dependent upon the assumption of radial flow from the injection well, as the Q_i term associated with V_n (Eq. 5 and 6) cancels with the Q_i in the denominator, indicating that the time needed for dissolution under ambient conditions can be determined without this assumption.

The calculated DNAPL dissolution timeframes are provided in Table 5.12. It is noted that these time frames do not account for any dechlorination reactions, additional uptake into the rock matrix, or decreases in aqueous concentration as the DNAPL mass diminishes; thus, these timeframes are for screening and comparative purposes only. The two findings of note are that 1) despite the very low DNAPL saturations in the fractures, dissolution timeframes are very long, and 2) DNAPL present in the low transmissivity fractures appears to be responsible for sustaining the contaminant plume. These results suggest that the presence of DNAPL in low permeability fractures can sustain plumes for timeframes similar to that of contaminants present in the rock matrix (57). The persistence of DNAPL in the low flow fractures is similar to the persistence of DNAPL in low permeability zones observed in unconsolidated materials (58).

Applying Eq. 10 to PCE under ambient flow conditions results in values >1 for times in excess of 1 year. This suggests that DNAPL sources, rather than matrix back-diffusion, is controlling the sustained mass discharge from the source area. PCE concentrations in the rock matrix adjacent to conductive fractures showed constant concentrations of approximately 120 $\mu\text{g kg}^{-1}$ moving inwards from the fracture interface (Supplemental Information). If matrix back-diffusion was sustaining the elevated PCE levels in the fractures, then a gradient in increasing PCE concentrations into the rock matrix would be expected. Thus, removal of DNAPL sources likely will result in a decrease in mass discharge from the source area. It is also notable that the mass of PCE DNAPL in the fractures (Table 5.12) is conservatively 10-times greater than that estimated in the rock matrix (assuming a uniform 4.9% matrix porosity and 120 $\mu\text{g/kg}$ PCE in the matrix).

Given the long DNAPL dissolution timeframes described in the previous paragraphs and shown in Table 5.12, dissolution into bypassing groundwater was not responsible for reducing the residual saturation from levels of DNAPL mobility (typically greater than S_n values of 0.03 to 0.1) to the current levels. Reductive dechlorination daughter products typically observed during biodegradation of PCE were not observed during baseline sampling of groundwater, thus it is unlikely that enhanced DNAPL removal via biodegradation facilitated DNAPL removal to any appreciable extent. Testing to assess abiotic dechlorination reactions within the rock matrix, using batch testing methods previously described (59), also indicated that abiotic process had minimal impact on DNAPL dissolution. Examination of the simulation work performed by Parker et al. (48) shows that diffusive uptake into the rock matrix alone could not account for depletion of the DNAPL source, assuming S_n values were originally at least 0.03. The PCE mass within the rock matrix, based on a uniform PCE concentration of 120 $\mu\text{g kg}^{-1}$, confirms that matrix diffusion alone could not have accounted for such a large decrease in S_n . We speculate that the value of S_n originally entrapped within the fractures was much lower than the range of residual S_n observed in laboratory studies (17,60), as very discrete fingers of DNAPL may have entered the fracture planes targeted in this field study. Alternately, or perhaps in addition, it is plausible that only a very small fraction of the DNAPL mass is near the flow path of the tracers, and much of the DNAPL resides in low-flow or no-flow zones within the fracture planes. This alternate possibility is consistent with previous bench-scale studies using fractured sandstone blocks that showed most of the residual PCE DNAPL in a single fracture plane was located in low flow zones (18). While it is possible that DNAPL in such very low-flow (or no-flow zones, such as dead-end fractures) may be present and not detected via the partitioning tracer technique, the impact of such DNAPL on the groundwater plume also would be limited by the same diffusional mass transfer processes that “hide” these sources from the partitioning tracers. Thus, in this respect, the partitioning tracer tests in fractured bedrock likely identify and quantify the DNAPL sources that most readily impact the dissolved plume, which are those along a measureable flow path. However, diffusional mass discharge from DNAPL in these stagnant zones could still have a measureable (albeit significantly less than DNAPL present along the measureable flow path) long-term impact on the dissolved plume.

6.2 BIOAUGMENTATION TREATMENT

6.2.1 DNAPL Mass Removal

Based on the PCE present in the extracted groundwater, and assuming conversion of this PCE to DCE, 25 mg/L of chloride would be generated. The chloride generation observed at both the shallow and deep intervals at 37-B11 (Figure 5.26) exceeded this value by 2- to 6-times, indicating the dechlorination of PCE DNAPL. Assuming the excess chloride is the result of PCE DNAPL dissolution and subsequent conversion to DCE, the maximum observed chloride generation (143 mg/L) at 37-B11s represents approximately 2.1 mM PCE, which indicates a dissolution enhancement of the PCE DNAPL of approximately 5 when compared to the PCE molar concentrations measured prior to bioaugmentation at 37-B11s (Figure 5.24). This level of DNAPL dissolution enhancement is similar to those observed by others (12,13,18).

While the measured increases in chloride provide useful information regarding DNAPL dissolution, the molar increases in DCE were approximately equal to the dissolved PCE concentrations prior to bioaugmentation, and thus were not indicative of any DNAPL dissolution enhancement.

Previous studies have suggested that DCE generated at the DNAPL-water interface likely back-partitions into the DNAPL, and is not observed in the bulk aqueous phase (18,41). Once partitioned into the DNAPL, DCE may diffuse through thin DNAPL layers/ganglia into the rock matrix or other low permeability zones.

Based on the chloride generation observed during active treatment, and applying Eq. 9, 1.1 and 0.6 kg of DNAPL were removed in 37-B11s and 37-B11d, respectively. Thus, treatment was effective for removing the DNAPL in the shallow zone, but only about 45% of the DNAPL was removed from the deep zone. It is noted that, due to the scatter in the chloride data, the DNAPL mass removal for the deep interval is only an estimated value, with an estimated error of up to 50%. The estimated DNAPL mass in each of these zones was based on partitioning tracer testing, which only accounts for the DNAPL mass that is in close proximity to the fracture flow paths. Thus, DNAPL may still remain within the shallow fracture zone, but in zones that are not hydraulically conductive relative to the primary flow path and that minimally impact groundwater quality.

6.2.2 Rebound

The behavior during the 10-month rebound period was similar for both 37-B11s and 37-B11d. Both the shallow and deep zones showed an increased conversion to VC and ethene after cessation of groundwater re-circulation and amendment addition, and both zones showed a substantial decrease in the molar balance (of chlorinated ethenes and ethene) as accumulation of VC and ethene occurred. The former observation can be readily explained by the increase in residence time (42) between the injection well and 37-B11 after cessation of groundwater recirculation. This increase in residence time allowed for further microbially-enhanced dechlorination. It is noted that a slow accumulation of VC and ethene had begun prior to the rebound period; this slow initial increase in VC and DCE likely was due to increases in biomass over time.

The decrease in the molar balance after rebound is explained by 1) eliminating the re-injection of high concentration PCE groundwater from the extractions wells as ambient flow conditions were resumed, and 2) VC and ethene diffusive uptake into the rock matrix. Assessment of elevated sodium levels (from addition of sodium lactate during the re-circulation phase), showed that approximately half of the sodium was depleted by 8 months into the rebound period in both the shallow and deep zones. Thus, the decrease in the elevated chlorinated ethenes + ethene is only partially explained by dilution due to ambient groundwater flow. Comparison of the relative importance of matrix diffusion effects on solute transport has been previously performed for both the shallow and deep fracture zones (42). Using this approach, but applying a mean residence time of 8 months, dimensional analysis suggests that matrix diffusion effects in the shallow zone will be significant. Due to the complex flow paths present in the deep zone (Table 5.12), a similar assessment is not possible, but the mass transfer limitations observed during the tracer test in the deep zone suggests diffusive controls on solute migration are likely. Thus, dissipation of the generated VC in both the shallow and deep zones is likely due to both dilution and diffusion into low flow zones.

While rebound behavior in 37-B11s and 37-B11d were similar, there were some important differences. In the shallow zone, the increase in sulfate, decrease in ferrous iron, and depletion of volatile fatty acids suggests that strongly reducing conditions did not persist throughout the rebound period. The shallow zone may have been more exposed to low levels of dissolved oxygen during rainfall events than the deep zone, which may explain why strongly reducing conditions were not maintained in the shallow zone, but yet were maintained in the deep zone. With conditions no longer supporting sulfate and iron reduction five months into the rebound period, it is unlikely that conditions were favorable for continued ethene generation in the shallow zone. The continued decreases in ethene and the lack of observed increases in any of the chlorinated ethenes are consistent with DNAPL source removal. The ethene remaining in the shallow zone likely persists because it has not yet been fully flushed from the system and/or due to matrix back diffusion.

In contrast, as indicated by the persistence of volatile fatty acids and continued sulfate depletion, strongly reducing conditions persisted in the deep zone. Such conditions support the continued dechlorination of chlorinated ethenes to ethene. The increasing trend in both ethene and the total molar balance suggest that an ongoing chlorinated ethene source is present. Based on the fact that only 45% of the PCE DNAPL was removed during active treatment, it is plausible that this ongoing source is residual PCE DNAPL, but it is also plausible that the continued ethene generation is from matrix back-diffusion and/or back-diffusion from other mass transfer limited zones.

6.2.3 Implications for Groundwater Quality

Overall, considering the specific fracture intervals targeted for this study, treatment in the shallow zone was more effective than in the deep zone with respect to DNAPL removal. In addition, while the shallow and deep zones showed decreases in chlorinated ethenes of 97 and 99.9%, respectively, the increasing ethene concentrations in the deep zone suggest that continuing microbially-enhanced dechlorination may be “masking” PCE rebound. This rebound process has been described conceptually and mathematically by Chambon et al. (2010) (61) and Manoli et al. (2012) (62). The difference in behavior, with respect to both the DNAPL removal and rebound, between 37-B11s and 37-B11d is likely due to the DNAPL architecture. For the shallow zone, DNAPL sources were along a flow path that did not show any mass-transfer limited behavior during the partitioning tracer test, while the DNAPL sources located in the deep zone showed “tailing” behavior that is indicative of mass transfer controlled processes (42). These mass transfer limitations likely inhibited the dissolution and removal of the PCE DNAPL sources in the deep zone during active treatment.

Page Intentionally Left Blank

7.0 COST ASSESSMENT

7.1 COST MODEL

In order to evaluate the cost of a potential full-scale bioremediation program, and compare it against other remedial approaches, costs associated with various aspects of the demonstration were tracked throughout the course of the project. Table 7.1 summarizes the various cost elements and total cost of the demonstration project. The costs have been grouped by categories as recommended in the Federal Remediation Technologies Roundtable Guide to Documenting and Managing Cost and Performance Information for Remediation Projects (63). Many of the costs shown on this table are a product of the innovative and technology validation aspects of this project, and would not be applicable to a typical site application. Therefore, a separate “discounted costs” column that excludes or appropriately discounts these costs has been included in Table 7.1 to provide a cost estimate for implementing this technology at the same scale as the demonstration (i.e., pilot scale).

Costs associated with the bioaugmentation for treatment of DNAPL in fractured bedrock demonstration were tracked from April 2012 to November 2016. The total cost of the demonstration was \$1,217,300, which included \$371,500 in capital costs, \$255,100 in operation and maintenance (O&M) costs, and \$590,700 in demonstration-specific costs (cost related to ESTCP requirements, site selection and characterization). A total of approximately 2,618 cubic yards (based on a 30 radius of influence from the single injection well and a 25-foot vertical treatment interval), or 2,115 gallons (assuming a 0.4% fracture porosity) of DNAPL-impacted contaminated aquifer were treated during the demonstration. This corresponds to a unit cost of approximately \$465 per cubic yard or \$575 per gallon of contaminated aquifer (Table 7.1). By excluding an estimated \$638,700 of research-oriented costs (primarily the costs associated with the installation and sampling of extra monitoring wells, down-hole geophysical surveys, contaminant flux investigations, molecular biology studies and ESTCP reporting requirements), unit costs are estimated at approximately \$221 per cubic yard, or \$274 per gallon of DNAPL-impacted contaminated aquifer for a project of this scale (Table 7.1).

7.1.1 Capital Costs

Capital costs (primarily system design and installation) accounted for \$371,500 (or 31 percent) of the total demonstration costs. As indicated in Table 7.1, these costs exceed what would be expected during a typical remediation project due partially to the larger number of performance monitoring wells (8) installed within the relatively small demonstration area versus those anticipated to be required for a more typical project of this scale.

7.1.2 O&M Costs

O&M costs accounted for \$255,100 (or 21 percent) of the total demonstration cost. These costs consisted primarily of groundwater monitoring (including labor, materials and analytical), system O&M, reporting, and travel costs. System O&M costs were \$106,000, or 9 percent of total demonstration costs. The cost of the 605 pounds of sodium lactate product added during the demonstration was \$2,900, or 0.2 percent of total demonstration costs.

Treatment dosage during the demonstration is estimated at approximately 0.23 pounds of sodium lactate product per cubic yard of treated aquifer. Extensive performance monitoring activities were conducted to effectively validate this technology; including 14 groundwater sampling events (2 baseline and 12 performance).

Table 7.1. Demonstration Cost Components

Cost Element	Details	Tracked Demonstration Costs	Discounted Costs ¹
CAPITAL COSTS			
System Design	Labor	\$41,500	\$41,500
	Labor	\$49,500	\$37,000
Well Installation, Development & Surveying ²	Materials	\$16,500	\$12,500
	Subcontracts (driller/surveyor)	\$76,000	\$57,000
System Fabrication & Installation (recirculation system)	Labor	\$75,500	\$75,500
	Equipment & Materials	\$54,500	\$54,500
	Subcontracts (electrical, Conex box/PLC)	\$45,500	\$45,500
	Travel	\$12,500	\$12,500
	Subtotal	\$371,500	\$336,000
OPERATION AND MAINTENANCE COSTS			
Groundwater Sampling ³	Labor	\$54,500	\$27,250
	Materials	\$7,500	\$3,750
Analytical	In-House Labor	\$10,500	\$0
	Outside Labs	\$20,600	\$15,500
System O&M (including testing & start-up)	Labor	\$61,500	\$46,125
	Materials	\$44,500	\$33,375
Utilities	Electric	\$0	\$3,600
Reporting & Data Management	Labor	\$47,500	\$23,750
Travel		\$8,500	\$4,250
	Subtotal	\$255,100	\$157,600
OTHER TECHNOLOGY-SPECIFIC COSTS			
Site Selection	Labor & Travel	\$24,600	\$0
Site Characterization (pump testing, downhole geophysical surveys, microbiological studies, and tracer testing)	Labor (including in-house analytical)	\$46,000	\$20,000
	Materials	\$15,000	\$5,000
	Subcontractors (driller, geophysical, tracer)	\$255,000	\$0
	Travel	\$3,500	\$0
Treatability Testing	Labor (including in-house analytical)	\$24,500	\$0
IPR Meeting & Reporting	Labor & Travel	\$10,500	\$0
Technology Transfer (presentations, papers)	Labor & Travel	\$11,000	\$0
Demonstration Plan/Work Plan	Labor	\$96,500	\$30,000
Final Report	Labor	\$85,600	\$30,000
Cost and Performance Report	Labor	\$18,500	\$0
	Subtotal	\$590,700	\$85,000
	TOTAL COSTS	\$1,217,300	\$578,600
ESTIMATED TREATMENT VOLUME (cubic yards)		2,618	2,618
ESTIMATED TREATMENT VOLUME (gallons)		2,115	2,115
APPROXIMATE TREATMENT COST (per cubic yard)		\$464.97	\$221.01
APPROXIMATE TREATMENT COST (per gallon)		\$575.56	\$273.57

Notes:

¹Discounted costs are defined as estimated costs to implement this technology at the same scale as the demonstration. These costs do not include extensive groundwater sampling, demonstration reporting, interim progress reviews, and preparation of technical and cost and performance reports.

²Demonstration includes 8 bedrock wells to 100 feet (includes 1 injection and 2 extraction wells). 5 bedrock wells are assumed for discounted costing.

³Two baseline and twelve performance monitoring events were performed during the demonstration. Six sampling events are assumed for discounted costing.

7.1.3 Demonstration-Specific Costs

Other demonstration-specific costs (a portion of which are not expected to be incurred during non-research-oriented remediation projects for the most part) accounted for \$590,000 (or 49 percent) of the total demonstration cost. These costs included site selection, laboratory treatability studies, down-hole geophysical surveys, tracer testing to determine DNAPL architecture, molecular biology studies, ESTCP demonstration reporting and meeting (IPR) requirements, and preparation of extensive technical and cost and performance reports.

7.2 COST DRIVERS

7.2.1 General Considerations

The expected cost drivers for installation and operation of a bedrock groundwater recirculation and amendment delivery system for the remediation of contaminated groundwater, and those that will determine the cost/selection of this technology over other options include the following:

- Depth of the DNAPL source below ground surface;
- Width, length, and thickness of the DNAPL source area;
- Aquifer lithology and hydrogeology;
- Regulatory/acceptance of groundwater extraction and re-injection;
- Regulatory considerations concerning secondary groundwater impacts (i.e. metals mobilization, sulfate reduction, etc.);
- Length of time for clean-up (e.g., necessity for accelerated clean-up);
- The presence of indigenous bacteria capable of degrading cVOCs;
- Concentrations of contaminants and alternate electron acceptors (e.g., NO_3^- , SO_4^{2-} and O_2);
- The type(s) of co-substrates determined to be effective at promoting the biodegradation at a given site (i.e. those that are packaged in soluble form vs. those that need to be mixed into solution prior to injection); and
- O&M costs.

As discussed in detail in Section 5.3, microcosm screening and column treatability testing showed that sodium lactate was an effective substrate for promoting biological reduction. Based on the laboratory studies, sodium lactate was chosen as the substrate for field injection.

7.2.2 Competing Treatment Technologies

The two other technologies (in addition to bioaugmentation with groundwater recirculation) that have been shown to treat DNAPL in fractured bedrock at the field scale include (1) Thermal Conductive Heating (TCH) and (2) Active Pump and Treat (P&T) with air stripping and carbon treatment.

TCH vaporizes volatile contaminants, and when coupled with SVE may be an effective means to remove contaminants as shown by ESTCP Project ER-200715 (64). The technology may be limited by the ability to achieve targeted temperature and the ability to remove contaminant from the rock matrix. Important parameters include the type of rock and its fracture porosity and heat capacity. Fracture patterns and their interconnectedness are also important.

Pump and treat technologies provide capture of contaminated groundwater, and above-ground treatment of the extracted water prior to discharge or re-injection into the subsurface. While these systems can provide protection to downgradient receptors if designed properly, they are inefficient at removing contaminant mass from a plume and/or source zone, and often require operation for decades, leading to high overall costs.

Zero-valent iron (ZVI) permeable reactive barriers, biowalls, and biobarriers treat contaminated groundwater as it flows through the wall/barrier. While these approaches can provide protection to downgradient receptors, they are even less effective than P&T at removing contaminant mass from the plume and/or source zone. These technologies are impractical at bedrock sites due to the difficulty of trenching through bedrock.

As previously discussed, bioremediation approaches can be either “active”, where distribution of amendments is achieved using groundwater recirculation, or “passive”, where distribution is accomplished during initial injection and/or via ambient groundwater flow. Active groundwater treatment approaches often involve pairs or groups of injection and extraction wells to recirculate groundwater and effectively distribute injected amendments within the subsurface. Passive treatment approaches generally involve injection of amendments via closely-spaced injection wells or direct-push technology. In each of the above three approaches, a carbon source is typically added in order to promote and maintain the reducing, anoxic conditions and supply carbon needed for *in situ* growth of bacteria capable of degrading target contaminants. A slow-release carbon source such as an emulsified vegetable oil (EVO) is often utilized with passive treatment approaches to reduce injection frequency.

Bioremediation (either active, passive, or semi-passive approaches) can be utilized to treat source areas and diffuse plumes or as a barrier to protect downgradient receptors. For deeper plumes (e.g. >50 ft. bgs) or those that are large or very thick, passive approaches are often not technically feasible and are cost-prohibitive (e.g., injecting passive substrates at closely spaced intervals to > 50 ft bgs). Active or semi-passive treatment systems may be technically and economically more attractive under these conditions. Active or semi-passive treatment approaches may also be better suited for heterogeneous geologies or sites where pH adjustment is required, as groundwater recirculation improves mixing and distribution of injected amendments within the subsurface. Longer treatment time frames, high contaminant concentrations, and secondary reactions may also present conditions favorable for utilizing an active approach, since amendment addition and mixing rates can be adjusted more easily than with passive approaches which often utilize less frequent injection of amendments at high concentrations. However, these approaches may be limited where re-injection of contaminated water with amendments is either prohibited or subject to regulatory injection permits.

7.3 COST ANALYSIS

A thorough cost analysis of various *in situ* treatment approaches, including active-pumping systems, passive systems, and semi-passive designs is provided in Chapter 10 of Krug et al. (2009) (65). Various approaches are compared technically and economically with each other and under a variety of different contamination scenarios. The base case and cost analysis presented in the publication referenced above was modified as a template for the cost analysis of the technology tested during this demonstration, as well as the other technologies discussed above. A cost analysis for the base case was performed for the following technologies:

1. Bioremediation Recirculation System
2. Thermal Conductive Heating
3. Active Pump and Treat

The cost analyses comparing the above approaches are presented below based on a 30-year operating scenario. It should be noted that detailed characterization activities, particularly the partitioning tracer tests discussed earlier in this report, are an important precursor to remediation technology selection and implementation, particularly at fractured bedrock sites. This characterization will allow a more focused remedial approach in specific fracture zones where DNAPL sources reside, reducing the treatment area and ultimately shortening remedial timeframes and potentially realizing significant cost savings for any treatment approach selected.

7.3.1 Base Cost Template

As discussed above, the base case presented in Krug et al. (2009) (65) is modified as a template for the cost analysis of the above technologies/approaches. The base case presents a situation where a bedrock aquifer is contaminated with residual TCE DNAPL (not exceeding 1% of the fracture volume) in the source. The TCE source area plume extends to 150 feet bgs, and is 150 feet long and 60 wide, perpendicular to groundwater flow (**Figure 7.1**). The specific base case site characteristics, including aquifer characteristics and design parameters for each of the remedial approaches analyzed are summarized in **Table 7.2**.

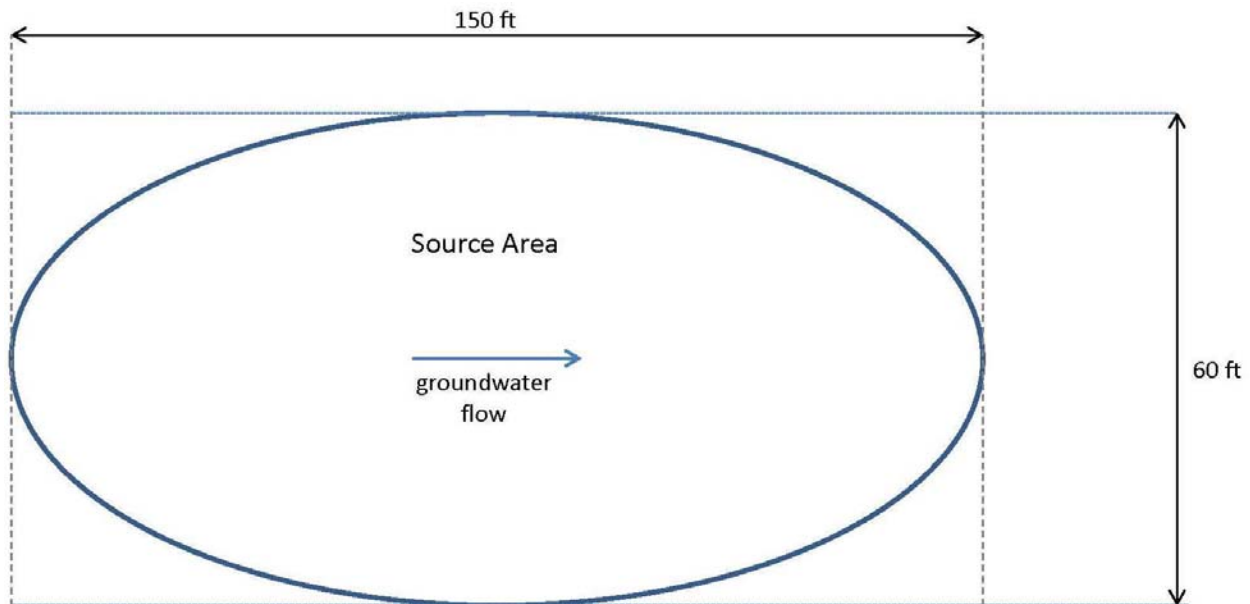


Figure 7.1. Base Plume Characteristics

The following subsections provide cost estimates for implementation of each the three treatment approaches for the base case. The cost estimates provide insight into the comparative capital, O&M, and long term monitoring costs to better identify cost drivers for each technology/ approach.

Total costs and the Net Present Value (NPV) of future costs were calculated for each of treatment approaches. Future costs (O&M and long term monitoring costs) are discounted, using a 2% discount rate, to determine the NPV estimates of these costs. Specifically excluded from consideration are the costs of pre-remedial investigations and treatability studies, assuming the costs for these activities would be similar for each alternative.

Table 7.2. Summary of Base Case Site Characteristics and Design Parameters

Design Parameter	Units	Alternative		
		Bioremediation Recirculation System	Thermal Conductive Heating	Pump and Treat
Width of Plume	feet	60	60	60
Length of Plume	feet	150	150	150
Treatment area	square feet	9000	9000	9000
Upper depth of treatment	feet	0	0	0
Lower depth of treatment	feet	150	150	150
Thickness of overburden	feet	50	50	50
Thickness of bedrock	feet	100	100	100
Porosity	dimensionless	0.05	0.05	0.05
Number of extraction wells	each	6	2	6
Number of injection wells	each	7	0	8
Number of Monitoring Wells	each	6	10	6
Number of heater borings	each	0	52	0
Number of SVE Wells	each	0	52	0
Number of steam injection wells	each	0	8	0
Number temperature monitoring wells	each	0	12	0
Number of pressure monitoring wells	each	0	5	0

7.3.2 Bioremediation Recirculation System

The Bioremediation Recirculation System alternative assumes that two rows of three extraction wells and three row of two or three injection wells will be installed in the source area as shown in Figure 7.2. Groundwater will be recirculated between the rows of extraction and injection wells, and substrate added every 2 months for a period of 3 years, after which time the system will be shut down and decommissioned. This alternative also assumes 30 years of associated long term monitoring costs.

As summarized in Table 7.3, the estimated total costs for this alternative over 30 years are \$1,400,725 with a total NPV of lifetime costs of \$1,299,777. The capital cost including design, work plan, installation of recirculation and monitoring wells, construction of the groundwater recirculation and amendment mixing systems, and system start up and testing are approximately \$511,000.

The NPV of the O&M is estimated at approximately \$388,000 for the 3 years of treatment. The O&M costs include the labor costs associated with regular rounds (every 2 months) of substrate mixing and injection, labor for system O&M, costs for equipment repair and replacement, and cost for substrate. The NPV of the 30 years of monitoring and reporting costs is estimated to be \$401,000.

This alternative ranks lowest in estimated total remedy cost and also lowest in NPV of lifetime costs (see Table 7.6). This technology has both lowest capital costs and the lowest long term O&M costs of the alternatives evaluated.

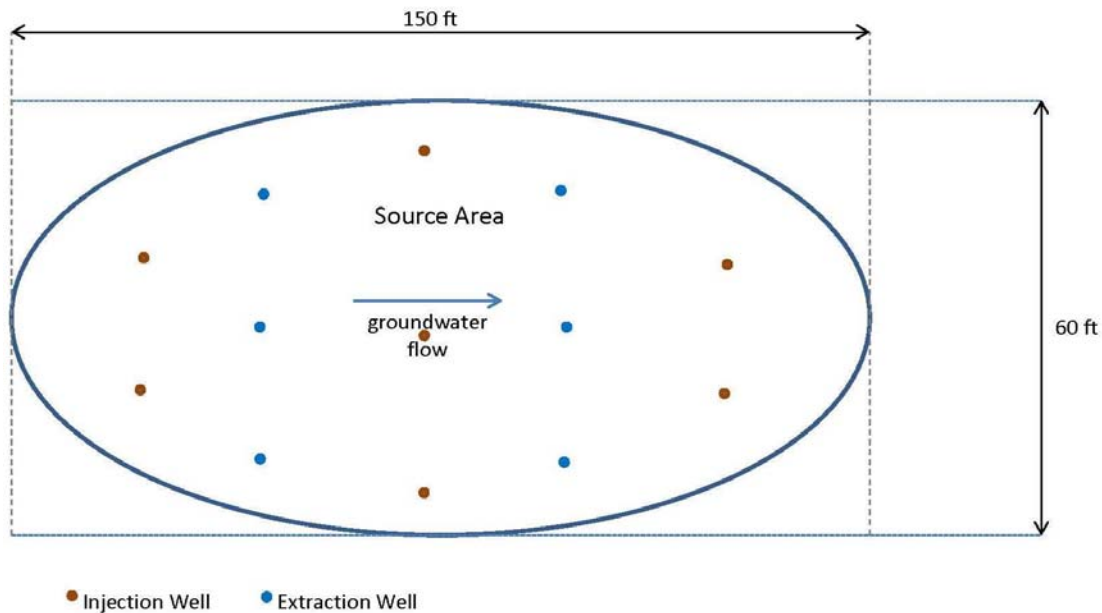


Figure 7.2. Bioremediation Recirculation System Alternative

Table 7.3. Cost Components for Bioremediation Recirculation System

	Year Cost is Incurred							NPV of Costs*	Total Costs
	1	2	3	4	5	6	7 to 30		
CAPITAL COSTS									
System Design	67,142	-	-	-	-	-	-	67,142	67,142
Well Installation	237,738	-	-	-	-	-	-	237,738	237,738
System Installation	188,133	-	-	-	-	-	-	188,133	188,133
Start-up and Testing	17,978	-	-	-	-	-	-	17,978	17,978
SUBCOST (\$)	510,990	-	-	-	-	-	-	510,990	510,990
OPERATION AND MAINTENANCE COSTS									
System Operation and Maintenance	131,833	131,833	131,833	-	-	-	-	387,796	395,500
Decommissioning	-	-	-	117,629	-	-	-	-	-
SUBCOST (\$)	131,833	131,833	131,833	117,629	0	0	0	387,796	395,500
LONG TERM MONITORING COSTS									
Sampling/Analysis/Reporting (Quarterly through 5 years then Annually)	37,002	37,002	37,002	37,002	37,002	12,369	12,369 every year	400,991	494,235
SUBCOST (\$)	37,002	37,002	37,002	37,002	37,002	12,369	12,369	400,991	494,235
TOTAL COST (\$)	679,826	168,835	168,835	154,631	37,002	12,369	12,369	1,299,777	1,400,725

Notes:
NPV - Net Present Value

7.3.3 Thermal Conductive Heating

The conceptual design and cost estimate for the Thermal Conductive Heating alternative are derived from the Cost and Performance Report for ESTCP Project ER-200715 (ESTCP, 2013). The alternative assumes the installation of 51 heater borings and 51 SVE wells installed in an array throughout the source area plume (Figure 7.3). The system will be maintained for a period of 1 year. This alternative also assumes 30 years of associated O&M and long term monitoring costs.

As summarized in Table 7.4, the estimated total costs for this alternative over 30 years are \$5,256,000 with a total NPV of lifetime costs of \$5,150,000. The capital cost including design, work plan, installation of steam injection wells, SVE wells and system infrastructure are approximately \$3,024,000. The NPV of the O&M is estimated at approximately \$1,725,000 for the 1 year of active treatment. The O&M costs primarily include the labor and material costs associated the labor required for system operations. Electrical consumption is a major component of the cost with an estimated cost of \$533,000 over the 1-year operating period. The NPV of the 30 years of monitoring and reporting costs is estimated to be \$401,000.

This alternative ranks highest in estimated total remedy cost and also the highest in NPV of lifetime costs (see Table 7.6). The estimated capital costs for this approach are the highest of the three alternatives because of the extensive infrastructure required. The estimated long term O&M costs associated with operating the system make this one of the highest expensed alternatives, with total remedy costs similar to the pump and treat alternative. As with the other approaches, total remedy costs will increase if the treatment needs to extend beyond 1 year.

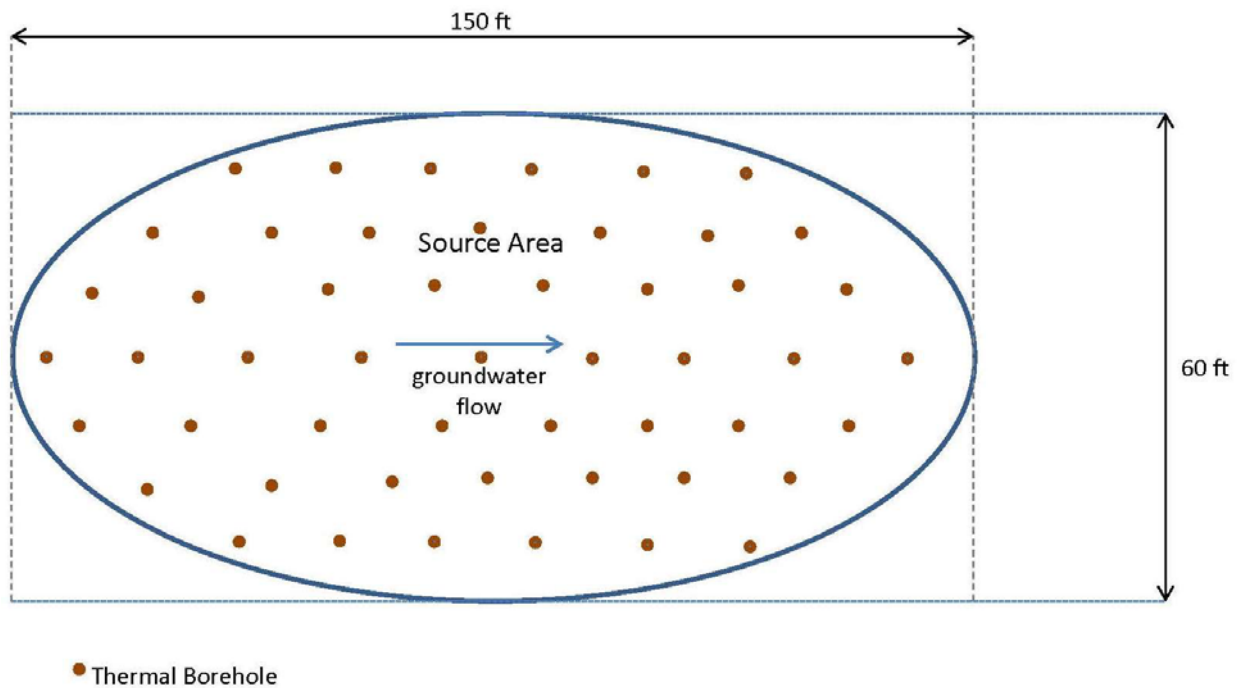


Figure 7.3. Thermal Conductive Heating Alternative

Table 7.4. Cost Components for Thermal Conductive Heating

	Year Cost is Incurred							NPV of Costs*	Total Costs
	1	2	3	4	5	6	7 to 30		
CAPITAL COSTS									
System Design	365,426	-	-	-	-	-	-	365,426	365,426
Well Installation (30 1" PVC Wells)	1,559,000	-	-	-	-	-	-	1,559,000	1,559,000
System installation	1,054,858	-	-	-	-	-	-	1,054,858	1,054,858
Start-up and Testing**	45,000	-	-	-	-	-	-	45,000	45,000
SUBCOST (\$)	3,024,284	-	-	-	-	-	-	3,024,284	3,024,284
OPERATION AND MAINTENANCE COSTS									
System Operation and Maintenance	1,091,485	646,000	-	-	-	-	-	1,724,819	1,737,485
Decommissioning									
SUBCOST (\$)	1,091,485	646,000	-	-	-	-	-	1,724,819	1,737,485
LONG TERM MONITORING COSTS									
Sampling/Analysis/Reporting (Quarterly through 5 years then Annually)	37,002	37,002	37,002	37,002	37,002	12,369	12,369 every year	400,991	494,235
SUBCOST (\$)	37,002	37,002	37,002	37,002	37,002	12,369		400,991	494,235
TOTAL COST (\$)	4,152,771	683,002	37,002	37,002	37,002	12,369		5,150,094	5,256,004

Notes:

NPV - Net Present Value

7.3.4 Active Pump and Treat

The P&T system alternative would include ten source area extraction wells and four injection wells outside the pumping zone of influence (Figure 7.4). In this case the extracted groundwater would be treated above ground by air stripping and passing it through GAC; and the treated groundwater is re-injected providing hydraulic control and mass removal. The pump and treat system will be maintained for a period of 30 years. This alternative also assumes 30 years of associated O&M and long term monitoring costs.

As summarized in Table 7.5, the estimated total costs for this alternative over 30 years are \$3,705,000 with a total NPV of lifetime costs of \$3,019,000. The capital cost including design, work plan, installation of extraction/injection and monitoring wells, construction of the groundwater treatment system, and system start up and testing are approximately \$791,000. The NPV of the O&M is estimated at approximately \$1,826,000. The O&M costs include the labor costs associated with system O&M, costs for equipment repair and replacement, electrical costs, and cost for the replacement and disposal of the GAC. The NPV of the 30 years of monitoring and reporting costs is estimated to be \$401,000.

This alternative ranks second in both estimated total remedy cost and NPV of lifetime costs (Table 7.6). The estimated capital costs for this alternative are higher than those of the bioremediation alternative because of the higher costs associated with constructing a groundwater treatment system, compared to constructing the recirculation system.

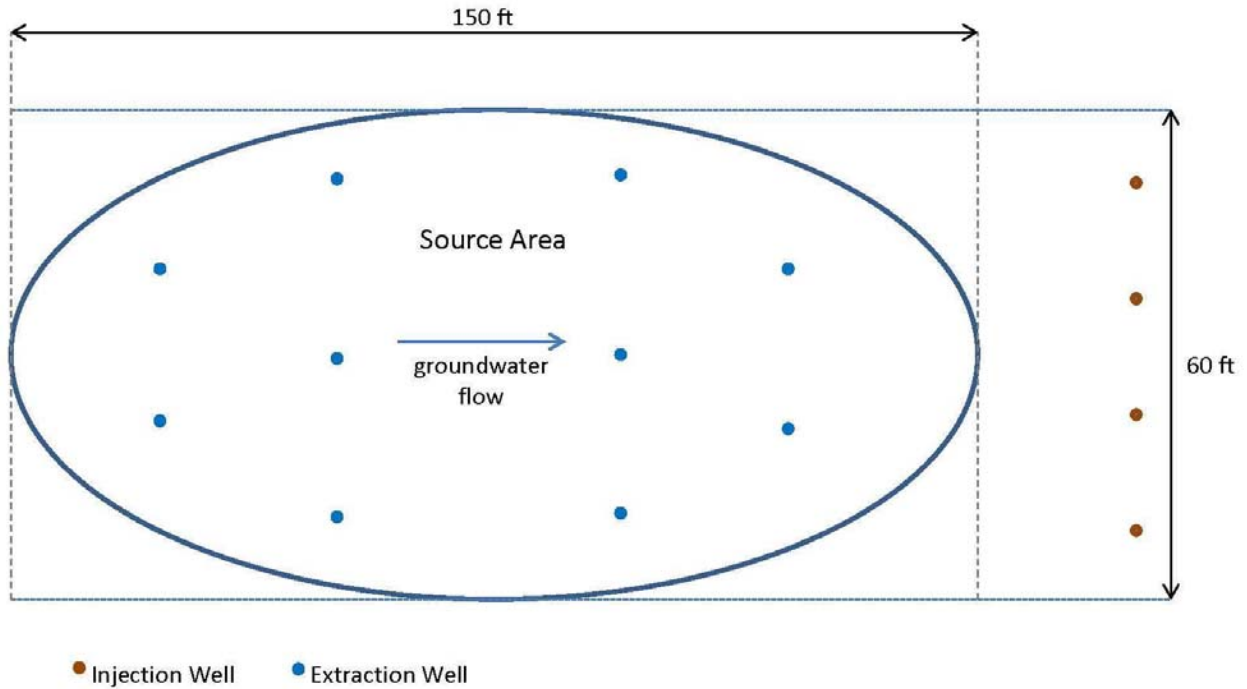


Figure 7.4. Active Pump and Treat Alternative

Table 7.5. Cost Components for Active Pump and Treat

	Year Cost is Incurred							NPV of Costs*	Total Costs
	1	2	3	4	5	6	7 to 30		
CAPITAL COSTS									
System Design	95,142	-	-	-	-	-	-	95,142	95,142
Well Installation	264,738	-	-	-	-	-	-	264,738	264,738
System Installation	405,300	-	-	-	-	-	-	405,300	405,300
Start-up and Testing	26,250	-	-	-	-	-	-	26,250	26,250
SUBCOST (\$)	791,430	-	-	-	-	-	-	791,430	791,430
OPERATION AND MAINTENANCE COSTS									
System Operation and Maintenance	55,809	82,059	82,059	82,059	82,059	82,059	82,059 every year	1,826,527	2,419,834
SUBCOST (\$)	55,809	82,059	82,059	82,059	82,059	82,059		1,826,527	2,419,834
LONG TERM MONITORING COSTS									
Sampling/Analysis/Reporting (Quarterly through 5 years then Annually)	37,002	37,002	37,002	37,002	37,002	12,369	12,369 every year	400,991	494,235
SUBCOST (\$)	37,002	37,002	37,002	37,002	37,002	12,369		400,991	494,235
TOTAL COST (\$)	884,241	119,061	119,061	119,061	119,061	94,428		3,018,947	3,705,498

Notes:

NPV - Net Present Value

* - NPV calculated based on a 2% discount rate

Table 7.6. Summary of Costs for Treatment Alternatives

Alternative	Capital Costs	NPV of 30 Years of O&M Costs	NPV of 30 Years of Monitoring Costs	NPV of 30 Years of Total Remedy Costs	Total 30-Year Remedy Costs
Bioremediation Recirculation System	\$510	\$390	\$400	\$1,300	\$1,400
Thermal Conductive Heating	\$3,020	\$1,720	\$400	\$5,150	\$5,260
Active Pump and Treat	\$790	\$1,830	\$400	\$3,020	\$3,710

Notes:

All costs are in thousands of dollars

NPV - Net Present Value; current value of future costs based on a 2% annual discount rate

Page Intentionally Left Blank

8.0 IMPLEMENTATION ISSUES

The primary issues related to implementation of the DNAPL architecture characterization and bioaugmentation treatment of the DNAPL sources were:

- ***Complexity of the fracture flow paths.*** Despite considerable efforts to characterize the fracture flow field (e.g., hydraulic testing, borehole geophysical testing), anticipating the distribution of tracers and amendments proved challenging. Thus, most of the interpretation of results from this study were limited to within 15 feet of the injection well. Improved methods to cost-effectively determine fracture flow paths remain a high priority for addressing contaminated groundwater in fractured rock.
- ***Multi-level borehole sampling.*** Inflatable packers were used to facilitate multi-level sampling, targeting specific fracture zones, for this demonstration. While this approach worked, the ability to examine more than 3 zones becomes impractical due to the number of packer pass-throughs. Also, there is always concern that the packers become deflated due to leakage (we had the packers connected to a gas tank). While FLUTe has developed a multi-level sampling system for bedrock borehole wells that offers some significant benefits, its use (based on personal experience) is not always cost effective or practical. Development of improved tools for multilevel borehole sampling would be beneficial to bedrock investigation and treatment.
- ***Biofouling within injection wells.*** Biofouling has often been an issue for active bioremediation systems. Not surprisingly, biofouling was a challenge in this demonstration. Unfortunately, the intrinsically low transmissivity of the fracture system limited the effectiveness of well regeneration techniques. Approaches using automated or periodic biocide treatment to limit microbial biomass accumulation within injection wells is likely needed to mitigate this issue in future bioremediation applications.

Page Intentionally Left Blank

9.0 REFERENCES

- (1) Schaefer, C.E., C.W. Condee, S. Vainberg, and R.J. Steffan. Bioaugmentation for chlorinated ethenes using *Dehalococcoides* sp.: comparison between batch and column experiments. *Chemosphere*. **2009**, 75, 141-148.
- (2) Schaefer, C.E., D. Lippincott, and R.J. Steffan. Field scale evaluation of bioaugmentation dosage for treating chlorinated ethenes. *Ground Water Monitoring and Remediation*. **2010**, 113-124.
- (3) Harkness, M.R., A.A. Bracco, M.J. Brennan Jr., K.A. DeWeerd, and J.L. Spivack. Use of bioaugmentation to stimulate complete reductive dechlorination of trichloroethene in Dover soil columns. *Environ. Sci. Technol.* **1999**, 33, 1100-1109.
- (4) Major, D.W., M.L. McMaster, E.E. Cox, E.A. Edwards, S.M. Dworatzek, E.R. Hendrickson, M.G. Starr, J.A. Payne, and L.W. Buonamici. Field demonstration of a successful bioaugmentation to achieve dechlorination of tetrachloroethene to ethene. *Environ. Sci. Technol.* **2002**, 36, 5106-5116.
- (5) Lendvay, J.M., F.E. Löffler, M. Dollhopf, M.R. Aiello, G. Daniels, B.Z. Fathepure, M. Gebhard, R. Heine, R. Helton, J. Shi, R. Krajmalnik-Brown, C.L. Major, Jr., M.J. Barcelona, E. Petrovskis, R. Hickey, J.M. Tiedje, and P. Adriaens. Bioreactive barriers: a comparison of bioaugmentation and biostimulation for chlorinated solvent remediation. *Environ. Sci. Technol.* **2003**, 37, 1422-1431.
- (6) United States Environmental Protection Agency. Demonstration of bioaugmentation of DNAPL through biostimulation and bioaugmentation at Launch Complex 34 Cape Canaveral Air Force station, Florida. **2004**, EPA/540/R-07/007.
- (7) Interstate Technology & Regulatory Council. Overview of in situ bioremediation of chlorinated ethene DNAPL source zones. **2005**, BioDNAPL-1. Washington, D.C.
- (8) Interstate Technology & Regulatory Council. In situ bioremediation of chlorinated ethene DNAPL source zones: case studies. **2007**, BioDNAPL-2. Washington, D.C.
- (9) Yang, Y. and P.L. McCarty. Biologically enhanced dissolution of tetrachloroethene DNAPL. *Environ. Sci. Technol.* **2005**, 34, 2979-2984.
- (10) Adamson, D.T., J.M. McDade, and J.B. Hughes. Inoculation of a DNAPL source zone to initiate reductive dechlorination of PCE. *Environ. Sci. Technol.* **2003**, 37, 2525-2533.
- (11) Amos, B.K., E.J. Suchomel, K.D. Pennell, and F.E. Löffler. Microbial activity and distribution during enhanced contaminant dissolution from a NAPL source zone. *Water Res.* **2008**, 42, 2963-2974.
- (12) Amos, B.K., E.J. Suchomel, K.D. Pennell, and F.E. Löffler. Spatial and temporal distributions of *Geobacter lovleyi* and *Dehalococcoides* spp. during bioenhanced PCE-DNAPL dissolution. *Environ. Sci. Technol.* **2009**, 43, 1977-1985.

- (13) Glover, K.C., J. Munakata-Marr, and T.H. Illangasekare. Biologically enhanced mass transfer of tetrachloroethene from DNAPL in source zones: experimental evaluation and influence of pool morphology. *Environ. Sci. Technol.* **2007**, 41, 1384-1389.
- (14) ITRC, In situ bioremediation of chlorinated ethene DNAPL source zones: Case studies. Washington, D.C., **2007**.
- (15) Mourzenko, V.V., F. Yousefian, B. Kolbah, J.-F. Thovert, P.M. Adler. Solute transport at fracture intersections. *Wat. Resour. Res.* **2002**, 38, 1000-1013.
- (16) Cho, H.J., R.J. Fiacco Jr., and M. Daly. Characterization of crystalline bedrock contaminated by dense nonaqueous liquid. *Ground Water Monitoring and Remediation.* **2008**, 28, 49-59.
- (17) Schaefer, C.E., A.V. Callaghan, J.D. King, and J.E. McCray. Dense nonaqueous phase liquid architecture and dissolution in discretely fractured sandstone blocks. *Environ. Sci. Technol.* **2009**, 43, 1877-1883.
- (18) Schaefer, C.E., R.M. Towne, S. Vainberg, J.E. McCray, and R.J. Steffan. Bioaugmentation for treatment of dense non-aqueous phase liquid in fractured sandstone blocks. *Environ. Sci. Technol.* **2010**, 44, 4958-4964.
- (19) Difilippo, E.L. and M. Brusseau. Time-continuous analysis of mass flux reduction as a function of mass removal at two field sites. SERDP/ESTCP Symposium, **2008**.
- (20) Fure, A.D., J.W. Jawitz, and M.D. Annable. DNAPL source depletion: Linking architecture and flux response. *J. Contam. Hydrol.* 85, 118-140, **2006**.
- (21) Rivett, M. and S. Feenstra, "Dissolution of an emplaced source of DNAPL in a natural aquifer setting", *Environ. Sci. Technol.*, 39, 447-455, **2005**.
- (22) Guilbeault, M.A., B.L. Parker, and J.A. Cherry. Mass and flux distributions from DNAPL zones in sandy aquifers. *Ground Water* 43, 70-86, **2005**.
- (23) AECOM. South AFRL First Five-Year Review Report (Sites 37, 133, 120, and 321) Air Force Research Laboratory Detachment 7 Operable Units 4 and 9 Edwards Air Force Base, California, **2012b**.
- (24) AECOM. Annual Groundwater Monitoring Report for 2010, Sites 37, 120, 133, 162 and 461 (Operable Unit 4) and 325 (Operable Unit 9), **2012a**.
- (25) Dibblee, T.W. Jr. *Geology of the Rogers Lake and Kramer Quadrangles, California: U.S. Geological Survey Bulletin I 089-B, 139, 1960*.
- (26) AECOM. *Annual Groundwater Monitoring Report for 2008, Sites 37, 120, 133, 162, 177, 328, and 461 (Operable Unit 4) and Site 325 (Operable Unit 9), Air Force Research Laboratory, Edwards Air Force Base, CA – FINAL, 2010b*.

- (27) Carlson, Carl S., David A. Leighton, Steven P. Phillips, and Loren F. Metzger. *Regional Water Table (1996) and Water-table Changes in the Antelope Valley Ground-Water Basin, California*. USGS Water-Resources Investigations Report 98-4022, **1998**.
- (28) AECOM. *Environmental Restoration Program, Groundwater Modeling Report for the Northeast AFRL, Air Force Research Laboratory, Operable Unit 4 and 9, Edwards Air Force Base, California*. Draft. Prepared for 95 ABW/CEVR, Edwards AFB, CA and AFCEE/EXEW, Lackland Air Force Base, TX. Orange, CA, **2011**.
- (29) Earth Tech. *Environmental Restoration Program, Site 162 and Site 177/325 In Situ Bioremediation Treatability Study Report, Air Force Research Laboratory, Operable Units 4 and 9, Edwards Air Force Base, California*. Prepared for 95 ABW/EMR, Edwards Air Force Base, CA and AFCEE/EXEW, Brooks City-Base, TX. Long Beach, CA, **2008b**.
- (30) Earth Tech. *Environmental Restoration Program, Site 162 and Site 177/325 In Situ Bioremediation Treatability Study Work Plan Addendum, Air Force Research Laboratory, Operable Units 4 and 9, Edwards Air Force Base, California*. Prepared for 95 ABW/EMR, Edwards Air Force Base, CA and AFCEE/EXEW, Brooks City-Base, TX. Long Beach, CA, **2008c**.
- (31) Earth Tech. *Environmental Restoration Program, Focused Feasibility Study to Support a Technical Impracticability Evaluation/Containment Zone Application for the South AFRL (Sites 37, 133, 120, and 321), Volume I, Text and Appendices, Air Force Research Laboratory, Operable Units 4 and 9, Edwards Air Force Base, California*. Prepared for 95 ABW/CEVR, Edwards AFB, CA and AFCEE/ISM, Brooks City-Base, TX. Long Beach, CA, **2005a**.
- (32) Earth Tech. *Environmental Restoration Program, Site 37 Fractured Bedrock Lime Treatability Study Evaluation Report, Air Force Research Laboratory, Operable Unit 4, Edwards Air Force Base, California*. Prepared for 95 ABW/EMR, Edwards Air Force Base, CA and USACE, Sacramento District, Sacramento, CA. Long Beach, CA, **2008a**.
- (33) Earth Tech. *Environmental Restoration Program, Focused Feasibility Study to Support a Technical Impracticability Evaluation/Containment Zone Application for the South AFRL (Sites 37, 133, 120, and 321), Volume I, Text and Appendices, Air Force Research Laboratory, Operable Units 4 and 9, Edwards Air Force Base, California*. Prepared for 95 ABW/CEVR, Edwards AFB, CA and AFCEE/ISM, Brooks City-Base, TX. Long Beach, CA, **2005c**.
- (34) Brooks, M.C., M.D. Annable et al. Controlled release, blind tests of DNAPL characterization using partitioning tracers. *J. Contam. Hydrol.* 59, 187-210, **2002**.
- (35) Istok, J.D., J.A. Field, M.H. Schroth, B.M. Davis, and V. Dwarakanath. Single-well "Push-Pull" partitioning tracer test for NAPL detection in the subsurface. *Environ. Sci. Technol.* 36, 2708-2716, **2002**.

- (36) Hatfield, K., M.D. Annable, J. Cho, P.S.C. Rao, and H. Klammler. A Direct Passive Method for Measuring Water and Contaminant Fluxes in Porous Media. *Journal of Contaminant Hydrology* Vol. 75, No. 3-4, **2004**, pp. 155-181.
- (37) Annable, M.D., K. Hatfield, J. Cho, H. Klammler, B.L. Parker, J.A. Cherry, and P.S.C. Rao. Field-Scale Evaluation of the Passive Flux Meter for Simultaneous Measurement of Groundwater and Contaminant Fluxes, *Environ. Sci. Technol.* **2005**, 39, 7194-7201.
- (38) Jin, M.; Delshad, M.; Dwarakanath, V.; McKinney, D.C.; Pope, G.A.; Sepehrnoori, K.; Tilburg, C.E.; Jackson, R.E. Partitioning tracer test for detection, estimation, and remediation performance assessment of subsurface nonaqueous phase liquids. *Water Resour. Res.* 1995 31, 1201-1211.
- (39) Annable, M.D., P.S.C. Rao, W.D. Graham, K. Hatfield, and A.L. Wood. Use of Partitioning Tracers for Measuring Residual NAPL: Results from a Field-Scale Test. *Journal of Environmental Engineering*, Vol. 124, No.6, **1998**, pp. 498-503.
- (40) Hartog, N.; Cho, J.; Parker, B.L.; Annable, M.D. Characterization of a heterogeneous DNAPL source zone in the Borden aquifer using partitioning and interfacial tracers: residual morphologies and background sorption. *J. Contam. Hydrol.* 2010 115, 79-89.
- (41) Torlapati, J., T.P. Clement, C.E. Schaefer, C.E., and K.K. Lee. 2012. Modeling *Dehalococcoides* Sp. augmented bioremediation in a single fracture system. *Ground Water Monitoring and Remediation* 32:75-83.
- (42) Schaefer, C.E., E.B. White, G.M. Lavorgna, and M.D. Annable. 2016. Dense nonaqueous-phase liquid architecture in fractured bedrock: implications for treatment and plume longevity. *Environmental Science & Technology* 50:207-213.
- (43) Novak, J.T.; Goldsmith, C.D.; Benoit, R.E.; O'Brien, J.H. Biodegradation of methanol and tertiary butyl alcohol in subsurface systems. *Water Sci. Technol.* 1985 17, 71-85.
- (44) Cho, J.; Annable, M.D.. Characterization of pore scale NAPL morphology in homogeneous sands as a function of grain size and NAPL dissolution. *Chemosphere* 2005 61, 899-908.
- (45) Cápiro, N.L., F.E. Löffler, and K.D. Pennell. 2015. Spatial and temporal dynamics of organohalide-respiring bacteria in a heterogeneous PCE-DNAPL source zone. *Journal of Contaminant Hydrology* 182:78-90.
- (46) Haest, P.J., D. Springael, and E. Smolders. 2010. Dechlorination kinetics of TCE at toxic TCE concentrations: Assessment of different models. *Water Research* 44:332-339.
- (47) Feth, J.H., C.E. Roberson, and W.L. Polzer. *Sources of Mineral Constituents in Water from Granitic Rocks, Sierra Nevada, California and Nevada*. USGS Water-Supply Paper 1535-I, **1964**, 70p.
- (48) Parker, B.L.; Gillham, R.W.; Cherry, J.A. Diffusive disappearance of immiscible-phase organic liquids in fractured geologic media. *Ground Water* 1994 35, 805-820.

- (49) Schaefer, C.E.; Towne, R.M.; Lazouskaya, V.; Bishop, M.E.; Dong, H. Diffusive flux and pore anisotropy in sedimentary rocks. *J. Contam. Hydrol.* 2012, 131, 1-8.
- (50) Boving, T.B.; Grathwohl, P. Tracer diffusion coefficients in sedimentary rocks: correlation to porosity and hydraulic conductivity. *J. Contam. Hydrol.* 2001, 53, 85-100.
- (51) Hao, L; Leaist, D.G. Binary mutual diffusion coefficients of aqueous alcohols. Methanol to 1-heptanol. *J. Chem. Eng. Data* 1996 41, 210-213.
- (52) Jardine, P.M.; Sanford, W.E.; Gwo, J.P.; Reedy, O.C.; Hicks, D.S.; Riggs, J.S.; Bailey, W.B. Quantifying diffusive mass transfer in fractured shale bedrock. *Water Resour. Res.* 1999 35, 2015-2030.
- (53) Lide, D.R. (ed). *CRC Handbook of Chemistry and Physics – 80th edition.* 1999 CRC Press, Boca Raton, FL.
- (54) Seyedabbasi, M.A.; Kulkarni, P.R.; McDade, J.M.; Newell, C.J.; Gandhi, D.; Gallinatti, J.D.; Cocianni, V.; Ferguson, D.J. Matrix diffusion modeling applied to long-term pump-and-treat data: 2. Results from three sites. *Remediation J.* 2013 23, 93-109.
- (55) Rodríguez, D.J.; Kueper, B.H. Specification of matrix cleanup goals in fractured porous media. *Ground Water* 2013 51, 58-65.
- (56) Earth Tech, Inc. Environmental Restoration Program, Record of Decision, South Air Force Research Laboratory, Operable Units 4 and 9, Edwards Air Force Base, California. 2008.
- (57) West, M.R.; Kueper, B.H. Plume detachment and recession times in fractured rock. *Ground Water* 2010, 48, 416-426.
- (58) Wang, F.; Annable, M.D.; Schaefer, C.E.; Ault, T.D.; Cho, J.; Jawitz, J.W. Enhanced aqueous dissolution of a DNAPL source to characterize the source strength function. *J. Contam. Hydrol.* 2014 169, 75–89.
- (59) Schaefer, C.E.; Towne, R.M.; Lippincott, D.R.; Lacombe, P.; Bishop, M.E.; Dong, H. Abiotic dechlorination in rock matrices impacted by long-term exposure to TCE. *Chemosphere* 2015 119, 744-749.
- (60) Longino, B.L.; Kueper, B.H. Nonwetting phase retention and mobilization in rock fractures. *Water Resour. Res.* 1999 35, 2085-2093.
- (61) [Chambon](#), J.C., [M.M. Broholm](#), [P.J. Binning](#), and P.L Bjerg. 2010. Modeling multi-component transport and enhanced anaerobic dechlorination processes in a single fracture–clay matrix system. *Journal of Contaminant Hydrology* [112](#):77–90.
- (62) Manoli, G., J.C. Chambon, J.C., P.L. Bjerg, C. Scheutz, P.J. Binning, and M.M. Broholm. 2012. A remediation performance model for enhanced metabolic reductive dechlorination of chloroethenes in fractured clay till. *Journal of Contaminant Hydrology* 131:64-78.

- (63) Federal Remediation Technologies Roundtable. 1998. Guide to Documenting and Managing Cost and Performance Information for Remediation Projects, Revised Version. EPA 542-B-98-007.
- (64) ESTCP, January 2013, ESTCP Cost and Performance Report (ER-200715) Dense Non Aqueous Phase Liquid (DNAPL) Removal from Fractured Rock Using Thermal; Conductive Heating (TCH).
- (65) Krug, T.A., C. Wolfe, R.D. Norris, and C.J. Winstead. 2009. Cost Analysis of In Situ Perchlorate Bioremediation Technologies. In In Situ Remediation of Perchlorate in Groundwater. H.F. Stroo and C.H. Ward, Eds. SERDP/ESTCP Environmental Remediation Technology.

APPENDIX A POINTS OF CONTACT

Point of Contact Name	Organization Name Address	Phone Fax Email	Role in Project
Charles Schaefer	CDM Smith 110 Fieldcrest Avenue, #8 6th Floor Edison, NJ 08837	732-590-4633 direct 609-332-0346 cell schaeferce@cdmsmith.com	Principal Investigator
Graig Lavorgna	CB&I Federal Services 17 Princess Road Lawrenceville, NJ 08648	609-895-5343 direct 908-309-7651 cell graug.lavorgna@cbifederalservices.com	Project Manager Project Engineer
Michael Annable	University of Florida 1949 Stadium Road 365 Weil Hall Gainesville, FL 32611	352-392-3294 direct 352-278-8693 cell annable@ufl.edu	Technical Support
Erin White	University of Florida 1949 Stadium Road 502 Weil Hall Gainesville, FL 32611	352-443-0082 cell erinw@ufl.edu	Technical Support
Andrea Leeson	SERDP/ESTCP 901 N Stuart Street, Suite 303 Arlington VA 22203	703-696-2118 direct 703-696-2114 fax andrea.leeson@osd.mil	ESTCP Environmental Restoration Program Manager
Nashat Saleh	Edwards Air Force Base Environmental Management 120 N. Rosamond Blvd. Edwards AFB, CA 93524	661-277-1401 main nashat.saleh@us.af.mil	Environmental Coordinator – Edwards Air Force Base

Page Intentionally Left Blank

APPENDIX B BORING LOGS

Page Intentionally Left Blank



BORING NO. 37-B06

Coordinates¹: N.
E.

Project: Edwards AFRC Project Number: 146185 Field Geologist: T. Ault, W. Werner
 Location: Drilling Method: Diamond Core Checked By:
 Drill Co.: Woodward Logging Method: HQ Continuous Core Approved By:
 Driller: Kris Nolan Boring Diameter: 3.78" Total Depth: 115 Feet
 Conductor Borehole Diameter: 10 in. Casing: None
 Conductor Casing Diameter: 6 in. Length: 7 Feet Type: Steel Filter Pack: None

TOC Elev²:
 GS Elev²:
 Date Began: 01/10/2013
 Date Finished: 01/11/2013
 Note 1 NAD 83 CALZ4
 Note 2 NAVD 88 ft amsl

Elevation (ft amsl)	Depth (feet)	Well Completion	Recovery (ft)	% Recovery	% RQD	Joint Spacing	Description	Comments
0							Sandy fill with broken granitic rocks.	Auger with 10" augers to set conductor casing
-1	1.0							
-2	2.0							
-3	3.0							
-4	4.0							
-5	5.0							
-6	6.0						Very coarse gravel and broken granitic rocks, 10% brown sand.	
-7	7.0		6/12	50	0		7-8': Bedrock, fresh to slightly weathered (on fractured surface), yellowish gray, hard, <1% distinct crystal mineral constituents, intergrown and non distinct, <50% biotite, quartz and plagioclase not easily distinguished.	Bedrock Fracture - 80° dip (from horizontal), single plane - distinct, 60% plagioclase, 30% quartz, ~5% k-spar, 5% biotite.
-8	8.0		2.1/3	60	16		8-11': Aphanitic, no distinct crystal forms except biotite, moderately weathered, fractures, surfaces are weathered (iron oxide), two fracture sets through core - break on fractures when drilled, high angle - 3rd lower angle set 60% from vertical.	8-10.5': Core segments w/zones of gravel sized pieces, fractures ~80°
-9	9.0							
-10	10.0							
-11	11.0							
-12	12.0							
-13	13.0		4/4	100	42		11-15': Fresh core, weathered on fractured surfaces, two sets of high angle fractures, one lower angle and minor horizontal fractures - random. 70% plagioclase, 20% k-spar, 8% quartz, 2% biotite.	10.5-15': Up section 8-9" intact, angular breakage to 14', intact 14-15', manganese dendrites, PID=0.0 ppm.
-14	14.0							
-15	15.0							
-16	16.0		2.5/2.5	100	83		15-16.8': Fresh core, hard non-weathered core, weathered on fractures - tertiary fracture set with rotational component joints, spider like. 60% plagioclase, 30% quartz, 10% k-spar.	Fracture sets: -Primary 10° from vertical -Secondary 40°, same azimuth. -Tertiary 20°, azimuth 90° out.
-17	17.0							
-18	18.0							
-19	19.0		2.6/3	86.7	83		16.8-20.5': Core has more fractures generally.	
-20	20.0							
-21	21.0							
-22	22.0							
-23	23.0		4.8/5	96	2.2/5		20.5-26.5': Grayish orange, hard, slightly weathered, generally more intact, fractures weathered, rock mass hard. 60% plagioclase, 10% k-spar, 20% quartz, 10% biotite. weathering rind on fracture	-One major fracture set - filled with quartz -High angle, similar to predominant sets seen above, 90° dip -Horizontal breaks
-24	24.0							
-25	25.0							
-26	26.0							
-27	27.0							
-28	28.0		5/5	100	3.5/5		26.5-30.5': Dark yellowish orange, core largely intact, quartz filled fractures, weathered at 30', large (~1") granular material filled fracture at 30': potential water producing zone, mylonitic sand like material probably from tectonic grinding.	
-29	29.0							
-30	30.0						Potential permeable zone at 30'	



BORING NO. 37-B06

Coordinates¹: N.
E.
TOC Elev²:
GS Elev²:
Date Began: 01/10/2013
Date Finished: 01/11/2013
Note 1 NAD 83 CALZ4
Note 2 NAVD 88 ft amsl

Project: Edwards AFRC Project Number: 146185 Field Geologist: T. Ault, W. Werner
Location: Drill Co.: Woodward Driller: Kris Nolan
Drilling Method: HQ Continuous Core Boring Diameter: 3.78" Total Depth: 115 Feet
Casing: None Filter Pack: None
Conductor Borehole Diameter: 10 in. Length: 7 Feet Type: Steel

Elevation (ft amsl)	Depth (feet)	Well Completion	Recovery (ft)	% Recovery	% RQD	Joint Spacing	Description	Comments
-31	-31.0						30.5-35': Similar to above, higher fracture density between 31' and 35'. Fractures weathered similar to above, mineralogy similar, rock mass inge??? , hard - fresh.	Zone 1-2': -Fracture at 90° and 60°, horizontal fracture also present
-32	-32.0		4.5/4.5	100	1.5/4.5			
-33	-33.0							
-34	-34.0						34': Potential permeable fracture similar to one at 30' but thinner.	Zone 1" or less
-35	-35.0							
-36	-36.0						35-40': Similar to above mineralogically, fractures similar to above but higher angled fractures are healed - no breakage, some breakage near the base of the interval - hard. - Clay filled fracture at 37', significant weathering near the fracture although still hard in strength. -Primary 10° fractures are largely healed, secondary 40° fractures sit at 1/2 to 1' intervals (irregular) - sharp break.	
-37	-37.0		5/5	100	5/5			
-38	-38.0							
-39	-39.0							
-40	-40.0						Not logged.	
-41	-41.0							
-42	-42.0		3.9/4	97.5	0.8/4			
-43	-43.0							
-44	-44.0						Zone at 44': Larger crystal form, loose in appearance from core barrel, may be slough or rubble zone.	44': Possible permeable zone
-45	-45.0		2.6/3	86.7	0.0			
-46	-46.0						46': Thin zone with clay material in a 40° fracture set.	
-47	-47.0							
-48	-48.0						47-51': Similar to above, weathered fracture zone - blocky 1x2" fracture ¹ , thin clay filled fracture at 48' - 1/4" or less.	¹ : Not likely to be permeable. PID=0.0 ppm
-49	-49.0		2.5/4	62.5	1.6			
-50	-50.0							
-51	-51.0							
-52	-52.0						51-56.2': Dark yellowish orange, significant change in rock texture - granular texture, hard, fracture with slickensides at 51.5'. clay filled fracture at 52'/slice of ovely lithology at 53' (1/2 foot) then returns to a coarse grained dark yellow unit. About 1' of coarse grain (53.5'). Fracture at 54.5' to 55', 1/2" filled. Above is loose breccia, possible permeable zone. Below is soil breccia (sm).	Box #5
-53	-53.0		4.5/4.5	100	84			
-54	-54.0							
-55	-55.0						55': Interfingering of fine and coarse grains	
-56	-56.0							
-57	-57.0						56.2-63': Coarse grained unit, hard, dark yellow orange, moderately hard, pinkish gray 5YR81, phaneritic - anastomosing remnants of darker country rock visible in core. 60% k-spar, 20% plagioclase, 15% quartz, 5% biotite and iron oxide. Slightly weathered.	
-58	-58.0		4.5/4.5	100	90			
-59	-59.0							
-60	-60.0							



BORING NO. 37-B06

Coordinates¹: N.
E.

Project: Edwards AFRC Project Number: 146185 Field Geologist: T. Ault, W. Werner
 Location: Woodward Drilling Method: Diamond Core Checked By:
 Drill Co.: Woodward Logging Method: HQ Continuous Core Approved By:
 Driller: Kris Nolan Boring Diameter: 3.78" Total Depth: 115 Feet
 Conductor Borehole Diameter: 10 in. Casing: None
 Conductor Casing Diameter: 6 in. Length: 7 Feet Type: Steel Filter Pack: None

TOC Elev²:
 GS Elev²:
 Date Began: 01/10/2013
 Date Finished: 01/11/2013
 Note 1 NAD 83 CALZ4
 Note 2 NAVD 88 ft amsl

Elevation (ft amsl)	Depth (feet)	Well Completion	Recovery (ft)	% Recovery	% RQD	Joint Spacing	Description	Comments
-61	61.0			See Above				
-62	62.0							
-63	63.0		2.5/3.5	71.4	0		63-64.5': Broken clayey zone, 1-1.5" blocky fragments, clay filled interstites . Probably fracture zone with permeable properties.	Permeable zone.
-64	64.0							
-65	65.0							
-66	66.0						64.5-69.5': Back into competent material, phaneritic, very light gray (N8), strong slightly weathered. 80% k-spar, 5% plagioclase, 10% quartz, 5% biotite, trace iron-oxide.	2 low fracture sets 45% and 15-20°
-67	67.0		5/5	100	2.4/5			
-68	68.0							
-69	69.0							
-70	70.0		1/1.5	66.7	4"/1.5' (0.22)		69.5-71': Rubble zone, may be drill ??? grinding.	Possible rubble zone, easier drilling, poor recovery on next run from 71-75'
-71	71.0						Poor recovery, solid 4" piece at top, platy and weathered below. No recovery over most of the interval.	
-72	72.0							
-73	73.0		1/5	20	0			
-74	74.0							
-75	75.0						75-78': Same as 64.5-69.5'	
-76	76.0							
-77	77.0		4.7/5	94	4/5			
-78	78.0						Distinct contact at 78'	
-79	79.0						78-82': Heavily weathered zone, ground up mylonitic appearance, zones weathered to clay, dark yellow orange (10YR6/6), considerable alteration, very loose, breaks easily with fingers. Very good recovery over the interval.	78-85': Permeable zone
-80	80.0						Intervals contain considerable clay, vertical fractures heavily oxidized.	
-81	81.0						82-85': As above, vertical (85°) fractures still present, 45° fractures not.	
-82	82.0		4.6/5	92	0.9			
-83	83.0							
-84	84.0							
-85	85.0							
-86	86.0		3/3	100	0.6/3		85-88': Intact rock mass - distinct boundary. Hard, dusky yellow green (5GY5/2), 70% plagioclase, 20% quartz, 10% k-spar, minor biotite and iron oxide, moderately weathered.	Fractures 60% only, no 80°
-87	87.0							
-88	88.0							
-89	89.0		5/5	100	1.6/5		88-103': As above, some 80° fractures, fine grained.	
-90	90.0							



BORING NO. 37-B06

Coordinates¹: N.
E.

Project: Edwards AFRC Project Number: 146185 Field Geologist: T. Ault, W. Werner
 Location: Woodward Drilling Method: Diamond Core Checked By:
 Drill Co.: Woodward Logging Method: HQ Continuous Core Approved By:
 Driller: Kris Nolan Boring Diameter: 3.78" Total Depth: 115 Feet
 Conductor Borehole Diameter: 10 in. Casing: None
 Conductor Casing Diameter: 6 in. Length: 7 Feet Type: Steel Filter Pack: None

TOC Elev²:
 GS Elev²:
 Date Began: 01/10/2013
 Date Finished: 01/11/2013
 Note 1 NAD 83 CALZ4
 Note 2 NAVD 88 ft amsl

Elevation (ft amsl)	Depth (feet)	Well Completion	Recovery (ft)	% Recovery	% RQD	Joint Spacing	Description	Comments
-91	91.0			See Above				
-92	92.0							
-93	93.0							
-94	94.0							Fracture 80° at 4 foot spacing horizontal fractures 45%
-95	95.0		5/5	100	2.5/5			
-96	96.0							
-97	97.0							
-98	98.0						End of first run.	
-99	99.0							
-100	100.0		5/5	100				
-101	101.0							
-102	102.0							
-103	103.0							
-104	104.0						103-108': Similar to unit above. Very hard, 2' nearly vertical clay filled fracture (upper 2'). 90% plagioclase, 5% k-spar, 5% quartz.	Fractures in lower segment 70°-60°
-105	105.0		5/5	100	2/5			
-106	106.0							
-107	107.0							
-108	108.0							
-109	109.0						108-112': Similar to above, pale green (10G6/2), very hard, crypto crystalline?	
-110	110.0		5/5	100				
-111	111.0							
-112	112.0						112-113': Hard, dark, even sized micro/macro crystals, in dark ground mass granular texture, sparkles in the sun, medium bluish gray (5B5/1). Mafic dike.	Distinct boundary, sandstone granular texture.
-113	113.0						113': End of second run.	
-114	114.0						113-115': Hard, similar to plagioclase rich rock (country rock) above. Thin two inch stringer of mafic dike material 0.4' below the top of the run, conclusion is that mafic material is an intrusive dike.	
-115	115.0						TD=115'	
-116	116.0							
-117	117.0							
-118	118.0							
-119	119.0							
-120	120.0							



BORING NO. 37-B07

Coordinates¹: N.
E.

Project: Edwards AFRC Project Number: 146185 Field Geologist: T. Ault
 Location: Drilling Method: Diamond Core Checked By:
 Drill Co.: Woodward Logging Method: HQ Continuous Core Approved By:
 Driller: Kris Nolan Boring Diameter: 3.78" Total Depth: 95.5 Feet
 Conductor Borehole Diameter: 10 in. Casing: None
 Conductor Casing Diameter: 6 in. Length: 8 Feet Type: Steel Filter Pack: None

TOC Elev²:
 GS Elev²:
 Date Began: 01/17/2013
 Date Finished: 01/18/2013
 Note 1 NAD 83 CALZ4
 Note 2 NAVD 88 ft amsl

Elevation (ft amsl)	Depth (feet)	Well Completion	Recovery (ft)	% Recovery	% RQD	Joint Spacing	Description	Comments
0								Hand Auger to 5'
-1	1.0							
-2	2.0							
-3	3.0						3-8': Start drilling, grout in boring.	
-4	4.0							
-5	5.0							
-6	6.0							Top of ????
-7	7.0							
-8	8.0		5/5	100	1/5		Top of bedrock 8-8.5': Hard, 90% plagioclase, 10% k-spar, fractured, non-weathered. 8.5-14': Medium hard, weathered, moderately medium bluish gray, 30% k-spar, 60% plagioclase, 5% quartz, 5% biotite.	Top of ???? Light bluish gray ????
-9	9.0							
-10	10.0							
-11	11.0							Core pinkish ????
-12	12.0							
-13	13.0		5/5	100	2.4/5			
-14	14.0							
-15	15.0							Base of ????
-16	16.0							
-17	17.0							
-18	18.0		4.5/5	90%	0.7/5		Fracturing at 45° and 90° 18-19': Coarse crystalline, brutal backs, 60% plagioclase, 30% k-spar, 10% biotite/quartz, fractured. 19-21': 80% plagioclase, 10% k-spar, 5% quartz, 5% biotite, moderately weathered. 1-2" coarse grained rubble zone at 20'. 21-25': Moderately hard, some what weathered upon fractures, medium gray, 60% k-spar, 40% plagioclase, trace quartz and biotite, light bluish gray (5B7/1) on fresh fractures, platy biotite.	
-19	19.0							
-20	20.0							
-21	21.0							
-22	22.0		4.5/5	90%	1/5			Core is yellowish gray (5Y8/1)
-23	23.0							
-24	24.0							
-25	25.0						25-26.5': Greenish tint to core at base, 60% k-spar, 30% plagioclase, 5% quartz, 5% biotite. Rubble zone at base, some clay 4" thick.	Hole tagged at 25.5
-26	26.0							
-27	27.0							
-28	28.0		4.8/5	96%	4.5/5		26.5-32': Hard, pale reddish purple on fractured face (5RP6/2), fewer fractures, minerals not well segregated, estimated 65% plagioclase, 30% k-spar, 5% biotite. Fresh surface bluish grain in white, slightly weathered.	
-29	29.0							
-30	30.0							



BORING NO. 37-B07

Coordinates¹: N.
E.

Project: Edwards AFRC Project Number: 146185 Field Geologist: T. Ault
 Location: Woodward Drilling Method: Diamond Core Checked By:
 Drill Co.: Woodward Logging Method: HQ Continuous Core Approved By:
 Driller: Kris Nolan Boring Diameter: 3.78" Total Depth: 95.5 Feet
 Conductor Borehole Diameter: 10 in. Casing: None
 Conductor Casing Diameter: 6 in. Length: 8 Feet Type: Steel Filter Pack: None

TOC Elev²:
 GS Elev²:
 Date Began: 01/17/2013
 Date Finished: 01/18/2013
 Note 1 NAD 83 CALZ4
 Note 2 NAVD 88 ft amsl

Elevation (ft amsl)	Depth (feet)	Well Completion	Recovery (ft)	% Recovery	% RQD	Joint Spacing	Description	Comments
-31	31.0							
-32	32.0							
-33	33.0		5.5/5.5	100	4/5.5		32-40': Fractured randomly - many heated with iron oxide stain. Fracture at 45°, same mineralogy as above, light gray on fresh fractures (5B7/1).	
-34	34.0							
-35	35.0							
-36	36.0							
-37	37.0							
-38	38.0		5/5	100	4.5/5			
-39	39.0							
-40	40.0							
-41	41.0						40-46': Distinct change to coarse grained rock matrix, 80% k-spar, 10% plagioclase, 5% quartz, 5% biotite, dark yellowish orange (10YR6/6), very granular, ????, 1-2" clay zones, interstitial iron oxide stains, loose coarse sand sized grains at base.	Contact: change to weathered coarse grains.
-42	42.0		3/3	100	0.5/3			
-43	43.0							
-44	44.0							
-45	45.0							
-46	46.0							
-47	47.0		4/6	66.7	2/6		46-48': Hard, medium bluish gray (5B) on fresh fracture, 90% plagioclase.	Contact: appears to intrude into bluish gray.
-48	48.0						48': Contact	
-49	49.0						48-56' grades back to coarse grained. 60% k-spar, 30% plagioclase, 5% quartz, trace epidote, small flex, minor biotite and manganese, moderately weathered.	
-50	50.0							
-51	51.0							
-52	52.0		5/5	100	1.5/5			
-53	53.0							
-54	54.0							
-55	55.0							
-56	56.0							
-57	57.0		5/5	100	2.5/5		56-60': Dark yellowish orange (10YR5/6), soft, very weathered, 90% k-spar, granular, coarse grained sand like zone at 59.5'.	Contact at 56'
-58	58.0							
-59	59.0							
-60	60.0							59.5-60': Permeable zone
				See below				



BORING NO. 37-B07

Coordinates¹: N.
E.

Project: Edwards AFRC Project Number: 146185 Field Geologist: T. Ault
 Location: Drilling Method: Diamond Core Checked By:
 Drill Co.: Woodward Logging Method: HQ Continuous Core Approved By:
 Driller: Kris Nolan Boring Diameter: 3.78" Total Depth: 95.5 Feet
 Conductor Borehole Diameter: 10 in. Length: 8 Feet Type: Steel
 Conductor Casing Diameter: 6 in. Filter: None
 Casing Pack: None

TOC Elev²:
 GS Elev²:
 Date Began: 01/17/2013
 Date Finished: 01/18/2013
 Note 1 NAD 83 CALZ4
 Note 2 NAVD 88 ft amsl

Elevation (ft amsl)	Depth (feet)	Well Completion	Recovery (ft)	% Recovery	% RQD	Joint Spacing	Description	Comments
-61	61.0						60-65': Dark yellowish orange (10YR5/6), same as above, hard at 60', vertical iron oxide filled fracture. Clayey zone starts at 63' in fracture, core is very soft at 63'	
-62	62.0							
-63	63.0		5/5	100	3/5			63': PID=19 ppm PIDA (598-76-1) 76-1 sample taken at 63' 64': PID=5.2 ppm
-64	64.0							
-65	65.0						65-69.5': Solid again by 65'. Hard, few fractures, granular, small size, slightly weathered, iron oxide stains in rock mass, 80% k-spar, 15% plagioclase, 5% oxides, fine grained mafics and iron.	
-66	66.0							
-67	67.0		4.5/4.5	100	3.4/4.5			
-68	68.0							
-69	69.0							
-70	70.0		0.4/0.5	80	0		69.5-70': Chert like on surface of fracture, may be a quartz vein. 70-74.5': Hard, medium bluish gray stained fine grains.	Short run - 1/2 foot Fracture map below 70' only
-71	71.0						4" dark granular (fine) mafic material, greenish black, crumbles in hand at 71.5' (mafic dike)	70': 30% plagioclase, 10% k-spar, ?% quartz, moderately weathered.
-72	72.0		4.7/5	94	1.7/5			71.5': PID=0.2 ppm 71.5': 5G2/1
-73	73.0							
-74	74.0							
-75	75.0						74.5-77': Weathered, coarse grained, large biotite books (phenocrysts), 65% k-spar, 30% plagioclase, 5% biotite, grayish orange, granular texture, moderately weathered. Ferro fractures buttons present are distinct with iron oxide full, 80% biotite books disappear below 76', fracture surfaces appear very coarse.	Contact - crumbly 74.5': 10YR7/4 (6" zone) granite? - granular
-76	76.0							
-77	77.0		4.6/5	92	NA		77-79.5': ??? plagioclase dominated, light bluish gray (5B7/1), unweathered.	Dipping at 77' Contact
-78	78.0							
-79	79.0							
-80	80.0						79.5-80': 90% plagioclase, 10% k-spar, 5% quartz, 5% biotite. 80-81': Contact at 80'. Granular feature, 80% k-spar, 15% plagioclase, 5% or less of quartz, weathered.	Coarse feature unweathered Contact at 80', return to granular granite
-81	81.0						81-84': Contact at 81'. 95% plagioclase, 5% quartz, hard, light bluish gray, (5B7/1), unweathered.	
-82	82.0		5/5	100	3.9/5			
-83	83.0							
-84	84.0						84-85': hard, un weathered, light greenish gray (5G8/1).	
-85	85.0							
-86	86.0						85-95.5': Wet core, grayish orange (10YR7/4), moderately weathered, 85% k-spar, 10% plagioclase, 5% quartz	Change back to k-spar rich material
-87	87.0							
-88	88.0		4.5/5.5	81.8	3.3/5.5		87': Slickensides on fracture, 45° fractures, granular texture, iron oxide on rock mass surfaces.	
-89	89.0							
-90	90.0							90.5' tagged by driller



BORING NO. 37-B07

Coordinates¹: N.
E.

Project: Edwards AFRC Project Number: 146185 Field Geologist: T. Ault
 Location: Drilling Method: Diamond Core Checked By:
 Drill Co.: Woodward Logging Method: HQ Continuous Corr Approved By:
 Driller: Kris Nolan Boring Diameter: 3.78" Total Depth: 95.5 Feet
 Conductor Borehole Diameter: 10 in. Casing: None
 Conductor Casing Diameter: 6 in. Length: 8 Feet Type: Steel Filter Pack: None

TOC Elev²:
 GS Elev²:
 Date Began: 01/17/2013
 Date Finished: 01/18/2013
 Note 1 NAD 83 CALZ4
 Note 2 NAVD 88 ft amsl

Elevation (ft amsl)	Depth (feet)	Well Completion	Recovery (ft)	% Recovery	% RQD	Joint Spacing	Description	Comments
-91	91.0							
-92	92.0							
-93	93.0		2.5/5	50	0.7			
-94	94.0							
-95	95.0							
-96	96.0						TD=95.5'	
-97	97.0							
-98	98.0							
-99	99.0							
-100	100.0							
-101	101.0							
-102	102.0							
-103	103.0							
-104	104.0							
-105	105.0							
-106	106.0							
-107	107.0							
-108	108.0							
-109	109.0							
-110	110.0							
-111	111.0							
-112	112.0							
-113	113.0							
-114	114.0							
-115	115.0							
-116	116.0							
-117	117.0							
-118	118.0							
-119	119.0							
-120	120.0							



BORING NO. 37-B08

Coordinates¹: N.
E.

Project: Edwards AFRC Project Number: 146185 Field Geologist: T. Ault/W. Werner
 Location: Woodward Drilling Method: Diamond Core Checked By:
 Drill Co.: Kris Nolan Logging Method: HQ Continuous Core Approved By:
 Driller: Kris Nolan Boring Diameter: 3.78" Total Depth: 101 Feet
 Conductor Borehole Diameter: 10 in. Length: 24 Feet Type: Steel Casing: None
 Conductor Casing Diameter: 6 in. Filter Pack: None

TOC Elev²:
 GS Elev²:
 Date Began: 01/22/2013
 Date Finished: 01/23/2013
 Note 1 NAD 83 CALZ4
 Note 2 NAVD 88 ft amsl

Elevation (ft amsl)	Depth (feet)	Well Completion	Recovery (ft)	% Recovery	% RQD	Joint Spacing	Description	Comments
-31	31.0							
-32	32.0							31'-41': Poor recovery, ground up by bit, etc.
-33	33.0		2.5/5	50	0			
-34	34.0							
-35	35.0							
-36	36.0							
-37	37.0							
-38	38.0		1/5	20	0			
-39	39.0							
-40	40.0							
-41	41.0							
-42	42.0						Granite and clay, yellowish gray (5Y5/2), pieces of broken granite in a white-yellow clay matrix.	41'-46': Lots of clay coming up in mud pan, poor recovery.
-43	43.0		1/5	20	0			
-44	44.0							
-45	45.0							
-46	46.0						Multiple parallel high angle fractures, somewhat clay filled.	
-47	47.0		2/2.5	80	10			
-48	48.0							
-49	49.0						Broken granite, yellowish gray (5Y8/1).	
-50	50.0		1/2.5	40	0			
-51	51.0							
-52	52.0		2.2/2.5	88	16			
-53	53.0							
-54	54.0							
-55	55.0		2.4/2.5	96	0			
-56	56.0							
-57	57.0							
-58	58.0							
-59	59.0		3.5/5	70	36			
-60	60.0							



BORING NO. 37-B08

Coordinates¹: N.
E.

Project: Edwards AFRC Project Number: 146185 Field Geologist: T. Ault/W. Werner
 Location: Drill Co.: Woodward Logging Method: HQ Continuous Core Approved By: TOC Elev²:
 Driller: Kris Nolan Boring Diameter: 3.78" Total Depth: 101 Feet GS Elev²:
 Conductor Borehole Diameter: 10 in. Length: 24 Feet Type: Steel Casing: None Date Began: 01/22/2013
 Conductor Casing Diameter: 6 in. Filter Pack: None Date Finished: 01/23/2013
 Note 1 NAD 83 CALZ4
 Note 2 NAVD 88 ft amsl

Elevation (ft amsl)	Depth (feet)	Well Completion	Recovery (ft)	% Recovery	% RQD	Joint Spacing	Description	Comments
-61	61.0							
				See above				
-62	62.0		2.5/2.5	100	0			
-63	63.0							
-64	64.0						Numerous thin clay filled fractures from 45 to 25 degrees from vertical.	
-65	65.0		2.5/2.5	100	0			
-66	66.0						Almost completely altered to clay, yellowish gray (5Y7/2).	
-67	67.0							
-68	68.0		4.5/5	90	0			
-69	69.0							
-70	70.0							
-71	71.0							
-72	72.0						As above, 71' to 72' is clay, dusky yellow (5Y6/4), red contact at 72.5', dark reddish brown (10R3/4) then back to yellowish gray, biotite still present.	
-73	73.0		5/5	100	0			
-74	74.0							
-75	75.0							
-76	76.0						As above - granitic clay.	
-77	77.0							
-78	78.0		5/5	100	0			
-79	79.0							
-80	80.0							
-81	81.0							
-82	82.0						As above, slightly less altered to clay but still easily broken by hand.	
-83	83.0		5/5	100	0			
-84	84.0							
-85	85.0							
-86	86.0						As above except with green vertical seam, slightly harder.	0.6/0.7 ppm
-87	87.0							
-88	88.0		5/5	100	0			
-89	89.0							
-90	90.0							



BORING NO. 37-B08

Coordinates¹: N.
E.

Project: Edwards AFRC Project Number: 146185 Field Geologist: T. Ault/W. Werner
 Location: Woodward Drilling Method: Diamond Core Checked By:
 Drill Co.: Woodward Logging Method: HQ Continuous Core Approved By:
 Driller: Kris Nolan Boring Diameter: 3.78" Total Depth: 101 Feet
 Conductor Borehole Diameter: 10 in. Casing: None
 Conductor Casing Diameter: 6 in. Length: 24 Feet Type: Steel Filter Pack: None

TOC Elev²:
 GS Elev²:
 Date Began: 01/22/2013
 Date Finished: 01/23/2013
 Note 1 NAD 83 CALZ4
 Note 2 NAVD 88 ft amsl

Elevation (ft amsl)	Depth (feet)	Well Completion	Recovery (ft)	% Recovery	% RQD	Joint Spacing	Description	Comments	
-91	91.0		See above				As above.		
-92	92.0								
-93	93.0		5/5	100	0				
-94	94.0								
-95	95.0								
-96	96.0					As above, clay, hard section at 98', very few fractures.			0.4 ppm
-97	97.0								
-98	98.0		5/5	100	0				
-99	99.0								
-100	100.0								
-101	101.0						Total depth = 101'		
-102	102.0								
-103	103.0								
-104	104.0								
-105	105.0								
-106	106.0								
-107	107.0								
-108	108.0								
-109	109.0								
-110	110.0								
-111	111.0								
-112	112.0								
-113	113.0								
-114	114.0								
-115	115.0								
-116	116.0								
-117	117.0								
-118	118.0								
-119	119.0								
-120	120.0								



BORING NO. 37-B09

Coordinates¹: N.
E.

Project: Edwards AFRC Project Number: 146185 Field Geologist: T. Ault/W. Werner
 Location: Drilling Method: Diamond Core Checked By: TOC Elev²:
 Drill Co.: Woodward Logging Method: HQ Continuous Core Approved By: GS Elev²:
 Driller: Kris Nolan Boring Diameter: 3.78" Total Depth: 89 Feet Date Began: 01/16/2013
 Conductor Borehole Diameter: 10 in. Casing: None Date Finished: 01/16/2013
 Conductor Casing Diameter: 6 in. Length: 16.5 Feet Type: Steel Filter Pack: None Note 1 NAD 83 CALZA
 Note 2 NAVD 88 ft amsl

Elevation (ft amsl)	Depth (feet)	Well Completion	Recovery (ft)	% Recovery	% RQD	Joint Spacing	Description	Comments
-31	31.0		See above				Dark yellowish orange, brittle, heavily tectonized, brittle zones, granular material, slickensides.	
-32	32.0							
-33	33.0		1.4/5?	93?	0.2			
-34	34.0							
-35	35.0							
-36	36.0							
-37	37.0		3/3?	100?	0.16		Hard, dense, fine grained, 45 degree fracture, moderately weathered, distinct 45 degree slickenside, 50% k-spar, 50% plagioclase.	
-38	38.0							
-39	39.0						70% plagioclase.	
-40	40.0		2/2.5?	80?	0.16		Green layer at 38.5', distinct slickenside, rubbly below, pale purple on fracture and rock mass, clay filled fractures.	
-41	41.0							
-42	42.0		1.5/2.5?	0.6?	0		60 degree fracture set, weathered, 70% k-spar, 30% plagioclase.	
-43	43.0							
-44	44.0		0.5/0.5	100	0		Grades into 90% plagioclase, 10% quartz - then to equal parts plagioclase and k-spar with biotite.	
-45	45.0		1.7/2.5	68	0		44': 80% plagioclase, 5% k-spar, 5% quartz, brownish gray on fractures, blue deposit in fracture, globs?	
-46	46.0						6" rubble zone.	7.7 ppm
-47	47.0						Fractured, hard matrix, ~50% fractures and loose , 9% broken up, fractures have green, mineralogy same as above.	
-48	48.0		1.6/2.5	64	0			
-49	49.0						Thin rubble zone, clasts moderate pale reddish brown (10R5/4) zone, clay weathered ground mass, very soft, sediment like , blue paint chip minerals, pale yellowish brown with dark gray.	Driller indicates soft drilling at 48'.
-50	50.0		2/2	100	1/2		1" rubble zone at 50'.	
-51	51.0						Iron oxide through out rock mass, 80% k-spar, 15% plagioclase and 5% quartz at 51', 5% biotite, zones of higher plagioclase, difficult to get a fresh sample surface.	45 ppm 33 ppm 52 ppm
-52	52.0						Fractured rock, semi broken coarse rubble at 51.5',	1 ppm 1 ppm
-53	53.0		3/3.5	86	0		90% plagioclase, 5% k-spar, 5% quartz.	
-54	54.0						6" rubble zone at 54', clay to coarse sand sized material, rock matrix weathered, difficult to get a fresh sample surface.	Permeable zone , 31 ppm
-55	55.0						54.5': Texture change, fractured but healed, 80% distinct fractures, 1.5 foot interval is clay filled on distinct fractures, weathered, difficult to determine mineralogy, appears to be 60% k-spar, 45% plagioclase, 5% quartz , 1/4 inch distinct clay fracture at about 57'.	Moderately hard, crumbles when hit repeatedly
-56	56.0		3.5/3.5	100	1.6			
-57	57.0							7 ppm 0.4 ppm
-58	58.0						Less weathered at base, 70% k-spar, 35% plagioclase , moderately hard at 58', light yellowish gray (5Y8/1), to light greenish gray (5GY8/1), moderately granular, not heavily weathered.	0.1 ppm Minor slickensides
-59	59.0							
-60	60.0		4.9/5	98	2.8/5		Biotite ???	



BORING NO. 37-B09

Coordinates¹: N.
E.

Project: Edwards AFRC Project Number: 146185 Field Geologist: T. Ault/W. Werner TOC Elev²:
 Location: Drilling Method: Diamond Core Checked By: GS Elev²:
 Drill Co.: Woodward Logging Method: HQ Continuous Core Approved By: Date Began: 01/16/2013
 Driller: Kris Nolan Boring Diameter: 3.78" Total Depth: 89 Feet Date Finished: 01/16/2013
 Conductor Borehole Diameter: 10 in. Casing: None Note 1 NAD 83 CALZ4
 Conductor Casing Diameter: 6 in. Length: 16.5 Feet Type: Steel Filter Pack: None Note 2 NAVD 88 ft amsl

Elevation (ft amsl)	Depth (feet)	Well Completion	Recovery (ft)	% Recovery	% RQD	Joint Spacing	Description	Comments
-61	61.0						See above	
-62	62.0						Distinct slickenside with ??? At 62'. 60% k-spar, 40% plagioclase, 10% quartz, minor ???	
-63	63.0						Coarse grained, weathered, texture change, some ??? residual crystals, may be ??? Plagioclase, dark yellowish brown (10YR5/4).	contact, coarse to fine grained.
-64	64.0		2/3	67	1.2/3		63.5': Hard, medium bluish gray (5B5/1), fine grained.	
-65	65.0						6" fracture zone at 65', blocky fracture 0.5" to 1", 90% plagioclase, 5% k-spar, 5% quartz, occasional zeolite crystal.	2 ppm
-66	66.0						Pale yellow brown, slightly weathered.	
-67	67.0		2.8/3	93	0.5		Rubble zone, distinct clay filled fracture, 1 foot zone of coarse sand sized material, clay rich.	7 ppm.
-68	68.0						K-spar rich material, 80% k-spar, 15% plagioclase, 5% quartz, moderate yellow brown, moderately weathered.	67.5' - 68': Permeable zone.
-69	69.0						Hard, slightly weathered, irregular fractures, weathered zone at 72', dark yellow orange, 60% k-spar, 35 % plagioclase, 5% quartz.	68': Contact - possible fault/ fracture plane 69': Note change to plagioclase %.
-70	70.0		3.2/4	80	0.8/2			
-71	71.0							
-72	72.0						6" fracture zone - solid blocks bounded by clay filled fractures.	72' - 72.5' some potential for permeation (question)
-73	73.0						85% k-spar, 10% plagioclase, 5% quartz.	
-74	74.0						Distinct green slickensides from 74' to 75', grayish green (10GY5/2).	
-75	75.0		3.6/5	72	1.2		Very pale orange (10YR8/2) rock mass generally, 2" clay and sand sized material filled fracture at 75' - very pale orange. Green color on fracture surface.	Thin permeable zone.
-76	76.0							
-77	77.0							
-78	78.0						Granular clay rich weathered zone, loose, wet, dusky yellow orange (10YR4/6).	77.5' - 78': permeable zone, 3.0 ppm, 26.3 ppm in glove.
-79	79.0						78'-83': Suspect much of the material is lost due to soft character.	78': 6.8 ppm
-80	80.0		2.5/5	50	1.2			
-81	81.0						Distinct thick iron oxide filled fracture, solid material, sandstone ???, hard, fine sand, granular texture, weathered, rock mass is light greenish gray (5GY8/1).	
-82	82.0							
-83	83.0						Coarse granular clayey permeable material, ??? ???, clayey, granular, epidote gives green ??? at 83' and transitions to granular clay. See above.	82.5' - 83': Permeable zone.
-84	84.0						Poor recovery - recovered material hard, broken up, rock core base grayish green (5G5/2), weathered, minerals difficult to distinguish, fresh break is grayish orange (10YR7/4), 70% k-spar, 25% plagioclase, 5% quartz, all exposed surfaces have a green color.	Solvent odor.
-85	85.0		1.5/6	25	0			
-86	86.0							
-87	87.0							
-88	88.0							
-89	89.0						Well TD = 89 feet bgs.	
-90	90.0							



BORING NO. 37-B10

Coordinates¹: N.
E.

Project: Edwards AFRC Project Number: 146185 Field Geologist: M. Glas, T. Ault
 Location: Drilling Method: Diamond Core Checked By:
 Drill Co.: Woodward Logging Method: HQ Continuous Corr Approved By:
 Driller: Kris Nolan Boring Diameter: 3.78" Total Depth: 106 Feet
 Conductor Borehole Diameter: 10 in. Casing: None
 Conductor Casing Diameter: 6 in. Length: 12 Feet Type: Steel Filter Pack: None

TOC Elev²:
 GS Elev²:
 Date Began: 12/13/2013
 Date Finished: 12/16/2013
 Note 1 NAD 83 CALZ4
 Note 2 NAVD 88 ft amsl

Elevation (ft amsl)	Depth (feet)	Well Completion	Recovery (ft)	% Recovery	% RQD	Joint Spacing	Description	Comments
0							0-12" Top soil (asphalt surface).	Air Knife to 5'
-1	1.0							
-2	2.0							
-3	3.0							
-4	4.0							
-5	5.0							
-6	6.0							
-7	7.0							
-8	8.0							
-9	9.0							
-10	10.0							
-11	11.0							
-12	12.0							
-13	13.0						12-16': Highly fractured granitic rock. No recovery from 13.5-16'.	PID = 0.6 ppm 0.0 ppm 0.0 ppm
-14	14.0							
-15	15.0							
-16	16.0						16-21': Fractured granitic rock. Rubble zone from 16-16.5'.	0.0 ppm 0.7 ppm 0.0 ppm 0.0 ppm 0.0 ppm 0.0 ppm
-17	17.0							0.0 ppm
-18	18.0							0.0 ppm
-19	19.0							0.0 ppm
-20	20.0							0.0 ppm
-21	21.0							0.0 ppm
-22	22.0						Solid rock core, light blue-green.	
-23	23.0		4.5/5	90				16.1 ppm
-24	24.0							
-25	25.0							
-26	26.0							
-27	27.0						28': Rock character changes to ???? brown - light.	
-28	28.0		5/5	100				0.0 ppm
-29	29.0							
-30	30.0						30': Fracture, clay-filled - slight PID.	2.0 ppm



BORING NO. 37-B10

Coordinates¹: N.
E.

Project: Edwards AFRC Project Number: 146185 Field Geologist: M. Glas, T. Ault
 Location: Woodward Drilling Method: Diamond Core Checked By:
 Drill Co.: Woodward Logging Method: HQ Continuous Core Approved By:
 Driller: Kris Nolan Boring Diameter: 3.78" Total Depth: 106 Feet
 Conductor Borehole Diameter: 10 in. Casing: None
 Conductor Casing Diameter: 6 in. Length: 12 Feet Type: Steel Filter Pack: None

TOC Elev²:
 GS Elev²:
 Date Began: 12/13/2013
 Date Finished: 12/16/2013
 Note 1 NAD 83 CALZ4
 Note 2 NAVD 88 ft amsl

Elevation (ft amsl)	Depth (feet)	Well Completion	Recovery (ft)	% Recovery	% RQD	Joint Spacing	Description	Comments
-31	31.0							
-32	32.0							
-33	33.0		5/5	100			33': Distinct lithology change - dark streaks.	0.5 ppm
-34	34.0						33.5': Clay-filled fracture - fat clay red oxidized (1-2" clay zone) - dark streaks.	
-35	35.0						34': Rubble zone 1-2" - sand-sized grains.	
-36	36.0						35.5': Low angle fractures - sand-sized	
-37	37.0						37': Low angle fracture - very coarse sand-sized rubble - zone 3" - may be wide (20 degree angle).	1.0 ppm
-38	38.0		2.5/5	50			38.5': Rubble zone similar to one above.	
-39	39.0							4.0 ppm
-40	40.0							
-41	41.0							
-42	42.0							
-43	43.0		3/3.5	86				
-44	44.0						44': Rubble zone (coarse sand-sized).	15 ppm
-45	45.0		1.9/2	95				
-46	46.0							
-47	47.0						46.5': Rubble zone - ? - same as above. Series of fractures, PID 5-10 ppm in fractures.	5.0 ppm 5.0 ppm 10.0 ppm
-48	48.0							
-49	49.0							
-50	50.0							10.0 ppm
-51	51.0							
-52	52.0							10.0 ppm. Near vertical fracture through core ????? ??
-53	53.0							5.0 ppm
-54	54.0							1.0 ppm
-55	55.0							
-56	56.0							2.0 ppm
-57	57.0							14.0 ppm
-58	58.0		5/5	100				
-59	59.0							15.0 ppm
-60	60.0						60': High angle contact - from solid rock to 1" tabular slab - to	70.0 ppm



BORING NO. 37-B10

Coordinates¹: N.
E.

Project: Edwards AFRC Project Number: 146185 Field Geologist: M. Glas, T. Ault
 Location: Drilling Method: Diamond Core Checked By:
 Drill Co.: Woodward Logging Method: HQ Continuous Core Approved By:
 Driller: Kris Nolan Boring Diameter: 3.78" Total Depth: 106 Feet
 Conductor Borehole Diameter: 10 in. Casing: None
 Conductor Casing Diameter: 6 in. Length: 12 Feet Type: Steel Filter Pack: None

TOC Elev²:
 GS Elev²:
 Date Began: 12/13/2013
 Date Finished: 12/16/2013
 Note 1 NAD 83 CALZ4
 Note 2 NAVD 88 ft amsl

Elevation (ft amsl)	Depth (feet)	Well Completion	Recovery (ft)	% Recovery	% RQD	Joint Spacing	Description	Comments
-61	61.0						0.8' zone of clay with granular texture clasts with clays.	
-62	62.0							1.0 ppm
-63	63.0		5/5	100				5.0 ppm
-64	64.0							2.0 ppm
-65	65.0						65': Large clast rubble zone. Angular clasts, 1" 40% with coarse sand-sized matrix, angular also (est. 0.5" thick).	8.0 ppm
-66	66.0							65': Clay-filled fracture. 7.0 ppm
-67	67.0							14.0 ppm
-68	68.0		4.5/5	90			68': Clay zone.	30.0 ppm
-69	69.0						68.5': Dark laminate biotite - fine-grained crystalline.	40.0 ppm
-70	70.0						69': Alternation rock-clay zone - loose granular - light-colored material at 70-71'.	50.0 ppm
-71	71.0							90.0 ppm
-72	72.0							68.5': Distinct horizontal contact.
-73	73.0		3/3	100				10.0 ppm
-74	74.0						73': Mottled brown-white zone - 6" to 1' wide - red oxide on surfaces.	15.0 ppm
-75	75.0		2/2	100				10.0 ppm
-76	76.0						75': Rubble zone 1-2" clasts with granular matrix.	
-77	77.0						76': High angle fracture - 60 ppm on fracture surface - dissipates quickly to 10 ppm.	60.0 ppm/10.0 ppm
-78	78.0		3.5/3.5	100				
-79	79.0						78': hor. Fracture	
-80	80.0						79': 70 ppm initially, dissipates to 4.5 ppm broken.	70.0 ppm/10.0 ppm
-81	81.0						Rock hard - somewhat broken in upper foot.	
-82	82.0		5/5	100				
-83	83.0							1.5 ppm
-84	84.0							3.6 ppm
-85	85.0							
-86	86.0		2.5/3	83				3.8 ppm
-87	87.0							4.0 ppm
-88	88.0							2.0 ppm
-89	89.0							6.1 ppm
-90	90.0		3.5/3.5	100				4.4 ppm



BORING NO. 37-B10

Coordinates¹: N.
E.

Project: Edwards AFRC Project Number: 146185 Field Geologist: M. Glas, T. Ault
 Location: Drilling Method: Diamond Core Checked By:
 Drill Co.: Woodward Logging Method: HQ Continuous Core Approved By:
 Driller: Kris Nolan Boring Diameter: 3.78" Total Depth: 106 Feet
 Conductor Borehole Diameter: 10 in. Casing: None
 Conductor Casing Diameter: 6 in. Length: 12 Feet Type: Steel Filter Pack: None

TOC Elev²:
 GS Elev²:
 Date Began: 12/13/2013
 Date Finished: 12/16/2013
 Note 1 NAD 83 CALZ4
 Note 2 NAVD 88 ft amsl

Elevation (ft amsl)	Depth (feet)	Well Completion	Recovery (ft)	% Recovery	% RQD	Joint Spacing	Description	Comments
-91	91.0							3.0 ppm 3.5 ppm
-92	92.0							
-93	93.0							
-94	94.0		5/5	100				
-95	95.0							
-96	96.0							
-97	97.0							
-98	98.0							
-99	99.0		5/5	100			98.5': Fracture set over about 0.5' interval with persistent elevated PID hits - solid rock mass but distinct fracturing is yielding high VOC detections on PID.	360 ppm 400 ppm 250 ppm Very hot persistent zone.
-100	100.0							
-101	101.0							
-102	102.0		1.8/2	90			Solid rock mass above - granular clayish material below 102' - oxidized	12.0 ppm 44.0 ppm 16.0 ppm 50.0 ppm
-103	103.0							
-104	104.0		2.5/2.5	100				
-105	105.0							
-106	106.0						TD = 106'	Multiple fractures Hole tagged at 106'.
-107	107.0							
-108	108.0							
-109	109.0							
-110	110.0							
-111	111.0							
-112	112.0							
-113	113.0							
-114	114.0							
-115	115.0							
-116	116.0							
-117	117.0							
-118	118.0							
-119	119.0							
-120	120.0							



BORING NO. 37-B11

Coordinates¹: N.
E.

Project: Edwards AFRC Project Number: 146185 Field Geologist: M. Glas
 Location: Drilling Method: Diamond Core Checked By:
 Drill Co.: Woodward Logging Method: HQ Continuous Core Approved By:
 Driller: Kris Nolan Boring Diameter: 3.78" Total Depth: 23.5 Feet
 Conductor Borehole Diameter: 10 in. Casing: None
 Conductor Casing Diameter: 6 in. Length: 6.5 Feet Type: Steel Filter Pack: None

TOC Elev²:
 GS Elev²:
 Date Began: 12/05/2013
 Date Finished: 12/05/2013
 Note 1 NAD 83 CALZ4
 Note 2 NAVD 88 ft amsl

Elevation (ft amsl)	Depth (feet)	Well Completion	Recovery (ft)	% Recovery	% RQD	Joint Spacing	Description	Comments
0							Asphalt over soil.	Air Knife to 5'
-1	1.0							
-2	2.0							
-3	3.0							
-4	4.0							
-5	5.0							
-6	6.0							
-7	7.0						Top of bedrock.	PID = 0.0 ppm
-8	8.0						6.5': 80% quartz, 20% k-spar, trace biotite, very light gray (N7).	0.0 ppm
-9	9.0						8.5': 80% k-spar, 20% quartz, trace biotite, light gray (N7).	0.0 ppm
-10	10.0							0.0 ppm
-11	11.0							0.0 ppm
-12	12.0							0.0 ppm
-13	13.0							0.0 ppm
-14	14.0							0.0 ppm
-15	15.0							0.0 ppm
-16	16.0							0.0 ppm
-17	17.0							0.0 ppm
-18	18.0							0.0 ppm
-19	19.0							0.0 ppm
-20	20.0							0.0 ppm
-21	21.0							0.0 ppm
-22	22.0						21.5': Primarily plagioclase with trace k-spar and quartz, light gray (N7) and grayish orange (10YR7/4).	0.0 ppm
-23	23.0						22.5': Medium gray (N5).	0.0 ppm
-24	24.0						23.5': Metal object, stop drilling. Abandon hole due to obstructions. Grout hole with tremie grout mix on 12/16/2013.	
-25	25.0							
-26	26.0							
-27	27.0							
-28	28.0							
-29	29.0							
-30	30.0							



BORING NO. 37-B12

Coordinates¹: N.
E.

Project: Edwards AFRC Project Number: 146185 Field Geologist: M. Glas
 Location: Drilling Method: Diamond Core Checked By:
 Drill Co.: Woodward Logging Method: HQ Continuous Core Approved By:
 Driller: Kris Nolan Boring Diameter: 3.78" Total Depth: 161 Feet
 Conductor Borehole Diameter: 10 in. Casing: None
 Conductor Casing Diameter: 6 in. Length: 19 Feet Type: Steel Filter Pack: None

TOC Elev²:
 GS Elev²:
 Date Began: 12/06/2013
 Date Finished: 12/13/2013
 Note 1 NAD 83 CALZ4
 Note 2 NAVD 88 ft amsl

Elevation (ft amsl)	Depth (feet)	Well Completion	Recovery (ft)	% Recovery	% RQD	Joint Spacing	Description	Comments
0							Top soil to 19'.	Air Knife to 5'
-1	1.0							
-2	2.0							
-3	3.0							
-4	4.0							
-5	5.0							
-6	6.0							
-7	7.0							
-8	8.0							
-9	9.0							
-10	10.0							
-11	11.0							
-12	12.0							
-13	13.0							
-14	14.0							
-15	15.0							
-16	16.0							
-17	17.0							
-18	18.0							
-19	19.0						19': Only recover 3" of the 19-21.5' run, no joints visible, rock is highly weathered.	PID = 0.0 ppm
-20	20.0							
-21	21.0							
-22	22.0						21.5': Recovered approximately 1' of the 21.5-26.5' run, rock is highly weathered for -6', no obvious joints, most likely a fault zone because of the presence of clays and slickensides.	
-23	23.0							
-24	24.0							
-25	25.0							
-26	26.0							
-27	27.0						26.5': Highly weathered granite (fault zone?), PID measurements were collected by cutting into the clay and reading in the split area.	66 ppm 1.2 ppm 2.1 ppm 24.4 ppm
-28	28.0							26.7 ppm
-29	29.0						29': Rock becomes competent at 29.75'.	63.3 ppm
-30	30.0						29.5': Rubble zone. 29.75-31.25': Mafic intrusions, rock has a green tint.	0.0 ppm



BORING NO. 37-B12

Coordinates¹: N.
E.

Project: Edwards AFRC Project Number: 146185 Field Geologist: M. Glas
 Location: Woodward Drilling Method: Diamond Core Checked By:
 Drill Co.: Kris Nolan Logging Method: HQ Continuous Core Approved By:
 Driller: Kris Nolan Boring Diameter: 3.78" Total Depth: 161 Feet
 Conductor Borehole Diameter: 10 in. Casing: None
 Conductor Casing Diameter: 6 in. Length: 19 Feet Type: Steel Filter Pack: None

TOC Elev²:
 GS Elev²:
 Date Began: 12/06/2013
 Date Finished: 12/13/2013
 Note 1 NAD 83 CALZ4
 Note 2 NAVD 88 ft amsl

Elevation (ft amsl)	Depth (feet)	Well Completion	Recovery (ft)	% Recovery	% RQD	Joint Spacing	Description	Comments
-31	31.0							0.5 ppm 0.0 ppm
-32	32.0						31.5-32': Granite. 32-33.5': Basalt.	0.0 ppm 0.0 ppm
-33	33.0							0.0 ppm
-34	34.0						33.5-35.5': Decomposed granite.	2.0 ppm 5.9 ppm
-35	35.0							0.4 ppm 0.4 ppm
-36	36.0						35.5-36.5': Granite.	0.0 ppm 0.0 ppm
-37	37.0						36.5-41.5': Granite decomposed to clay.	0.0 ppm 0.3 ppm
-38	38.0							1.0 ppm 0.0 ppm
-39	39.0							2.9 ppm 3.3 ppm
-40	40.0							10.3 ppm 6.2 ppm
-41	41.0							5.3 ppm 2.1 ppm
-42	42.0						41.5-42.5': Granite weathered to ???a clay.	16.5 ppm 3.4 ppm
-43	43.0						42.5-43.5': Partially weathered granite.	3.7 ppm
-44	44.0						43.5-44.25': Highly weathered granitic clay. 44.25-45': Rubble zone.	43.1 ppm 17.3 ppm
-45	45.0						45-45.75': Partially weathered granite. 45.75-46.5': Rubble zone.	7.3 ppm 2.0 ppm
-46	46.0							0.0 ppm 0.8 ppm
-47	47.0						46.5-48': Competent rock.	0.0 ppm
-48	48.0							7.1 ppm
-49	49.0						48-50': Highly weathered granitic clay.	30.8 ppm 0.2 ppm
-50	50.0							
-51	51.0						50-51.5': No recovery.	0.3 ppm
-52	52.0						51.5-52.25': Rubble zone. 52.25-54.5': Fractured competent rock.	0.0 ppm 0.0 ppm
-53	53.0							0.0 ppm 1.0 ppm
-54	54.0							0.0 ppm
-55	55.0						54.5-56.5': No recovery.	
-56	56.0							
-57	57.0						56.5-58.5': Highly weathered granitic clay.	3.2 ppm 18.2 ppm
-58	58.0							
-59	59.0						58.5-60': Competent granitic rock.	0.0 ppm
-60	60.0							0.0 ppm



BORING NO. 37-B12

Coordinates¹: N.
E.

Project: Edwards AFRC Project Number: 146185 Field Geologist: M. Glas
 Location: Woodward Drilling Method: Diamond Core Checked By:
 Drill Co.: Kris Nolan Logging Method: HQ Continuous Core Approved By:
 Driller: Kris Nolan Boring Diameter: 3.78" Total Depth: 161 Feet
 Conductor Borehole Diameter: 10 in. Casing: None
 Conductor Casing Diameter: 6 in. Length: 19 Feet Type: Steel Filter Pack: None

TOC Elev²:
 GS Elev²:
 Date Began: 12/06/2013
 Date Finished: 12/13/2013
 Note 1 NAD 83 CALZ4
 Note 2 NAVD 88 ft amsl

Elevation (ft amsl)	Depth (feet)	Well Completion	Recovery (ft)	% Recovery	% RQD	Joint Spacing	Description	Comments
-61	61.0						60-65': Competent granitic rock.	0.0 ppm 0.0 ppm
-62	62.0							0.0 ppm 0.0 ppm
-63	63.0							0.0 ppm 0.0 ppm
-64	64.0							0.0 ppm 0.0 ppm
-65	65.0							0.0 ppm 0.0 ppm
-66	66.0						65-70': ~3' of recovery, fractured granitic rock, ~2" mafic intrusion at 65.5', became more fractured when transferred to core box.	0.0 ppm 0.0 ppm
-67	67.0							0.0 ppm 0.0 ppm
-68	68.0							0.0 ppm 0.0 ppm
-69	69.0							0.0 ppm 0.0 ppm
-70	70.0						70-75': Competent granitic rock.	0.0 ppm 0.0 ppm
-71	71.0							0.0 ppm 0.0 ppm
-72	72.0							0.0 ppm 0.0 ppm
-73	73.0							0.0 ppm 0.0 ppm
-74	74.0							0.0 ppm 0.0 ppm
-75	75.0						75-76.5': Competent granitic rock.	0.0 ppm 0.0 ppm
-76	76.0							0.0 ppm 0.0 ppm
-77	77.0						76.5-80': Weathered granitic clay, clay is very stiff and dry.	0.0 ppm 0.0 ppm
-78	78.0							4.3 ppm 13.8 ppm 2.4 ppm
-79	79.0							
-80	80.0						80-83.5': Slightly weathered granitic rock, clay 80.5-80.75'.	1.4 ppm 2.6 ppm 18.1 ppm 8.4 ppm
-81	81.0							
-82	82.0							7.8 ppm 0.0 ppm
-83	83.0							
-84	84.0						83.5-84.5': Fractured competent granitic rock.	0.0 ppm
-85	85.0						84.5-85': Competent granitic rock.	
-86	86.0						85-90': Competent granitic rock with zones of clay from 86.25-86.5' and 89.25-89.5'. Clay is contaminated. Rock is highly fractured from 89.5-90'.	0.0 ppm 9.7 ppm 5.3 ppm
-87	87.0							
-88	88.0							
-89	89.0							
-90	90.0							12 ppm
							90-95': No recovery because the core was lost in the mud pit	



BORING NO. 37-B12

Coordinates¹: N.
E.

Project: Edwards AFRC Project Number: 146185 Field Geologist: M. Glas
 Location: Woodward Drilling Method: Diamond Core Checked By:
 Drill Co.: Kris Nolan Logging Method: HQ Continuous Core Approved By:
 Driller: Kris Nolan Boring Diameter: 3.78" Total Depth: 161 Feet
 Conductor Borehole Diameter: 10 in. Casing: None
 Conductor Casing Diameter: 6 in. Length: 19 Feet Type: Steel Filter Pack: None

TOC Elev²:
 GS Elev²:
 Date Began: 12/06/2013
 Date Finished: 12/13/2013
 Note 1 NAD 83 CALZ4
 Note 2 NAVD 88 ft amsl

Elevation (ft amsl)	Depth (feet)	Well Completion	Recovery (ft)	% Recovery	% RQD	Joint Spacing	Description	Comments
-91	91.0						during extraction.	
-92	92.0							
-93	93.0							
-94	94.0							
-95	95.0						95-97': Highly fractured granitic rock (competent).	12.0 ppm
-96	96.0							26.5 ppm
-97	97.0						97-97.5': Competent rock.	167 ppm
-98	98.0						97.5-100': Stiff granitic clay.	432 ppm
-99	99.0							0.0 ppm
-100	100.0							0.0 ppm
-101	101.0							55.5 ppm
-102	102.0						101-101.5': Weathered granitic rock.	65.6 ppm
-103	103.0						101.5-103.5': Highly weathered granitic clay.	63.1 ppm
-104	104.0							70.7 ppm
-105	105.0						103.5-104.25': Highly weathered granitic clay.	6.9 ppm
-106	106.0						104.25-105': Competent granitic rock.	18.0 ppm
-107	107.0							39.7 ppm
-108	108.0						105-105.5': Clay as above.	3.6 ppm
-109	109.0						105.5-106': Rock as above.	73.3 ppm
-110	110.0						106-107.25': Competent granitic rock.	63.4 ppm
-111	111.0							467 ppm
-112	112.0						107.25-109': Slightly weathered granitic rock (breaks apart easily).	23.7 ppm
-113	113.0							6.1 ppm
-114	114.0						109-111': Competent granitic rock.	18.5 ppm
-115	115.0							82.3 ppm
-116	116.0						111-116': Competent granitic rock with high angle fractures.	40.0 ppm
-117	117.0						No recovery from 115.5-116'.	14.4 ppm
-118	118.0							1.8 ppm
-119	119.0							0.3 ppm
-120	120.0						116-118': Competent granitic rock.	0.0 ppm
							118-118.5': Rubble zone comprised of mafic rock (peridotite).	0.0 ppm
							118.5-119.5': Competent mafic rock (peridotite)	5.6 ppm
							119.5-120': Stiff mafic clay.	0.4 ppm
							120-120.25': Rubble zone comprised of mafic gravel with a	4.4 ppm



BORING NO. 37-B12

Coordinates¹: N.
E.

Project: Edwards AFRC Project Number: 146185 Field Geologist: M. Glas
 Location: Drilling Method: Diamond Core Checked By:
 Drill Co.: Woodward Logging Method: HQ Continuous Core Approved By:
 Driller: Kris Nolan Boring Diameter: 3.78" Total Depth: 161 Feet
 Conductor Borehole Diameter: 10 in. Casing: None
 Conductor Casing Diameter: 6 in. Length: 19 Feet Type: Steel Filter Pack: None

TOC Elev²:
 GS Elev²:
 Date Began: 12/06/2013
 Date Finished: 12/13/2013
 Note 1 NAD 83 CALZ4
 Note 2 NAVD 88 ft amsl

Elevation (ft amsl)	Depth (feet)	Well Completion	Recovery (ft)	% Recovery	% RQD	Joint Spacing	Description	Comments
-121	121.0						clay matrix.	0.0 ppm
-122	122.0						120.25-120.75': Weathered mafic rock.	0.0 ppm
-123	123.0						121-124': Competent granitic rock.	0.0 ppm
-124	124.0						121-124': Competent granitic rock, mostly dark reddish brown (10R3/4), high in k-spar.	0.0 ppm
-125	125.0						124-126': Competent granitic rock.	0.0 ppm
-126	126.0						126-130.5': Competent granitic rock with fractures. Highly fractured zone from 128-129'.	0.0 ppm
-127	127.0							0.0 ppm
-128	128.0							1.8 ppm
-129	129.0							7.5 ppm
-130	130.0							0.0 ppm
-131	131.0						130.5-134.5': Competent granitic rock with fractures. No recovery from 134-134.5'.	0.0 ppm
-132	132.0							0.0 ppm
-133	133.0							0.8 ppm
-134	134.0							0.0 ppm
-135	135.0						134.5-139.5': Competent granitic rock with fractures.	0.0 ppm
-136	136.0							0.0 ppm
-137	137.0							0.0 ppm
-138	138.0							0.0 ppm
-139	139.0							0.0 ppm
-140	140.0						139.5-144.5': Competent granitic rock with fractures, small amount of clay in the fracture at 143.5'.	0.0 ppm
-141	141.0							0.0 ppm
-142	142.0							0.0 ppm
-143	143.0							2.1 ppm
-144	144.0							0.0 ppm
-145	145.0						144.5-147.5': Competent granitic rock with fractures.	4.2 ppm
-146	146.0							21.1 ppm
-147	147.0							0.0 ppm
-148	148.0						147.5-148': No recovery.	0.0 ppm
-149	149.0						148-152': Competent granitic rock with fractures. Rubble zones from 150.75-151' and 151.5-152'.	0.0 ppm
-150	150.0							1.5 ppm
								0.5 ppm



BORING NO. 37-B12

Coordinates¹: N.
E.

Project: Edwards AFRC Project Number: 146185 Field Geologist: M. Glas
 Location: Woodward Drilling Method: Diamond Core Checked By:
 Drill Co.: Woodward Logging Method: HQ Continuous Core Approved By:
 Driller: Kris Nolan Boring Diameter: 3.78" Total Depth: 161 Feet
 Conductor Borehole Diameter: 10 in. Casing: None
 Conductor Casing Diameter: 6 in. Length: 19 Feet Type: Steel Filter Pack: None

TOC Elev²:
 GS Elev²:
 Date Began: 12/06/2013
 Date Finished: 12/13/2013
 Note 1 NAD 83 CALZ4
 Note 2 NAVD 88 ft amsl

Elevation (ft amsl)	Depth (feet)	Well Completion	Recovery (ft)	% Recovery	% RQD	Joint Spacing	Description	Comments
-151	151.0							17.7 ppm 2.3 ppm
-152	152.0						152-153': Highly fractured granitic rock.	1.2 ppm 0.0 ppm
-153	153.0						153-154.5': Mafic intrusion (peridotite).	0.0 ppm 2.3 ppm
-154	154.0							
-155	155.0						154.5-154.75': Mafic clay. 154.75-156': Competent granitic rock.	0.0 ppm 79.2 ppm 0.0 ppm
-156	156.0						156-161': Competent granitic rock with high angle fractures. Fractures contain granitic gravel and clay. No recovery from 160.5-161'.	0.0 ppm 0.3 ppm 1.3 ppm
-157	157.0							
-158	158.0							
-159	159.0							0.0 ppm
-160	160.0							0.0 ppm 0.7 ppm
-161	161.0							Tagged bottom at 161'.
-162	162.0							
-163	163.0							
-164	164.0							
-165	165.0							
-166	166.0							
-167	167.0							
-168	168.0							
-169	169.0							
-170	170.0							
-171	171.0							
-172	172.0							
-173	173.0							
-174	174.0							
-175	175.0							
-176	176.0							
-177	177.0							
-178	178.0							
-179	179.0							
-180	180.0							



BORING NO. 37-B13

Coordinates¹: N.
E.

Project: Edwards AFRC Project Number: 146185 Field Geologist: M. Glas
 Location: Drilling Method: Diamond Core Checked By:
 Drill Co.: Woodward Logging Method: HQ Continuous Core Approved By:
 Driller: Kris Nolan Boring Diameter: 3.78" Total Depth: 100 Feet
 Conductor Borehole Diameter: 10 in. Casing: None
 Conductor Casing Diameter: 6 in. Length: 6 Feet Type: Steel Filter Pack: None

TOC Elev²:
 GS Elev²:
 Date Began: 12/10/2013
 Date Finished: 12/11/2013
 Note 1 NAD 83 CALZ4
 Note 2 NAVD 88 ft amsl

Elevation (ft amsl)	Depth (feet)	Well Completion	Recovery (ft)	% Recovery	% RQD	Joint Spacing	Description	Comments
0							0-6" Top soil.	Air Knife to 5'
-1	1.0							
-2	2.0							
-3	3.0							
-4	4.0							
-5	5.0							
-6	6.0						6-7.25': Rubble zone, competent granitic rock.	PID = 2.2 ppm
-7	7.0						7.25-11': Competent granitic rock.	1.9 ppm
-8	8.0							1.6 ppm
-9	9.0							9.1 ppm
-10	10.0							5.1 ppm
-11	11.0						11-16': Competent granitic rock.	5.3 ppm
-12	12.0							1.5 ppm
-13	13.0							0.5 ppm
-14	14.0							0.3 ppm
-15	15.0							0.2 ppm
-16	16.0						16-21': Competent granitic rock.	0.0 ppm
-17	17.0							0.0 ppm
-18	18.0							0.0 ppm
-19	19.0							0.0 ppm
-20	20.0							0.0 ppm
-21	21.0							0.0 ppm
-22	22.0						21-26': Bedrock with high angle fractures, rubble zone from 22-24' due to large fracture.	0.5 ppm
-23	23.0							0.0 ppm
-24	24.0							0.3 ppm
-25	25.0							0.6 ppm
-26	26.0							0.4 ppm
-27	27.0						26-31': Competent granitic rock with high angle fractures, rubble zone from 26-27.5'. Brown stained fracture surfaces from 28-31'.	14.4 ppm
-28	28.0							9.2 ppm
-29	29.0							2.2 ppm
-30	30.0							127 ppm
								128 ppm
								37.9 ppm
								12.8 ppm
								66.7 ppm
								69.1 ppm
								1527 ppm
								649 ppm
								374 ppm



BORING NO. 37-B13

Coordinates¹: N.
E.

Project: Edwards AFRC Project Number: 146185 Field Geologist: M. Glas
 Location: Drilling Method: Diamond Core Checked By:
 Drill Co.: Woodward Logging Method: HQ Continuous Core Approved By:
 Driller: Kris Nolan Boring Diameter: 3.78" Total Depth: 100 Feet
 Conductor Borehole Diameter: 10 in. Casing: None
 Conductor Casing Diameter: 6 in. Length: 6 Feet Type: Steel Filter Pack: None

TOC Elev²:
 GS Elev²:
 Date Began: 12/10/2013
 Date Finished: 12/11/2013
 Note 1 NAD 83 CALZ4
 Note 2 NAVD 88 ft amsl

Elevation (ft amsl)	Depth (feet)	Well Completion	Recovery (ft)	% Recovery	% RQD	Joint Spacing	Description	Comments
-61	61.0							
-62	62.0						61.5-64': Competent granitic rock with high angle fractures.	
-63	63.0							12.4 ppm 28.1 ppm
-64	64.0							2.7 ppm 30.2 ppm
-65	65.0						64.5-66.5': Weathered granitic clay.	4.9 ppm 64.1 ppm
-66	66.0							26.4 ppm
-67	67.0						66.5-71.5': Slightly weathered to very weathered granitic rock (can easily break with tools to clay).	21.0 ppm 58.8 ppm
-68	68.0							0.2 ppm 1.8 ppm
-69	69.0							40.0 ppm
-70	70.0							5.1 ppm 0.0 ppm
-71	71.0							3.2 ppm 0.2 ppm
-72	72.0						71.5-72.25': Weathered granitic clay ending at a high angle fracture.	0.0 ppm
-73	73.0						72.25-75.5': Competent fractured granitic rock. No recovery from 75-75.5'.	1.4 ppm
-74	74.0							0.6 ppm 3.1 ppm
-75	75.0							0.8 ppm 2.0 ppm
-76	76.0						75.5-80': Competent granitic rock with high angle fractures. No recovery from 79.5-80'.	7.2 ppm
-77	77.0							0.4 ppm
-78	78.0							0.0 ppm
-79	79.0							2.3 ppm 0.6 ppm
-80	80.0							0.0 ppm
-81	81.0						80-82.5': Competent granitic rock with fractures. Rubble zone from 81.5-82.5'.	0.0 ppm 1.2 ppm
-82	82.0							0.0 ppm 0.0 ppm
-83	83.0						82.5-86.5': Highly fractured competent granitic rock. Clay zone from 84.5-84.75'.	0.0 ppm 0.0 ppm
-84	84.0							0.0 ppm 0.5 ppm
-85	85.0							0.5 ppm 0.3 ppm
-86	86.0							0.1 ppm
-87	87.0						86.5-91.5': Competent granitic rock with fractures. Highly fractured zone from 88.75-89.5'.	
-88	88.0							0.0 ppm
-89	89.0							0.0 ppm 0.0 ppm
-90	90.0							0.0 ppm



BORING NO. 37-B13

Coordinates¹: N.
E.

Project: Edwards AFRC Project Number: 146185 Field Geologist: M. Glas
 Location: Drilling Method: Diamond Core Checked By:
 Drill Co.: Woodward Logging Method: HQ Continuous Core Approved By:
 Driller: Kris Nolan Boring Diameter: 3.78" Total Depth: 100 Feet
 Conductor Borehole Diameter: 10 in. Casing: None
 Conductor Casing Diameter: 6 in. Length: 6 Feet Type: Steel Filter Pack: None

TOC Elev²:
 GS Elev²:
 Date Began: 12/10/2013
 Date Finished: 12/11/2013
 Note 1 NAD 83 CALZ4
 Note 2 NAVD 88 ft amsl

Elevation (ft amsl)	Depth (feet)	Well Completion	Recovery (ft)	% Recovery	% RQD	Joint Spacing	Description	Comments
-91	91.0							0.0 ppm
-92	92.0						91.5-96.5': Competent granitic rock with fractures. Thin clay layers at 93.75', 94.5'.	0.0 ppm
-93	93.0							0.0 ppm
-94	94.0							0.6 ppm
-95	95.0							9.5 ppm
-96	96.0							1.5 ppm
-97	97.0						96.5-100': Competent granitic rock with shallow angle fractures, stiff clay from 99.75-100'.	17.7 ppm
-98	98.0							3.3 ppm
-99	99.0						Extra 9" of core (shoe?) comprised of competent granitic rock.	1.0 ppm
-100	100.0							0.2 ppm
-101	101.0							0.0 ppm
-102	102.0							3.6 ppm. TD=100'.
-103	103.0							
-104	104.0							
-105	105.0							
-106	106.0							
-107	107.0							
-108	108.0							
-109	109.0							
-110	110.0							
-111	111.0							
-112	112.0							
-113	113.0							
-114	114.0							
-115	115.0							
-116	116.0							
-117	117.0							
-118	118.0							
-119	119.0							
-120	120.0							



BORING NO. 37-B14

Coordinates¹: N. not determined

E. not determined

TOC Elev²: not applicable

GS Elev²: not determined

Date Began: 09/28/2016

Date Finished: 09/29/2016

Note 1

Note 2

Project: Edwards AFRL Project Number: 146185 Field Geologist: Mark Tucker
 Location: Building 8595 Drilling Method: Diamond Core Checked By:
 Drill Co.: Woodward Logging Method: HQ Continuous Core Approved By:
 Driller: Robert Wharf Boring Diameter: 3.78" Total Depth: 87.5 Feet
 Conductor Borehole Diameter: 10 in. Casing: None
 Conductor Casing Diameter: 6 in. Length: 6.5 Feet Type: Steel Filter Pack: None

Elevation (ft amsl)	Depth (feet)	Well Completion	Recovery (ft)	% Recovery	% RQD	Joint Spacing	Description	Fracture Data (depth in feet, dip in degrees)
		None						
	—1.0						Pavement	
	—2.0		NA				Coarse gravel and angular cobbles with sand	
	—3.0							
	—4.0		NA				Brown sand and coarse gravel	
	—5.0							
	—6.0						6.5 top of rock	
	—7.0		2.5	100%	44%		Light gray granite, highly fractured	7.8, 80 8.0, 20 8.5, 30 8.6, 30 8.6, 80 9.2, 5
	—8.0							
	—9.0							
	—10.0		4.9	98%	69%		Light bluish gray granite, highly fractured, becoming more competent with depth	9.7, 30 10.0, 15 10.4, 50 10.6, 30 10.8, 45 11.45, 20 12.7, 5 12.75, 35 13.5, 15 14.2, 60; 14.3, 60
	—11.0							
	—12.0							
	—13.0							
	—14.0							
	—15.0		3.1	78%	13%		Light gray granite	15., 5, 70 16.3, 70 16.7, 30 17.3, 70
	—16.0							
	—17.0							
	—18.0							
	—19.0		2.5	63%	32%		Light gray granite	19.9, 70
	—20.0						20.4 - 20.9 White quartz vein in 40% of core	
	—21.0							
	—22.0							
	—23.0		2	100%	100%		Light gray granite	22.9, 40 23.7, 40
	—24.0							



BORING NO. 37-B14

Coordinates¹: N. not determined

E. not determined

TOC Elev²: not applicable

GS Elev²: not determined

Date Began: 09/28/2016

Date Finished: 09/29/2016

Note 1

Note 2

Project: Edwards AFRL Project Number: 146185 Field Geologist: Mark Tucker
 Location: Building 8595 Drilling Method: Diamond Core Checked By:
 Drill Co.: Woodward Logging Method: HQ Continuous Core Approved By:
 Driller: Robert Wharf Boring Diameter: 3.78" Total Depth: 87.5 Feet
 Conductor Borehole Diameter: 10 in. Casing: None
 Conductor Casing Diameter: 6 in. Length: 6.5 Feet Type: Steel Filter Pack: None

Elevation (ft amsl)	Depth (feet)	Well Completion	Recovery (ft)	% Recovery	% RQD	Joint Spacing	Description	Fracture Data (depth in feet, dip in degrees)
	—25.0		4.3	86%	60%		Light gray granite	25.6, 60 26.3, 70 27.0, 70
	—26.0							
	—27.0							
	—28.0						27.8 - 28.7 Incompetent granite, crumbly	
	—29.0							
	—30.0		5	100%	100%		Light gray granite	30.1, 30 31.3, 70 32.5, 60 33.7, 10 34.1, 30
	—31.0							
	—32.0							
	—33.0							
	—34.0							
	—35.0		5	100%	94%		Light gray granite	35.0, 50 36.3, 45 37.3, 60 38.0, 45 38.4, 70 39.3, 60
	—36.0							
	—37.0							
	—38.0							
	—39.0							
	—40.0		4	100%	100%		Light gray granite	39.6, 70 40.5, 80 40.8, 20 40.9, 20 41.4, 50 41.7, 50 43.0, 60
	—41.0							
	—42.0							
	—43.0							
	—44.0		4.2	84%	52%		Light gray granite	44.4, 75 44.1, 45 44.7, 70 45.3, 60
	—45.0							
	—46.0						46.0 - 46.1 Brecciated, soft	
	—47.0						47.2 - 47.5 Brecciated	
	—48.0							



BORING NO. 37-B14

Coordinates¹: N. not determined

E. not determined

TOC Elev²: not applicable

GS Elev²: not determined

Date Began: 09/28/2016

Date Finished: 09/29/2016

Note 1

Note 2

Project: Edwards AFRL Project Number: 146185 Field Geologist: Mark Tucker
 Location: Building 8595 Drilling Method: Diamond Core Checked By:
 Drill Co.: Woodward Logging Method: HQ Continuous Core Approved By:
 Driller: Robert Wharf Boring Diameter: 3.78" Total Depth: 87.5 Feet
 Conductor Borehole Diameter: 10 in. Casing: None
 Conductor Casing Diameter: 6 in. Length: 6.5 Feet Type: Steel Filter Pack: None

Elevation (ft amsl)	Depth (feet)	Well Completion	Recovery (ft)	% Recovery	% RQD	Joint Spacing	Description	Fracture Data (depth in feet, dip in degrees)
	—49.0		3.3	94%	42%		Light gray granite	49.1, 50
	—50.0						48.5 - 49.5 Brecciated and re-healed	49.2, 40
	—51.0						49.5 - 50.9 Brecciated, broken, sandy texture	
	—52.0		2.5	100%	80%		Light gray granite	52.6, 60
	—53.0						52.8, 0; 53.1, 0	
	—54.0						53.3, 20	
	—54.0						53.7, 70	
	—55.0		2.8	56%	68%		Light gray granite	54.7, 60
	—56.0						54.9, 30	
	—56.0						56.8 - 57.2 Soft and clayey	55.2, 40
	—57.0						56.1, 45	
	—58.0						56.6, 20	
	—59.0							
	—60.0	3.6	72%	53%		Light gray granite	59.8, 0	
	—61.0					60.4, 60		
	—61.0					61.0, 50		
	—62.0					61.3, 80		
	—62.0					62.8, 50		
	—63.0	2.7	54%	48%		Light gray granite	64.9, 100	
	—65.0					64.5 - 66.1 Brecciated and re-healed	65.2, broken	
	—66.0					66.1 - 67.2 Brecciated, half of core clayey	66.1, 85	
	—67.0						66.5, 60	
	—68.0							
	—69.0							
	—70.0	2.5	50%	52%		Light gray granite	70.2, 35	
	—71.0					70.8 - 72.0 Loose and granular		
	—72.0							



BORING NO. 37-B14

Coordinates¹: N. not determined

E. not determined

TOC Elev²: not applicable

GS Elev²: not determined

Date Began: 09/28/2016

Date Finished: 09/29/2016

Note 1

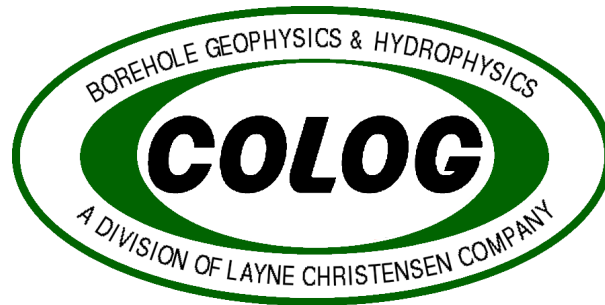
Note 2

Project: Edwards AFRL Project Number: 146185 Field Geologist: Mark Tucker
 Location: Building 8595 Drilling Method: Diamond Core Checked By:
 Drill Co.: Woodward Logging Method: HQ Continuous Core Approved By:
 Driller: Robert Wharf Boring Diameter: 3.78" Total Depth: 87.5 Feet
 Conductor Borehole Diameter: 10 in. Casing: None
 Conductor Casing Diameter: 6 in. Length: 6.5 Feet Type: Steel Filter Pack: None

Elevation (ft amsl)	Depth (feet)	Well Completion	Recovery (ft)	% Recovery	% RQD	Joint Spacing	Description	Fracture Data (depth in feet, dip in degrees)
	73.0							
	74.0							
	75.0		5	100%	50%		74.5 - 76.2 Brown weathered granite 76.2 - 79.5 Light gray granite, solid	74.9, 45 76.0, 45
	76.0						76.2 - 79.2 Solid granite with void lined by black crystals	76.6, 0 79.2, 70
	77.0							
	78.0							
	79.0							
	80.0		3.4	68%	38%		Light gray granite 79.5 - 80.3 Multiple fractures 79.7 - 80.3 Core sample sliced for VOC analysis (samples 1 - 5)	79.7, 5 80.3, 30 (Fracture F1)
	81.0						80.3 - 80.8 Soft, granular and clayey	80.7, 45 80.9, 30
	82.0						80.8 - 81.4 Multiple fractures 81.4 - 81.8 Solid	81.4, 30 81.8, 45
	83.0						81.4 - 81.9 Core Sample 11 for iron analysis	82.4, 45
	84.0						81.8 - 82.4 Soft, sandy texture 82.4 - 82.8 Solid	
	85.0		3	100%	43%		Light gray granite 85.3 - 85.8 Core Sample sliced for VOC analysis (Samples 6 - 10)	85.8, 20 (Fracture F2) 86.2, 70
	86.0						86.4 - 86.9 Core Sample 12 for iron analysis	86.4, 5 86.8, 25
	87.0							87.2, 65
	88.0						87.5 End of boring	
	89.0							
	90.0							

APPENDIX C BOREHOLE GEOPHYSICAL LOGS

Page Intentionally Left Blank



**Geophysical Logging Results
Hermosa
Edwards Air Force Base**

Prepared for
Shaw
February 19, 2013

Prepared by
COLOG Division of Layne Christensen Company
810 Quail Street Suite E, Lakewood, CO, 80215
Phone: (303) 279-0171 Fax: (303) 278-0135

Table of Contents

Geophysical Logging Results, Hermosa, Edwards Air Force Base

1.0 Introduction

2.0 Methodology

2.1 Optical and Acoustic Televiewer

2.2 Natural Gamma

2.3 Single Point Resistance (SPR) & Spontaneous Potential (SP)

2.4 Heat Pulse Flow Meter

3.0 37-B06 Geophysical Logging Results

3.1 Geophysical Logging

3.2 Optical Televiewer (OBI) & Acoustic Televiewer (ABI)

3.3 Natural Gamma

3.4 Single Point Resistance (SPR) & Spontaneous Potential (SP)

3.5 Heat Pulse Flow Meter

4.0 37-B09 Geophysical Logging Results

4.1 Geophysical Logging

4.2 Optical Televiewer (OBI) & Acoustic Televiewer (ABI)

4.3 Natural Gamma

5.0 Limitations

Appendices

Appendix A Logging Results (plots) from 37-B06

Appendix B Logging Results (plots) from 37-B09

List of Acronyms

gpm – gallons per minute

ft – feet

min. – minute

CPS – counts per second

OBI – Optical Borehole Imager, or generically, optical televiewer

ABI – Acoustic Borehole Imager, or generically, acoustic televiewer

Geophysical Logging Results Hermosa, Edwards Air Force Base

1.0 Introduction

In accordance with COLOG's proposal dated December 10, 2012, and Shaw's purchase order #828847-000 OP, COLOG has applied geophysical logging methods to two wellbores at the Edwards Air Force Base in California. The objectives of the investigation were to:

- Identify fractures and features intersecting the borehole and evaluate their orientation.
- Characterize and quantify vertical flow in the wellbores under both non-stressed (ambient) and stressed (pumping) conditions.
- Evaluate the lithology through which the borehole penetrates and assist in correlating lithology and possible flow zones.

The subject wellbores geophysically logged at the Hermosa site were: 37-B06 and 37-B09. At the time of logging the boreholes were HQ size (3.78").

The geophysical logging methods used were: acoustic televiewer, optical televiewer, natural gamma, single point resistance, spontaneous potential, and heat-pulse flowmeter. Flowmeter tests were performed under both non-stressed (ambient) conditions, and under stressed (pumping) conditions to evaluate the water-bearing horizons intersecting the wellbore.

COLOG's logging of the subject wellbore was performed over the period of January 17-18, 2013.

2.0 Methodology

2.1 Optical and Acoustic Televiewers

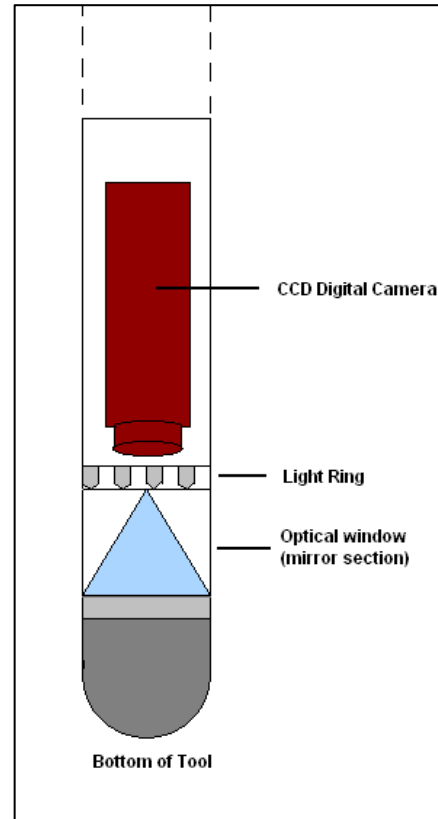
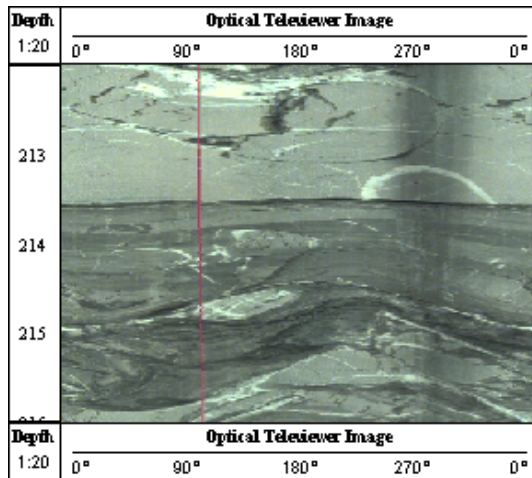
The OBI-40 optical televiewer and the ABI-40 acoustic televiewer (and its predecessor, the FAC40), from Advanced Logic Technologies (ALT), provide the highest resolution available for fracture and feature analysis in boreholes. Precise dip direction and angle measurements of bedding, fractures, and joint planes, along with other geological analyses, are possible.

The optical televiewer technology is based on direct optical observation of the borehole wall face and can be utilized in both air and clear fluid filled boreholes. The acoustic televiewer technology is based on the return amplitude and time of an acoustic wave reflected off the borehole wall face; it can be utilized in clear or murky fluid-filled boreholes, but not in air.

Varying borehole conditions often exist which preclude the usage of one or the other tool; therefore, the optical televiewer and acoustic televiewer are often used in conjunction to image the entire borehole. When doing so, it must be kept in mind that optical and acoustic properties are not necessarily yielding the same data set. For example, a transition between two similarly-colored beds may not stand out visually, but it may stand out acoustically if the densities of the two materials are different.

Optical Televiwer – Theory of Operation

The OBI-40 optical televiwer provides a detailed, oriented optical image of the borehole wall. A small ring of lights illuminates the borehole wall allowing a camera to directly image the borehole wall face. A conical mirror housed in a clear cylindrical window focuses a 360° optical “slice” of the borehole wall onto the camera’s lens. As the optical televiwer tool is lowered down the hole, the video signal from the camera is transmitted uphole via the wireline to the recording instrumentation.



Figures: Example of OBI40 optical Televiwer data (left) and sketch of OBI40 optical tool head (right). The signal is digitized in real time by capturing up to 720 pixels from the conical optical image. A digital magnetometer and accelerometer package is used to determine the orientation of the probe, and thus the digital image, for each conical image capture. The conical image rings are stacked and unwrapped to a 2-D, oriented image of the borehole wall.

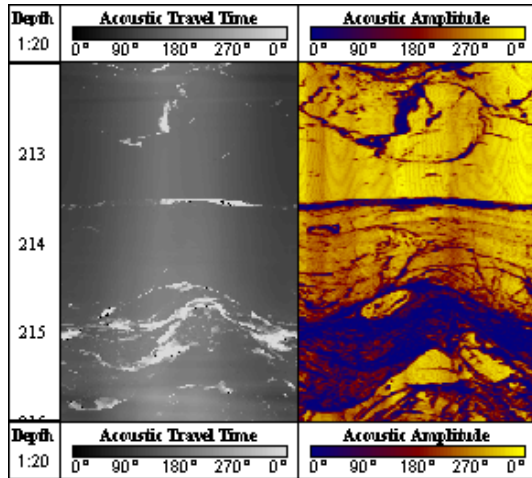
Precise borehole trajectory/deviation and image orientation are achieved using a 3-axis magnetometer and three accelerometers. When the tool is well-centralized, azimuthal accuracy is to ± 1.0 degrees and inclination accuracy is to ± 0.5 degrees. Deviated or rugous boreholes and outside magnetic interference can contribute to reduced orientation accuracy of the tool, and thus the oriented image. The pink line seen in the example data above represents a fixed point on the tool; it is used in orienting the data with respect to magnetic north.

Tool image colors are calibrated in shop to true-color, however, varying light conditions downhole often lead to color images that are somewhat false-colored. This should be taken into account when reviewing images.

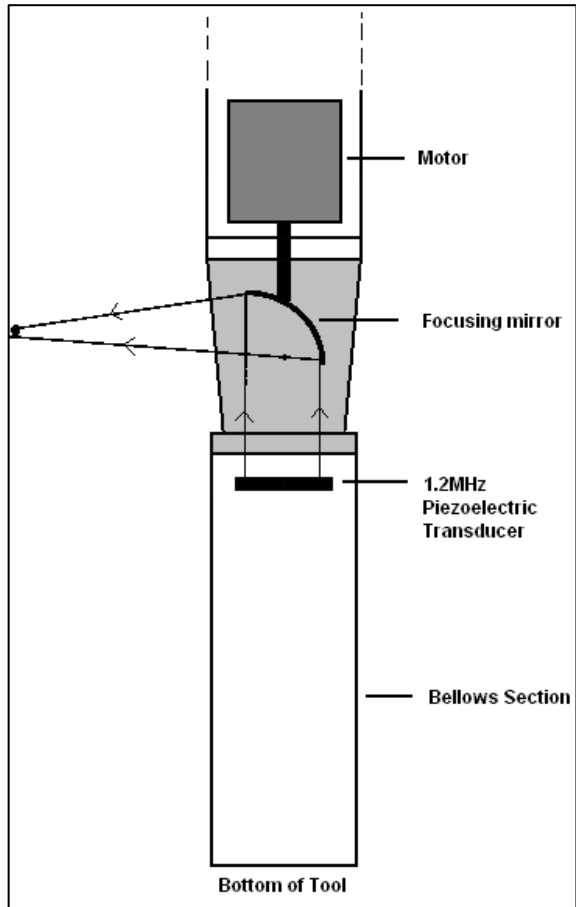
Main applications of the optical televiwer include: fracture detection and evaluation, detection of thin beds, determination of bedding dip, lithological characterization, and casing inspection.

Acoustic Televiwer (ATV) – Theory of Operation

The ABI-40 acoustic televiewer, from Advanced Logic Technologies (ALT), provides a detailed, oriented image of acoustic reflections from the borehole wall. A unique focusing system resolves bedding features as small as 2 mm and is capable of detecting fractures with apertures as small as 0.1 mm.



Figures: Example ABI40 acoustic televiewer data (left) and sketch of ABI40 acoustic head (right).



The acoustic televiewer transmits ultrasonic pulses from a rotating sensor (mirror) and records the signals reflected from the interface between the borehole fluid and the borehole wall. The amplitude of these reflections is representative of the hardness of the formation surrounding the borehole, while the travel time represents the borehole shape and diameter. As many as 288 reflections may be recorded per revolution at up to 10 revolutions per second. The conical image rings are stacked and unwrapped to a 2-D, oriented image of the borehole wall. The digital amplitude and travel time data are presented using a variety of color schemes.

Precise borehole trajectory/deviation and acoustic image orientation are achieved using a 3-axis magnetometer and three accelerometers. When the tool is well-centralized, azimuthal accuracy is to ± 1.0 degrees and inclination accuracy is to ± 0.5 degrees. Deviated or rugous boreholes and outside magnetic interference can contribute to reduced orientation accuracy of the tool, and thus the oriented image.

The high-resolution reflection images and the precise travel time measurements make the ABI-40 acoustic televiewer a versatile tool. Possible applications include: fracture detection and evaluation, detection of thin beds, determination of bedding dip, lithological characterization, casing inspection, and high-resolution caliper measurements.

Acoustic Televiewer Caliper Log

An unconventional caliper log may be generated from the travel time data acquired by the ABI-40 acoustic televiewer. Using WellCAD software, an estimation of the distance from the probe to

the borehole wall can be made by incorporating the travel time of the acoustic signal with an estimation of the velocity of the borehole fluid. The time it takes the acoustic signal to travel through a known viscous medium and back to the probe is directly related to the distance between the signal generator and the borehole wall provided the borehole fluid viscosity remains constant and the probe is properly centralized. The distance from the probe to the borehole wall is then corrected for the radius of the probe, producing a borehole diameter value.

Understanding 2-D Televiewer Images

For both the optical and acoustic televiewer, the 2-D picture of the borehole wall is unwrapped from north to north. Planar features that intersect the borehole appear to be sinusoids on the unwrapped image. To calculate the dip angle of a fracture or bedding feature, the amplitude of the sinusoid (h) and the borehole diameter (d) are required. The angle of dip is equal to the arc tangent of h/d , and the dip direction is picked at the trough of the sinusoid.

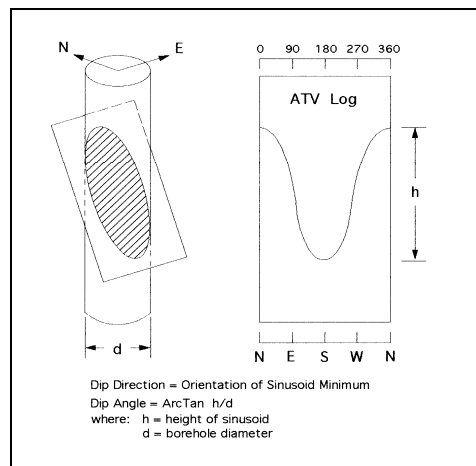


Figure: Geometric representation of a north-dipping fracture plane and corresponding log.

Interpreting Optical and/or Acoustic Televiewer Data

Sinusoidal features are picked throughout the boreholes by visual inspection of the digital optical and acoustic televiewer images using the interactive software WellCAD. These sinusoidal feature *projections* can directly overlay the televiewer images or be plotted alongside the televiewer images.

The features can also be represented by *tadpoles*. The tail of the tadpole points in the azimuthal direction of dip, where north is up, east is 90° to the right, etcetera. The head of the tadpole is located vertically on the plot, at the projection's inflection point, that is, halfway between the peak and the trough depth of the sinusoidal projection. The horizontal head location represents the dip angle, with shallow features near the left side of the plot and steeper features near the right side.

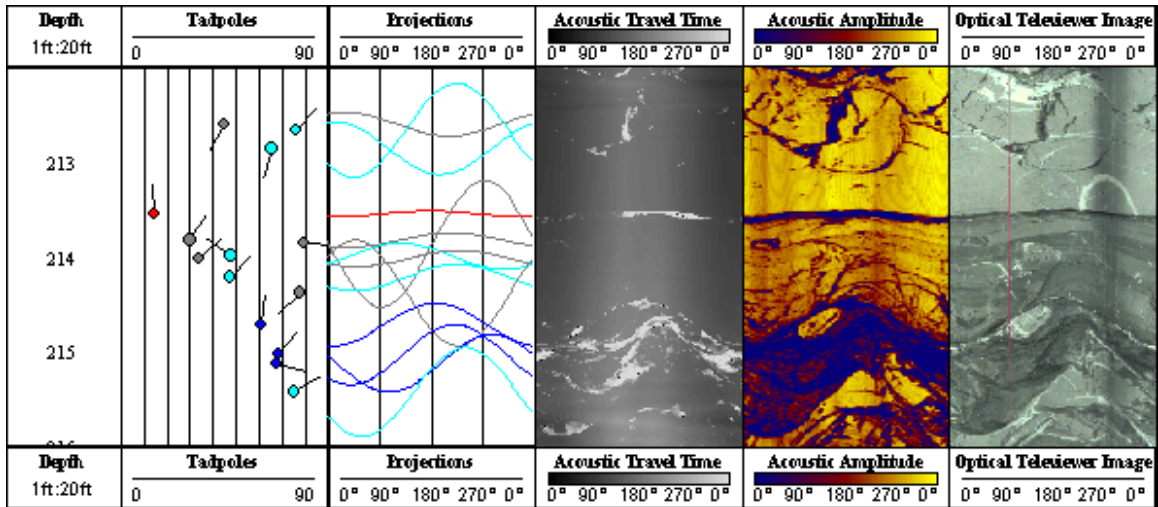


Figure: Example projections and tadpoles for corresponding optical and acoustic televiewer data sets.

The WellCAD software calculates the true feature orientation (dip direction and angle) in either deviated or vertical boreholes. Depths are assigned to the fractures or bedding features at the inflection points (middles) of the sinusoids. Features are subjectively ranked for flow potential using *COLOG's Ranking System for Optical Televiewer Features*, included in this report. The features picked, along with their assigned ranks, orientations and depths are exported and presented in tables for each well. Orientations are based on magnetic north and are not corrected for magnetic declination, unless specified.

From the feature data tables, stereonet plots and rose diagrams are generated, as necessary. Stereonet plots and rose diagrams provide useful information concerning the statistical distribution and possible patterns or trends that may exist from the optical and/or acoustic televiewer feature orientation data set.

Rose Diagrams

A rose diagram is a polar diagram in which radial length of the petals indicates the relative frequency (percentage) of observation of a particular angle or fracture dip direction or range of angles or dip directions. Rose diagrams are used to identify patterns (if any) in the frequency of dip angles or directions for a particular data set. The following rose diagrams and stereonet plots all come from the same data set to help illustrate the relationships between the plot types.

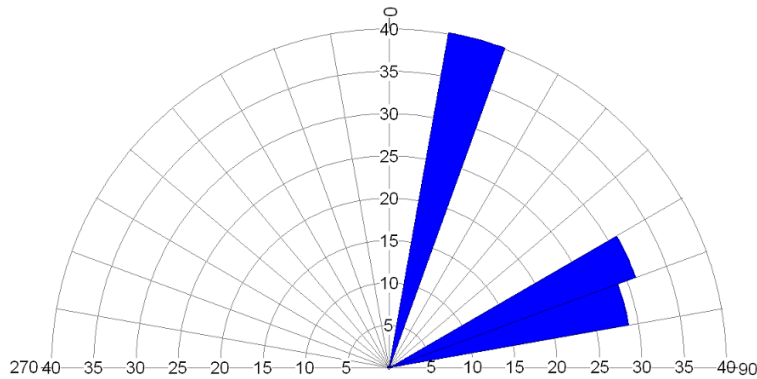


Figure: Example rose diagram from an optical televiewer data set illustrating the frequency (%) of dip angles.

With a quick glance at the above rose diagram of dip angle values, one can see two distinct sets of dip angles; one set with lower dip angles and one set with higher dip angles. Specifically, 40 percent of the features have a dip angle between 10° and $<20^\circ$, and 60 percent of the features have a dip angle between 60° and $<80^\circ$. The left-hand side of the above rose diagram will always be blank by convention of positive dip angle values only.

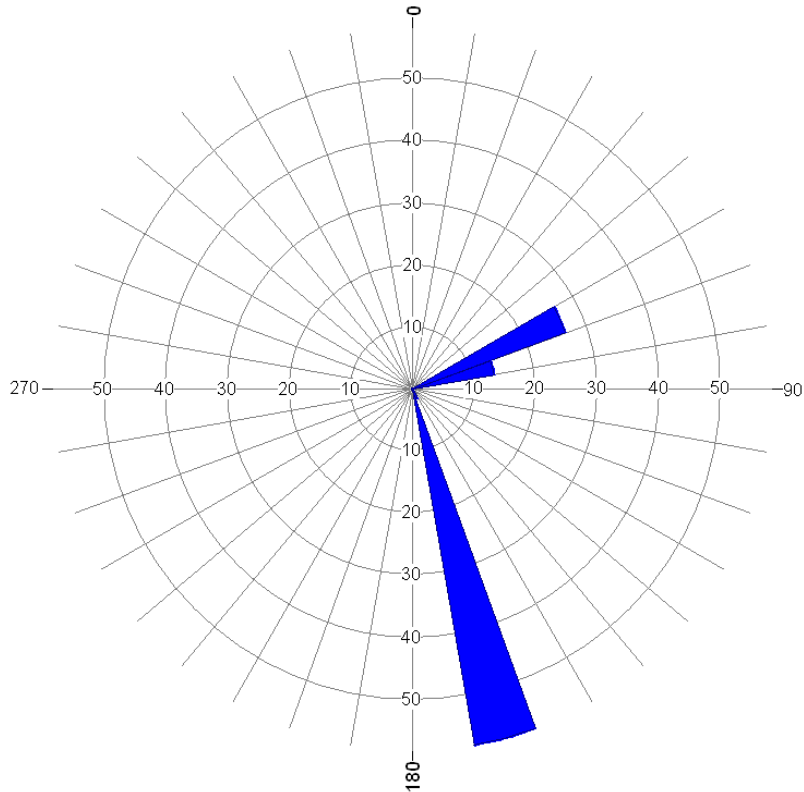


Figure: Example rose diagram from an optical televiwer data set illustrating the frequency (%) of dip direction (azimuth).

With a quick glance at the above rose diagram of dip direction values, one can see that the features (and/or fractures) in this data set have two primary dip directions. Specifically, 40 percent of the features dip to the east-northeast between 60° degrees and $<80^\circ$ in azimuth and 60 percent of the features dip to the south-southeast between 160° and $<170^\circ$ in azimuth.

Stereonets

For stereonets, Colog utilizes a southern-hemisphere projected, equal-area Schmidt net to plot the poles to the feature planes. These plots are often used in plotting geologic data such as the dips and orientations of structural features. Here, the azimuthal angle indicates dip direction of the plane's pole (which dips 180 degrees opposite in azimuth from the plane's dip direction at a complementary angle). The distance from the center indicates the dip magnitude. The further from the center the steeper the dip angle; the closer to the center the more horizontal the feature is.

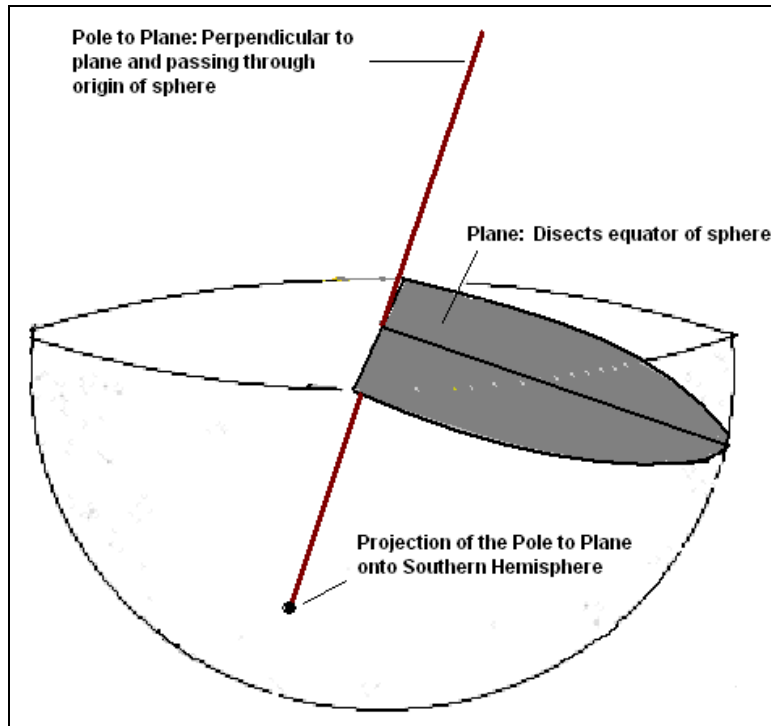


Figure: The above cartoon demonstrates the relationship between a plane and its pole, as projected onto the southern hemisphere of a sphere.

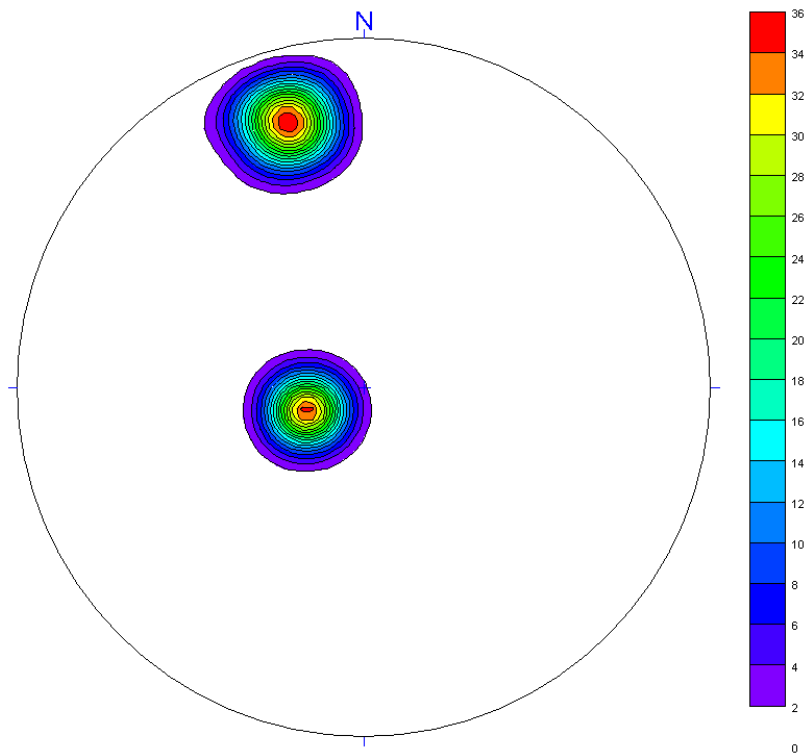
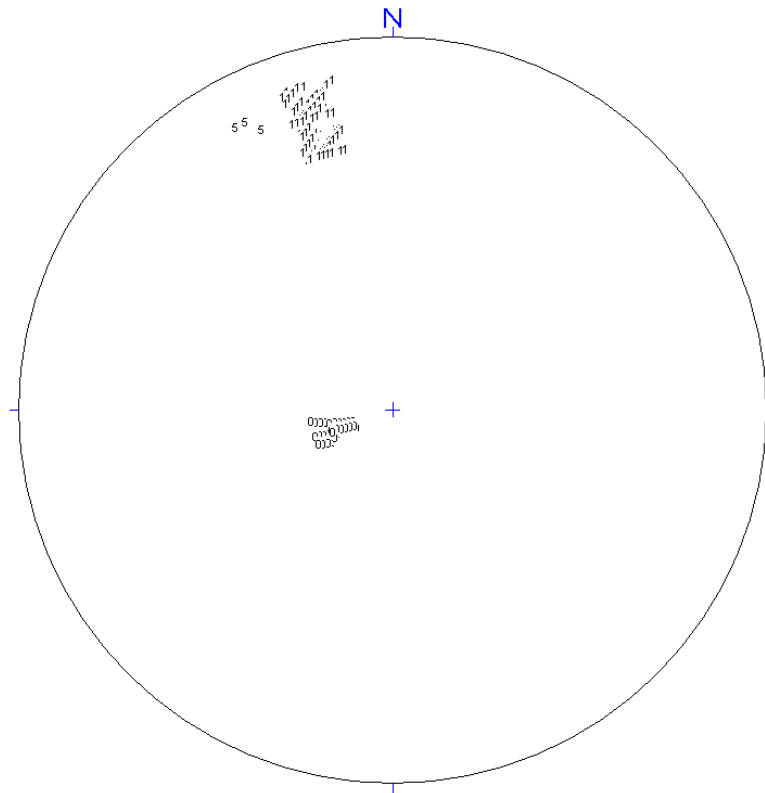


Figure: Example stereonet from an optical televiewer data set illustrating the frequency (%) of dip direction and dip angle.

The figure above is an example stereonet diagram from the same televiewer data set of fractures and features as used previously to describe rose diagrams. It was created by binning the density (frequency) of poles per area. The figure below indicates, with a quick glance, that two distinct patterns exist in the example data set. A cluster of fractures/features with similar dip directions of approximately 160-170 degrees with steep dip angles of around 60-80 degrees is apparent. A second cluster is apparent with similar dip directions of approximately 60-80 degrees with moderate dip angles of approximately 10-20 degrees. The white areas indicate low to zero density of poles.



Colog also often provides a Schmidt net with the qualitative rank of each fracture/feature plotted at the location of its planar pole. Please refer to the *Ranking System for Optical/Acoustic Televiewer Features*, included in the report, for an explanation of the qualitative ranks assigned each optical/acoustic televiewer feature identified.

With a quick glance at the above Schmidt net, one can see that the low dip angle features which dip to the east-northeast are bedding features, ranked “0”; the high dip angle features dipping to the south-southeast are primarily weak or partial fractures, ranked “1”; and there are several major fracture zones, ranked “5”, with strike/dip very similar to the majority of the partial/weak fractures in the well.

2.2 Natural Gamma

The natural gamma log (also known as gamma or gamma ray log) provides a measurement recorded in counts per second (CPS), that is proportional to the natural radioactivity of the formation. Actual counts depend upon the detector size and. The depth of investigation for the

gamma log is typically 10 to 12 inches. Gamma logs provide formation clay and shale content and general stratigraphic correlation in sedimentary formations. In general, the natural gamma ray activity of clay-bearing sediments is much higher than that of quartz sands and carbonates. Gamma logs are also used in hard rock environments to differentiate between different rock types and in mining applications for assessment of radioactive mineralization such as uranium, potash, etc.

Gamma radiation is measured with scintillation NaI detectors. The gamma-emitting radioisotopes that naturally occur in geologic materials are Potassium40 and nuclides in the Uranium238 and Thorium232 decay series. Potassium40 occurs with all potassium minerals, including potassium feldspars. Uranium238 is typically associated with dark shales and uranium mineralization. Thorium232 is typically associated with biotite, sphene, zircon and other heavy minerals.

The usual interpretation of the gamma log, for hydrogeology applications, is that measured counts are proportional to the quantity of clay minerals present. This assumes that the natural radioisotopes of potassium, uranium, and thorium occur in exchange ions, which are attached to the clay particles. Thus, the correlation is between gamma counts and the cation exchange capacity (CEC). Usually gamma logs show an inverse linear correlation between gamma counts and the average grain size (higher counts indicate smaller grain size, lower counts indicate larger grain size). This relation can become invalid if there are radioisotopes in the mineral grains themselves (immature sandstones or arkose), and if there are differences in the CEC of clay minerals in the different parts of the formation. Both of these situations are possible in many environments. The former situation would most likely occur in basal conglomerates composed of granitic debris, and the latter where clay occurs as a primary sediment in shale and another as an authigenic mineral deposited in pore spaces during diagenesis.

Calibration of the gamma logging tool may be performed in large physical models such as the API test pits in Houston, or the DOE uranium calibration test pits. In hydrogeology, the gamma measurement is usually a relative log and quantitative calibrations are not routinely performed. However, the stability and repeatability of the natural gamma measurement is routinely checked with a sleeve of known radioactivity. It is also common to routinely check the gamma log by repeat logging a section of a well. Natural radioactive decay follows a Gaussian distribution; that is, approximately 67% of the radioactive response occurs within \pm the square root of the count rate. For instance, if a background radiation of 100 CPS is being measured, there is approximately \pm 10 CPS variability.

Fundamental assumptions and limitations inherent in these procedures are as follows:

- The natural gamma ray log, as with all nuclear or radiation logs, have a fundamental advantage over most other logs in that they may be recorded in either cased or open holes that are fluid or air filled. Borehole fluid and casing may attenuate the gamma values.

Excessive borehole rugosity, often caused by air drilling, may degrade natural gamma ray log.

2.3 Single Point Resistance (SPR) and Spontaneous Potential (SP)

Single Point Resistance (SPR)

The SPR measurement is controlled by rock and fluid parameters in much the same way as resistivity logs. SPR is a simple system of two electrodes (the resistivity current electrode) and a surface electrode. Current is passed through the formation and voltage differences are measured between the two electrodes. The measured resistance includes the resistance of the cable, borehole fluid, and the formation around the borehole. The current density is higher near the borehole electrode and surface electrode. Since the current density at the surface electrode is constant, formation variations close to the probe produce the resistance changes visible on the logs. Since there is a single downhole electrode, not an array, the log effectively shows a point measurement. This gives a very "responsive", high vertical resolution measurement. Though the single point resistance cannot be calibrated quantitatively, its instantaneous response is a good boundary indicator, and does show a more well defined response than the 16" or 64" Normal Resistivities

Spontaneous Potential (SP)

The SP is a measurement of the naturally occurring potential in the borehole. This naturally occurring potential is most often caused by a concentration gradient between the borehole fluid and formation fluid (electro-chemical), and requires the presence of a clay rich/porous media interface to occur. Reduction/oxidation (redox) interfaces and streaming potentials (electro-kinetic), caused by the flow of fluid in or out of the borehole, are also causes for the occurrence of spontaneous potential.

In fresh water environments where the drilling fluid is natural or the salinity is near the formation pore fluid salinity the electro-chemical potential is minimized. The absence of sulfide mineralization or fluid movement into or out of the formation may minimize the redox and streaming potentials.

2.4 Heat Pulse Flowmeter

The Heat Pulse Flowmeter (HFP-4293), from Mount Sopris Instruments is a high resolution device for measuring vertical fluid movement within the borehole. This flowmeter is based upon the proven USGS design and works on the thermal fluid tracer concept. Borehole fluid is heated or thermally tagged by as much as 1° F with an electrical heater grid. The flow rate is determined by measuring the time between the grid discharge and the peak of the thermal pulse of water reaching an upper or lower thermistor sensor. MSI utilizes flow concentrating diverters to direct fluid flowing in the borehole through the probe flow tube (Figure).

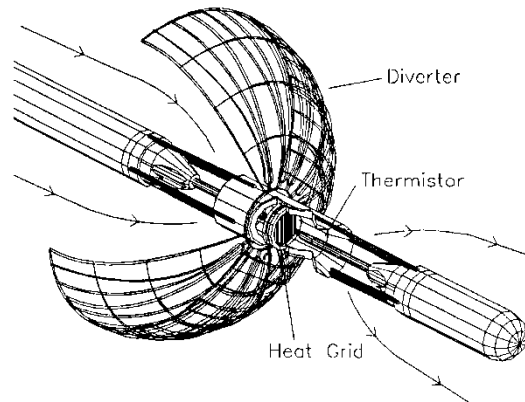


Figure: Heat pulse flowmeter diverter diagram showing fluid flow

The HFP-4293 is calibrated in a flow chamber where flow rate can be controlled and measured. Values for response time are taken for a wide range of flow rates and applied in an empirical curve-fit solution (Figure H-2). The calibration coefficients are entered into the processing software to determine vertical flow rates in gallons/minute. Thermal buoyancy of the heat pulse imposes a small asymmetry on the flow calibration so that the device is slightly less sensitive to upflow than to downflow.

Presently the HFP measures flow from 0.01 to 1.5 gallons/minute (0.038 to 5.69 liters/min) with 0.005 gpm resolution using a 1.125 inch diameter flow tube and standard multilayered flow diverter. The low end flow limit of 0.01 gpm is a function of the current calibration facility in which convective eddy currents as great as 0.01 gpm are generated by differences between water temperature in the calibration device and surrounding air. A more thermally insulated calibration chamber or smaller diameter probe flow tube could allow for significantly lower flow limit with this tool. Higher flow rates can be achieved by increasing thermistor spacing or flow tube and heating grid diameter.

In practice the HFP is run at discrete intervals within a borehole. Intervals are selected based upon review of fluid column logs (temperature, fluid resistivity, etc.), a caliper log and optimally a borehole imaging log (video or acoustic televiewer). Flow is measured at each interval and each test repeated until at least two measurements are recorded within given tolerances. Time to collect flow data is subject to the flow rate and number of intervals tested. While the actual time to record a flow rate of 0.01 gpm is less than 30 seconds, it may take up to 15 minutes per station for the borehole to stabilize and to obtain repeatable data. At higher flow rates, the borehole stabilizes more quickly and obtaining good data may take only a few minutes per station.

Heat Pulse Calibration Curves (Up and Down Flow)

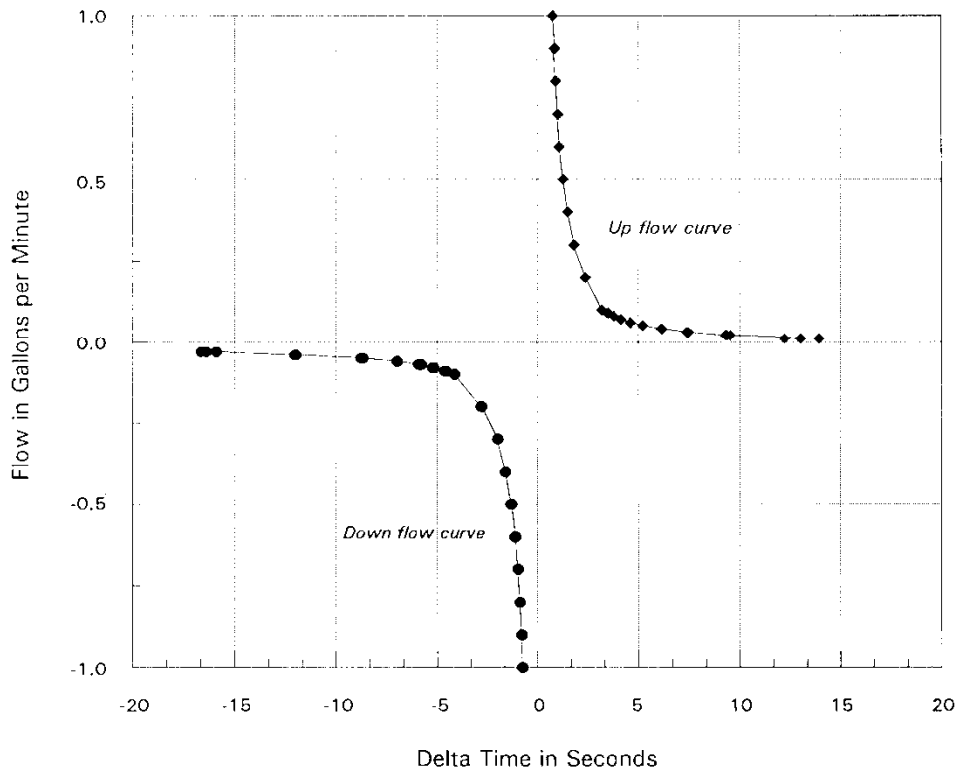


Figure: Heat pulse flowmeter calibration curves used to translate response time to gpm.

A number of factors must be considered when interpreting high-resolution flow data including: 1) the effect of the open borehole on the flow regime in the vicinity of the well bore; 2) the effects of turbulent thermal convection and other secondary flow circulations; 3) real flow regimes are often changing with time as measurements are being made; and, 4) not all permeable intervals may be producing vertical flow under ambient conditions. (Paillet et al, 1994)¹ describes these factors in detail which should be reviewed for a more thorough discussion.

Some of these factors can be minimized by using a flow concentrating diverter and by locating the diverter in a portion of the borehole that is not fractured or rugose (by analyzing the caliper and a borehole imaging log). More importantly, flow measurements should be collected in the same intervals under different head conditions. In areas where the flow regime is changing with time, a number of flow measurements should be measured at the same intervals over time and the resulting flow transients interpreted. Other variations include cross-borehole experiments where one borehole is pumped and the changes in flow are detected in the surrounding boreholes. This can provide a quick assessment of the hydraulic connections between boreholes.

¹ Paillet, Crowder and Hess, 1994, High-Resolution Flowmeter Logging - A Unique Combination of Borehole Geophysics and Hydraulics: Part II - Borehole Applications with the Heat-Pulse Flowmeter, Proceedings of the Symposium on the Application of Geophysics to Engineering and Environmental Problems, Boston, Massachusetts, pages 381-404.

3.0 37-B06 Logging Results

3.1 Geophysical Logging

On January 17 and 18, 2013, downhole geophysical investigations were performed in boring 37-B06. The geophysical logs performed were: optical televiewer (OBI), acoustic televiewer, natural gamma, single point resistance (SPR), spontaneous potential (SP), and heat pulse flow meter. The data for these logs are presented in the 37-B06 Geophysical and Flow Logs plot, the Acoustic and Optical Televiewers Plot, the stereonet and rose diagrams, and the orientation summary table of televiewer features. Please see Appendix A to view these plots and diagrams.

3.2 Optical Televiewer (OBI) & Acoustic Televiewer (ABI)

On January 17 and 18, 2013, OBI and ABI logging was performed in 37-B06. The OBI was logged from 4.1 feet to a depth of 108.1 feet while the ABI was logged from 51.1 feet to 110.1 feet.

The OBI and ABI dataset indicates features at depths which correlate well with the water-bearing intervals identified from the heat pulse flow meter data. In general, the OBI and ABI identified fractures/features with aperture at water producing zones. Fracture density and fracture orientation were evaluated over the entire OBI and ABI dataset. The Rose Diagram – Dip Directions image indicates approximately 32.4% of the identified features in 37-B06 dip in the direction of 50 to 100 degrees (East-Northeast and East-Southeast).

The Rose Diagram – Dip Angles image indicates over approximately 86% of the features in 37-B06 are dipping at more than 40° from horizontal, while the remaining features are dipping at less than 40° from horizontal.

There are 103 high-angle fractures or features (dip angles greater than 45°) identified in 37-B06. These 103 high-angle features represent 76.2% of all identified features from the OBI and ABI data set. The 103 high-angle features are qualitatively ranked 0 to 3, suggesting minimal flow potential from these features. Please see the Rose Diagrams, Stereonets and the Fracture Feature Table for a complete summary of all fracture and feature orientations.

3.3 Natural Gamma

On January 17 and 18, 2013, natural gamma logging was performed in 37-B06 to a depth of 104.8 feet. The natural gamma log is relatively featureless and registers a nominal counts per second (CPS) rate of approximately 65 CPS. Minor fluctuations in CPS are observed and expected due to heterogeneities in the formation and/or changes in the clay volume around the logging probe.

3.4 Single Point Resistance (SPR) & Spontaneous Potential (SP)

On January 17 and 18, 2013, Single Point Resistance (SPR) and Spontaneous Potential (SP) logging was performed in 37-B06 from a depth of 71.0 to 107.9 feet (SPR log) and 65.7 to 102.3 feet (SP). The SP log shows a steady decline from approximately 825 mV to 398 mV at the bottom of the borehole. The SPR log ranges from approximately 50 to 250 Ohms and does not indicate a trend.

3.5 Heat Pulse Flow Meter

The Heat-Pulse Flowmeter indicated no flow during ambient conditions between approximately 51 and 58 feet. Minor flow was indicated at 60.7, 66.1, 71.0, 76.6, 96.0, and 102.0 feet with flow ranging from 0.02 to 0.04 gpm. During pumping, water was drawn up the borehole, and extracted at 1.07 gpm. The Heat-Pulse tests in the deepened borehole, during pumping, indicated upflow with a maximum of 0.03 gpm at 71.0 feet and a minimum of 0.01 gpm at 83.9 feet. This decreasing flow with depth indicates that the entire interval was contributing to the flow of fluid into the borehole and adding to the flow rate with successively shallower tests.

4.0 37-B09 Logging Results

4.1 Geophysical Logging

On January 18, 2013, downhole geophysical investigations were performed in boring 37-B09. The geophysical logs performed were: optical televiewer (OBI), acoustic televiewer (ABI), and natural gamma. The data for these logs are presented in the 37-B09 Geophysical Logs Plot, the Acoustic and Optical Televiewer Image Plot, the stereonet and rose diagrams, and the orientation summary table of televiewer features. Please see Appendix B to view these plots and diagrams.

4.2 Optical Televiewer (OBI) & Acoustic Televiewer (ABI)

On January 18, 2013, optical OBI and ABI logging were performed in 37-B09. The OBI was logged from 11.8 feet to a depth of 88.9 feet while the ABI was logged from 78.6 feet to 89.3 feet.

In general, the OBI and ABI identified fractures/features with aperture at possible water producing zones. Fracture density and fracture orientation were evaluated over the entire OBI and ABI dataset. The Rose Diagram – Dip Directions image indicates approximately 26% of the identified features in 37-B06 dip in the direction of 320 to 360 degrees (Northwest) and 25.5% dip in the direction of 140 to 200 degrees (Southeast).

The Rose Diagram – Dip Angles image indicates over approximately 66% of the features in 37-B09 are dipping at more than 50° from horizontal, while the remaining features are dipping at less than 50° from horizontal.

There are 97 high-angle fractures or features (dip angles greater than 45°) that were identified in 37-B09. These 97 high-angle features represent 79.5% of all identified features from the OBI and ABI data set. The 97 high-angle features are qualitatively ranked 0 to 3, suggesting minimal flow potential from these features, with the exception of one high-angle feature ranked 4, suggesting a

nominal flow potential. Please see the Rose Diagrams, Stereonets and the Fracture Feature Table for a complete summary of all fracture and feature orientations

4.3 Natural Gamma

On January 18, 2013, natural gamma logging was performed in 37-B09 to a depth of 83.3 feet. The natural gamma profile is relatively featureless and registers a nominal counts per second (CPS) reading of approximately 28 to 139 CPS throughout the borehole. Minor fluctuations in CPS are observed and expected due to heterogeneities in the formation and/or changes in the clay volume around the logging probe. Two significant gamma peaks are observed at 28 and 52 feet, indicating increased clay content at these depths.

5.0 Limitations

COLOG's logging was performed in accordance with generally accepted industry practices. COLOG has observed that degree of care and skill generally exercised by others under similar circumstances and conditions. Interpretations of logs or interpretations of test or other data, and any recommendation or hydrogeologic description based upon such interpretations, are opinions based upon inferences from measurements, empirical relationships and assumptions. These inferences and assumptions require engineering judgment, and therefore, are not scientific certainties. As such, other professional engineers or analysts may differ as to their interpretation. Accordingly, COLOG cannot and does not warrant the accuracy, correctness or completeness of any such interpretation, recommendation or hydrogeologic description.

All technical data, evaluations, analysis, reports, and other work products are instruments of COLOG's professional services intended for one-time use on this project. Any reuse of work product by Client for other than the purpose for which they were originally intended will be at Client's sole risk and without liability to COLOG. COLOG makes no warranties, either express or implied. Under no circumstances shall COLOG or its employees be liable for consequential damages.

Appendix A



Acoustic and Optical Televiewers

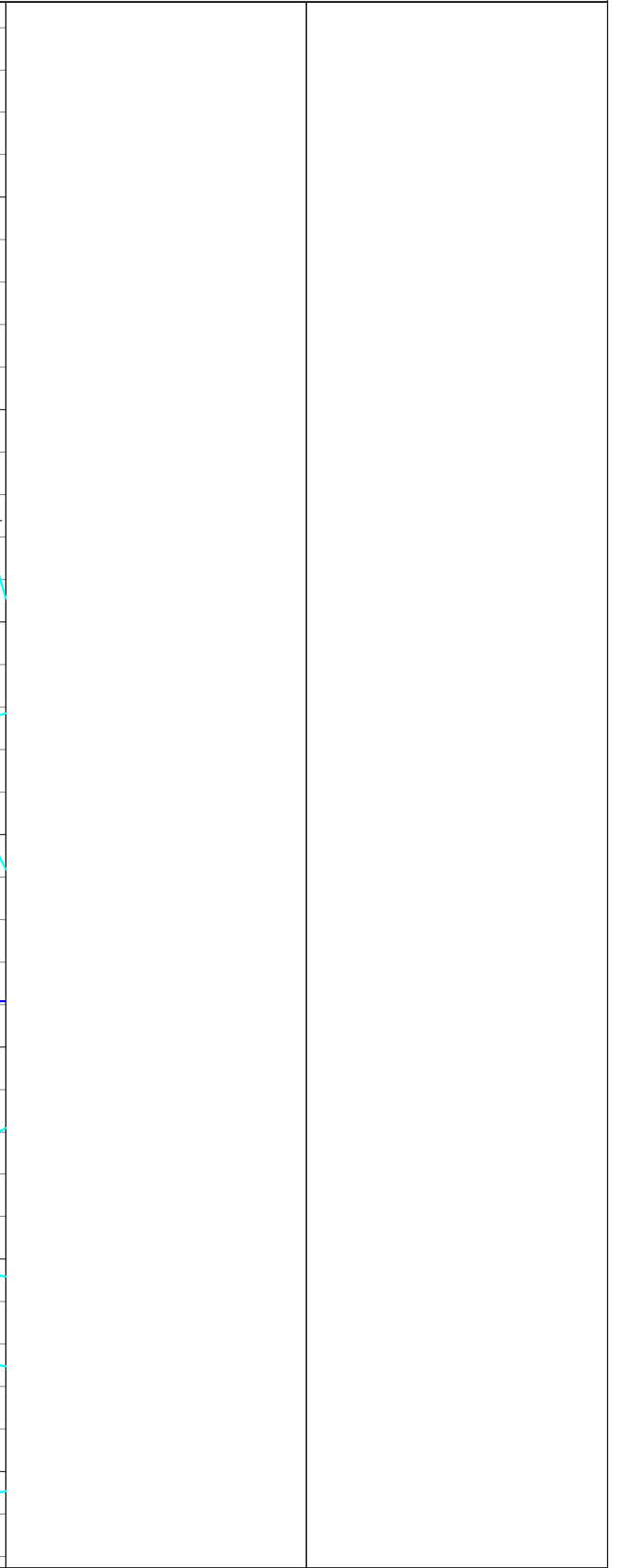
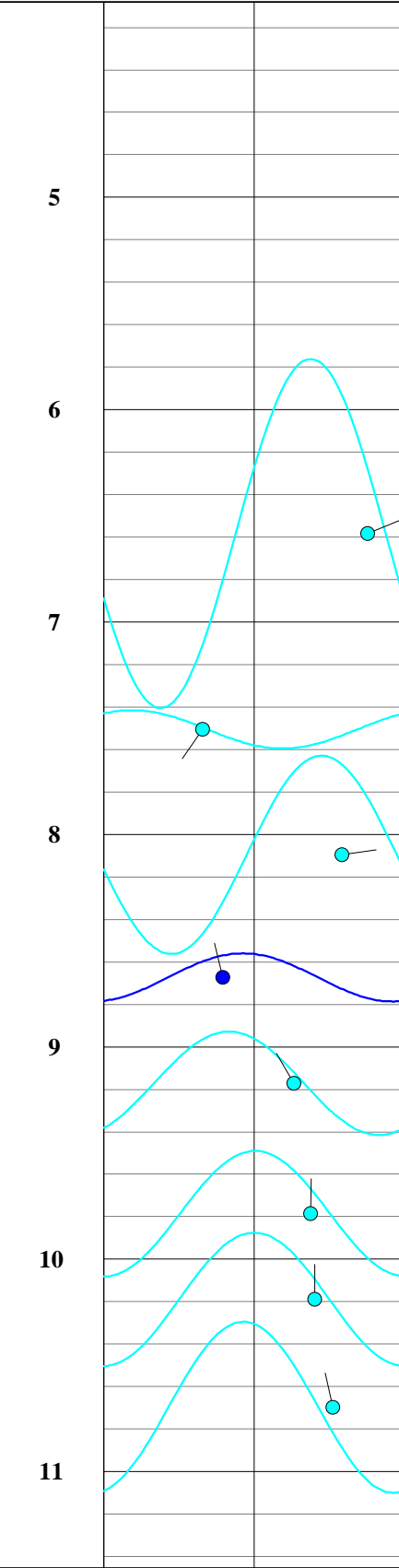
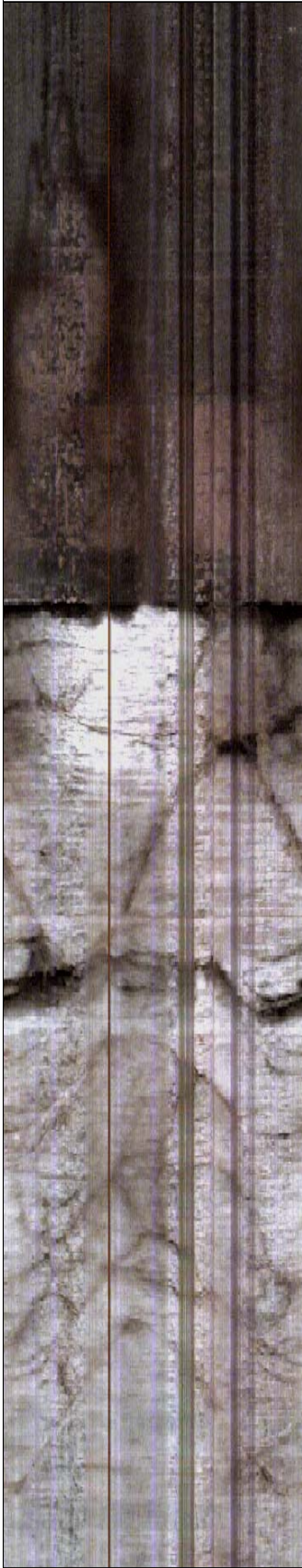
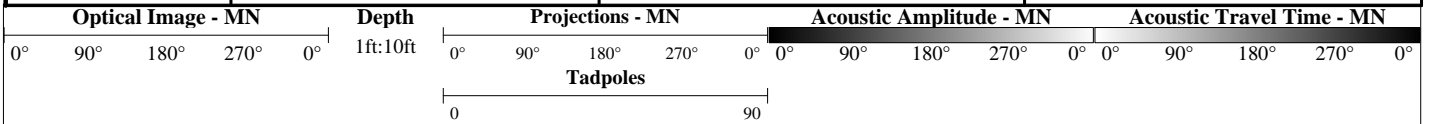
COLOG Main Office
810 Quail Street, Suite E, Lakewood, CO 80215
Phone: (303) 279-0171, Fax: (303) 278-0135
www.colog.com

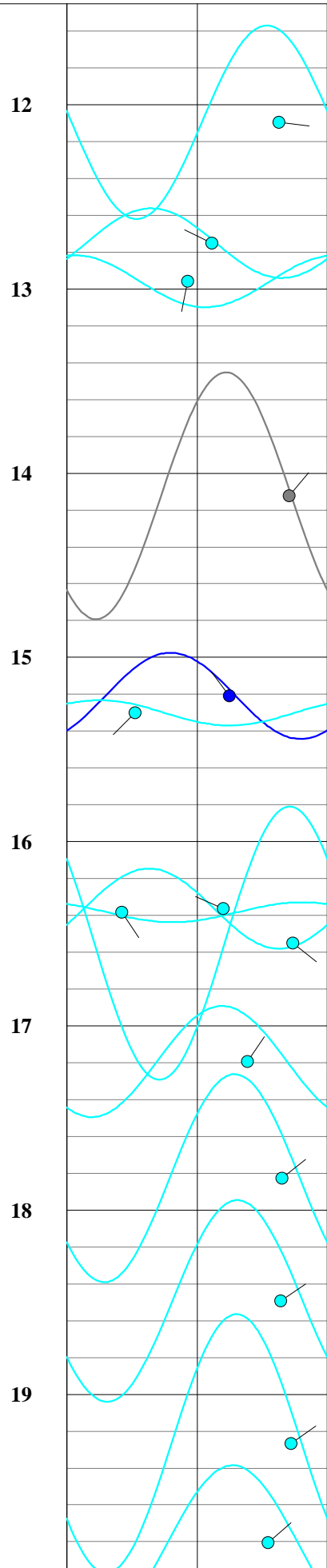
COMPANY: Shaw

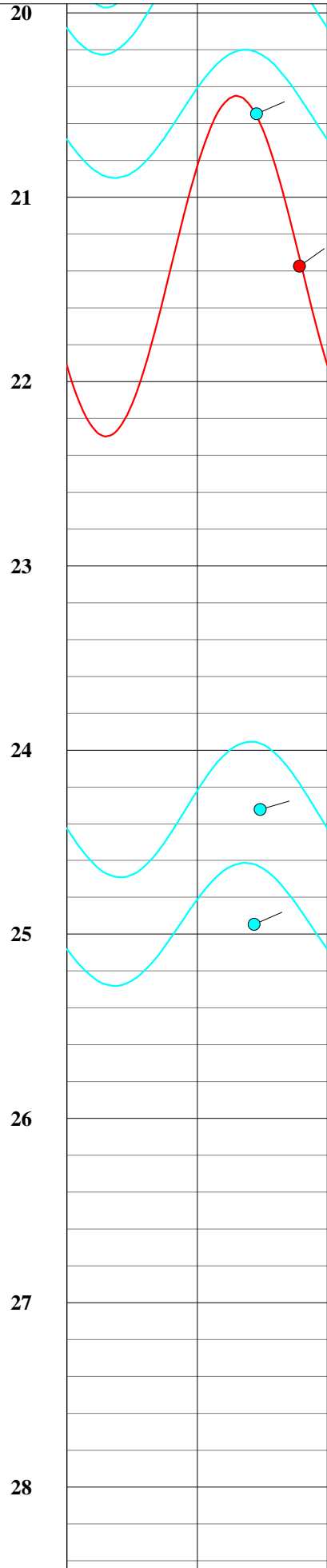
PROJECT: Hermosa

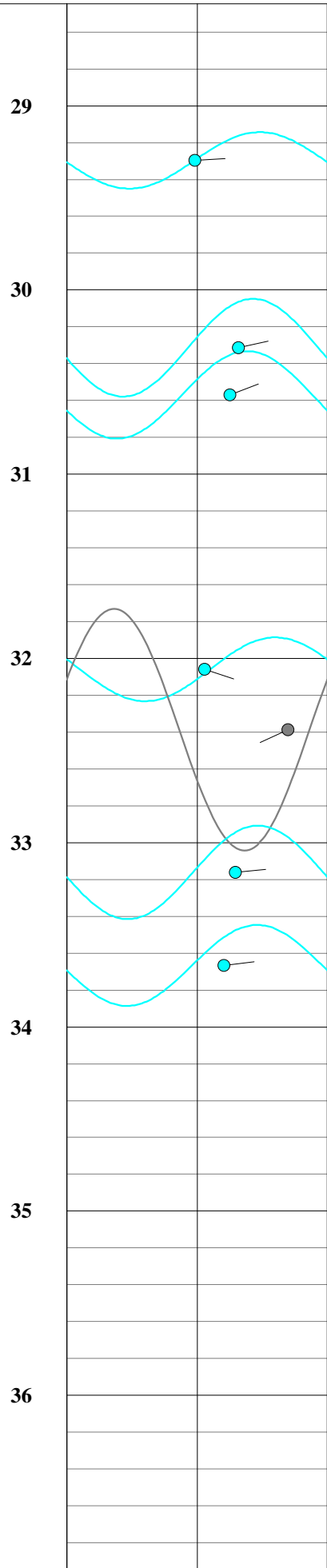
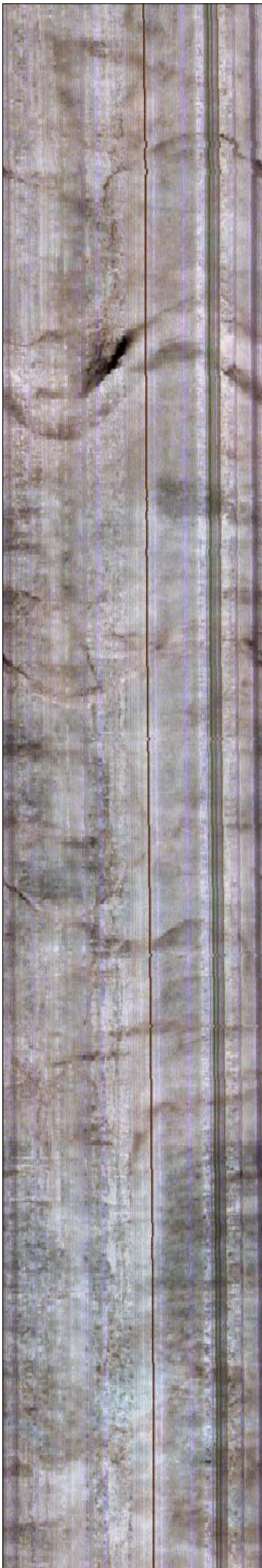
DATE LOGGED: 17-18 Jan 2013

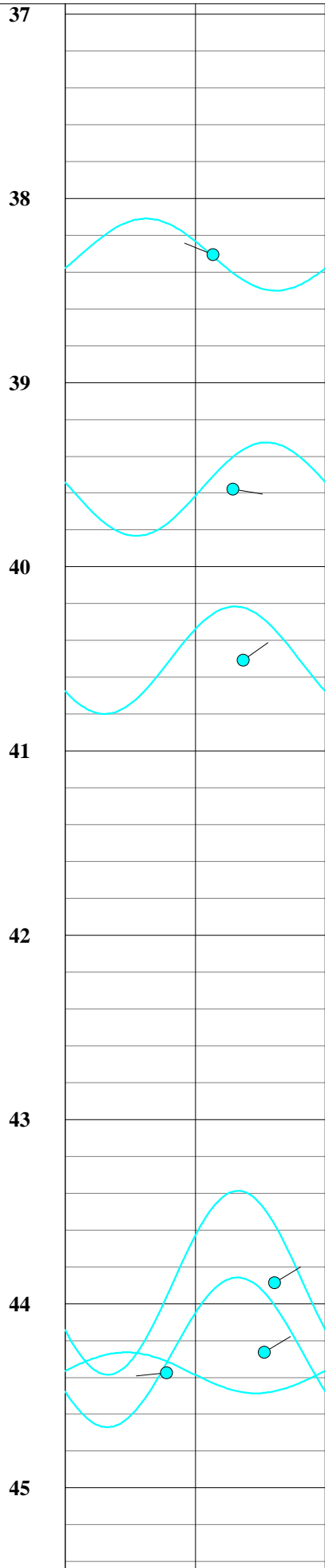
WELL: 37-B06

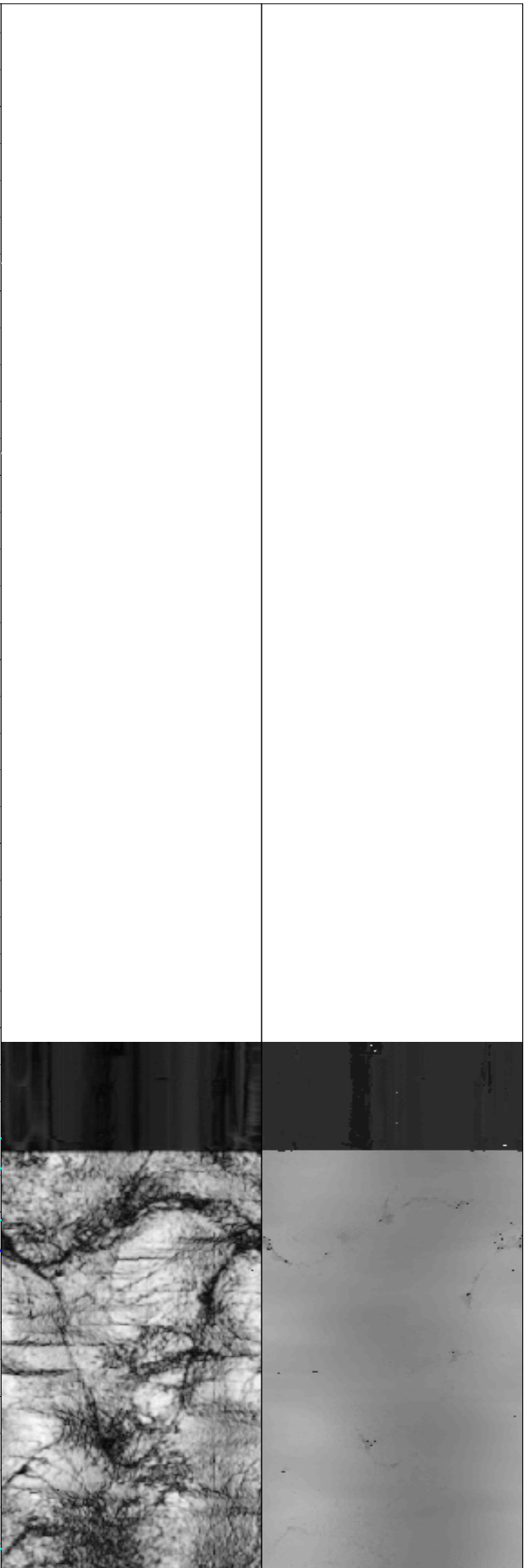
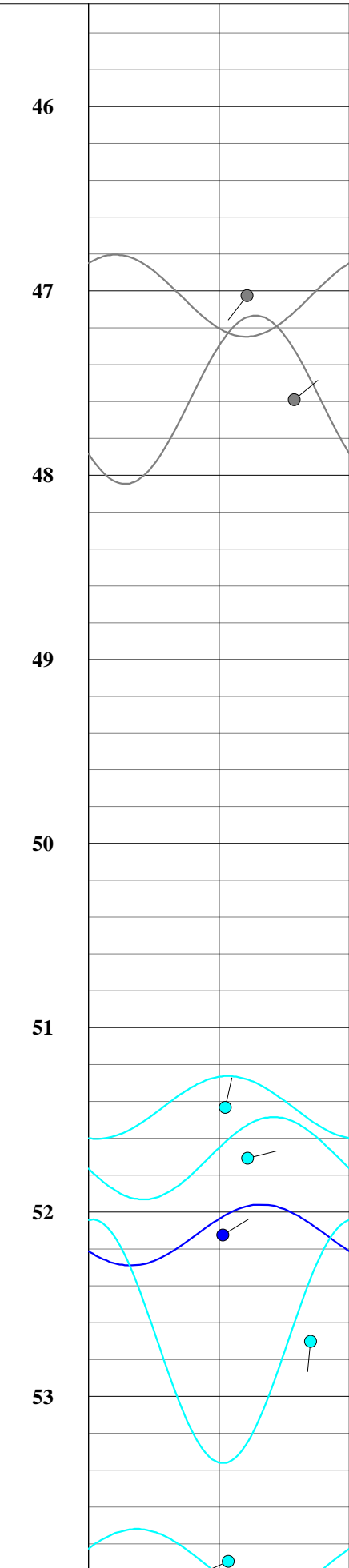
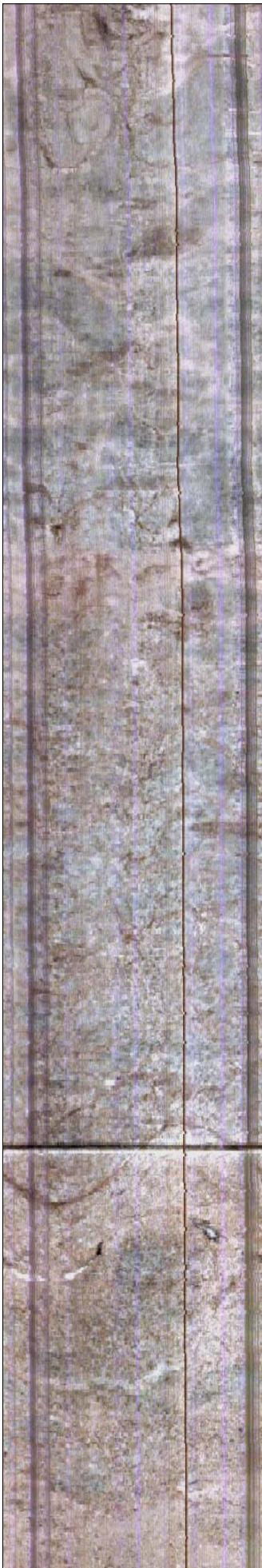


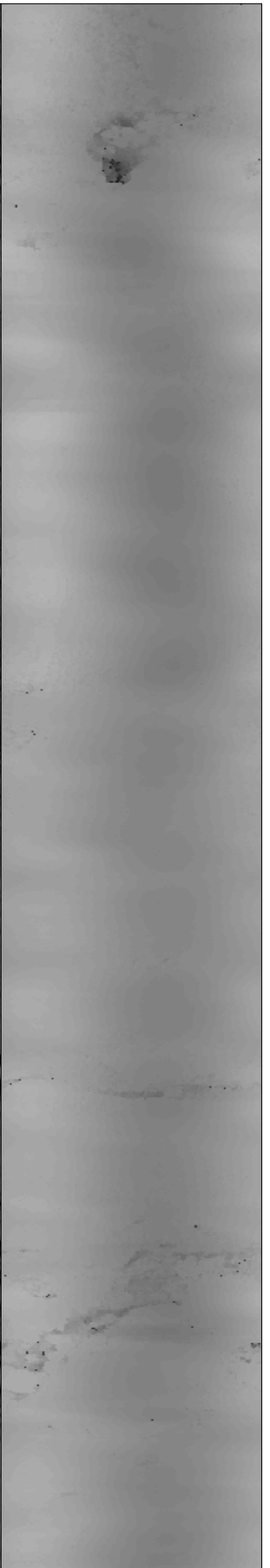
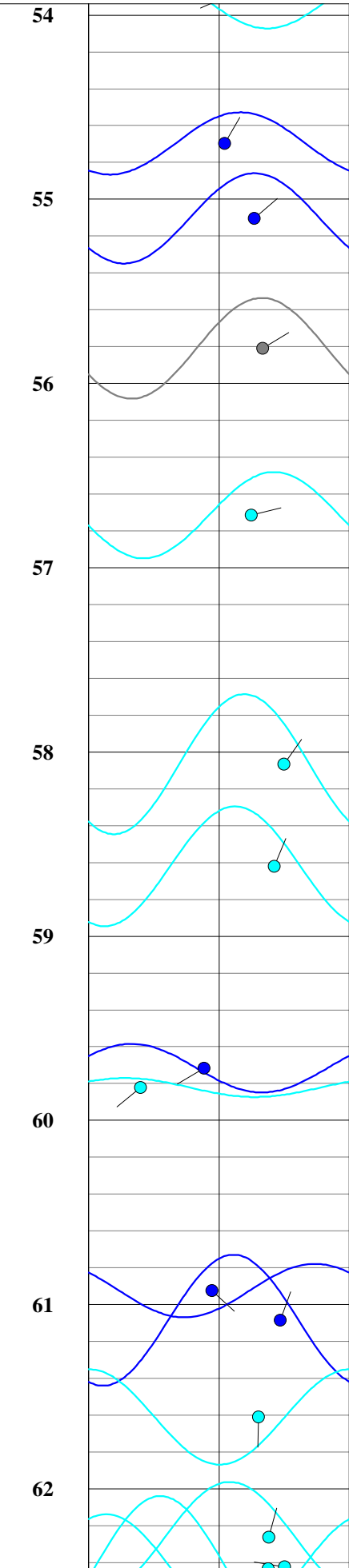


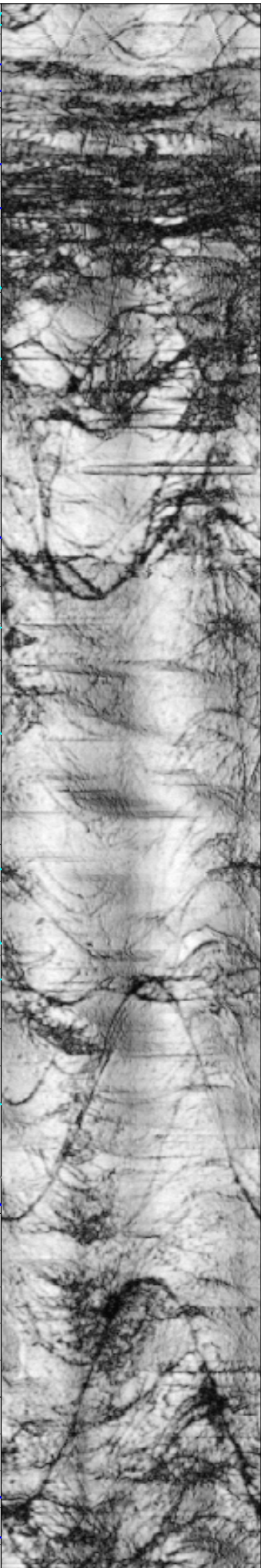
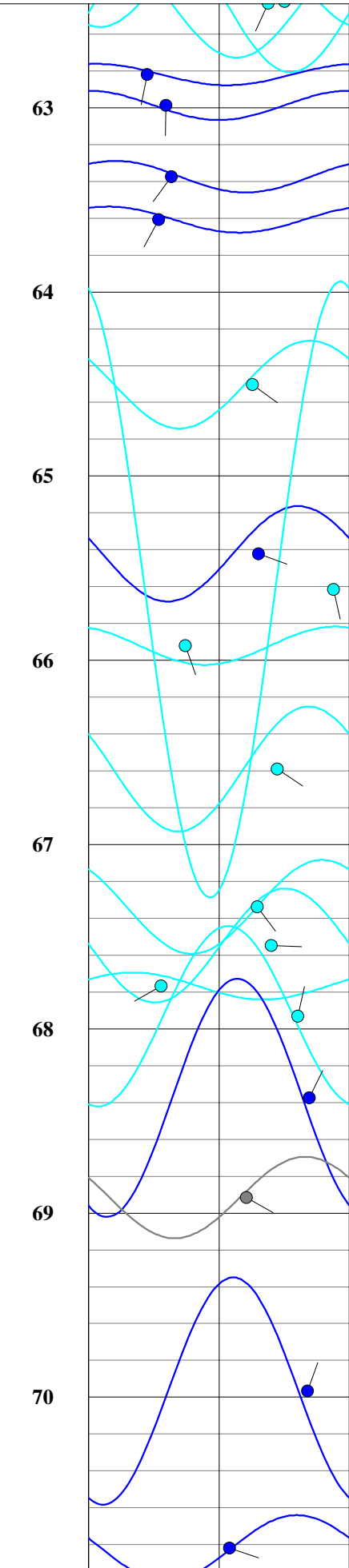
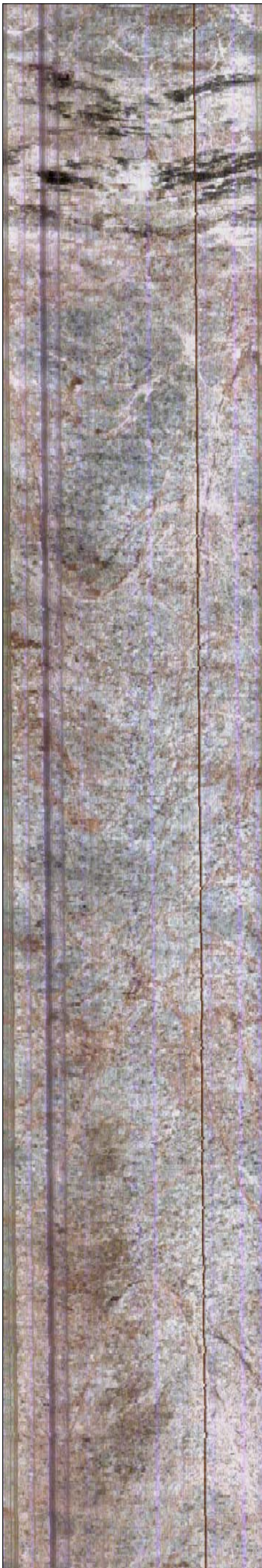


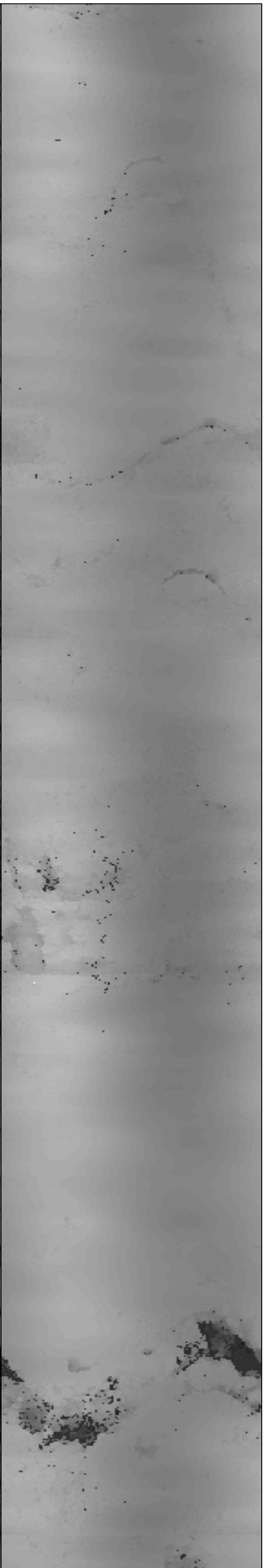
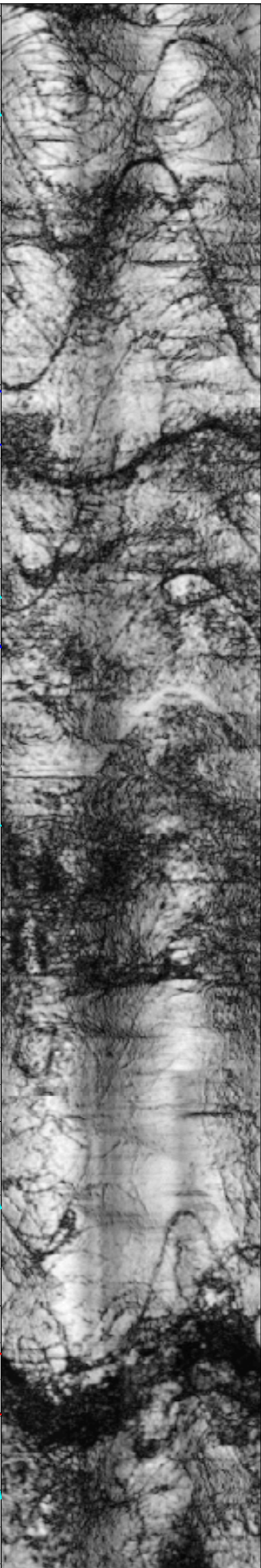
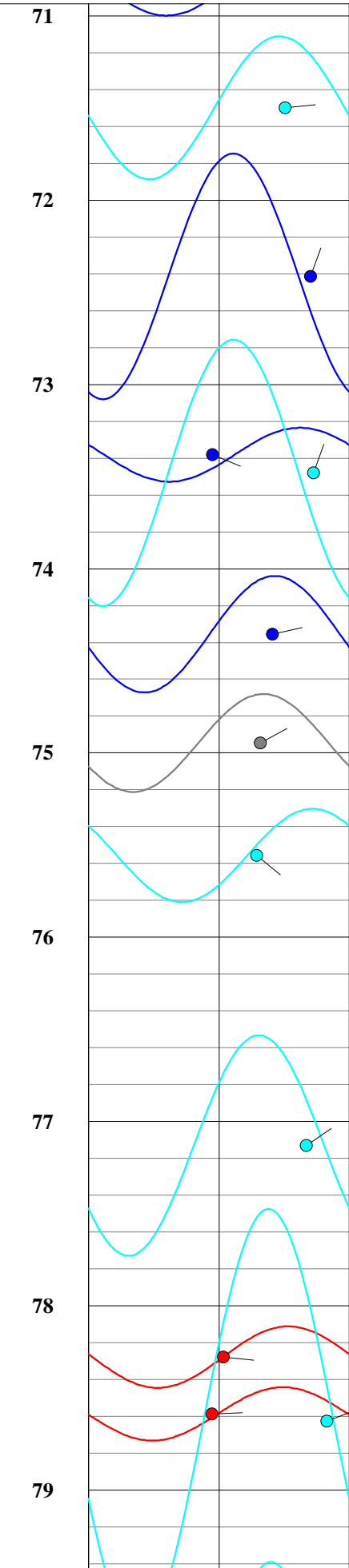


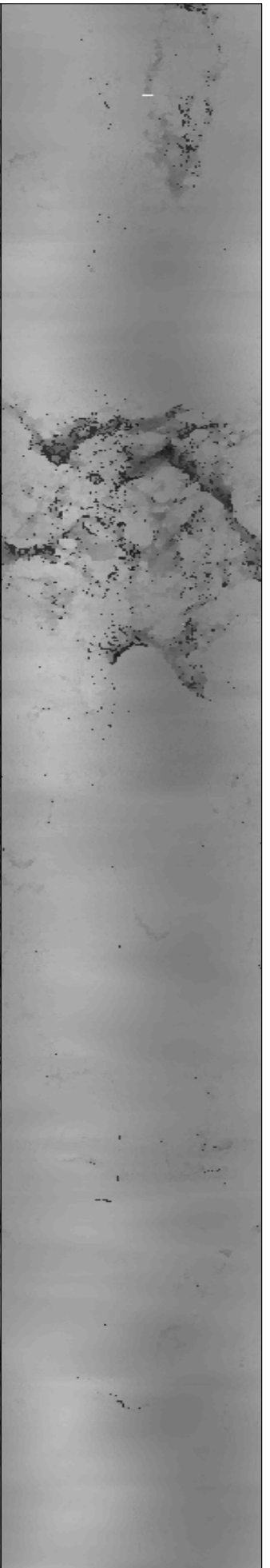
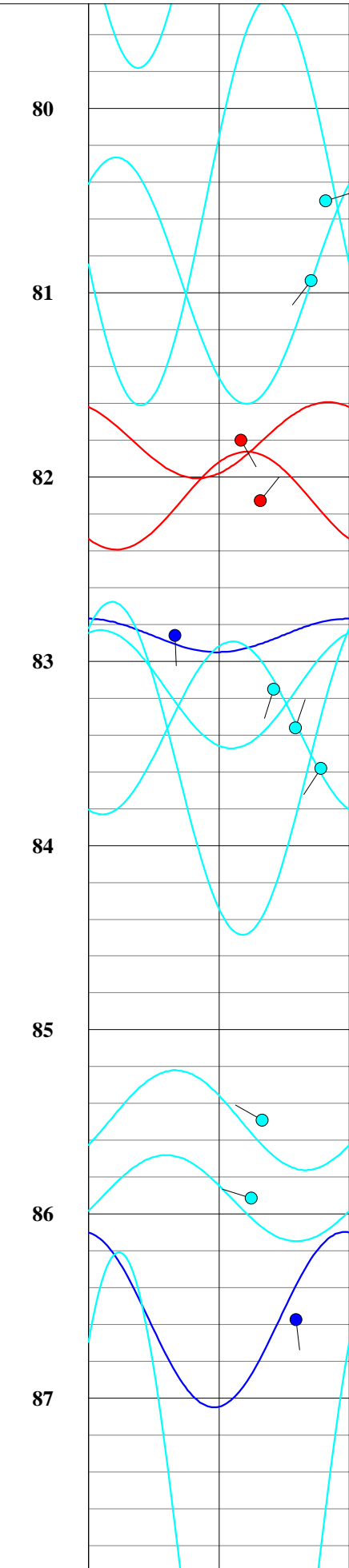
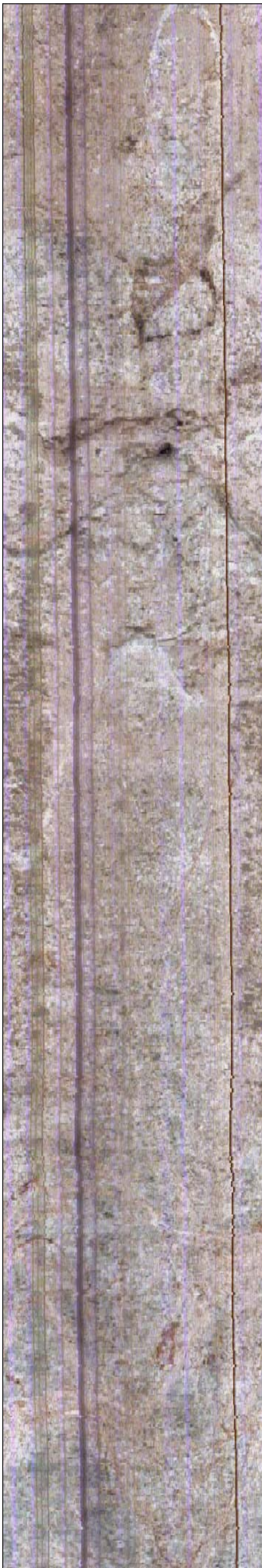


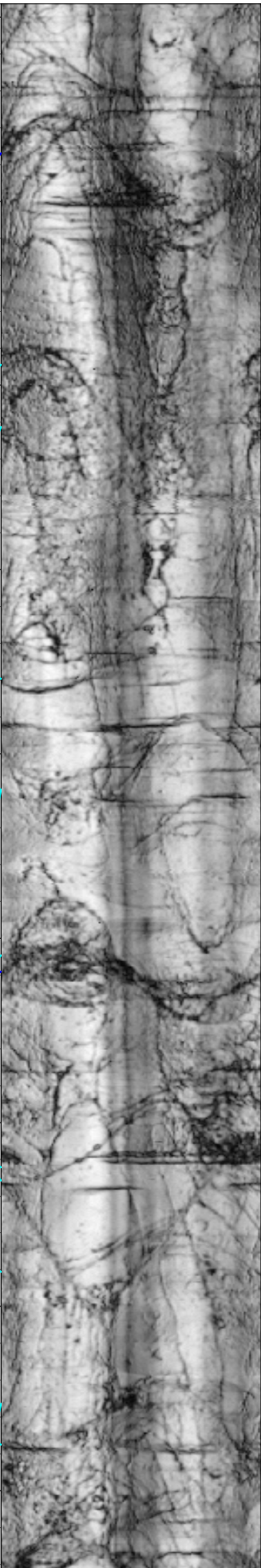
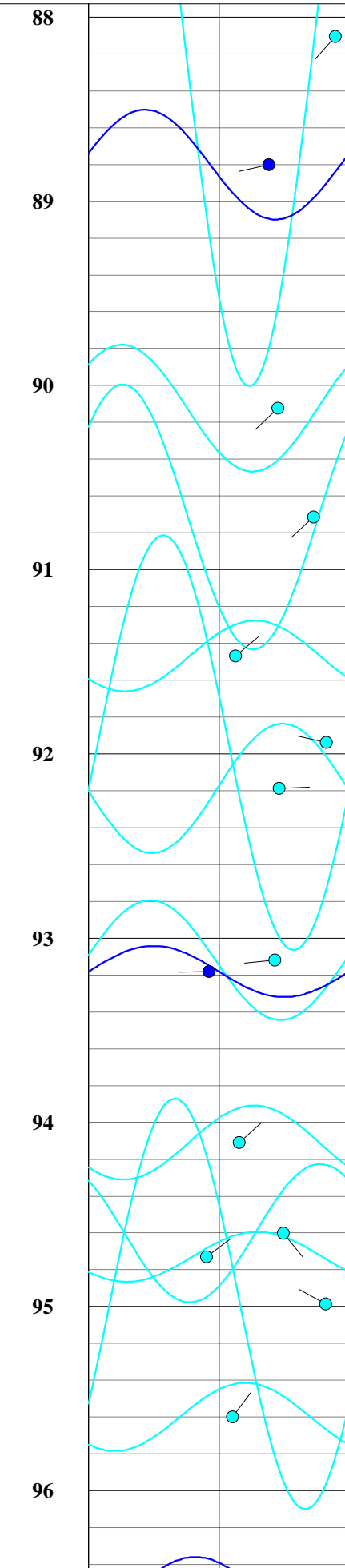
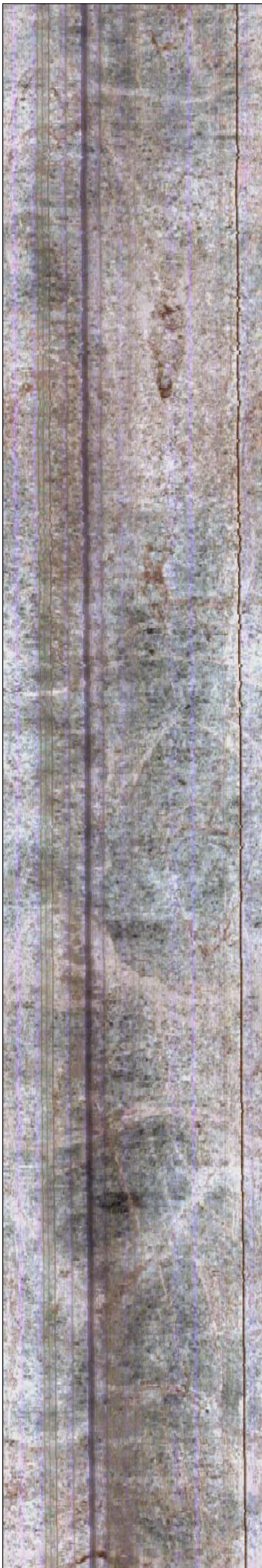


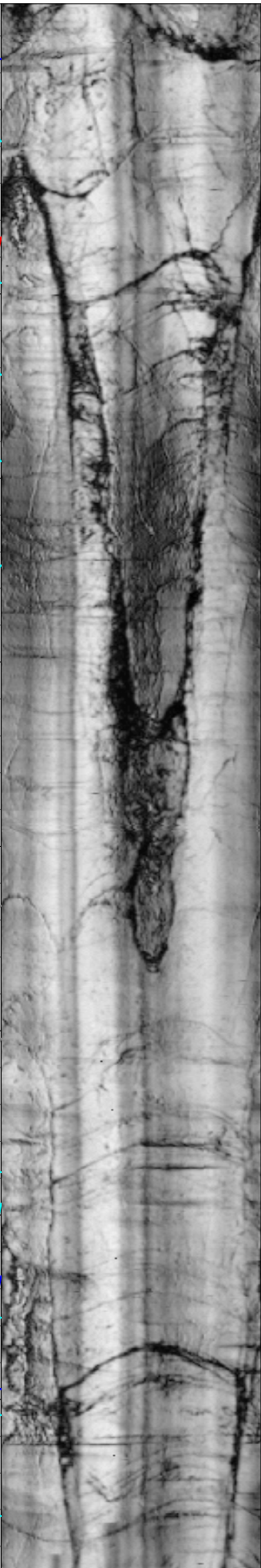
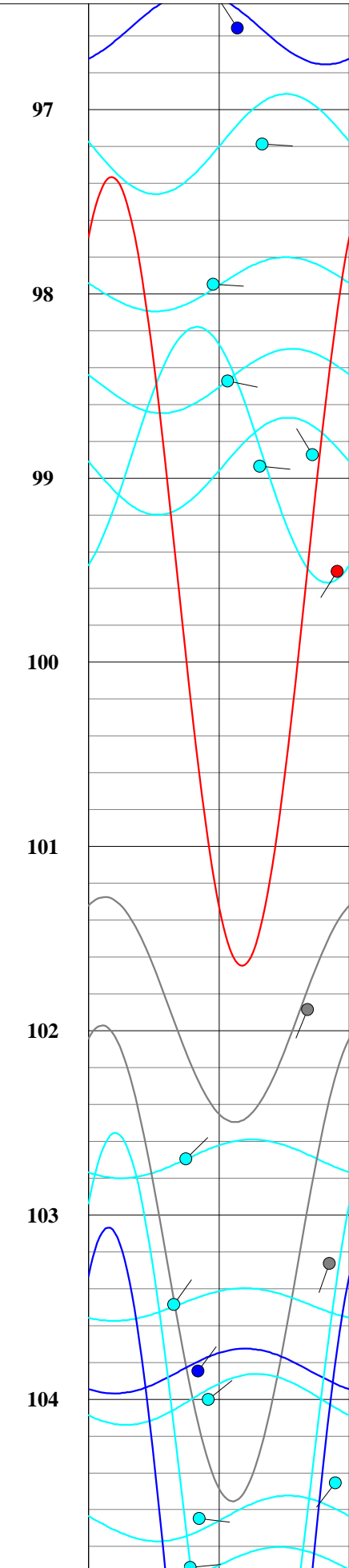
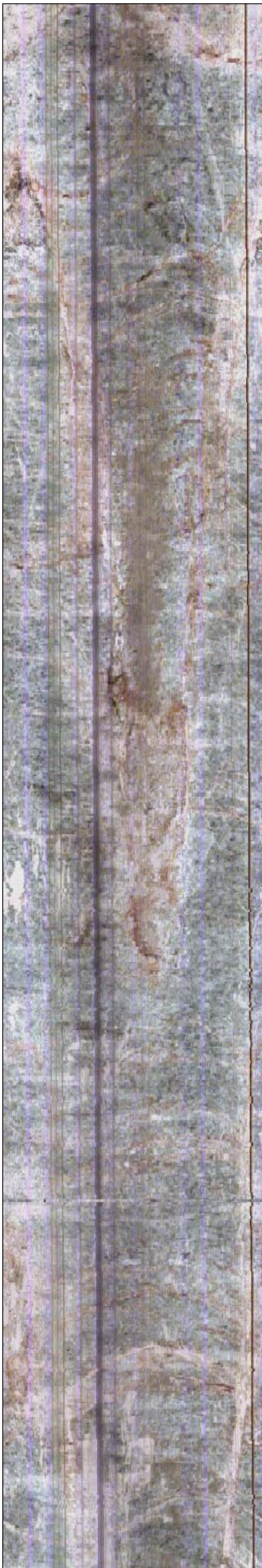


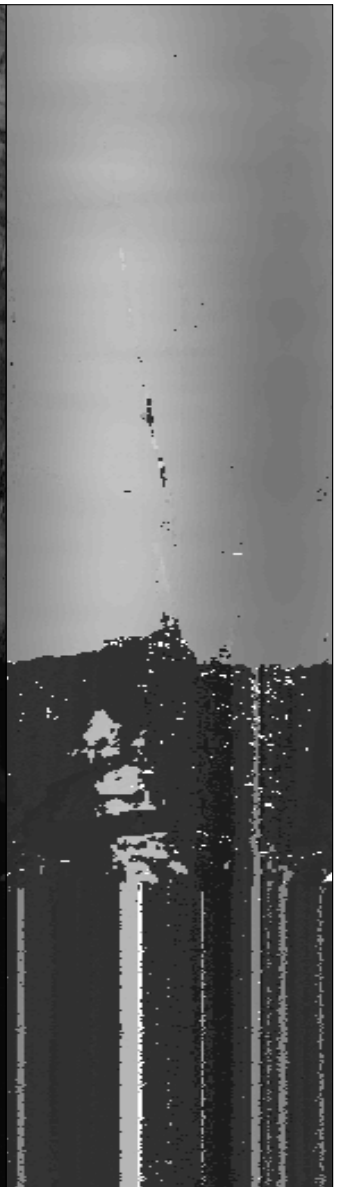
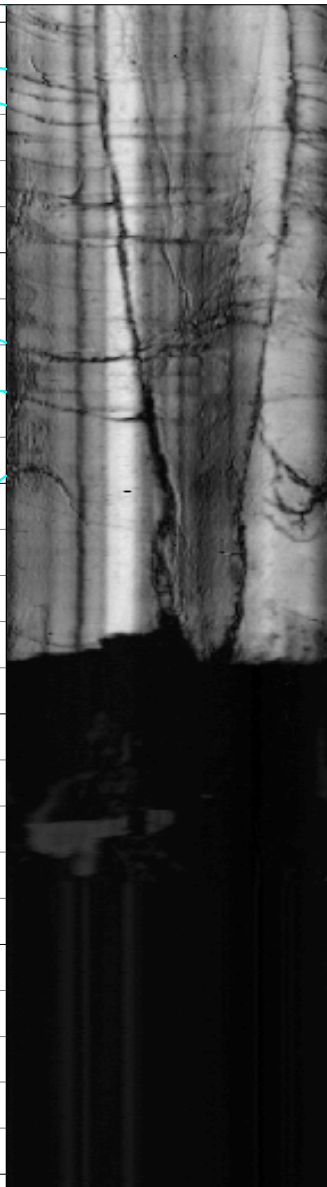
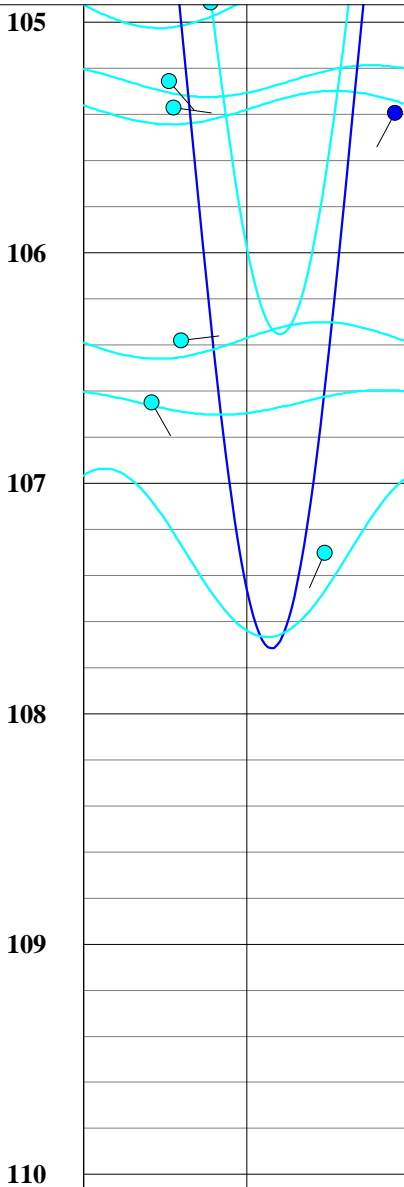












Optical Image - MN					Depth 1ft:10ft	Tadpoles					Acoustic Amplitude - MN					Acoustic Travel Time - MN				
0°	90°	180°	270°	0°		0	90	180	270	90	0°	90°	180°	270°	0°	0°	90°	180°	270°	0°

Orientation Summary Table
Televiewer Features
Shaw
Hermosa
Well: 37-B06
January 17-18, 2013

Feature No.	Depth (meters)	Depth (feet)	Dip Direction (degrees)	Dip Angle (degrees)	Feature Rank (0 to 5)
1	2.01	6.6	68	79	1
2	2.29	7.5	214	30	1
3	2.47	8.1	81	71	1
4	2.64	8.7	347	36	2
5	2.80	9.2	330	57	1
6	2.98	9.8	1	62	1
7	3.11	10.2	1	63	1
8	3.26	10.7	347	69	1
9	3.69	12.1	97	73	1
10	3.89	12.8	297	50	1
11	3.95	13.0	191	42	1
12	4.30	14.1	40	77	0
13	4.64	15.2	323	56	2
14	4.66	15.3	225	24	1
15	4.99	16.4	294	54	1
16	4.99	16.4	146	19	1
17	5.04	16.6	128	78	1
18	5.24	17.2	34	62	1
19	5.43	17.8	52	74	1
20	5.64	18.5	56	74	1
21	5.87	19.3	55	77	1
22	6.04	19.8	49	69	1
23	6.26	20.6	67	66	1
24	6.51	21.4	54	80	3
25	7.41	24.3	74	67	1
26	7.60	25.0	66	65	1
27	8.93	29.3	87	44	1
28	9.24	30.3	78	59	1
29	9.32	30.6	69	56	1
30	9.77	32.1	108	48	1
31	9.87	32.4	245	77	0
32	10.11	33.2	84	58	1
33	10.26	33.7	83	54	1
34	11.68	38.3	292	51	1
35	12.06	39.6	99	58	1
36	12.35	40.5	55	62	1
37	13.38	43.9	59	72	1
38	13.49	44.3	59	69	1
39	13.53	44.4	265	35	1
40	14.33	47.0	217	55	0
41	14.51	47.6	50	71	0
42	15.68	51.4	12	47	1
43	15.76	51.7	76	55	1
44	15.89	52.1	58	46	2
45	16.06	52.7	185	77	1

All directions are with respect to magnetic north.

Orientation Summary Table
Televiewer Features
Shaw
Hermosa
Well: 37-B06
January 17-18, 2013

Feature No.	Depth (meters)	Depth (feet)	Dip Direction (degrees)	Dip Angle (degrees)	Feature Rank (0 to 5)
46	16.43	53.9	247	48	1
47	16.67	54.7	30	47	2
48	16.79	55.1	49	57	2
49	17.01	55.8	59	60	0
50	17.29	56.7	76	56	1
51	17.70	58.1	35	67	1
52	17.87	58.6	23	64	1
53	18.20	59.7	240	40	2
54	18.23	59.8	230	18	1
55	18.57	60.9	132	43	2
56	18.62	61.1	20	66	2
57	18.78	61.6	181	59	1
58	18.98	62.3	15	62	1
59	19.03	62.4	279	68	1
60	19.03	62.4	204	62	1
61	19.15	62.8	191	20	2
62	19.20	63.0	180	27	2
63	19.32	63.4	217	29	2
64	19.39	63.6	208	24	2
65	19.66	64.5	126	57	1
66	19.94	65.4	109	59	2
67	20.00	65.6	168	85	1
68	20.09	65.9	161	33	1
69	20.30	66.6	124	65	1
70	20.53	67.3	143	58	1
71	20.59	67.6	92	63	1
72	20.66	67.8	241	25	1
73	20.71	67.9	13	72	1
74	20.84	68.4	26	76	2
75	21.01	68.9	119	55	0
76	21.33	70.0	20	76	2
77	21.59	70.8	108	49	2
78	21.79	71.5	84	68	1
79	22.07	72.4	20	77	2
80	22.37	73.4	112	43	2
81	22.40	73.5	20	78	1
82	22.66	74.4	77	64	2
83	22.84	75.0	62	59	0
84	23.03	75.6	129	58	1
85	23.51	77.1	55	75	1
86	23.86	78.3	96	47	3
87	23.95	78.6	88	43	3
88	23.97	78.6	69	82	1
89	24.54	80.5	72	82	1
90	24.67	80.9	218	77	1

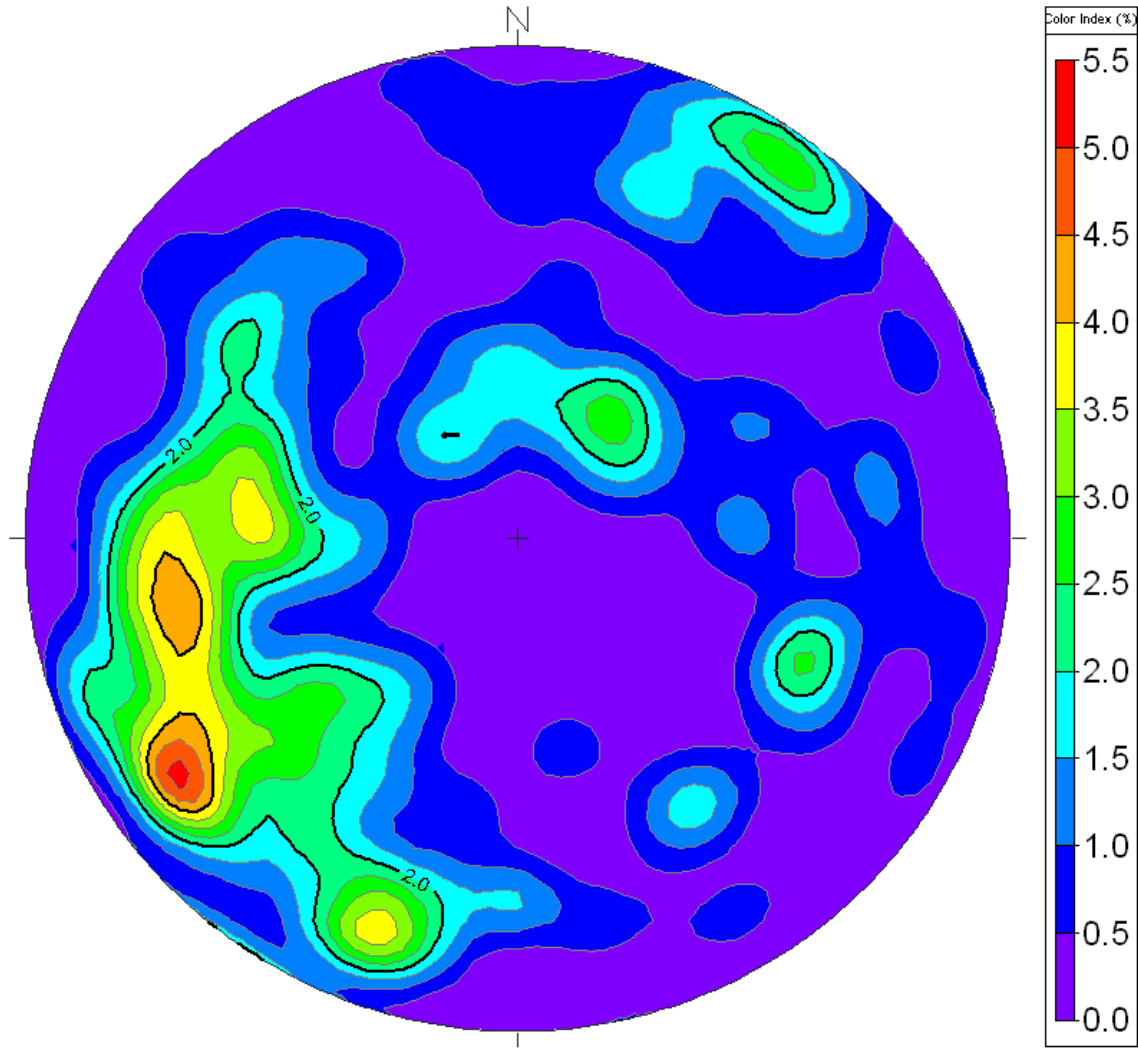
All directions are with respect to magnetic north.

Orientation Summary Table
Televiewer Features
Shaw
Hermosa
Well: 37-B06
January 17-18, 2013

Feature No.	Depth (meters)	Depth (feet)	Dip Direction (degrees)	Dip Angle (degrees)	Feature Rank (0 to 5)
91	24.93	81.8	151	53	3
92	25.03	82.1	38	59	3
93	25.26	82.9	178	30	2
94	25.34	83.2	197	64	1
95	25.41	83.4	19	71	1
96	25.48	83.6	213	80	1
97	26.06	85.5	300	60	1
98	26.19	85.9	287	56	1
99	26.39	86.6	173	72	2
100	26.85	88.1	222	85	1
101	27.07	88.8	258	62	2
102	27.47	90.1	226	65	1
103	27.65	90.7	227	78	1
104	27.88	91.5	50	51	1
105	28.02	91.9	283	82	1
106	28.10	92.2	88	66	1
107	28.38	93.1	265	64	1
108	28.40	93.2	270	41	2
109	28.68	94.1	48	52	1
110	28.83	94.6	140	67	1
111	28.87	94.7	53	41	1
112	28.95	95.0	299	82	1
113	29.14	95.6	36	50	1
114	29.43	96.6	328	51	2
115	29.62	97.2	93	60	1
116	29.86	98.0	92	43	1
117	30.01	98.5	101	48	1
118	30.14	98.9	330	77	1
119	30.16	98.9	96	59	1
120	30.33	99.5	212	86	3
121	31.06	101.9	202	76	0
122	31.30	102.7	46	34	1
123	31.47	103.3	199	83	0
124	31.54	103.5	35	29	1
125	31.65	103.9	36	38	2
126	31.70	104.0	52	41	1
127	31.84	104.5	217	85	1
128	31.90	104.7	96	38	1
129	31.98	104.9	84	35	1
130	32.08	105.3	138	24	1
131	32.12	105.4	98	25	1
132	32.12	105.4	208	86	2
133	32.42	106.4	83	27	1
134	32.51	106.7	150	19	1
135	32.71	107.3	203	67	1

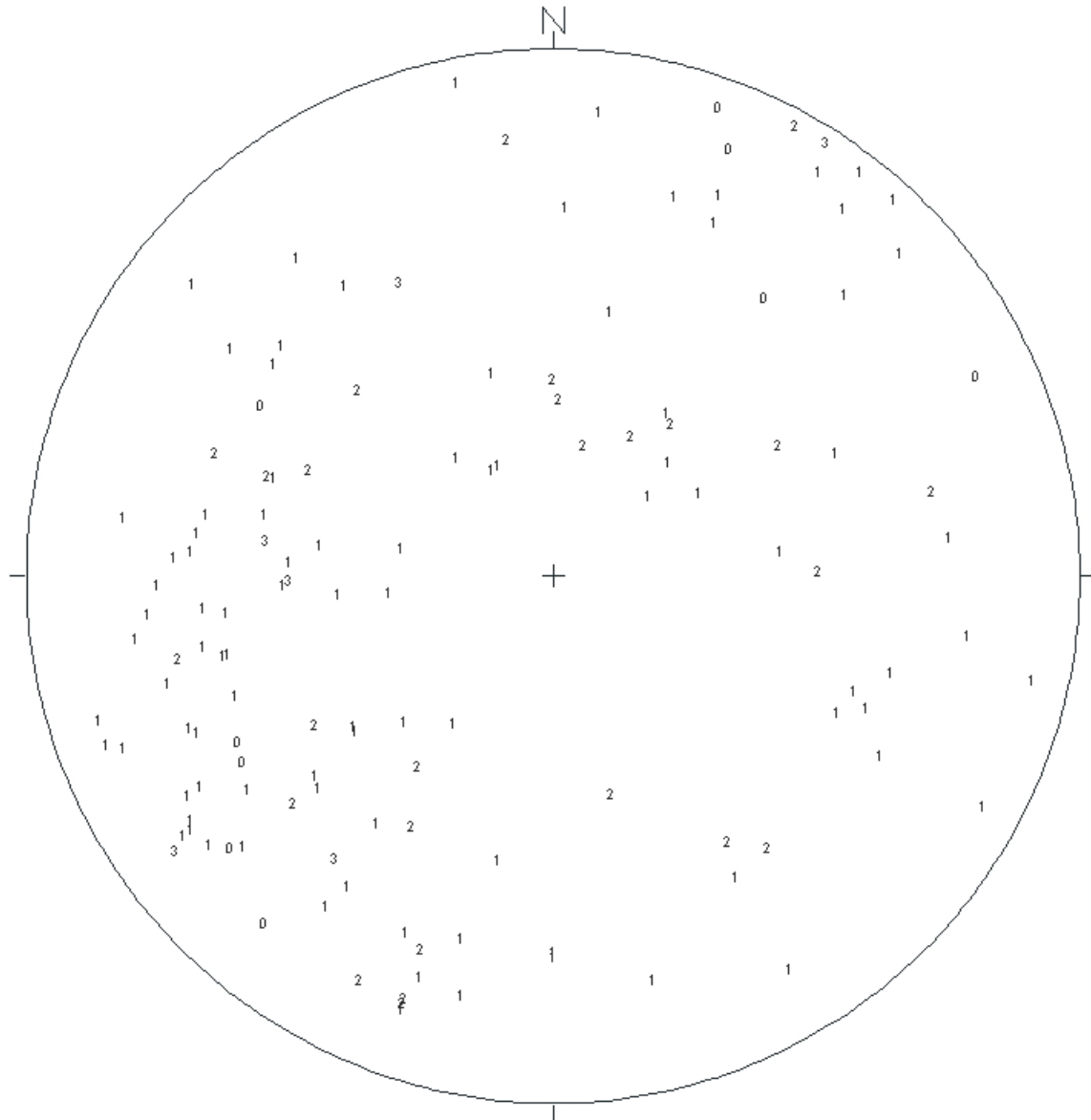
All directions are with respect to magnetic north.

Stereonet Diagram – Schmidt Projection
Image Features
Shaw
Project: Hermosa
Well: 37-B06
17 & 18 January 2013



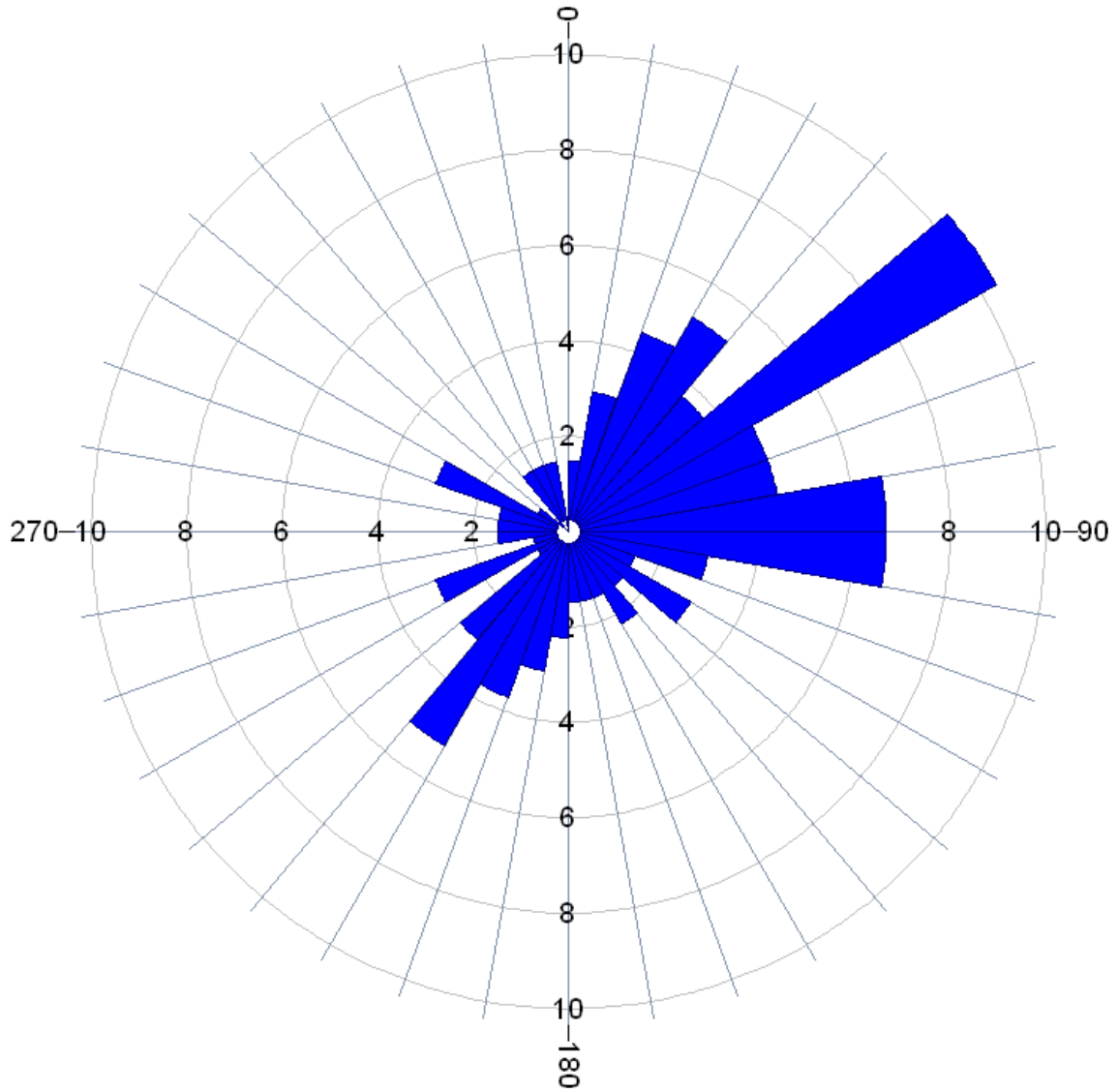
All directions are with respect to Magnetic North.

**Stereonet Diagram – Schmidt Projection
Image Features
Shaw
Project: Hermosa
Well: 37-B06
17 & 18 January 2013**



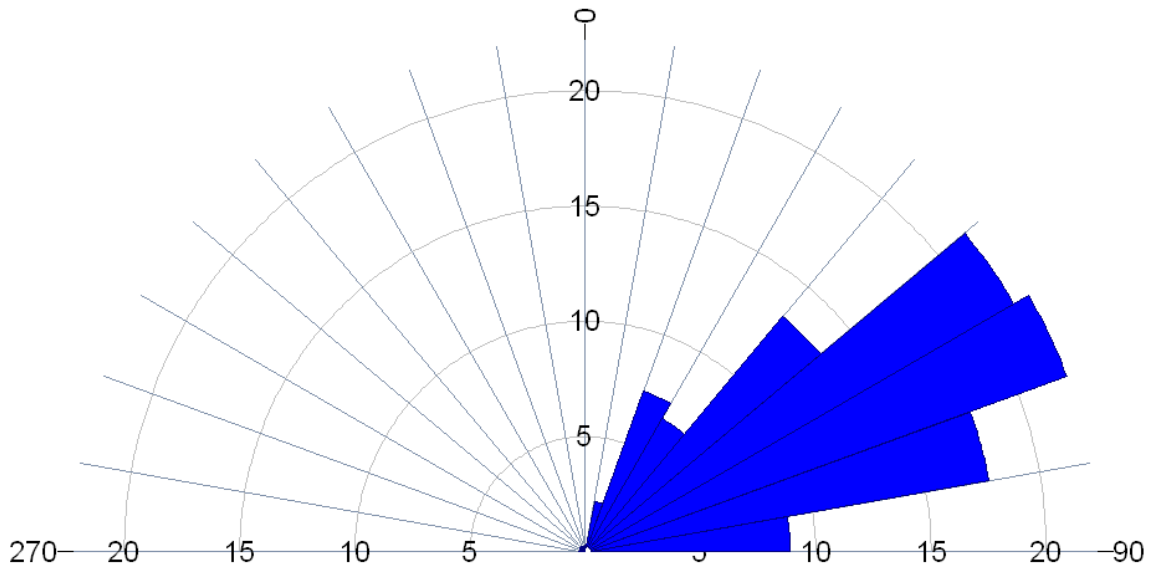
All directions are with respect to Magnetic North.

Rose Diagram – Dip Directions
Image Features
Shaw
Project: Hermosa
Well: 37-B06
17 & 18 January 2013

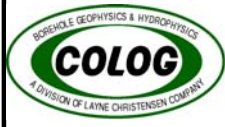


All directions are with respect to Magnetic North.

Rose Diagram – Dip Angles
Image Features
Shaw
Project: Hermosa
Well: 37-B06
17 & 18 January 2013



All directions are with respect to Magnetic North.



Geophysical and Flow Logs

COMPANY: Shaw

PROJECT: Hermosa

DATE LOGGED: 17-18 Jan 2013

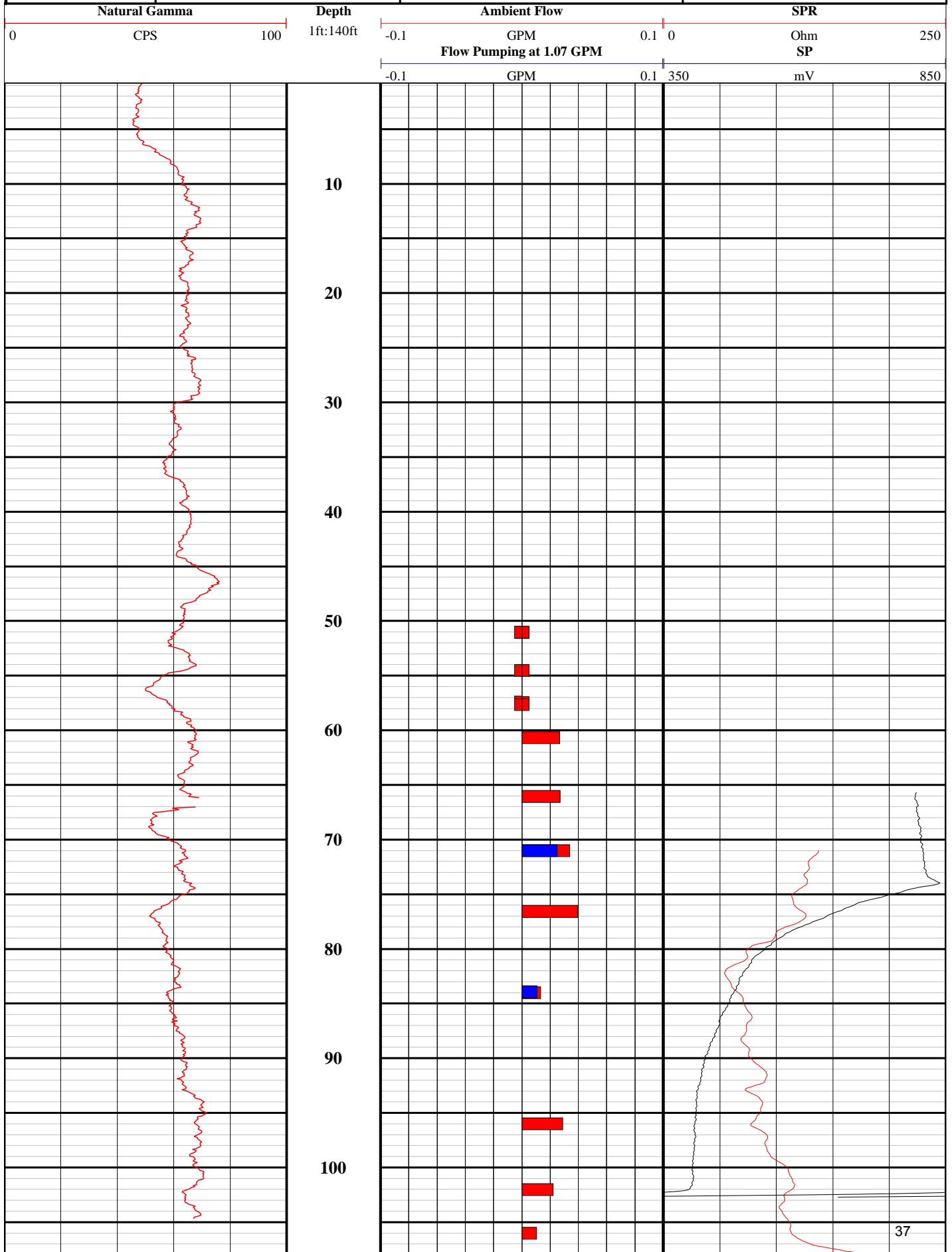
WELL: 37-B06

COLOG Main Office

810 Quail Street, Suite E, Lakewood, CO 80215

Phone: (303) 279-0171, Fax: (303) 278-0135

www.colog.com



Appendix B



Acoustic and Optical Televiewers

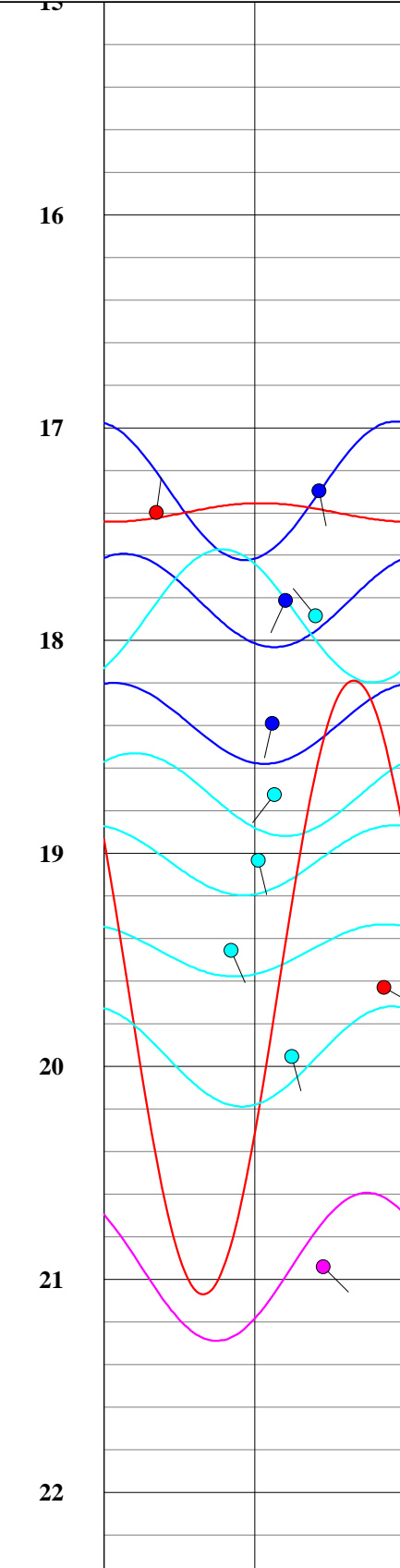
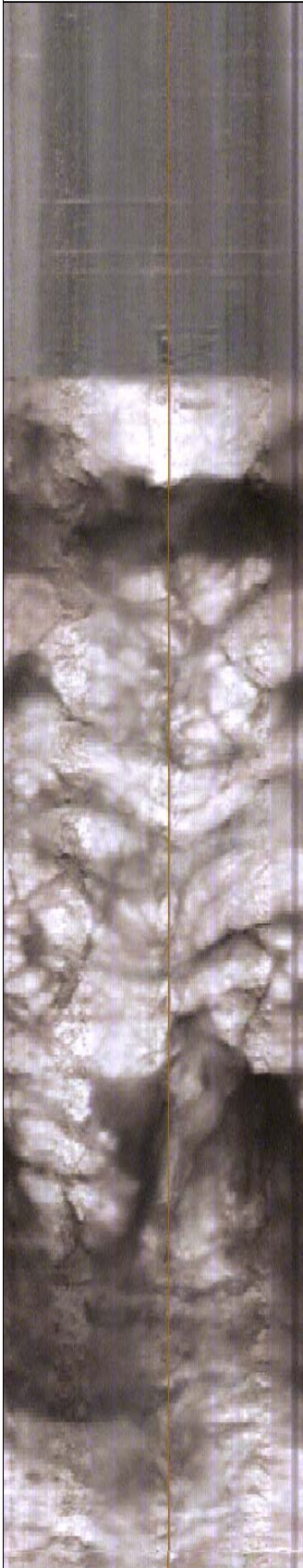
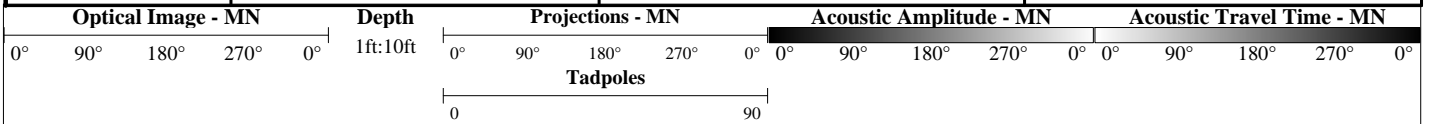
COLOG Main Office
810 Quail Street, Suite E, Lakewood, CO 80215
Phone: (303) 279-0171, Fax: (303) 278-0135
www.colog.com

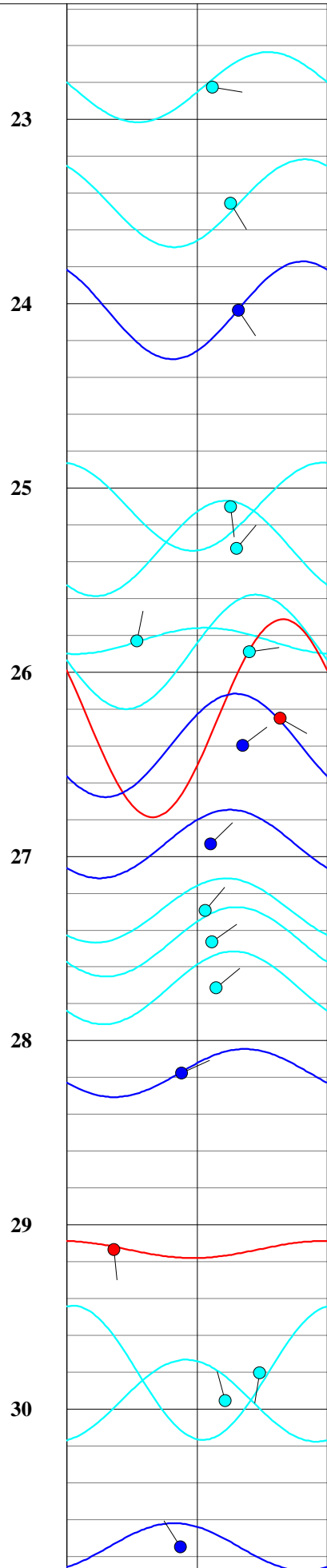
COMPANY: Shaw

PROJECT: Hermosa

DATE LOGGED: 17-18 Jan 2013

WELL: 37-B09







31

32

33

34

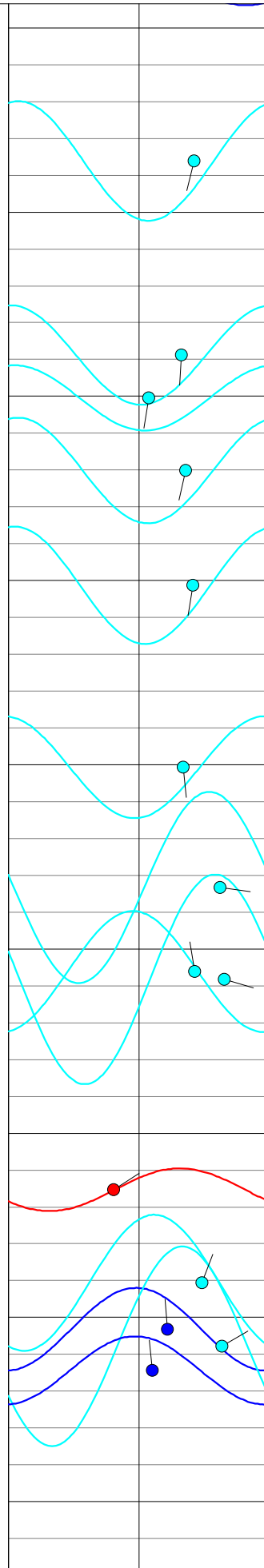
35

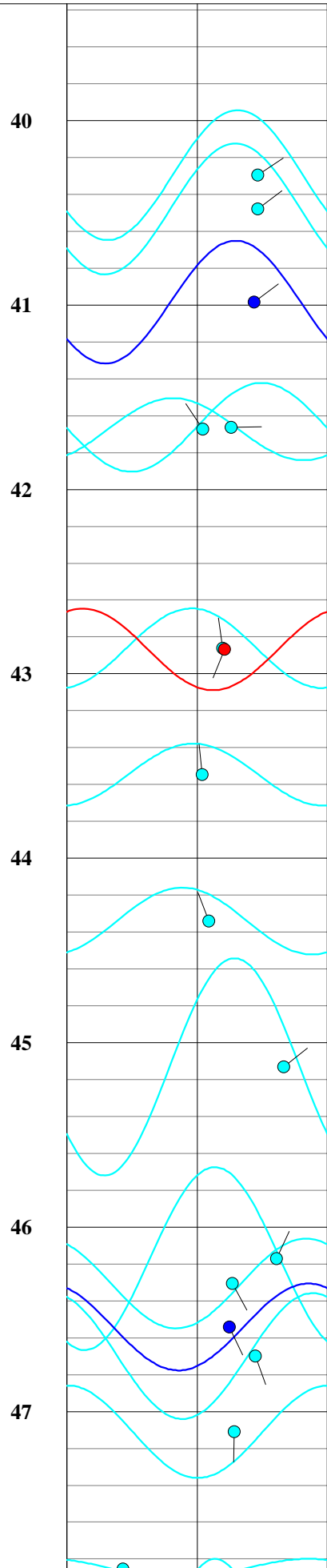
36

37

38

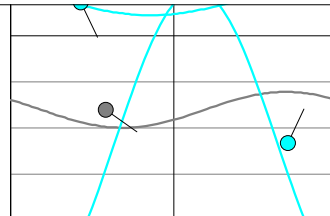
39



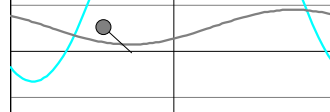




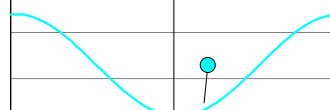
48



49



50



51



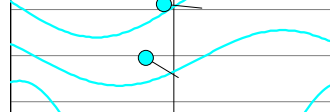
52



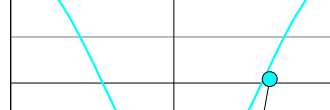
53



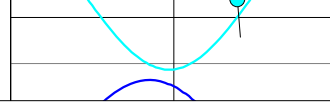
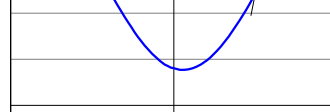
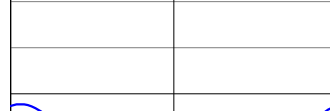
54

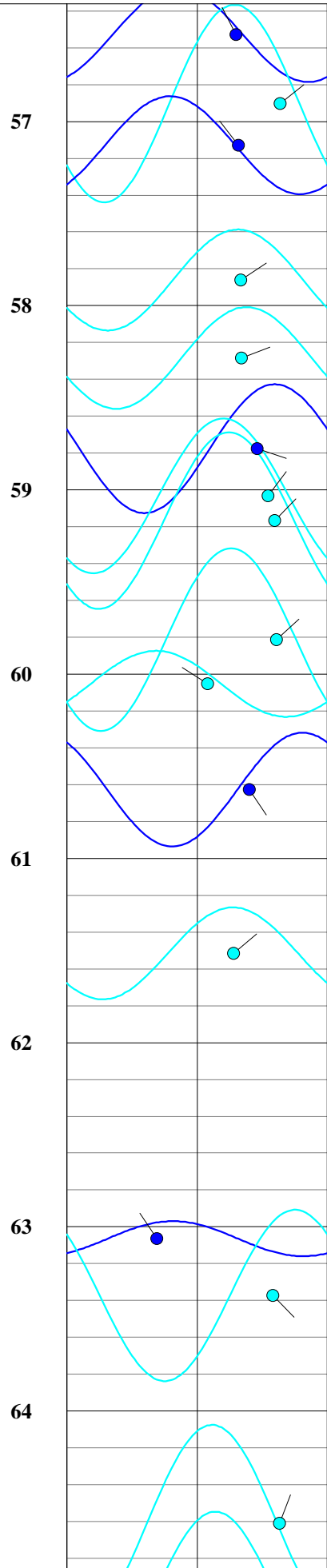


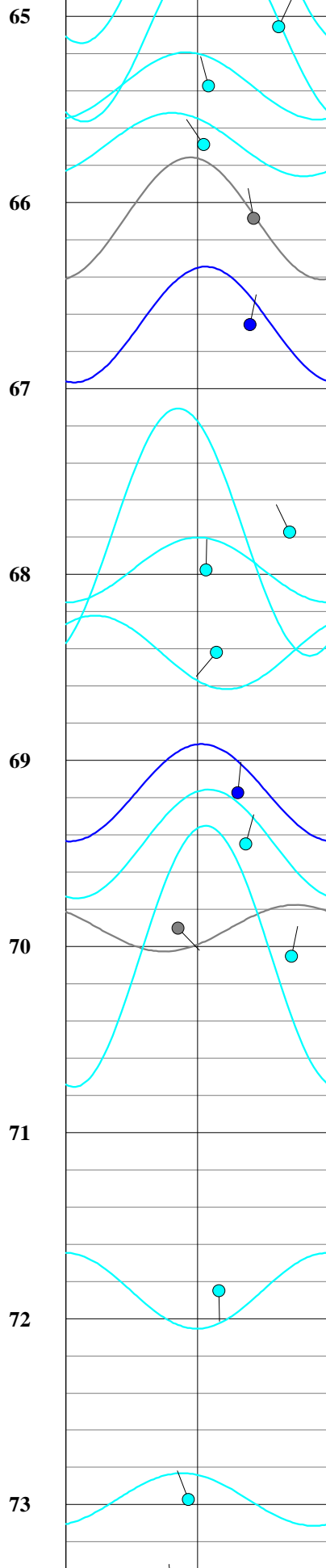
55

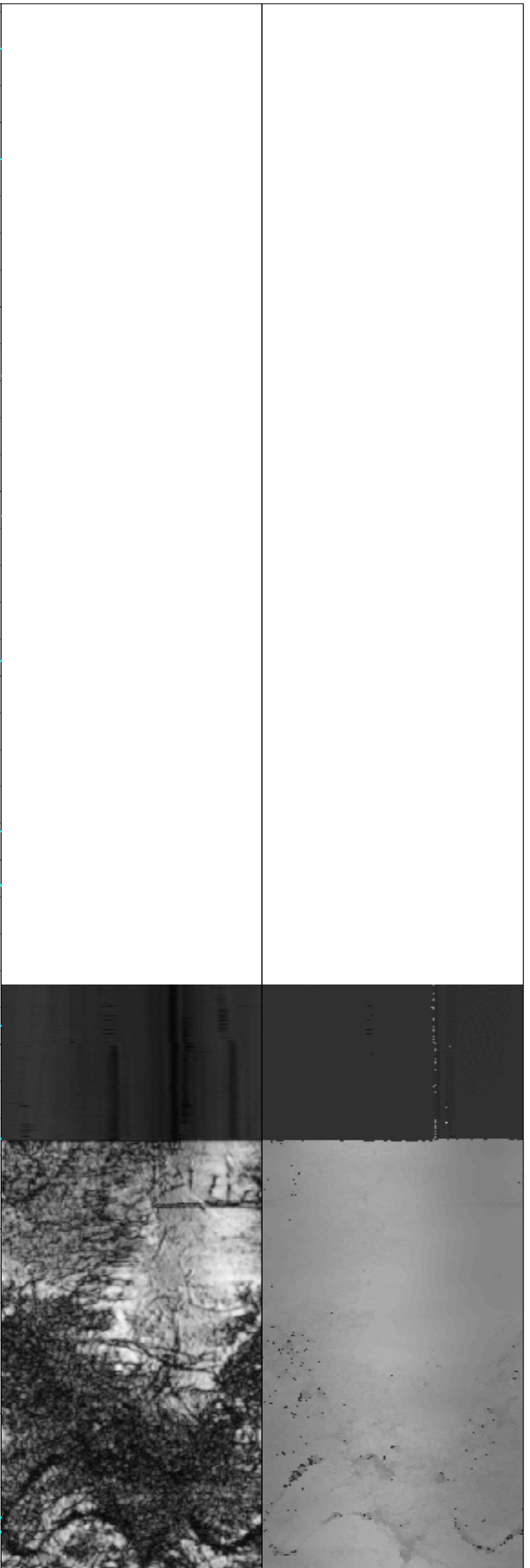
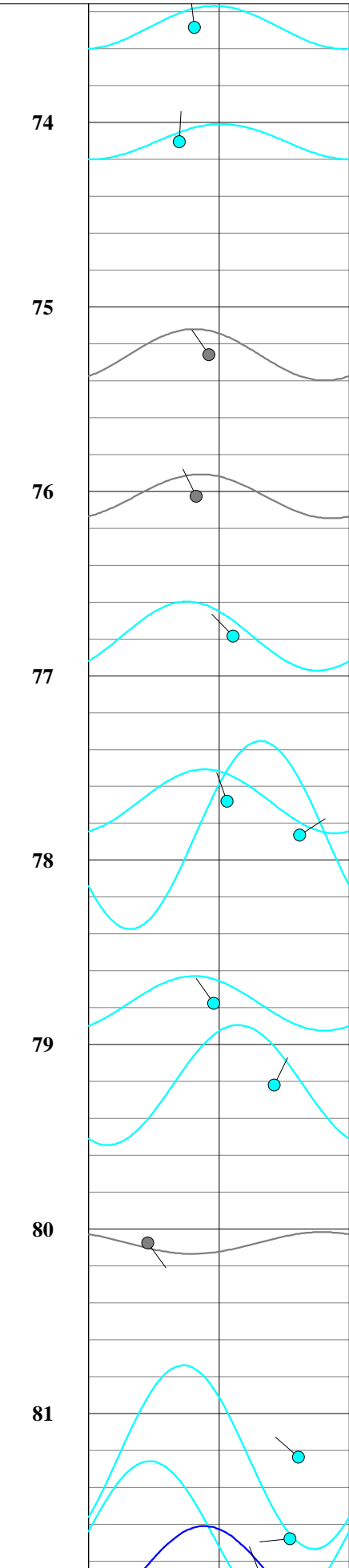


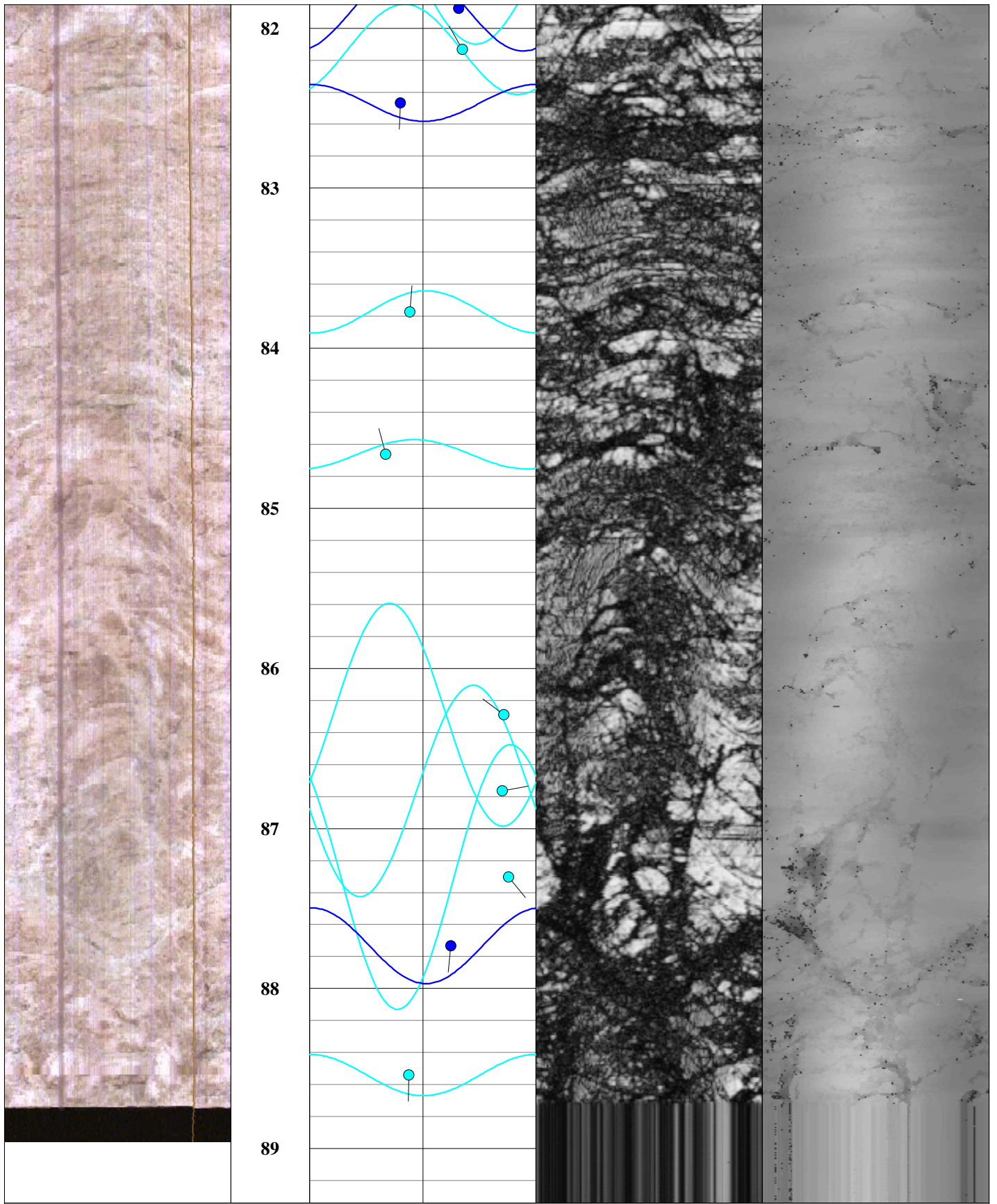
56











Tadpoles

Optical Image - MN
0° 90° 180° 270° 0°

Depth
1ft:10ft

Projections - MN
0 90 180 270 0

Acoustic Amplitude - MN
0° 90° 180° 270° 0°

Acoustic Travel Time - MN
0° 90° 180° 270° 0°

Orientation Summary Table
Televiewer Features
Shaw
Hermosa
Well: 37-B09
January 17-18, 2013

Feature No.	Depth (meters)	Depth (feet)	Dip Direction (degrees)	Dip Angle (degrees)	Feature Rank (0 to 5)
1	5.27	17.3	169	64	2
2	5.30	17.4	8	16	3
3	5.43	17.8	204	54	2
4	5.45	17.9	322	63	1
5	5.61	18.4	192	50	2
6	5.71	18.7	217	51	1
7	5.80	19.0	167	46	1
8	5.93	19.5	156	38	1
9	5.98	19.6	119	84	3
10	6.08	20.0	165	56	1
11	6.38	20.9	135	66	4
12	6.96	22.8	98	50	1
13	7.15	23.5	148	57	1
14	7.32	24.0	146	59	2
15	7.65	25.1	174	57	1
16	7.72	25.3	40	59	1
17	7.87	25.8	11	24	1
18	7.89	25.9	82	63	1
19	8.00	26.3	119	74	3
20	8.05	26.4	53	61	2
21	8.21	26.9	45	50	2
22	8.32	27.3	40	48	1
23	8.37	27.5	54	50	1
24	8.45	27.7	51	51	1
25	8.59	28.2	66	40	2
26	8.88	29.1	175	16	3
27	9.08	29.8	188	67	1
28	9.13	30.0	345	55	1
29	9.37	30.8	328	39	2
30	9.67	31.7	193	64	1
31	9.99	32.8	183	60	1
32	10.06	33.0	188	48	1
33	10.18	33.4	192	61	1
34	10.37	34.0	189	64	1
35	10.67	35.0	174	60	1
36	10.87	35.7	97	73	1
37	11.01	36.1	352	64	1
38	11.02	36.2	105	75	1
39	11.37	37.3	57	36	3
40	11.52	37.8	22	67	1
41	11.60	38.1	356	55	2
42	11.63	38.2	60	74	1
43	11.67	38.3	355	50	2
44	12.28	40.3	56	66	1
45	12.34	40.5	53	66	1

All directions are with respect to magnetic north.

Orientation Summary Table
Televiewer Features
Shaw
Hermosa
Well: 37-B09
January 17-18, 2013

Feature No.	Depth (meters)	Depth (feet)	Dip Direction (degrees)	Dip Angle (degrees)	Feature Rank (0 to 5)
46	12.49	41.0	53	65	2
47	12.70	41.7	89	57	1
48	12.70	41.7	327	47	1
49	13.06	42.9	352	54	1
50	13.07	42.9	202	55	3
51	13.27	43.6	355	47	1
52	13.51	44.3	339	49	1
53	13.76	45.1	52	75	1
54	14.07	46.2	25	72	1
55	14.12	46.3	151	57	1
56	14.19	46.5	154	56	2
57	14.23	46.7	160	65	1
58	14.36	47.1	181	58	1
59	14.58	47.9	154	19	1
60	14.73	48.3	124	26	0
61	14.77	48.5	25	77	1
62	14.90	48.9	132	26	0
63	15.10	49.5	185	55	1
64	15.31	50.2	59	57	1
65	15.49	50.8	343	61	1
66	15.60	51.2	95	42	1
67	15.67	51.4	120	37	1
68	15.85	52.0	190	72	1
69	16.29	53.5	191	69	2
70	16.61	54.5	115	58	1
71	17.04	55.9	175	63	1
72	17.23	56.5	333	58	2
73	17.34	56.9	52	74	1
74	17.41	57.1	323	59	2
75	17.64	57.9	57	60	1
76	17.76	58.3	69	60	1
77	17.91	58.8	108	66	2
78	17.99	59.0	37	69	1
79	18.04	59.2	44	72	1
80	18.23	59.8	47	72	1
81	18.30	60.1	303	49	1
82	18.48	60.6	146	63	2
83	18.75	61.5	50	58	1
84	19.22	63.1	326	31	2
85	19.32	63.4	135	71	1
86	19.69	64.6	21	74	1
87	19.83	65.1	25	73	1
88	19.92	65.4	345	49	1
89	20.02	65.7	326	47	1
90	20.14	66.1	351	64	0

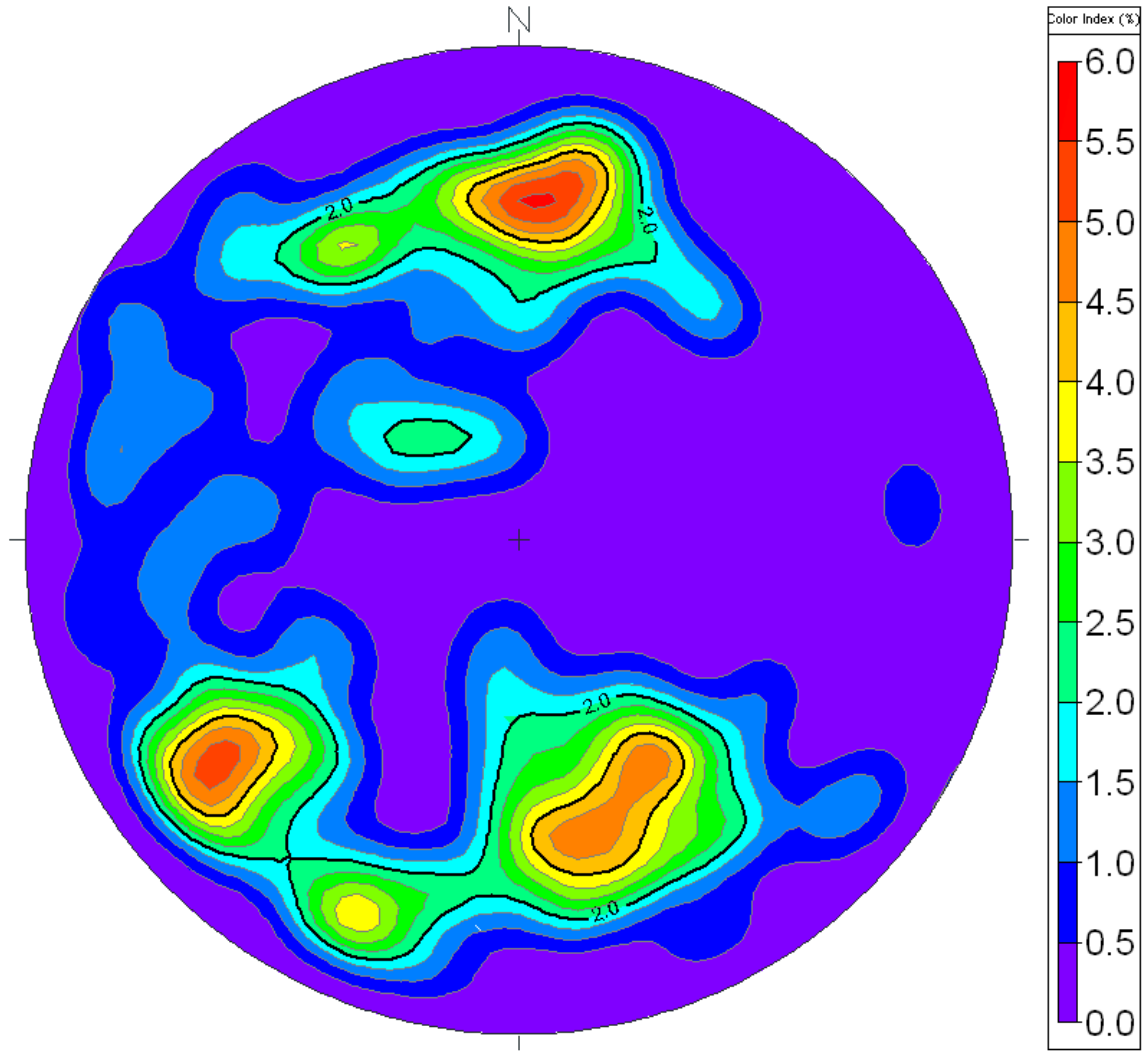
All directions are with respect to magnetic north.

Orientation Summary Table
Televiewer Features
Shaw
Hermosa
Well: 37-B09
January 17-18, 2013

Feature No.	Depth (meters)	Depth (feet)	Dip Direction (degrees)	Dip Angle (degrees)	Feature Rank (0 to 5)
91	20.32	66.7	11	63	2
92	20.66	67.8	334	77	1
93	20.72	68.0	1	48	1
94	20.85	68.4	220	51	1
95	21.08	69.2	6	59	2
96	21.17	69.5	15	62	1
97	21.31	69.9	135	39	0
98	21.35	70.1	12	77	1
99	21.90	71.9	179	52	1
100	22.24	73.0	340	42	1
101	22.40	73.5	354	37	1
102	22.59	74.1	3	31	1
103	22.94	75.3	326	42	0
104	23.17	76.0	334	37	0
105	23.41	76.8	316	50	1
106	23.68	77.7	340	48	1
107	23.73	77.9	58	73	1
108	24.01	78.8	326	43	1
109	24.15	79.2	26	64	1
110	24.41	80.1	143	21	0
111	24.76	81.2	311	72	1
112	24.90	81.7	265	69	1
113	24.96	81.9	340	59	2
114	25.03	82.1	331	61	1
115	25.14	82.5	181	36	2
116	25.53	83.8	4	40	1
117	25.80	84.7	346	30	1
118	26.30	86.3	307	77	1
119	26.44	86.8	80	77	1
120	26.61	87.3	140	79	1
121	26.74	87.7	185	56	2
122	26.99	88.5	181	39	1

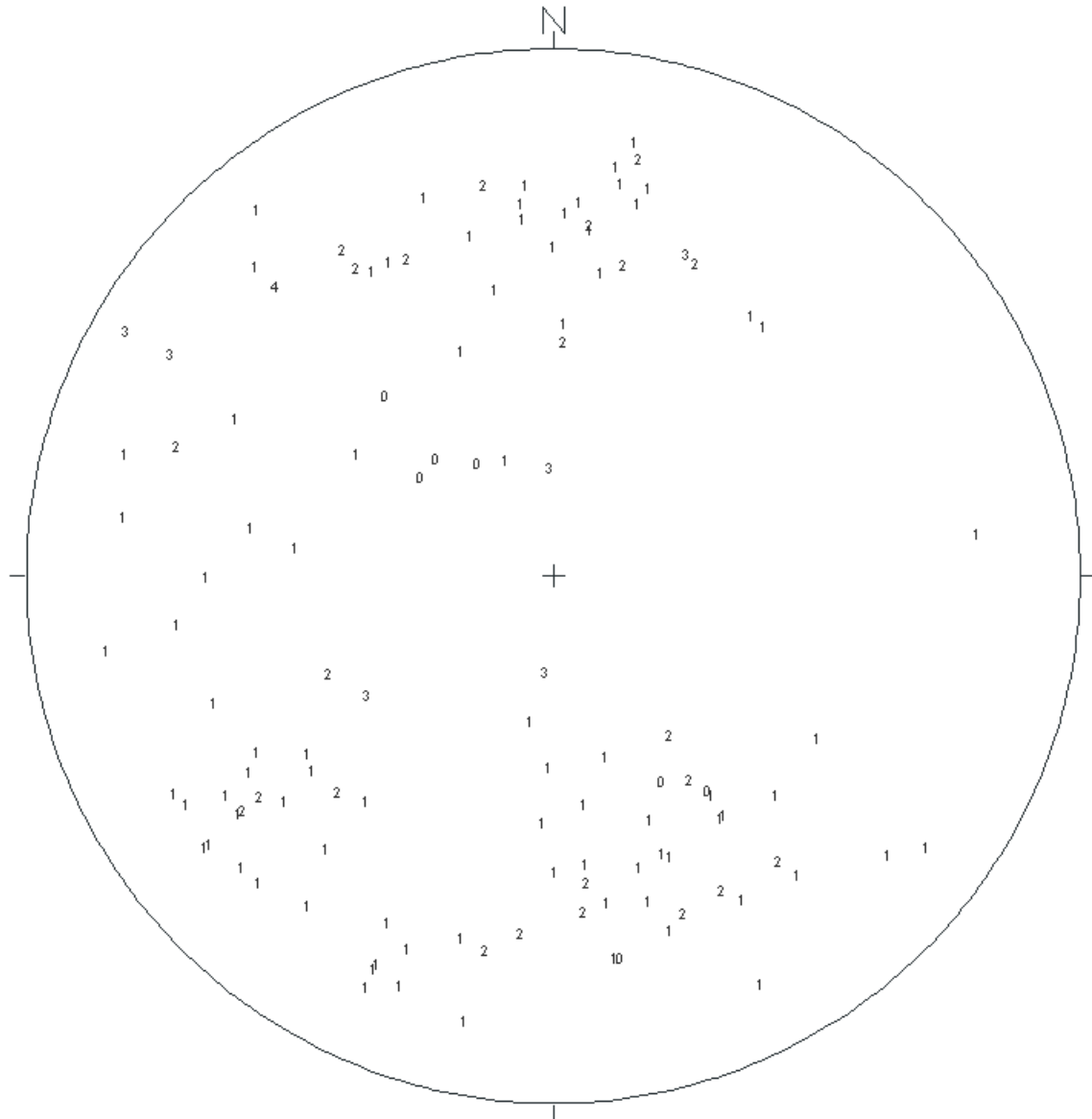
All directions are with respect to magnetic north.

Stereonet Diagram – Schmidt Projection
Image Features
Shaw
Project: Hermosa
Well: 37-B09
17 & 18 January 2013



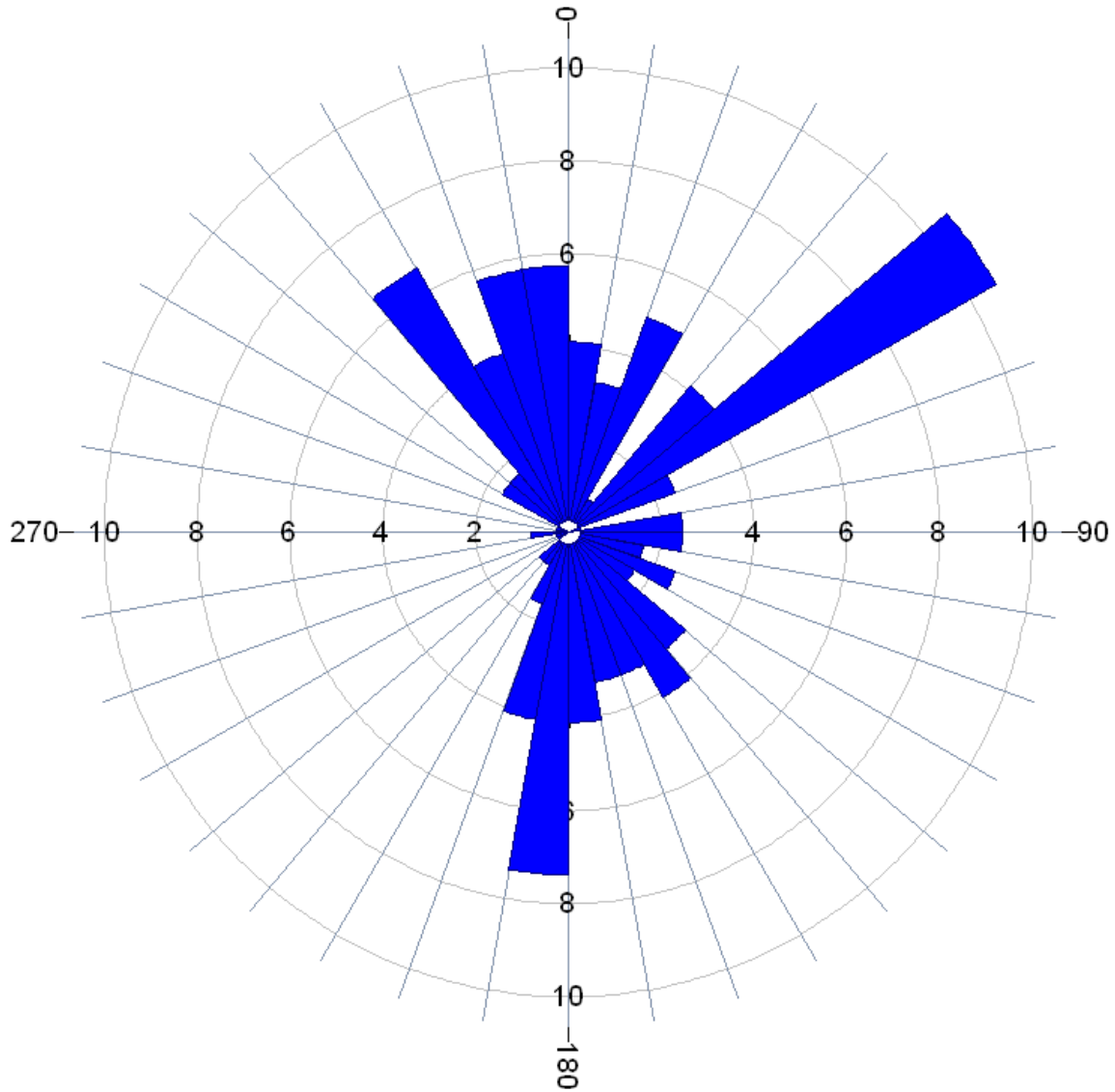
All directions are with respect to Magnetic North.

**Stereonet Diagram – Schmidt Projection
Image Features
Shaw
Project: Hermosa
Well: 37-B09
17 & 18 January 2013**



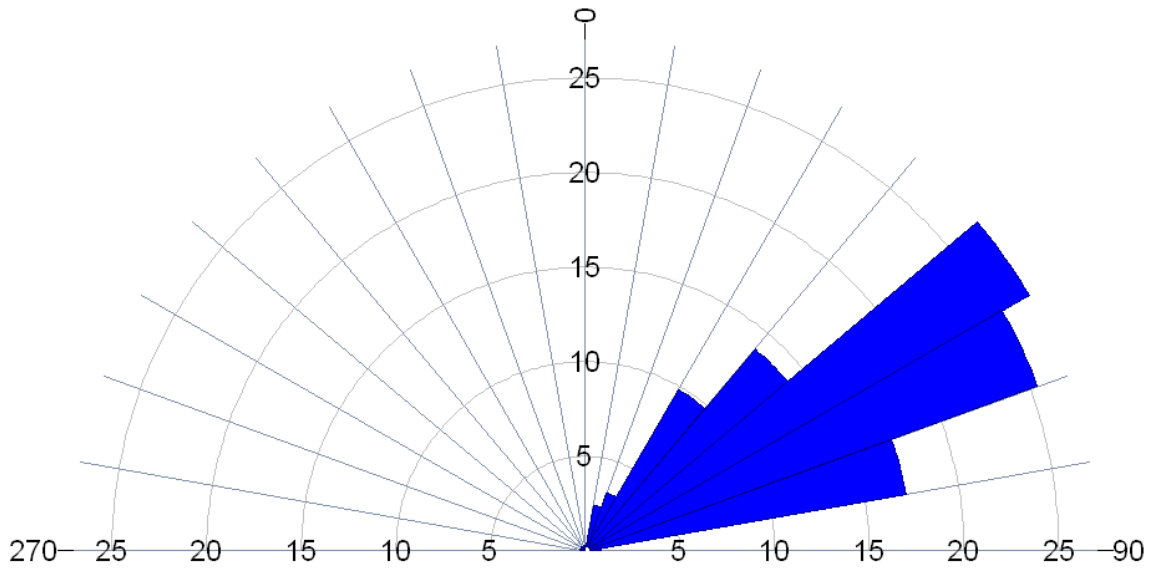
All directions are with respect to Magnetic North.

Rose Diagram – Dip Directions
Image Features
Shaw
Project: Hermosa
Well: 37-B09
17 & 18 January 2013

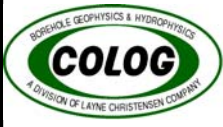


All directions are with respect to Magnetic North.

Rose Diagram – Dip Angles
Image Features
Shaw
Project: Hermosa
Well: 37-B09
17 & 18 January 2013



All directions are with respect to Magnetic North.



Geophysical Logs

COMPANY: Shaw

PROJECT: Hermosa

DATE LOGGED: 17-18 Jan 2013

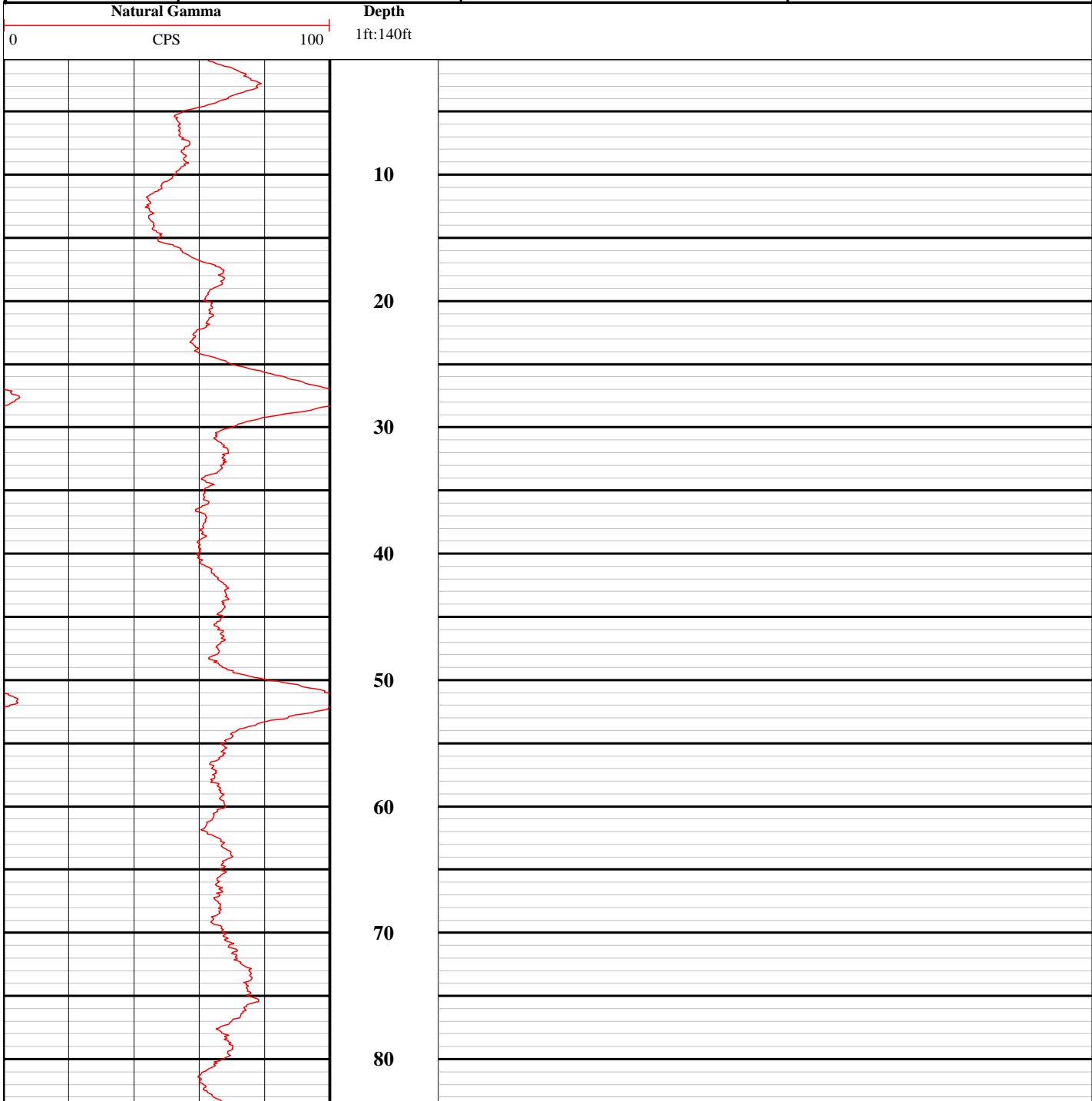
WELL: 37-B09

COLOG Main Office

810 Quail Street, Suite E, Lakewood, CO 80215

Phone: (303) 279-0171, Fax: (303) 278-0135

www.colog.com





**Geophysical Logging Results
Hermosa
Edwards Air Force Base**

Prepared for
CB & I
January 21, 2014

Prepared by
International Directional Services
Colog Geophysics Group
810 Quail Street Suite E, Lakewood, CO, 80215
Phone: (303) 279-0171 Fax: (303) 278-0135

Table of Contents

Geophysical Logging Results, Hermosa, Edwards Air Force Base

1.0 Introduction

2.0 Methodology

2.1 Optical and Acoustic Televiwer

2.2 Heat Pulse Flow Meter

3.0 37-B07 Geophysical Logging Results

3.1 Geophysical Logging

3.2 Optical Televiwer (OBI) & Acoustic Televiwer (ABI)

3.3 Heat Pulse Flow Meter

4.0 37-B10 Geophysical Logging Results

4.1 Geophysical Logging

4.2 Acoustic Televiwer (ABI)

5.0 37-B12 Geophysical Logging Results

5.1 Geophysical Logging

5.2 Optical Televiwer (OBI) & Acoustic Televiwer (ABI)

5.3 Heat Pulse Flow Meter

6.0 37-B13 Geophysical Logging Results

6.1 Geophysical Logging

6.2 Optical Televiwer (OBI) & Acoustic Televiwer (ABI)

6.3 Heat Pulse Flow Meter

7.0 Limitations

Appendices

Appendix A Logging Results (plots) from 37-B07

Appendix B Logging Results (plots) from 37-B10

Appendix C Logging Results (plots) from 37-B12

Appendix D Logging Results (plots) from 37-B13

List of Acronyms

gpm – gallons per minute

ft – feet

min. – minute

OBI – Optical Borehole Imager, or generically, optical televiewer

ABI – Acoustic Borehole Imager, or generically, acoustic televiewer

Geophysical Logging Results Hermosa, Edwards Air Force Base

1.0 Introduction

In accordance with IDS proposal dated 22 October 2013, and CBI purchase order #828847-000 OP, the Colog Group has applied geophysical logging methods to two wellbores at the Edwards Air Force Base in California. The objectives of the investigation were to:

- Identify fractures and features intersecting the borehole and evaluate their orientation.
- Characterize and quantify vertical flow in the wellbores under both non-stressed (ambient) and stressed (pumping) conditions.
- Evaluate the lithology through which the borehole penetrates and assist in correlating lithology and possible flow zones.

The subject wellbores geophysically logged at the Hermosa site were: 37-B07, 37-B10, 37-B12 and 37-B13. At the time of logging the boreholes were HQ size (3.78”).

The geophysical logging methods used were: acoustic televiewer, optical televiewer, and heat-pulse flowmeter. Flowmeter tests were performed under both non-stressed (ambient) conditions, and under stressed (pumping) conditions to evaluate the water-bearing horizons intersecting the wellbore.

The Colog Group’s logging of the subject wellbores was performed between the 18th and 20th of December, 2013.

2.0 Methodology

2.1 Optical and Acoustic Televiewers

The OBI-40 optical televiewer and the ABI-40 acoustic televiewer (and its predecessor, the FAC40), from Advanced Logic Technologies (ALT), provide the highest resolution available for fracture and feature analysis in boreholes. Precise dip direction and angle measurements of bedding, fractures, and joint planes, along with other geological analyses, are possible.

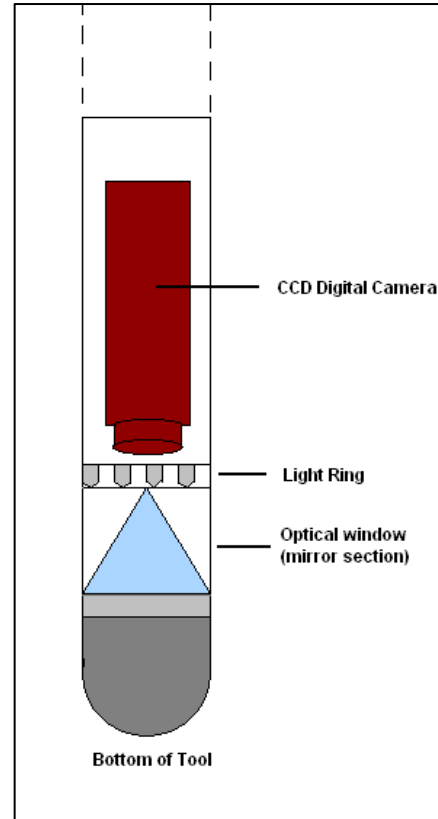
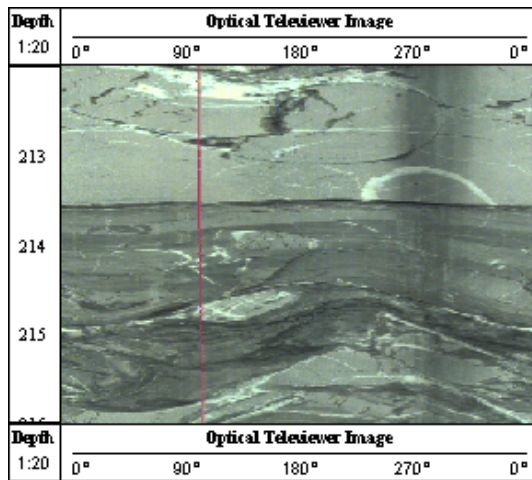
The optical televiewer technology is based on direct optical observation of the borehole wall face and can be utilized in both air and clear fluid filled boreholes. The acoustic televiewer technology is based on the return amplitude and time of an acoustic wave reflected off the borehole wall face; it can be utilized in clear or murky fluid-filled boreholes, but not in air.

Varying borehole conditions often exist which preclude the usage of one or the other tool; therefore, the optical televiewer and acoustic televiewer are often used in conjunction to image the entire borehole. When doing so, it must be kept in mind that optical and acoustic properties are not necessarily yielding the same data set. For example, a transition between two similarly-

colored beds may not stand out visually, but it may stand out acoustically if the densities of the two materials are different.

Optical Televiwer – Theory of Operation

The OBI-40 optical televiwer provides a detailed, oriented optical image of the borehole wall. A small ring of lights illuminates the borehole wall allowing a camera to directly image the borehole wall face. A conical mirror housed in a clear cylindrical window focuses a 360° optical “slice” of the borehole wall onto the camera’s lens. As the optical televiwer tool is lowered down the hole, the video signal from the camera is transmitted uphole via the wireline to the recording instrumentation.



Figures: Example of OBI40 optical Televiwer data (left) and sketch of OBI40 optical tool head (right). The signal is digitized in real time by capturing up to 720 pixels from the conical optical image. A digital magnetometer and accelerometer package is used to determine the orientation of the probe, and thus the digital image, for each conical image capture. The conical image rings are stacked and unwrapped to a 2-D, oriented image of the borehole wall.

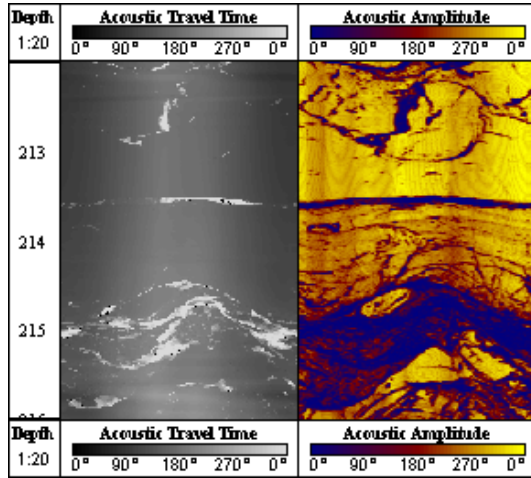
Precise borehole trajectory/deviation and image orientation are achieved using a 3-axis magnetometer and three accelerometers. When the tool is well-centralized, azimuthal accuracy is to ± 1.0 degrees and inclination accuracy is to ± 0.5 degrees. Deviated or rugous boreholes and outside magnetic interference can contribute to reduced orientation accuracy of the tool, and thus the oriented image. The pink line seen in the example data above represents a fixed point on the tool; it is used in orienting the data with respect to magnetic north.

Tool image colors are calibrated in shop to true-color, however, varying light conditions downhole often lead to color images that are somewhat false-colored. This should be taken into account when reviewing images.

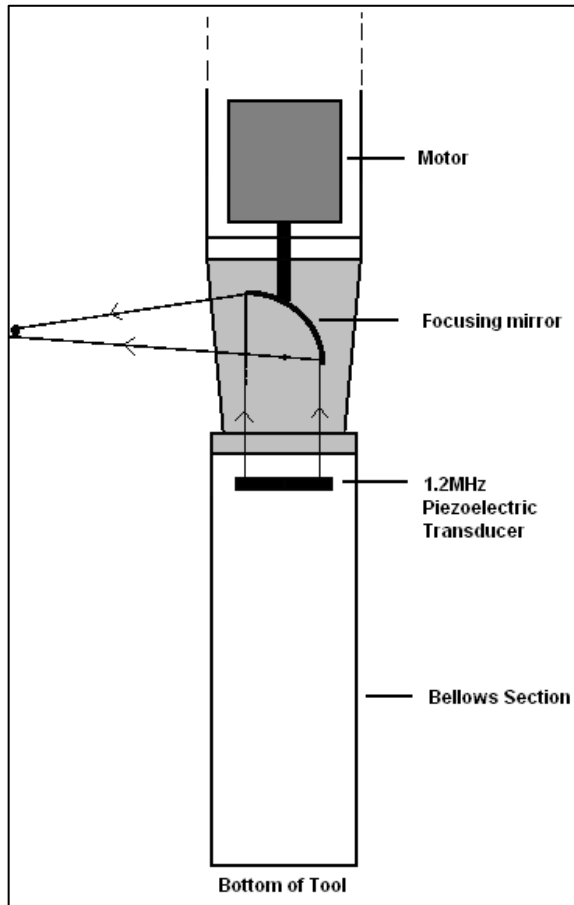
Main applications of the optical televiwer include: fracture detection and evaluation, detection of thin beds, determination of bedding dip, lithological characterization, and casing inspection.

Acoustic Televiwer (ATV) – Theory of Operation

The ABI-40 acoustic televiwer, from Advanced Logic Technologies (ALT), provides a detailed, oriented image of acoustic reflections from the borehole wall. A unique focusing system resolves bedding features as small as 2 mm and is capable of detecting fractures with apertures as small as 0.1 mm.



Figures: Example ABI40 acoustic televiwer data (left) and sketch of ABI40 acoustic head (right).



The acoustic televiwer transmits ultrasonic pulses from a rotating sensor (mirror) and records the signals reflected from the interface between the borehole fluid and the borehole wall. The amplitude of these reflections is representative of the hardness of the formation surrounding the borehole, while the travel time represents the borehole shape and diameter. As many as 288 reflections may be recorded per revolution at up to 10 revolutions per second. The conical image rings are stacked and unwrapped to a 2-D, oriented image of the borehole wall. The digital amplitude and travel time data are presented using a variety of color schemes.

Precise borehole trajectory/deviation and acoustic image orientation are achieved using a 3-axis magnetometer and three accelerometers. When the tool is well-centralized, azimuthal accuracy is to ± 1.0 degrees and inclination accuracy is to ± 0.5 degrees. Deviated or rugous boreholes and outside magnetic interference can contribute to reduced orientation accuracy of the tool, and thus the oriented image.

The high-resolution reflection images and the precise travel time measurements make the ABI-40 acoustic televiwer a versatile tool. Possible applications include: fracture detection and evaluation, detection of thin beds, determination of bedding dip, lithological characterization, casing inspection, and high-resolution caliper measurements.

Acoustic Televiwer Caliper Log

An unconventional caliper log may be generated from the travel time data acquired by the ABI-40 acoustic televiewer. Using WellCAD software, an estimation of the distance from the probe to the borehole wall can be made by incorporating the travel time of the acoustic signal with an estimation of the velocity of the borehole fluid. The time it takes the acoustic signal to travel through a known viscous medium and back to the probe is directly related to the distance between the signal generator and the borehole wall provided the borehole fluid viscosity remains constant and the probe is properly centralized. The distance from the probe to the borehole wall is then corrected for the radius of the probe, producing a borehole diameter value.

Understanding 2-D Televiewer Images

For both the optical and acoustic televiewer, the 2-D picture of the borehole wall is unwrapped from north to north. Planar features that intersect the borehole appear to be sinusoids on the unwrapped image. To calculate the dip angle of a fracture or bedding feature, the amplitude of the sinusoid (h) and the borehole diameter (d) are required. The angle of dip is equal to the arc tangent of h/d , and the dip direction is picked at the trough of the sinusoid.

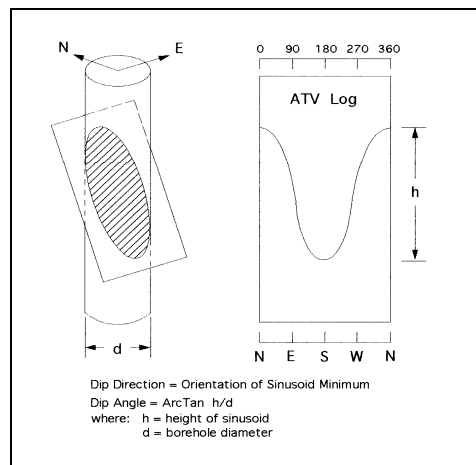


Figure: Geometric representation of a north-dipping fracture plane and corresponding log.

Interpreting Optical and/or Acoustic Televiewer Data

Sinusoidal features are picked throughout the boreholes by visual inspection of the digital optical and acoustic televiewer images using the interactive software WellCAD. These sinusoidal feature *projections* can directly overlay the televiewer images or be plotted alongside the televiewer images.

The features can also be represented by *tadpoles*. The tail of the tadpole points in the azimuthal direction of dip, where north is up, east is 90° to the right, etcetera. The head of the tadpole is located vertically on the plot, at the projection's inflection point, that is, halfway between the peak and the trough depth of the sinusoidal projection. The horizontal head location represents the dip angle, with shallow features near the left side of the plot and steeper features near the right side.

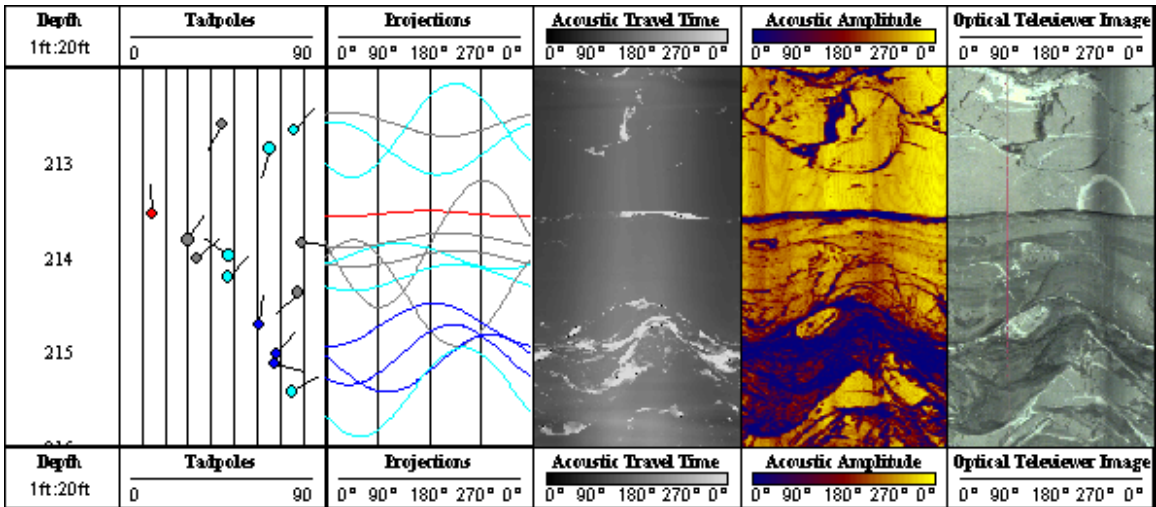


Figure: Example projections and tadpoles for corresponding optical and acoustic televiewer data sets.

The WellCAD software calculates the true feature orientation (dip direction and angle) in either deviated or vertical boreholes. Depths are assigned to the fractures or bedding features at the inflection points (middles) of the sinusoids. Features are subjectively ranked for flow potential using *IDS's Ranking System for Optical Televiewer Features*, included in this report. The features picked, along with their assigned ranks, orientations and depths are exported and presented in tables for each well. Orientations are based on magnetic north and are not corrected for magnetic declination, unless specified.

From the feature data tables, stereonet plots and rose diagrams are generated, as necessary. Stereonet plots and rose diagrams provide useful information concerning the statistical distribution and possible patterns or trends that may exist from the optical and/or acoustic televiewer feature orientation data set.

Rose Diagrams

A rose diagram is a polar diagram in which radial length of the petals indicates the relative frequency (percentage) of observation of a particular angle or fracture dip direction or range of angles or dip directions. Rose diagrams are used to identify patterns (if any) in the frequency of dip angles or directions for a particular data set. The following rose diagrams and stereonet plots all come from the same data set to help illustrate the relationships between the plot types.

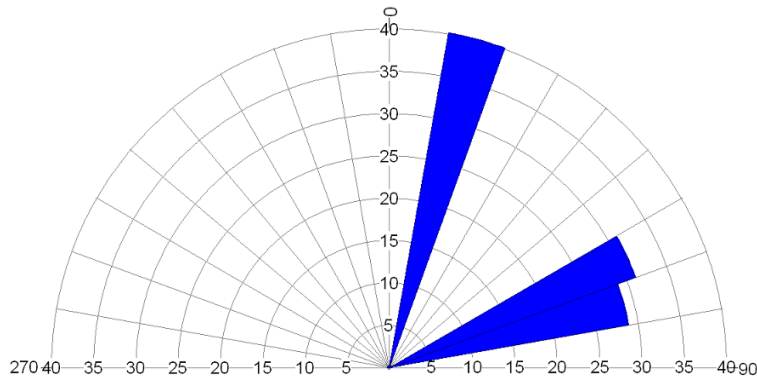


Figure: Example rose diagram from an optical televiewer data set illustrating the frequency (%) of dip angles.

With a quick glance at the above rose diagram of dip angle values, one can see two distinct sets of dip angles; one set with lower dip angles and one set with higher dip angles. Specifically, 40 percent of the features have a dip angle between 10° and $<20^{\circ}$, and 60 percent of the features have a dip angle between 60° and $<80^{\circ}$. The left-hand side of the above rose diagram will always be blank by convention of positive dip angle values only.

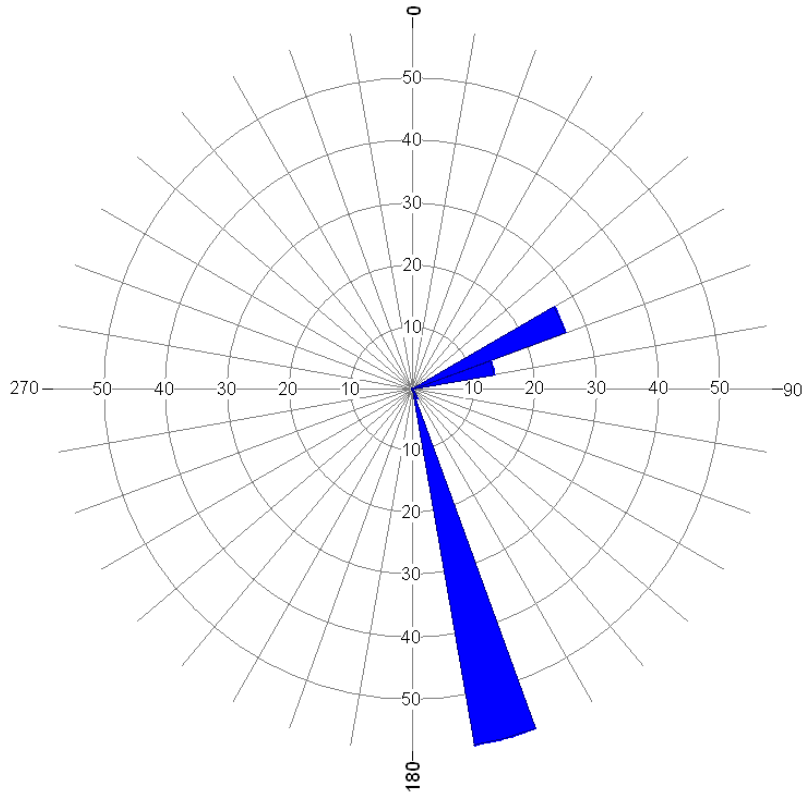


Figure: Example rose diagram from an optical televiwer data set illustrating the frequency (%) of dip direction (azimuth).

With a quick glance at the above rose diagram of dip direction values, one can see that the features (and/or fractures) in this data set have two primary dip directions. Specifically, 40 percent of the features dip to the east-northeast between 60° degrees and $<80^{\circ}$ in azimuth and 60 percent of the features dip to the south-southeast between 160° and $<170^{\circ}$ in azimuth.

Stereonets

For stereonets, The Colog Group utilizes a southern-hemisphere projected, equal-area Schmidt net to plot the poles to the feature planes. These plots are often used in plotting geologic data such as the dips and orientations of structural features. Here, the azimuthal angle indicates dip direction of the plane's pole (which dips 180 degrees opposite in azimuth from the plane's dip direction at a complementary angle). The distance from the center indicates the dip magnitude. The further from the center the steeper the dip angle; the closer to the center the more horizontal the feature is.

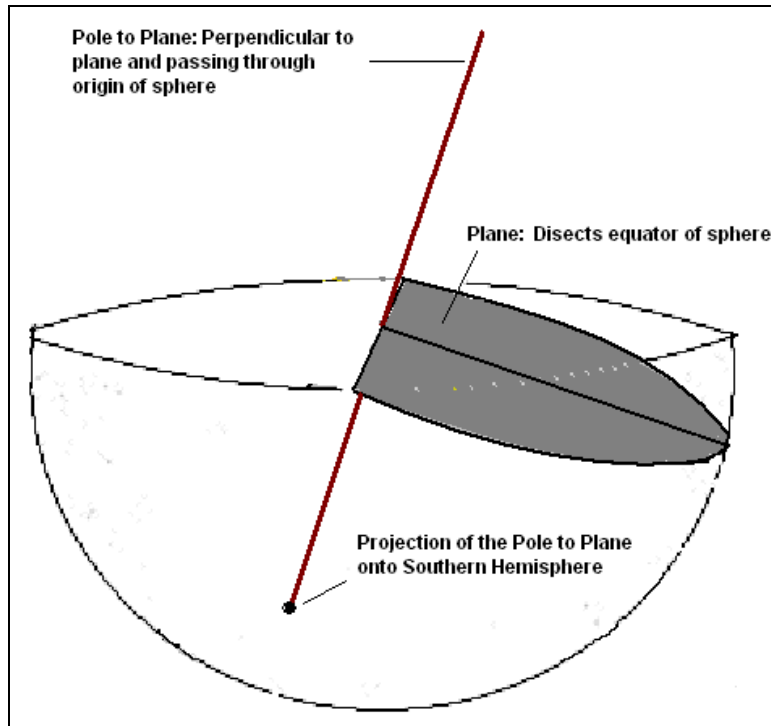


Figure: The above cartoon demonstrates the relationship between a plane and its pole, as projected onto the southern hemisphere of a sphere.

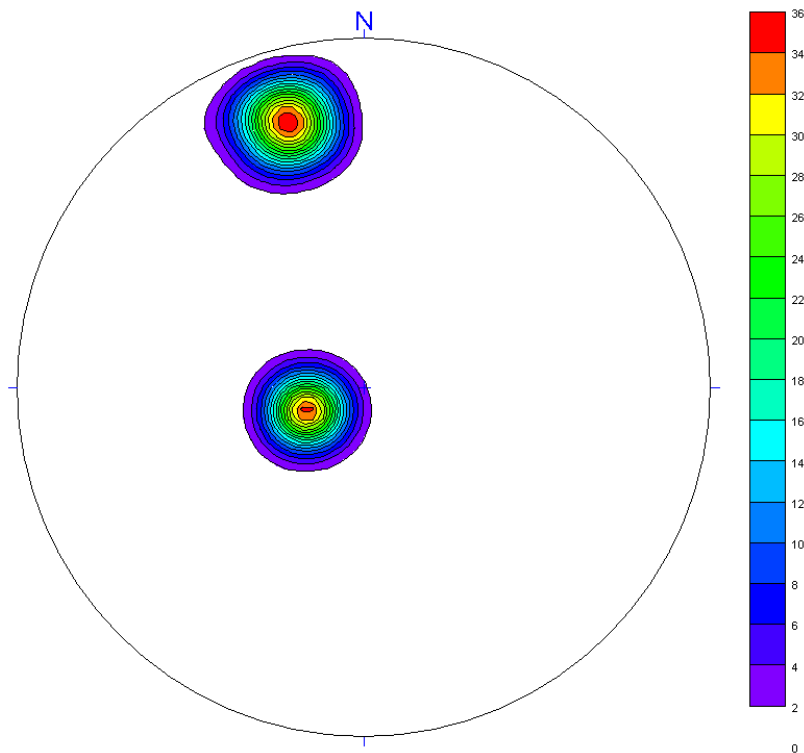
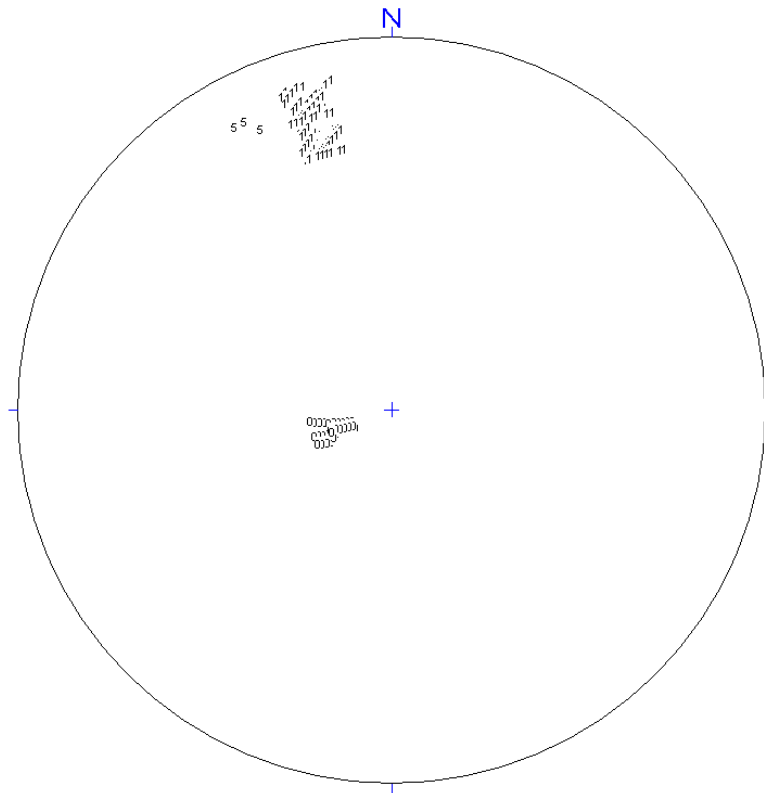


Figure: Example stereonet from an optical televiewer data set illustrating the frequency (%) of dip direction and dip angle.

The figure above is an example stereonet diagram from the same televiewer data set of fractures and features as used previously to describe rose diagrams. It was created by binning the density (frequency) of poles per area. The figure below indicates, with a quick glance, that two distinct patterns exist in the example data set. A cluster of fractures/features with similar dip directions of approximately 160-170 degrees with steep dip angles of around 60-80 degrees is apparent. A second cluster is apparent with similar dip directions of approximately 60-80 degrees with moderate dip angles of approximately 10-20 degrees. The white areas indicate low to zero density of poles.



The Colog Group also often provides a Schmidt net with the qualitative rank of each fracture/feature plotted at the location of its planar pole. Please refer to the *Ranking System for Optical/Acoustic Televiewer Features*, included in the report, for an explanation of the qualitative ranks assigned each optical/acoustic televiewer feature identified.

With a quick glance at the above Schmidt net, one can see that the low dip angle features which dip to the east-northeast are bedding features, ranked “0”; the high dip angle features dipping to the south-southeast are primarily weak or partial fractures, ranked “1”; and there are several major fracture zones, ranked “5”, with strike/dip very similar to the majority of the partial/weak fractures in the well.

2.2 Heat Pulse Flowmeter

The Heat Pulse Flowmeter (HFP-4293), from Mount Sopris Instruments is a high resolution device for measuring vertical fluid movement within the borehole. This flowmeter is based upon the proven USGS design and works on the thermal fluid tracer concept. Borehole fluid is heated or thermally

tagged by as much as 1° F with an electrical heater grid. The flow rate is determined by measuring the time between the grid discharge and the peak of the thermal pulse of water reaching an upper or lower thermistor sensor. MSI utilizes flow concentrating diverters to direct fluid flowing in the borehole through the probe flow tube (Figure).

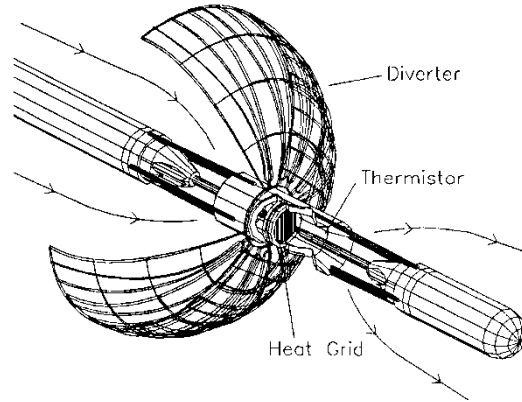


Figure: Heat pulse flowmeter diverter diagram showing fluid flow

The HFP-4293 is calibrated in a flow chamber where flow rate can be controlled and measured. Values for response time are taken for a wide range of flow rates and applied in an empirical curve-fit solution (Figure H-2). The calibration coefficients are entered into the processing software to determine vertical flow rates in gallons/minute. Thermal buoyancy of the heat pulse imposes a small asymmetry on the flow calibration so that the device is slightly less sensitive to upflow than to downflow.

Presently the HFP measures flow from 0.01 to 1.5 gallons/minute (0.038 to 5.69 liters/min) with 0.005 gpm resolution using a 1.125 inch diameter flow tube and standard multilayered flow diverter. The low end flow limit of 0.01 gpm is a function of the current calibration facility in which convective eddy currents as great as 0.01 gpm are generated by differences between water temperature in the calibration device and surrounding air. A more thermally insulated calibration chamber or smaller diameter probe flow tube could allow for significantly lower flow limit with this tool. Higher flow rates can be achieved by increasing thermistor spacing or flow tube and heating grid diameter.

In practice the HFP is run at discrete intervals within a borehole. Intervals are selected based upon review of fluid column logs (temperature, fluid resistivity, etc.), a caliper log and optimally a borehole imaging log (video or acoustic televiewer). Flow is measured at each interval and each test repeated until at least two measurements are recorded within given tolerances. Time to collect flow data is subject to the flow rate and number of intervals tested. While the actual time to record a flow rate of 0.01 gpm is less than 30 seconds, it may take up to 15 minutes per station for the borehole to stabilize and to obtain repeatable data. At higher flow rates, the borehole stabilizes more quickly and obtaining good data may take only a few minutes per station.

Heat Pulse Calibration Curves (Up and Down Flow)

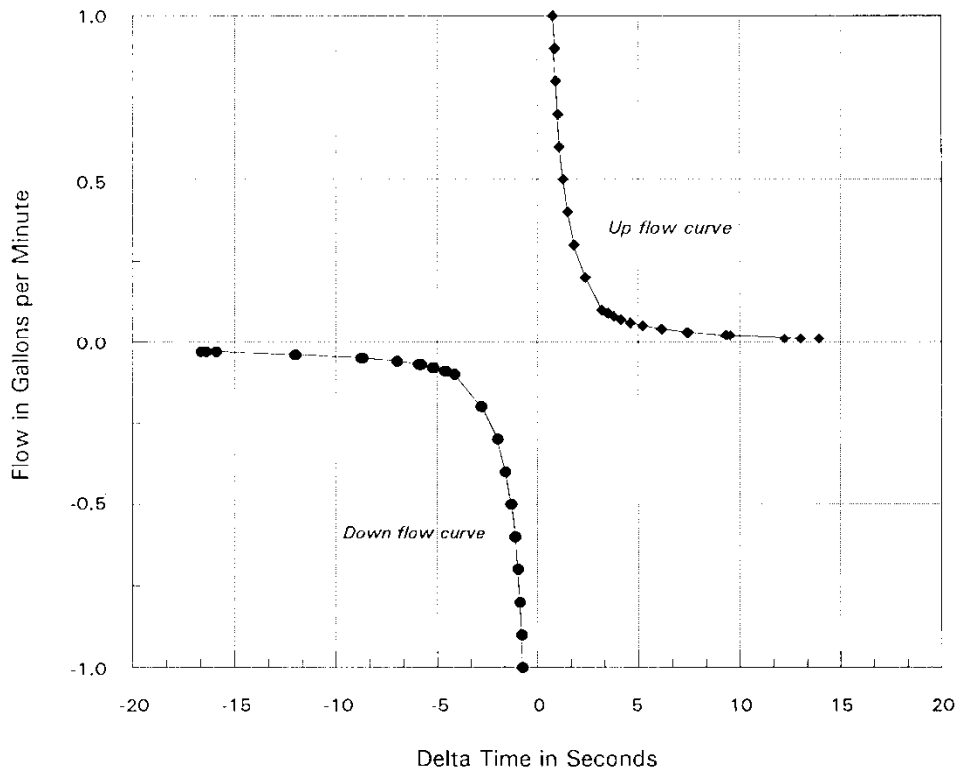


Figure: Heat pulse flowmeter calibration curves used to translate response time to gpm.

A number of factors must be considered when interpreting high-resolution flow data including: 1) the effect of the open borehole on the flow regime in the vicinity of the well bore; 2) the effects of turbulent thermal convection and other secondary flow circulations; 3) real flow regimes are often changing with time as measurements are being made; and, 4) not all permeable intervals may be producing vertical flow under ambient conditions. (Paillet et al, 1994)¹ describes these factors in detail which should be reviewed for a more thorough discussion.

Some of these factors can be minimized by using a flow concentrating diverter and by locating the diverter in a portion of the borehole that is not fractured or rugose (by analyzing the caliper and a borehole imaging log). More importantly, flow measurements should be collected in the same intervals under different head conditions. In areas where the flow regime is changing with time, a number of flow measurements should be measured at the same intervals over time and the resulting flow transients interpreted. Other variations include cross-borehole experiments where one borehole is pumped and the changes in flow are detected in the surrounding boreholes. This can provide a quick assessment of the hydraulic connections between boreholes.

¹ Paillet, Crowder and Hess, 1994, High-Resolution Flowmeter Logging - A Unique Combination of Borehole Geophysics and Hydraulics: Part II - Borehole Applications with the Heat-Pulse Flowmeter, Proceedings of the Symposium on the Application of Geophysics to Engineering and Environmental Problems, Boston, Massachusetts, pages 381-404.

3.0 37-B07 Logging Results

3.1 Geophysical Logging

On December 18, 2013, downhole geophysical investigations were performed in boring 37-B07. The geophysical logs performed were: optical televiewer (OBI), acoustic televiewer, and heat pulse flow meter. The data for these logs are presented in the 37-B07 Flow Logs plot, the Acoustic and Optical Televiewers Plot, the stereonet and rose diagrams, and the orientation summary table of televiewer features. Please see Appendix A to view these plots and diagrams.

3.2 Optical Televiewer (OBI) & Acoustic Televiewer (ABI)

On December 18, 2013, OBI and ABI logging was performed in 37-B07. The OBI was logged from 4.1 feet to a depth of 92.0 feet while the ABI was logged from 49.5 feet to 91.6 feet.

The OBI and ABI dataset indicates features at depths which correlate well with the water-bearing intervals identified from the heat pulse flow meter data. In general, the OBI and ABI identified fractures/features with aperture at water producing zones. Fracture density and fracture orientation were evaluated over the entire OBI and ABI dataset. The Rose Diagram – Dip Directions image indicates approximately 35.3% of the identified features in 37-B07 dip in the direction of 50 to 100 degrees (East-Northeast and East-Southeast).

The Rose Diagram – Dip Angles image indicates over approximately 80% of the features in 37-B07 are dipping at more than 50° from horizontal, while the remaining features are dipping at less than 50° from horizontal.

There are 151 high-angle fractures or features (dip angles greater than 45°) identified in 37-B07. These 151 high-angle features represent 86.3% of all identified features from the OBI and ABI data set. The 151 high-angle features are qualitatively ranked 0 to 4, suggesting minimal to nominal flow potential from these features. Please see the Rose Diagrams, Stereonets and the Fracture Feature Table for a complete summary of all fracture and feature orientations.

3.3 Heat Pulse Flow Meter

The Heat-Pulse Flowmeter indicated no flow during ambient conditions between approximately 53.0 and 90.9 feet. Ambient testing was only conducted in 37-B07 due to time constraints.

4.0 37-B10 Logging Results

4.1 Geophysical Logging

On December 18, 2013, downhole geophysical investigations were performed in boring 37-B10. The geophysical logging performed was acoustic televiewer (ABI). The data for this log is presented in the 37-B10 Acoustic Televiewer Image Plot, the stereonet and rose diagrams, and the orientation summary table of televiewer features. Please see Appendix B to view these plots and diagrams.

4.2 Acoustic Televiewer (ABI)

On December 18, 2011, ABI logging was performed in 37-B10. The ABI was logged from 5.0 feet to 104.2 feet.

In general, the ABI identified fractures/features with aperture at possible water producing zones. Fracture density and fracture orientation were evaluated over the entire ABI dataset. The Rose Diagram – Dip Directions image indicates approximately 39.1% of the identified features in 37-B10 dip in the direction of 180 to 240 degrees (South and Southwest) and 18.5% dip in the direction of 50 to 90 degrees (Northeast).

The Rose Diagram – Dip Angles image indicates over approximately 76% of the features in 37-B10 are dipping at more than 50° from horizontal, while the remaining features are dipping at less than 50° from horizontal.

There are 243 high-angle fractures or features (dip angles greater than 45°) that were identified in 37-B10. These 243 high-angle features represent 81.8% of all identified features from the ABI data set. The 243 high-angle features are qualitatively ranked 0 to 3, suggesting minimal flow potential from these features. Please see the Rose Diagrams, Stereonets and the Fracture Feature Table for a complete summary of all fracture and feature orientations.

5.0 37-B12 Logging Results

5.1 Geophysical Logging

On December 17 and 19, 2013, downhole geophysical investigations were performed in boring 37-B12. The geophysical logs performed were: optical televiewer (OBI), acoustic televiewer, and heat pulse flow meter. The data for these logs are presented in the 37-B12 Flow Logs plot, the Acoustic and Optical Televiewers Plot, the stereonet and rose diagrams, and the orientation summary table of televiewer features. Please see Appendix C to view these plots and diagrams.

5.2 Optical Televiewer (OBI) & Acoustic Televiewer (ABI)

On December 17, 2013, OBI and ABI logging was performed in 37-B12. The OBI was logged from 17.1 feet to a depth of 52.0 feet while the ABI was logged from 47.4 feet to 153.5 feet.

The OBI and ABI dataset indicates features at depths which correlate well with the water-bearing intervals identified from the heat pulse flow meter data. In general, the OBI and ABI identified fractures/features with aperture at water producing zones. Fracture density and fracture orientation were evaluated over the entire OBI and ABI dataset. The Rose Diagram – Dip Directions image indicates approximately 29% of the identified features in 37-B12 dip in the direction of 300 to 360 degrees (Northwest).

The Rose Diagram – Dip Angles image indicates over approximately 90% of the features in 37-B12 are dipping at more than 50° from horizontal, while the remaining features are dipping at less than 50° from horizontal.

There are 249 high-angle fractures or features (dip angles greater than 45°) identified in 37-B12. These 249 high-angle features represent 92.5% of all identified features from the OBI and ABI

data set. The 249 high-angle features are qualitatively ranked 0 to 4, suggesting minimal to nominal flow potential from these features. Please see the Rose Diagrams, Stereonets and the Fracture Feature Table for a complete summary of all fracture and feature orientations.

5.3 Heat Pulse Flow Meter

The Heat-Pulse Flowmeter indicated no flow during ambient conditions between approximately 52.1 and 58.0 feet and again at 118.4 feet. The Flowmeter indicated minor flow at approximately 74.9, 96.9, 109.9, 122.9, 133.0, 142.9, and 149.9 feet with flow ranging from 0.01 to 0.06gpm. During pumping, water was drawn up the borehole, and extracted at 0.365gpm.

6.0 37-B13 Logging Results

6.1 Geophysical Logging

On December 18 and 19, 2013, downhole geophysical investigations were performed in boring 37-B13. The geophysical logs performed were: optical televiewer (OBI), acoustic televiewer, and heat pulse flow meter. The data for these logs are presented in the 37-B13 Flow Logs plot, the Acoustic and Optical Televiewers Plot, the stereonet and rose diagrams, and the orientation summary table of televiewer features. Please see Appendix D to view these plots and diagrams.

6.2 Optical Televiewer (OBI) & Acoustic Televiewer (ABI)

On December 18, 2013, OBI and ABI logging was performed in 37-B13. The OBI was logged from 4.0 feet to a depth of 99.0 feet while the ABI was logged from 36.5 feet to 98.1 feet.

The OBI and ABI dataset indicates features at depths which correlate well with the water-bearing intervals identified from the heat pulse flow meter data. In general, the OBI and ABI identified fractures/features with aperture at water producing zones. Fracture density and fracture orientation were evaluated over the entire OBI and ABI dataset. The Rose Diagram – Dip Directions image indicates approximately 24.8% of the identified features in 37-B13 dip in the direction of 20 to 70 degrees (Northeast) and 18.5% of the identified features dip in the direction of 200 to 240 degrees (Southwest).

The Rose Diagram – Dip Angles image indicates over approximately 70% of the features in 37-B13 are dipping at more than 50° from horizontal, while the remaining features are dipping at less than 50° from horizontal.

There are 143 high-angle fractures or features (dip angles greater than 45°) identified in 37-B13. These 143 high-angle features represent 70.1% of all identified features from the OBI and ABI data set. The 143 high-angle features are qualitatively ranked 0 to 2, suggesting minimal to nominal flow potential from these features. Please see the Rose Diagrams, Stereonets and the Fracture Feature Table for a complete summary of all fracture and feature orientations.

6.3 Heat Pulse Flow Meter

The Heat-Pulse Flowmeter indicated no flow during ambient conditions between approximately 39.0 and 95.0 feet. The Flowmeter indicated minor flow at approximately 60.1, and 83.2 feet with flow ranging from 0.02 to 0.03gpm. During pumping, water was drawn up the borehole, and extracted at

0.365gpm. The Heat-Pulse tests in the deepened borehole, during pumping, indicated downflow with a maximum of 0.03 gpm at 83.2 feet and a minimum of 0.02 gpm at 60.1 feet.

7.0 Limitations

IDS's logging was performed in accordance with generally accepted industry practices. IDS has observed that degree of care and skill generally exercised by others under similar circumstances and conditions. Interpretations of logs or interpretations of test or other data, and any recommendation or hydrogeologic description based upon such interpretations, are opinions based upon inferences from measurements, empirical relationships and assumptions. These inferences and assumptions require engineering judgment, and therefore, are not scientific certainties. As such, other professional engineers or analysts may differ as to their interpretation. Accordingly, IDS cannot and does not warrant the accuracy, correctness or completeness of any such interpretation, recommendation or hydrogeologic description.

All technical data, evaluations, analysis, reports, and other work products are instruments of IDS's professional services intended for one-time use on this project. Any reuse of work product by Client for other than the purpose for which they were originally intended will be at Client's sole risk and without liability to IDS. IDS makes no warranties, either express or implied. Under no circumstances shall IDS or its employees be liable for consequential damages.

Appendix A



Optical & Acoustic Televiewer

COMPANY: CB&I

PROJECT: Edwards Air Force Base

DATE LOGGED: 18 December 2013

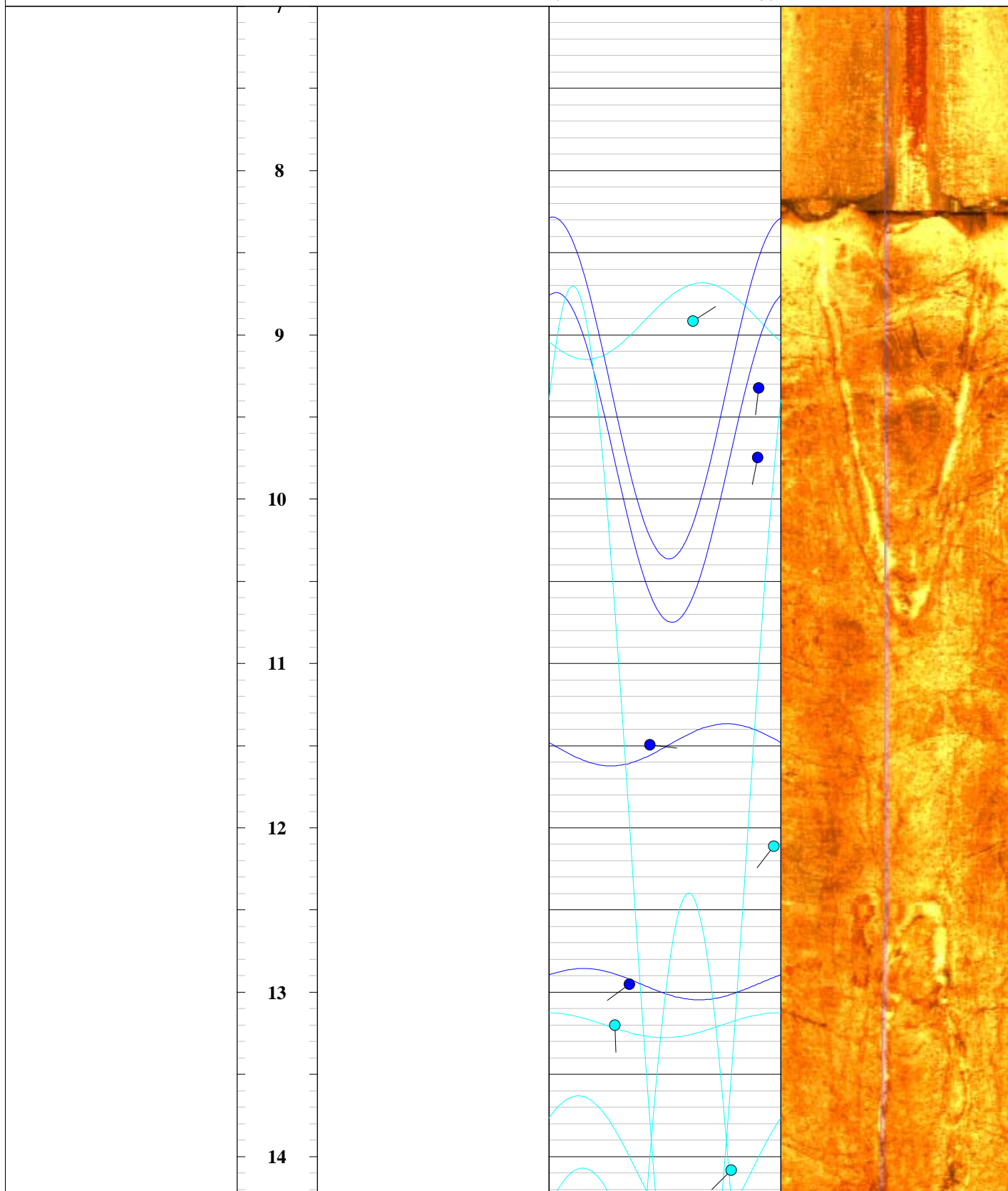
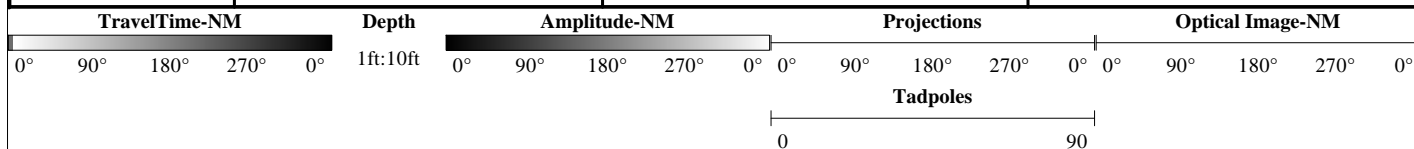
WELL: 37-B07

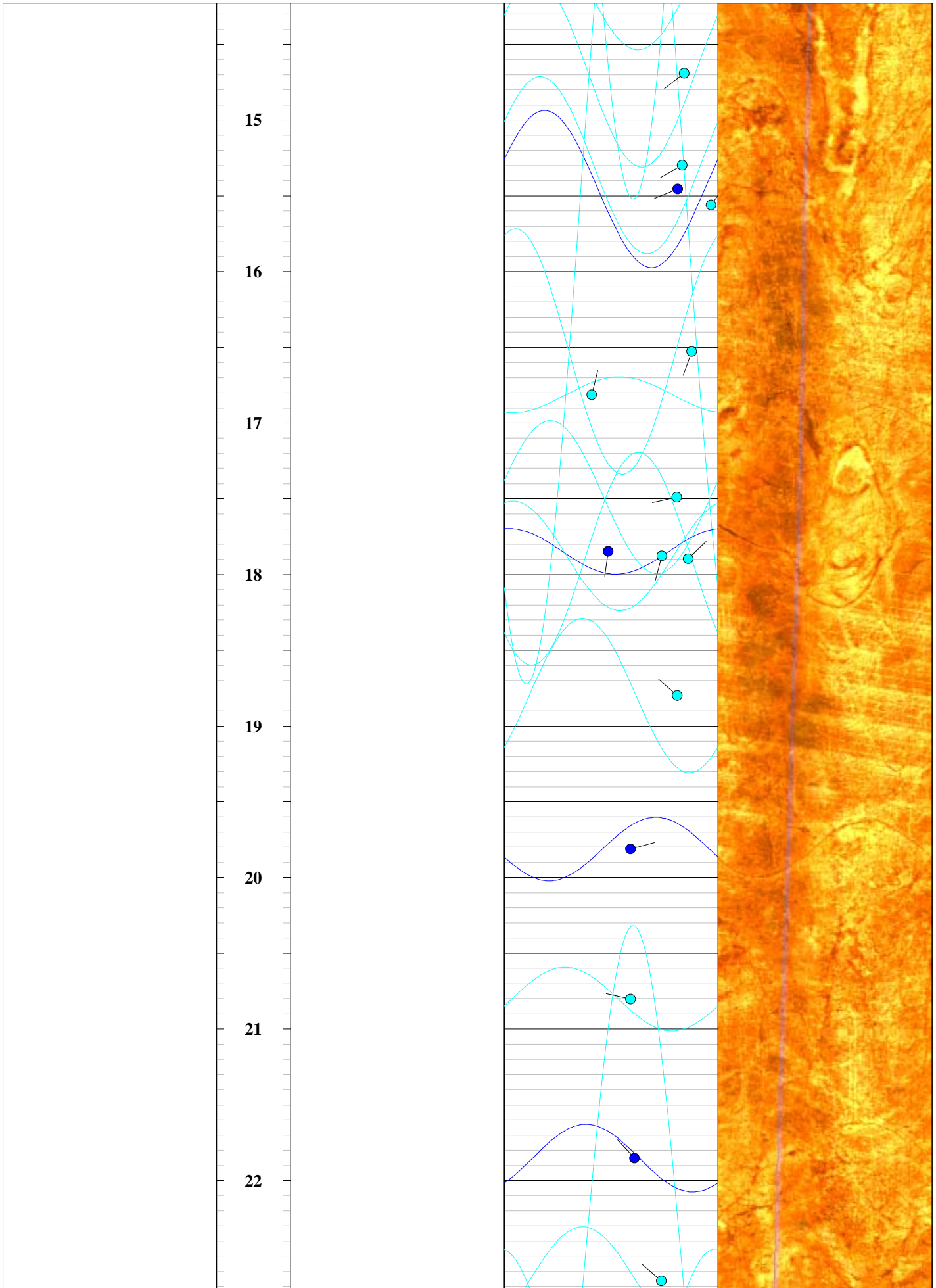
IDS - Colog Group

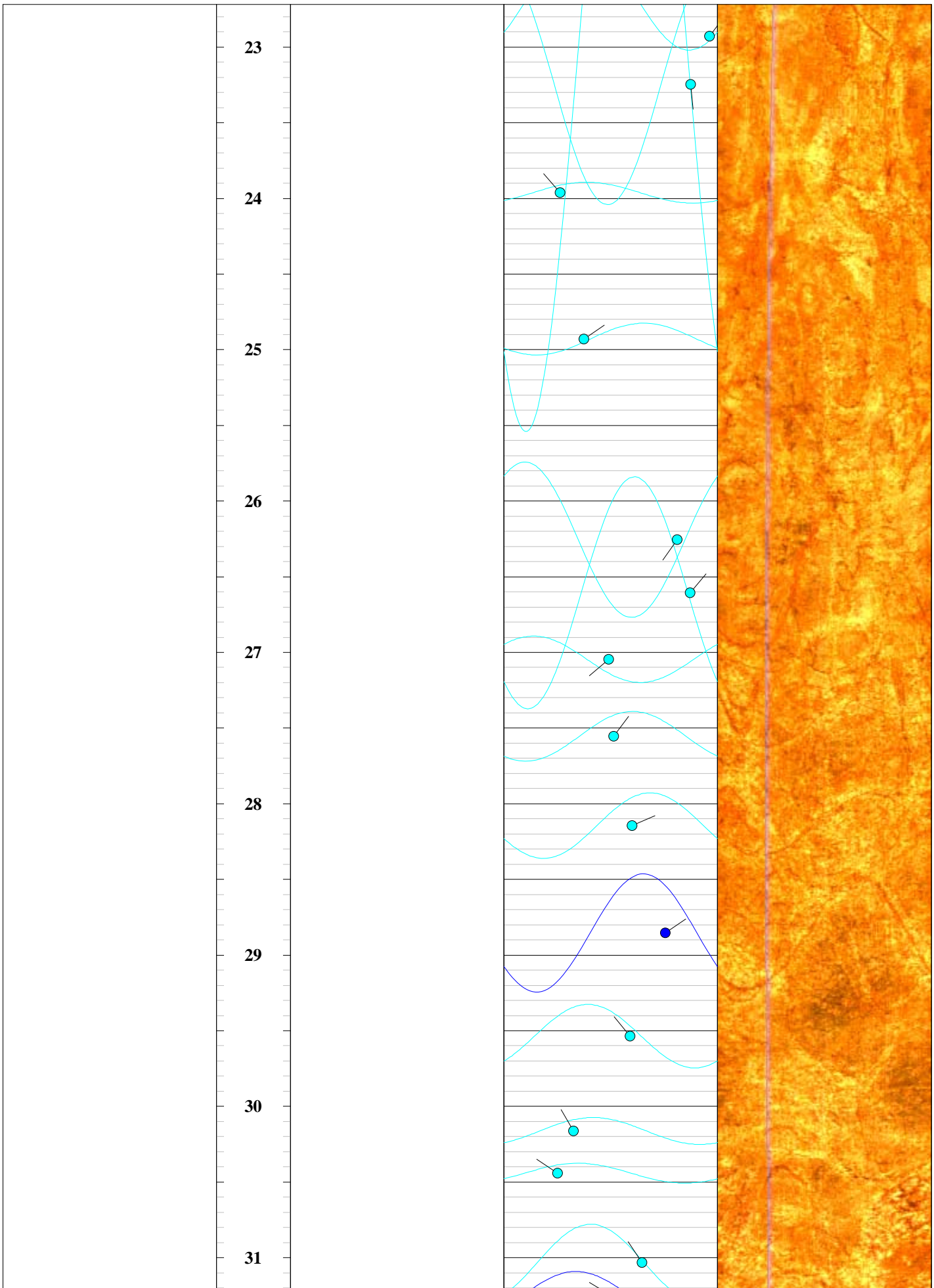
810 Quail Street, Suite E, Lakewood, CO 80215

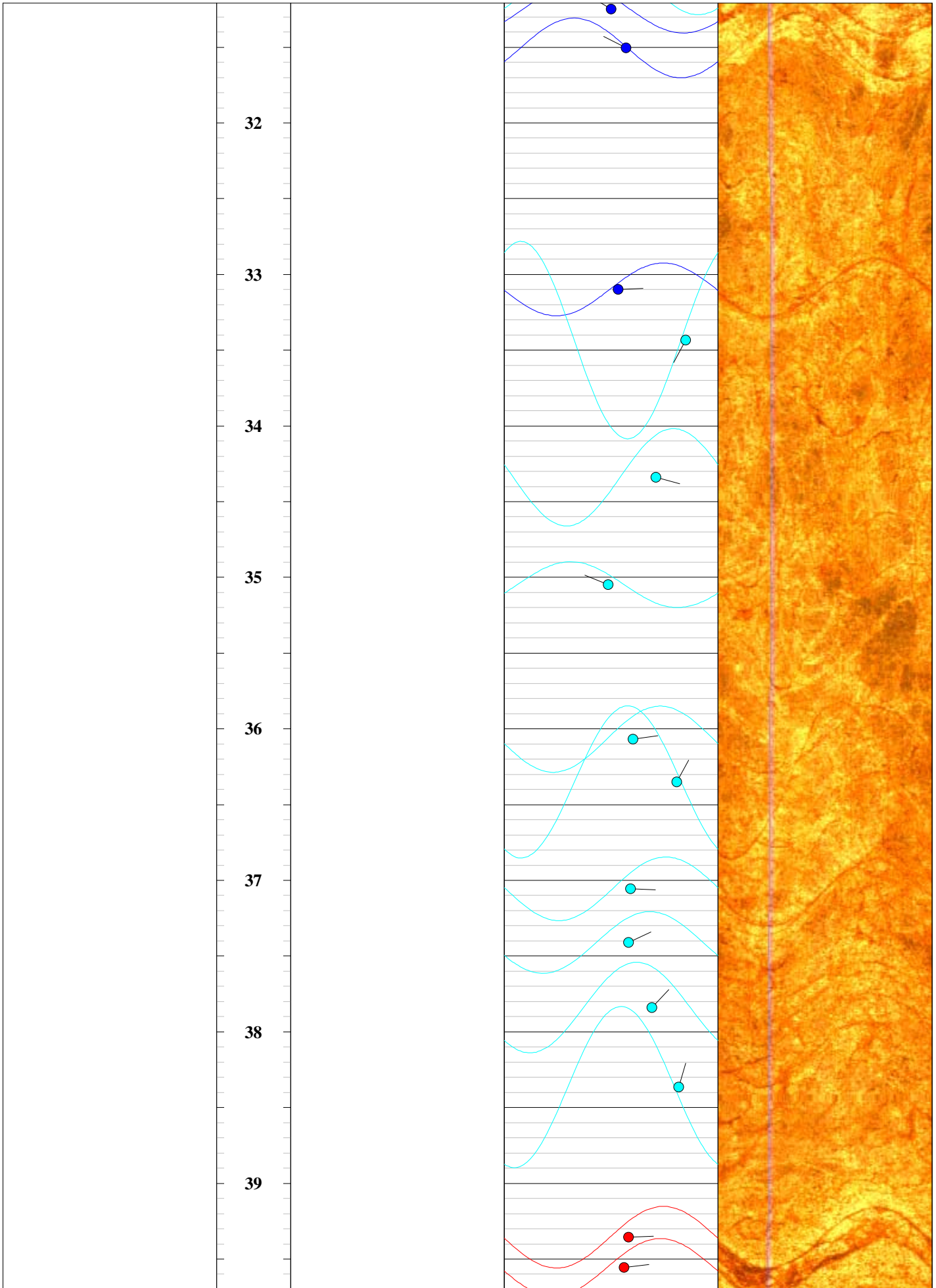
Phone: (303) 279-0171, Fax: (303) 278-0135

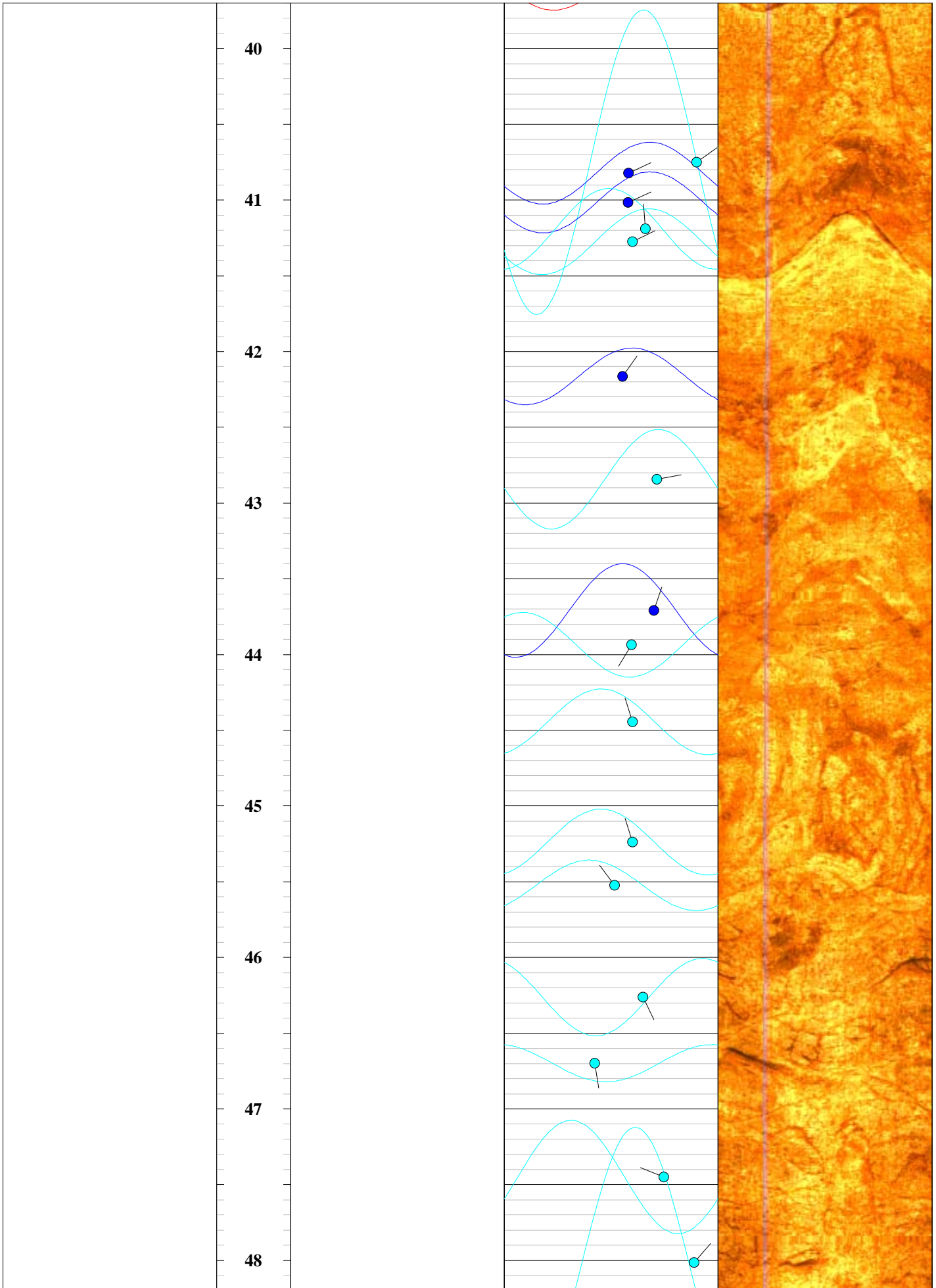
www.idsdrill.com

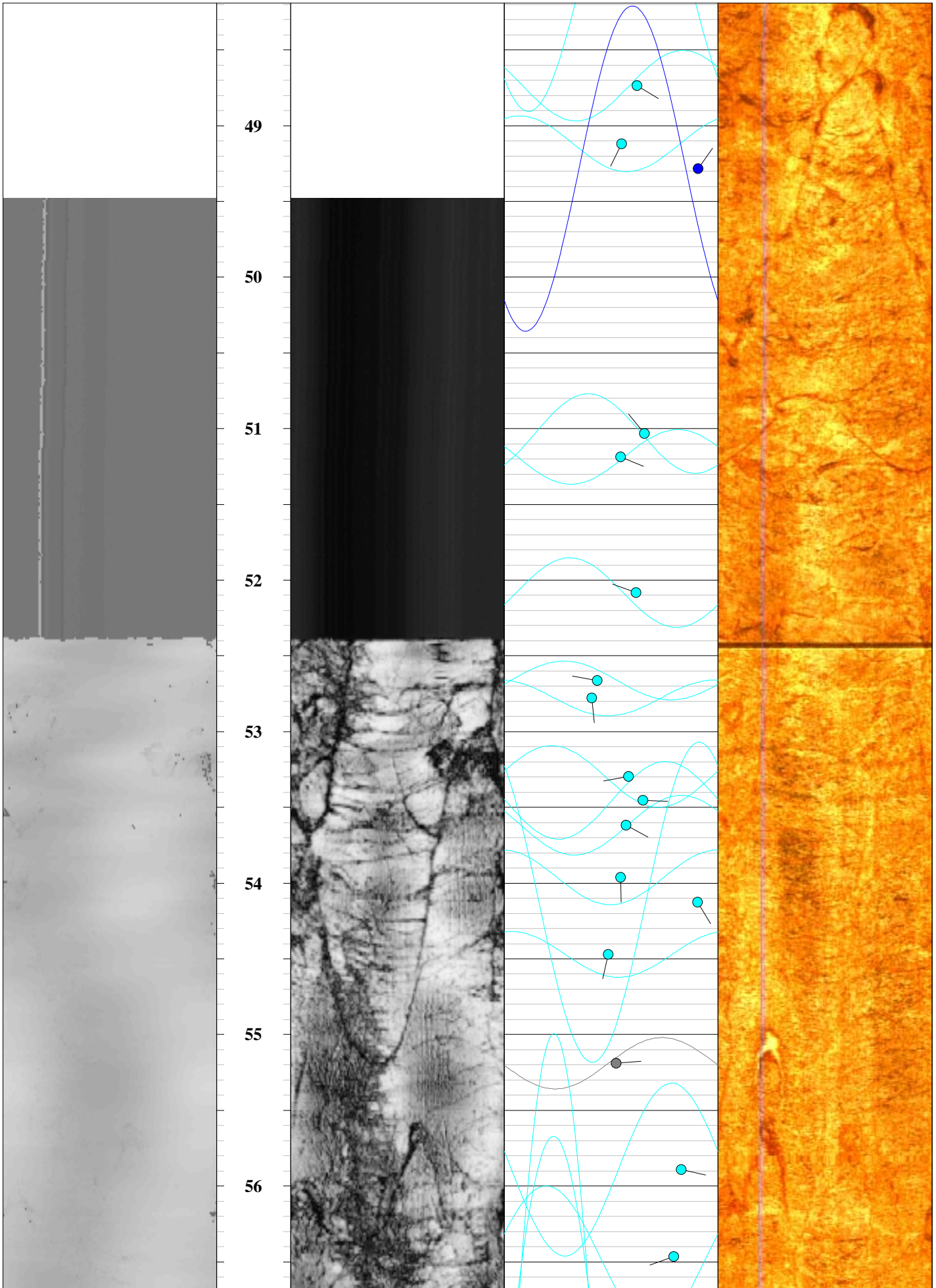


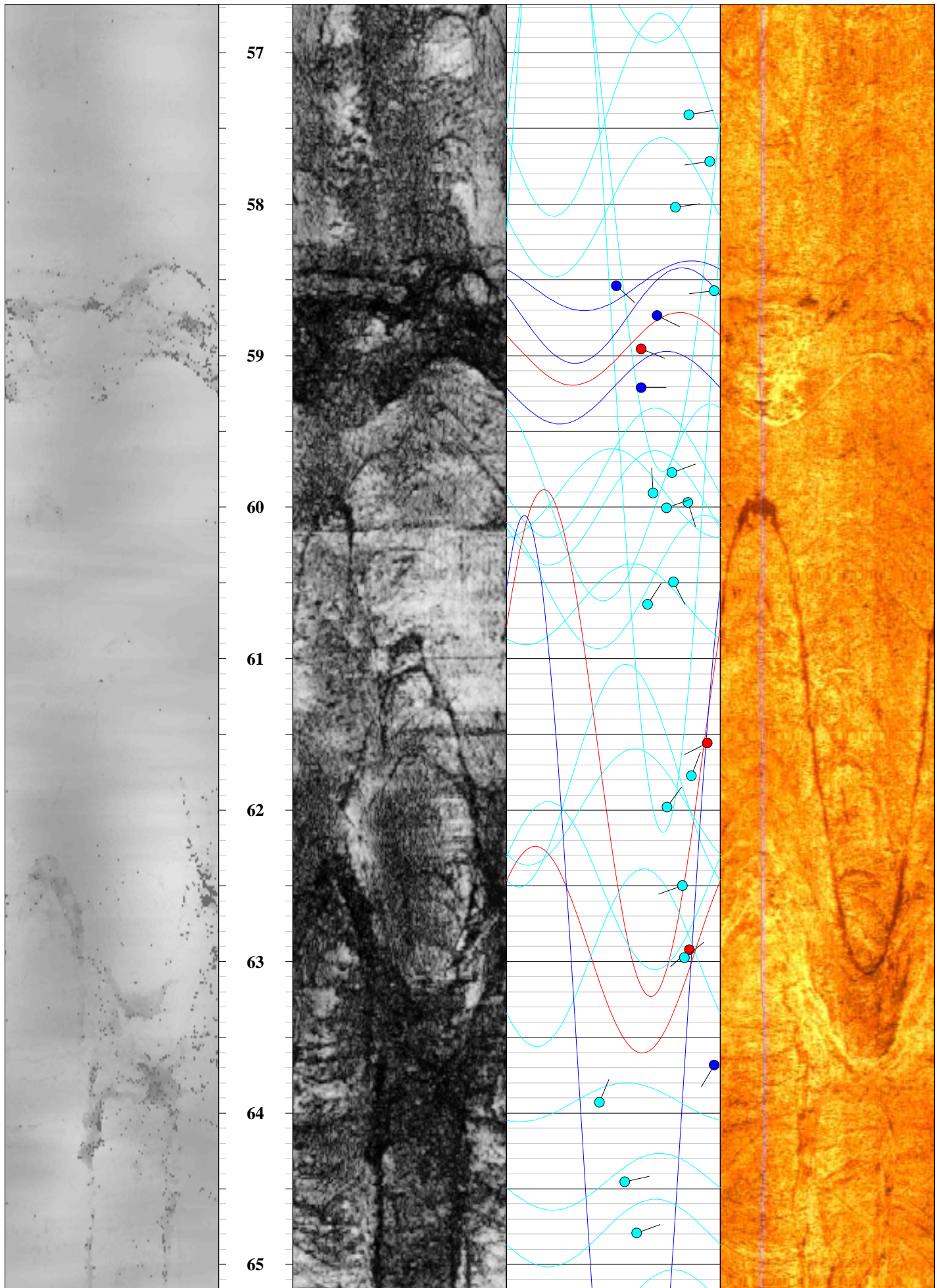


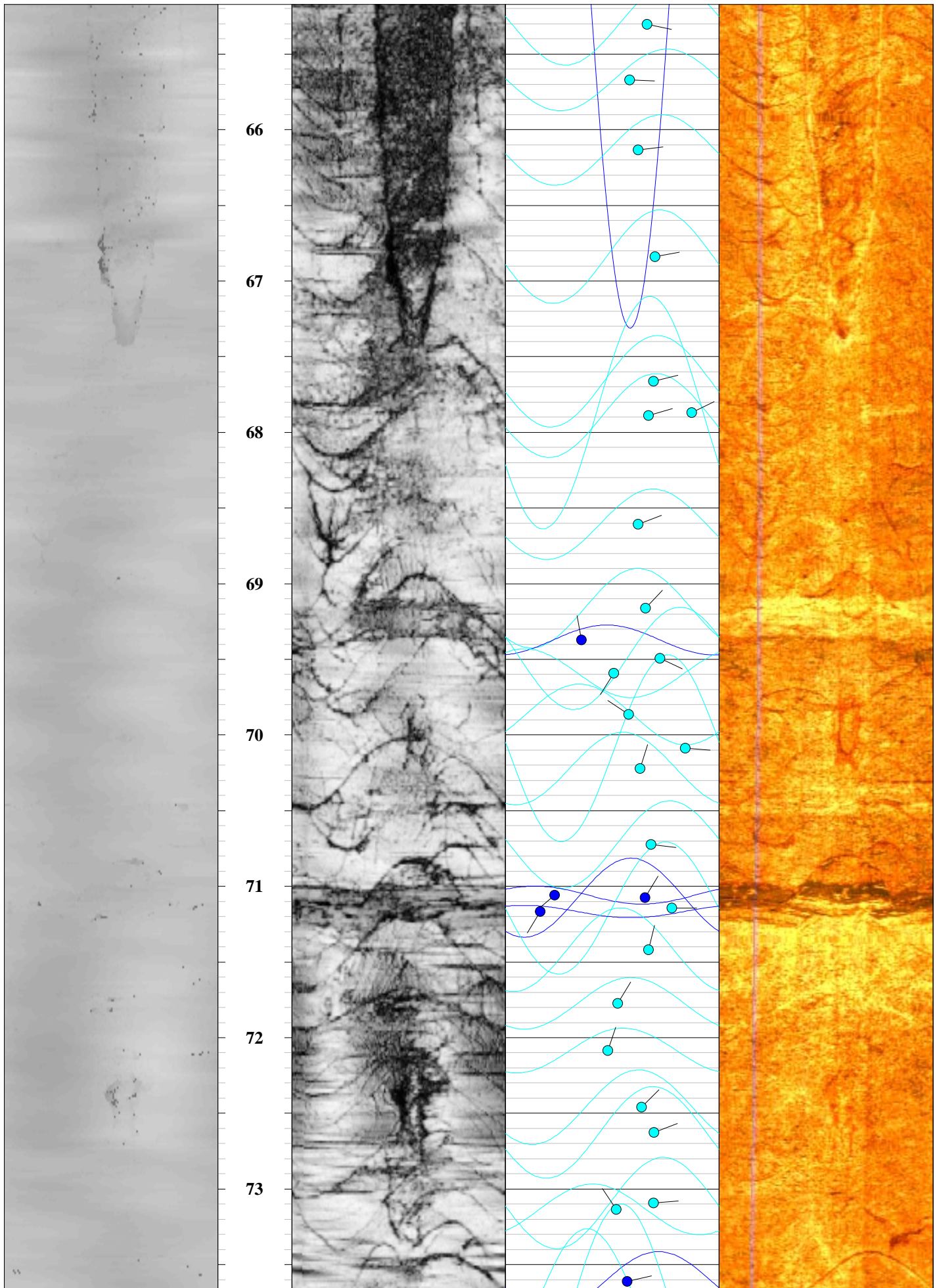


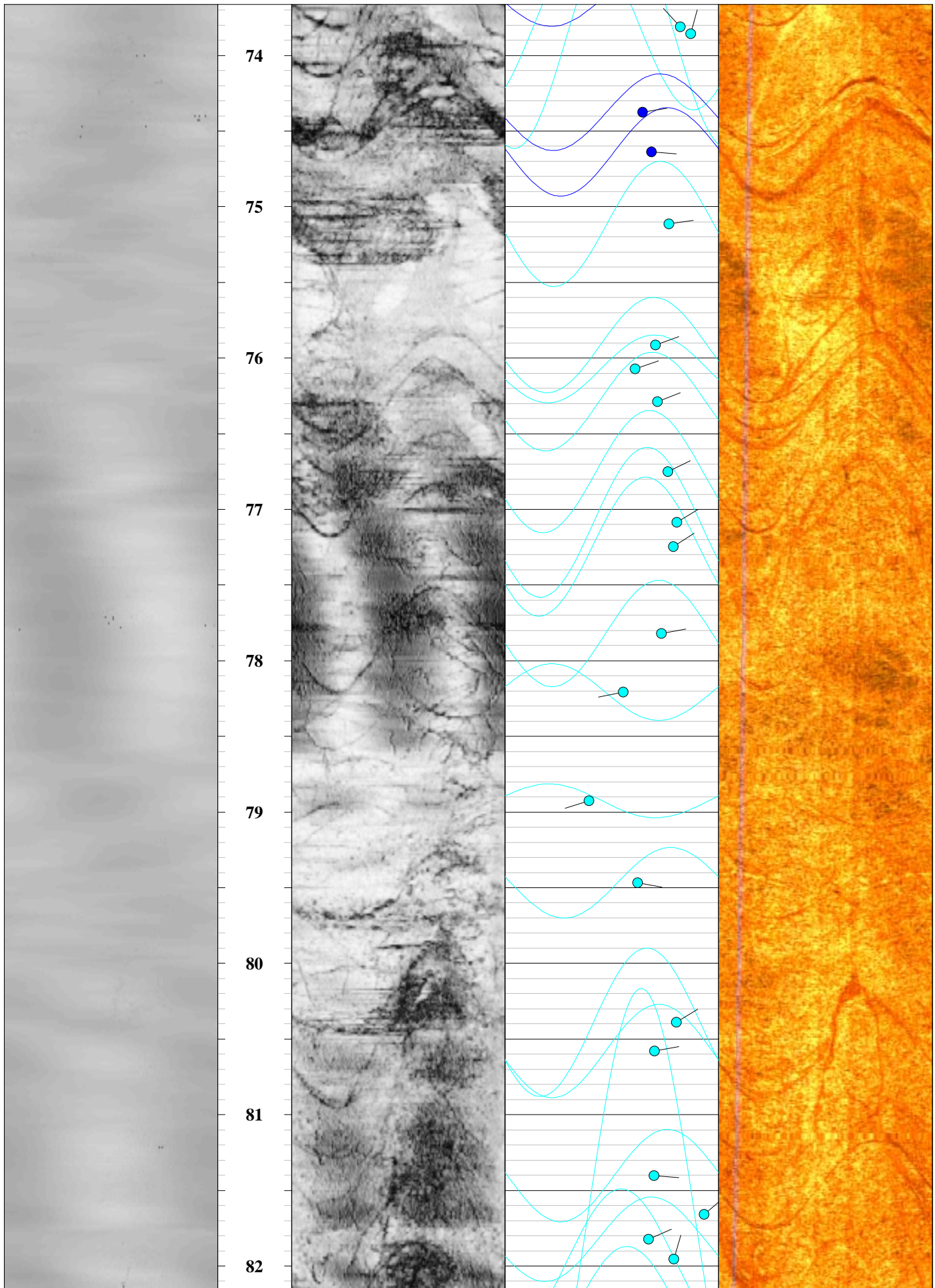


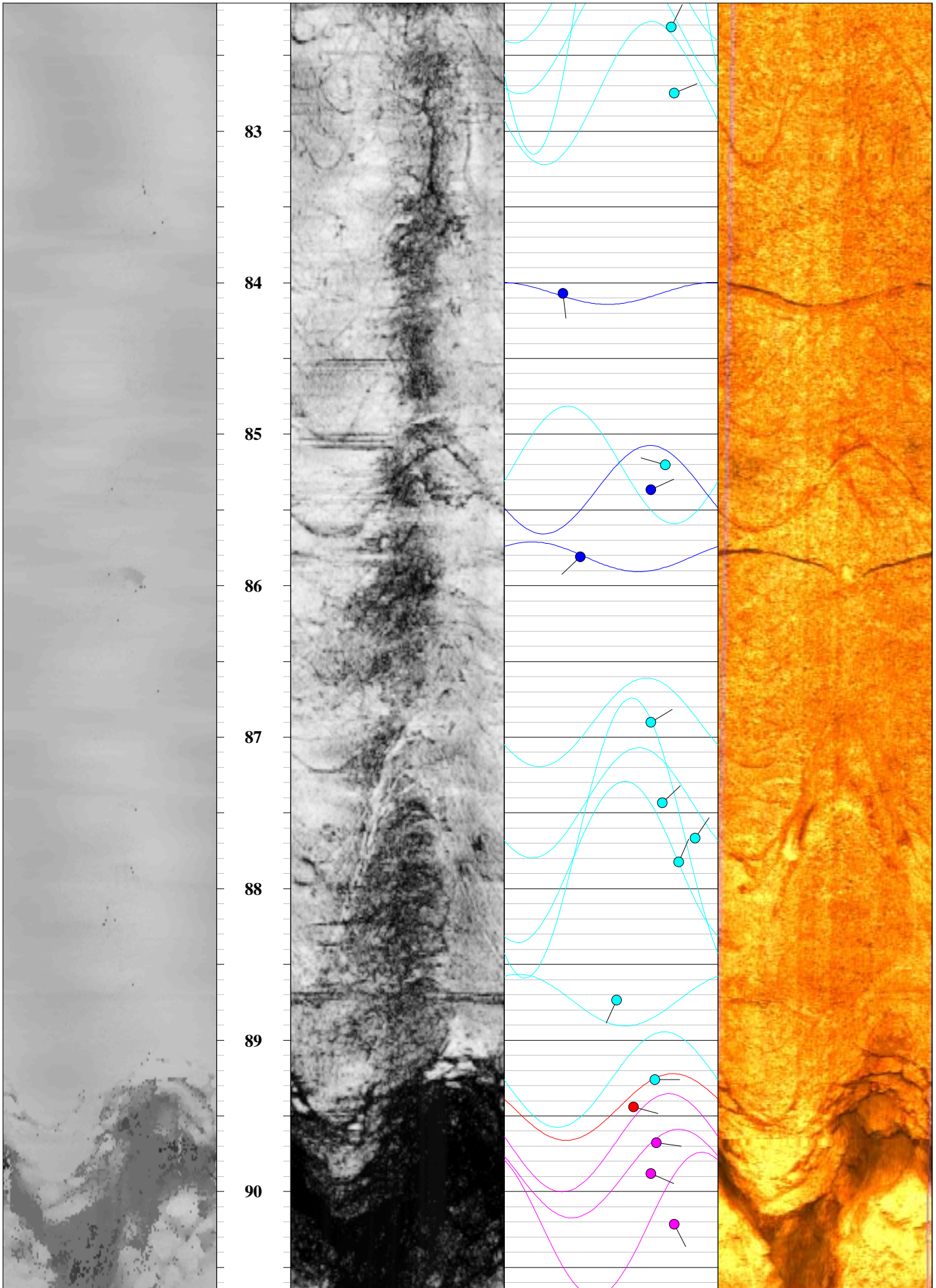


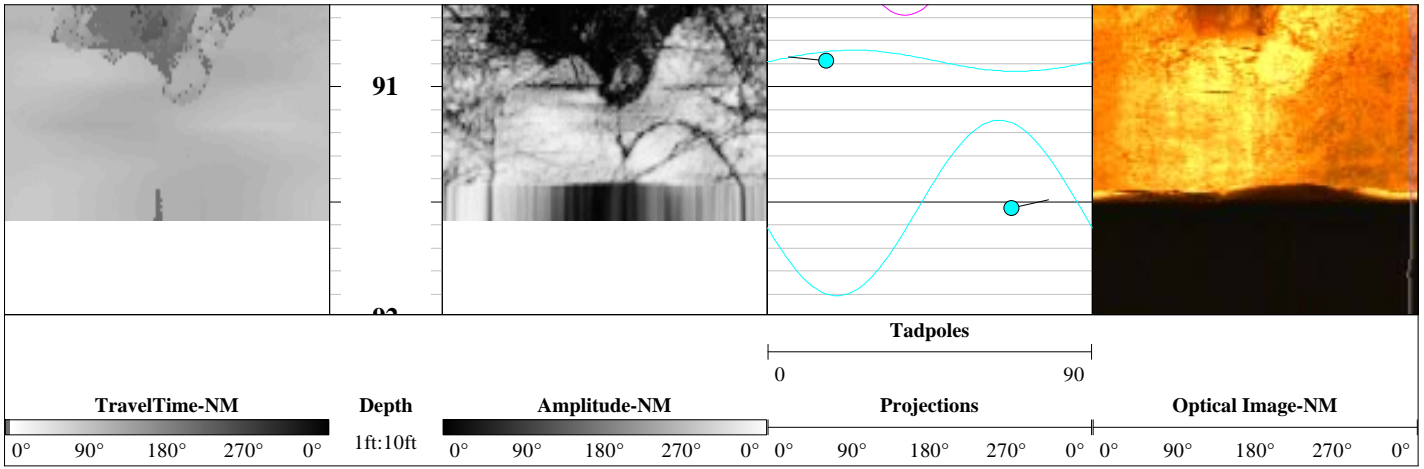












Orientation Summary Table
Televiewer Features
CB and I
Edwards Air Force Base
Well: 37-B07
December 18, 2013

Feature No.	Depth (meters)	Depth (feet)	Dip Direction (degrees)	Dip Angle (degrees)	Feature Rank (0 to 5)
1	2.72	8.9	58	56	1
2	2.84	9.3	186	81	2
3	2.97	9.7	191	81	2
4	3.50	11.5	96	39	2
5	3.69	12.1	217	87	1
6	3.95	13.0	233	31	2
7	4.02	13.2	178	26	1
8	4.29	14.1	225	71	1
9	4.48	14.7	232	76	1
10	4.66	15.3	241	75	1
11	4.71	15.5	248	73	2
12	4.74	15.6	37	87	1
13	5.04	16.5	199	79	1
14	5.12	16.8	14	37	1
15	5.33	17.5	257	73	1
16	5.44	17.8	188	44	2
17	5.45	17.9	195	66	1
18	5.45	17.9	46	77	1
19	5.73	18.8	312	73	1
20	6.04	19.8	75	53	2
21	6.34	20.8	282	53	1
22	6.66	21.9	318	55	2
23	6.91	22.7	312	66	1
24	6.99	22.9	37	87	1
25	7.09	23.3	175	79	1
26	7.30	24.0	319	24	1
27	7.60	24.9	55	34	1
28	8.00	26.3	215	73	1
29	8.11	26.6	40	78	1
30	8.24	27.1	230	44	1
31	8.40	27.6	37	46	1
32	8.58	28.1	67	54	1
33	8.79	28.9	55	68	2
34	9.00	29.5	322	53	1
35	9.19	30.2	330	29	1
36	9.28	30.4	305	23	1
37	9.46	31.0	326	58	1
38	9.53	31.3	301	45	2
39	9.60	31.5	297	51	2
40	10.09	33.1	88	48	2
41	10.19	33.4	208	76	1
42	10.47	34.3	105	64	1
43	10.68	35.1	292	44	1
44	10.99	36.1	82	54	1
45	11.08	36.4	28	73	1

All directions are with respect to magnetic north.

Orientation Summary Table
Televiewer Features
CB and I
Edwards Air Force Base
Well: 37-B07
December 18, 2013

Feature No.	Depth (meters)	Depth (feet)	Dip Direction (degrees)	Dip Angle (degrees)	Feature Rank (0 to 5)
46	11.29	37.1	92	53	1
47	11.40	37.4	65	52	1
48	11.53	37.8	43	62	1
49	11.69	38.4	17	73	1
50	12.00	39.4	88	52	3
51	12.06	39.6	83	50	3
52	12.42	40.8	55	81	1
53	12.44	40.8	65	52	2
54	12.50	41.0	66	52	2
55	12.55	41.2	356	59	1
56	12.58	41.3	63	54	1
57	12.85	42.2	35	50	2
58	13.06	42.8	79	64	1
59	13.32	43.7	19	63	2
60	13.39	43.9	211	54	1
61	13.55	44.4	343	54	1
62	13.79	45.2	343	54	1
63	13.87	45.5	323	47	1
64	14.10	46.3	154	58	1
65	14.23	46.7	171	38	1
66	14.46	47.5	293	67	1
67	14.63	48.0	41	80	1
68	14.86	48.7	121	56	1
69	14.97	49.1	206	49	1
70	15.02	49.3	36	82	2
71	15.55	51.0	322	59	1
72	15.60	51.2	112	49	1
73	15.87	52.1	290	56	1
74	16.05	52.7	281	39	1
75	16.09	52.8	174	37	1
76	16.24	53.3	260	52	1
77	16.29	53.5	91	58	1
78	16.34	53.6	118	51	1
79	16.45	54.0	179	49	1
80	16.50	54.1	148	82	1
81	16.60	54.5	192	44	1
82	16.82	55.2	86	47	0
83	17.04	55.9	102	75	1
84	17.21	56.5	251	71	1
85	17.50	57.4	79	77	1
86	17.59	57.7	263	86	1
87	17.68	58.0	82	71	1
88	17.84	58.5	131	46	2
89	17.85	58.6	264	87	1
90	17.90	58.7	115	63	2

All directions are with respect to magnetic north.

Orientation Summary Table
Televiewer Features
CB and I
Edwards Air Force Base
Well: 37-B07
December 18, 2013

Feature No.	Depth (meters)	Depth (feet)	Dip Direction (degrees)	Dip Angle (degrees)	Feature Rank (0 to 5)
91	17.97	59.0	111	57	3
92	18.05	59.2	90	57	2
93	18.22	59.8	71	70	1
94	18.26	59.9	358	62	1
95	18.28	60.0	163	76	1
96	18.29	60.0	70	67	1
97	18.44	60.5	153	70	1
98	18.48	60.6	32	59	1
99	18.76	61.6	243	85	3
100	18.83	61.8	21	78	1
101	18.89	62.0	36	68	1
102	19.05	62.5	250	74	1
103	19.18	62.9	229	77	3
104	19.20	63.0	51	75	1
105	19.41	63.7	210	88	2
106	19.49	63.9	22	39	1
107	19.64	64.5	78	50	1
108	19.75	64.8	71	55	1
109	19.90	65.3	101	60	1
110	20.02	65.7	92	52	1
111	20.16	66.1	83	56	1
112	20.37	66.8	80	63	1
113	20.62	67.7	76	62	1
114	20.69	67.9	63	78	1
115	20.69	67.9	74	60	1
116	20.91	68.6	69	56	1
117	21.08	69.2	43	59	1
118	21.14	69.4	350	32	2
119	21.18	69.5	115	65	1
120	21.21	69.6	212	46	1
121	21.29	69.9	304	52	1
122	21.36	70.1	94	76	1
123	21.40	70.2	18	57	1
124	21.56	70.7	97	61	1
125	21.66	71.1	229	21	2
126	21.67	71.1	32	59	2
127	21.68	71.1	89	70	1
128	21.69	71.2	211	15	2
129	21.77	71.4	14	60	1
130	21.88	71.8	31	47	1
131	21.97	72.1	18	43	1
132	22.09	72.5	45	57	1
133	22.14	72.6	69	63	1
134	22.28	73.1	86	62	1
135	22.29	73.1	327	47	1

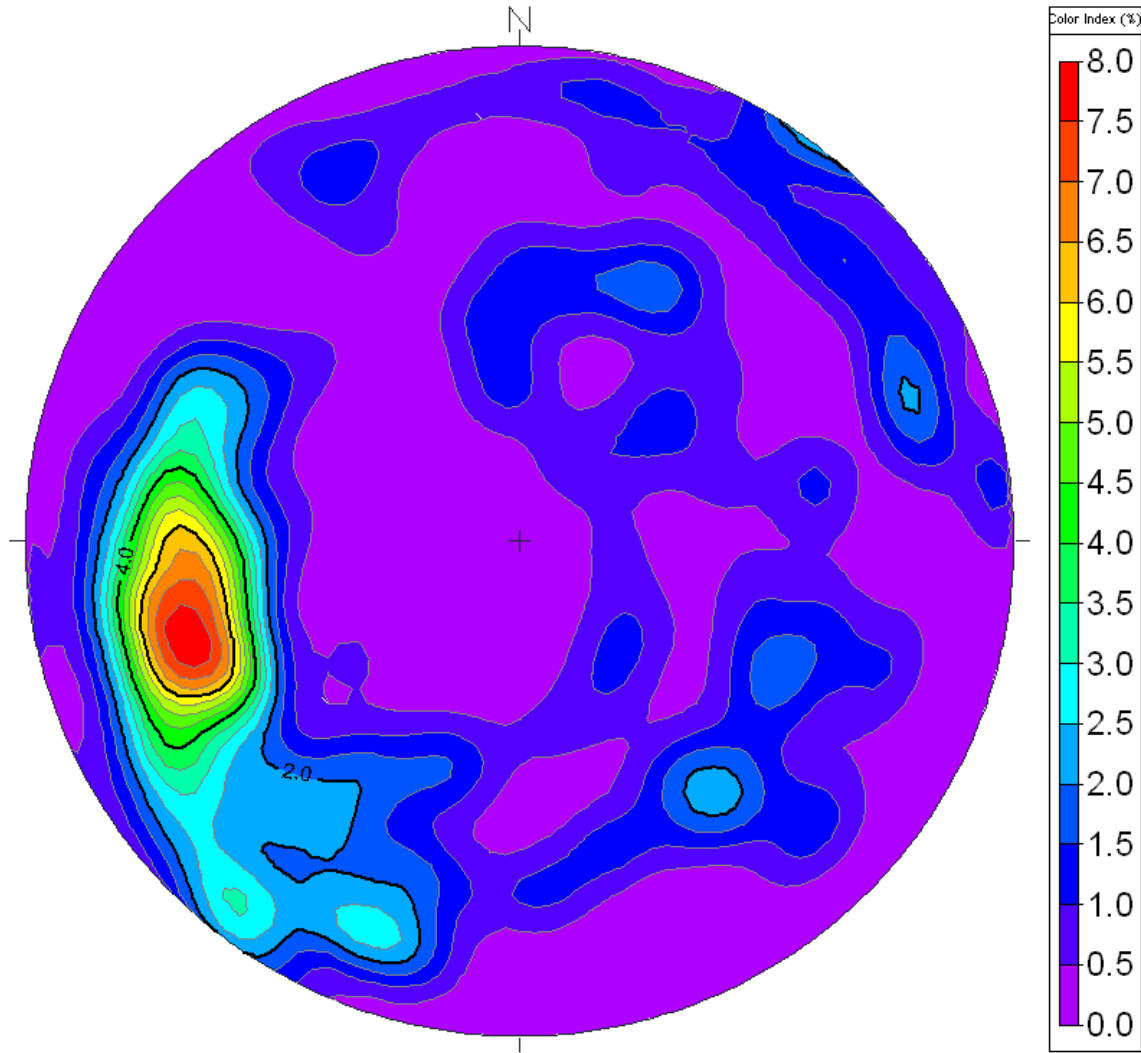
All directions are with respect to magnetic north.

Orientation Summary Table
Televiewer Features
CB and I
Edwards Air Force Base
Well: 37-B07
December 18, 2013

Feature No.	Depth (meters)	Depth (feet)	Dip Direction (degrees)	Dip Angle (degrees)	Feature Rank (0 to 5)
136	22.44	73.6	78	51	2
137	22.50	73.8	318	74	1
138	22.51	73.9	15	78	1
139	22.67	74.4	81	58	2
140	22.75	74.6	94	62	2
141	22.89	75.1	82	69	1
142	23.14	75.9	71	63	1
143	23.19	76.1	72	55	1
144	23.25	76.3	68	64	1
145	23.39	76.8	64	69	1
146	23.49	77.1	59	72	1
147	23.55	77.3	57	71	1
148	23.72	77.8	79	66	1
149	23.84	78.2	259	50	1
150	24.05	78.9	253	35	1
151	24.22	79.5	99	56	1
152	24.50	80.4	59	72	1
153	24.56	80.6	79	63	1
154	24.81	81.4	94	63	1
155	24.89	81.7	50	84	1
156	24.94	81.8	67	61	1
157	24.98	82.0	16	71	1
158	25.09	82.3	26	70	1
159	25.22	82.8	68	72	1
160	25.62	84.1	173	25	2
161	25.97	85.2	286	68	1
162	26.02	85.4	66	62	2
163	26.15	85.8	226	32	2
164	26.49	86.9	59	62	1
165	26.65	87.4	47	67	1
166	26.72	87.7	35	80	1
167	26.77	87.8	23	74	1
168	27.04	88.7	204	47	1
169	27.21	89.3	90	63	1
170	27.26	89.4	104	54	3
171	27.33	89.7	97	64	4
172	27.40	89.9	113	62	4
173	27.50	90.2	153	72	4
174	27.70	90.9	276	16	1
175	27.90	91.5	77	68	1

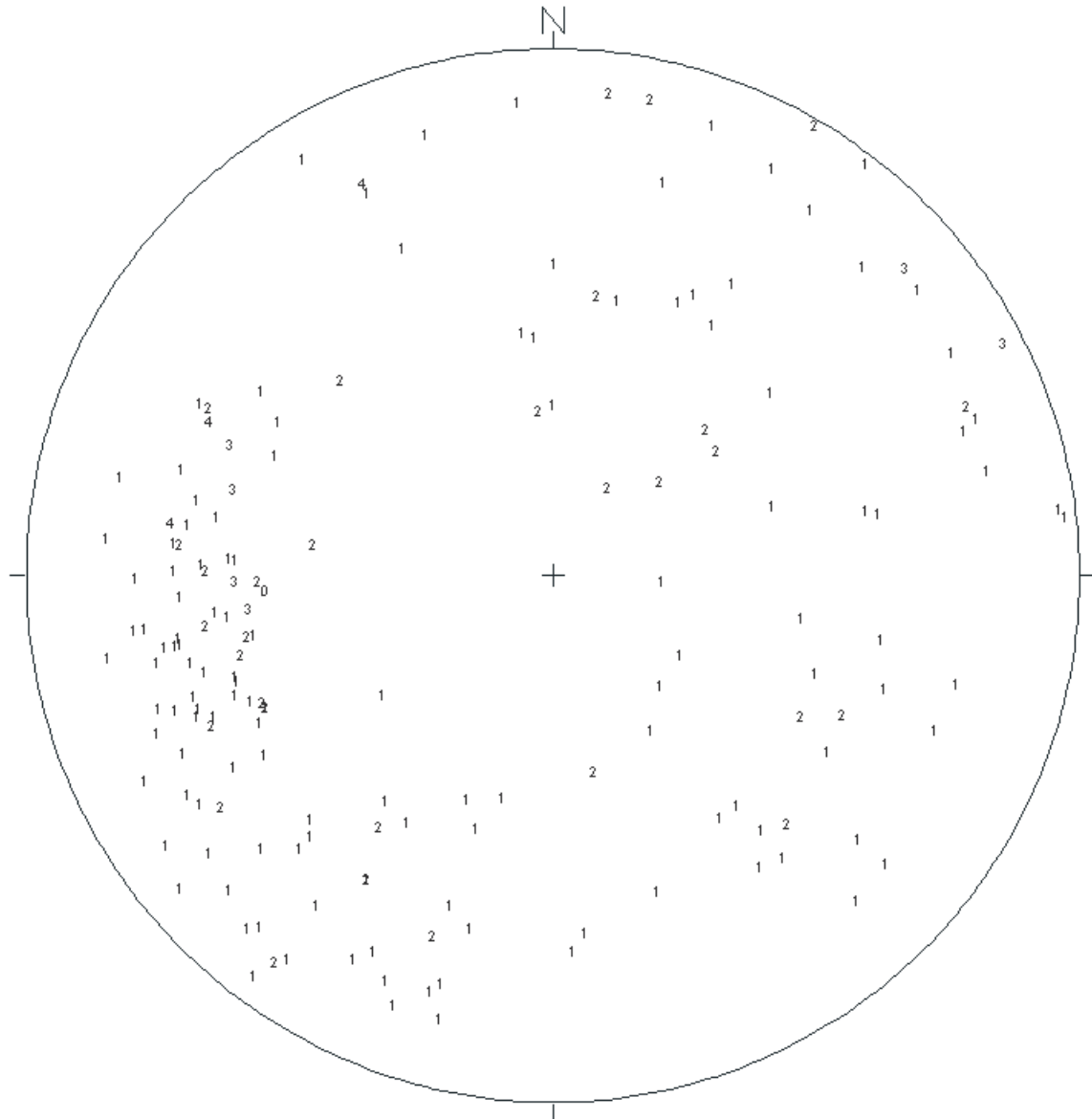
All directions are with respect to magnetic north.

**Stereonet Diagram – Schmidt Projection
Image Features
CB & I
Project: Edwards Air Force Base
Well: 37-B07
December 18, 2013**



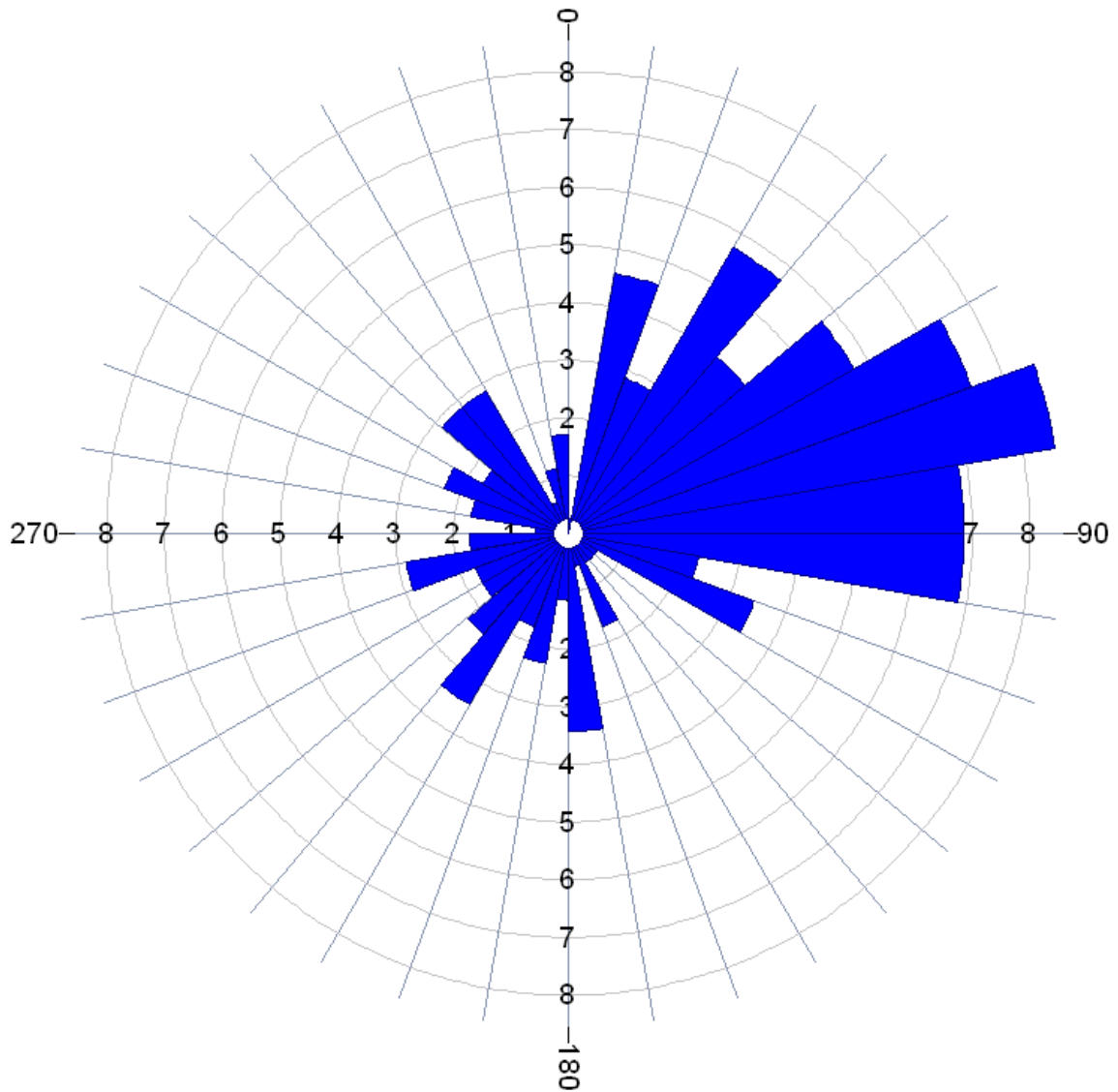
All directions are with respect to Magnetic North.

**Stereonet Diagram – Schmidt Projection
Image Features
CB & I
Project: Edwards Air Force Base
Well: 37-B07
December 18, 2013**



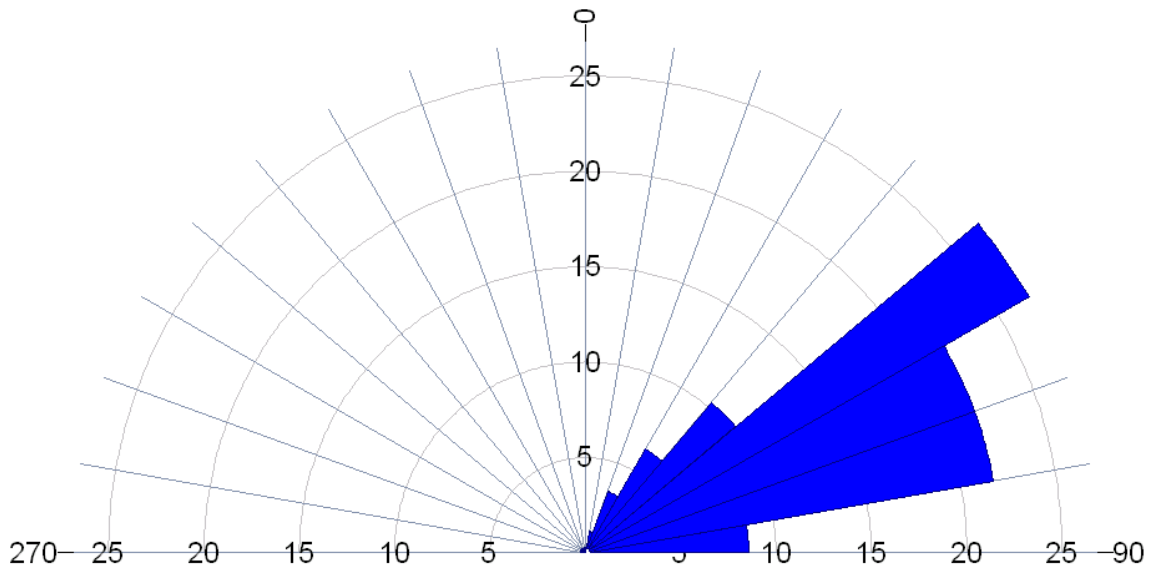
All directions are with respect to Magnetic North.

**Rose Diagram – Dip Directions
Image Features
CB & I
Project: Edwards Air Force Base
Well: 37-B07
December 18, 2013**



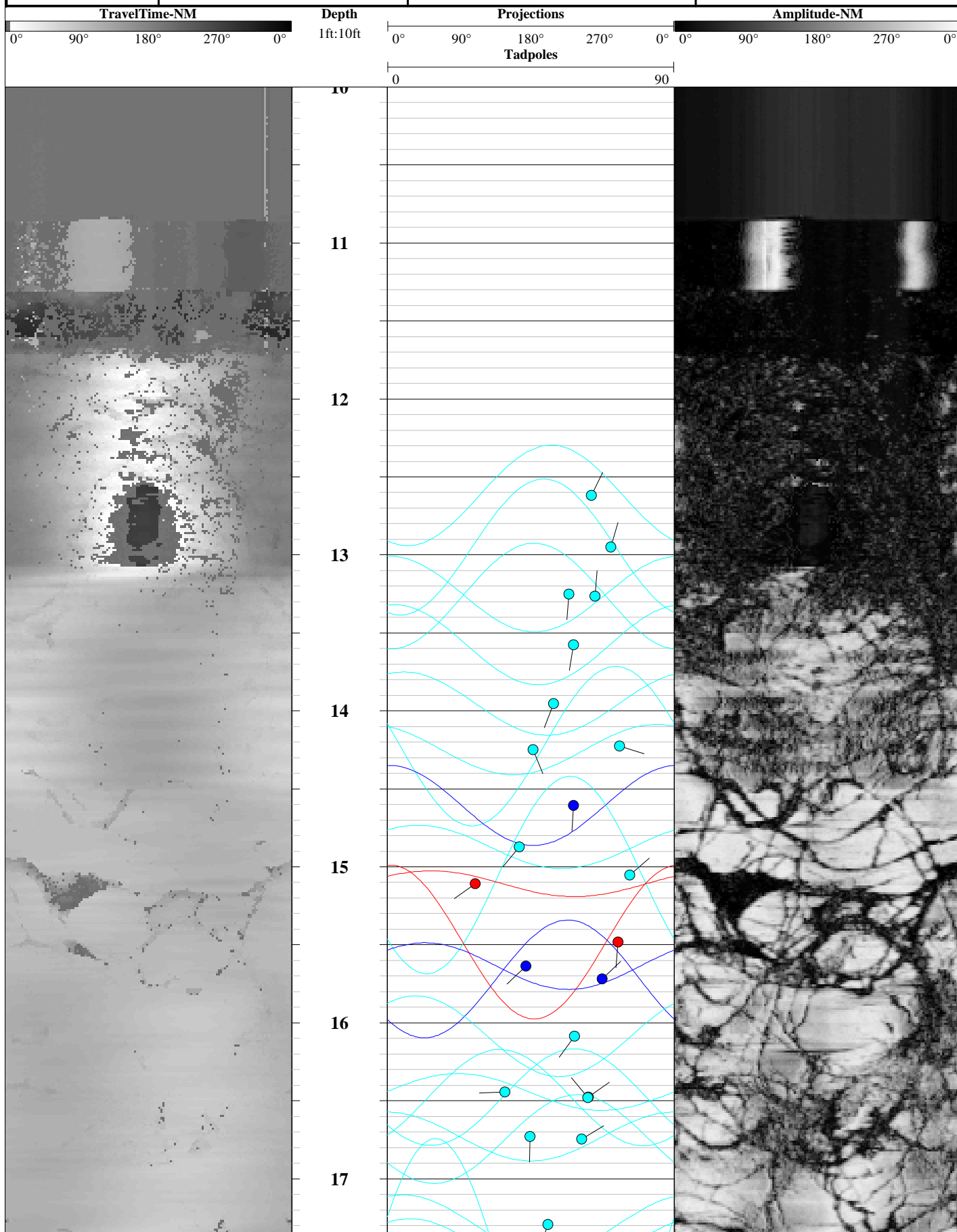
All directions are with respect to Magnetic North.

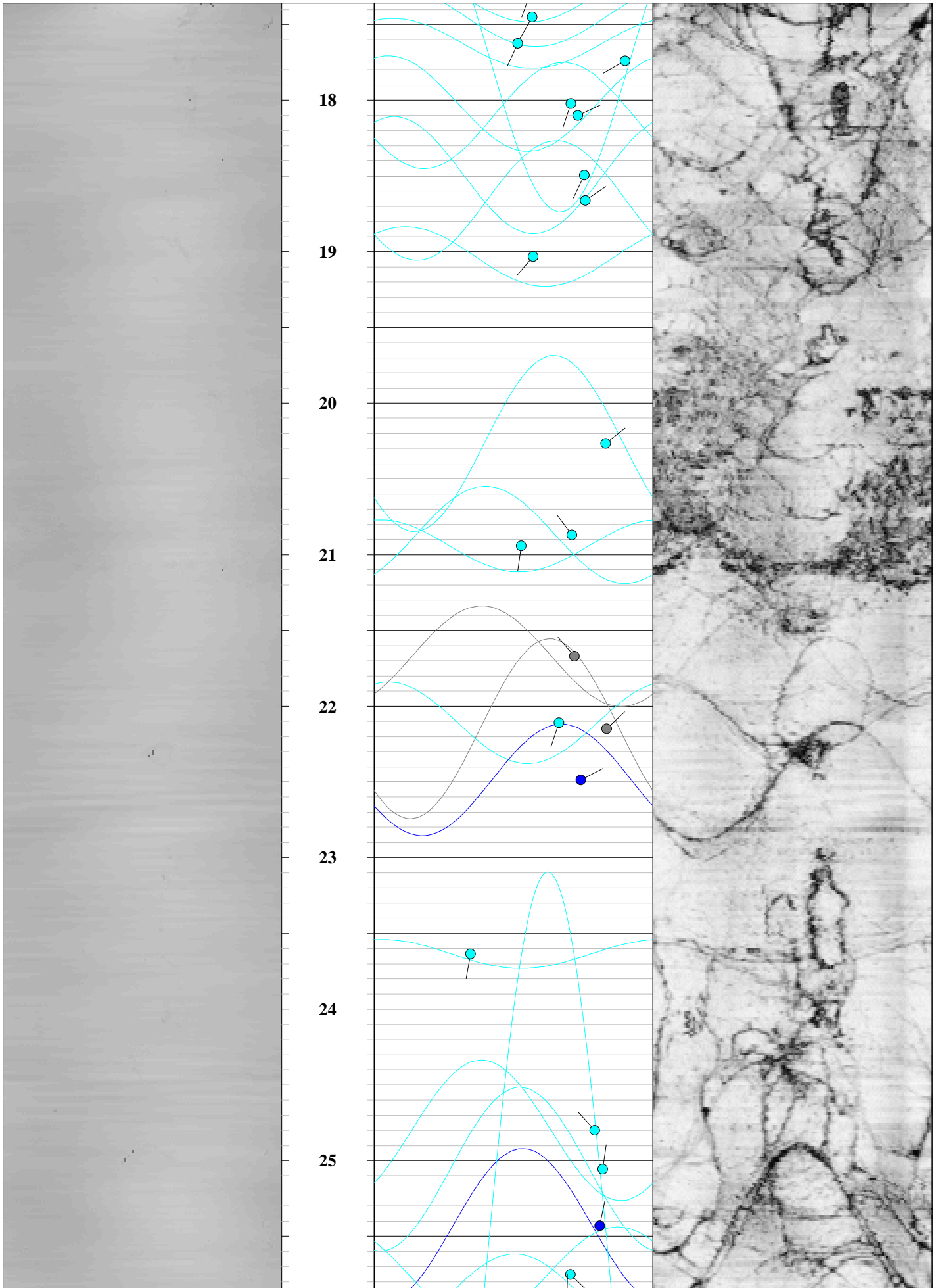
Rose Diagram – Dip Angles
Image Features
CB & I
Project: Edwards Air Force Base
Well: 37-B07
December 18, 2013

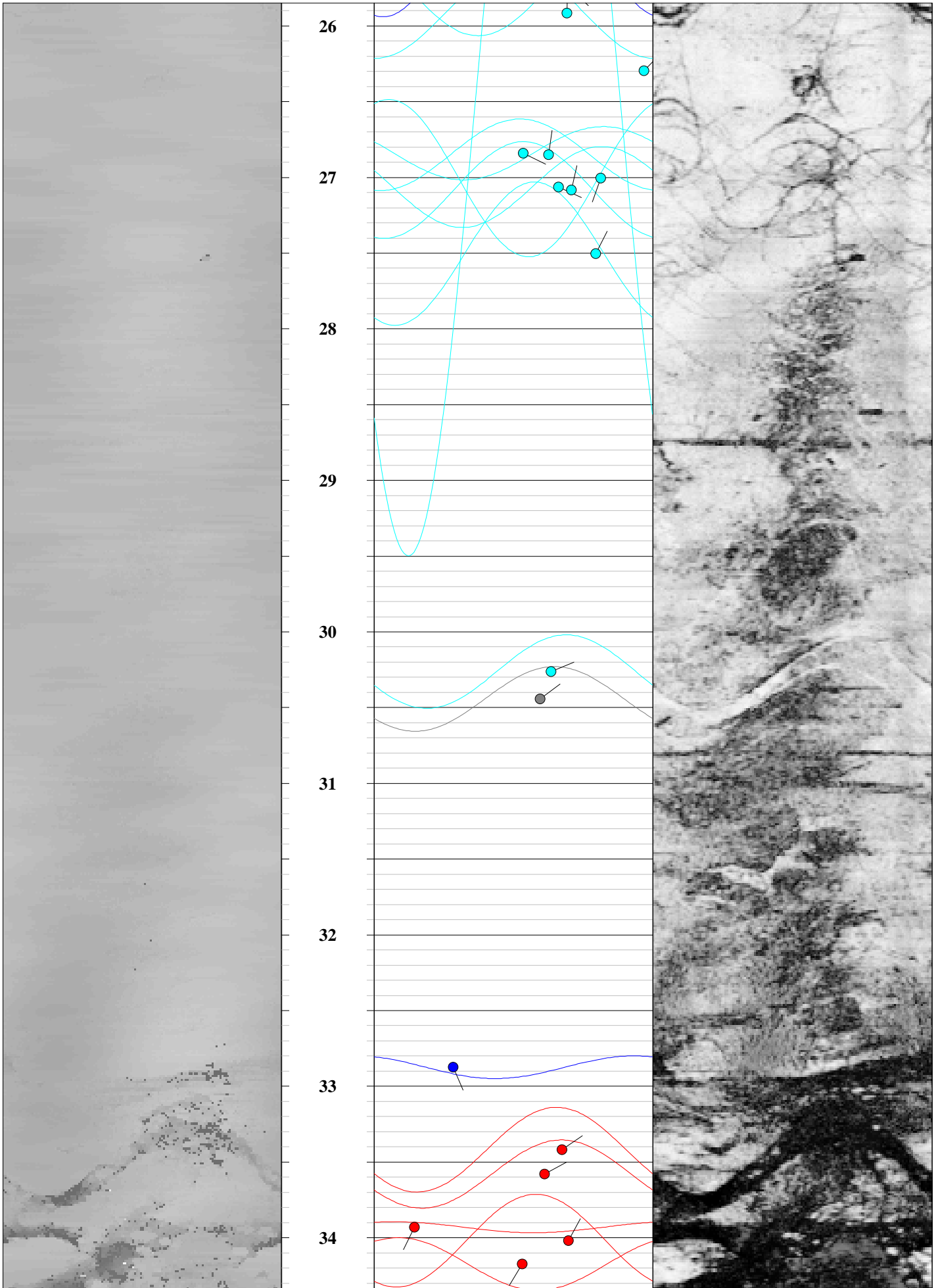


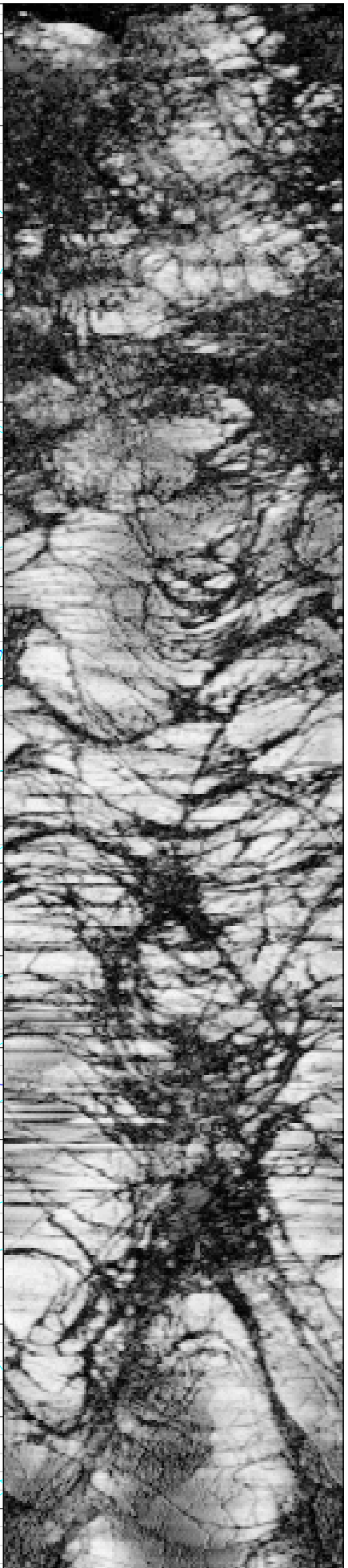
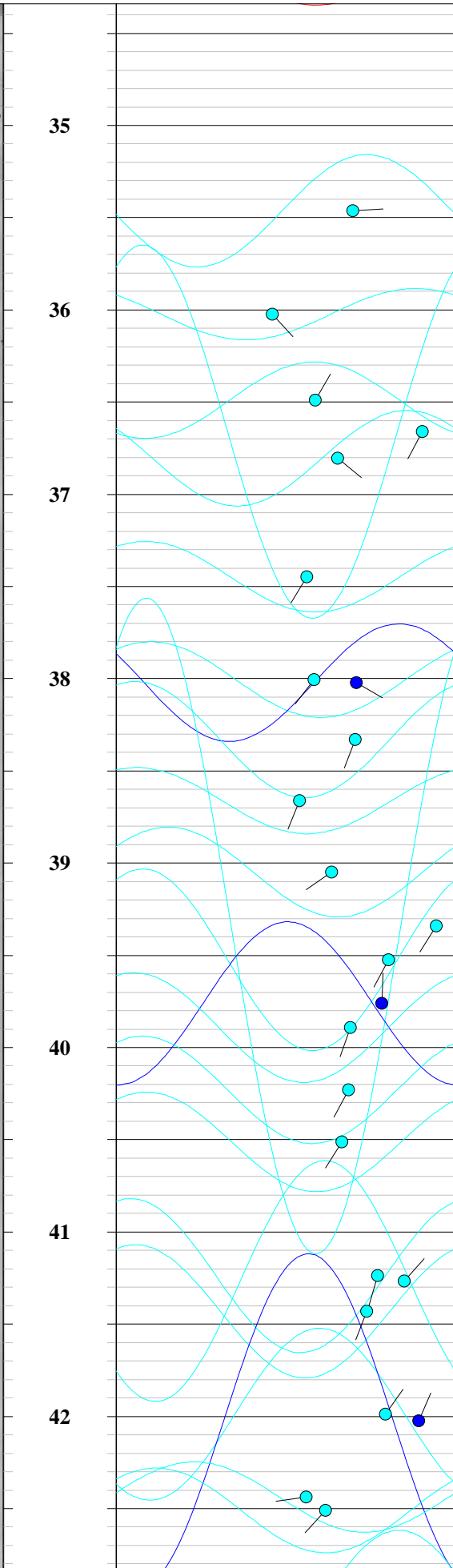
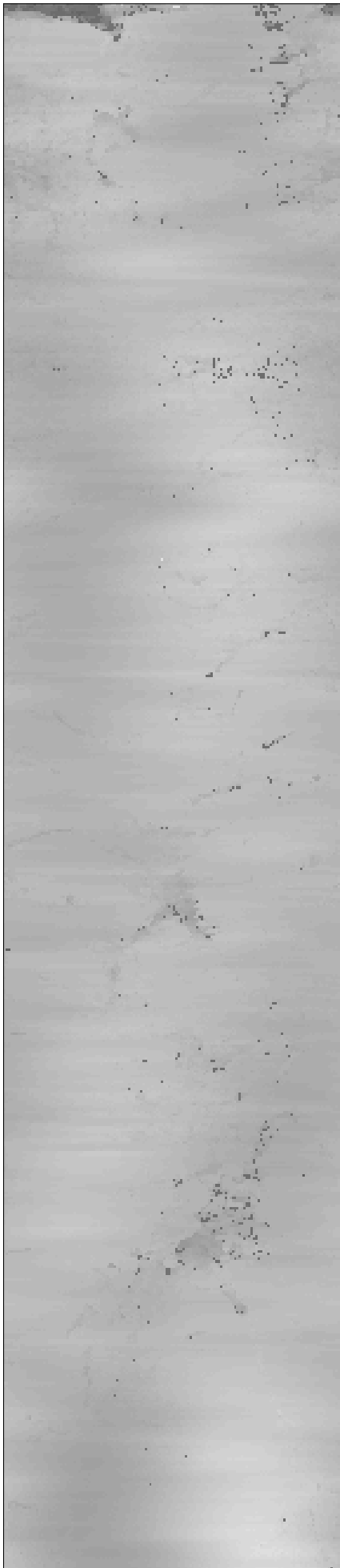
All directions are with respect to Magnetic North.

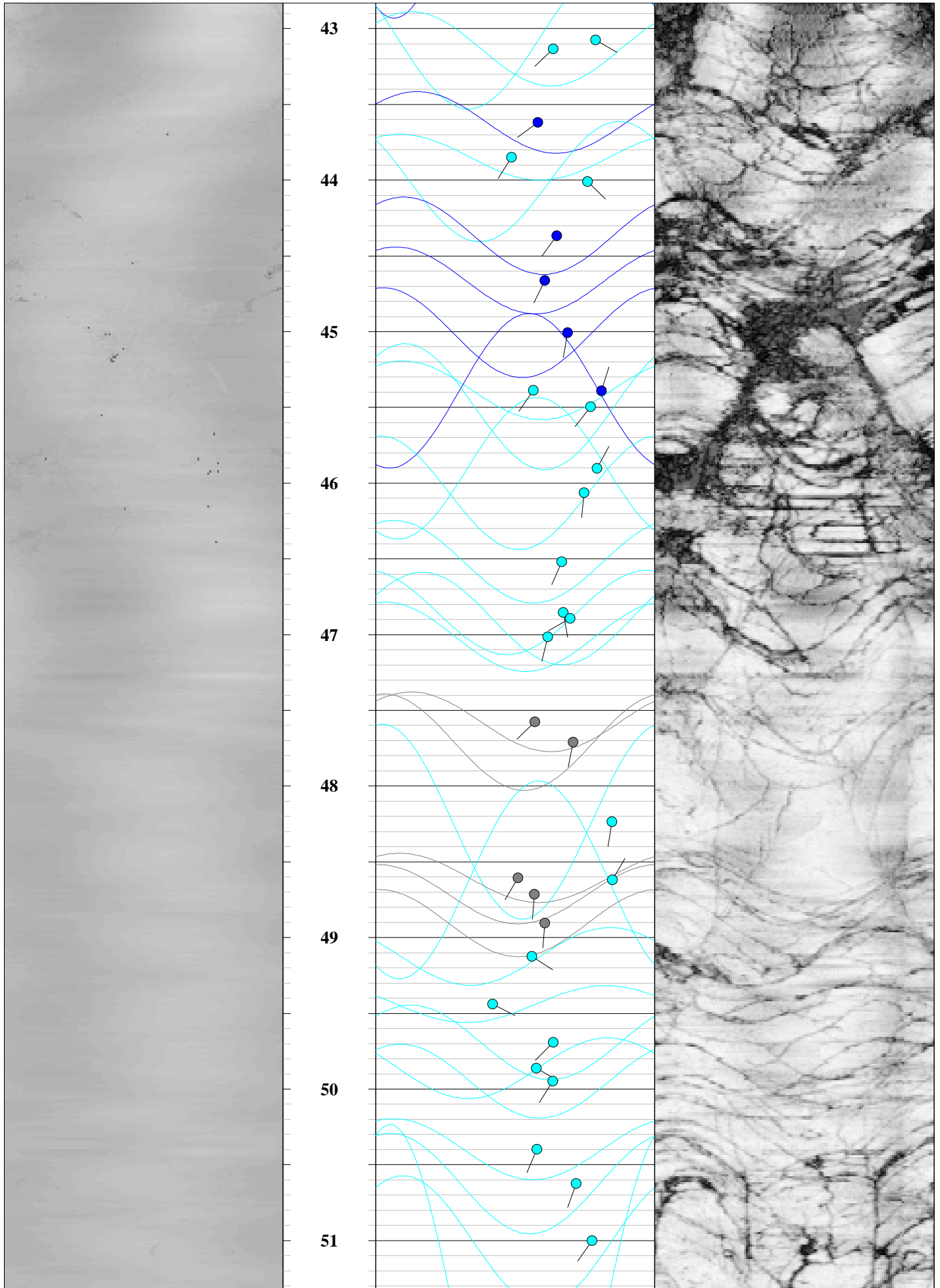
Appendix B

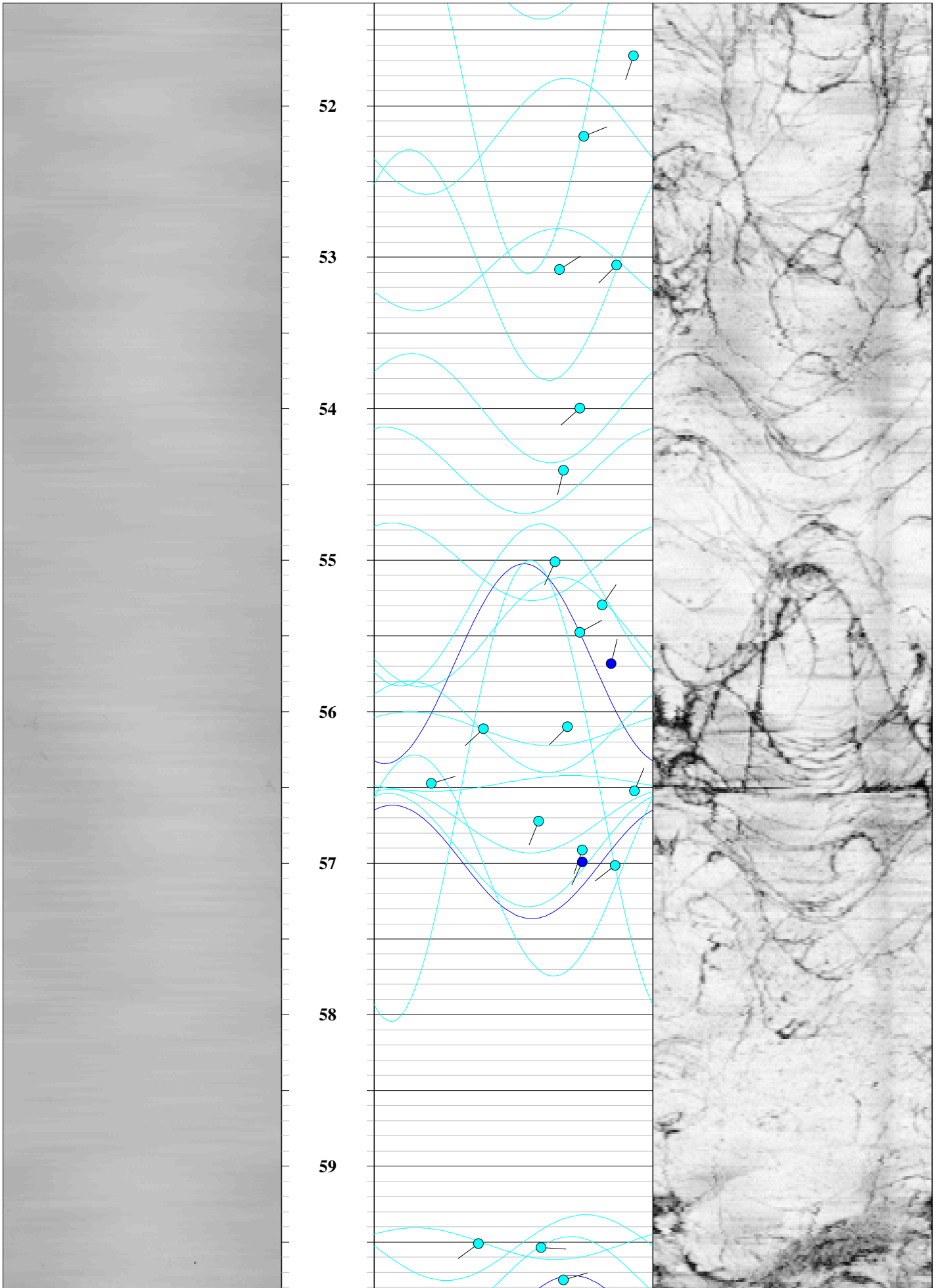


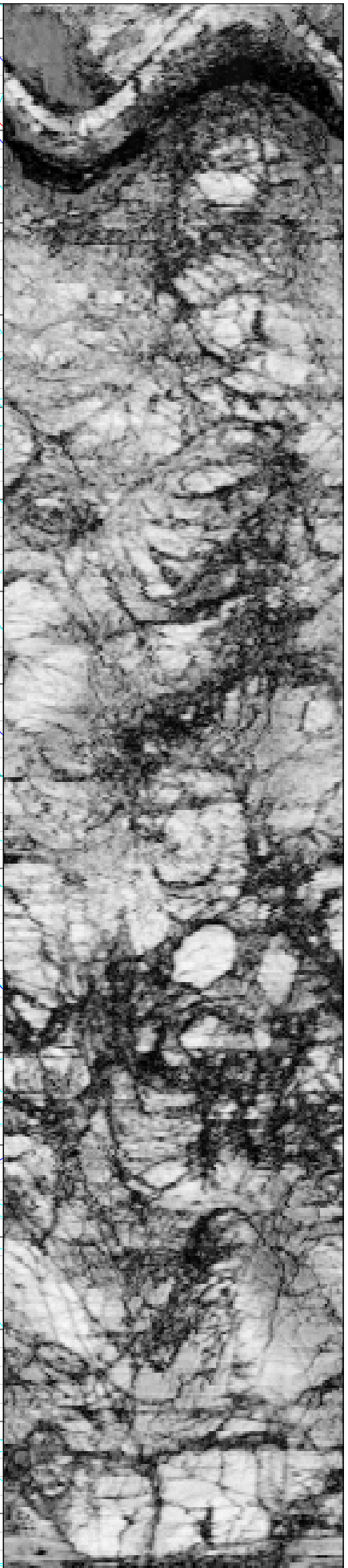
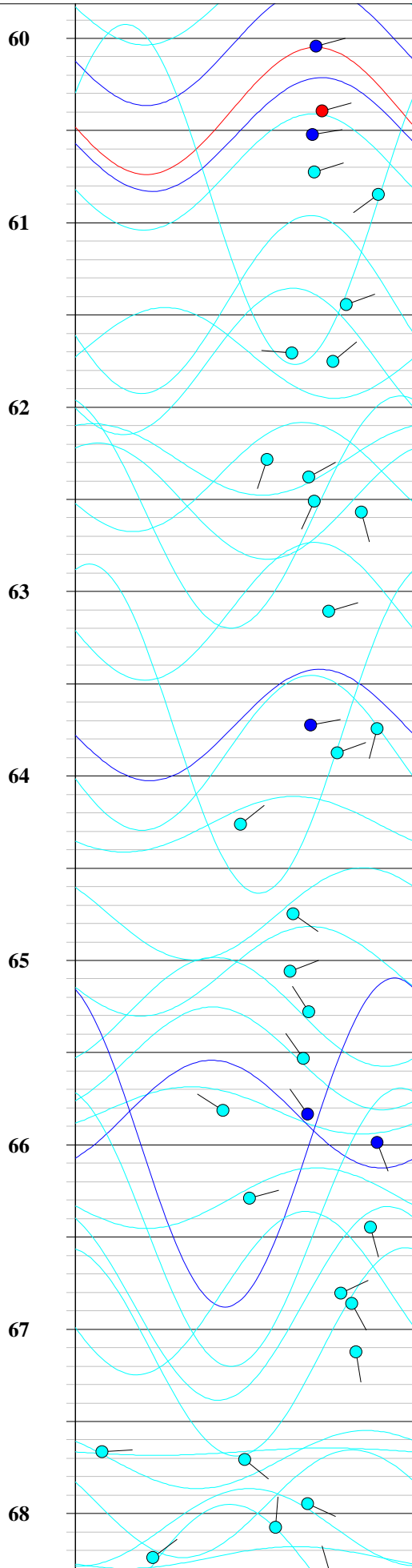


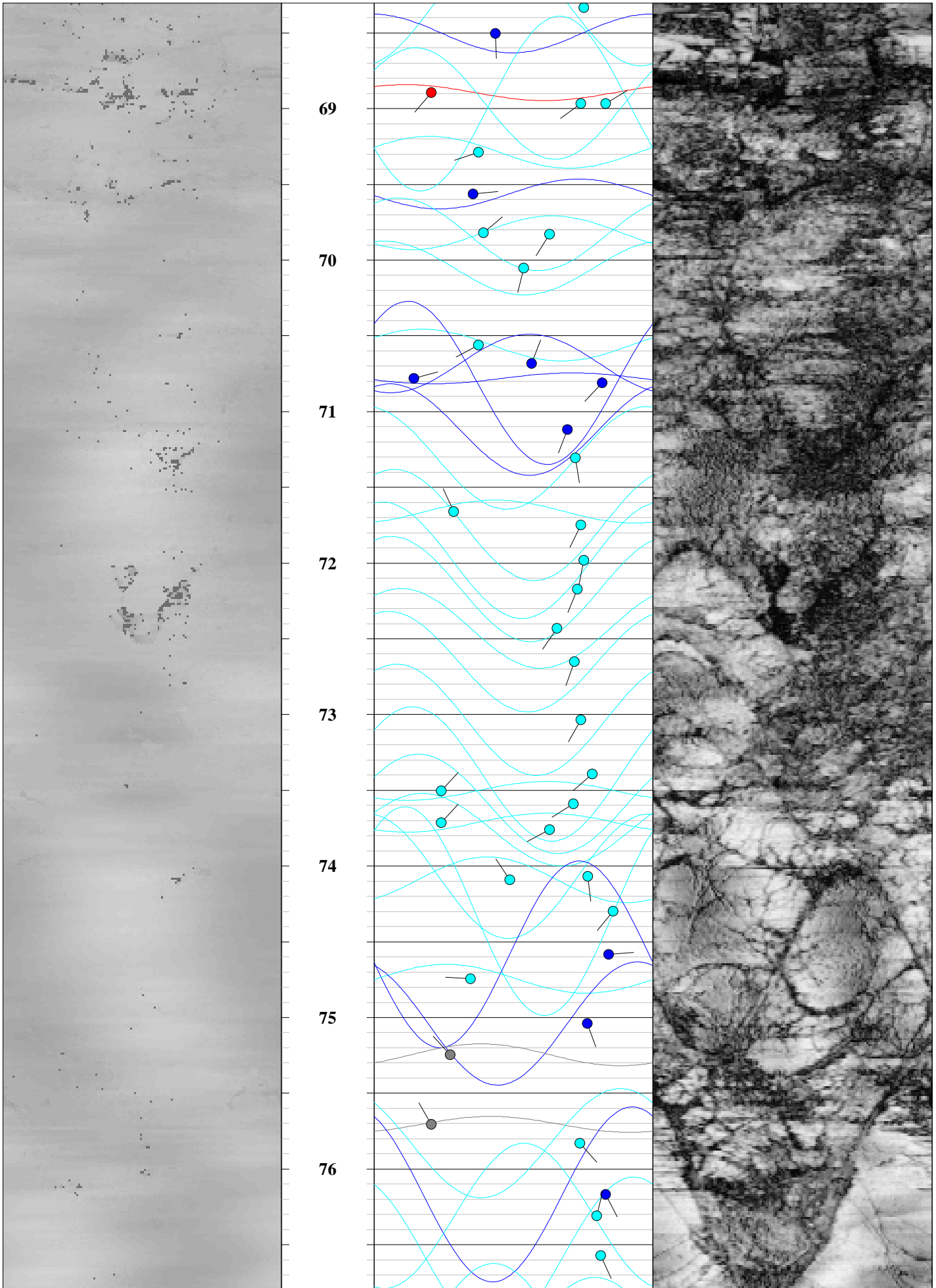


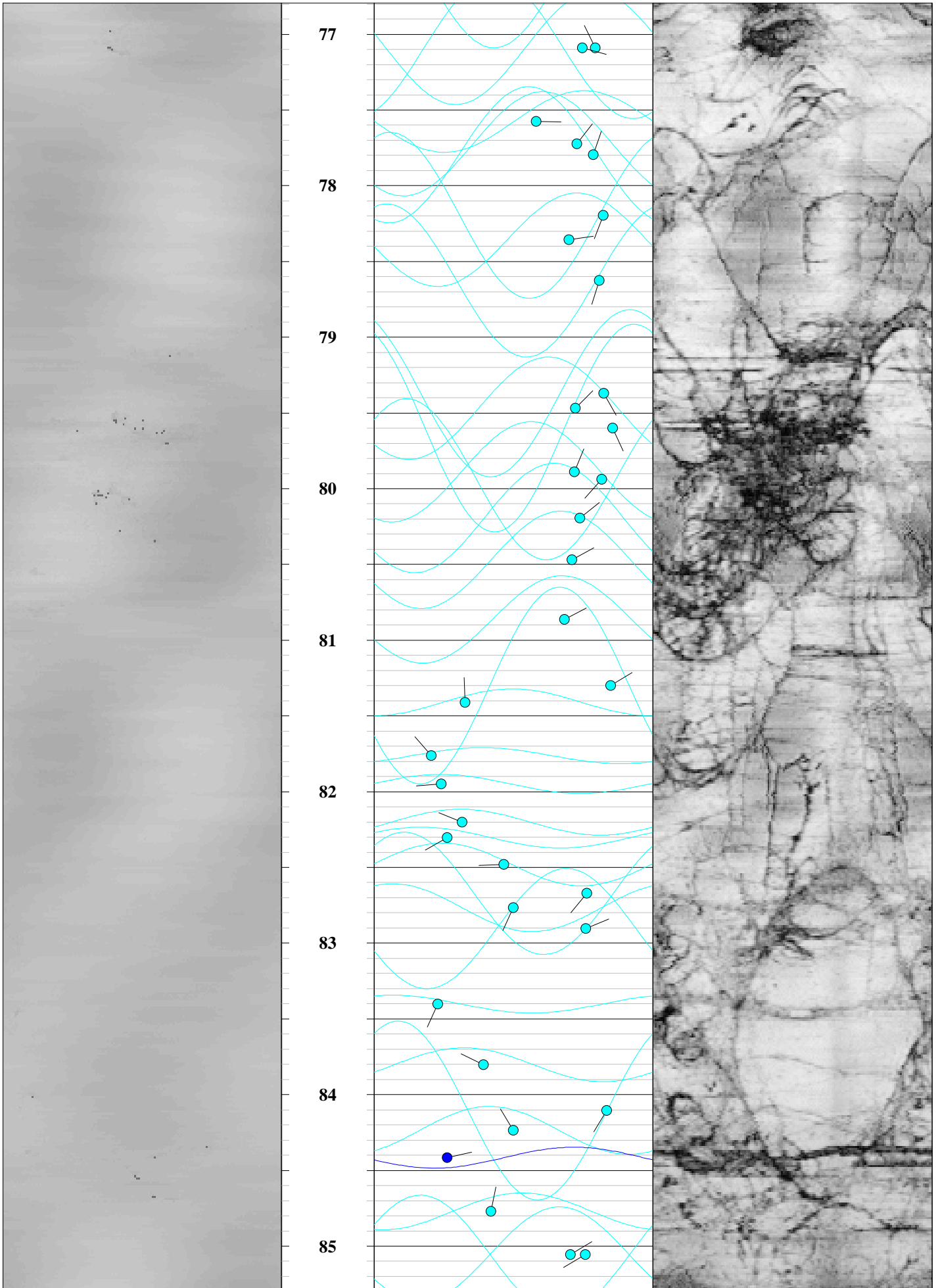


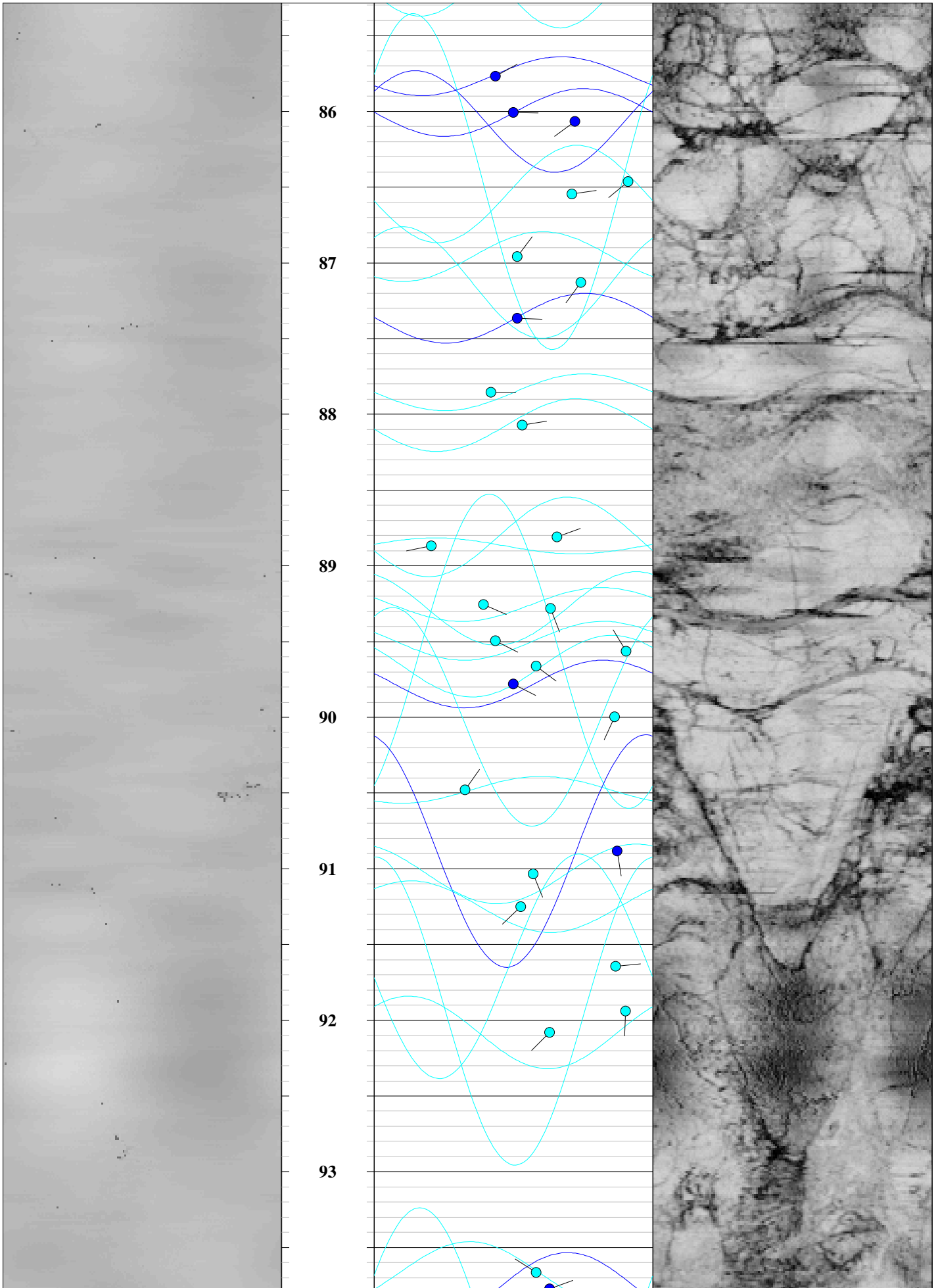


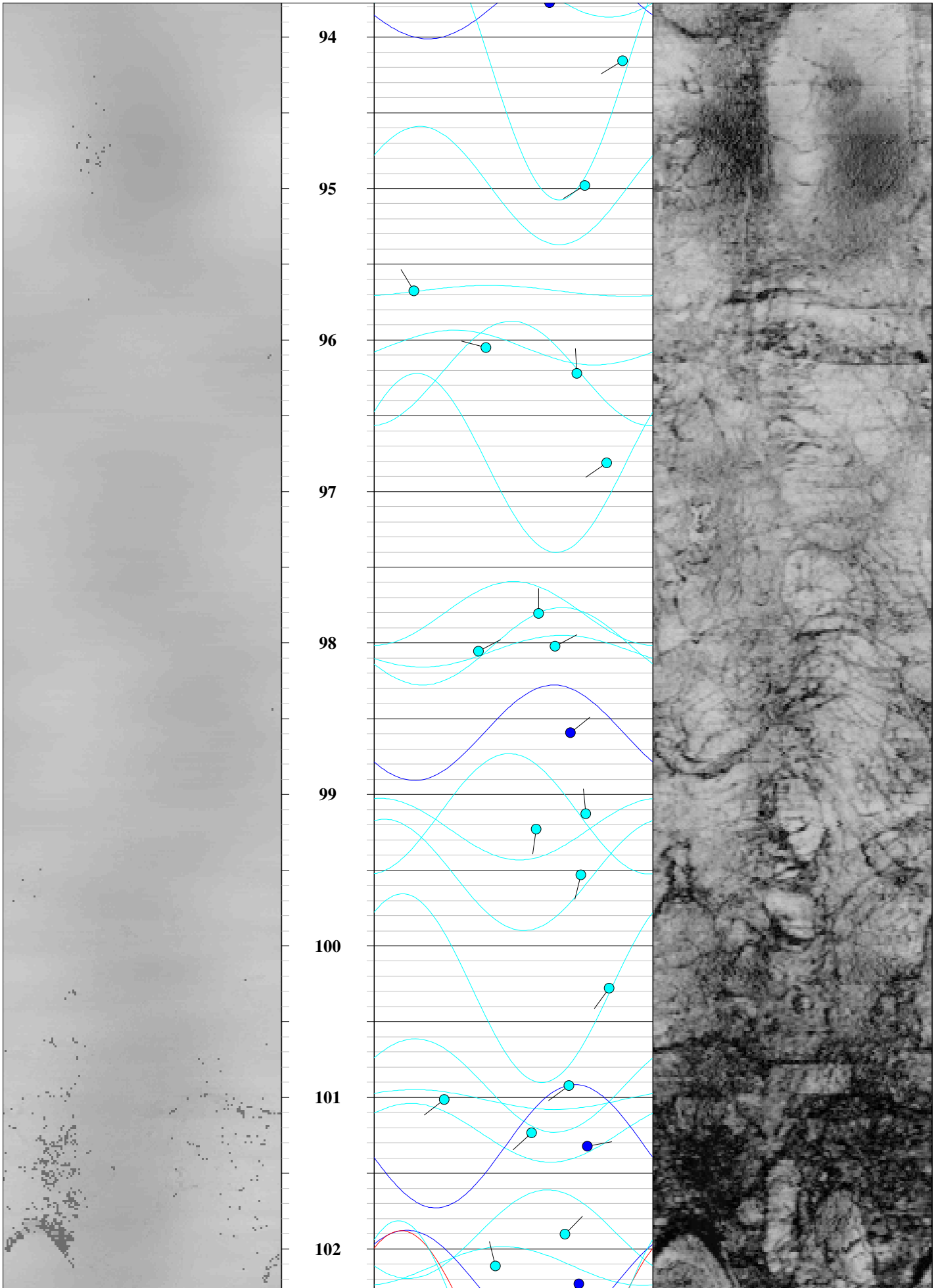


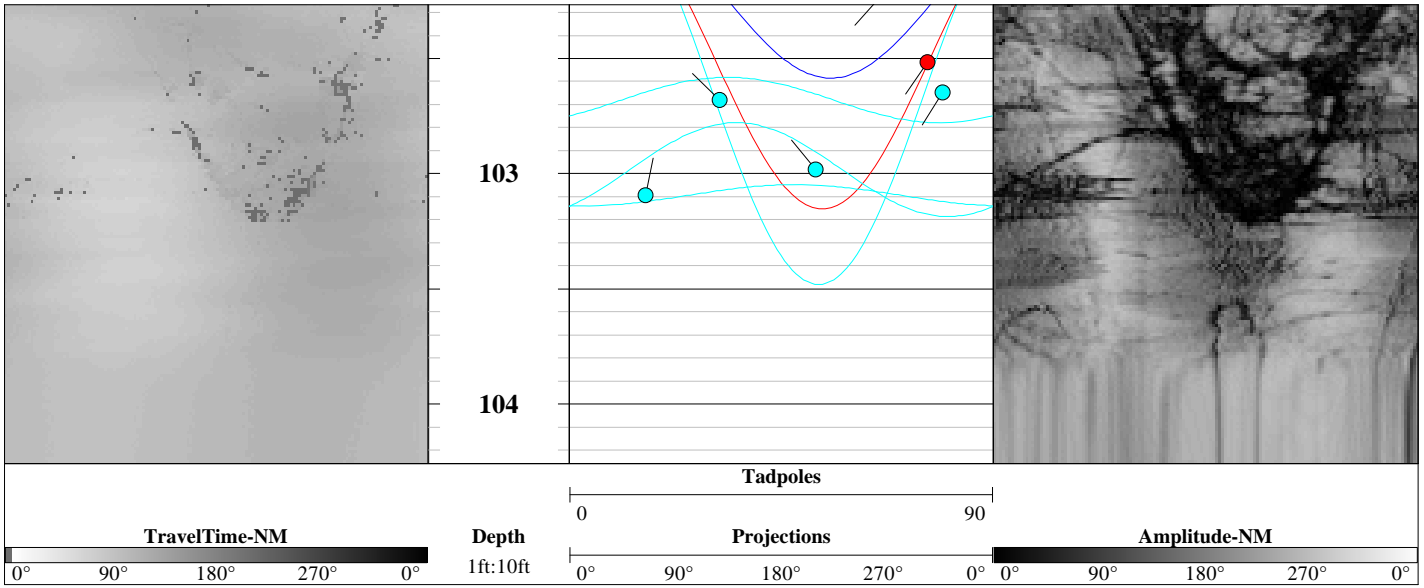












Orientation Summary Table
Televiewer Features
CB and I
Edwards Air Force Base
Well: 37-B10
December 18, 2013

Feature No.	Depth (meters)	Depth (feet)	Dip Direction (degrees)	Dip Angle (degrees)	Feature Rank (0 to 5)
1	3.85	12.6	26	64	1
2	3.95	13.0	16	70	1
3	4.04	13.3	184	57	1
4	4.04	13.3	4	65	1
5	4.14	13.6	189	58	1
6	4.25	14.0	201	52	1
7	4.34	14.2	106	73	1
8	4.34	14.3	158	46	1
9	4.45	14.6	183	58	2
10	4.53	14.9	219	41	1
11	4.59	15.1	49	76	1
12	4.61	15.1	235	28	3
13	4.72	15.5	184	72	3
14	4.77	15.6	227	43	2
15	4.79	15.7	47	67	2
16	4.90	16.1	216	59	1
17	5.01	16.4	269	37	1
18	5.02	16.5	55	63	1
19	5.02	16.5	321	63	1
20	5.10	16.7	180	45	1
21	5.10	16.7	58	61	1
22	5.27	17.3	199	50	1
23	5.32	17.5	209	51	1
24	5.37	17.6	204	46	1
25	5.41	17.7	240	81	1
26	5.49	18.0	198	63	1
27	5.52	18.1	65	66	1
28	5.64	18.5	206	68	1
29	5.69	18.7	55	68	1
30	5.80	19.0	221	51	1
31	6.18	20.3	52	75	1
32	6.36	20.9	324	64	1
33	6.38	20.9	187	48	1
34	6.61	21.7	319	65	0
35	6.74	22.1	198	60	1
36	6.75	22.2	47	75	0
37	6.85	22.5	62	67	2
38	7.20	23.6	190	31	1
39	7.56	24.8	318	71	1
40	7.64	25.1	8	74	1
41	7.75	25.4	12	73	2
42	7.85	25.8	134	63	1
43	7.90	25.9	2	62	1
44	8.02	26.3	44	87	1
45	8.18	26.8	116	48	1

All directions are with respect to magnetic north.

Orientation Summary Table
Televiewer Features
CB and I
Edwards Air Force Base
Well: 37-B10
December 18, 2013

Feature No.	Depth (meters)	Depth (feet)	Dip Direction (degrees)	Dip Angle (degrees)	Feature Rank (0 to 5)
46	8.18	26.9	8	56	1
47	8.23	27.0	199	73	1
48	8.25	27.1	114	60	1
49	8.25	27.1	13	64	1
50	8.38	27.5	27	72	1
51	9.22	30.3	68	57	1
52	9.28	30.4	53	54	0
53	10.02	32.9	156	25	2
54	10.19	33.4	55	61	3
55	10.24	33.6	62	55	3
56	10.34	33.9	206	13	3
57	10.37	34.0	29	63	3
58	10.42	34.2	211	48	3
59	10.81	35.5	86	63	1
60	10.98	36.0	138	41	1
61	11.12	36.5	30	53	1
62	11.17	36.7	208	81	1
63	11.22	36.8	128	59	1
64	11.41	37.5	211	51	1
65	11.59	38.0	217	53	1
66	11.59	38.0	120	64	2
67	11.68	38.3	200	63	1
68	11.78	38.7	202	49	1
69	11.90	39.1	235	57	1
70	11.99	39.3	212	85	1
71	12.05	39.5	208	72	1
72	12.12	39.8	2	70	2
73	12.16	39.9	199	62	1
74	12.26	40.2	208	62	1
75	12.35	40.5	212	60	1
76	12.57	41.2	196	69	1
77	12.58	41.3	42	76	1
78	12.63	41.4	200	66	1
79	12.80	42.0	36	71	1
80	12.81	42.0	24	80	2
81	12.94	42.4	263	50	1
82	12.96	42.5	222	56	1
83	13.13	43.1	120	71	1
84	13.15	43.1	226	57	1
85	13.30	43.6	233	52	2
86	13.37	43.9	212	44	1
87	13.41	44.0	134	68	1
88	13.52	44.4	216	58	2
89	13.61	44.7	206	55	2
90	13.72	45.0	189	62	2

All directions are with respect to magnetic north.

**Orientation Summary Table
 Televiewer Features
 CB and I
 Edwards Air Force Base
 Well: 37-B10
 December 18, 2013**

Feature No.	Depth (meters)	Depth (feet)	Dip Direction (degrees)	Dip Angle (degrees)	Feature Rank (0 to 5)
91	13.83	45.4	214	51	1
92	13.83	45.4	18	73	2
93	13.87	45.5	218	69	1
94	13.99	45.9	28	71	1
95	14.04	46.1	185	67	1
96	14.18	46.5	203	60	1
97	14.28	46.9	170	60	1
98	14.29	46.9	240	63	1
99	14.33	47.0	193	56	1
100	14.50	47.6	226	51	0
101	14.54	47.7	191	64	0
102	14.70	48.2	189	76	1
103	14.81	48.6	210	46	0
104	14.82	48.6	31	76	1
105	14.85	48.7	184	51	0
106	14.90	48.9	184	55	0
107	14.97	49.1	122	50	1
108	15.07	49.4	117	38	1
109	15.15	49.7	225	57	1
110	15.20	49.9	119	52	1
111	15.22	50.0	212	57	1
112	15.36	50.4	203	52	1
113	15.43	50.6	199	65	1
114	15.54	51.0	215	70	1
115	15.75	51.7	199	84	1
116	15.91	52.2	68	68	1
117	16.17	53.1	225	78	1
118	16.18	53.1	57	60	1
119	16.46	54.0	228	66	1
120	16.58	54.4	194	61	1
121	16.77	55.0	204	58	1
122	16.86	55.3	34	74	1
123	16.91	55.5	61	66	1
124	16.97	55.7	14	77	2
125	17.10	56.1	225	62	1
126	17.10	56.1	228	35	1
127	17.21	56.5	74	18	1
128	17.23	56.5	22	84	1
129	17.29	56.7	202	53	1
130	17.35	56.9	199	67	1
131	17.37	57.0	204	67	2
132	17.38	57.0	232	78	1
133	18.14	59.5	233	34	1
134	18.15	59.5	93	54	1
135	18.21	59.8	74	61	1

All directions are with respect to magnetic north.

Orientation Summary Table
Televiewer Features
CB and I
Edwards Air Force Base
Well: 37-B10
December 18, 2013

Feature No.	Depth (meters)	Depth (feet)	Dip Direction (degrees)	Dip Angle (degrees)	Feature Rank (0 to 5)
136	18.30	60.0	75	64	2
137	18.41	60.4	75	65	3
138	18.45	60.5	81	63	2
139	18.51	60.7	72	63	1
140	18.54	60.8	233	80	1
141	18.73	61.4	70	72	1
142	18.81	61.7	275	57	1
143	18.82	61.8	51	68	1
144	18.98	62.3	198	51	1
145	19.01	62.4	61	62	1
146	19.05	62.5	204	63	1
147	19.07	62.6	165	76	1
148	19.24	63.1	74	67	1
149	19.42	63.7	79	62	2
150	19.43	63.7	195	80	1
151	19.47	63.9	71	69	1
152	19.59	64.3	52	44	1
153	19.74	64.8	125	58	1
154	19.83	65.1	69	57	1
155	19.90	65.3	328	62	1
156	19.97	65.5	326	61	1
157	20.06	65.8	303	39	1
158	20.06	65.8	325	62	2
159	20.11	66.0	159	80	2
160	20.21	66.3	75	46	1
161	20.25	66.5	165	78	1
162	20.36	66.8	65	70	1
163	20.38	66.9	152	73	1
164	20.46	67.1	171	74	1
165	20.62	67.7	87	7	1
166	20.64	67.7	129	45	1
167	20.71	67.9	114	62	1
168	20.75	68.1	5	53	1
169	20.80	68.2	54	21	1
170	20.83	68.3	344	68	1
171	20.88	68.5	178	39	2
172	21.00	68.9	220	18	3
173	21.02	69.0	233	67	1
174	21.02	69.0	59	75	1
175	21.12	69.3	252	34	1
176	21.20	69.6	84	32	2
177	21.28	69.8	50	35	1
178	21.28	69.8	212	57	1
179	21.35	70.1	193	48	1
180	21.51	70.6	242	34	1

All directions are with respect to magnetic north.

Orientation Summary Table
Televiewer Features
CB and I
Edwards Air Force Base
Well: 37-B10
December 18, 2013

Feature No.	Depth (meters)	Depth (feet)	Dip Direction (degrees)	Dip Angle (degrees)	Feature Rank (0 to 5)
181	21.54	70.7	21	51	2
182	21.57	70.8	75	13	2
183	21.58	70.8	223	74	2
184	21.68	71.1	200	62	2
185	21.73	71.3	171	65	1
186	21.84	71.7	336	26	1
187	21.87	71.8	206	67	1
188	21.94	72.0	191	68	1
189	22.00	72.2	202	66	1
190	22.08	72.4	215	59	1
191	22.14	72.7	199	65	1
192	22.26	73.0	209	67	1
193	22.37	73.4	229	70	1
194	22.40	73.5	42	22	1
195	22.43	73.6	237	64	1
196	22.47	73.7	42	22	1
197	22.48	73.8	242	57	1
198	22.58	74.1	173	69	1
199	22.58	74.1	326	44	1
200	22.65	74.3	220	77	1
201	22.73	74.6	85	76	2
202	22.78	74.7	273	31	1
203	22.87	75.0	160	69	2
204	22.93	75.2	318	25	0
205	23.07	75.7	330	18	0
206	23.11	75.8	138	66	1
207	23.22	76.2	153	75	2
208	23.26	76.3	14	72	1
209	23.34	76.6	155	73	1
210	23.50	77.1	334	71	1
211	23.50	77.1	105	67	1
212	23.64	77.6	91	52	1
213	23.69	77.7	38	65	1
214	23.71	77.8	19	71	1
215	23.83	78.2	200	74	1
216	23.88	78.4	82	63	1
217	23.96	78.6	196	73	1
218	24.19	79.4	150	74	1
219	24.22	79.5	45	65	1
220	24.26	79.6	156	77	1
221	24.35	79.9	22	65	1
222	24.37	79.9	222	73	1
223	24.44	80.2	52	66	1
224	24.53	80.5	61	64	1
225	24.65	80.9	63	61	1

All directions are with respect to magnetic north.

Orientation Summary Table
Televiewer Features
CB and I
Edwards Air Force Base
Well: 37-B10
December 18, 2013

Feature No.	Depth (meters)	Depth (feet)	Dip Direction (degrees)	Dip Angle (degrees)	Feature Rank (0 to 5)
226	24.78	81.3	59	76	1
227	24.81	81.4	358	29	1
228	24.92	81.8	319	18	1
229	24.98	82.0	266	22	1
230	25.05	82.2	292	28	1
231	25.09	82.3	241	24	1
232	25.14	82.5	268	42	1
233	25.20	82.7	219	69	1
234	25.23	82.8	204	45	1
235	25.27	82.9	68	68	1
236	25.42	83.4	204	21	1
237	25.54	83.8	296	35	1
238	25.63	84.1	211	75	1
239	25.67	84.2	329	45	1
240	25.73	84.4	78	24	2
241	25.84	84.8	11	38	1
242	25.92	85.1	59	63	1
243	25.93	85.1	240	68	1
244	26.14	85.8	61	39	2
245	26.22	86.0	91	45	2
246	26.23	86.1	233	65	2
247	26.35	86.5	230	82	1
248	26.38	86.5	82	64	1
249	26.51	87.0	37	46	1
250	26.56	87.1	216	67	1
251	26.63	87.4	92	46	2
252	26.78	87.9	91	38	1
253	26.84	88.1	81	48	1
254	27.07	88.8	70	59	1
255	27.09	88.9	259	18	1
256	27.20	89.3	113	35	1
257	27.21	89.3	159	57	1
258	27.28	89.5	116	39	1
259	27.30	89.6	329	81	1
260	27.33	89.7	127	52	1
261	27.36	89.8	116	45	2
262	27.43	90.0	204	78	1
263	27.58	90.5	35	29	1
264	27.70	90.9	171	78	2
265	27.75	91.0	158	51	1
266	27.81	91.3	227	47	1
267	27.93	91.6	84	78	1
268	28.02	91.9	182	81	1
269	28.07	92.1	225	57	1
270	28.55	93.7	303	52	1

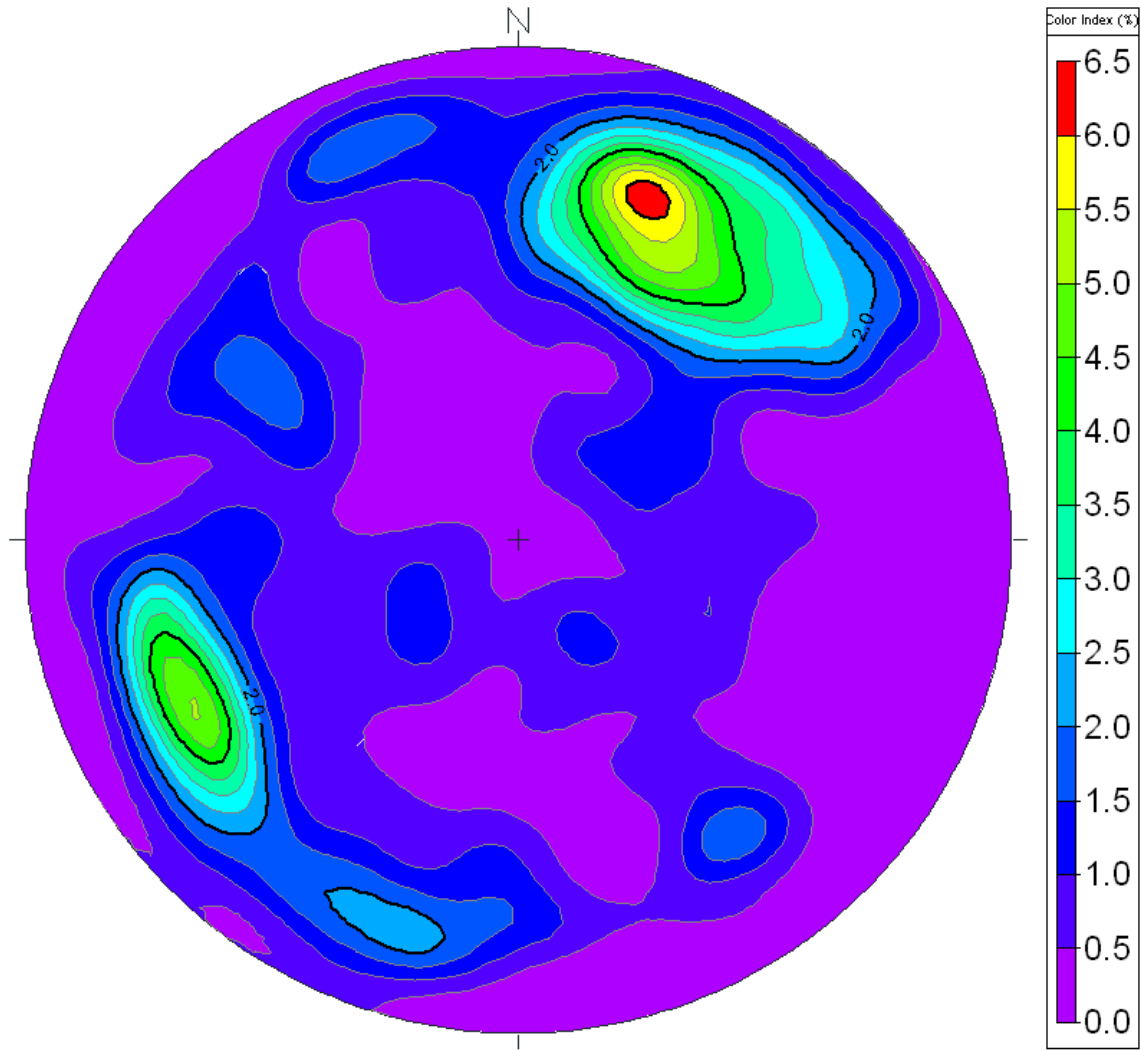
All directions are with respect to magnetic north.

Orientation Summary Table
Televiewer Features
CB and I
Edwards Air Force Base
Well: 37-B10
December 18, 2013

Feature No.	Depth (meters)	Depth (feet)	Dip Direction (degrees)	Dip Angle (degrees)	Feature Rank (0 to 5)
271	28.58	93.8	70	57	2
272	28.70	94.2	239	80	1
273	28.95	95.0	239	68	1
274	29.16	95.7	329	13	1
275	29.28	96.1	285	36	1
276	29.33	96.2	357	65	1
277	29.51	96.8	235	75	1
278	29.81	97.8	0	53	1
279	29.88	98.0	63	58	1
280	29.89	98.1	63	34	1
281	30.05	98.6	52	63	2
282	30.21	99.1	354	68	1
283	30.25	99.2	188	52	1
284	30.34	99.5	193	67	1
285	30.57	100.3	216	76	1
286	30.76	100.9	233	63	1
287	30.79	101.0	232	23	1
288	30.85	101.2	228	51	1
289	30.88	101.3	79	69	2
290	31.06	101.9	44	62	1
291	31.12	102.1	346	39	1
292	31.16	102.2	222	66	2
293	31.25	102.5	215	76	3
294	31.29	102.7	212	79	1
295	31.30	102.7	314	32	1
296	31.39	103.0	322	52	1
297	31.42	103.1	11	16	1

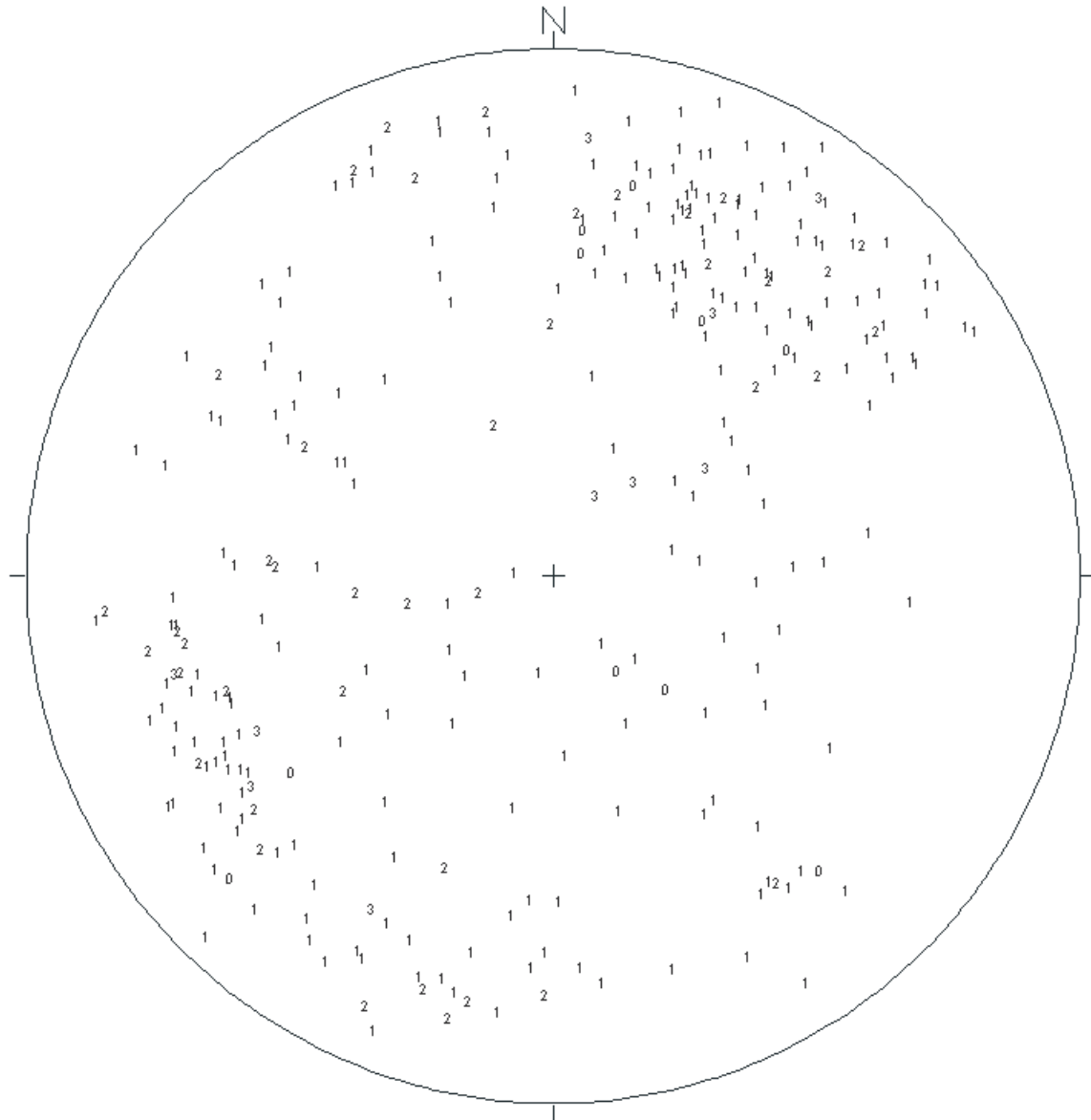
All directions are with respect to magnetic north.

**Stereonet Diagram – Schmidt Projection
Image Features
CB & I
Project: Edwards Air Force Base
Well: 37-B10
December 18, 2013**



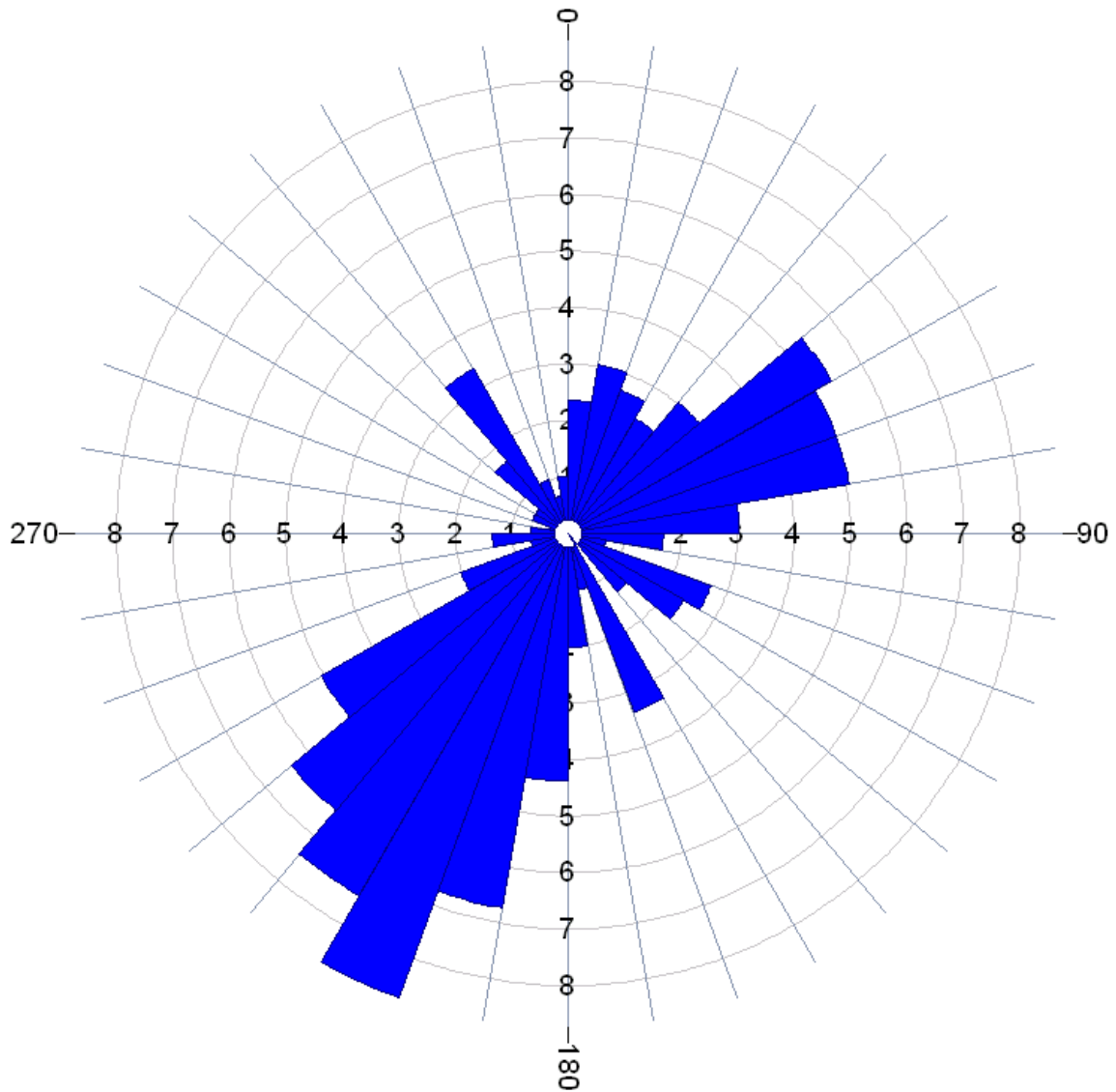
All directions are with respect to Magnetic North.

**Stereonet Diagram – Schmidt Projection
Image Features
CB & I
Project: Edwards Air Force Base
Well: 37-B10
December 18, 2013**



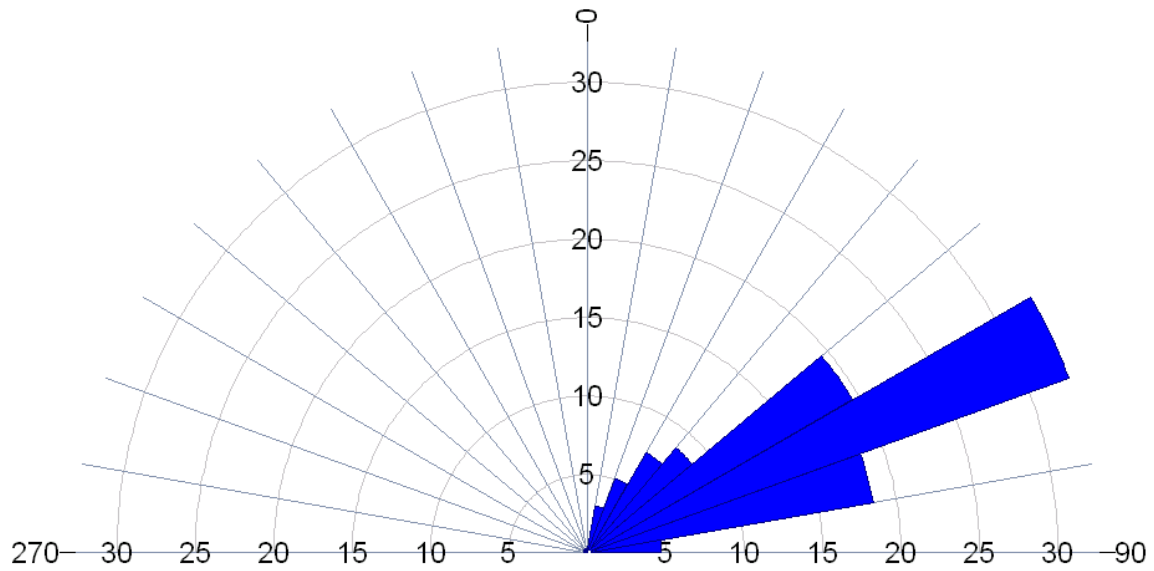
All directions are with respect to Magnetic North.

**Rose Diagram – Dip Directions
Image Features
CB & I
Project: Edwards Air Force Base
Well: 37-B10
December 18, 2013**



All directions are with respect to Magnetic North.

Rose Diagram – Dip Angles
Image Features
CB & I
Project: Edwards Air Force Base
Well: 37-B10
December 18, 2013



All directions are with respect to Magnetic North.

Appendix C



Optical & Acoustic Televiewer

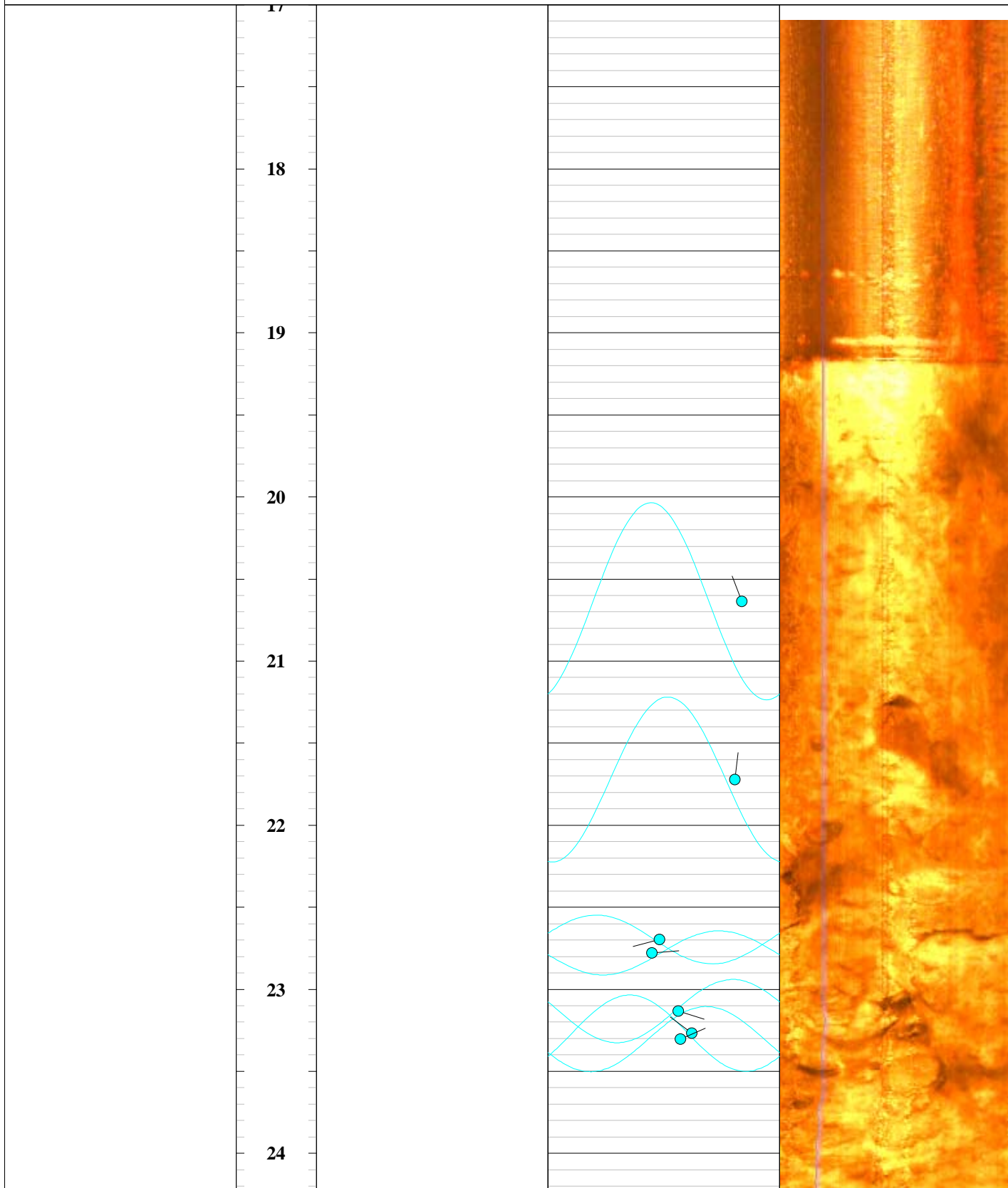
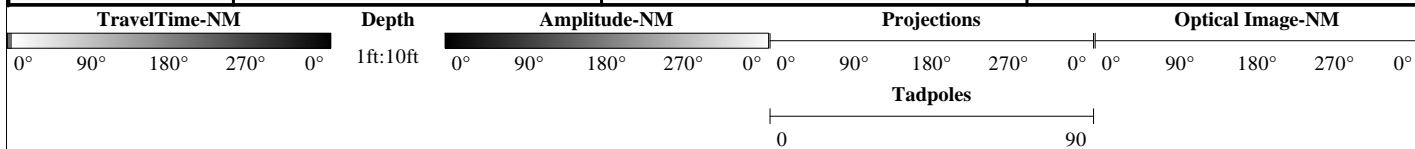
COMPANY: CB&I

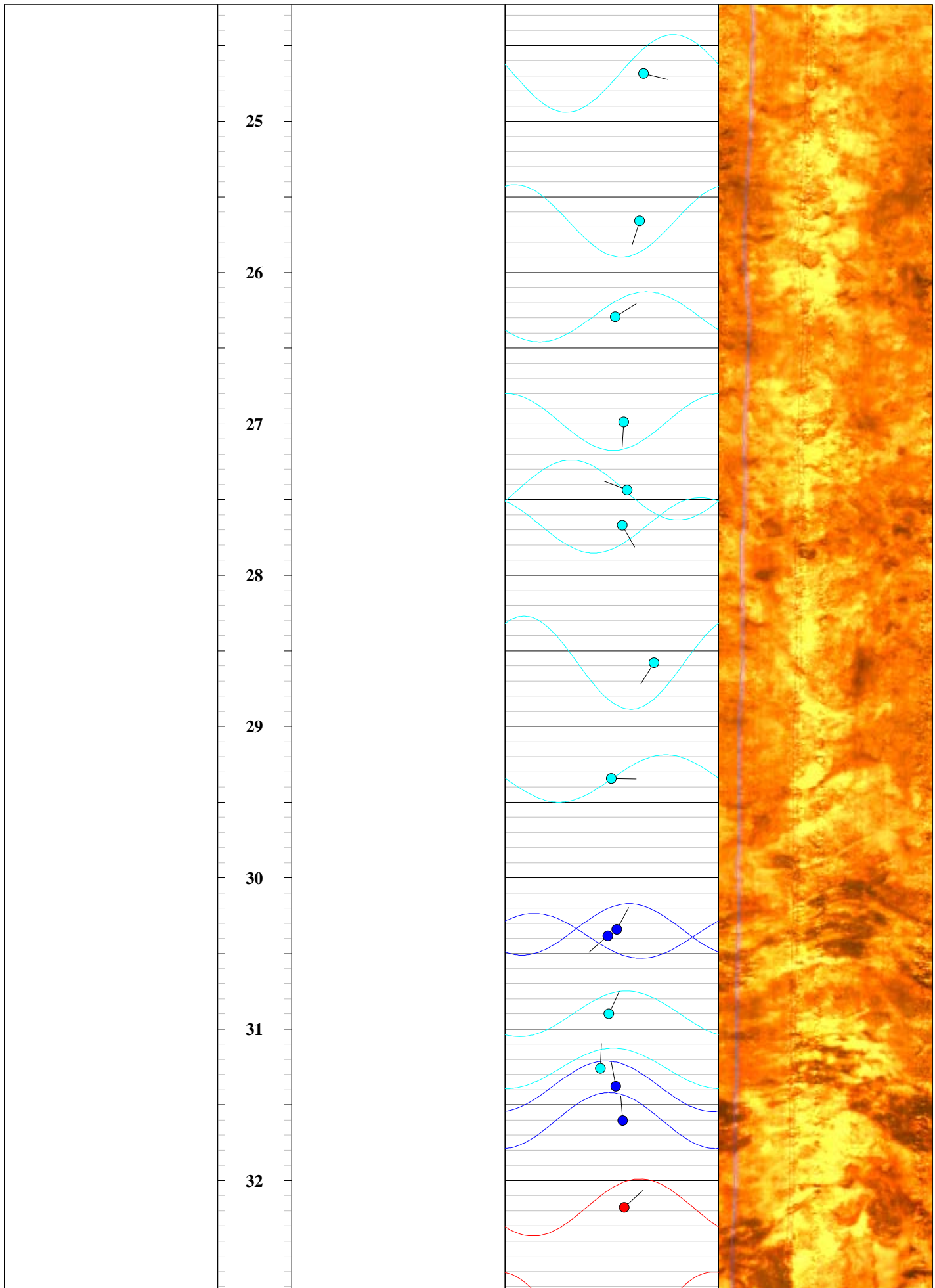
PROJECT: Edwards Air Force Base

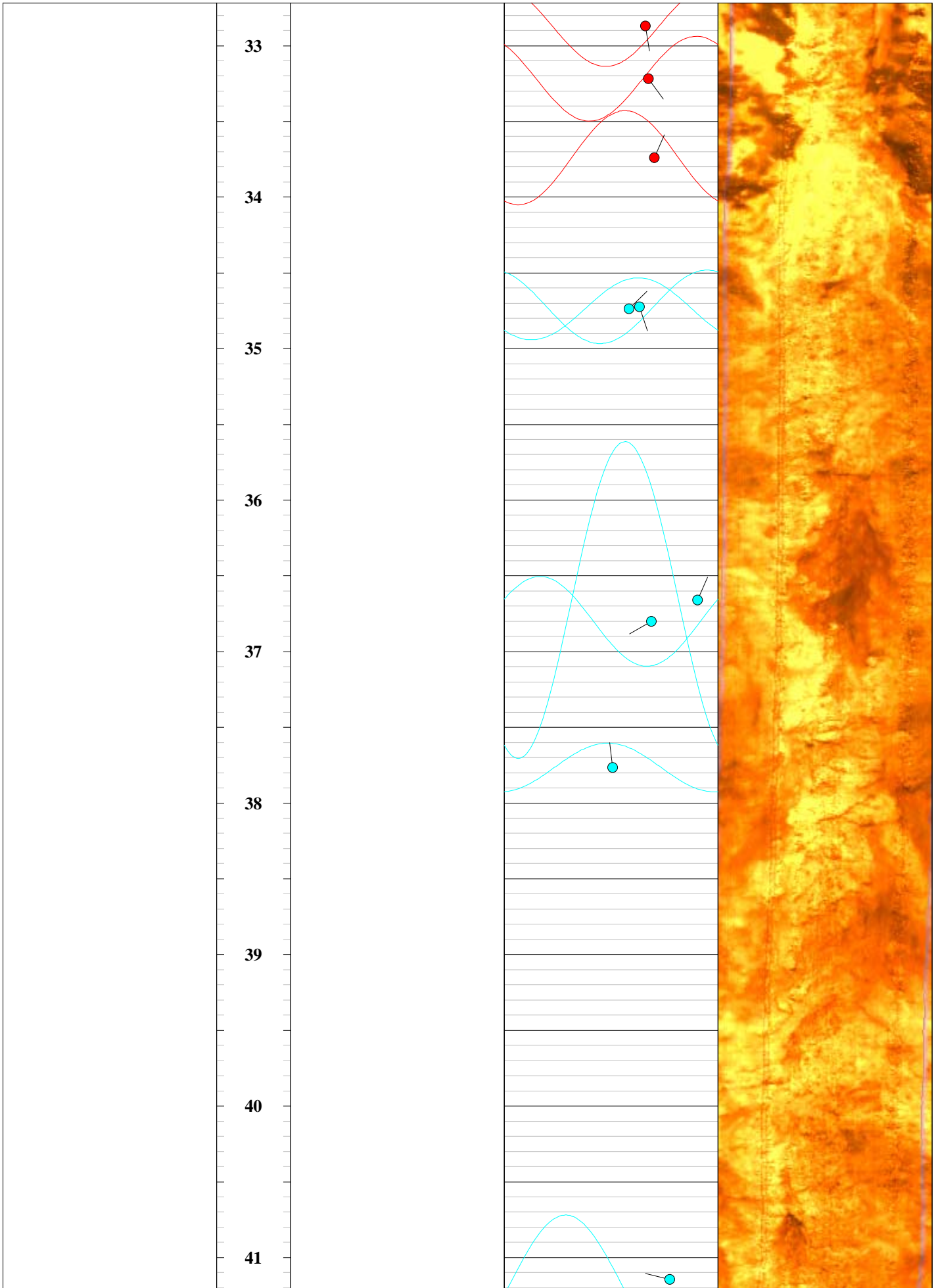
DATE LOGGED: 17 December 2013

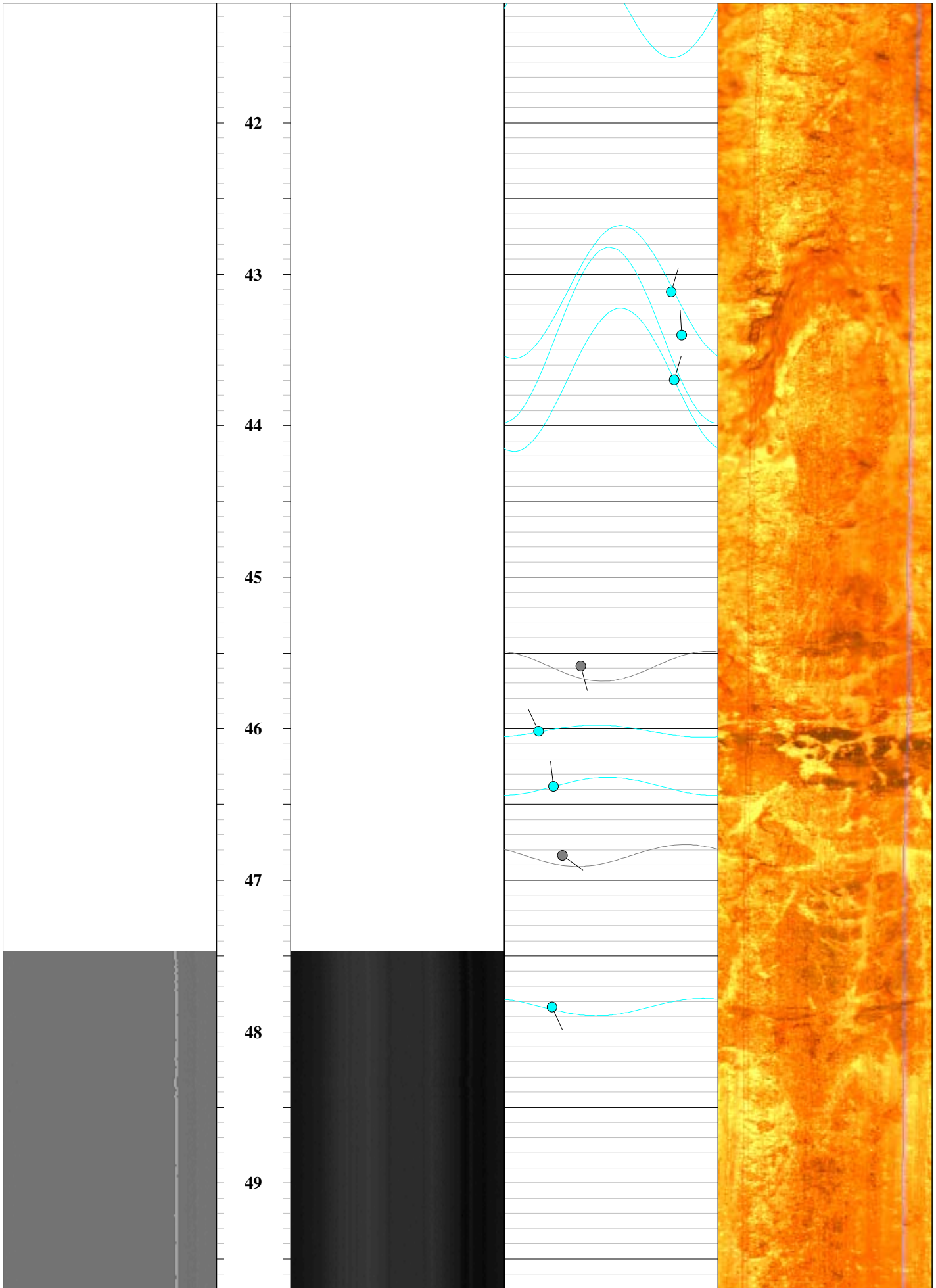
WELL: 37-B12

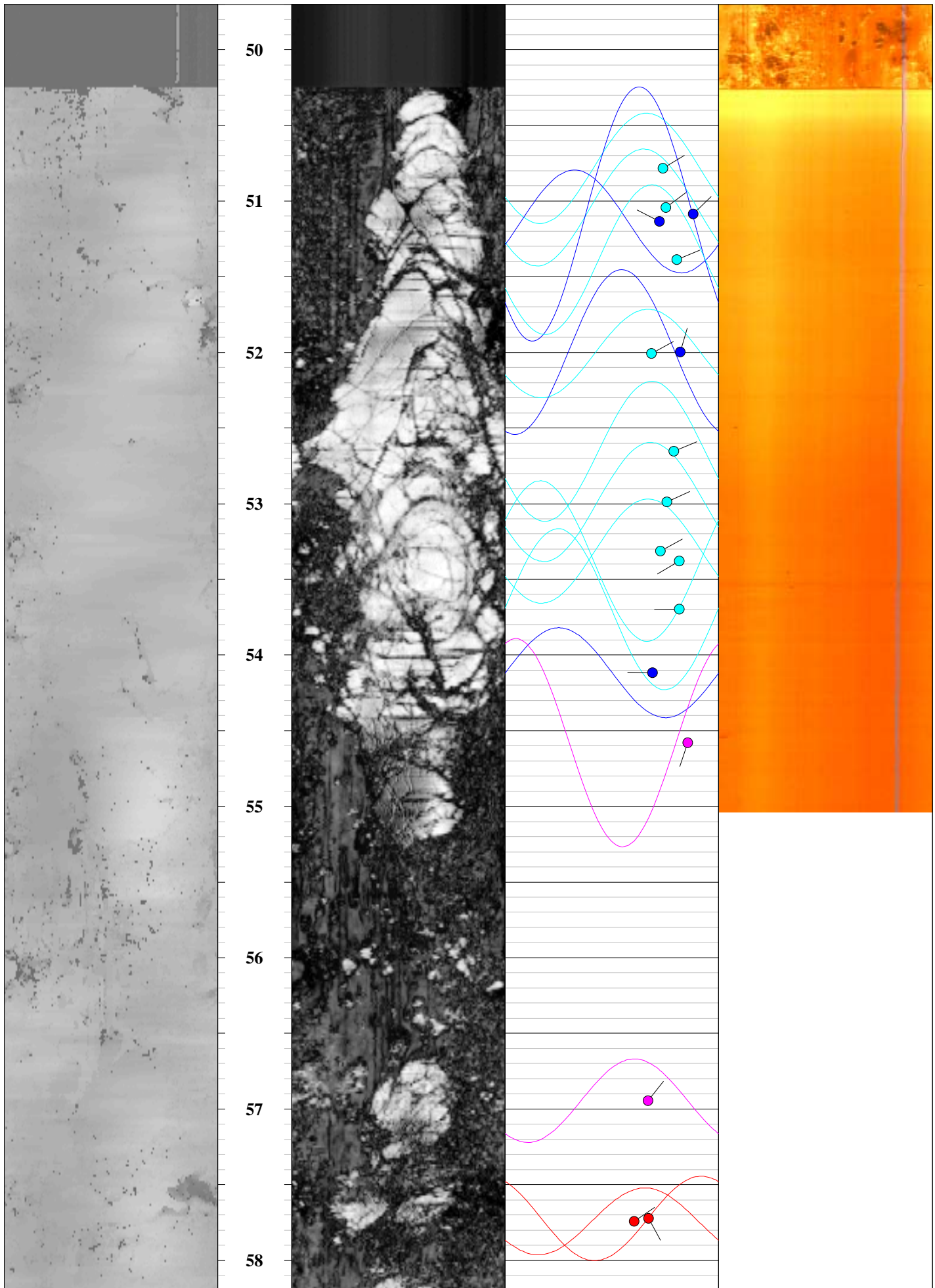
IDS - Colog Group
810 Quail Street, Suite E, Lakewood, CO 80215
Phone: (303) 279-0171, Fax: (303) 278-0135
www.idsdrill.com

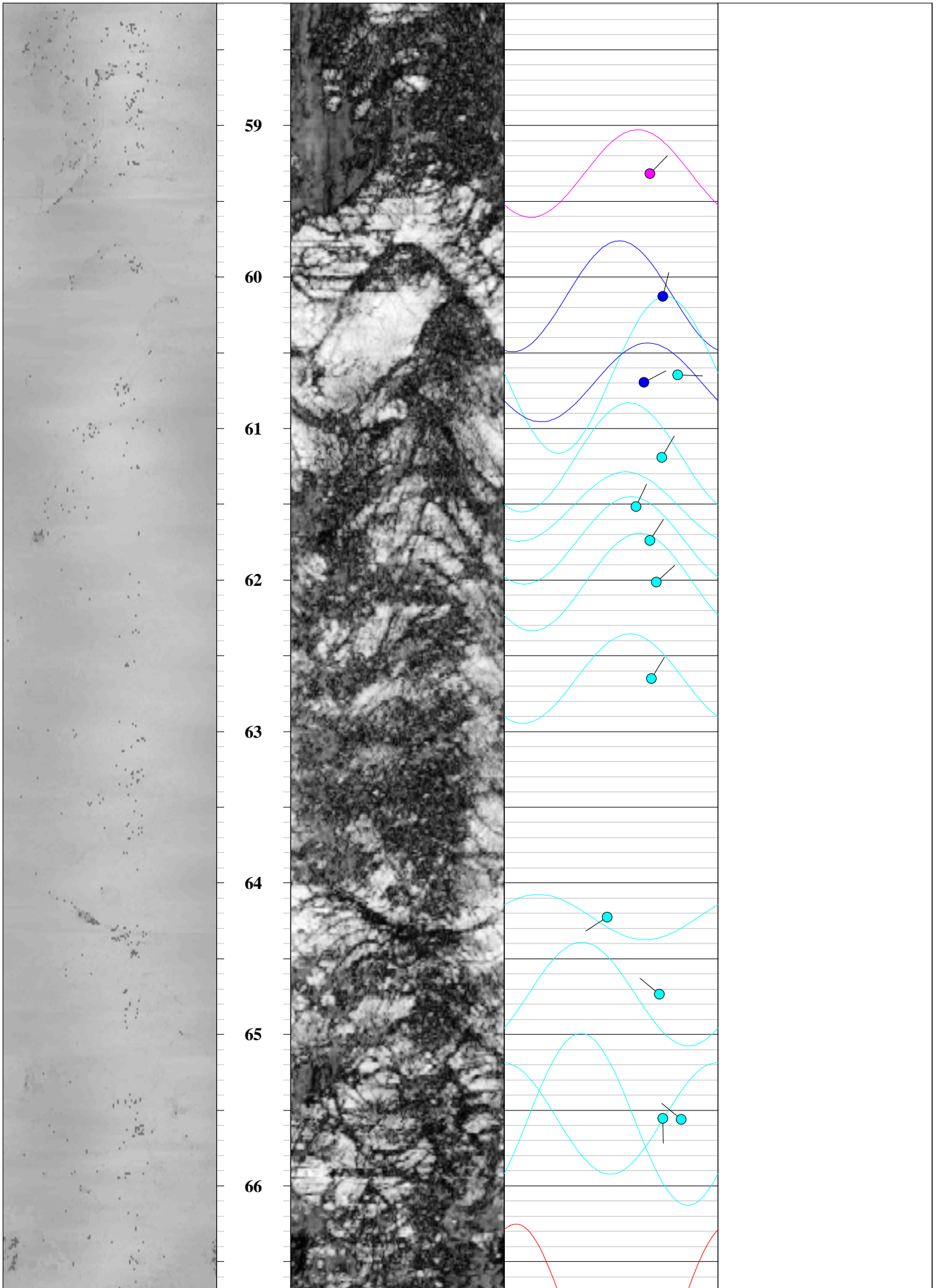


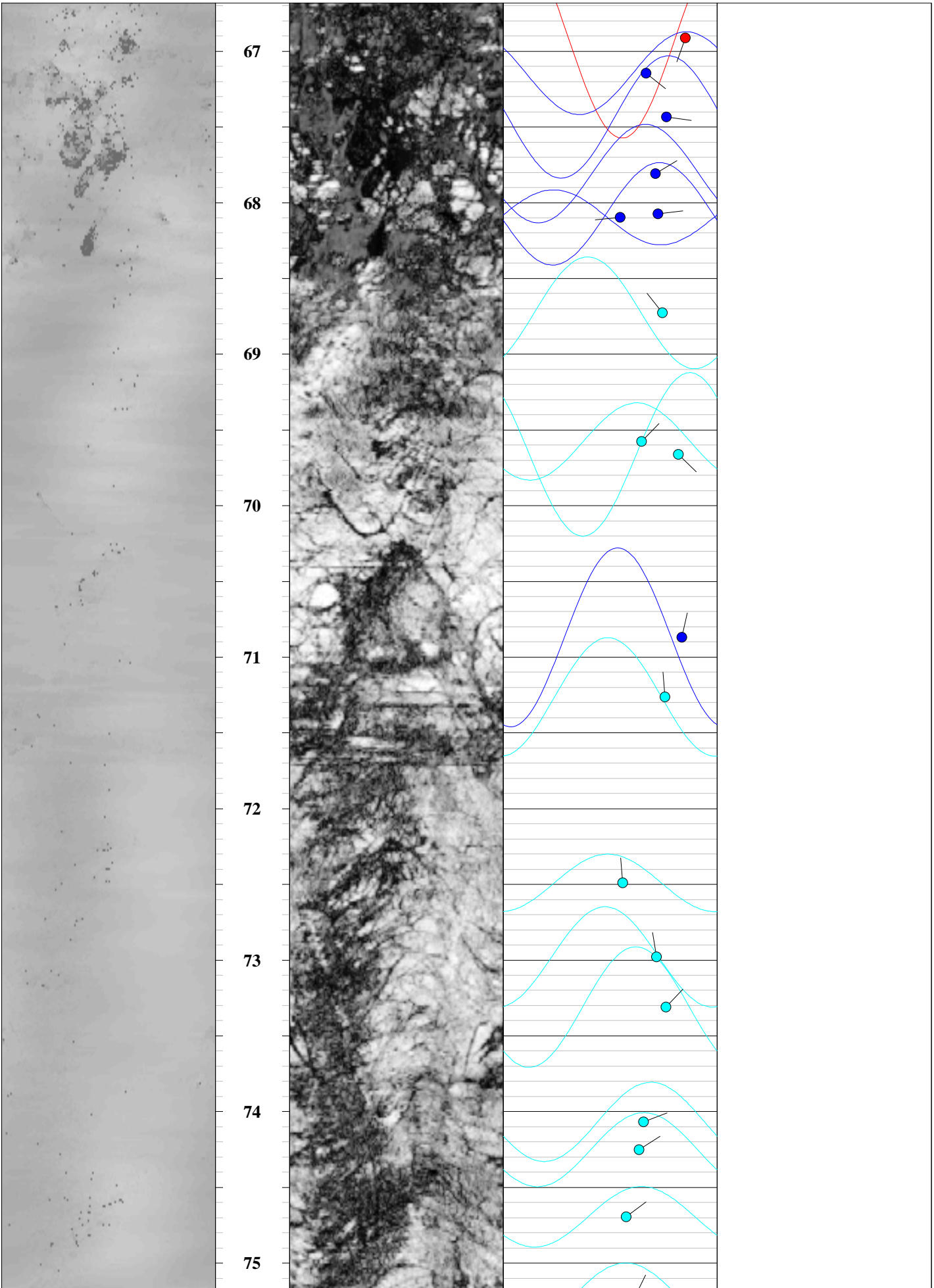


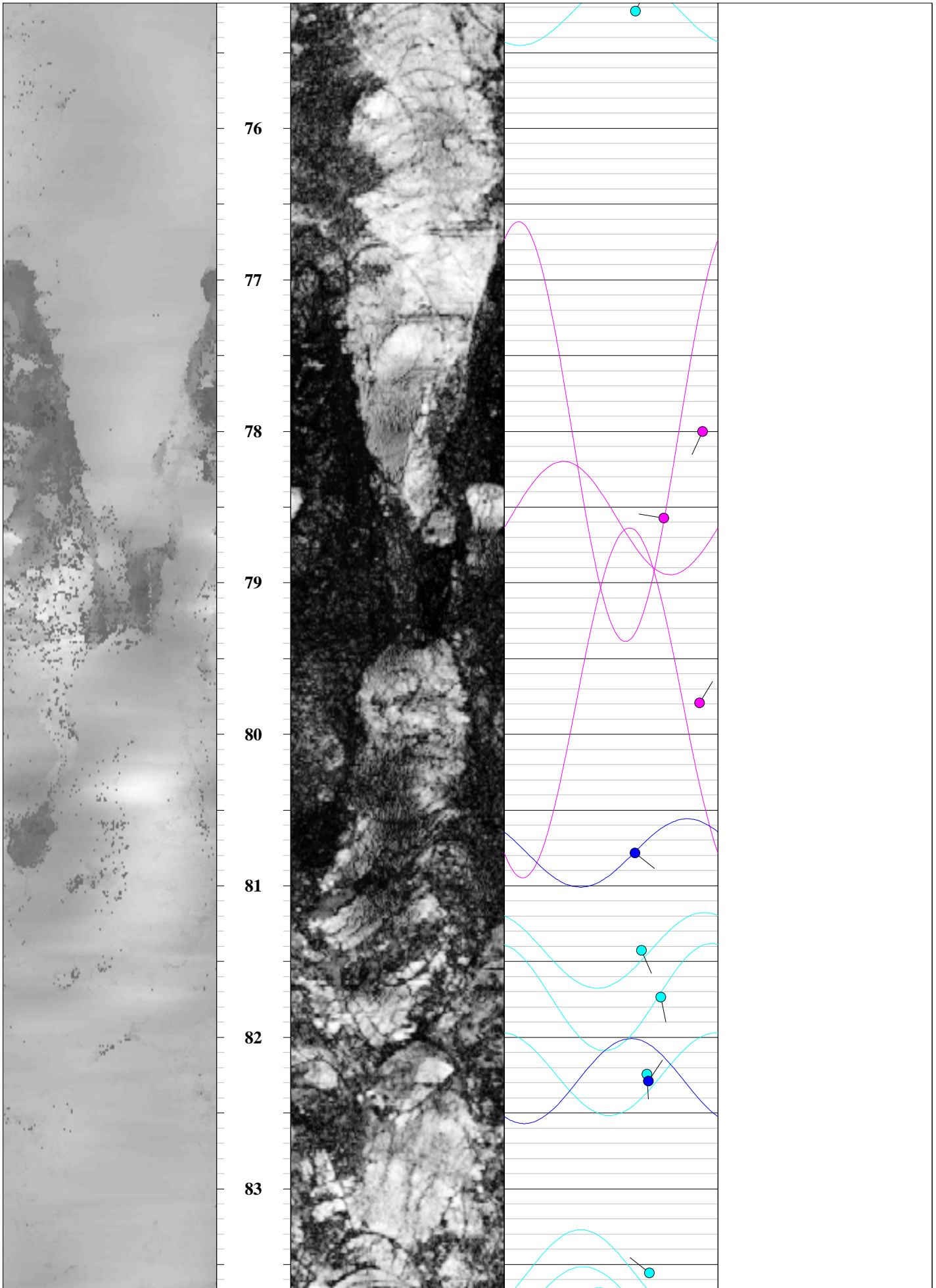


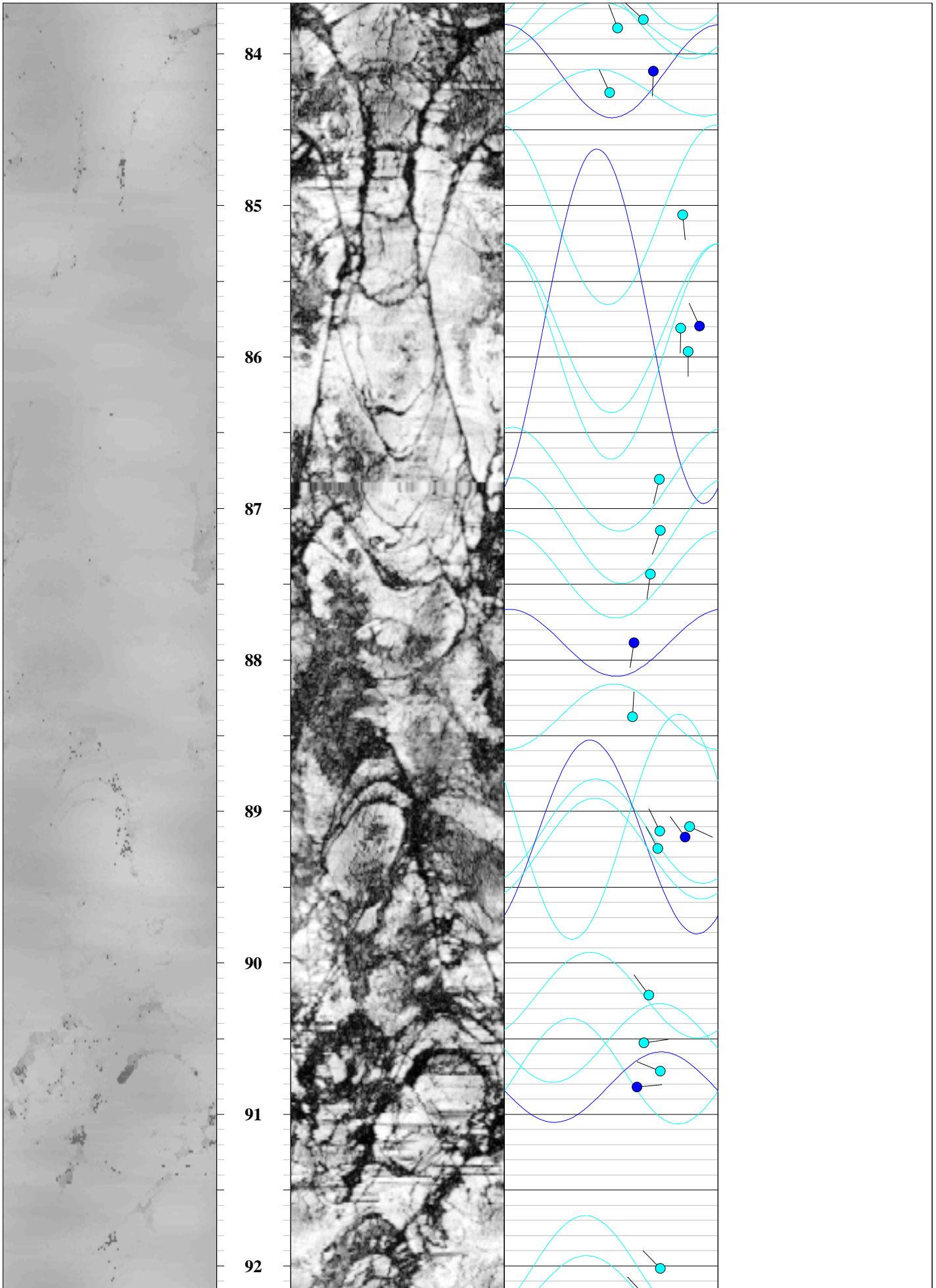


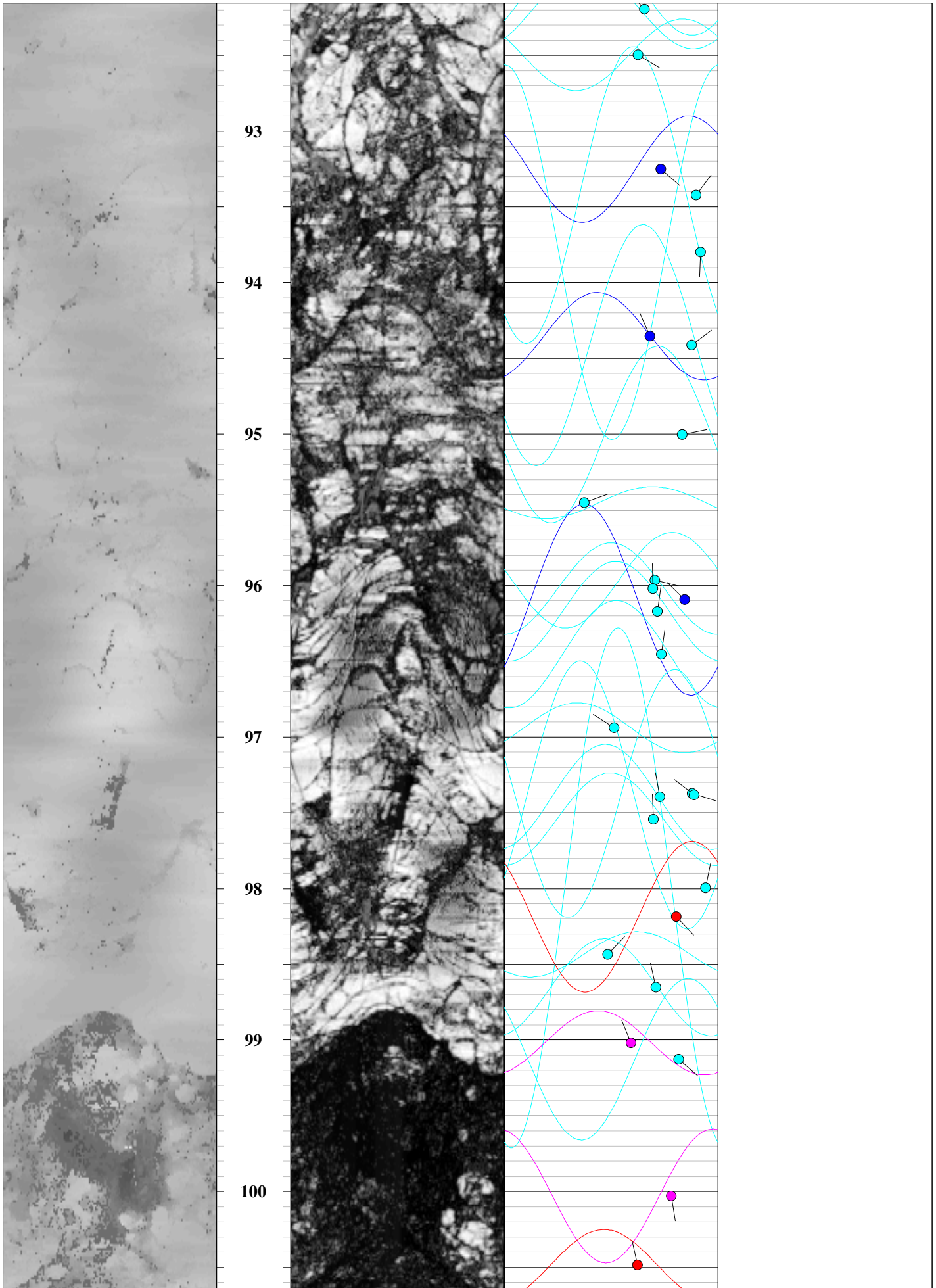


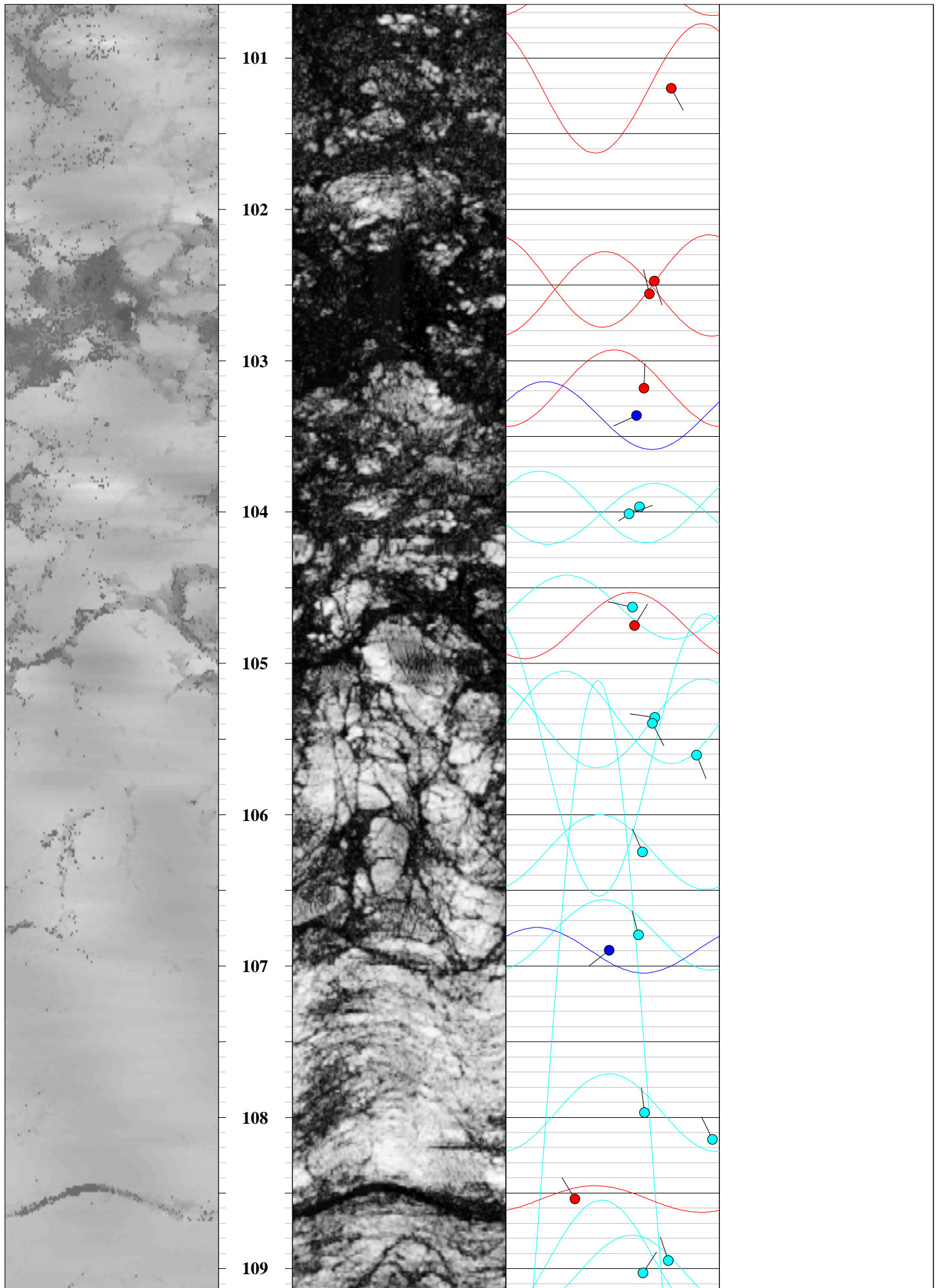


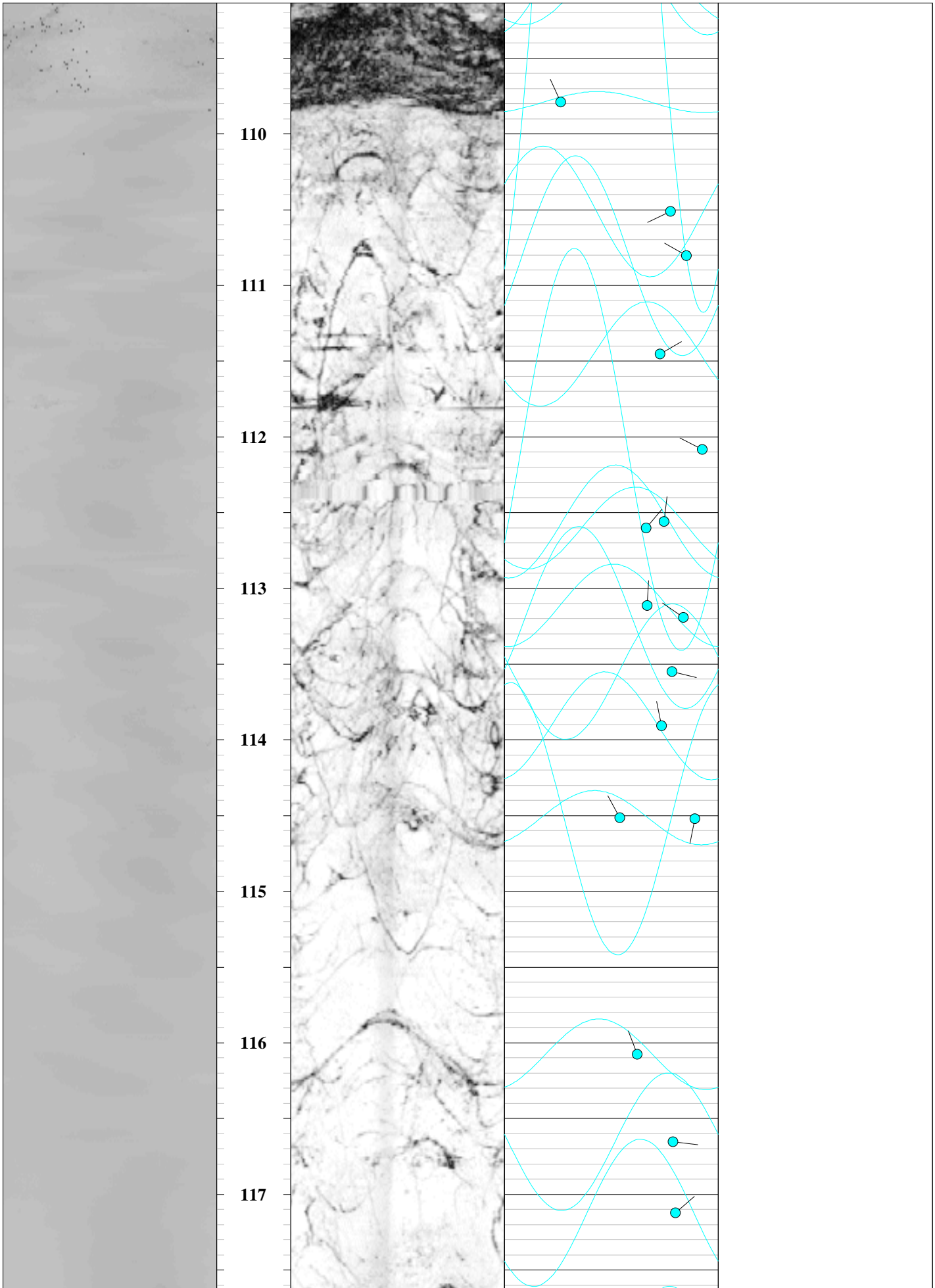


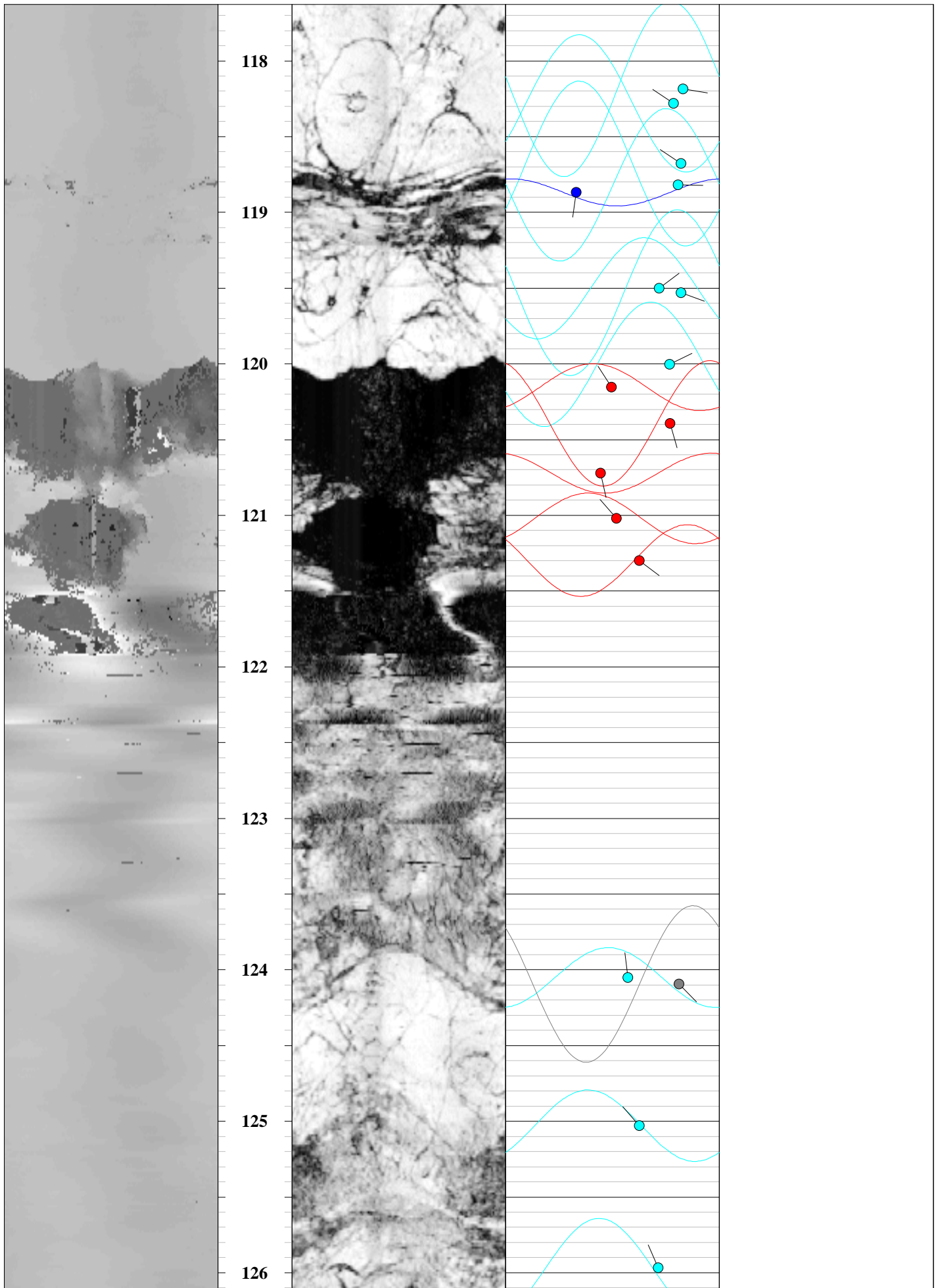


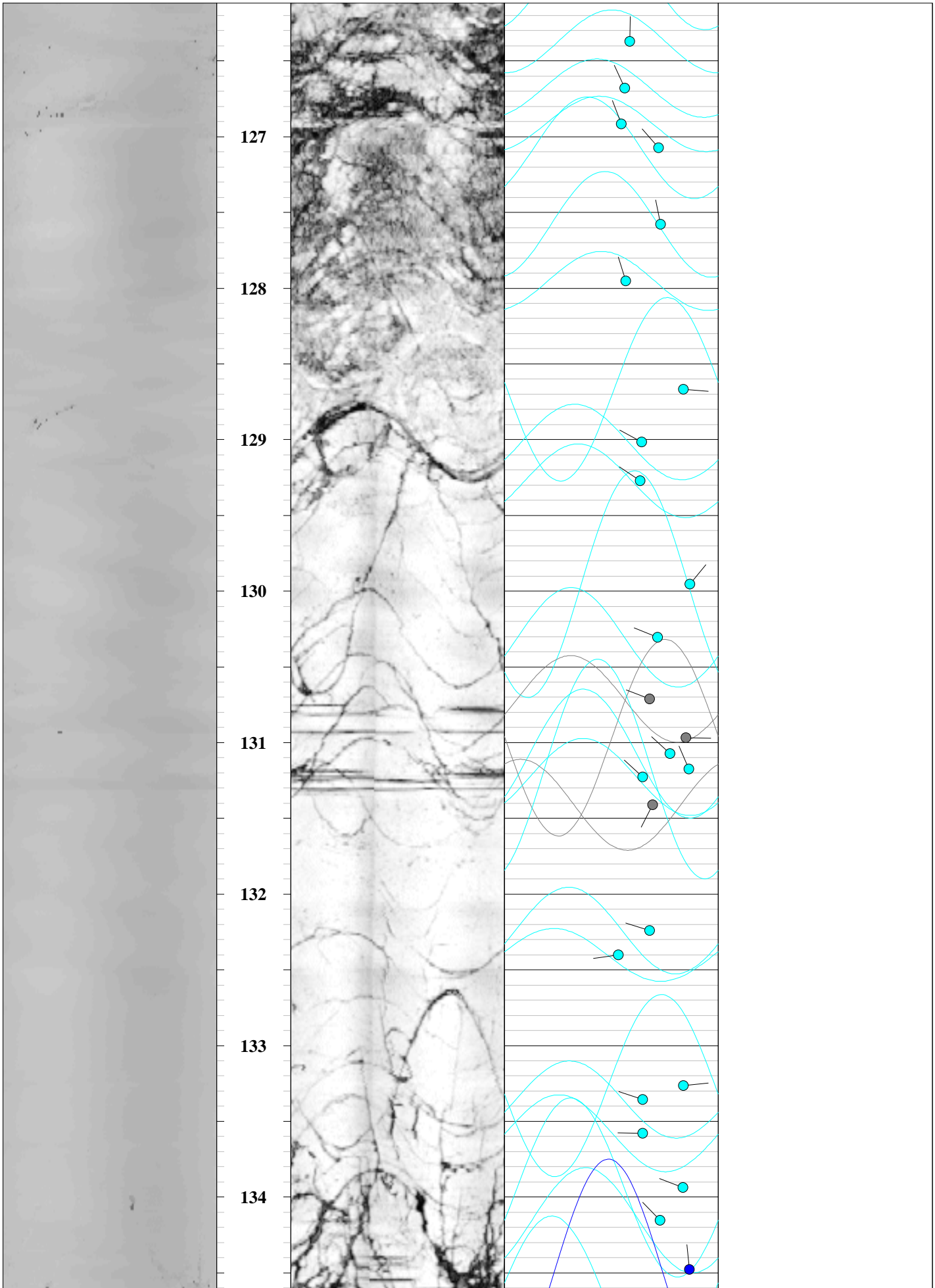


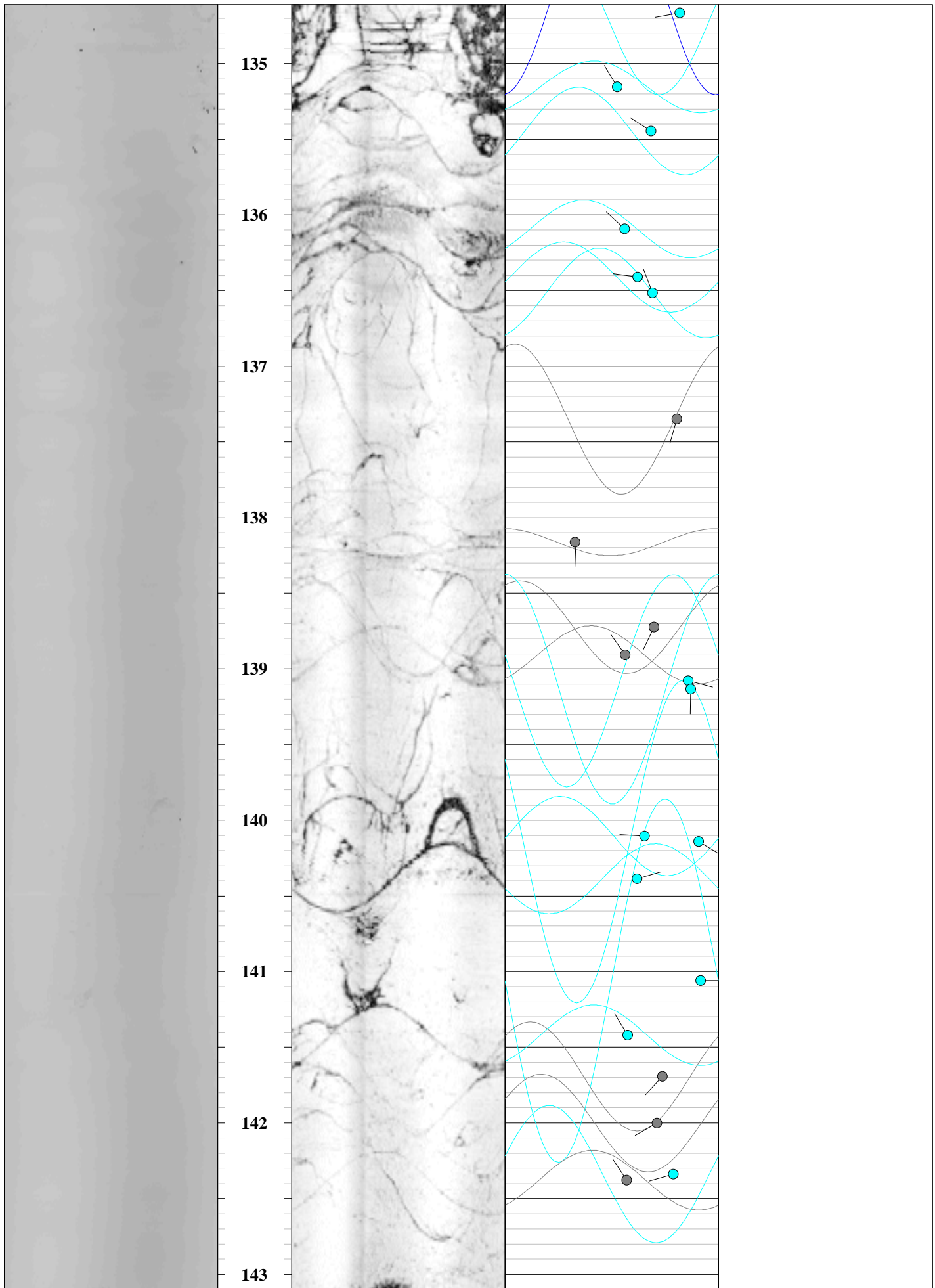


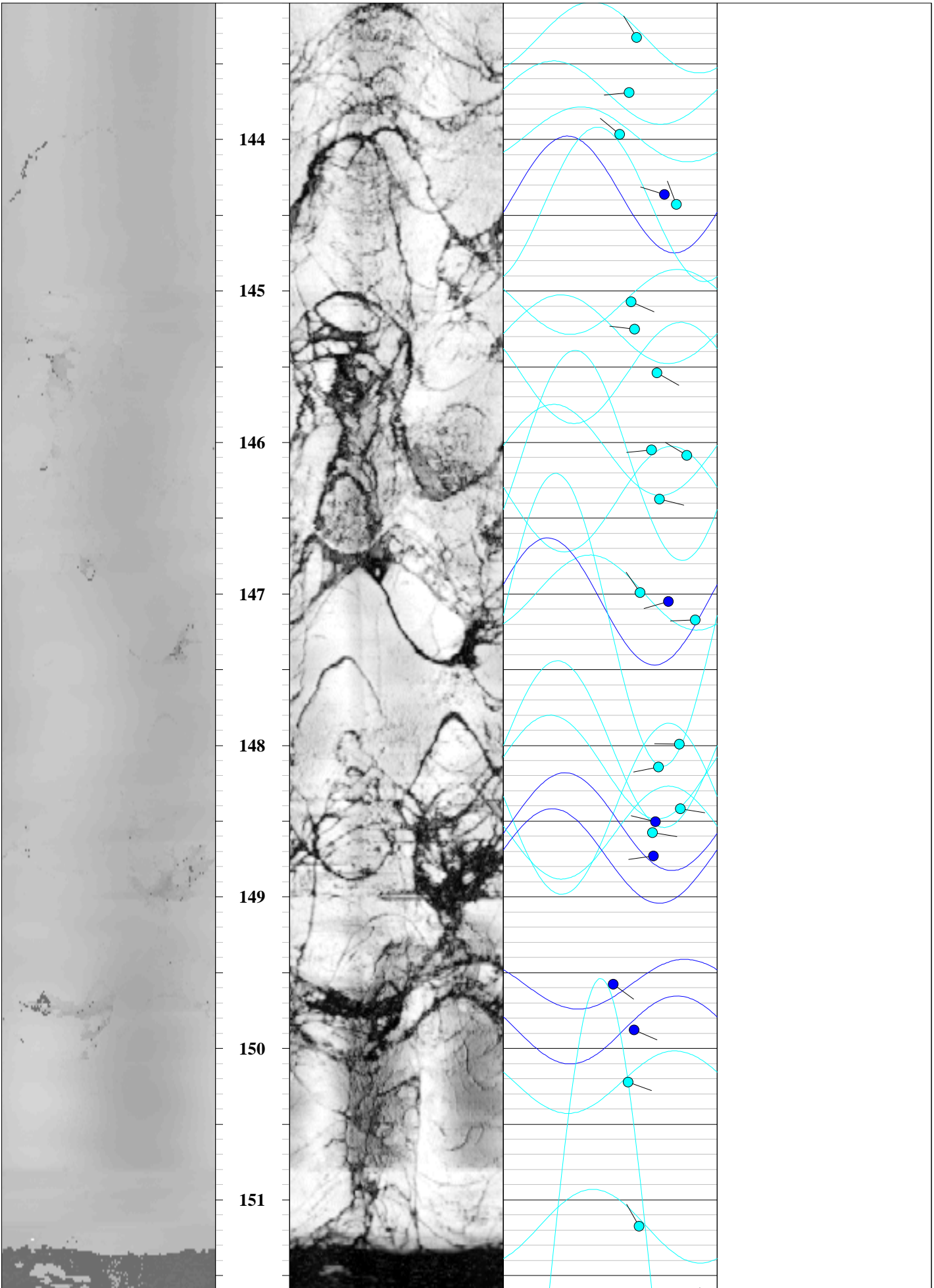


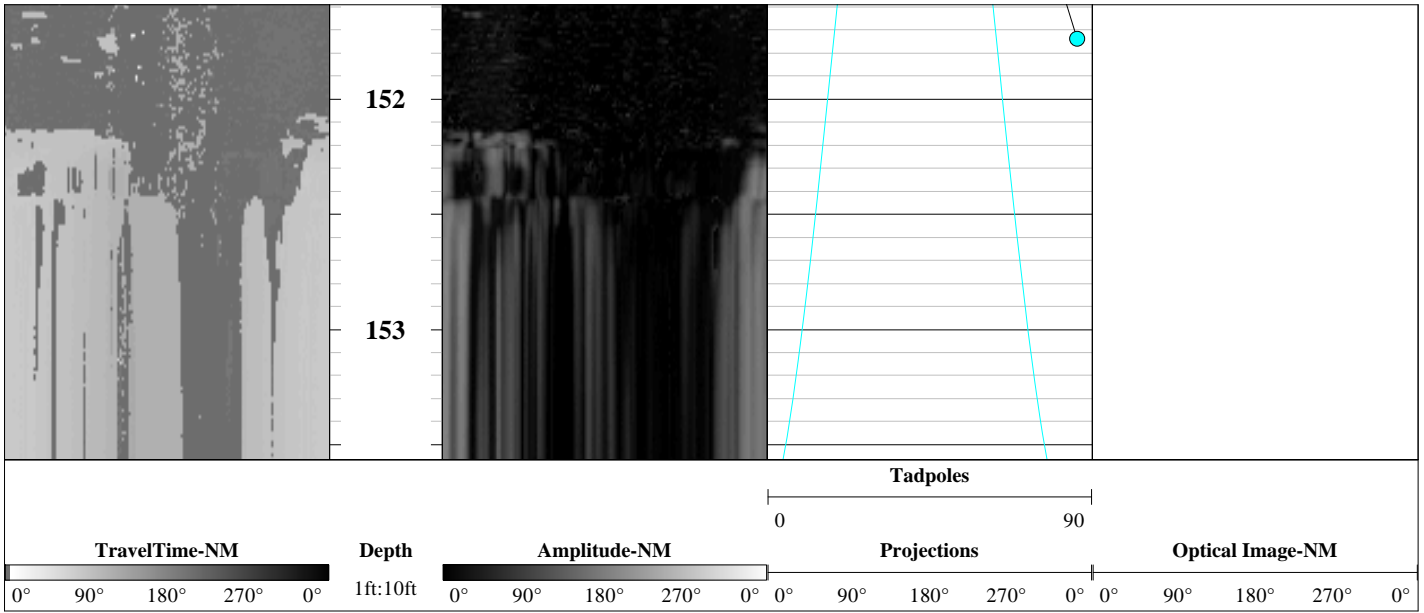












Orientation Summary Table
Televiewer Features
CB and I
Edwards Air Force Base
Well: 37-B12
December 17, 2013

Feature No.	Depth (meters)	Depth (feet)	Dip Direction (degrees)	Dip Angle (degrees)	Feature Rank (0 to 5)
1	6.29	20.6	340	75	1
2	6.62	21.7	6	73	1
3	6.92	22.7	255	43	1
4	6.94	22.8	85	40	1
5	7.05	23.1	107	51	1
6	7.09	23.3	307	56	1
7	7.10	23.3	66	52	1
8	7.52	24.7	104	58	1
9	7.82	25.7	196	57	1
10	8.01	26.3	58	46	1
11	8.23	27.0	182	50	1
12	8.36	27.4	291	52	1
13	8.43	27.7	150	49	1
14	8.71	28.6	212	63	1
15	8.94	29.3	91	45	1
16	9.25	30.3	29	47	2
17	9.26	30.4	229	43	2
18	9.42	30.9	25	44	1
19	9.53	31.3	3	40	1
20	9.56	31.4	350	47	2
21	9.63	31.6	355	50	2
22	9.81	32.2	47	50	3
23	10.02	32.9	171	59	3
24	10.13	33.2	143	61	3
25	10.28	33.7	23	63	3
26	10.58	34.7	161	57	1
27	10.59	34.7	46	52	1
28	11.17	36.7	23	81	1
29	11.22	36.8	240	62	1
30	11.51	37.8	354	46	1
31	12.54	41.1	283	70	1
32	13.14	43.1	16	70	1
33	13.23	43.4	357	75	1
34	13.32	43.7	16	72	1
35	13.90	45.6	165	32	0
36	14.03	46.0	335	15	1
37	14.14	46.4	354	21	1
38	14.28	46.8	124	25	0
39	14.58	47.8	155	20	1
40	15.48	50.8	59	67	1
41	15.56	51.0	54	68	1
42	15.57	51.1	46	79	2
43	15.58	51.1	297	65	2
44	15.66	51.4	68	72	1
45	15.85	52.0	17	74	2

All directions are with respect to magnetic north.

Orientation Summary Table
Televiewer Features
CB and I
Edwards Air Force Base
Well: 37-B12
December 17, 2013

Feature No.	Depth (meters)	Depth (feet)	Dip Direction (degrees)	Dip Angle (degrees)	Feature Rank (0 to 5)
46	15.85	52.0	61	62	1
47	16.05	52.7	67	71	1
48	16.15	53.0	66	68	1
49	16.25	53.3	61	65	1
50	16.27	53.4	240	73	1
51	16.37	53.7	269	74	1
52	16.50	54.1	271	62	2
53	16.64	54.6	198	77	4
54	17.36	57.0	38	60	4
55	17.59	57.7	151	61	3
56	17.60	57.7	56	54	3
57	18.08	59.3	45	61	4
58	18.33	60.1	14	67	2
59	18.49	60.7	92	73	1
60	18.50	60.7	62	59	2
61	18.65	61.2	30	66	1
62	18.75	61.5	25	55	1
63	18.82	61.7	33	61	1
64	18.90	62.0	47	64	1
65	19.10	62.7	31	62	1
66	19.58	64.2	237	43	1
67	19.73	64.7	310	65	1
68	19.98	65.6	179	67	1
69	19.98	65.6	309	74	1
70	20.39	66.9	200	77	3
71	20.47	67.2	128	60	2
72	20.55	67.4	98	69	2
73	20.67	67.8	59	64	2
74	20.75	68.1	83	65	2
75	20.76	68.1	265	49	2
76	20.95	68.7	322	67	1
77	21.21	69.6	45	58	1
78	21.23	69.7	134	74	1
79	21.60	70.9	13	75	2
80	21.72	71.3	356	68	1
81	22.09	72.5	356	50	1
82	22.24	73.0	351	65	1
83	22.34	73.3	43	68	1
84	22.58	74.1	69	59	1
85	22.63	74.3	57	57	1
86	22.77	74.7	53	52	1
87	22.93	75.2	26	55	1
88	23.77	78.0	204	84	4
89	23.95	78.6	280	67	4
90	24.32	79.8	31	82	4

All directions are with respect to magnetic north.

Orientation Summary Table
Televiewer Features
CB and I
Edwards Air Force Base
Well: 37-B12
December 17, 2013

Feature No.	Depth (meters)	Depth (feet)	Dip Direction (degrees)	Dip Angle (degrees)	Feature Rank (0 to 5)
91	24.62	80.8	128	55	2
92	24.82	81.4	156	58	1
93	24.91	81.7	169	66	1
94	25.07	82.2	177	60	1
95	25.08	82.3	33	61	2
96	25.47	83.6	309	61	1
97	25.53	83.8	313	59	1
98	25.55	83.8	339	48	1
99	25.64	84.1	182	63	2
100	25.68	84.3	336	44	1
101	25.93	85.1	175	75	1
102	26.15	85.8	336	82	2
103	26.15	85.8	180	74	1
104	26.20	86.0	180	78	1
105	26.46	86.8	193	65	1
106	26.56	87.2	198	66	1
107	26.65	87.4	188	61	1
108	26.79	87.9	188	55	2
109	26.94	88.4	4	54	1
110	27.16	89.1	114	78	1
111	27.17	89.1	334	65	1
112	27.18	89.2	324	76	2
113	27.20	89.2	332	65	1
114	27.50	90.2	324	61	1
115	27.59	90.5	81	59	1
116	27.65	90.7	292	66	1
117	27.68	90.8	84	56	2
118	28.05	92.0	316	66	1
119	28.10	92.2	318	59	1
120	28.19	92.5	120	56	1
121	28.42	93.3	131	66	2
122	28.47	93.4	37	81	1
123	28.59	93.8	181	83	1
124	28.76	94.4	337	61	2
125	28.78	94.4	54	79	1
126	28.96	95.0	79	75	1
127	29.09	95.5	70	34	1
128	29.25	96.0	103	64	1
129	29.27	96.0	360	62	1
130	29.29	96.1	314	76	2
131	29.31	96.2	8	64	1
132	29.40	96.5	8	66	1
133	29.55	96.9	303	46	1
134	29.68	97.4	107	79	1
135	29.68	97.4	308	80	1

All directions are with respect to magnetic north.

Orientation Summary Table
Televiewer Features
CB and I
Edwards Air Force Base
Well: 37-B12
December 17, 2013

Feature No.	Depth (meters)	Depth (feet)	Dip Direction (degrees)	Dip Angle (degrees)	Feature Rank (0 to 5)
136	29.68	97.4	350	66	1
137	29.73	97.5	358	63	1
138	29.87	98.0	12	85	1
139	29.93	98.2	136	72	3
140	30.00	98.4	44	44	1
141	30.07	98.7	348	64	1
142	30.18	99.0	338	53	4
143	30.21	99.1	130	74	1
144	30.49	100.0	171	70	4
145	30.63	100.5	348	56	3
146	30.85	101.2	151	70	3
147	31.23	102.5	162	63	3
148	31.26	102.6	347	61	3
149	31.45	103.2	2	58	3
150	31.50	103.4	246	55	2
151	31.69	104.0	236	56	1
152	31.70	104.0	71	52	1
153	31.89	104.6	282	53	1
154	31.93	104.8	31	54	3
155	32.11	105.4	278	63	1
156	32.13	105.4	152	62	1
157	32.19	105.6	157	80	1
158	32.39	106.3	337	58	1
159	32.55	106.8	345	56	1
160	32.58	106.9	232	44	2
161	32.91	108.0	354	58	1
162	32.96	108.2	335	87	1
163	33.08	108.5	330	29	3
164	33.21	109.0	342	68	1
165	33.23	109.0	32	58	1
166	33.46	109.8	336	24	1
167	33.68	110.5	245	70	1
168	33.77	110.8	300	77	1
169	33.97	111.5	60	65	1
170	34.16	112.1	298	83	1
171	34.31	112.6	7	67	1
172	34.32	112.6	40	60	1
173	34.48	113.1	3	60	1
174	34.50	113.2	305	75	1
175	34.61	113.6	103	71	1
176	34.72	113.9	349	66	1
177	34.90	114.5	332	49	1
178	34.91	114.5	191	80	1
179	35.38	116.1	339	56	1
180	35.55	116.7	96	71	1

All directions are with respect to magnetic north.

Orientation Summary Table
Televiewer Features
CB and I
Edwards Air Force Base
Well: 37-B12
December 17, 2013

Feature No.	Depth (meters)	Depth (feet)	Dip Direction (degrees)	Dip Angle (degrees)	Feature Rank (0 to 5)
181	35.70	117.1	49	72	1
182	36.02	118.2	98	75	1
183	36.05	118.3	304	71	1
184	36.17	118.7	304	74	1
185	36.22	118.8	91	73	1
186	36.23	118.9	187	30	2
187	36.42	119.5	53	65	1
188	36.43	119.5	109	74	1
189	36.58	120.0	64	69	1
190	36.62	120.2	328	45	3
191	36.69	120.4	164	69	3
192	36.80	120.7	167	40	3
193	36.89	121.0	319	47	3
194	36.97	121.3	126	56	3
195	37.81	124.1	353	51	1
196	37.82	124.1	136	73	0
197	38.11	125.0	319	56	1
198	38.40	126.0	338	64	1
199	38.52	126.4	1	53	1
200	38.61	126.7	336	51	1
201	38.68	126.9	339	49	1
202	38.73	127.1	319	65	1
203	38.89	127.6	349	66	1
204	39.00	128.0	343	51	1
205	39.22	128.7	94	75	1
206	39.33	129.0	299	58	1
207	39.40	129.3	304	57	1
208	39.61	130.0	39	78	1
209	39.72	130.3	292	64	1
210	39.84	130.7	291	61	0
211	39.92	131.0	91	76	0
212	39.95	131.1	312	70	1
213	39.98	131.2	337	78	1
214	40.00	131.2	312	58	1
215	40.05	131.4	207	62	0
216	40.31	132.2	288	61	1
217	40.36	132.4	263	48	1
218	40.62	133.3	85	75	1
219	40.65	133.4	289	58	1
220	40.72	133.6	271	58	1
221	40.82	133.9	291	75	1
222	40.89	134.2	316	66	1
223	40.99	134.5	355	78	2
224	41.04	134.7	260	74	1
225	41.19	135.2	330	47	1

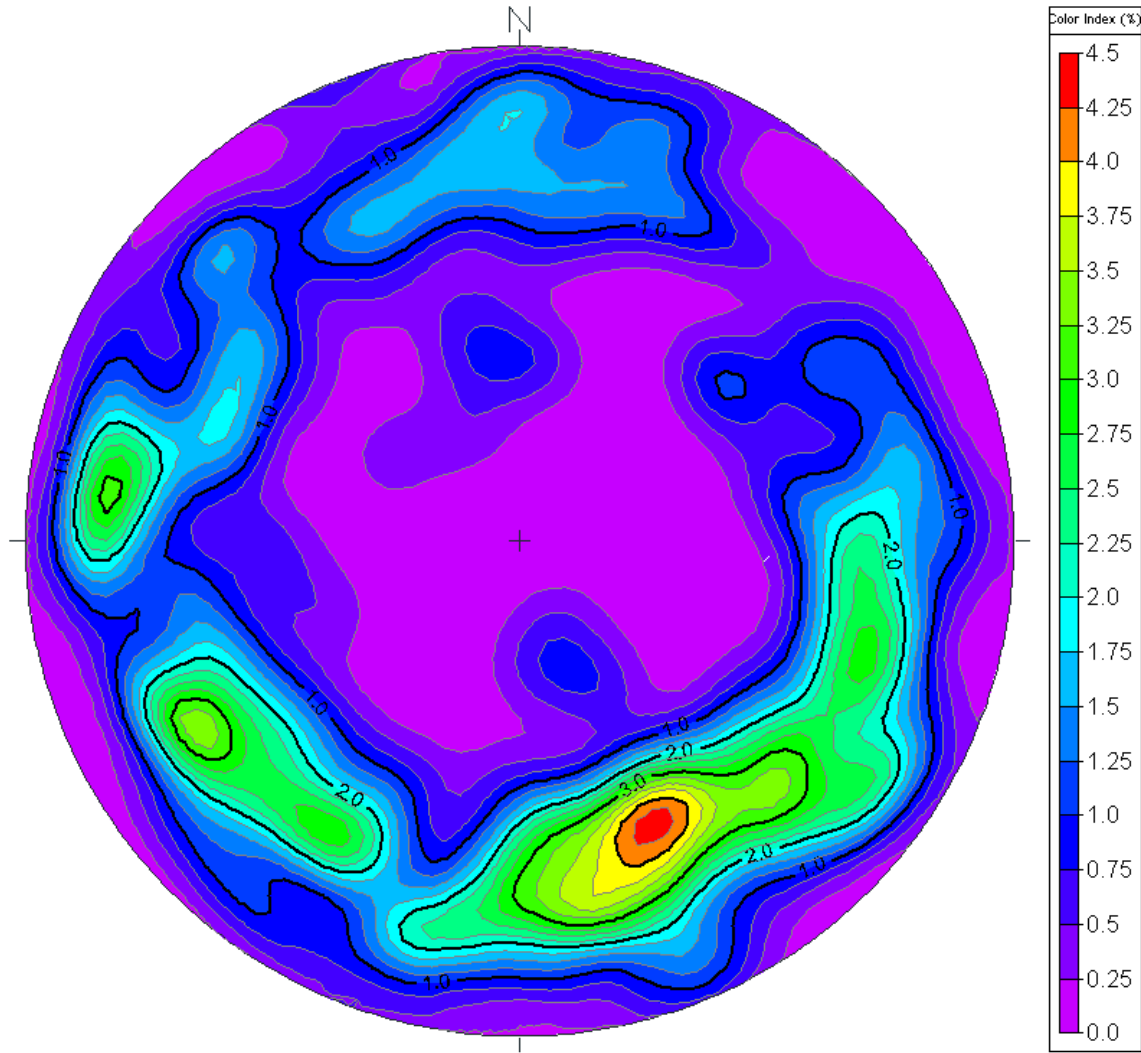
All directions are with respect to magnetic north.

Orientation Summary Table
Televiewer Features
CB and I
Edwards Air Force Base
Well: 37-B12
December 17, 2013

Feature No.	Depth (meters)	Depth (feet)	Dip Direction (degrees)	Dip Angle (degrees)	Feature Rank (0 to 5)
226	41.29	135.5	303	61	1
227	41.48	136.1	312	51	1
228	41.58	136.4	278	56	1
229	41.61	136.5	339	62	1
230	41.86	137.4	196	72	0
231	42.11	138.2	177	30	0
232	42.28	138.7	205	63	0
233	42.34	138.9	325	51	0
234	42.39	139.1	104	77	1
235	42.41	139.1	181	78	1
236	42.71	140.1	273	59	1
237	42.71	140.1	121	82	1
238	42.79	140.4	74	56	1
239	43.00	141.1	90	83	1
240	43.10	141.4	329	52	1
241	43.19	141.7	222	66	0
242	43.28	142.0	241	64	0
243	43.39	142.3	255	71	1
244	43.40	142.4	327	51	0
245	43.68	143.3	329	56	1
246	43.80	143.7	265	53	1
247	43.88	144.0	310	49	1
248	44.00	144.4	288	68	2
249	44.02	144.4	339	73	1
250	44.22	145.1	113	54	1
251	44.27	145.3	277	55	1
252	44.36	145.5	119	65	1
253	44.52	146.1	264	62	1
254	44.53	146.1	301	77	1
255	44.61	146.4	103	66	1
256	44.80	147.0	326	58	1
257	44.82	147.1	255	69	2
258	44.86	147.2	268	81	1
259	45.11	148.0	271	74	1
260	45.15	148.1	259	65	1
261	45.24	148.4	98	74	1
262	45.26	148.5	284	64	2
263	45.28	148.6	98	63	1
264	45.33	148.7	263	63	2
265	45.59	149.6	126	46	2
266	45.68	149.9	113	55	2
267	45.79	150.2	109	53	1
268	46.08	151.2	331	57	1
269	46.25	151.7	344	86	1

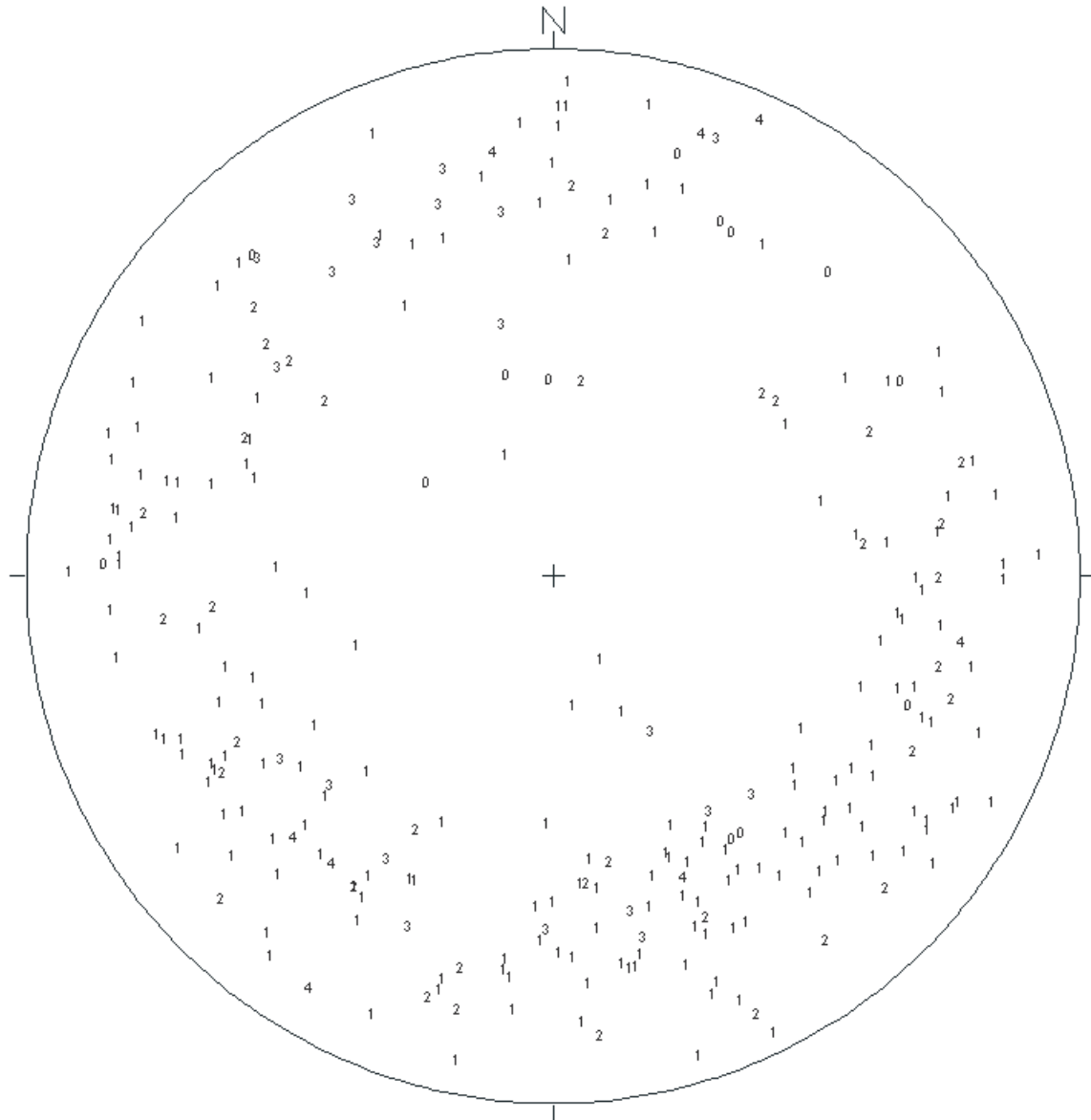
All directions are with respect to magnetic north.

**Stereonet Diagram – Schmidt Projection
Image Features
CB & I
Project: Edwards Air Force Base
Well: 37-B12
December 17, 2013**



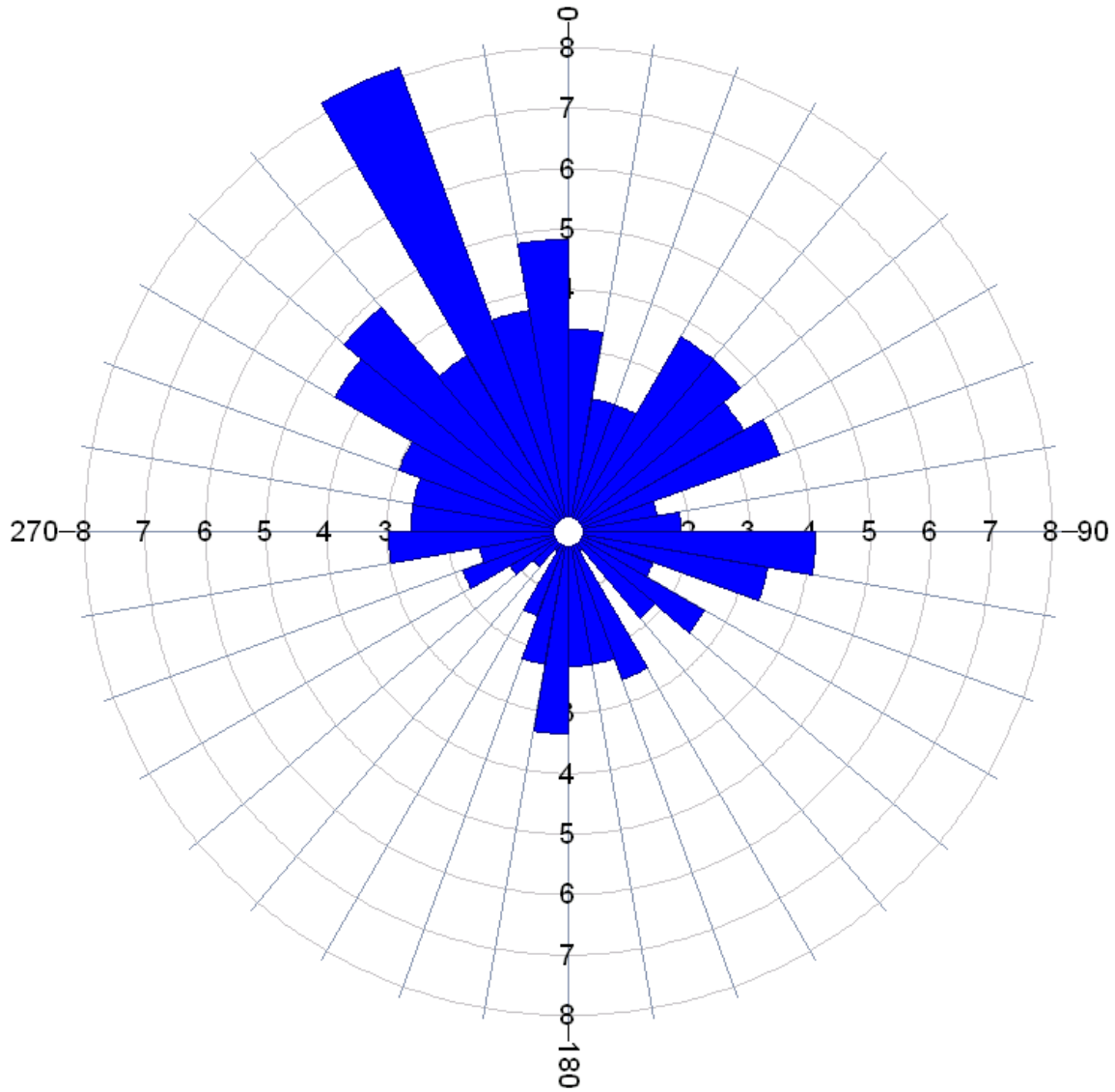
All directions are with respect to Magnetic North.

Stereonet Diagram – Schmidt Projection
Image Features
CB & I
Project: Edwards Air Force Base
Well: 37-B12
December 17, 2013



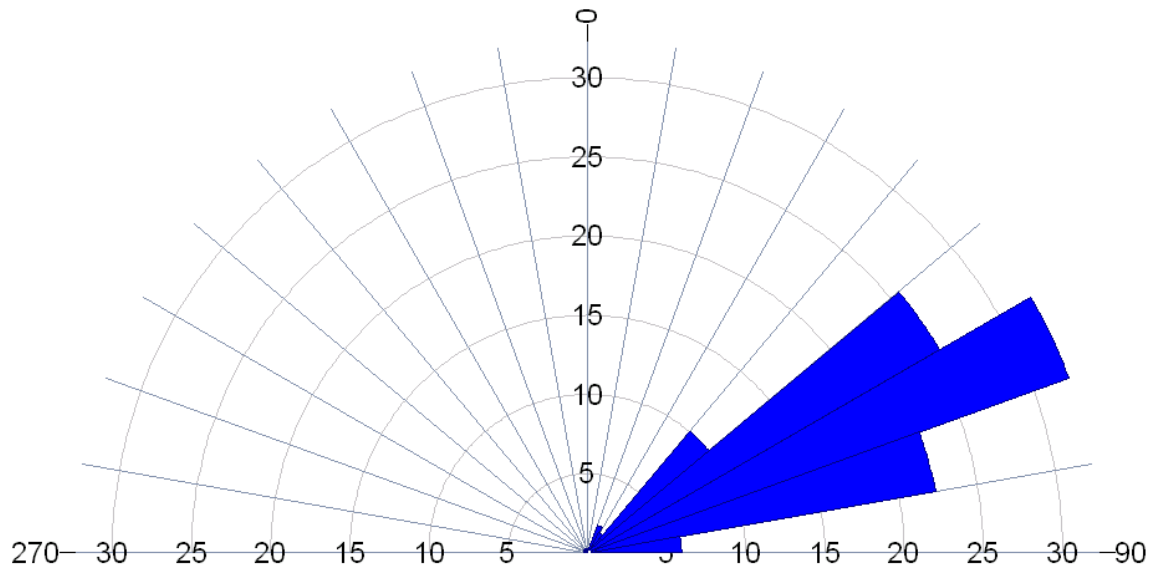
All directions are with respect to Magnetic North.

**Rose Diagram – Dip Directions
Image Features
CB & I
Project: Edwards Air Force Base
Well: 37-B12
December 17, 2013**



All directions are with respect to Magnetic North.

Rose Diagram – Dip Angles
Image Features
CB & I
Project: Edwards Air Force Base
Well: 37-B12
December 17, 2013



All directions are with respect to Magnetic North.



Flow Logs

COLOG Group

810 Quail Street, Suite E, Lakewood, CO 80215

Phone: (303) 279-0171, Fax: (303) 278-0135

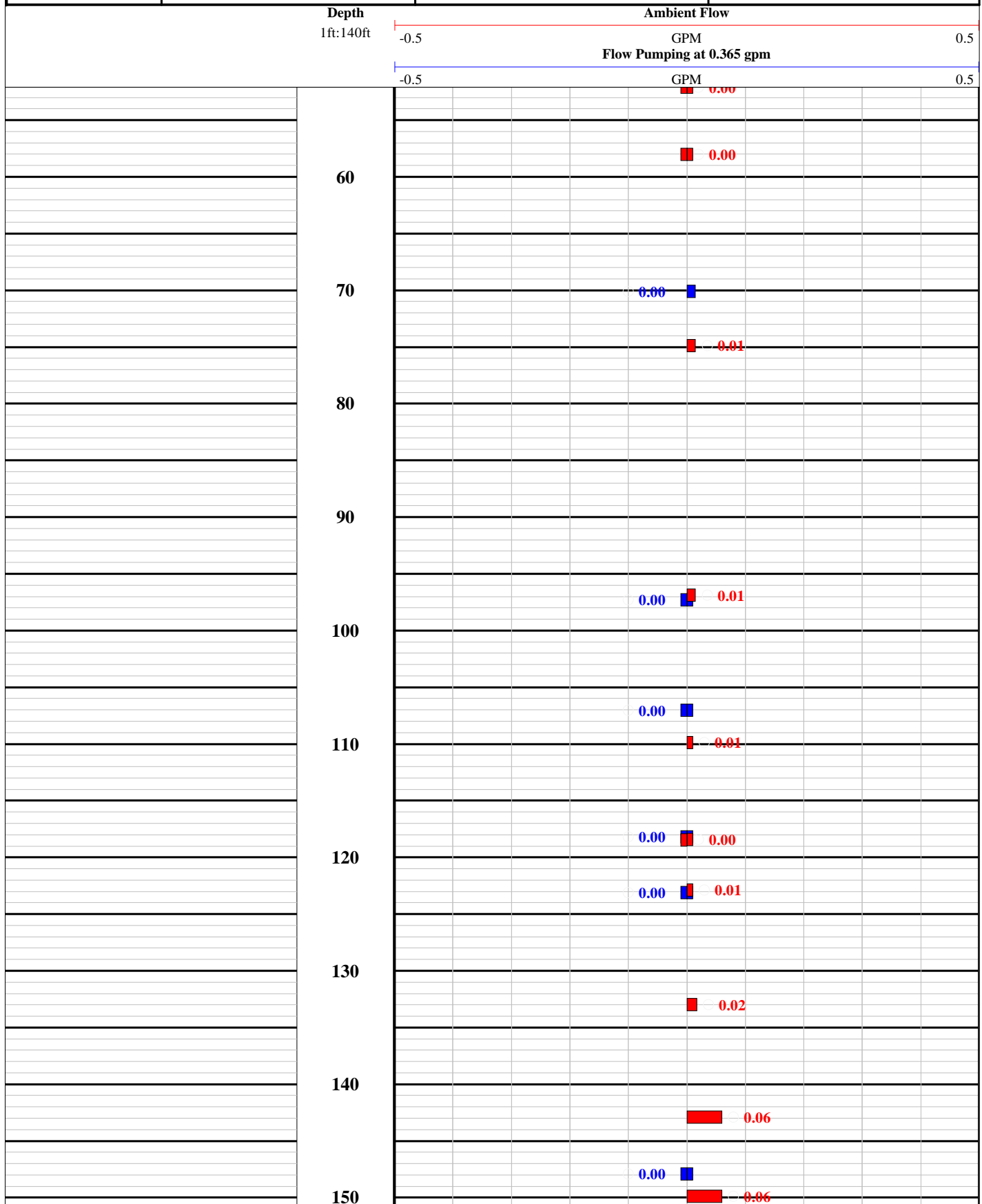
www.idsdrill.com

COMPANY: CB&I

PROJECT: Edwards AFB

DATE LOGGED: 19 December 2013

WELL: 37-B12



Appendix D



Optical & Acoustic Televiewer

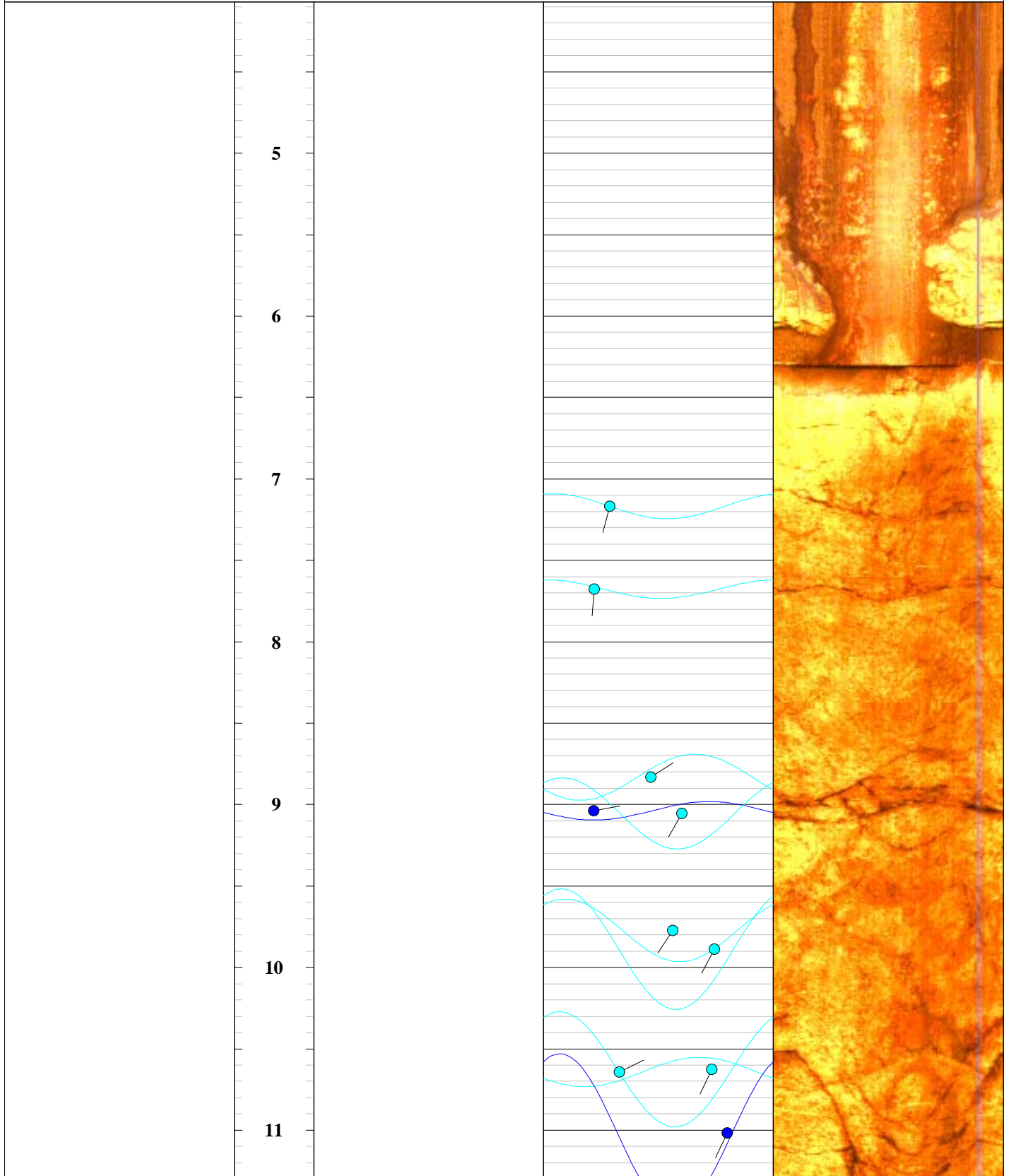
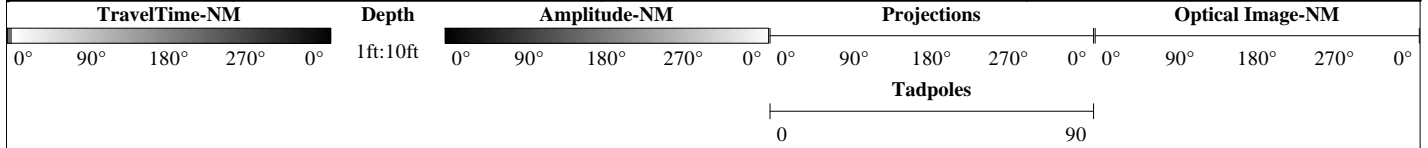
COMPANY: CB&I

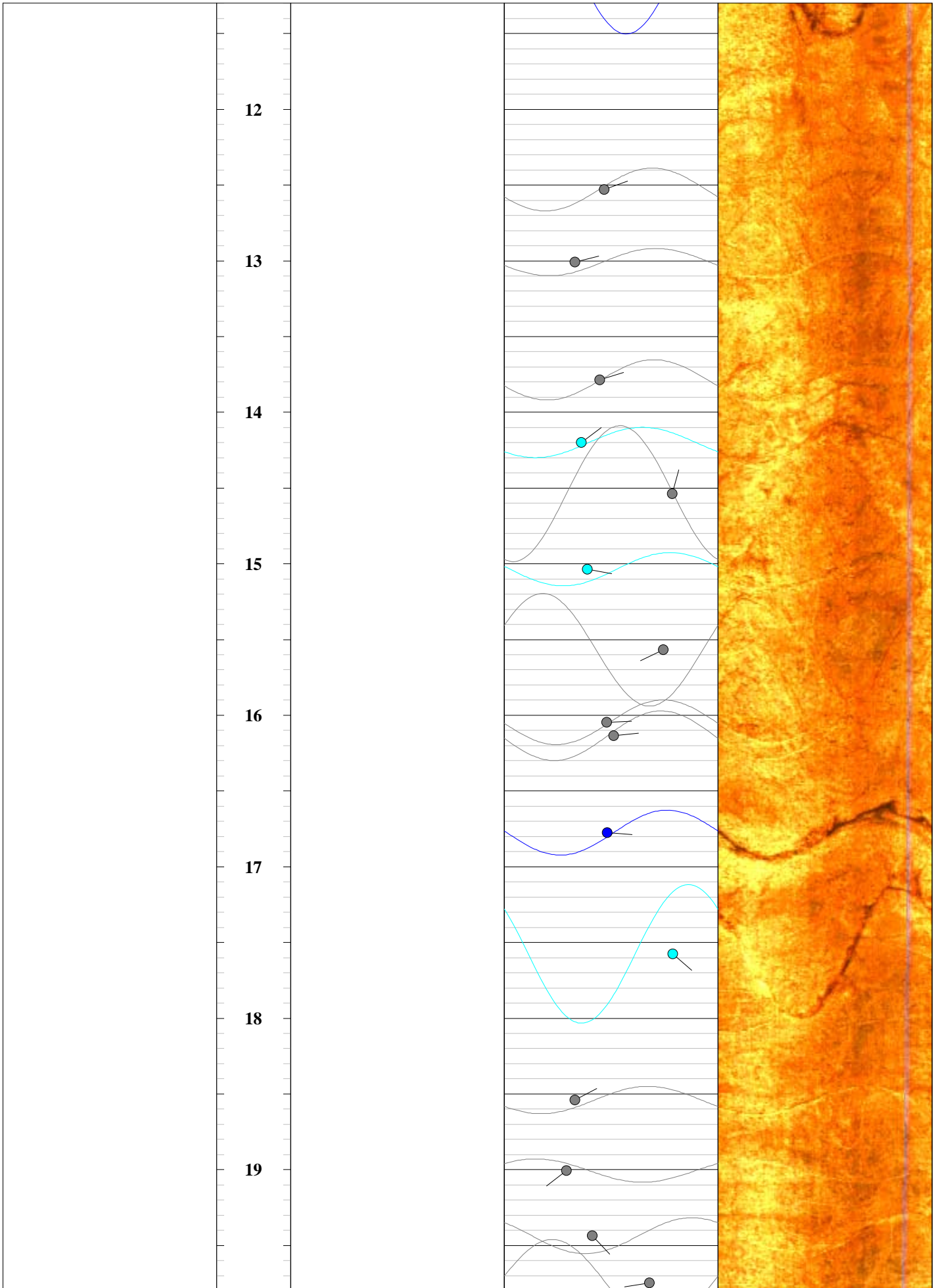
PROJECT: Edwards Air Force Base

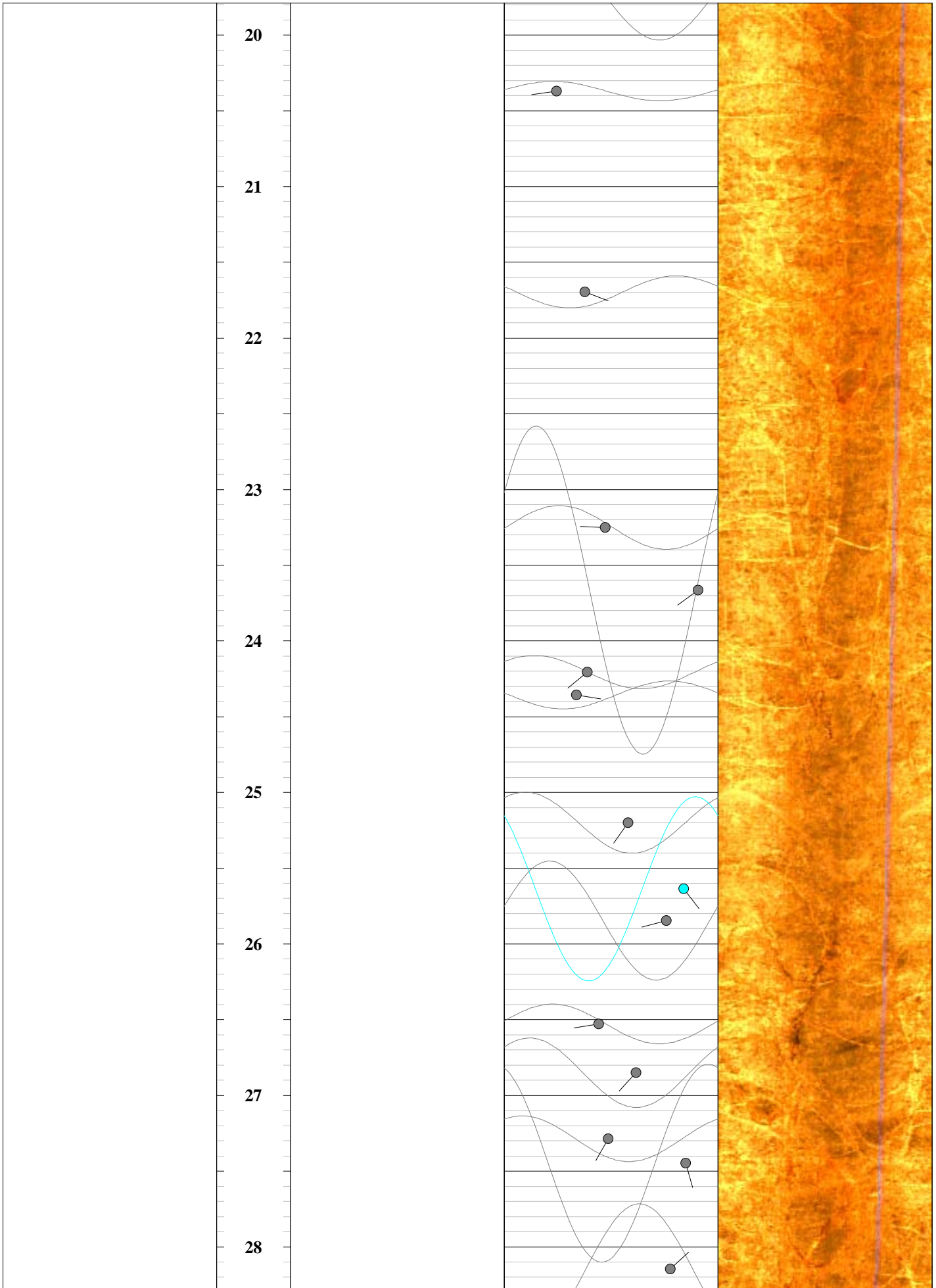
DATE LOGGED: 18 December 2013

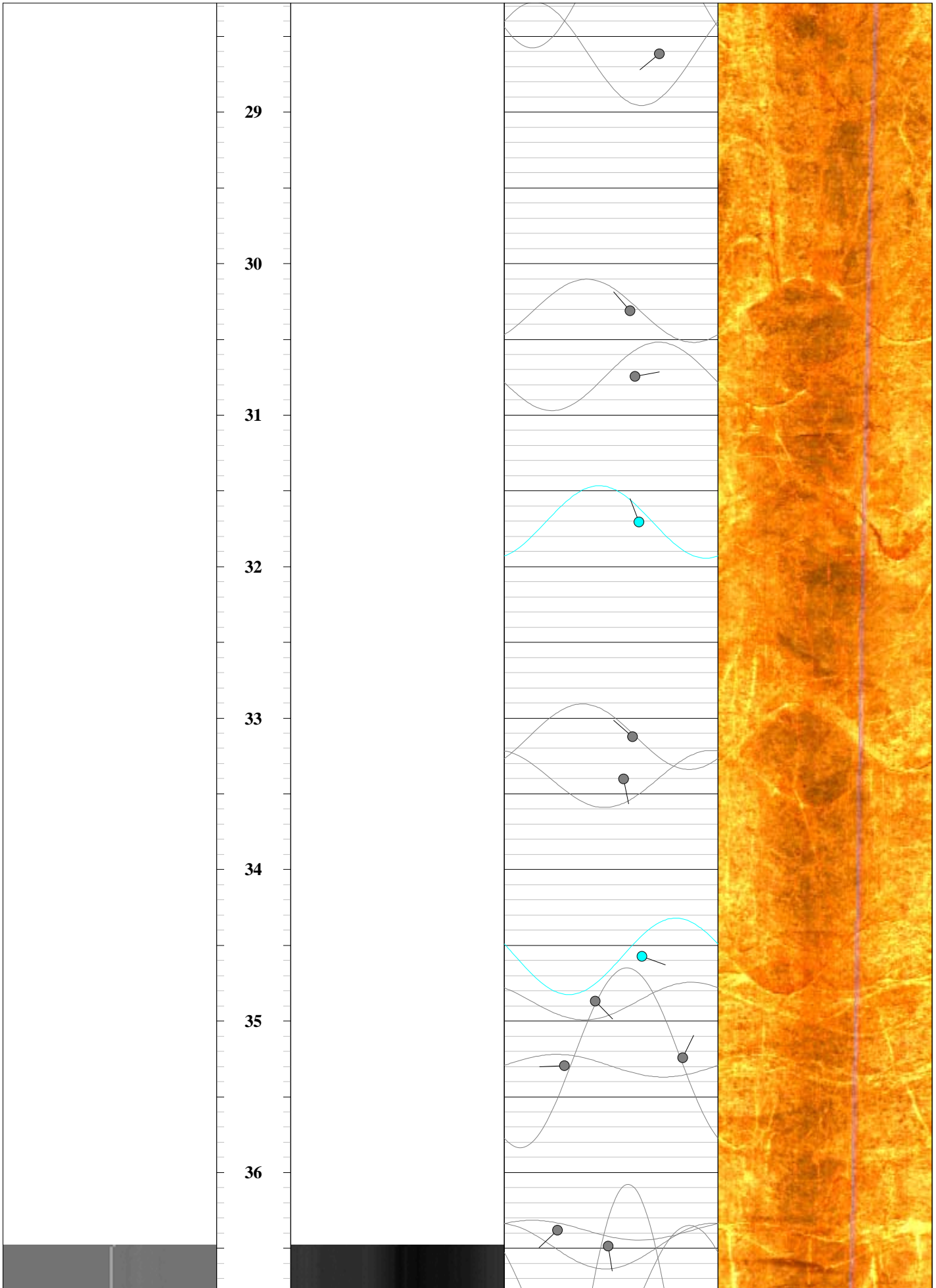
WELL: 37-B13

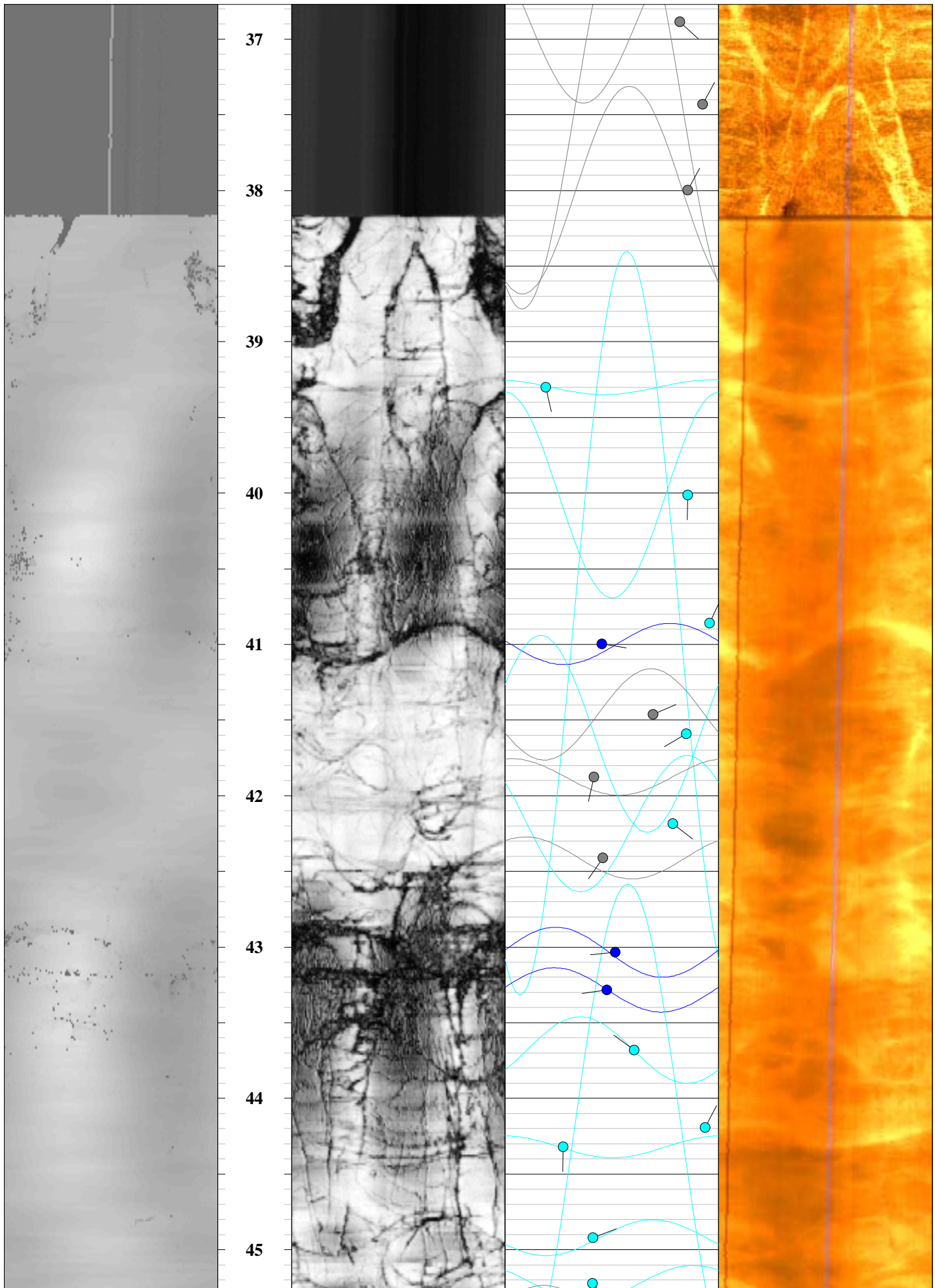
IDS - Colog Group
810 Quail Street, Suite E, Lakewood, CO 80215
Phone: (303) 279-0171, Fax: (303) 278-0135
www.idsdrill.com

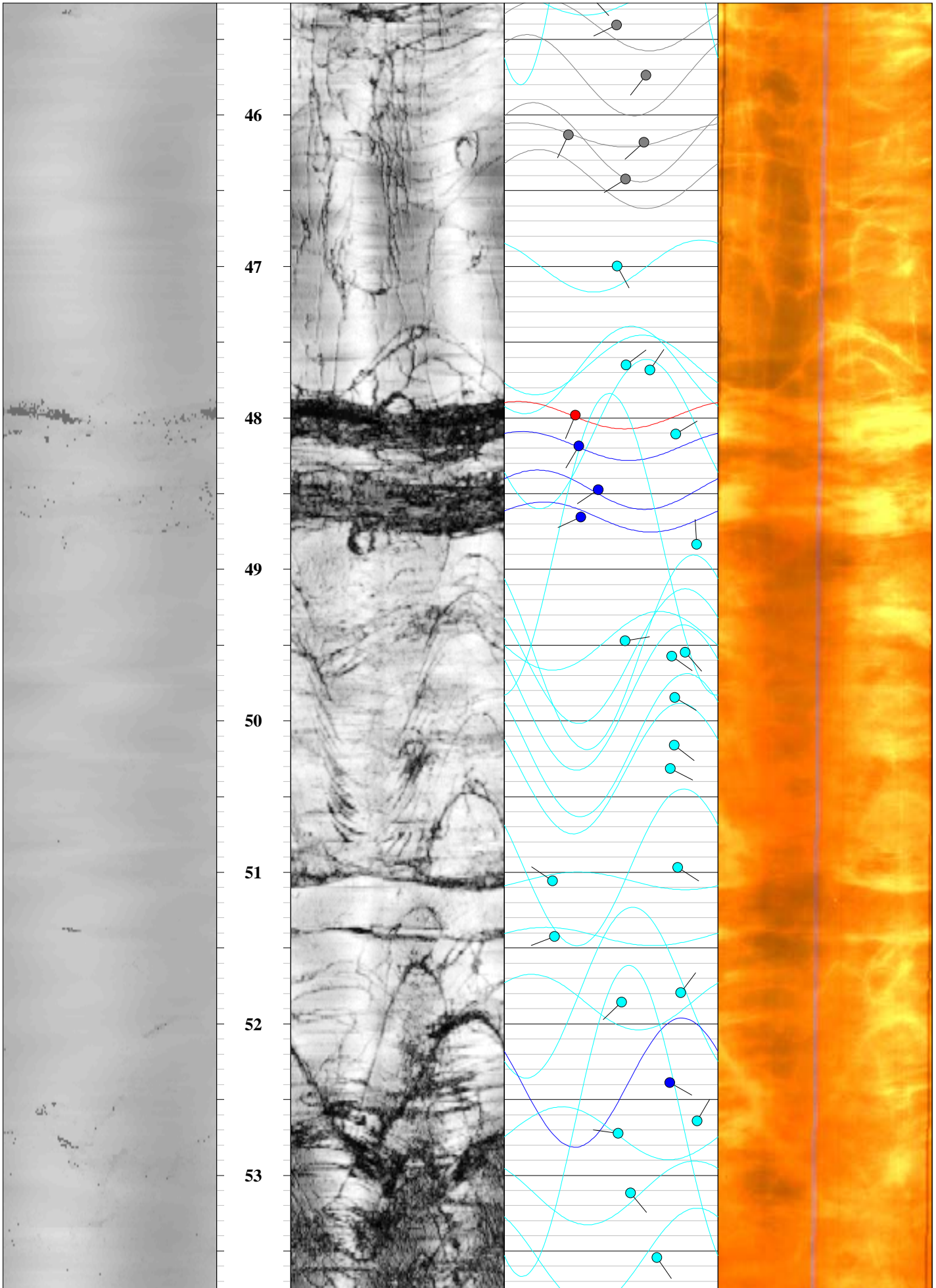


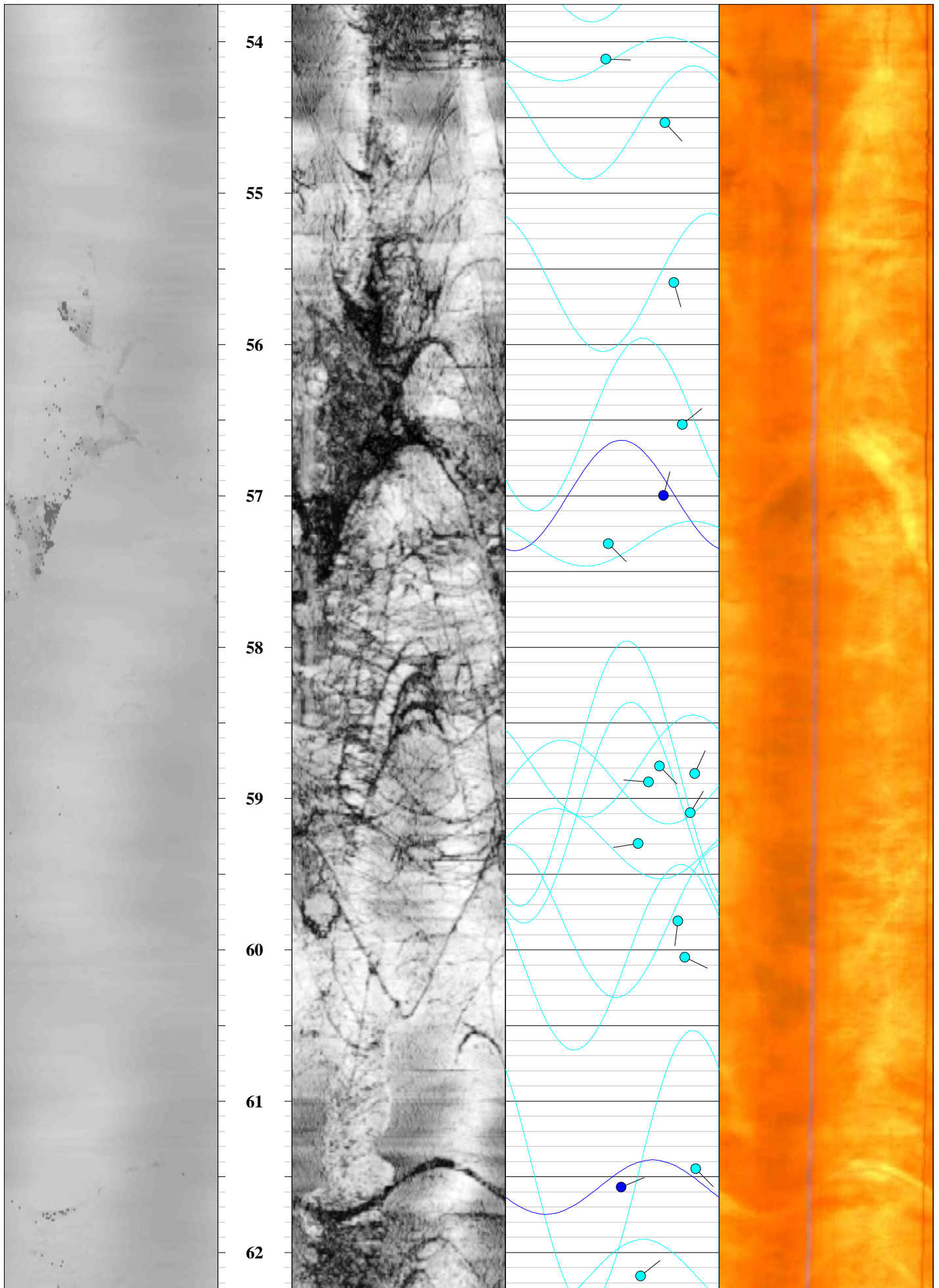


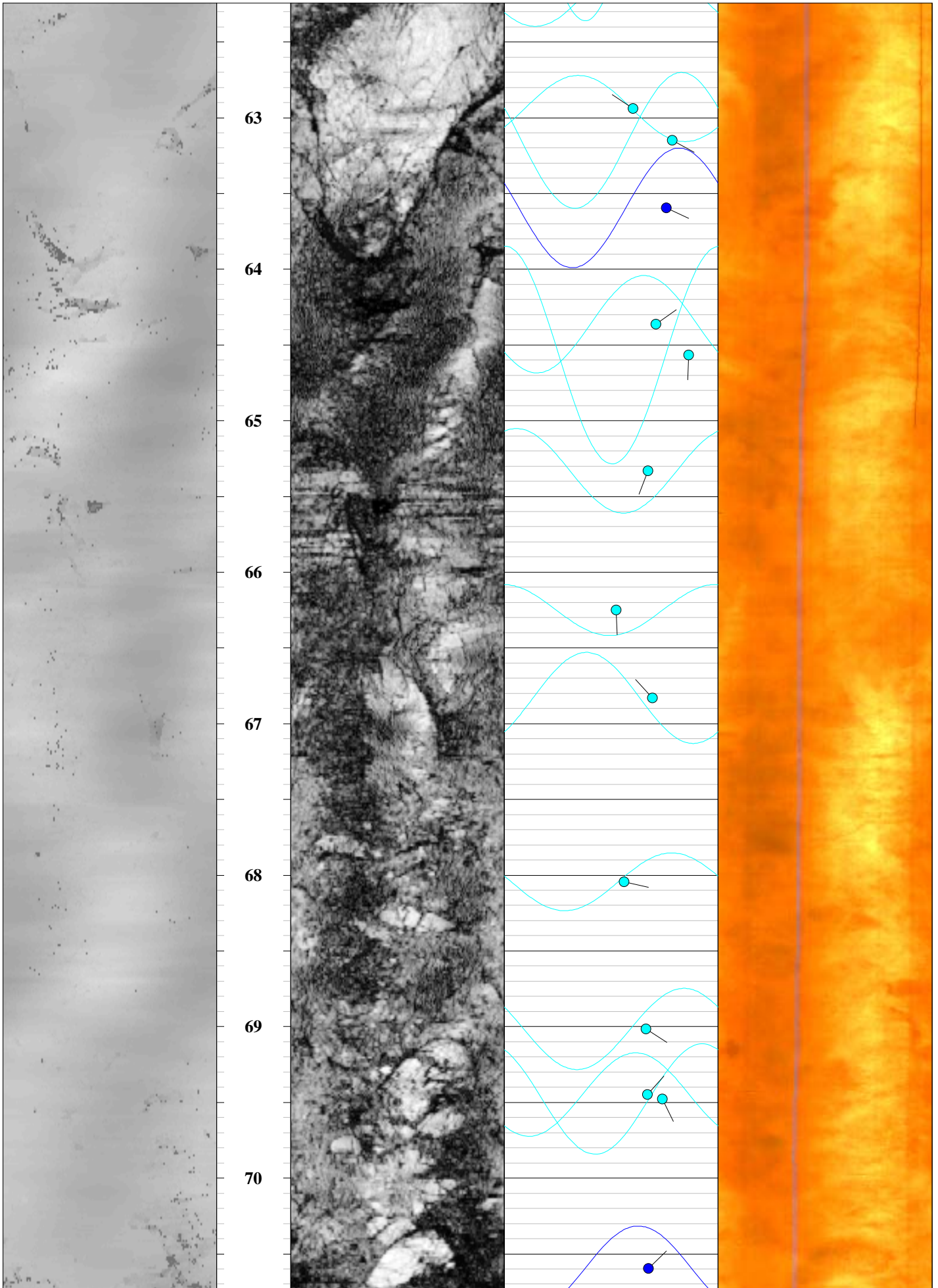


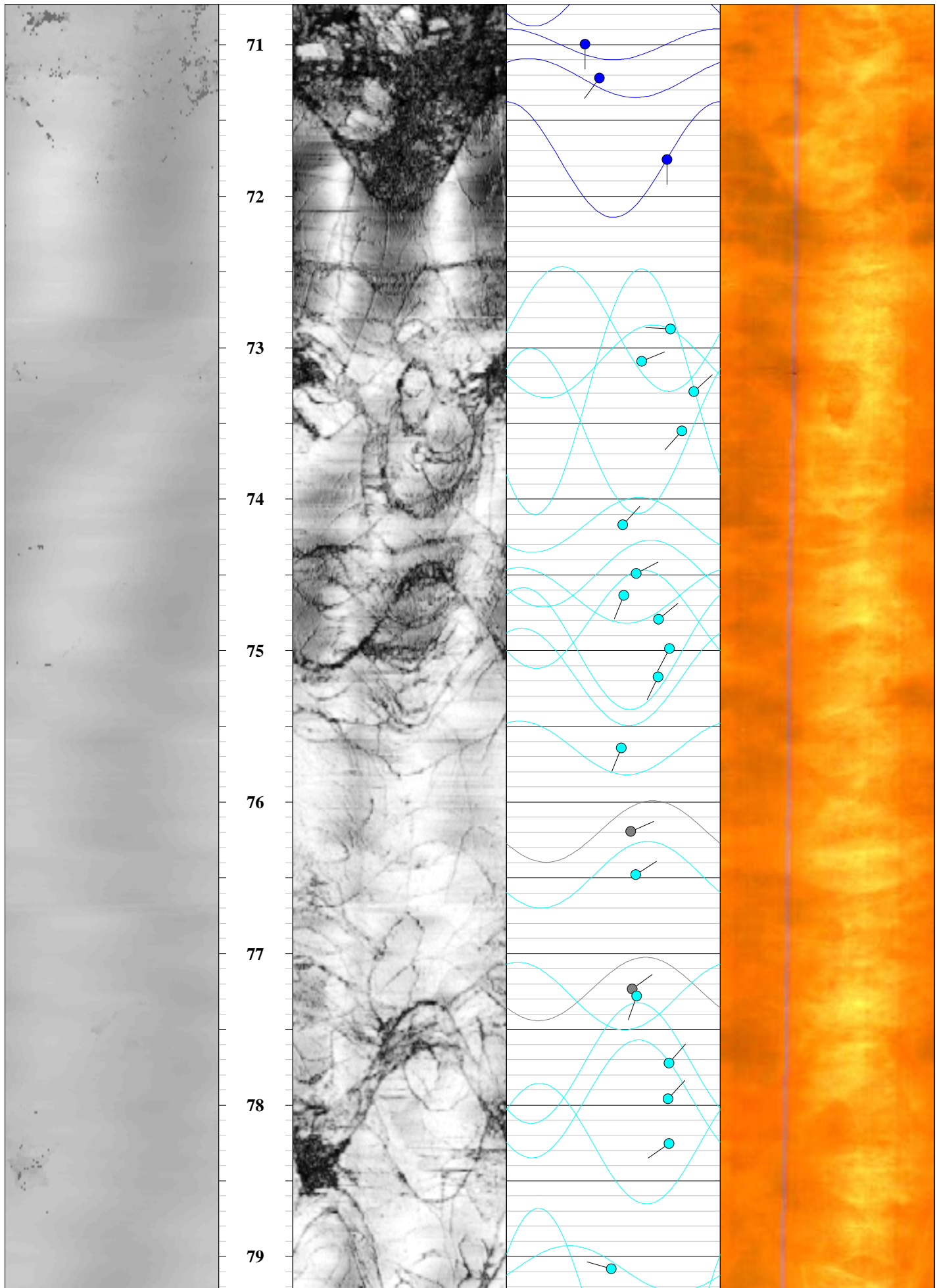


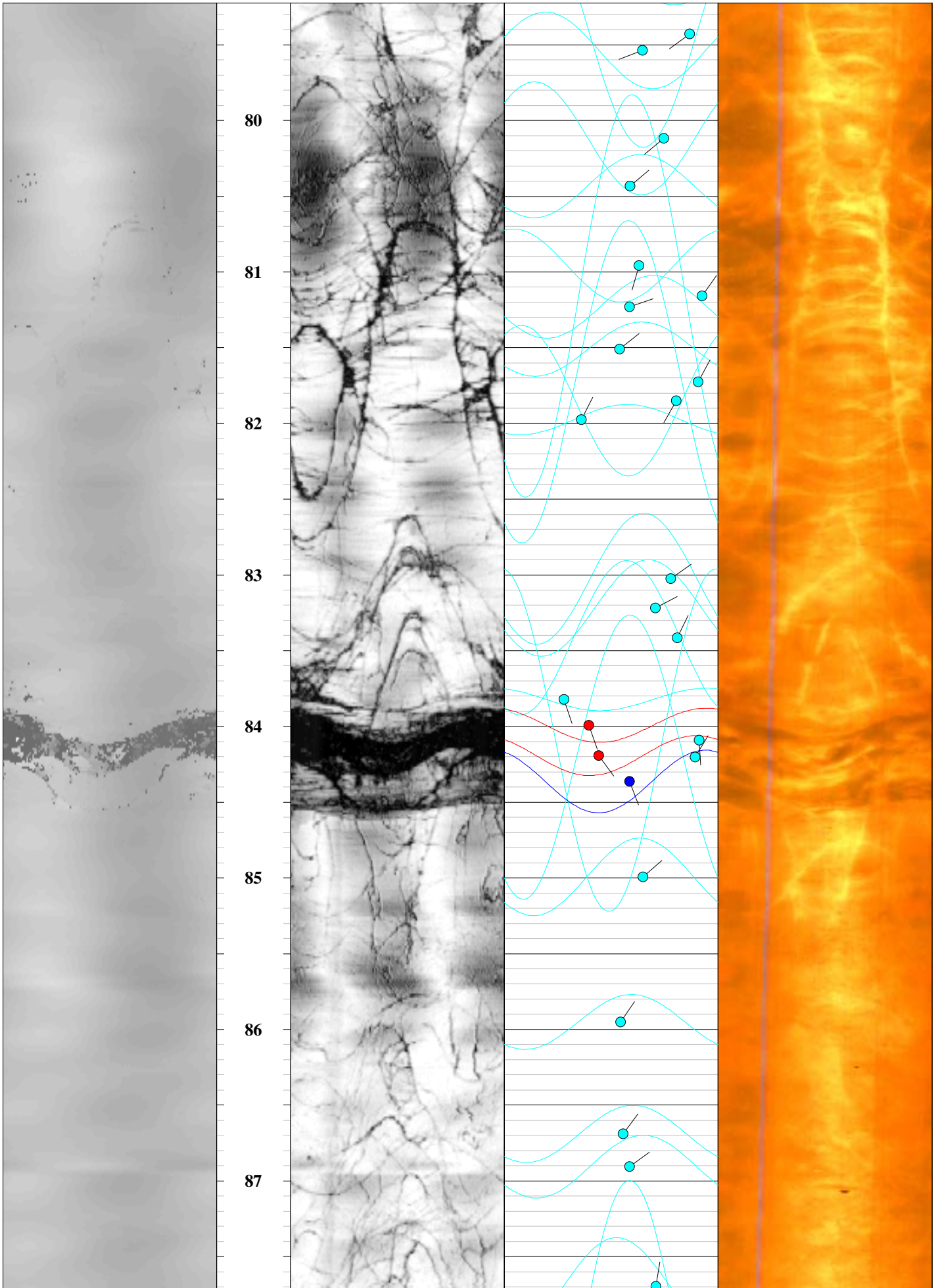


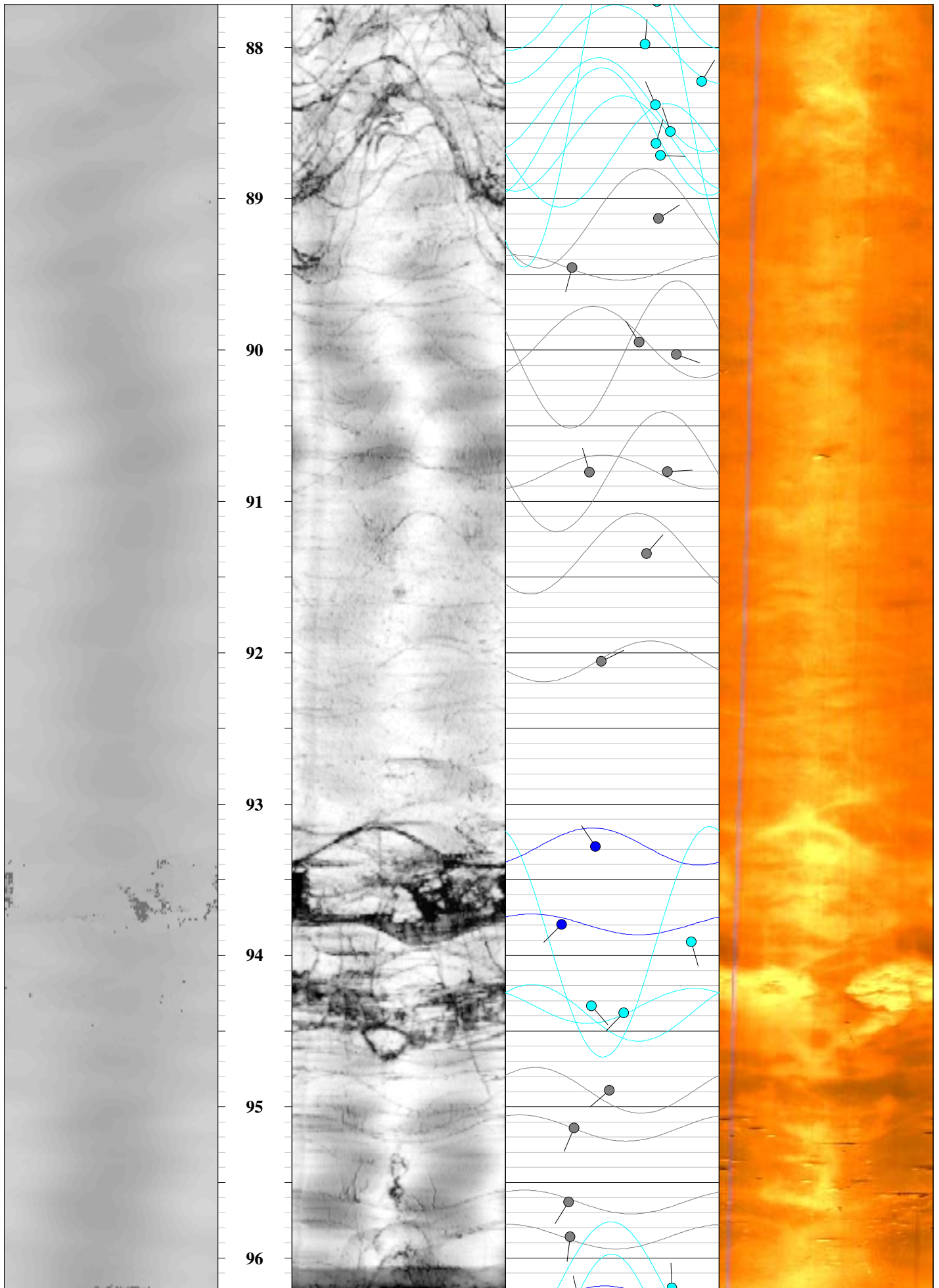


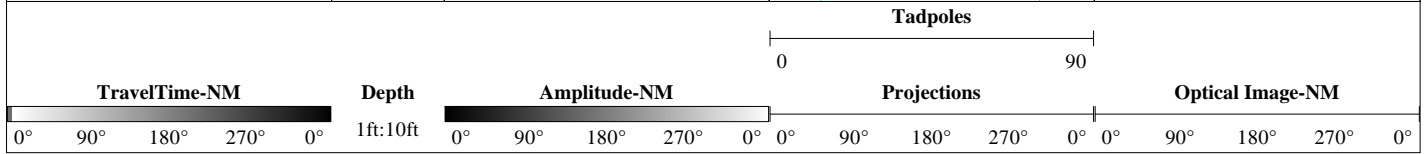
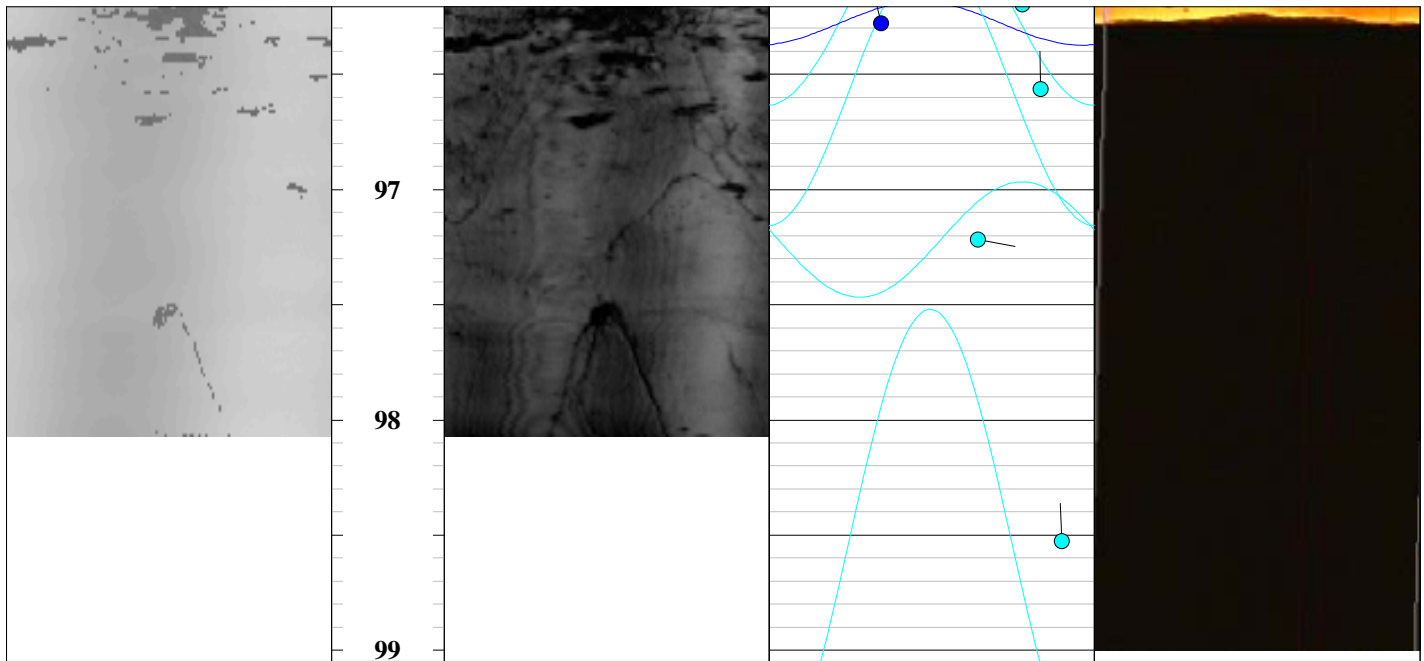












Orientation Summary Table
Televiewer Features
CB and I
Edwards Air Force Base
Well: 37-B13
December 18, 2013

Feature No.	Depth (meters)	Depth (feet)	Dip Direction (degrees)	Dip Angle (degrees)	Feature Rank (0 to 5)
1	2.19	7.2	194	26	1
2	2.34	7.7	184	20	1
3	2.69	8.8	57	42	1
4	2.76	9.0	79	20	2
5	2.76	9.1	210	54	1
6	2.98	9.8	214	51	1
7	3.01	9.9	208	67	1
8	3.24	10.6	205	66	1
9	3.24	10.6	65	30	1
10	3.36	11.0	206	72	2
11	3.82	12.5	70	42	0
12	3.97	13.0	76	30	0
13	4.20	13.8	72	40	0
14	4.33	14.2	53	32	1
15	4.43	14.5	15	71	0
16	4.58	15.0	99	35	1
17	4.75	15.6	244	67	0
18	4.89	16.1	88	43	0
19	4.92	16.1	84	46	0
20	5.11	16.8	94	43	2
21	5.36	17.6	130	71	1
22	5.65	18.5	62	30	0
23	5.79	19.0	233	26	0
24	5.93	19.4	136	37	0
25	6.02	19.8	261	61	0
26	6.21	20.4	262	22	0
27	6.61	21.7	110	34	0
28	7.09	23.3	273	42	0
29	7.21	23.7	234	82	0
30	7.38	24.2	231	35	0
31	7.42	24.4	98	30	0
32	7.68	25.2	215	52	0
33	7.82	25.6	142	75	1
34	7.88	25.9	256	68	0
35	8.09	26.5	261	40	0
36	8.18	26.9	222	55	0
37	8.32	27.3	210	44	0
38	8.37	27.5	164	76	0
39	8.58	28.2	47	70	0
40	8.72	28.6	231	65	0
41	9.24	30.3	319	53	0
42	9.37	30.7	80	55	0
43	9.67	31.7	340	57	1
44	10.09	33.1	312	54	0
45	10.18	33.4	169	50	0

All directions are with respect to magnetic north.

**Orientation Summary Table
 Televiewer Features
 CB and I
 Edwards Air Force Base
 Well: 37-B13
 December 18, 2013**

Feature No.	Depth (meters)	Depth (feet)	Dip Direction (degrees)	Dip Angle (degrees)	Feature Rank (0 to 5)
46	10.54	34.6	109	58	1
47	10.63	34.9	135	38	0
48	10.74	35.2	27	75	0
49	10.76	35.3	268	25	0
50	11.09	36.4	227	22	0
51	11.12	36.5	171	44	0
52	11.24	36.9	132	74	0
53	11.41	37.4	29	83	0
54	11.58	38.0	29	77	0
55	11.98	39.3	168	17	1
56	12.20	40.0	181	77	1
57	12.45	40.9	25	86	1
58	12.50	41.0	99	41	2
59	12.64	41.5	66	62	0
60	12.68	41.6	240	76	1
61	12.77	41.9	192	37	0
62	12.86	42.2	127	71	1
63	12.93	42.4	214	41	0
64	13.12	43.0	265	46	2
65	13.19	43.3	263	43	2
66	13.31	43.7	307	54	1
67	13.47	44.2	27	84	1
68	13.51	44.3	181	24	1
69	13.69	44.9	69	37	1
70	13.78	45.2	137	37	1
71	13.84	45.4	244	47	0
72	13.94	45.7	218	60	0
73	14.06	46.1	205	27	0
74	14.08	46.2	228	59	0
75	14.15	46.4	238	51	0
76	14.33	47.0	151	48	1
77	14.52	47.7	52	51	1
78	14.53	47.7	34	61	1
79	14.62	48.0	203	30	3
80	14.66	48.1	59	72	1
81	14.69	48.2	210	31	2
82	14.77	48.5	236	39	2
83	14.83	48.7	246	32	2
84	14.89	48.8	357	81	1
85	15.08	49.5	81	51	1
86	15.10	49.6	139	76	1
87	15.11	49.6	125	70	1
88	15.19	49.9	121	72	1
89	15.29	50.2	127	72	1
90	15.34	50.3	116	70	1

All directions are with respect to magnetic north.

Orientation Summary Table
Televiewer Features
CB and I
Edwards Air Force Base
Well: 37-B13
December 18, 2013

Feature No.	Depth (meters)	Depth (feet)	Dip Direction (degrees)	Dip Angle (degrees)	Feature Rank (0 to 5)
91	15.54	51.0	123	73	1
92	15.56	51.1	304	20	1
93	15.67	51.4	250	21	1
94	15.79	51.8	36	74	1
95	15.81	51.9	226	49	1
96	15.97	52.4	119	70	2
97	16.04	52.6	30	81	1
98	16.07	52.7	278	48	1
99	16.19	53.1	140	53	1
100	16.32	53.5	145	64	1
101	16.49	54.1	92	42	1
102	16.62	54.5	136	67	1
103	16.94	55.6	164	71	1
104	17.23	56.5	51	75	1
105	17.37	57.0	15	67	2
106	17.47	57.3	135	43	1
107	17.92	58.8	136	65	1
108	17.93	58.8	24	80	1
109	17.95	58.9	275	60	1
110	18.01	59.1	31	78	1
111	18.07	59.3	262	56	1
112	18.23	59.8	187	73	1
113	18.30	60.1	116	76	1
114	18.73	61.5	136	80	1
115	18.77	61.6	68	49	2
116	18.95	62.2	52	57	1
117	19.18	62.9	304	54	1
118	19.25	63.2	119	71	1
119	19.39	63.6	115	68	2
120	19.62	64.4	55	64	1
121	19.68	64.6	182	78	1
122	19.91	65.3	200	61	1
123	20.19	66.3	177	47	1
124	20.37	66.8	318	62	1
125	20.74	68.0	102	50	1
126	21.04	69.0	122	60	1
127	21.17	69.5	42	60	1
128	21.18	69.5	153	67	1
129	21.52	70.6	46	61	2
130	21.64	71.0	179	33	2
131	21.71	71.2	217	39	2
132	21.87	71.8	180	68	2
133	22.21	72.9	273	69	1
134	22.28	73.1	68	57	1
135	22.34	73.3	47	79	1

All directions are with respect to magnetic north.

Orientation Summary Table
Televiewer Features
CB and I
Edwards Air Force Base
Well: 37-B13
December 18, 2013

Feature No.	Depth (meters)	Depth (feet)	Dip Direction (degrees)	Dip Angle (degrees)	Feature Rank (0 to 5)
136	22.42	73.6	221	74	1
137	22.61	74.2	43	49	1
138	22.70	74.5	63	55	1
139	22.75	74.6	202	49	1
140	22.80	74.8	51	64	1
141	22.86	75.0	208	69	1
142	22.91	75.2	206	64	1
143	23.06	75.6	202	48	1
144	23.22	76.2	67	52	0
145	23.31	76.5	58	54	1
146	23.54	77.2	54	53	0
147	23.55	77.3	199	55	1
148	23.69	77.7	41	68	1
149	23.76	78.0	43	68	1
150	23.85	78.3	236	68	1
151	24.10	79.1	286	44	1
152	24.21	79.4	234	78	1
153	24.24	79.5	249	58	1
154	24.42	80.1	231	67	1
155	24.52	80.4	50	53	1
156	24.68	81.0	196	57	1
157	24.74	81.2	35	83	1
158	24.76	81.2	71	53	1
159	24.84	81.5	51	49	1
160	24.91	81.7	29	82	1
161	24.95	81.9	209	72	1
162	24.99	82.0	27	32	1
163	25.31	83.0	54	70	1
164	25.37	83.2	62	64	1
165	25.42	83.4	26	73	1
166	25.55	83.8	161	25	1
167	25.60	84.0	160	36	3
168	25.63	84.1	176	82	1
169	25.66	84.2	144	40	3
170	25.66	84.2	32	80	1
171	25.71	84.4	159	53	2
172	25.90	85.0	49	58	1
173	26.20	86.0	34	49	1
174	26.42	86.7	37	50	1
175	26.49	86.9	54	53	1
176	26.73	87.7	9	64	1
177	26.82	88.0	4	59	1
178	26.89	88.2	31	83	1
179	26.94	88.4	337	63	1
180	26.99	88.6	342	70	1

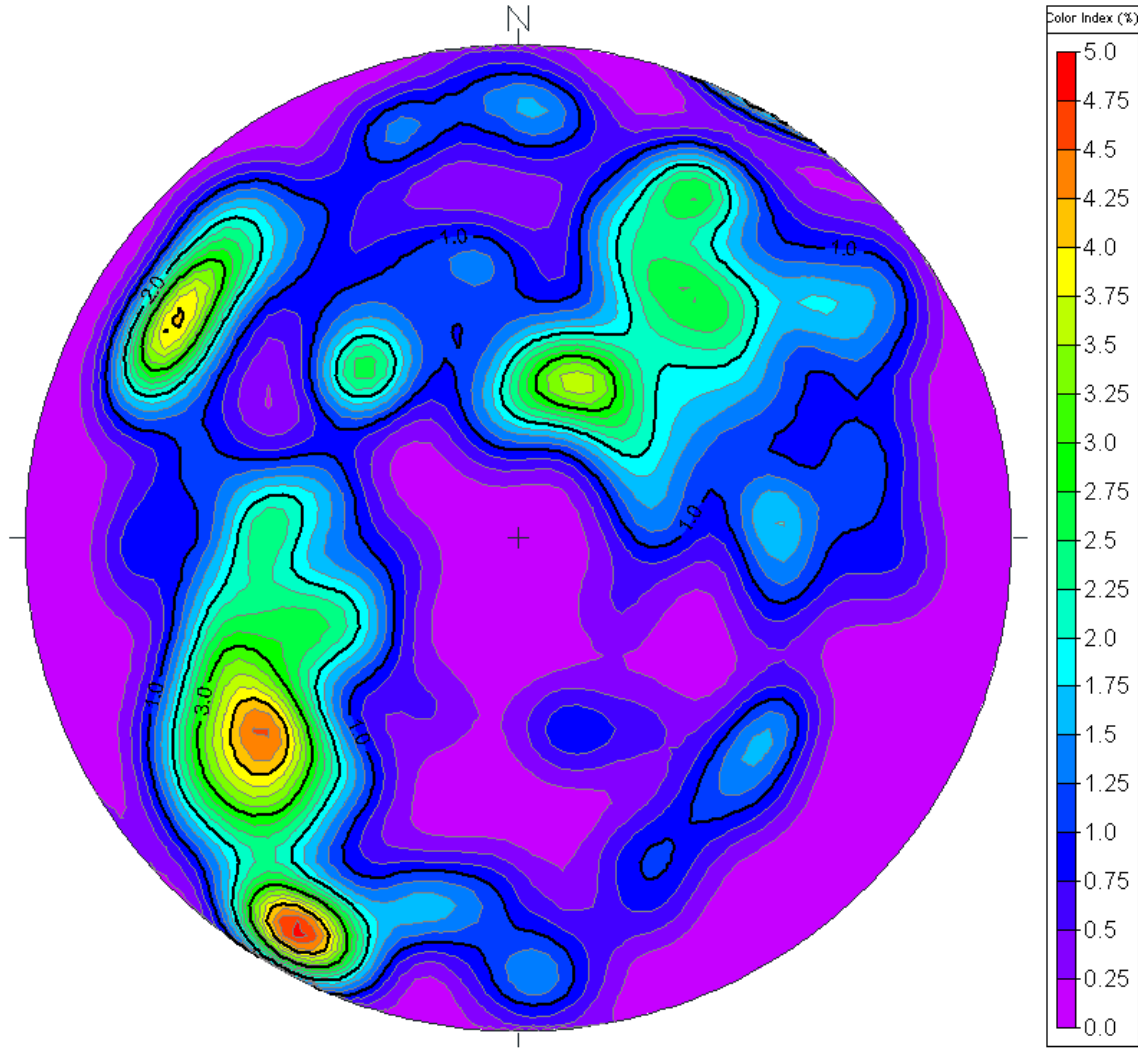
All directions are with respect to magnetic north.

**Orientation Summary Table
 Televiewer Features
 CB and I
 Edwards Air Force Base
 Well: 37-B13
 December 18, 2013**

Feature No.	Depth (meters)	Depth (feet)	Dip Direction (degrees)	Dip Angle (degrees)	Feature Rank (0 to 5)
181	27.01	88.6	17	63	1
182	27.04	88.7	92	65	1
183	27.17	89.1	57	64	0
184	27.26	89.5	195	28	0
185	27.42	90.0	328	56	0
186	27.44	90.0	109	72	0
187	27.68	90.8	86	68	0
188	27.68	90.8	344	35	0
189	27.84	91.4	41	60	0
190	28.06	92.1	64	40	0
191	28.43	93.3	326	38	2
192	28.59	93.8	225	24	2
193	28.62	93.9	164	78	1
194	28.75	94.3	138	36	1
195	28.77	94.4	224	50	1
196	28.92	94.9	229	44	0
197	29.00	95.1	203	29	0
198	29.15	95.6	212	27	0
199	29.22	95.9	186	27	0
200	29.32	96.2	358	70	1
201	29.35	96.3	347	31	2
202	29.43	96.6	359	75	1
203	29.63	97.2	100	58	1
204	30.03	98.5	358	81	1

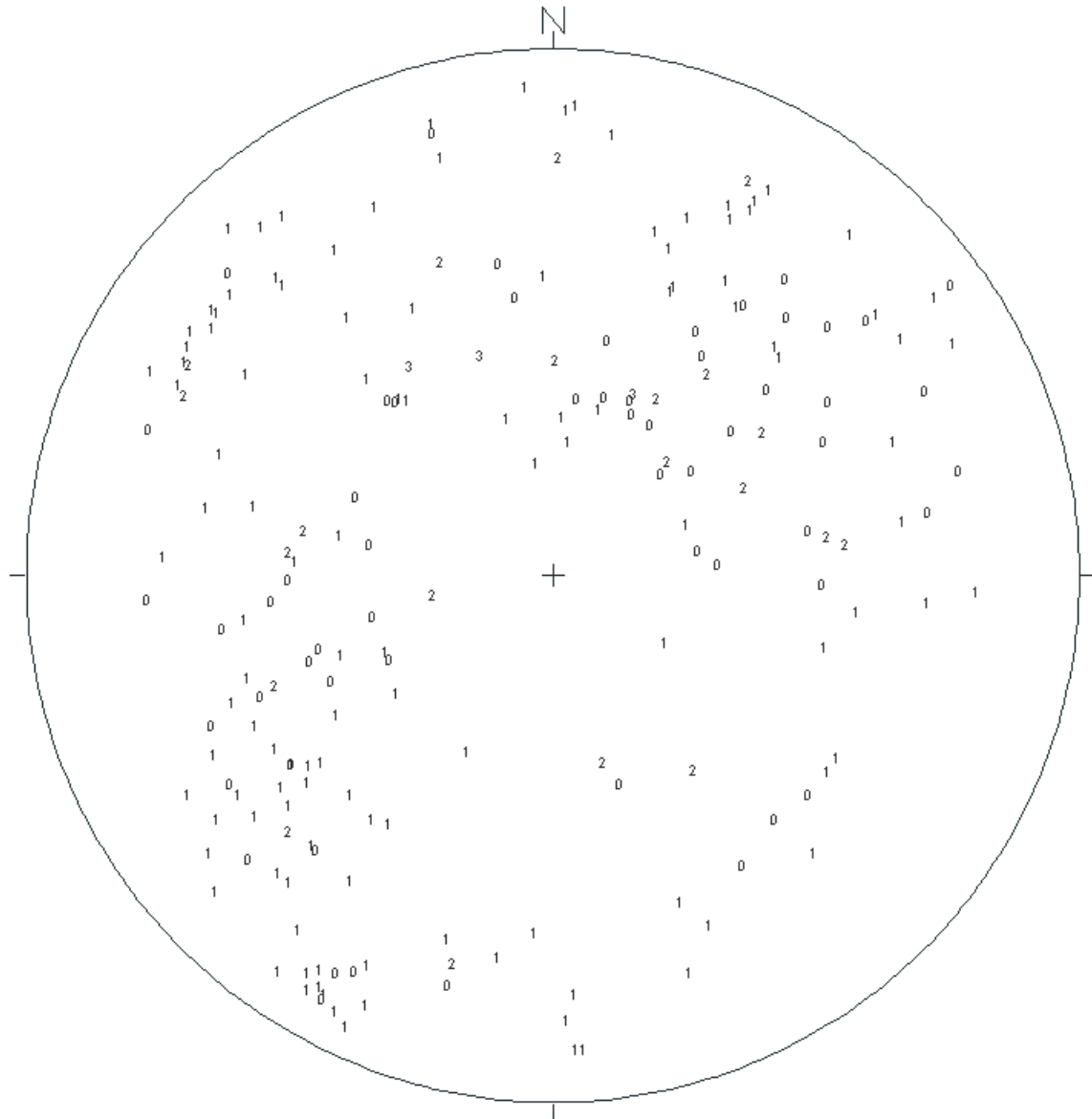
All directions are with respect to magnetic north.

**Stereonet Diagram – Schmidt Projection
Image Features
CB & I
Project: Edwards Air Force Base
Well: 37-B13
December 18, 2013**



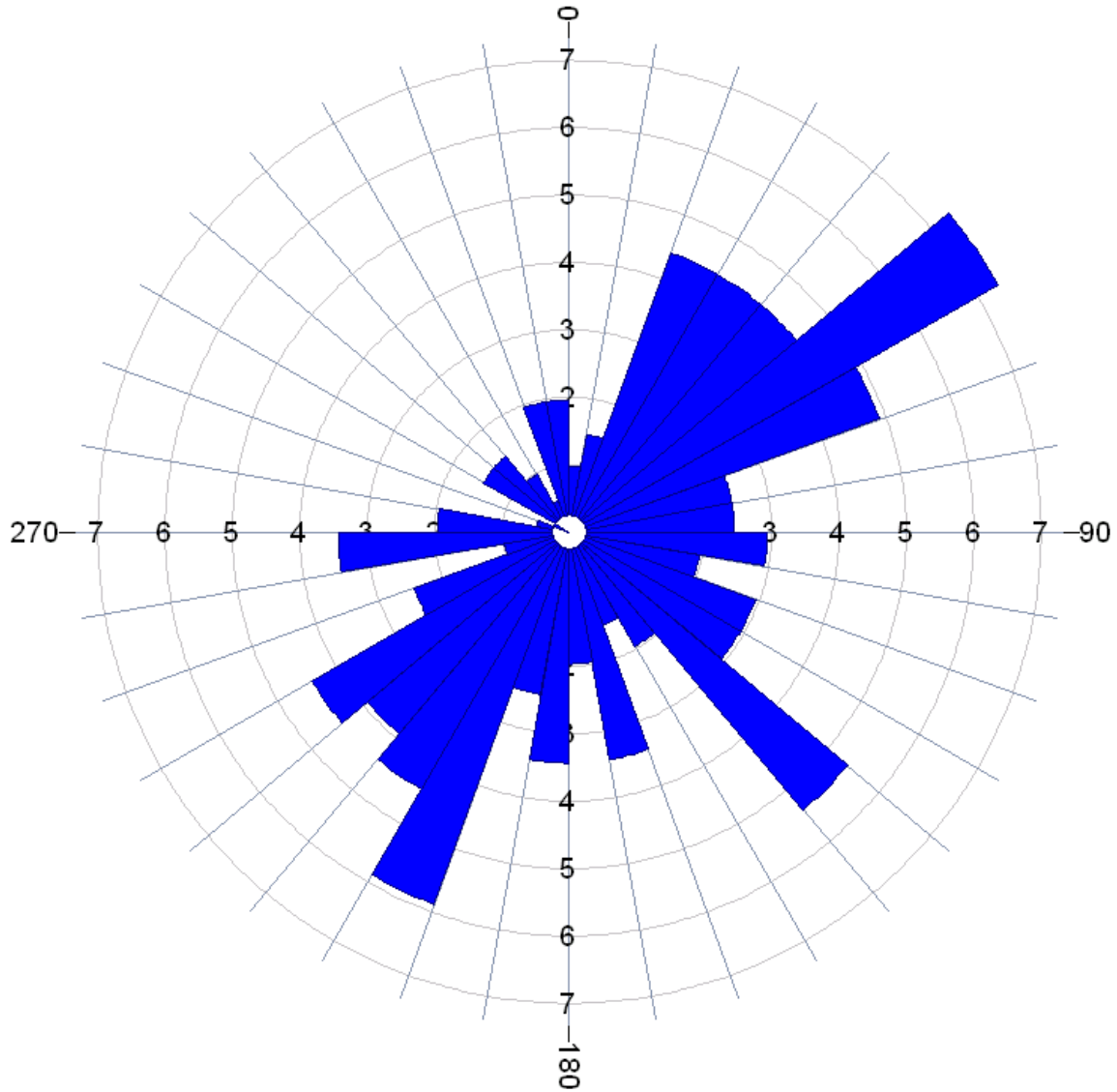
All directions are with respect to Magnetic North.

Stereonet Diagram – Schmidt Projection
Image Features
CB & I
Project: Edwards Air Force Base
Well: 37-B13
December 18, 2013



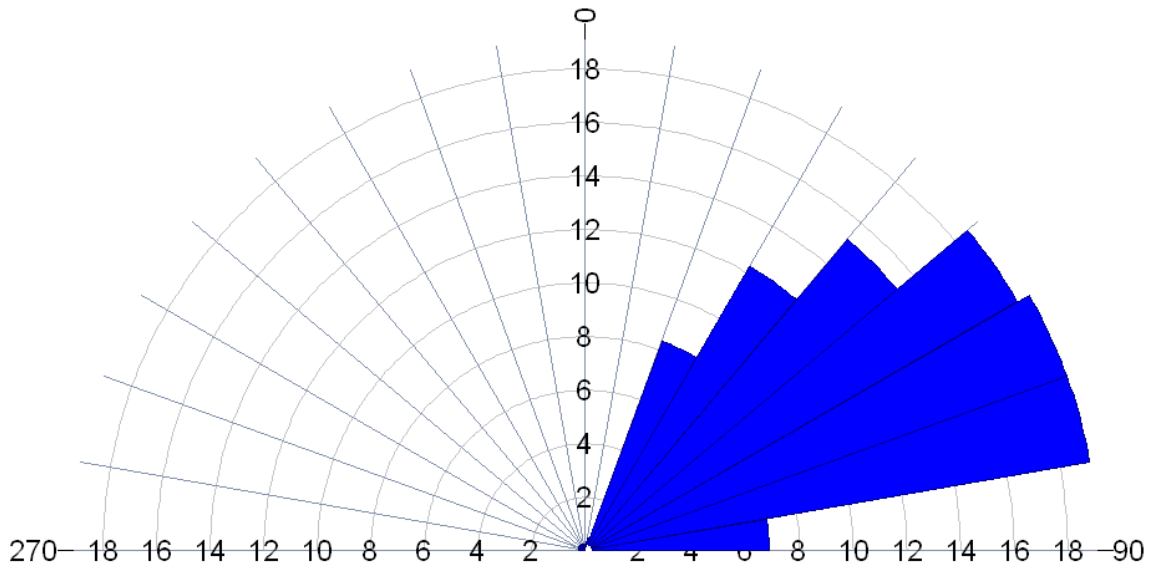
All directions are with respect to Magnetic North.

**Rose Diagram – Dip Directions
Image Features
CB & I
Project: Edwards Air Force Base
Well: 37-B13
December 18, 2013**



All directions are with respect to Magnetic North.

Rose Diagram – Dip Angles
Image Features
CB & I
Project: Edwards Air Force Base
Well: 37-B13
December 18, 2013



All directions are with respect to Magnetic North.



Flow Logs

COLOG Group

810 Quail Street, Suite E, Lakewood, CO 80215

Phone: (303) 279-0171, Fax: (303) 278-0135

www.idsdrill.com

COMPANY: CB&I

PROJECT: Edwards AFB

DATE LOGGED: 19 December 2013

WELL: 37-B13

Depth 1ft:140ft	Ambient Flow	
	-0.5	0.5
	GPM Flow Pumping at 0.365 gpm	
	-0.5	0.5
40		■ 0.00
50		■ 0.00
60	0.02	■ 0.00
70		■ 0.00
80	0.03	■ 0.00
90	0.00	■ 0.00
		■ 0.00

APPENDIX D FIELD OPERATIONS SUMMARY TABLE

Page Intentionally Left Blank

Date	Duration	Day Relative to Bioaugmentation	Activity	Extraction Well 37-B12				Extraction Well 37-B13				Comments
				Pump Cycle		Flowrate (mL/min)	Flow Totalizer (liters)	Pump Cycle		Flowrate (mL/min)	Flow Totalizer (liters)	
				Refill (min:sec)	Discharge (min:sec)			Refill (min:sec)	Discharge (min:sec)			
1/10/2013	13 days	-596	Install 37-B06, 37-B07, 37-B08, 37-B09									4 wells: 37-B06, 37-B07, 37-B08, 37-B09
1/17/2013	2 days	-589	Geophysical Testing									2 wells: 37-B06, 37-B09
1/23/2013	3 days	-583	Push-Pull Testing									3 intervals: 37-B06s, 37-B06d, 37-B07
3/5/2013	17 days	-542	Interwell Testing									2 wells: 37-B06, 37-B07
12/4/2013	13 days	-268	Install 37-B10, 37-B11, 37-B12, 37-B13									4 wells: 37-B10, 37-B11, 37-B12, 37-B13
12/18/2013	3 days	-254	Geophysical Testing									4 wells: 37-B07, 37-B10, 37-B12, 37-B13
1/8/2014	175 days	-233	STAGE 1 - Hydraulic Testing & Baseline Sampling									
1/8/2014	1 day	-233	Short-term pump test at 37-B12									
1/9/2014	1 day	-232	Short-term pump test at 37-B13									
1/10/2014	1 day	-231	Short-term pump test at 37-B06									
1/13/2014	1 day	-228	Short-term pump test at 37-B07									
5/28/2014	2 days	-93	Baseline Sampling Event No. 1									4 wells/7 intervals: 37-B07s, 37-B07i, 37-B07d, 37-B11s, 37-B11d, 37-B12, 37-B13
6/30/2014	2 days	-60	Groundwater Recirculation System Testing				205,495				148,626	
7/2/2014	1 day	-58	Baseline Sampling Event No. 2									4 wells/7 intervals: 37-B07s, 37-B07i, 37-B07d, 37-B11s, 37-B11d, 37-B12, 37-B13
7/2/2014	57 days		STAGE 2 - Groundwater Recirculation and PTT									
7/2/2014	1 day	-58	Groundwater Recirculation System Start-up	4:30	0:30	80	205,518	4:30	0:30	80	148,637	
7/3/2014		-57	System Operating	4:30	0:30	72	205,616	4:30	0:30	36	148,716	
7/6/2014		-54	System Operating	4:30	0:30	66		4:30	0:30	18		
7/8/2014		-52	System Operating	4:30	0:30	81	206,184	4:30	0:30	31	148,993	Deflate packer in 37-B13 due to low well production
7/10/2014		-50	System Operating	4:30	0:30	82	206,415	4:30	0:30	26	149,123	
7/15/2014	92 days	-45	Partitioning Tracer Testing	4:30	0:30	90	206,983	4:30	0:30	27	149,408	Multiple Sampling Rounds at 4 wells/7 intervals: 37-B07s, 37-B07i, 37-B07d, 37-B11s, 37-B11d, 37-B12, 37-B13
7/30/2014		-30	System Operating	4:30	0:30	100	209,236	4:30	0:30	22	150,218	
8/7/2014		-22	System Operating	4:30	0:30	98	210,445	4:30	0:30	26	150,740	
8/14/2014		-15	System Operating	4:30	0:30	98	211,501	4:30	0:30	26	151,219	
8/27/2014	1 day	-2	Pre-Bioaugmentation Sampling Event									5 wells/8 intervals: 37-B07s, 37-B07i, 37-B07d, 37-B11s, 37-B11d, 37-B12, 37-B13, 37-EW07
8/28/2014	264 days	-1	STAGE 3 - Bioaugmentation Treatment and Monitoring									
8/28/2014	1 day	-1	Initial Lactate/Nutrient Pulse Injection	4:30	0:30	86	213,532	4:30	0:30	28	152,192	57 liters of lactate/nutrients (1,000 mg/L lactate, 100 mg/L DAP, 100 mg/L yeast extract) injected at approximately 400 mL/min. Begin auto amendment injection.
8/29/2014	1 day	0	Bioaugmentation Injection									19 liters of SDC-9 culture injected at approximately 400 mL/min. Inject 38 liters of chase water containing 1,000 mg/L lactate, 100 mg/L DAP, 100 mg/L yeast extract. Increase pumping cycle time for 37-B12 from 12 mins (11:30 refill, 0:30 discharge) to decrease flow to injection well.
9/2/2014		4	System Operating	11:30	0:30	42	213,882	4:30	0:30	26	152,498	
9/9/2014	1 day	11	Post-Bioaugmentation Sampling Event No. 1	11:30	0:30	42	214,300	4:30	0:30	28	152,874	5 wells/8 intervals: 37-B07s, 37-B07i, 37-B07d, 37-B11s, 37-B11d, 37-B12, 37-B13, 37-EW07
9/24/2014		26	System Operating	11:30	0:30	42	214,714	4:30	0:30	52	153,365	
10/2/2014	1 day	34	Redevelop 37-B06 with surge block and pumping	11:30	0:30	42	214,841	4:30	0:30	58	153,549	System down during well redevelopment activities
10/13/2014	1 day	45	Post-Bioaugmentation Sampling Event No. 2	11:30	0:30	42	215,078	4:30	0:30	58	153,887	4 wells/7 intervals: 37-B07s, 37-B07i, 37-B07d, 37-B11s, 37-B11d, 37-B12, 37-B13

Date	Duration	Day Relative to Bioaugmentation	Activity	Extraction Well 37-B12				Extraction Well 37-B13				Comments
				Pump Cycle		Flowrate (mL/min)	Flow Totalizer (liters)	Pump Cycle		Flowrate (mL/min)	Flow Totalizer (liters)	
				Refill (min:sec)	Discharge (min:sec)			Refill (min:sec)	Discharge (min:sec)			
10/20/2014		52	System Operating	11:30	0:30	42	215,136	4:30	0:30	60	153,974	Mix new 50 gallon batch of amendments (1,000 mg/L lactate, 100 mg/L DAP, 100 mg/L yeast extract). Set chemical feed pump at 30 mL/min. Install anti-syphon valve on amendmnet injection line to stop syphoning of amendments into process stream.
11/5/2014		68	System Operating	11:30	0:30	42	215,390	4:30	0:30	60	154,355	
11/19/2014	1 day	82	Post-Bioaugmentation Sampling Event No. 3	11:30	0:30	42	215,651	4:30	0:30	60	154,743	4 wells/7 intervals: 37-B07s, 37-B07i, 37-B07d, 37-B11s, 37-B11d, 37-B12, 37-B13
12/17/2014	1 day	110	Post-Bioaugmentation Sampling Event No. 4									4 wells/7 intervals: 37-B07s, 37-B07i, 37-B07d, 37-B11s, 37-B11d, 37-B12, 37-B13
12/17/2014		110	System Operating	11:30	0:30	42	216,045	4:30	0:30	66	155,320	Add bicarbonate to achieve 200 mg/L in process stream. Set chemical feed pump to 2 mins ON, 118 mins OFF
1/13/2015		137	System Operating	11:30	0:30	42	216,236	4:30	0:30	75	155,608	Set chemical feed pump to 2 mins ON, 28 mins OFF
2/9/2015	4 days	164	Redevelope 37-B06 with Nu-Well products									System down during well redevelopment activities
2/13/2015		168	System Operating	11:30	0:30	42	216,462	4:30	0:30	80	155,920	Restart system, 37-B06 re-install bottom packer only, add 2 liters (in 19 liter keg) SDC-9 culture to 37-B06
2/16/2015		171	System Operating	11:30	0:30		216,639	4:30	0:30		156,112	
2/23/2015		178	System Operating	11:30	0:30	42	216,736	4:30	0:30	63	156,256	
3/5/2015	1 day	188	Post-Bioaugmentation Sampling Event No. 5	11:30	0:30	42	216,934	4:30	0:30	76	156,513	4 wells/7 intervals: 37-B07s, 37-B07i, 37-B07d, 37-B11s, 37-B11d, 37-B12, 37-B13
3/16/2015		199	System Operating	11:30	0:30	42	217,050	4:30	0:30	70	156,682	
3/17/2015		200	System Operating	11:30	0:30		217,068	4:30	0:30		156,707	
3/27/2015	1 day	210	Redevelope 37-B06 with surge block and wire brush									System down during well redevelopment activities
3/28/2015		211	System Operating	11:30	0:30	42	217,147	4:30	0:30	85	156,815	
4/13/2015	1 day	227	Post-Bioaugmentation Sampling Event No. 6	11:30	0:30	42	218,327	4:30	0:30	22	157,614	4 wells/6 intervals: 37-B07s, 37-B07d, 37-B11s, 37-B11d, 37-B12, 37-B13
4/18/2015		232	System Operating	11:30	0:30	42	218,662	4:30	0:30	20	157,858	Add 2 liters (in 19 liter keg) SDC-9 culture to 37-B06. Deflate packer in 37-B06. Mix 10 gallons of lactate/nutrients
4/21/2015		235	System Operating	11:30	0:30	42	218,868	4:30	0:30	20	158,003	Mix 40 gallons of lactate/nutrients
5/19/2015	1 day	263	Shut-down recirculation system	11:30	0:30	42	220,419	4:30	0:30	40	159,351	
5/19/2015	295 days	263	STAGE 4 - Post-Treatment Monitoring and Assessment									
5/19/2015	1 day	263	Rebound Baseline Sampling Event									4 wells/6 intervals: 37-B07s, 37-B07d, 37-B11s, 37-B11d, 37-B12, 37-B13
8/5/2015	1 day	341	Rebound Sampling Event No. 1									2 wells/3 intervals: 37-B07d, 37-B11s, 37-B11d
10/19/2015	1 day	416	Rebound Sampling Event No. 2									1 well/2 intervals: 37-B11s, 37-B11d
10/19/2015	3 days	416	Transport soil drums from staging area to site, spread soil onsite									Spreading of soil on-site approved by Base personnel
1/12/2016	1 day	501	Rebound Sampling Event No. 3									1 well/2 intervals: 37-B11s, 37-B11d
3/9/2016	1 day	558	Rebound Sampling Event No. 4									1 well/2 intervals: 37-B11s, 37-B11d
7/12/2016	1 day	683	Discharge IDW water to Base industrial sewer									Discharge approved under permit from Base
9/28/2016	2 days	761	Post-Treatment Rock Core Collection									37-B14: Collect samples for VOC and ferrous iron analysis

**APPENDIX E PERMIT FOR INDUSTRIAL WASTEWATER
DISCHARGE**

Page Intentionally Left Blank

APPENDIX F ANALYTICAL DATA TABLES

Page Intentionally Left Blank

Appendix F - Table 1: Analytical Results Summary - Stage 2 Partitioning Tracer Test

Sample ID	Sample Date	Sample Time	VOCs				Bromide (mg/L)	Alcohols			
			DCE (mg/L)	TCE (mg/L)	PCE (mg/L)	VC (mg/L)		Methanol (mg/L)	24DMP (mg/L)	2-octanol (mg/L)	355TMH (mg/L)
37-B07s	7/15/2014	9:00	<0.1	0.6	4.8	<0.1					
37-B07s	7/15/2014	10:00	<0.1	0.5	4.5	<0.1	2.00	0	0	0	0
37-B07s	7/15/2014	14:00	<0.1	0.7	8.3	<0.1	2.02	0	0	0	0
37-B07s	7/16/2014	17:00	<0.1	1.7	12.2	<0.1	2.04	0	0	0	0
37-B07s	7/17/2014	17:00	<0.1	0.9	12.2	<0.1	2.11	0	0	0	0
37-B07s	7/18/2014	11:30					1.83	0	0	0	0
37-B07s	7/19/2014	9:00	<0.1	0.9	13.0	<0.1	1.73	0	0	0	0
37-B07s	7/21/2014	7:00	<0.1	0.9	11.8	<0.1	1.70	0	0	0	0
37-B07s	7/22/2014	7:00	<0.1	1.1	13.2	<0.1	1.63	0	0	0	0
37-B07s	7/23/2014	9:00	<0.1	1.0	12.1	<0.1	1.47	0	0	0	0
37-B07s	7/24/2014	9:00	<0.1	1.1	10.6	<0.1	1.68	0	0	0	0
37-B07s	7/25/2014	9:00	<0.1	1.0	11.2	<0.1	1.45	0	0	0	0
37-B07s	7/31/2014	10:00	<0.1	0.9	11.5	<0.1	1.58	0	0	0	0
37-B07s	8/7/2014	10:00	<0.1	0.9	9.1	<0.1	1.69	0	0	0	0
37-B07s	8/14/2014	8:35	<0.1	0.8	8.4	<0.1		0	0.05	0	0
37-B07s	8/27/2014	11:35	<0.1	0.9	9.2	<0.1	2.16	0	0.09	0	0
37-B07s	9/9/2014	9:10	<0.1	1.1	10.6	<0.1	2.10	0	0	0	0
37-B07i	7/15/2014	9:00	<0.1	0.6	5.2	<0.1					
37-B07i	7/15/2014	10:00	<0.1	0.7	8.1	<0.1	2.20	0	0	0	0
37-B07i	7/15/2014	14:00	<0.1	0.6	6	<0.1	2.01	0	0	0	0
37-B07i	7/16/2014	17:00	<0.1	0.6	5.8	<0.1	1.89	0	0	0	0
37-B07i	7/17/2014	17:00	<0.1	0.5	5.3	<0.1	1.86	0	0	0	0
37-B07i	7/18/2014	11:30					1.97	0	0	0	0
37-B07i	7/19/2014	9:00	<0.1	0.5	6.1	<0.1	1.89	0	0	0	0
37-B07i	7/21/2014	7:00	<0.1	0.5	5.9	<0.1	1.49	0	0	0	0
37-B07i	7/21/2014	17:00					1.56	0	0	0	0
37-B07i	7/22/2014	7:00	<0.1	0.5	5.4	<0.1	1.51	0	0	0	0
37-B07i	7/22/2014	17:00					1.50	0	0	0	0
37-B07i	7/23/2014	9:00	<0.1	0.6	6	<0.1	1.38	0	0	0	0
37-B07i	7/23/2014	17:00					1.50	0	0	0	0
37-B07i	7/24/2014	9:00	<0.1	0.6	7.6	<0.1	1.44	0	0	0	0
37-B07i	7/24/2014	17:00					1.47	0	0	0	0
37-B07i	7/25/2014	9:00	<0.1	0.6	7.1	<0.1	1.53	0	0	0	0
37-B07i	7/31/2014	10:00	<0.1	0.3	4.0	<0.1	1.53	0	0	0	0
37-B07i	8/7/2014	10:00	<0.1	0.4	5.0	<0.1	1.59	0	0	0	0
37-B07i	8/14/2014	9:30	<0.1	0.5	4.5	<0.1		0	0	0	0
37-B07i	8/28/2014		<0.1	0.7	9.6	<0.1		0	0	0	0
37-B07i	9/9/2014	8:40	<0.1	0.5	6.8	<0.1		0	0	0	0
37-B07d	7/15/2014	9:00	<0.1	0.6	7.5	<0.1					
37-B07d	7/15/2014	10:00	<0.1	1.1	25.6	<0.1	1.60	0	0	0	0
37-B07d	7/15/2014	14:00	<0.1	1.0	24.8	<0.1	1.42	0	0	0	0
37-B07d	7/16/2014	17:00	<0.1	1.0	24.0	<0.1	1.47	0	0	0	0
37-B07d	7/17/2014	17:00	<0.1	1.1	25.3	<0.1	1.44	0	0	0	0
37-B07d	7/18/2014	11:30					1.64	0.2	0.2	0.0	0
37-B07d	7/19/2014	9:00	<0.1	1.1	28.1	<0.1	1.86	0.5	0.4	0.0	
37-B07d	7/21/2014	7:00	<0.1	1.1	27.0	<0.1	2.58	1.0	1.0	0.1	
37-B07d	7/21/2014	17:00					2.98	1.4	1.1	0.1	
37-B07d	7/22/2014	7:00	<0.1	1.4	34.1	<0.1	3.19	1.6	1.4	0.1	
37-B07d	7/22/2014	17:00					3.66	1.9	1.6	0.1	
37-B07d	7/23/2014	9:00	<0.1	1.2	30.7	<0.1	4.04	2.2	2.2	0.2	
37-B07d	7/23/2014	17:00					4.52	2.5	2.0	0.2	
37-B07d	7/24/2014	9:00	<0.1	1.4	35.3	<0.1	4.74	2.8	2.2	0.2	
37-B07d	7/24/2014	17:00					4.88	3.1	2.6	0.3	
37-B07d	7/25/2014	9:00	<0.1	1.4	34.3	<0.1	5.18	3.3	2.7	0.2	
37-B07d	7/31/2014	10:00	<0.1	1.1	27.4	<0.1	5.60	3.2	3.1	0.2	0.1
37-B07d	8/7/2014	10:00	<0.1	1.3	25.7	<0.1	6.29	2.2	3.8	0.0	0.0
37-B07d	8/14/2014	7:30	<0.1	1.4	32.2	<0.1		1.95	4.32	0.15	0.05
37-B07d	8/27/2014	12:40	<0.1	1.9	45.6	<0.1	5.65	1.00	4.00	0.15	0.07
37-B07d	9/9/2014	8:30	<0.1	2.3	68.7	<0.1	4.10	0.11	3.52	0.00	0.00

Appendix F - Table 1: Analytical Results Summary - Stage 2 Partitioning Tracer Test

Sample ID	Sample Date	Sample Time	VOCs				Bromide (mg/L)	Alcohols			
			DCE (mg/L)	TCE (mg/L)	PCE (mg/L)	VC (mg/L)		Methanol (mg/L)	24DMP (mg/L)	2-octanol (mg/L)	355TMH (mg/L)
37-B11s	7/15/2014	9:00	<0.1	0.0	2.6	<0.1					
37-B11s	7/15/2014	10:00	<0.1	2.6	43.4	<0.1	1.09	0	0	0	0
37-B11s	7/15/2014	12:00		0.6	7.3		1.75	0	0	0	0
37-B11s	7/15/2014	14:00	<0.1	2.6	44.6	<0.1	1.08	0.3	0.1	0.0	0.0
37-B11s	7/15/2014	17:00		2.6	41.5		8.44	22.4	11.7	3.7	2.0
37-B11s	7/16/2014	7:00		2.0	20.8		33.46	90.0	43.9	13.3	8.1
37-B11s	7/16/2014	12:00		1.7	25.6		187.85	532.7	246.3	79.1	46.7
37-B11s	7/16/2014	17:00	<0.1	1.4	22.6	<0.1	235.57	582.3	292.5	94.3	57.4
37-B11s	7/17/2014	7:00		2.3	36.8		84.44	212.0	103.8	32.7	20.1
37-B11s	7/17/2014	11:30		2.7	39.9		61.33	160.9	73.1	22.4	13.8
37-B11s	7/17/2014	17:00	<0.1	3.0	43.3	<0.1	43.99	116.5	55.4	16.6	10.0
37-B11s	7/18/2014	7:00		3.3	46.3		30.93	79.8	36.7	10.4	6.3
37-B11s	7/18/2014	11:30		3.3	46.8		25.50	62.5	29.8	8.5	5.2
37-B11s	7/18/2014	17:00		3.5	49.0		23.89	56.3	26.8	6.9	4.5
37-B11s	7/19/2014	9:00	<0.1	3.5	52.6	<0.1	18.50	45.1	20.2	5.7	3.7
37-B11s	7/20/2014	9:00		3.6	52.3		14.61	39.1	17.9	4.7	3.0
37-B11s	7/21/2014	7:00	<0.1	3.6	54.6	<0.1	9.50	23.6	11.0	2.7	1.9
37-B11s	7/21/2014	17:00		3.8	61.5		7.91	21.0	10.1	2.4	1.6
37-B11s	7/22/2014	7:00	<0.1	2.8	57.8	<0.1	6.65	16.8	8.6	1.8	1.3
37-B11s	7/22/2014	17:00		3.4	58.5		6.14	14.3	7.3	1.6	1.1
37-B11s	7/23/2014	9:00	<0.1	3.8	62.3	<0.1	5.58	10.3	6.6	1.1	1.0
37-B11s	7/23/2014	17:00		3.5	58.5		4.88	8.5	5.2	1.0	1.0
37-B11s	7/24/2014	9:00	<0.1	3.8	66.7	<0.1	3.95	5.8	4.2	0.8	0.7
37-B11s	7/25/2014	9:00	<0.1	3.7	60.0	<0.1	2.99	2.6	3.2	0.4	0.4
37-B11s	7/31/2014	10:00	<0.1	4.1	70.7	<0.1	1.50	0.0	1.0	0.1	0.03
37-B11s	8/7/2014	10:00	<0.1	4.5	70.7	<0.1	1.01	0.0	0.6	0.0	0.0
37-B11s	8/14/2014	7:50	<0.1	3.9	59.7	<0.1		0.00	0.22	0.00	0.00
37-B11s	8/27/2014	10:30	<0.1	4.6	81.0	<0.1	1.04	0.02	0.09	0.00	0.00
37-B11s	9/9/2014	10:30					1.73	0.00	0.00	0.00	0.00
37-B11d	7/15/2014	9:00	<0.1	0.7	13.8	<0.1					
37-B11d	7/15/2014	10:00	<0.1	0.9	16.6	<0.1	1.52	0	0	0	0
37-B11d	7/15/2014	12:00	<0.1	1.2	19.1	<0.1	1.21	0	0	0	0
37-B11d	7/15/2014	14:00	<0.1	1.3	20.6	<0.1	1.36	0	0	0	0
37-B11d	7/15/2014	17:00	<0.1	1.3	21.2	<0.1	1.76	0	0	0	0
37-B11d	7/16/2014	7:00	<0.1	1.4	22.5	<0.1	2.95	5.1	2.6	0.7	0.3
37-B11d	7/16/2014	12:00	<0.1	1.3	21.8	<0.1	13.21	20.8	10.6	3.1	1.9
37-B11d	7/16/2014	17:00	<0.1	1.4	21.9	<0.1	11.97	17.9	9.2	2.6	1.4
37-B11d	7/17/2014	7:00	<0.1	1.2	19.9	<0.1	7.52	14.7	7.7	1.7	1.0
37-B11d	7/17/2014	11:30	<0.1	1.4	22.0	<0.1	15.06	44.2	24.1	6.7	3.8
37-B11d	7/17/2014	17:00	<0.1	1.5	25.7	<0.1	112.00	321.2	153.2	46.8	28.4
37-B11d	7/18/2014	7:00	<0.1	1.9	26.4	<0.1	116.79	341.4	163.0	49.1	30.0
37-B11d	7/18/2014	11:30	<0.1	1.9	28.4	<0.1	121.37	284.6	136.0	44.3	26.5
37-B11d	7/18/2014	17:00	<0.1	1.8	26.8	<0.1	40.23	98.1	50.1	14.6	8.6
37-B11d	7/19/2014	9:00	<0.1	1.6	22.5	<0.1	38.14	97.1	44.8	13.0	7.9
37-B11d	7/20/2014	9:00	<0.1	1.9	26.6	<0.1	34.63	84.0	41.0	10.4	6.4
37-B11d	7/21/2014	7:00	<0.1	2.0	32.1	<0.1	32.75	81.5	38.0	9.1	5.1
37-B11d	7/21/2014	17:00	<0.1	2.1	31.5	<0.1	30.20	73.9	37.6	7.9	4.5
37-B11d	7/22/2014	7:00	<0.1	2.1	25.8	<0.1	31.31	72.4	36.2	7.0	4.2
37-B11d	7/22/2014	17:00	<0.1	2.3	32.2	<0.1	27.85	64.6	33.4	6.8	4.0
37-B11d	7/23/2014	9:00	<0.1	2.3	32.3	<0.1	26.45	60.6	31.7	6.5	3.8
37-B11d	7/23/2014	17:00	<0.1	2.5	34.0	<0.1	25.66	61.8	30.8	6.1	3.5
37-B11d	7/24/2014	9:00	<0.1	2.6	29.0	<0.1	24.97	58.8	29.6	5.6	3.4
37-B11d	7/25/2014	9:00	<0.1	2.6	37.7	<0.1	22.94	54.7	27.3	5.6	3.1
37-B11d	7/31/2014	10:00	<0.1	2.9	40.0	<0.1	16.57	37.9	19.5	3.8	1.8
37-B11d	8/7/2014	10:00	<0.1	3.3	45.8	<0.1	11.48	27.4	14.0	2.5	1.4
37-B11d	8/14/2014	8:15	<0.1	3.9	43.9	<0.1		17.3	8.8	0.6	0.0
37-B11d	8/27/2014	11:00	<0.1	4.6	54.7	<0.1	4.91	7.4	4.6	0.2	0.0
37-B11d	9/9/2014	10:15					2.65				

Appendix F - Table 1: Analytical Results Summary - Stage 2 Partitioning Tracer Test

Sample ID	Sample Date	Sample Time	VOCs				Bromide (mg/L)	Alcohols			
			DCE (mg/L)	TCE (mg/L)	PCE (mg/L)	VC (mg/L)		Methanol (mg/L)	24DMP (mg/L)	2-octanol (mg/L)	355TMH (mg/L)
37-B12	7/15/2014	9:00	<0.1	2.7	30.1	<0.1					
37-B12	7/15/2014	10:00	<0.1	4.3	109	<0.1	1.27	0	0	0	0
37-B12	7/15/2014	14:00	<0.1	5.0	117.8	<0.1	1.14	0	0	0	0
37-B12	7/16/2014	17:00	<0.1	5.4	113.3	<0.1	0.89	0	0	0	0
37-B12	7/17/2014	17:00	<0.1	5.2	110.0	<0.1	0.93	0	0	0	0
37-B12	7/18/2014	11:30	<0.1	4.7	104.4	<0.1	0.64	0	0	0	0
37-B12	7/19/2014	9:00	<0.1	5.5	117.3	<0.1	0.79	0	0	0	0
37-B12	7/21/2014	7:00	<0.1	5.4	119.3	<0.1	0.96	0	0	0	0
37-B12	7/22/2014	7:00	<0.1	5.4	129.6	<0.1	1.04	0	0	0	0
37-B12	7/23/2014	9:00	<0.1	4.8	125.4	<0.1	1.07	0	0	0	0
37-B12	7/24/2014	9:00	<0.1	4.4	129.3	<0.1	1.05	0	0	0	0
37-B12	7/25/2014	9:00	<0.1	4.4	119.7	<0.1	0.96	0	0	0	0
37-B12	7/31/2014	10:00	<0.1	6.2	157.5	<0.1	0.93	0	0	0	0
37-B12	8/7/2014	10:00	<0.1	5.1	121.5	<0.1	0.88	0	0	0	0
37-B12	8/14/2014	7:00	<0.1	5.6	121.4	<0.1		0	0	0	0
37-B12	8/27/2014	15:35	<0.1	6.8	150.0	<0.1	0.12	0	0	0	0
37-B12	9/9/2014		<0.1	8.6	173.6	<0.1		0	0	0	0
37-B13	7/15/2014	9:00	<0.1	0.1	15.6	<0.1					
37-B13	7/15/2014	10:00	<0.1	0.4	35.5	<0.1	1.12	0	0	0	0
37-B13	7/15/2014	14:00	<0.1	0.3	31.0	<0.1	1.23	0	0	0	0
37-B13	7/16/2014	17:00	<0.1	0.4	32.1	<0.1	1.03	0	0	0	0
37-B13	7/17/2014	17:00	<0.1	0.3	30.6	<0.1	1.10	0	0	0	0
37-B13	7/18/2014	11:30	<0.1	0.4	38.1	<0.1	1.03	0	0	0	0
37-B13	7/19/2014	9:00	<0.1	0.4	38.2	<0.1	0.95	0	0	0	0
37-B13	7/21/2014	7:00	<0.1	0.4	43.2	<0.1	0.56	0	0	0	0
37-B13	7/22/2014	7:00	<0.1	0.4	43.1	<0.1	0.78	0	0	0	0
37-B13	7/23/2014	9:00	<0.1	0.4	41.0	<0.1	0.51	0	0	0	0
37-B13	7/24/2014	9:00	<0.1	0.5	44.3	<0.1	0.51	0	0	0	0
37-B13	7/25/2014	9:00	<0.1	0.5	49.0	<0.1	0.56	0	0	0	0
37-B13	7/31/2014	10:00	<0.1	0.5	56.8	<0.1	0.54	0	0	0	0
37-B13	8/7/2014	10:00	<0.1	0.5	61.7	<0.1		0	0	0	0
37-B13	8/14/2014	7:05	<0.1	0.6	62.0	<0.1		0	0	0	0
37-B13	8/27/2014	14:42	<0.1	0.5	54.3	<0.1	1.02	0	0	0	0
37-B13	9/9/2014		<0.1	0.6	77.5	<0.1		0	0	0	0

